

ADAPTIVE CONTROL AND IDENTIFICATION
FOR ON-LINE DRUG INFUSION IN ANAESTHESIA

A thesis submitted to the
UNIVERSITY OF SHEFFIELD
for the degree of
DOCTOR OF PHILOSOPHY

by

Mahdi MAHFOUF, Ingenieur d'Etat, MPhil.

Department of Automatic Control
and Systems Engineering

October 1991.

To the memory of my
brother Azzeddine

Publications and Conference Presentations

Some of the results obtained during the course of this research have appeared (or will appear) in the following publications:

1. Linkens D.A., Mahfouf, M., Asbury, A.J., and Gray, W.M. (1991) "Generalized predictive control applied to muscle relaxant anaesthesia", IEE conference on adaptive control, Control 91, Edinburgh, March, pp 790-794 .
2. Linkens, D.A., Mahfouf, M., and Asbury, A.J. (1991) "Multivariable generalized predictive control for anaesthesia", Proc. First European Control Conference ECC1, Grenoble (France), 2nd. July, Vol.2, pp 1687-1683.
3. Linkens, D.A., Mahfouf, M., and Abbod, M. (1991) "Self-adaptive and self-organizing control applied to non-linear multivariable anaesthesia: a comparative model-based study", IEE Proc., submitted.
4. Linkens D.A., Mahfouf, M. (1991) "Generalized predictive control (GPC) in operating theatre", IEE Proc., in preparation.
5. Linkens D.A., Mahfouf, M. (1991) "Multivariable generalized predictive control using feedforward for anaesthesia", IEE Proc., in preparation.

Acknowledgements

I would like to express my most sincere gratitude to my supervisor, Professor D.A. Linkens, for his help, guidance, encouragement and stimulation throughout the course of this study.

My thanks are also extended to Dr. M. Menad, Dr. M. Khelfa, Dr. S. Greenhow, and Dr. M.J. Tham for many stimulating and fruitful discussions.

I am pleased to acknowledge the help of Dr. A.J. Asbury, and Dr. W.M. Gray from Western Infirmary Hospital, Glasgow without whom the clinical trials in theatre would not have been made possible. My thanks are also extended to their very kind and generous families. I also take the opportunity to thank Dr. J. Peacock from Hallamshire Hospital who helped with the trials in Sheffield.

I also wish to thank the technical and clerical staff of the Department of Automatic Control and Systems Engineering, particularly Mr. D. Cotterill, Mr. A. Green, Miss A. Kisby, Mrs. J. Stubbs, Mr. T. Cornah, Mrs. L. Gray, Miss Julie, and Mrs Carroll for their kindness and understanding.

Finally and most importantly, I wish to thank my mother, my father, my sisters, my nephew Azzeddine, my girlfriend Amanda and her family, my brothers Abdelkrim, Nourreddine, Slimane, and Abderrahmane and their families for their ever-lasting moral support.

ADAPTIVE CONTROL AND IDENTIFICATION
FOR ON-LINE DRUG INFUSION IN ANAESTHESIA

by

Mahdi MAHFOUF

SUMMARY

Anaesthesia is that part of the medical science profession which ensures that the patient's body is insensitive to pain and possibly other stimuli during surgical operations. It includes muscle relaxation (paralysis) and unconsciousness, both conditions being crucial for the operating surgeon. Maintaining a steady level of muscle relaxation as well as an acceptable depth of anaesthesia (unconsciousness), while keeping the dosage of administered drugs which induce those effects at a minimum level, have successfully been achieved using automatic control.

Fixed gain controllers such as P, PI, and PID strategies can perform well when used in clinical therapy and under certain conditions but on the other hand can lead to poor performances because of the large variability between subjects. This is the reason which led to the consideration of adaptive control techniques which seemed to overcome such problems.

Two control strategies falling into the above scheme and including the two newly developed techniques, i.e Proportional-Integral-Plus (PIP) control algorithm, and Generalized Predictive Control algorithm (GPC), are considered under extensive simulation studies using the muscle relaxation process associated with two drugs known as Pancuronium-Bromide and Atracurium. Both models exhibit

severe non-linearities as well as time-varying dynamics and delays.

Only the strategy corresponding to the GPC algorithm is retained for implementation on a 380Z disk-based microcomputer system, while the muscle relaxation process corresponding to either drugs is simulated on a VIDAC 336 analogue computer. The sensitivity of the algorithm is investigated when patient-to-patient parameter variability is evoked. The study is seen to provide the necessary basis for future clinical implementation of the scheme.

Following the satisfactory results obtained under such a real-time environment, the self-adaptive GPC algorithm has been successfully applied in theatre to control Atracurium infusion on humans during surgery.

This success later motivated further research work in which simultaneous control of muscle relaxation and anaesthesia (unconsciousness) was achieved. A good multivariable model has been derived and controlled via the multivariable version of the SISO GPC algorithm. The results obtained are very encouraging.

Table of Contents

Publications and Conference Presentations	i
Acknowledgements	ii
Summary	iii
CHAPTER 1: INTRODUCTION	1
 CHAPTER 2: PHYSIOLOGICAL BACKGROUND PERTAINING TO THE MUSCLE RELAXATION PROCESS	 10
2.1 INTRODUCTION	10
2.2 THE NEUROMUSCULAR TRANSMISSION	10
2.3 MUSCLE RELAXANT DRUGS AND THEIR MECHANISM OF ACTION	11
2.3.1 The Depolarizing Type of Muscle Relaxant Agents	12
2.3.2 The Non-Depolarizing Type of Muscle Relaxant Agents	12
2.3.3 The Margin of Safety of Neuromuscular Transmission	12
2.4 PHARMACOLOGY OF MUSCLE RELAXANTS	13
2.4.1 Pharmacokinetics	13
2.4.2 Pharmacodynamics	15
2.5 MANAGEMENT OF NEUROMUSCULAR BLOCKADE	17
2.5.1 Evaluation of Neuromuscular Blockade	17

2.5.2 Administration of Muscle Relaxant Drugs and Reversal of Neuromuscular Blockade	18
CHAPTER 3: CLOSED-LOOP CONTROL OF MUSCLE RELAXATION DRUG ADMINISTRATION	19
3.1 INTRODUCTION	19
3.2 THE MATHEMATICAL MODELS ASSOCIATED WITH MUSCLE RELAXATION PROCESSES	21
3.2.1 Identification of Pancuronium Dynamics in Dogs	21
3.2.2 Pharmacology and Dose Response Relationship of Atracurium Administered I.V.	23
3.3 CLASSIC CONTROL OF MUSCLE RELAXATION SYSTEM	26
3.3.1 A Simulation Study with PI and PID Controllers	26
3.3.2 Sensitivity Studies	28
3.4 INTRODUCTION TO ADAPTIVE FEEDBACK CONTROL	29
3.4.1 The Explicit Self-Adaptive Control Approach: 'The Pole-Placement Approach'	31
3.4.2 The Implicit Self-Adaptive Control Approach: 'Optimal Regulation and Control'	33
3.4.3 Parameter Estimation Methods	35

CHAPTER 4: POLE-PLACEMENT PROPORTIONAL- INTEGRAL-PLUS (PIP) APPLIED TO THE MUSCLE RELAXATION SYSTEM	42
4.1 INTRODUCTION	42
4.2 A REVIEW OF STATE-SPACE FORMULATION	42
4.3 NON-MINIMAL STATE-SPACE FORM	46
4.4 THE PROPORTIONAL-INTEGRAL-PLUS CONTROL SYSTEM	48
4.5 A SIMPLE EXAMPLE OF APPLICATION	51
4.6 ON-LINE PIP CONTROL OF MUSCLE RELAXATION SYSTEM	53
4.6.1 Self-Tuning Adaptive PIP Control of Muscle Relaxation System Associated with Pancuronium-Bromide	54
4.6.2 Self-Tuning Adaptive PIP Control of Muscle Relaxation System Associated with Atracurium	65
4.7 SENSITIVITY OF THE PIP DESIGN TO THE PRESENCE OF TIME-DELAY	70
4.8 PIP DESIGN WITH DEAD-TIME COMPENSATION	71
4.8.1 The Classical Smith Predictor Scheme	73
4.8.2 The Extended Smith Predictor (ESP)	76
4.8.3 The $B(z^{-1})$ Polynomial Expansion Method	81

**CHAPTER 5: GENERALIZED PREDICTIVE CONTROL
(GPC) OF MUSCLE RELAXANT**

ANAESTHESIA	90
5.1 INTRODUCTION	90
5.2 DEVELOPMENT OF THE BASIC SISO GPC ALGORITHM	93
5.2.1 The CARIMA Process Model Representation and Output Prediction	93
5.2.2 Recursion of the Diophantine Equation	97
5.2.3 The Long-Range Predictive Control Principle and the GPC Control Law	100
5.2.4 The GPC Algorithm and the Selection of its Tuning Parameters	107
5.3 EXAMPLES OF APPLICATION	109
5.3.1 Example 1 (Non-Minimum Phase Plant)	109
5.3.2 Example 2 (Muscle Relaxation Process Pharmacokinetics)	113
5.4 GENERALIZED PREDICTIVE CONTROL (GPC) APPLIED TO THE MUSCLE RELAXATION SYSTEM	114
5.4.1 The Pancuronium-Bromide Model	115
5.4.2 The Atracurium Model	120
5.5 THE EXTENDED GPC ALGORITHM	122
5.5.1 Inclusion of The Model-Reference Polynomial $P(z^{-1})$	123

5.5.2 GPC and The Observer Polynomial $T(z^{-1})$	127
5.6 GENERALIZED PREDICTIVE CONTROL	
WITH INPUT CONSTRAINTS	132
5.6.1 GPC and the Soft Rate Limits	133
5.6.2 GPC and Amplitude Limits	135
CHAPTER 6: MICROCOMPUTER IMPLEMENTATION	
AND PERFORMANCE EVALUATION	
OF THE GPC CONTROLLER:	
A SIMULATION STUDY FOR	
PANCURONIUM AND ATRACURIUM	139
6.1 INTRODUCTION	139
6.2 CONTROL OF PANCURONIUM	
ADMINISTRATION USING GPC	141
6.2.1 Model Representation on the VIDAC 336	141
6.2.2 Implementation and Application of the GPC	
Algorithm Using the 380Z Machine	143
6.3 MICROCOMPUTER-CONTROLLED ANALOGUE	
COMPUTER MODEL OF ATRACURIUM	
DYNAMICS	146
6.3.1 Simulation of Atracurium Model	
on the VIDAC 336	146
6.3.2 Control of Atracurium Administration	
Using GPC	149
6.3.3 Sensitivity of the Self-Adaptive	
GPC to Patient Variability	151

**CHAPTER 7: SELF-ADAPTIVE GENERALIZED PREDICTIVE
CONTROL (GPC) OF ATRACURIUM
INDUCED MUSCLE RELAXATION
IN OPERATING THEATRE**

	159
7.1 INTRODUCTION	159
7.2 MODIFICATION OF THE MUSCLE RELAXATION CONTROL SYSTEM PRIOR TO CLINICAL EVALUATION	160
7.2.1 The Relaxograph Measurement System	160
7.2.2 The Pump-Syringe Unit	162
7.2.3 The Control Algorithm and the Sampling Period	162
7.2.4 The Overall Control Program	165
7.3 CLINICAL PREPARATION OF THE PATIENTS BEFORE SURGERY	166
7.4 RESULTS AND DISCUSSIONS	167

**CHAPTER 8: IDENTIFICATION AND CONTROL
OF NON-LINEAR MULTIVARIABLE
ANAESTHETIC MODEL**

	187
8.1 INTRODUCTION	187
8.2 IDENTIFICATION OF THE NON-LINEAR MULTIVARIABLE ANAESTHETIC MODEL	187
8.2.1 The Atracurium Mathematical Model	189
8.2.2 The Isoflurane Unconsciousness Model	190
8.2.3 Interactive Component Model	193
8.2.4 The Overall Multivariable Anaesthetic Model	198

8.3 DEVELOPMENT OF THE MULTIVARIABLE	
GPC CONTROLLER	198
8.3.1 The Basic Algorithm	198
8.3.2 Inclusion of the Model Following	
Polynomial $P(z^{-1})$	202
8.3.3 Inclusion of the Observer Polynomial $T(z^{-1})$	203
8.4 SIMULATION RESULTS	208
8.4.1 Simulation Studies Using Nominal	
Parameter Values	208
8.4.2 Simulation Studies via Monte-Carlo Parameter	
Selection Method	211
8.4.3 Execution-Time Considerations	216
8.5 MULTIVARIABLE GPC ALGORITHM USING	
FEEDFORWARD	218
8.5.1 Development of the SISO GPC	
Algorithm with Feedforward	218
8.5.2 Development of the Multivariable GPC	
Algorithm with Feedforward (GPCF)	220
8.6 SIMULATION RESULTS WITH GPCF	221
CHAPTER 9: CONCLUSIONS AND RECOMMENDATIONS	226
REFERENCES	234
APPENDICES	246
A. Solution of the Diophantine Equation-	
The Extended Version	246

B. Recursive Least-Squares Algorithm-

The Multivariable Case 249

CHAPTER 1

INTRODUCTION

During a surgical operation, the operating surgeon is often involved in cutting large areas of a muscle. In some cases muscle movements can considerably hinder the surgeon's activities so much that access to deeper structures often results in considerable tissue damage. In order to make the surgeon's task easier and at the same time help avoid the pain that may result from such surgical manipulations, there is a need for muscle movement reduction, i.e muscle relaxation.

Muscle contraction is the result of a series of events which start with an impulse generated in the central nervous system and followed by a release of a chemical substance called Acetylcholine which produces a depolarization, a crucial phase in the above chain of events that eventually leads to muscle movement. Breaking this chain of events that normally lead to muscle contraction is the driving force behind muscle relaxation, i.e paralysis. It is achieved by administering a number of muscle relaxant drugs. These muscle relaxant drugs fall into two main categories: depolarizing and non-depolarizing agents.

Depolarizing drugs produce a continuous depolarization, whereas the non-depolarizing type of drugs compete with Acetylcholine for the receptor sites. For this reason they are better known as competitive agents. Pancuronium-Bromide and Atracurium included in the present study are non-depolarizing type of agents.

Whether a depolarizing or a non-depolarizing type, the administration of muscle relaxant drugs needs to be carried out efficiently, which also implies that maintaining acceptable levels of relaxation for the operating surgeon must also be a prime target. For this purpose, it is important to have at least some knowledge of the interaction of these drugs with the body. Pharmacology is used to interpret

the metabolism of such drugs. Pharmacology comprises two main categories known as pharmacokinetics and pharmacodynamics. Pharmacokinetics study the relationship that exists between drug dose and drug concentration in the blood plasma as well as other parts of the body. Interpretation of this relationship was given a mathematical meaning when the concept of compartment models was introduced. With this concept the body is said to consist of several compartments each representing one part of the body that involves the drug metabolism.

Pharmacodynamics, however, are concerned with the drug concentration and the effect produced. One key postulate of this category is that there is a considerable delay separating the first administration of the muscle relaxant drug and the onset of relaxation; this is known as the "margin of safety" (Paton and Waud, 1967; Waud and Waud, 1971), whereby no depression of twitch response can be detected until over 75% of the receptors are occluded, and once initiated, paralysis cannot increase indefinitely as the drug dosage increases.

For muscle relaxation, measurements are made via evoked electromyogram (EMG) responses (Epstein and Epstein, 1975) obtained from supramaximal stimulation at the wrist. Resulting EMG signals at the hand are rectified and integrated giving a proportional measurement of the degree of relaxation.

In operating theatre, muscle relaxation monitoring is a prime responsibility (among others) of the anaesthetist. It is he who administers muscle relaxant drugs. Based on his own experience and relying on a few indices relating to the patient's medical history and body weight, he determines the right doses of the intravenous boluses to be given at different intervals. However, this strategy does not always lead to satisfactory results as obtained levels of relaxation are not steady. In major operations, such as eye and heart surgeries, this may lead to undesirable consequences, while large doses of muscle relaxant drugs which are unnecessarily

administered can lead to postoperative complications.

As a result, and over the last ten years, constructive steps have been taken to ensure that other more efficient ways of drug administration can be considered. That is how the idea of using automatic feedback control was first introduced by Cass et al. (1976) and Brown et al. (1980). Further research work later followed mainly that by Ritchie et al. (1985), Webster et al. (1987), and MacLeod et al. (1989). The general structure of the controllers used in these studies ranged from fixed proportional (P) controllers to proportional-integral (PI) and proportional-integral-derivative (PID) strategies. Significant improvements have been reported with the use of such protocols including obtaining a reasonably steady level of paralysis together with the reduction of the total dosage of administered muscle relaxant drugs. However, because of patient-to-patient physiological differences, the above fixed strategies were considered to be unsuitable for application as occasional oscillations were recorded during clinical trials on humans (Webster et al., 1987; MacLeod et al., 1989). Because it is practically impossible to proceed to the manual tuning of such controllers during an operation, the concept of adaptive control was considered to be an attractive candidate for application in this particular area of life sciences. An adaptive scheme consists of identifying the system dynamics given an adopted structure and updating the control law each time a control input is required from the process. This idea was first explored by Linkens et al. (1982) who devised an explicit algorithm in the form of pole-placement (Wellstead, 1980). The control strategy, experimented on dogs, was successful in reaching the targets previously mentioned. Pancuronium was used as the muscle relaxant drug. Further research work, also led by the same author considered the application of a self-adaptive PID algorithm (Denai et al., 1990) on humans using the drug Atracurium. Acceptable levels of relaxation were obtained with most of the patients included in the study.

Prior to any controller design study, a knowledge of the mathematical model associated with the process under consideration is required. In the case of muscle relaxation, the process may be modelled in terms of pharmacokinetics and pharmacodynamics. To describe the pharmacokinetics of the drugs, a two-compartment model was found to be suitable for both drugs considered. To reflect the pharmacodynamics, the "margin of safety" concept is usually described by a Hill equation (Whiting and Kelman, 1980; Weatherley et al., 1983) or a dead-space in series with a saturation element. A study of the pharmacodynamics of Atracurium by the previous authors postulated the existence of a third compartment known as the "effect compartment".

The research work leading to this thesis is mainly concerned with the design of more robust self-adaptive control strategies than the self-adaptive PID algorithm which, because of its inherent structure, cannot consider systems whose order is higher than 2, and whose performance because of these unmodelled dynamics often degrades. Two recently developed techniques were considered. The first one, falling into the category of explicit self-tuning algorithms, is based in part on the earlier continuous-time approach of Young and Willems (1972), and because its superficial similarity with the conventional digitized Proportional-Integral (PI) controller, it is referred to as the Proportional-Integral-Plus (PIP) control algorithm. It is a new approach in the sense that, by defining a non-minimal state-space (NMSS) representation of the system, whose state-variables are defined only in terms of the present and past values of the output and past values of the input signals, it is possible to avoid the main problem of conventional state-variable feedback (SVF) law which requires measuring all the state-variables.

Automatic feedback control has always suffered from problems caused by dead-time, and this has been acknowledged by many researchers (Smith, 1957;

Marshall, 1979; Gawthrop, 1977). Several schemes centered around the idea which was first introduced by Smith (1957, 1959) and known as the Smith predictor have since been proposed. Because of the particular importance of such control protocol, the combination of the PIP approach with the Smith predictor and called by the authors Extended Smith Predictor algorithm (ESP) (Chotai and Young, 1988) is investigated and compared with the algorithm that emerges as an inherent structure of the PIP control algorithm in the presence of a delay and named Generalized Smith Predictor algorithm (GSP).

The second self-tuning technique studied is known as the Generalized Predictive Control (GPC) algorithm (Clarke et al., 1987a, 1987b) and is a direct successor of the well known Generalized Minimum Variance (GMV) algorithm (Clarke and Gawthrop, 1975, 1979). It is a technique that combines the advantages of explicit algorithms such as the pole-placement algorithm (Wellstead, 1980) together with those of implicit algorithms (predictive approaches). Moreover, it is based on a CARIMA* model representation (Tuffs and Clarke, 1985) of the process under consideration, a structure which is a refined version of the well known ARMA** model structure.

Both algorithms in question have been investigated under a wide range of conditions and using the non-linear models associated with the drugs Pancuronium and Atracurium. For the Pancuronium model, a second order linear model with time-delay was considered followed by a non-linearity represented by a Hill equation (Whiting and Kelman, 1980; Weatherley et al., 1983) or alternatively a dead-space in series with a saturation element. For the Atracurium model, a third order linear model with time-delay was found to be suitable. The same non-linearity as

*Controlled Auto-Regressive Integrated Moving Average

**Auto-Regressive Moving Average

above characterizes the pharmacodynamics of the drug.

Next, the study considered the implementation of the GPC algorithm on a Research Machines 380Z disk-based microcomputer system and its application to the above models. The muscle relaxant models were simulated on a VIDAC 336 analogue computer. A sensitivity study of the algorithm was carried out to reflect the large patient-to-patient parameters variability.

Because of the encouraging results obtained under real-time conditions, the GPC algorithm was considered to be a likely candidate for a clinical evaluation. To this effect, clinical trials in operating theatre on humans were conducted in collaboration with the Department of Anaesthesia (Western Infirmary Hospital, Glasgow) and the Department of Anaesthesia and Anaesthesiology (Hallamshire Hospital, Sheffield) and after local Ethics Committee approvals. The drug Atracurium which is a fast acting drug with a short onset was considered for continuous infusion. The designed GPC control strategy succeeded in maintaining a remarkably good steady level of paralysis with all of the 10 patients considered for operation, while the total dosage of Atracurium was kept to a minimum.

Besides muscle relaxation management, depth of anaesthesia (unconsciousness) represents another responsibility for anaesthetists in operating theatres. The successful results obtained with the single-input single-output (SISO) GPC algorithm led to considering simultaneous control of muscle relaxation and anaesthesia using the multivariable format of the above control strategy. Because depth of anaesthesia is difficult to quantify accurately, blood pressure (considered to give good indication of the state of unconsciousness) was used as the second variable for the multivariable model. Hence, a non-linear multivariable anaesthetic model using both variables has been elicited via literature surveys and clinical experiments conducted in hospital. The drug Atracurium was used to induce muscle

relaxation, whereas Isoflurane was used to induce unconsciousness.

Extensive simulation studies have been undertaken to verify the algorithm and provide guidelines for settings which will produce robust control conditions. Monte-Carlo simulations have also been undertaken to validate further the robustness of this control strategy which includes various 'jacketing' constraints in addition to the GPC algorithm commonly described.

Because the obtained non-linear multivariable model included one unique cross-interaction from one of the other loops, a different strategy in which two single GPC loops were considered and feedforward being added to one of the loops for the interaction. this was found to provide various advantages including:

- Better transient responses.
- Reduction of the interactions.
- Considerable reduction of the computer burden.

The hence obtained scheme was named Generalized Predictive Control with Feedforward (GPCF) in opposition to the simple multivariable GPC version.

The thesis is organized into 9 chapters which can be summarized as:

Chapter 2

The background relative to the mechanism of neuromuscular transmission is reviewed. Different aspects of muscle relaxant drugs pharmacology are given together with the problems encountered in the standard method of muscle relaxant drugs management. The need for automatic feedback control is therefore emphasized.

Chapter 3

In this chapter, details of the modelling study relative to the two muscle relaxant drugs Pancuronium-Bromide and Atracurium are first reviewed, then the problems associated with classic control method through simulations with fixed PI and PID controllers are outlined. The need for adaptive control strategies is reinforced with an introductory section dedicated to two well known protocols pertaining to this concept.

Chapter 4

The self-adaptive Proportional-Integral-Plus (PIP) control algorithm is presented together with its application to the muscle relaxation process. Its extension to handle unknown and varying time-delay is also reviewed under the Extended Smith Predictor (ESP) and Generalized Smith Predictor (GSP) schemes.

Chapter 5

This chapter is dedicated to the development of the second self-tuning control technique known as the Generalized Predictive Control algorithm (GPC) which is presented in its basic form as well as its extended versions to include model following and observer polynomials. The different versions are then applied to the muscle relaxation process associated with both drugs in a series of simulations to determine the best controller parameters settings.

Chapter 6

The performance of the self-adaptive GPC algorithm is evaluated under real-time simulations environment using an analogue computer.

Chapter 7

The implementation of the self-adaptive GPC algorithm in operating theatre during surgery on humans via Atracurium infusion is considered. Different aspects of the modified algorithm for such application are reviewed together with a general description of the hardware involved. The results obtained are presented, analysed, and discussed.

Chapter 8

A multivariable model combining muscle relaxation via Atracurium infusion and depth of anaesthesia via Isoflurane inhalation is identified. Simultaneous control of muscle relaxation as well as depth of anaesthesia (unconsciousness) is considered by using the multivariable version of the GPC algorithm. Simulation studies using nominal parameter values as well as Monte-Carlo method for parameter selection are performed. Further simulations using single-input single-output GPC with feedforward are also undertaken and a comparison is made between the two different strategies.

Chapter 9

The major conclusions of this study and recommendations for further research work are given.

CHAPTER 2

PHYSIOLOGICAL BACKGROUND PERTAINING TO THE MUSCLE RELAXATION PROCESS

2.1 INTRODUCTION

In order to help the surgeon perform an operation while minimizing the risks of tissue damage, there is a need for the muscle to be relaxed (paralysed). This is achieved by administering a number of drugs which induce muscle relaxation. To better understand this process, it was found useful to begin with the mechanism of neuromuscular transmission as the next section endeavours to show.

2.2 THE NEUROMUSCULAR TRANSMISSION

In the chain of events that starts with the stimulation of a motor nerve and ends with the contraction of a muscle, the most vulnerable link is the synapse between the nerve and the muscle- the neuromuscular junction. The motor nerve is separated from the muscle by the synaptic cleft. This cleft is in fact a sub-division of the extracellular fluid (ECF) from which it is separated by the Schwann cell membrane. The neurotransmitter Acetylcholine (Ach) is responsible for transmitting motor nerve activity across this junction. Early work by Birks et al. (1960) elucidated the fundamental anatomy of the neuromuscular junction, and modern techniques have allowed refinements of details relative to this structure. As shown in figure (2.1), the motor nerve ends at that part of the muscle membrane known as the motor end plate. In this area, the membrane is folded into longitudinal gutters; the ridges of each gutter conceal orifices to secondary clefts. Around these orifices, a high concentration of a chemical substance known as Cholinesterase

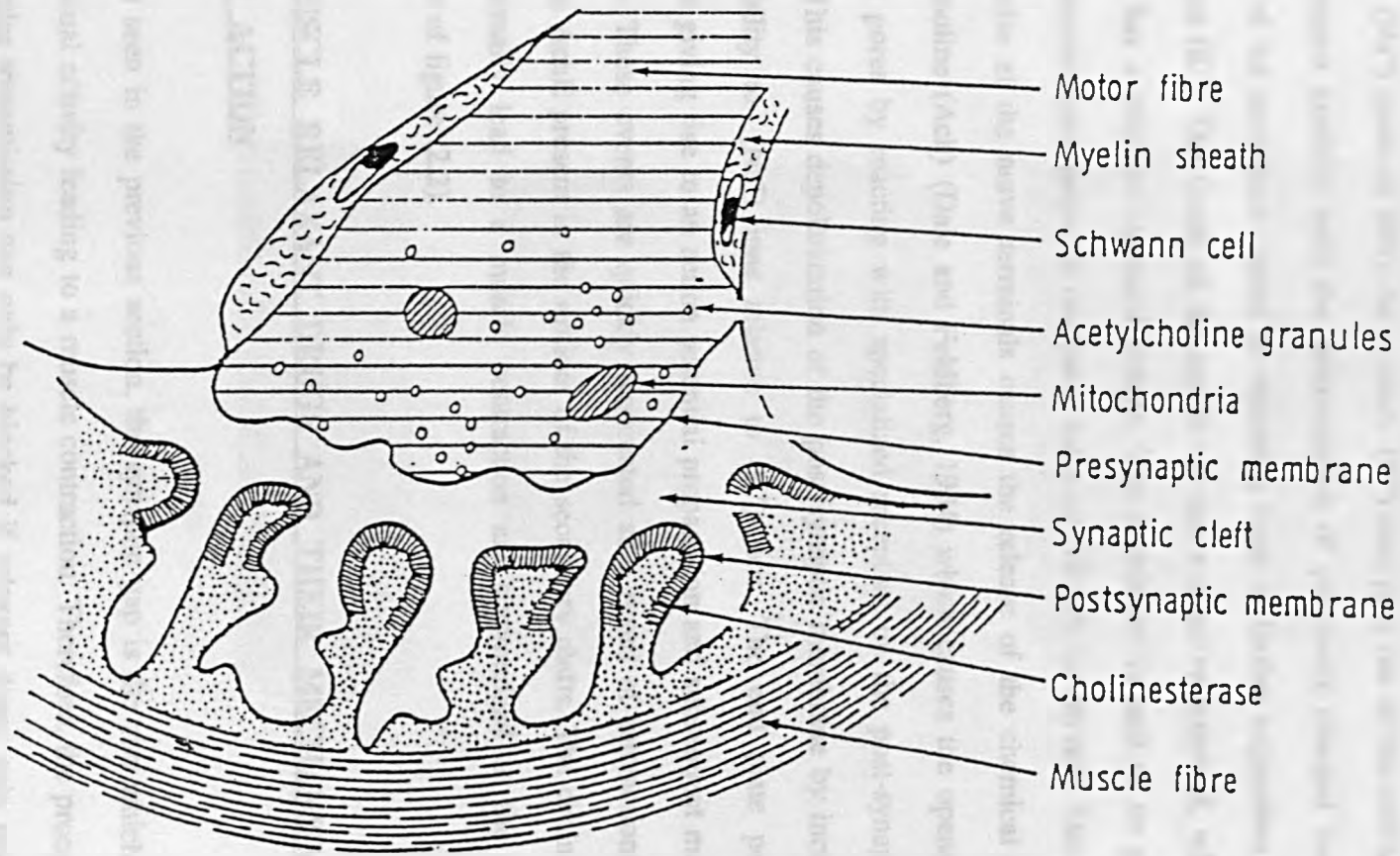


Figure 2.1. A schematic representation of the neuromuscular junction

(AChE) was proved to be present. The end plate membrane potential is a reflection of the uneven distribution of ions across the surface membrane. In its resting state, this membrane is far more permeable to Potassium ions (K^+) than those of Sodium (Na^+) (ratio of 100). As a result, (K^+) ions pass out of the cell along their concentration gradient until the accumulation of positively charged ions on the outside of the membrane causes an opposing force to further migrations of Potassium ions (K^+). The inside of the membrane has a negative potential, whereas the outside has a positive electrical charge. The membrane is said to be polarized. The transmembrane potential reaches a value of -70 mV to -90 mV. The arrival of an impulse at the nerve terminals causes the release of the chemical substance Acetylcholine (ACh) (Dale and Feldberg, 1934) which causes the opening of the Sodium pores by reacting with specialized receptors on the post-synaptic membrane. This causes depolarization of the post synaptic membrane by increasing its permeability to (Na^+) ions relative to (K^+) ions. The end plate potential is reversed giving rise to an action potential propagation and subsequent muscle contraction. These events are quickly terminated as a result of interactions between ACh and AChE present in the orifices of the secondary clefts. The chain of events that normally lead to a muscle contraction are summarized in the schematic diagram of figure (2.2).

2.3 MUSCLE RELAXANT DRUGS AND THEIR MECHANISM OF ACTION

As seen in the previous section, the synaptic gap is the site which witnesses the unusual activity leading to a muscle contraction. Therefore, the process of neuromuscular transmission can only be blocked if relaxant drugs gain access to the synaptic cleft and break the chain of events described in the diagram of figure

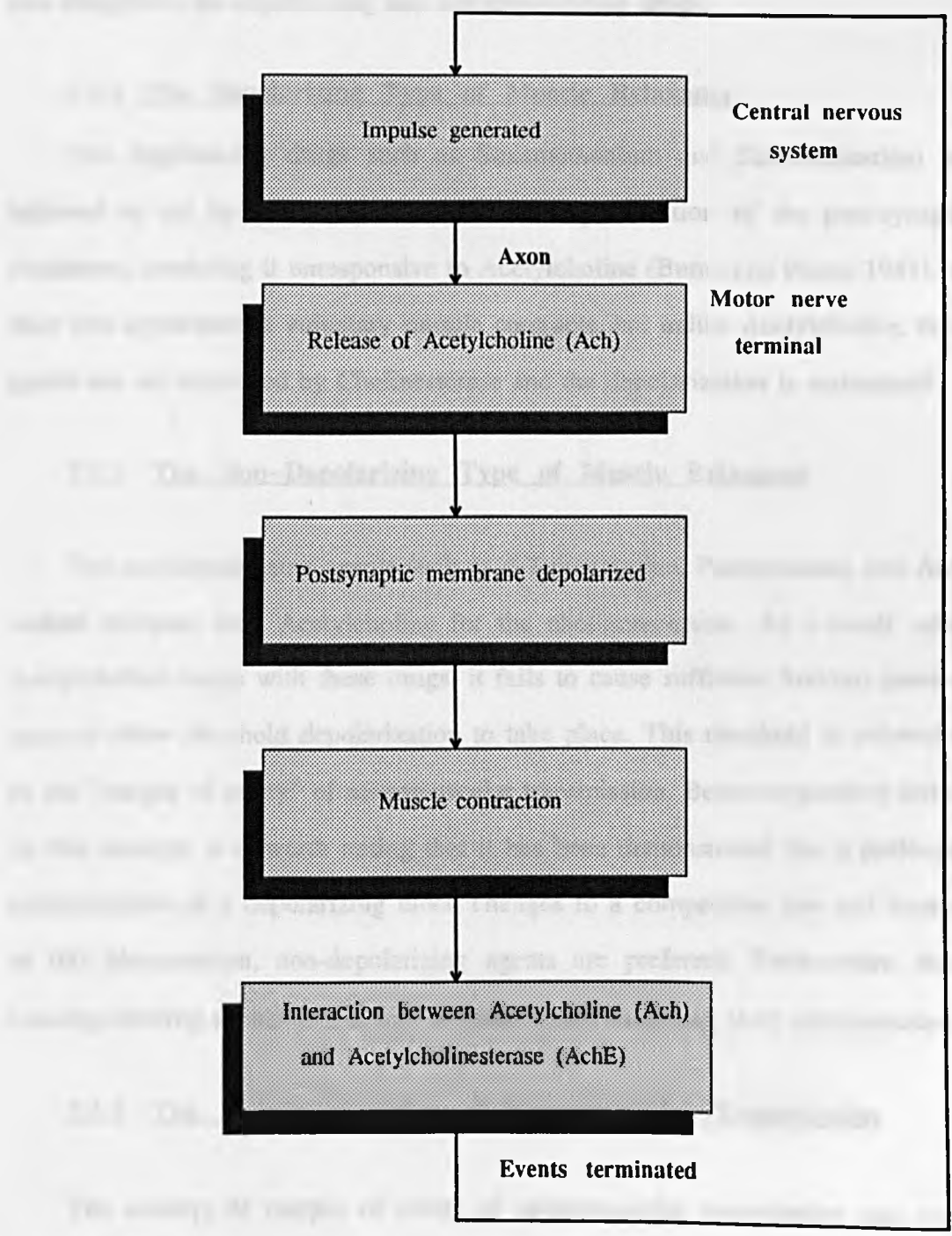


Figure 2.2. A schematic diagram describing the chain of events leading to muscle contraction

(2.2). Depending on their mechanism of action, muscle relaxant agents fall into two categories: the depolarizing and non-depolarizing drugs.

2.3.1 The Depolarizing Type of Muscle Relaxants

The depolarizing drugs such as Suxamethonium and Decamethonium are believed to act by producing a continuous depolarization of the post-synaptic membrane, rendering it unresponsive to Acetylcholine (Burns and Paton, 1951). At their first application a voluntary muscle contracts, but unlike Acetylcholine, these agents are not destroyed by Cholinesterase and the depolarization is maintained.

2.3.2 The Non-Depolarizing Type of Muscle Relaxants

The non-depolarizing agents such as d-Tubocurarine, Pancuronium, and Atracurium compete with Acetylcholine for the cholinoreceptors. As a result, when Acetylcholine reacts with these drugs, it fails to cause sufficient Sodium pores to open to allow threshold depolarization to take place. This threshold is referred to as the "margin of safety" of neuromuscular transmission. Before expanding further on this concept, it is worth noting that it has been demonstrated that a prolonged administration of a depolarizing block changes to a competitive one and because of this phenomenon, non-depolarizing agents are preferred. Furthermore, these non-depolarizing agents do not induce muscle pain following their administration.

2.3.3 The Margin of Safety of Neuromuscular Transmission

The concept of margin of safety of neuromuscular transmission was introduced by Paton and Waud (1967) who demonstrated that unless more than 75% of the receptors were occupied, it was not possible to detect a reduction in the indirectly elicited twitch response. Figure (2.3) illustrates this concept.

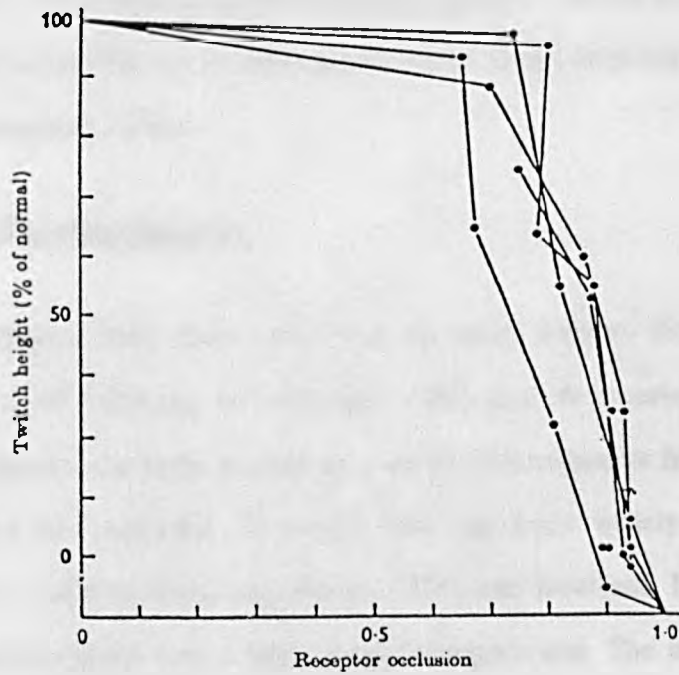


Figure 2.3. Margin of safety of neuromuscular transmission.
(Paton and Waud, 1967)

No depression of twitch response can be detected until over 75% of the receptors are occluded.

2.4 PHARMACOLOGY OF MUSCLE RELAXANTS

Pharmacology is that part of science that studies the relation between the administration of the drug and the pharmacological effect it produces. It falls into 2 categories: pharmacokinetics and pharmacodynamics. Pharmacokinetics concern the absorption, distribution, metabolism and excretion of the drugs, whereas pharmacodynamics describe the relationship between drug concentrations in the plasma and their therapeutic effect.

2.4.1 Pharmacokinetics

Drug kinetics have been considered by many authors (Stanski et al., 1979; Hull et al., 1980; Whiting and Kelman, 1980; and Weatherley et al., 1983). In these formulations the body is seen as a set of compartments from which the drug is distributed and excreted. A model that has been widely used is the one-compartment model (Gibaldi and Perrier, 1975; and Rowland, 1978). In this model the drug is introduced into a large single compartment. The concentration of the drug in this compartment is assumed to be equal to the plasma concentration of the drug. The drug is excreted from this compartment. The overall configuration is modelled by one exponential rate of decay of drug concentration in the blood expressed by the following differential equation:

$$\frac{d x_1}{dt} = - k_{10} x_1(t) + u_1(t) \quad (2.1)$$

where,

$u_1(t)$ represents the drug input

k_{10} is the transfer rate constant from the compartment to the environment

$x_1(t)$ is the total amount of drug in the body at time 't'

The overall configuration is shown in figure (2.4).

However, the model that allows one to better understand the early phases of drug distribution and plasma levels after intravenous injection is the two-compartment model. It is considered to be more realistic than the previous one (Rowland, 1978; Shanks et al., 1980). The model, illustrated in figure (2.5), includes a small central compartment equivalent to the plasma volume and perfused tissues (heart, lungs, liver, kidney, and endocrine glands) and a larger peripheral compartment corresponding to the rest of the body (muscle, skin, and fat). When a drug is injected into the central compartment, the drug concentration falls in a biphasic fashion: the first phase represents drug transfer from one compartment to another, whereas the second, which is slower, represents drug elimination from the body once a state of pseudo-equilibrium between the compartments has been achieved. All characteristics of drug transfer are assumed to be first order processes in which the rate of drug exit from a given space is proportional to the concentration of the drug in that space. The plasma concentration of drug versus time is given by the following biexponential equation:

$$C(t) = A e^{-\alpha t} + B e^{-\beta t} \quad (2.2)$$

where A, and B are complex functions of the inter-compartmental rate constants k_{ij} .

In the above equation $A e^{-\alpha t}$ characterizes the distribution phase, whereas $B e^{-\beta t}$ relates to the elimination phase.

Finally, a three-compartment model has been proposed by several authors: Gibaldi et al. (1972) who studied d-Tubocurarine in man, and Brown and Godfrey (1978) who considered the Bilirubin drug. In this representation, shown in figure (2.6), the central compartment (1) corresponds to the plasma, whereas compartments (2)

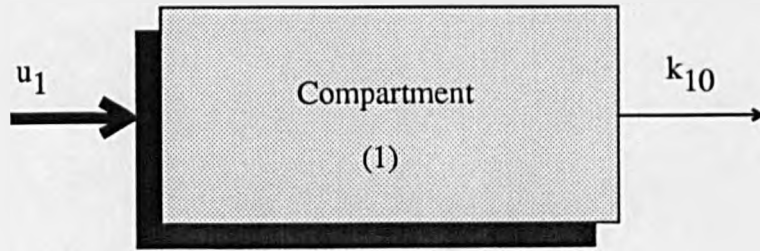


Figure 2.4. A one-compartment open model representation

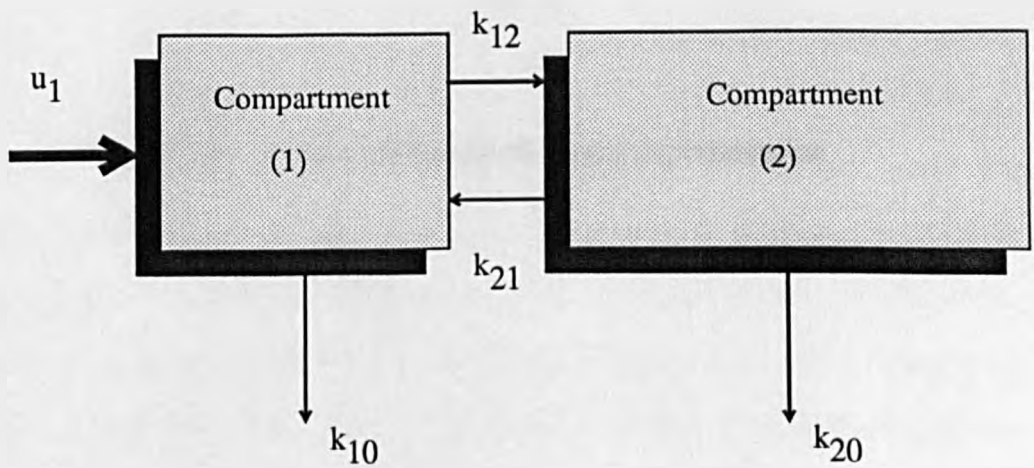


Figure 2.5. A two-compartment open model representation

and (3) represent other sites unaccounted for. They are often interpreted as being the extracellular and intracellular compartments of poorly perfused tissues.

The plasma concentration versus time in this case is given by the following sum of three decaying exponentials:

$$C(t) = A e^{-\alpha t} + B e^{-\beta t} + D e^{-\delta t} \quad (2.3)$$

where A , B , and D are complex functions of the inter-compartmental rate constants k_{ij} .

2.4.2 Pharmacodynamics

The fact that the drug effect cannot increase indefinitely as the amount of drug in the body increases is embodied in the Hill equation of the form:

$$E = \frac{E_{\max.}}{1 + \frac{C(50)^\alpha}{C^\alpha}} \quad (2.4)$$

where $E_{\max.}$ is the maximum effect possible, C the concentration in the plasma, $C(50)$ is the drug concentration which produces 50% of the maximum effect $E_{\max.}$, and α is a real positive constant power that governs the speed at which the response reaches its maximum as the concentration of drug in the plasma increases. Figure (2.7) shows the shape of the curves corresponding to the previous equation as α varies and for a given $C(50)$. Notice that all these curves have non-linear forms which characterize sigmoidicity of the concentration response relationship. It is however worth noting that Ham et al. (1979) modelled a complete pharmacological response using a three-compartment model together with equation (2.4) modified into the logistic function of equation (2.5) (Waud, 1972):

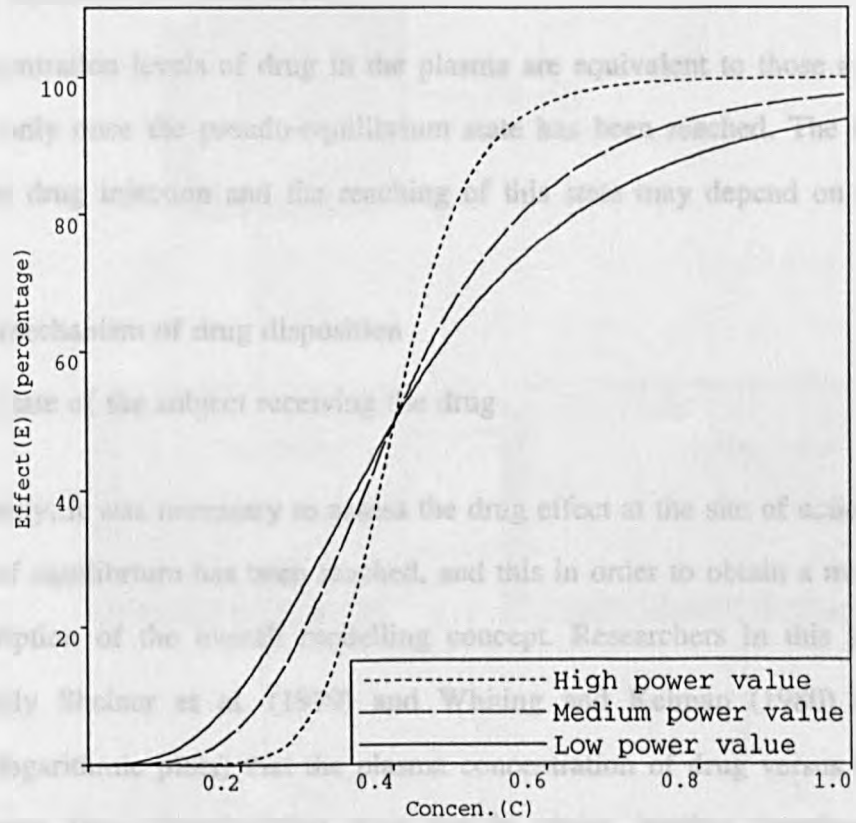


Figure 2.7. Shape of curves corresponding to Hill equation (2.4) as power α varies

$$\begin{cases} Y_h = \frac{1}{1 + e^{-X'}} \\ e^{-X'} = \frac{C(50)^\alpha}{C^\alpha} \end{cases} \quad (2.5)$$

where Y_h represents the drug effect.

Concentration levels of drug in the plasma are equivalent to those at the site of action only once the pseudo-equilibrium state has been reached. The time following the drug injection and the reaching of this state may depend on two factors:

- The mechanism of drug disposition
- The state of the subject receiving the drug

Consequently, it was necessary to assess the drug effect at the site of action before the state of equilibrium has been reached, and this in order to obtain a more accurate description of the overall modelling concept. Researchers in this particular field mainly Sheiner et al. (1979) and Whiting and Kelman (1980) observed (through logarithmic plots) that the plasma concentration of drug versus time and effect versus time characteristics were not in phase, leading therefore to the existence of another compartment- the effect compartment- linked to the pharmacokinetics model by a first order process with a constant k_{1E} (arbitrarily small compared to the smallest rate constant of the kinetics model), in such a way that it does not affect the parameters of the original model (Whiting and Kelman, 1980). Figure (2.8) illustrates such a configuration.

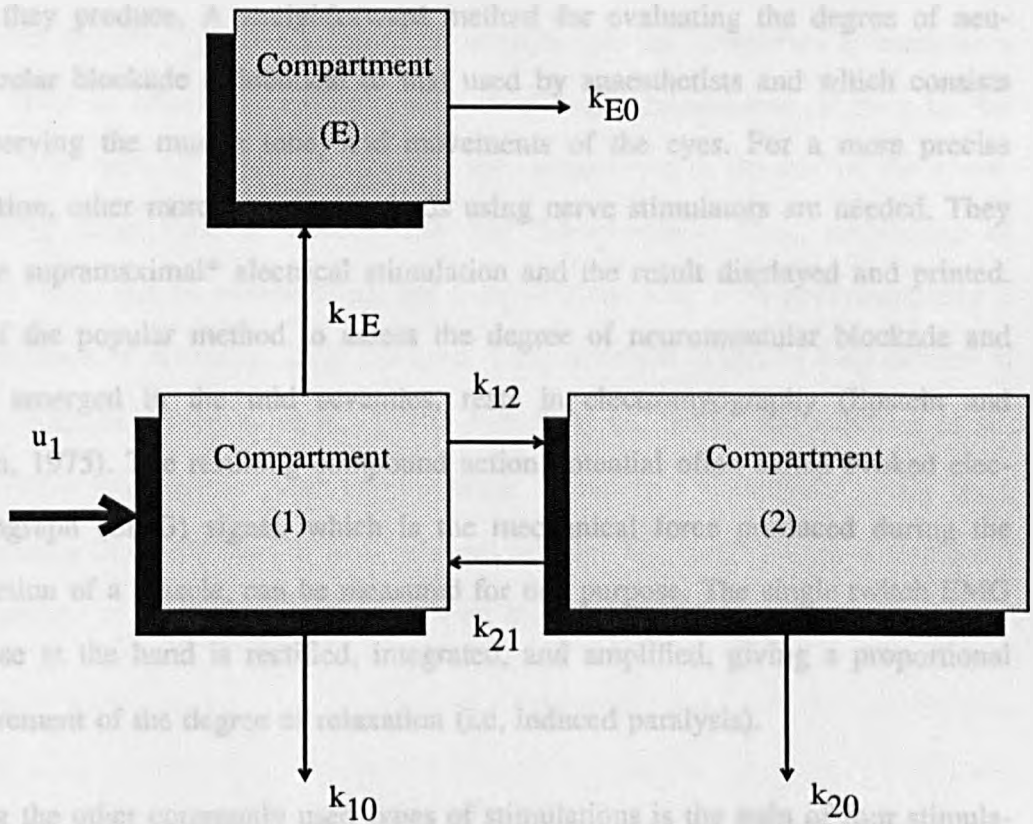


Figure 2.8. Modification of the two-compartment open model to include the 'effect compartment'

2.5 MANAGEMENT OF NEUROMUSCULAR BLOCKADE

2.5.1 Evaluation of Neuromuscular Blockade

Effective administration of muscle relaxant drugs requires monitoring of the effect they produce. A straightforward method for evaluating the degree of neuromuscular blockade is identical to that used by anaesthetists and which consists of observing the muscle tone, and movements of the eyes. For a more precise evaluation, other more accurate methods using nerve stimulators are needed. They involve supramaximal* electrical stimulation and the result displayed and printed. One of the popular method to assess the degree of neuromuscular blockade and which emerged in the mid seventies, rests in electromyography (Epstein and Epstein, 1975). The resulting compound action potential often called evoked electromyograph (EMG) signal, which is the mechanical force produced during the contraction of a muscle, can be measured for that purpose. The single twitch EMG response at the hand is rectified, integrated, and amplified, giving a proportional measurement of the degree of relaxation (i.e, induced paralysis).

Among the other commonly used types of stimulations is the train of four stimulation (TOF). It is performed by means of four supramaximal stimuli delivered at time intervals of 0.5 second over a period of 2 seconds (Ali et al., 1971). The TOF stimuli is repeated over 10 to 12 seconds. The amplitude of the fourth response gives the TOF ratio when expressed as a percentage of the first. Further details of this type of stimulation are given in chapter 7. Other types of stimulation include the single twitch and tetanic stimuli (succession of stimuli at very rapid rate).

* Stimulation whose intensity is bigger than that needed to evoke the maximal response

2.5.2 Administration of Muscle Relaxant Drugs and Reversal of Neuromuscular Blockade

Muscle relaxant drugs are conventionally administered by anaesthetists who, based on their own experience, determine the adequate dose in order to achieve a predefined degree of paralysis. However, anaesthetists fail sometimes to maintain a steady level of relaxation resulting often in a large consumption of drug by the patient. The residual effects of relaxants are antagonised at the end of the operation using drugs such as Neostigmine and Edrophonium. Thus, overdosing of relaxant drugs can be counteracted, but complications may arise postoperatively if large amounts of reversing drugs are used. Early attempts at closed-loop control of muscle relaxation (Brown et al., 1980; Asbury et al., 1980; and Linkens et al., 1981, 1982) have shown great improvements including a reasonably steady level of relaxation and reduction of total relaxant dosage. The next chapter is dedicated to the review of the control techniques used in achieving that.

CHAPTER 3

CLOSED-LOOP CONTROL OF MUSCLE RELAXATION DRUG ADMINISTRATION

3.1 INTRODUCTION

Closed-loop control has found many applications in every day life and emerged as a serious contender for all forms of control. However, in biomedicine, because it is such a highly sensitive area and because of all the risks involved, the research community were often reluctant in conducting experiments that could involve such a scheme. It is only in the late seventies that the gap existing between feedback control and continuous infusion of chemical substances necessary for regulating physiological variables (blood pressure, muscle relaxation) was bridged when research work conducted by pioneers in this field such as Sheppard et al., (1979); Asbury et al.; (1980); Brown et al., (1980); Linkens et al., (1981); and Zhang and Cameron (1989), proved through clinical experiments on humans as well as on animals that this form of control is safe and effective and in some cases better than manual control.

While the need for feedback control was emphasized in chapter 2 together with all the problems associated with conventional methods of administering muscle relaxant drugs, it is worth noting that the so-called three-term controller or PID algorithm was at the forefront of the commonly type of controllers used.

Brown et al. (1980) used a simple proportional control algorithm to regulate the muscle relaxation level around a 10% EMG set-point using infusions of Pancuronium. Although the authors reported offsets of 6% (due to the absence of integral action), the results were considered satisfactory.

In their trials on humans, Wait et al. (1987) reported a successful regulation around a reference set-point just by using an on-off relay controller to adjust the delivery of Atracurium, while Ebert et al. (1986) reported the use of a PID algorithm to achieve a level of 10% EMG by means of Vecuronium administration. Better performance was achieved. Finally, similar results were also reported by Webster et al. (1987) and MacLeod et al. (1989) who used a PID and PI algorithm respectively to control the infusion of Atracurium on humans. Again here, a comparative study performed by the last author demonstrated that simple feedback control was more superior than manual control performed by the anaesthetist.

When using the three-term controller of PID algorithm, the output is given by the following equation:

$$U_c = K_p e + K_I \int e dt + K_D \frac{de}{dt} \quad (3.1)$$

where e is the error signal given a reference output signal, K_p is a proportional gain constant, K_I the integral term constant, and K_D the derivative term constant.

Settings of the parameters K_p , K_I , and K_D are usually obtained using the Ziegler Nichols methods (Ziegler and Nichols, 1942) in an off-line study involving open-loop step responses. Although positive remarks were made by the previous authors who used these PID controllers, problems ranging from oscillations to offsets were also acknowledged (Brown et al., 1980; MacLeod et al., 1989) due to the considerable differences between individual subjects (Linkens et al., 1982), and the fact that the above parameter settings needed adjustments. Consequently, prior to any clinical evaluation, a computer simulation of the closed-loop infusion control system, with the patient replaced by a mathematical model is a safer, faster and altogether more convenient method, enabling one to assess any subsequent problems and to obtain a deeper insight into this complex mechanism which is the human

body. This is the subject of the next section which is concerned with the mathematical modelling of muscle relaxant dynamics, i.e: Pancuronium-Bromide and Atracurium using the concepts of pharmacokinetics and pharmacodynamics introduced in chapter 2.

3.2 THE MATHEMATICAL MODELS ASSOCIATED WITH MUSCLE RELAXATION PROCESSES

Referring to the study conducted in chapter 2, the process of muscle relaxation requires a model which comprises a linear part describing the pharmacokinetics and a non-linear part which concerns the pharmacodynamics of the drug. While the pharmacokinetics may be different from one type of muscle relaxant to another depending on how many compartments are associated with the drug, the pharmacodynamics are all modelled by the Hill equation or by a dead-space in series with a saturation element to account for the 'margin of safety' of the neuromuscular transmission (Paton and Waud, 1967). The section below considers two types of non-depolarizing drugs- Pancuronium-Bromide, and Atracurium, both having been the subject of much published research work (Linkens et al., 1982; Whiting and Kelman, 1980).

3.2.1 Identification of Pancuronium Dynamics in Dogs

In a study performed by Linkens et al. (1982), open-loop as well as closed-loop experiments on dogs were conducted to identify Pancuronium-Bromide dynamics. To avoid saturation problems and to enable sufficiently long sequences to be used under steady-state conditions, PRBS signals, through a peristaltic pump rather than bolus injections, were used as perturbations. The pump was considered as having nearly linear characteristics, with a small offset so that the motor drive

was operating over the linear region. Analysis of the data was performed using a generalized least-squares package (SPAID) (Billings and Sterling, 1975). Under both modes (open-loop and closed-loop), the linearized model indicated a two-time-constant system corresponding to a two-compartment model without the third effect compartment (see chapter 2), and with an estimated time-delay accounting for the transport of blood via the circulation system. Equation (3.2) describes such kinetics:

$$G_1(s) = \frac{K_1 e^{-\tau s}}{(1 + T_1 s) (1 + T_2 s)} \quad (3.2)$$

Within the six trials conducted, each of the identified parameters, i.e K_1 , τ , T_1 , and T_2 showed large patient-to-patient variability, this being a well known phenomenon in the life sciences, where parameter variations of 4:1 are endemic (Slate, 1980; and Linkens et al., 1981). However, the nominal values for the above parameters were:

$$\begin{cases} K_1 = 3.5 \\ \tau = 1 \text{ minute} \\ T_1 = 2 \text{ minutes} \\ T_2 = 20 \text{ minutes} \end{cases}$$

Finally, to complete the overall Wiener structure of the model, the dynamic effect of the drug was modelled by a dead-zone and a saturation element. Both of these reflect the 'margin of safety' concept as well as the fact that the drug effect cannot increase indefinitely as the amount of drug in the body increases respectively. Both characteristics could alternatively be embodied within the context of a Hill equation (2.4).

3.2.2 Pharmacology and Dose Response Relationship of Atracurium Administered I.V

- Pharmacokinetics

It has been shown that after a bolus-dose, the plasma concentration of Atracurium declines rapidly in two exponential phases corresponding to distribution and elimination (Ward et al., 1983). Therefore, the conventional two-compartment model is retained by adding an elimination path from the peripheral compartment obeying the so called "Hofmann elimination" (Ward et al., 1983; Weatherley et al., 1983). Figure (3.1) is a schematic diagram showing the different model components.

If x_i is the drug concentration at time "t" and \dot{x}_i its rate of change then:

$$\begin{aligned}\dot{x}_1 &= -(k_{10} + k_{12}) x_1 + k_{21} x_2 + u \\ \dot{x}_2 &= k_{12} x_1 - (k_{20} + k_{21}) x_2\end{aligned}\quad (3.3)$$

Using Laplace transforms, equation (3.3) can be rewritten as:

$$\begin{aligned}s X_1 &= -(k_{10} + k_{12}) X_1 + k_{21} X_2 + U \\ s X_2 &= k_{12} X_1 - (k_{20} + k_{21}) X_2 \\ X_1 &= L^{-1}(x_1) \\ X_2 &= L^{-1}(x_2)\end{aligned}\quad (3.4)$$

Hence,

$$\frac{X_1}{U} = \frac{s + k_{20} + k_{21}}{(s + k_{10} + k_{12})(s + k_{20} + k_{21}) - k_{12}k_{21}}\quad (3.5)$$

Experimental studies by Weatherley et al. (1983) gave the following mean values for the Pharmacokinetics parameters:

$$k_{12} = 0.20 \text{ min}^{-1}$$

$$k_{21} = 0.075 \text{ min}^{-1}$$

$$k_{10} = 0.015 \text{ min}^{-1}$$

Substituting in equation (3.5) yields:

$$\frac{C_2}{C_1} = \frac{0.20(1 - 0.015/0.075)e^{-0.015t}}{(0.20 - 0.015/0.075) + (0.015/0.075)e^{-0.075t}} \quad (3.6)$$

Equation (3.6) describes the pharmacokinetics of the central elimination compartment during the drug Atracurium.

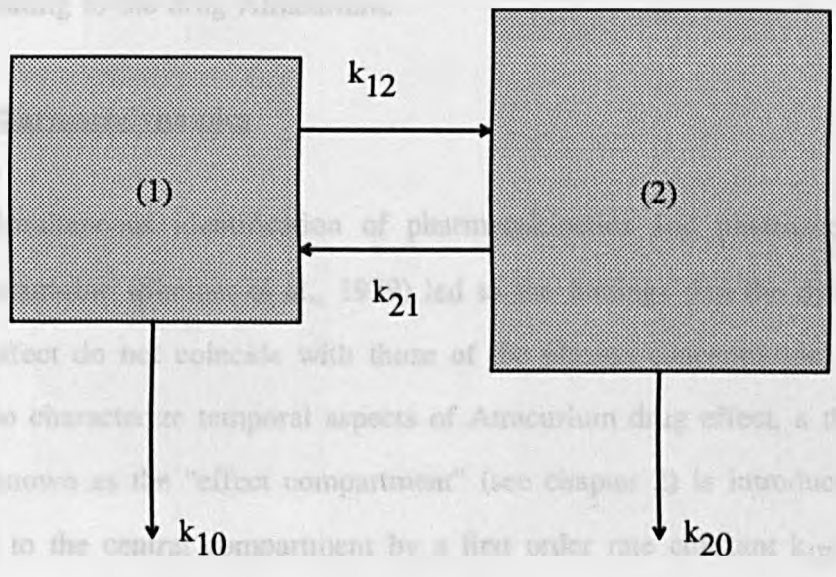


Figure 3.1. A two-compartment model for Atracurium with an additional elimination path (k_{20})

$$k_{12} = 0.20 \text{ min}^{-1} \quad (3.7)$$

Using equation (3.6) yields:

$$C_2 = \frac{0.20 C_1}{0.20 - 0.015/0.075} \left[1 - \frac{0.015/0.075}{0.20 - 0.015/0.075} e^{-0.075t} \right] \quad (3.8)$$

Thus, the 100% bioavailability is assumed to occur by a specific pathway.

$$k_{12} + k_{10} = 0.26 \text{ min.}^{-1}$$

$$k_{21} + k_{20} = 0.094 \text{ min.}^{-1}$$

$$k_{12} \times k_{21} = 0.015 \text{ min.}^{-2}$$

Substituting in equation (3.5) leads to:

$$\frac{X_1}{U} = \frac{9.9442 (1.0+10.6382 \text{ s})}{(1.0+3.0778 \text{ s}) (1.0+34.3642 \text{ s})} \quad (3.6)$$

Equation (3.6) describes the pharmacokinetics of the muscle relaxation system relating to the drug Atracurium.

- **Pharmacodynamics**

Simultaneous identification of pharmacokinetics and pharmacodynamics of d-Tubocurarine (Sheiner et al., 1979) led to the findings that the dynamics of the drug effect do not coincide with those of the plasma concentration. Similarly, in order to characterize temporal aspects of Atracurium drug effect, a third compartment known as the "effect compartment" (see chapter 2) is introduced. It is connected to the central compartment by a first order rate constant k_{1E} , whereas the rate constant k_{E0} characterizes the drug dissipation from the effect compartment, as shown in figure (3.2).

In this latter compartment, the drug concentration-change is governed by the equation:

$$\dot{x}_E = k_{1E} x_1 - k_{E0} x_E \quad (3.7)$$

Using Laplace transforms yields:

$$X_E = \frac{k_{1E} X_1}{s + k_{E0}} \quad (3.8)$$

Once again the Hill equation may be used to relate the effect to a specific concen-

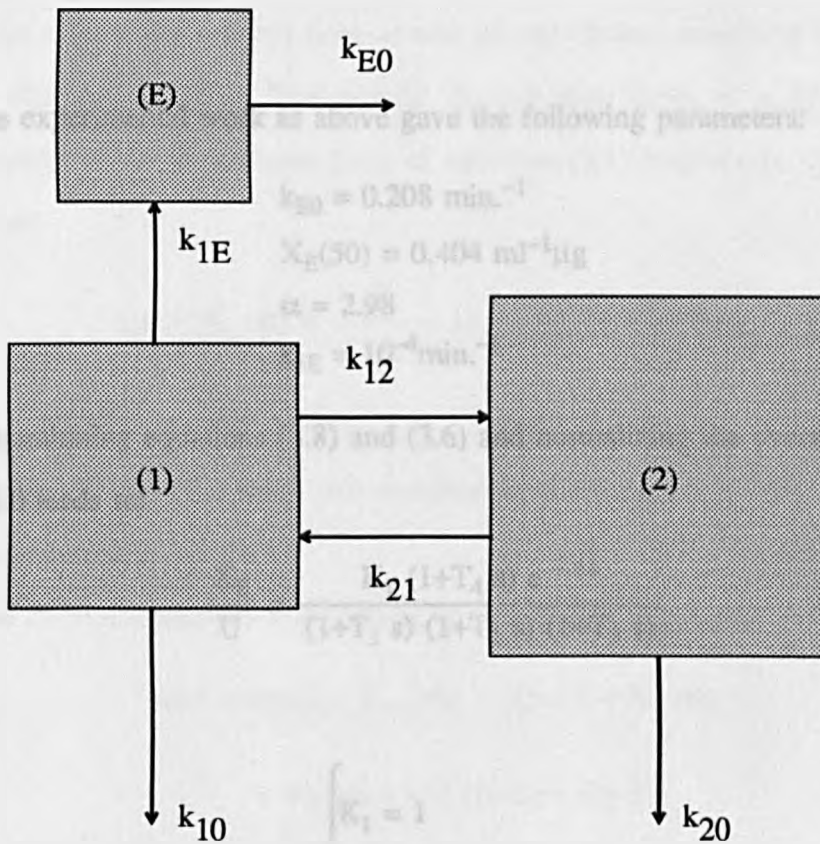


Figure 3.2. Modification of the Atracurium kinetics to include the 'effect' compartment (E)

tration.

$$E_{\text{eff}} = \frac{E_{\text{max}}}{1 + \frac{X_E(50)^\alpha}{X_E^\alpha}} \quad (3.9)$$

where X_E is the drug concentration and $X_E(50)$ is the drug concentration at a 50% effect.

The same experimental work as above gave the following parameters:

$$k_{E0} = 0.208 \text{ min.}^{-1}$$

$$X_E(50) = 0.404 \text{ ml}^{-1}\mu\text{g}$$

$$\alpha = 2.98$$

$$k_{1E} = 10^{-4} \text{ min.}^{-1}$$

Finally, combining equations (3.8) and (3.6) and normalizing the overall open-loop gain at 1.0 leads to:

$$\frac{X_E}{U} = \frac{K_1 (1+T_4 s) e^{-\tau s}}{(1+T_1 s) (1+T_2 s) (1+T_3 s)} \quad (3.10)$$

Where,

$$\left\{ \begin{array}{l} K_1 = 1 \\ \tau = 1 \text{ min.} \\ T_1 = 4.81 \text{ min.} \\ T_2 = 34.36 \text{ min.} \\ T_3 = 3.08 \text{ min.} \\ T_4 = 10.64 \text{ min.} \end{array} \right.$$

3.3 CLASSIC CONTROL OF MUSCLE RELAXATION SYSTEM

3.3.1 A Simulation Study with PI and PID Controllers

The overall muscle relaxation control system, shown in figure (3.3), was simulated using a fourth order Runge-Kutta integration method, with a step length of 0.1 and a sampling interval time of one minute chosen according to Shannon's theorem (Isermann, 1981). The general discrete-time form of a PID controller corresponding to the continuous form of equation (3.1) is given by the following expression:

$$u(t) = K_p e(t) + \frac{K_I}{1 - z^{-1}} e(t) + K_D (1 - z^{-1}) e(t) \quad (3.11)$$

where K_p , K_I , K_D are the proportional, integral, and derivative constant terms respectively, z^{-1} the backward shift operator in the form of $z^{-1} = e^{-s h}$, h being the sampling time.

Using the same denominator everywhere in equation (3.11) yields:

$$\begin{aligned} u(t) = & u(t-1) + K_p (e(t) - e(t-1)) + K_I e(t) \\ & + K_D (e(t) - 2 e(t-1) + e(t-2)) \end{aligned} \quad (3.12)$$

Developing and rearranging leads to the following expression:

$$u(t) = u(t-1) + p_0 e(t) + p_1 e(t-1) + p_2 e(t-2) \quad (3.13)$$

where,

$$p_0 = K_p + K_I + K_D$$

$$p_1 = -K_p - 2 K_D$$

$$p_2 = K_D$$

In order to obtain the best possible settings for the above parameters and for both systems considered, a hill-climbing optimisation routine provided by a package

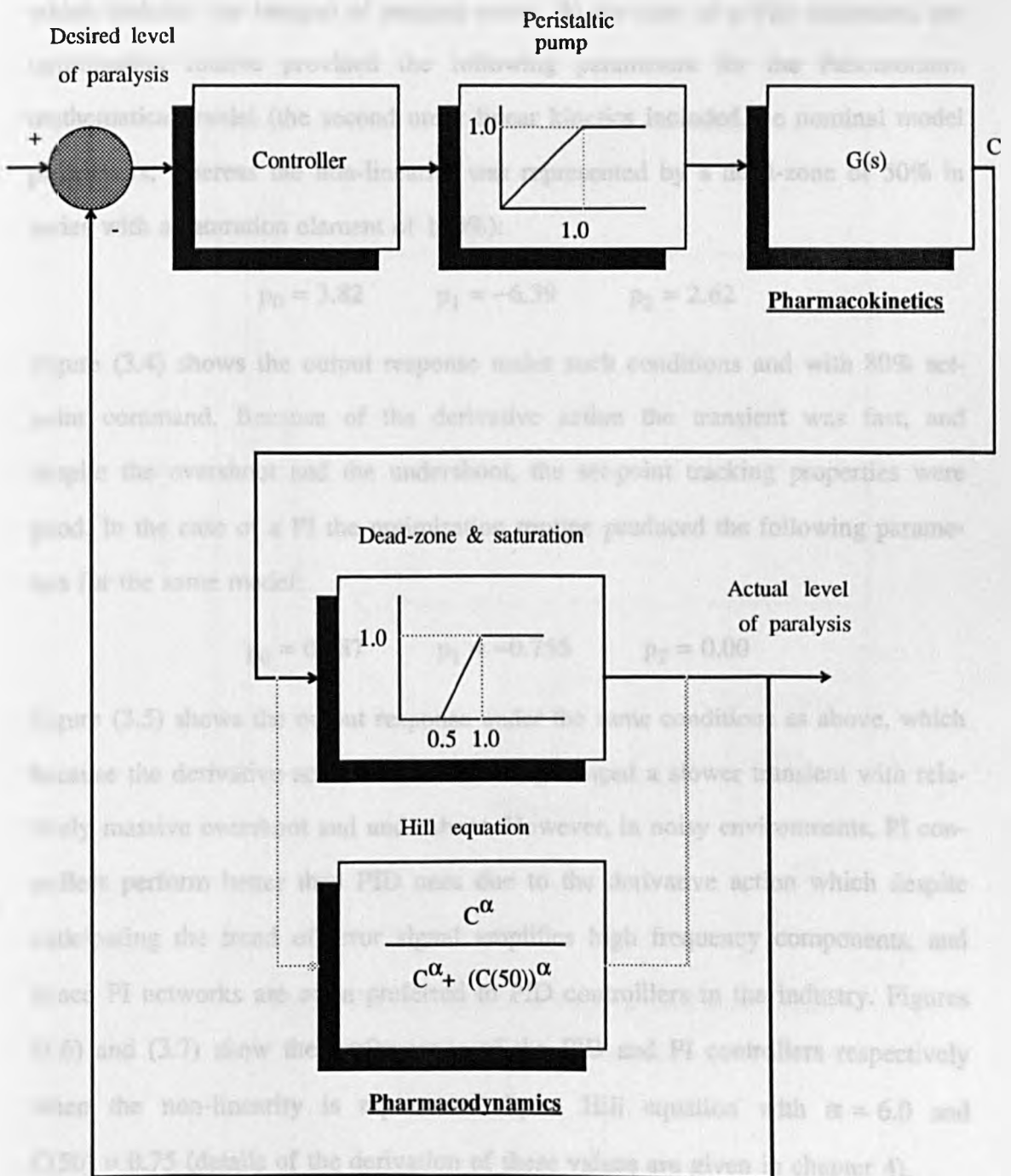


Figure 3.3. A schematic diagram representing the muscle relaxant model simulated under closed-loop conditions

called PSI (Van Den Bosch, 1979) and available in the Department of Automatic Control and Systems Engineering was used. This routine minimizes a cost function which includes the integral of squared errors. In the case of a PID controller, the optimisation routine provided the following parameters for the Pancuronium mathematical model (the second order linear kinetics included the nominal model parameters, whereas the non-linearity was represented by a dead-zone of 50% in series with a saturation element of 100%):

$$p_0 = 3.82 \quad p_1 = -6.39 \quad p_2 = 2.62$$

Figure (3.4) shows the output response under such conditions and with 80% set-point command. Because of the derivative action the transient was fast, and despite the overshoot and the undershoot, the set-point tracking properties were good. In the case of a PI the optimisation routine produced the following parameters for the same model:

$$p_0 = 0.787 \quad p_1 = -0.755 \quad p_2 = 0.00$$

Figure (3.5) shows the output response under the same conditions as above, which because the derivative action was removed, produced a slower transient with relatively massive overshoot and undershoot. However, in noisy environments, PI controllers perform better than PID ones due to the derivative action which despite anticipating the trend of error signal amplifies high frequency components, and hence PI networks are often preferred to PID controllers in the industry. Figures (3.6) and (3.7) show the performance of the PID and PI controllers respectively when the non-linearity is represented by a Hill equation with $\alpha = 6.0$ and $C(50) = 0.75$ (details of the derivation of these values are given in chapter 4).

Next, the system associated with a third order non-linear Atracurium model was considered under the same conditions as before but using the Hill equation to describe the pharmacodynamics of the drug. The optimization routine in the case

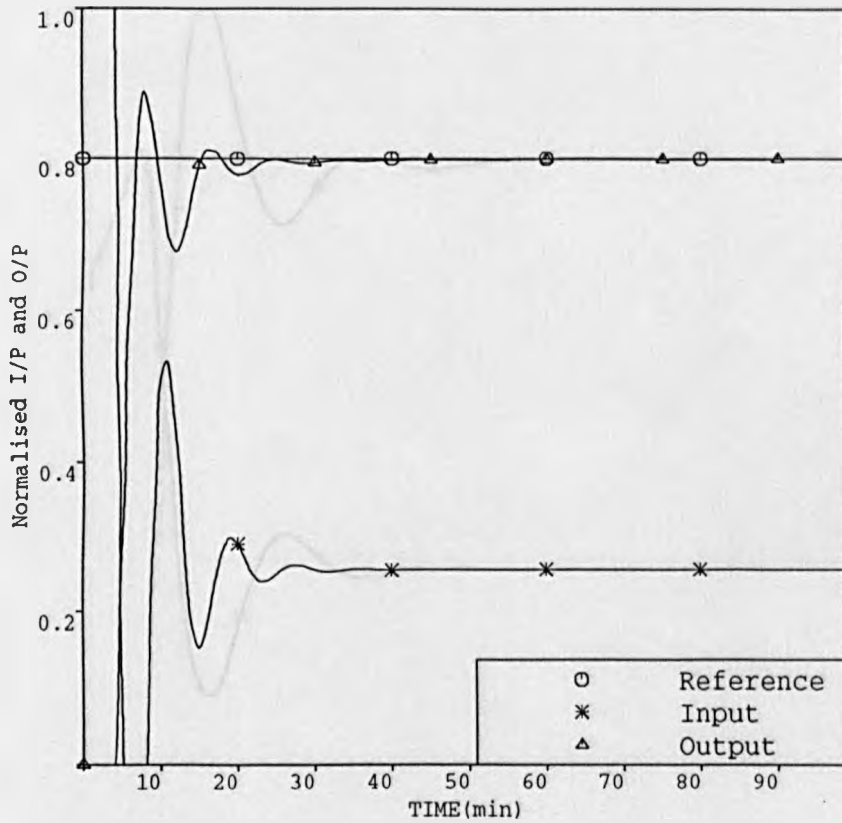


Figure 3.4. Closed-loop response of Pancuronium model under PID control

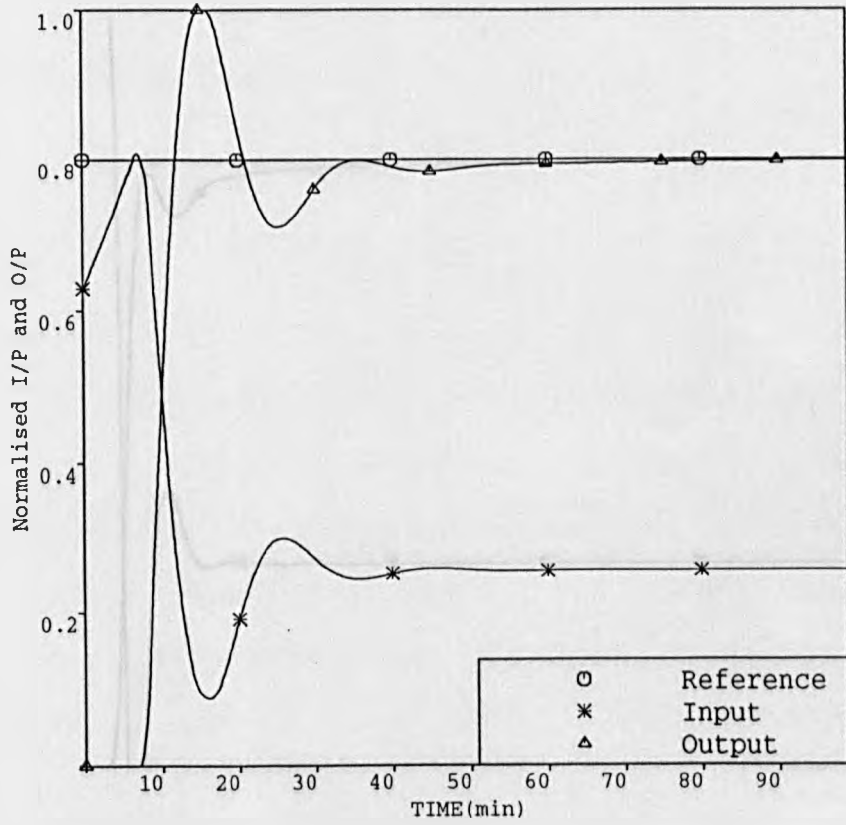


Figure 3.5. Closed-loop response of Pancuronium model under PI control

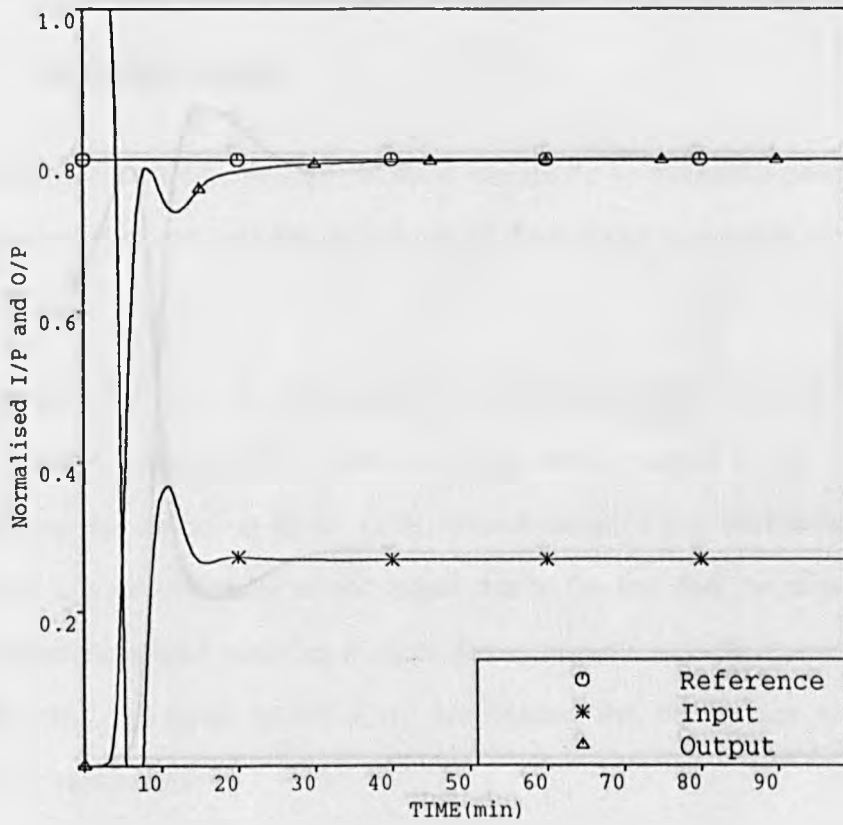


Figure 3.6. Same conditions as figure (3.4) but with non-linearity represented by Hill equation ($\alpha=6.0$; $C(50)=0.75$)

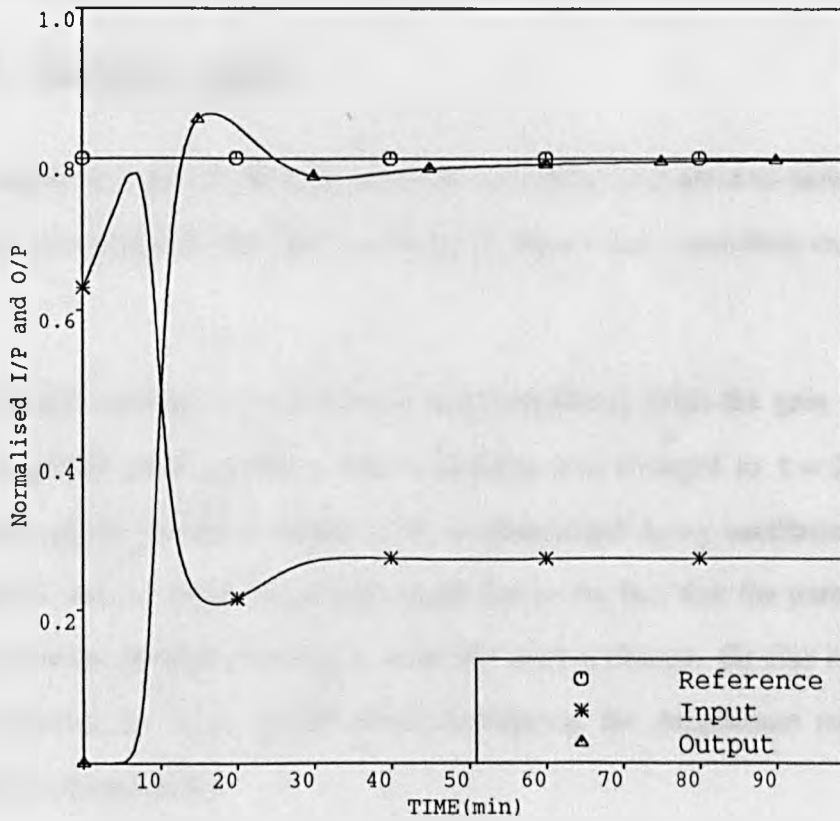


Figure 3.7. Same conditions as figure (3.5) but with non-linearity represented by Hill equation ($\alpha=6.0$; $C(50)=0.75$)

of a PI produced the following parameters:

$$p_0 = 0.84 \quad p_1 = -0.800 \quad p_2 = 0.00$$

Figure (3.8) shows the corresponding output response which demonstrated a rather slow transient due to the slow dominant time-constant of 34 minutes.

3.3.2 Sensitivity Studies

As pointed out earlier, because of large variability in patient-to-patient model parameters, investigations into the sensitivity of these fixed controllers were necessary.

First, the model relating to Pancuronium was considered. With the gain and time-constants kept the same as above, the time-delay was changed to $\tau = 2$ minutes. The system output, shown in figure (3.9), demonstrated dying oscillations of the control signal and consequently of the output due to the fact that the parameters of the PID controller needed retuning to cater for such a change. Similar results can also be observed on figure (3.10) when considering the Atracurium model with the following parameters:

$$\left\{ \begin{array}{l} K_1 = 1 \\ \tau = 1 \text{ min.} \\ T_1 = 1 \text{ min.} \\ T_2 = 2 \text{ min.} \\ T_3 = 10 \text{ min.} \\ T_4 = 30 \text{ min.} \end{array} \right.$$

Clearly, the previous simulation results showed that a fixed controller is not suitable for adequately regulating muscle relaxation around a predefined reference level due to the large inter-patient variability for which there is no information

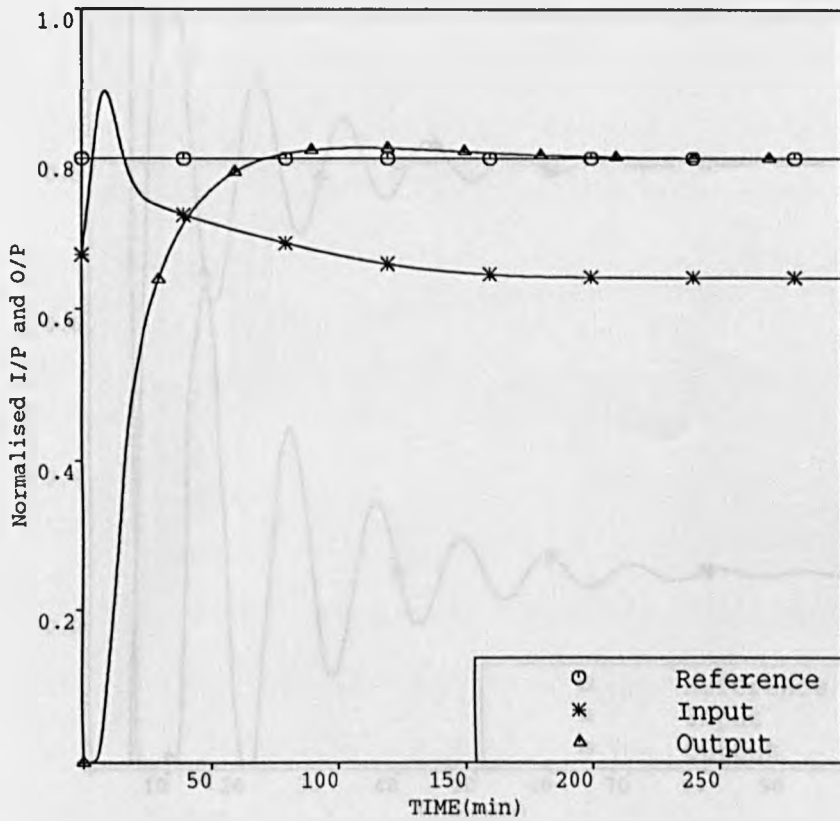


Figure 3.8. Closed-loop response of Atracurium model under PI control with non-linearity represented by Hill equation ($\alpha=2.98$; $C(50)=0.404$)

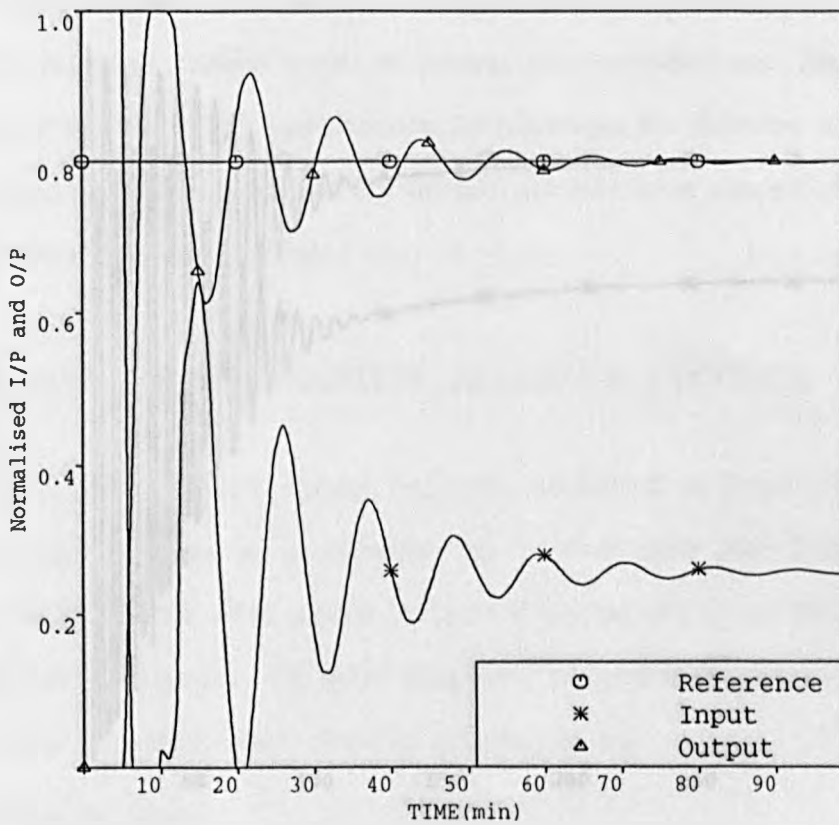


Figure 3.9. Closed-loop response of Pancuronium model under PID control when $\tau=2$ min.

process response. The first, which was not based on other processes in the field of process control (e.g. 1970, 1980, 1985, 1990, 1995, 2000) was concerned with the use of a control which could be used to control a process with a long time constant. This alone would be able to control the process.

Adaptive control seems to answer such expectations. The fact that it does is shown by such concepts by reviewing the different techniques that have been developed and that have shaped, since the late 1970s, the field of adaptive control.

ADAPTIVE FEEDBACK CONTROL

We have seen that adaptive control has been considered an important area of control systems. Its contribution can be seen with over 200 papers presented at the INSPEC service during the last decade alone. Many of these papers have been published in systems, the term "adaptive" is used to describe the control system.

The time which could be spent on this subject is limited. The time which could be spent on this subject is limited. The time which could be spent on this subject is limited.

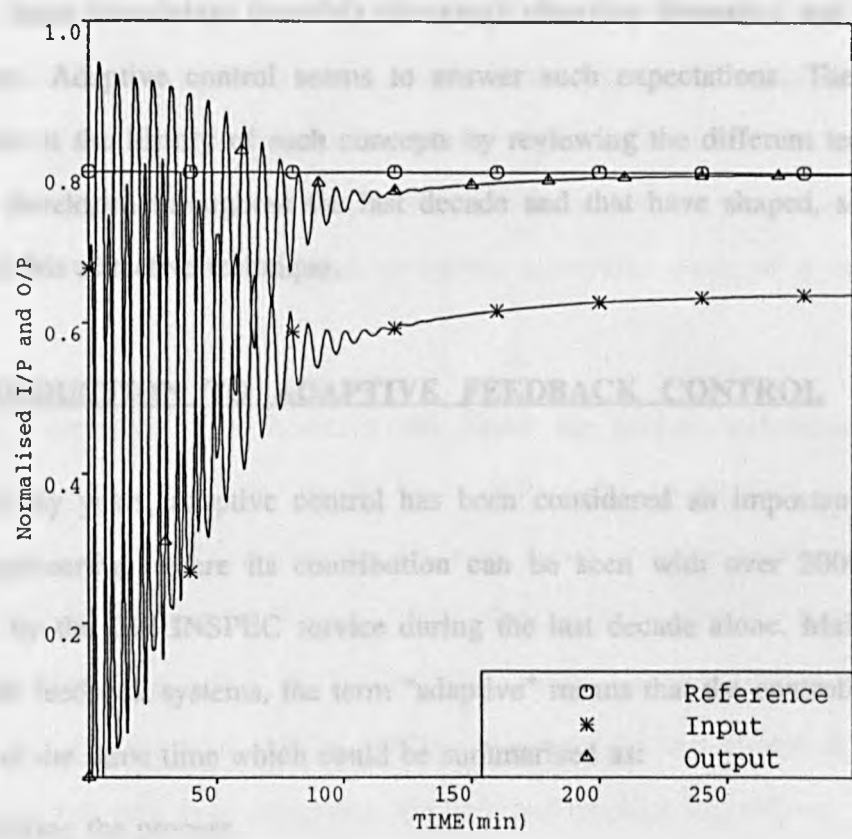


Figure 3.10. System response of Atracurium model under PI control when $T_1=1$ min. ; $T_2=2$ min. ; $T_3=10$ min. ; $T_4=30$ min.

The time which could be spent on this subject is limited. The time which could be spent on this subject is limited. The time which could be spent on this subject is limited.

prior to an operation. This fact, which was also backed by other researchers in the field of biomedicine (Sheppard et al., 1979; Slate, 1980; Linkens et al., 1982) only strengthens the case for a scheme which combines on-line process dynamics estimation together with control. This scheme would be able to account for nonlinearities, large time-delays (possibly changing), changing dynamics, and possible disturbances. Adaptive control seems to answer such expectations. The section below looks at the history of such concepts by reviewing the different techniques that were developed throughout the last decade and that have shaped, since, the skeleton of this attractive technique.

3.4 INTRODUCTION TO ADAPTIVE FEEDBACK CONTROL

For many years, adaptive control has been considered an important part of control engineering, where its contribution can be seen with over 2000 papers abstracted by the IEE INSPEC service during the last decade alone. Mainly concerned with feedback systems, the term "adaptive" means that the controller fulfils two tasks at the same time which could be summarized as:

1. controlling the process.
2. Adapting itself to that process and its disturbances in order to achieve satisfactory control.

Therefore, adaptive control can be described as being a generalization of classical linear feedback control, in the sense that in classical control the coefficients of the law are time-invariant and probably obtained during an off-line study, whereas adaptive control theory produces a controller which tunes itself as process parameters vary. The associated algorithms are called "self-tuning algorithms". The approach was first proposed by Kalman (1958) who made an attempt to implement

the algorithm on a computer. A block diagram of the self-tuning control system is shown in figure (3.11). At each sampling instant the parameters in an assumed dynamic model are estimated recursively from input-output data and the controller settings are then updated. The control design simply accepts current estimates and ignores their uncertainties by evoking the principle of certainty equivalence (Astrom and Wittenmark, 1989) which simply states that the self-tuning properties should still hold if the true parameter estimates are replaced by their estimated ones. The principle represents, in fact, the corner-stone of the theory as it facilitated the solving of many practical problems, especially those of a non-linear nature.

Self-tuning controllers can, however, be based on several techniques which although different in structure use the same philosophy, i.e regulating around a certain point, be it a SISO or a MIMO situation. Space prohibits mentioning all of them, but Pole-Placement (Wellstead, 1980), General Minimum Variance (GMV) (Clarke and Gawthrop, 1975, 1977; Gawthrop, 1979) and Generalized Predictive Control (GPC) (Clarke et al., 1987a, 1987b) are among the best known algorithms. They mainly fall into two categories: explicit and implicit algorithms. The first category, as schematically represented in figure (3.12), implies that the regulator parameters are updated indirectly via estimation of the process parameters, whereas in the second category, the control design stage is omitted by producing directly the coefficients of the required control law as figure (3.13) illustrates.

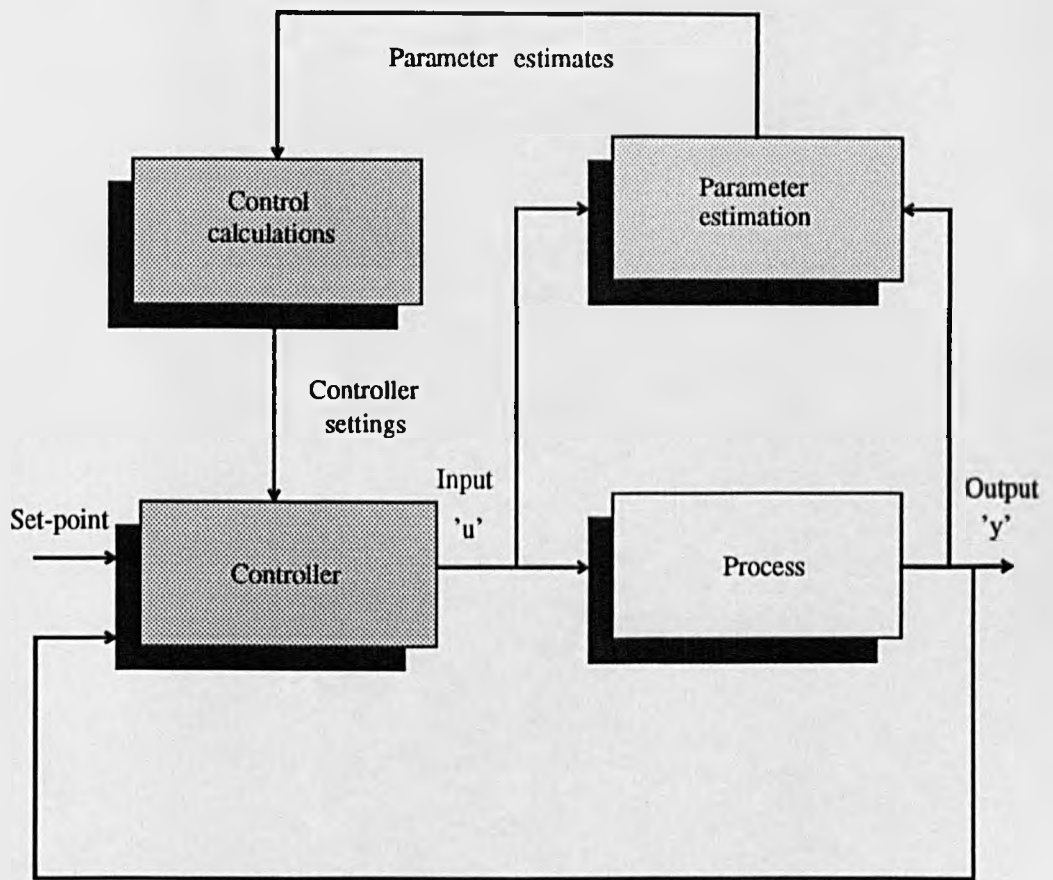


Figure 3.11. Self-tuning control system

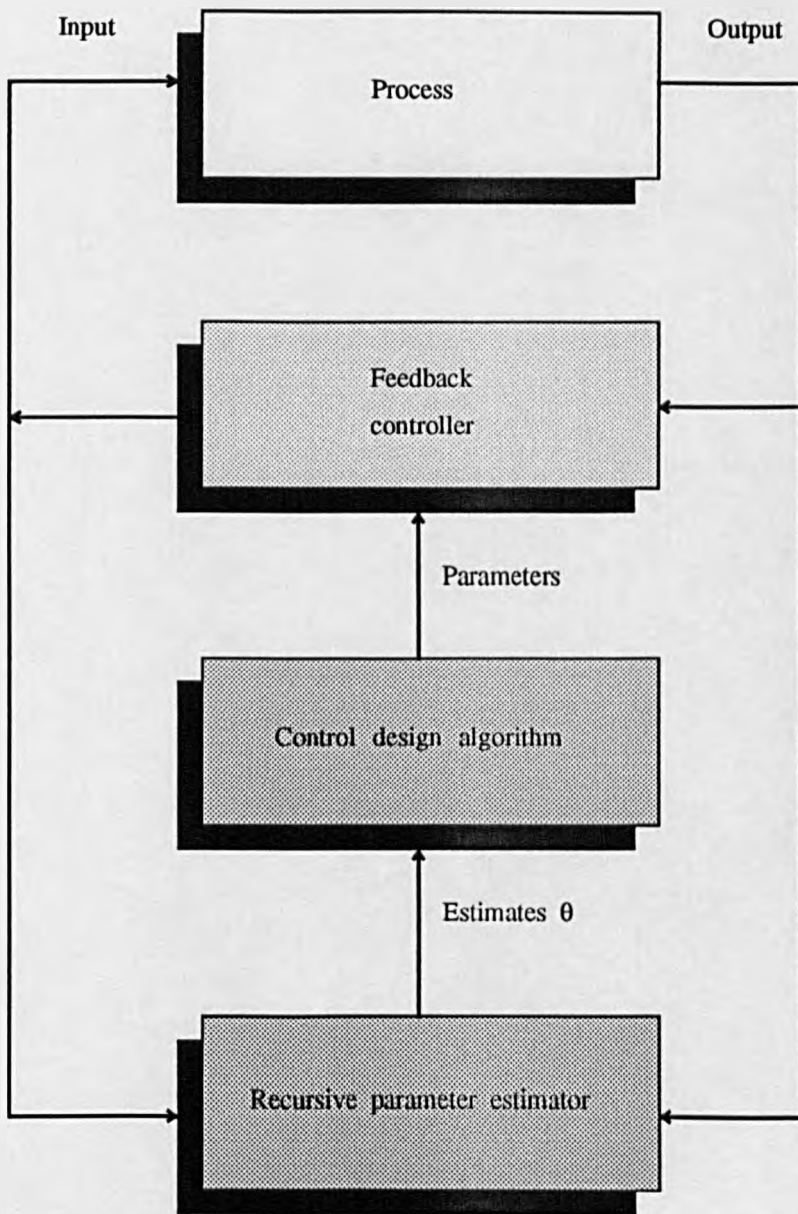


Figure 3.12. Structure of an explicit self-tuner

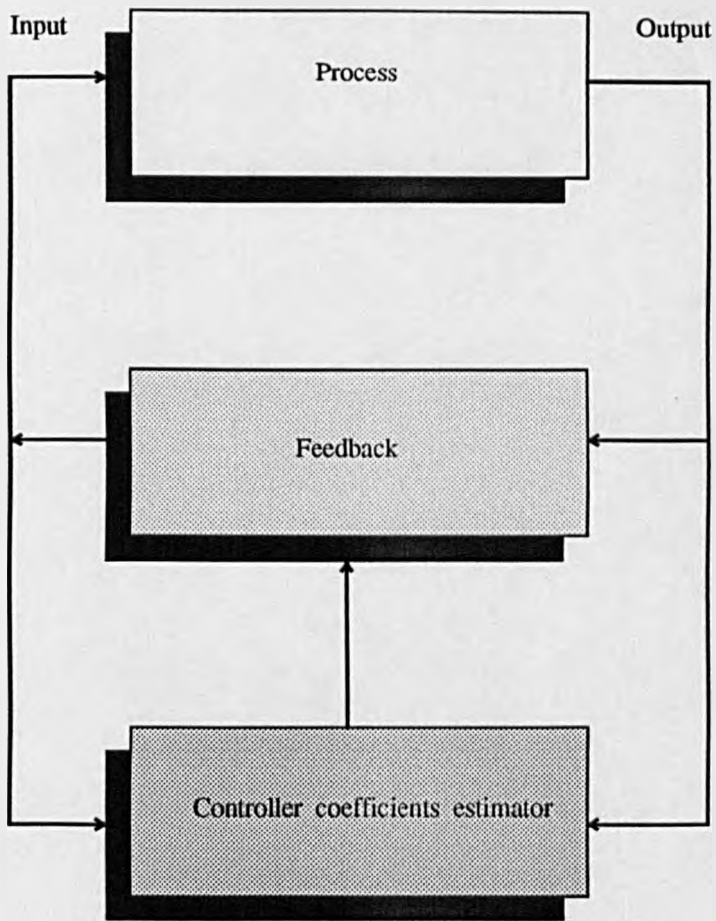


Figure 3.13. Structure of an implicit self-tuner

3.4.1 The Explicit Self-Adaptive Control Approach: 'The Pole-Placement Algorithm'

Before being involved in the different mathematical steps that normally lead to the formulation of the final control law, it is worth reviewing some of the basic results in process model theory.

- **Process Model**

Whether the time-delay is an integer multiple, or a fraction of the sampling time, the SISO model describing the continuous process dynamics in a discrete form is given by the structure known as the ARMAX model structure:

$$y(t) = \frac{B(z^{-1})}{A(z^{-1})} u(t - k) + \frac{C(z^{-1})}{A(z^{-1})} \zeta(t) \quad (3.14)$$

where $A(z^{-1})$, $B(z^{-1})$, and $C(z^{-1})$ are polynomials in the backward shift operator z^{-1} of the form:

$$\begin{aligned} A(z^{-1}) &= 1 + a_1 z^{-1} + a_2 z^{-2} + \dots + a_n z^{-n} \\ B(z^{-1}) &= b_0 + b_1 z^{-1} + b_2 z^{-2} + \dots + b_m z^{-m} \\ C(z^{-1}) &= 1 + c_1 z^{-1} + c_2 z^{-2} + \dots + c_p z^{-p} \end{aligned}$$

$y(t)$ is the process output, $u(t)$ is the control signal delayed by k samples, and $\zeta(t)$ is a sequence of random variables all having a variance σ^2 and a mean of zero. It is also assumed that all roots of the $C(z^{-1})$ lie inside the unit circle in the z -plane.

- **Control Objectives**

The general pole-placement algorithm for stochastic regulation or servo-tracking is derived by the following steps (Wellstead, 1980):

Assume incremental control (for zero steady-state error) such that a digital integrator is lumped with the system, thus,

$$y(t) = \frac{B(z^{-1})}{A(z^{-1})} \Delta u(t - k) + \frac{C(z^{-1})}{A(z^{-1})} \zeta(t) \quad (3.15)$$

Propose the control law given by:

$$\Delta u(t) = G(z^{-1}) \left[\frac{y_r(t) - y(t)}{1 + F(z^{-1})} \right] \quad (3.16)$$

where,

$y_r(t)$ is the command signal

$$G(z^{-1}) = 1 + g_1 z^{-1} + g_2 z^{-2} + \dots + g_{ng} z^{-ng}$$

$$F(z^{-1}) = f_0 + f_1 z^{-1} + f_2 z^{-2} + \dots + f_{nf} z^{-nf}$$

Combining the control law of equation (3.16) and equation (3.15) yields:

$$[(1 + F) A + z^{-k} B G] y(t) = z^{-k} B G y_r(t) + C (1 + F) \zeta(t) \quad (3.17)$$

where the operator z^{-1} has been dropped for simplicity's sake.

Equation (3.17) can be rewritten as:

$$\begin{aligned} y(t) &= \frac{N_1(z^{-1})}{D(z^{-1})} y_r(t) + \frac{N_2(z^{-1})}{D(z^{-1})} \zeta(t) \\ D(z^{-1}) &= (1 + F) A + z^{-k} B G \\ N_1(z^{-1}) &= z^{-k} B G \\ N_2(z^{-1}) &= C (1 + F) \end{aligned} \quad (3.18)$$

Now, $D(z^{-1})$ is the closed-loop characteristic polynomial of the servo system, thus, if it is wished to specify desired closed-loop poles positions corresponding to the roots of the polynomial $T(z^{-1})$ such that:

$$T(z^{-1}) = 1 + t_1 z^{-1} + t_2 z^{-2} + \dots + t_{nt} z^{-nt}$$

then, for good closed-loop regulation properties, the following identity is solved:

$$A (1 + F) + z^{-k} B G = CT \quad (3.19)$$

For this identity to have a unique solution, the order of the regulators must be set

to the following quantities:

$$\begin{aligned}n_g &= n_a - 1 \\n_f &= n_b + k - 1\end{aligned}$$

and the number of the assigned poles such that:

$$n_t \leq n_a + n_b + k - n_c$$

However, if the stochastic disturbance is negligible, the control law identity (3.19) becomes:

$$A(1 + F) + z^{-k} B G = T \quad (3.20)$$

leading to the following closed-loop transfer function:

$$\frac{y(t)}{y_r(t)} = z^{-k} \frac{B G}{T} \quad (3.21)$$

Further guidelines on the choice of the tailoring polynomial $T(z^{-1})$ are widely available in the literature (Wellstead, 1980). It is worth noting that equation (3.21) includes the zeros of the open-loop system, and because zeros cannot be shifted by feedback, it is usually suggested to cancel them. However, the polynomial $B(z^{-1})$ is very likely to be non-minimum phase, leading therefore to unstable control resulting from this cancellation attempt.

3.4.2 The Implicit Self-Adaptive Control Approach:

'Optimal Regulation and Control'

In the original self-tuning regulator of Astrom and Wittenmark (1973), the feedback was designed to minimize the variance of the output variable y . Thus, the control objective was to minimize the quadratic cost function of the form:

$$J_1 = E \left[y^2(t) \right] \quad (3.22)$$

For quality control problems, this expression is a logical choice: by reducing the output variance, the set-point can be moved closer to a limiting constraint (Astrom and Wittenmark, 1980b; Clarke, 1985a). However, the above algorithm had two basic limitations: it does not include set-point following, and it does not penalize excessive control efforts. In order to account for both deficiencies, Clarke and Gawthrop (1975, 1979) proposed the following generalized cost function:

$$J_2 = E \left[(P y(t) - R w(t))^2 + (Q u(t))^2 \right] \quad (3.23)$$

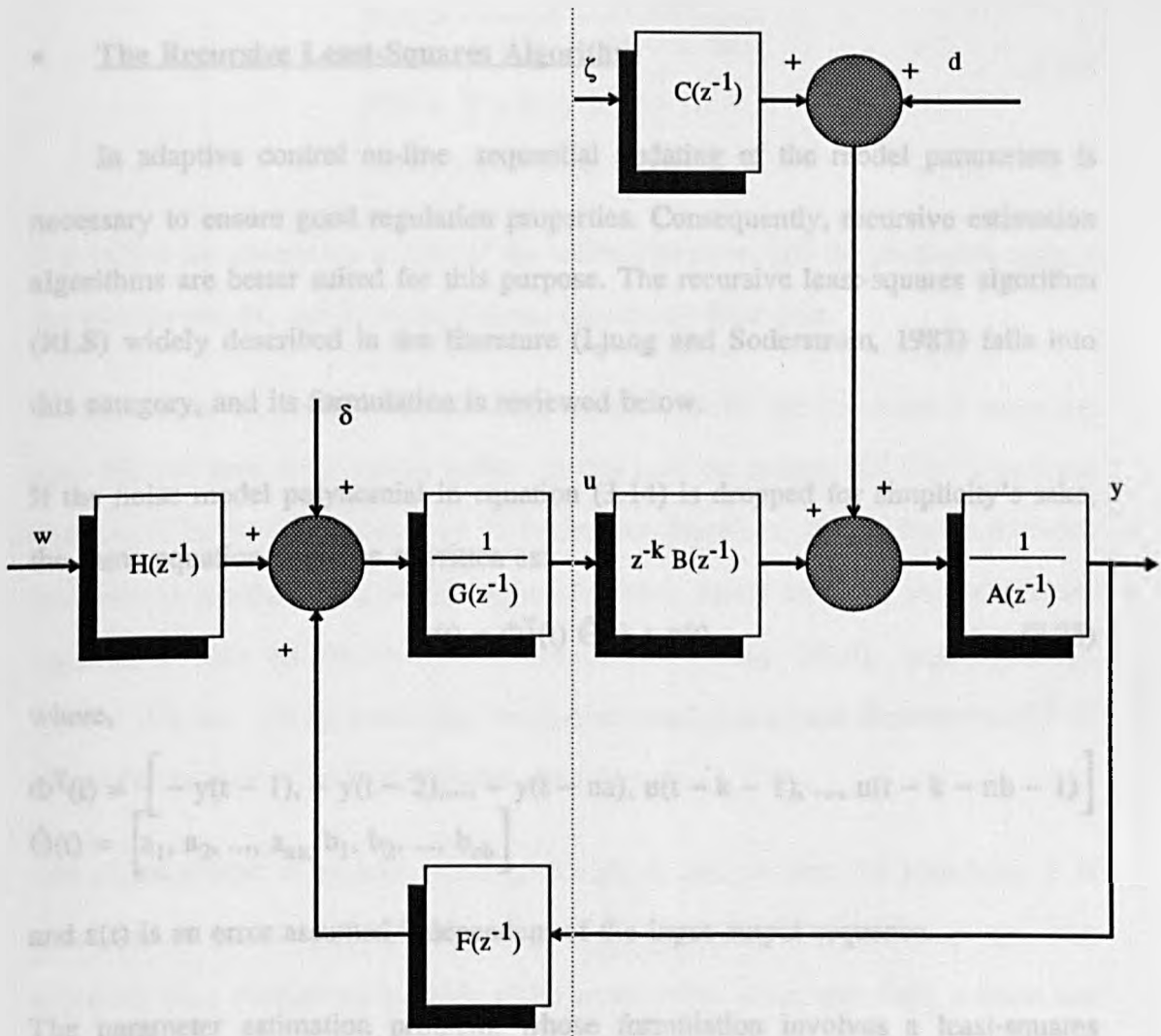
where $w(t)$ is the set-point, $u(t)$ the control signal, and P , Q , and R polynomials in the backward shift z^{-1} . The derived control law minimizing this cost function is shown to be of the form:

$$F y(t) + G u(t) + H w(t) = 0 \quad (3.24)$$

F , G , and H are polynomials in the backward shift z^{-1} related to the system and noise polynomials A , B , and C , as well as the polynomials P , Q , and R . Figure (3.14) shows the structure of this self-tuning optimal controller (STC). Further developments by Gawthrop (1977) extended the STC to include rational transfer functions for P , Q , and R as opposed to simple polynomials. For instance, taking the following expressions for these polynomials

$$P(z^{-1}) = \frac{1}{M(z^{-1})}; \quad Q(z^{-1}) = 0; \quad R(z^{-1}) = 1$$

brings out Landau's concept of model-following adaptive control (Landau, 1974). Finally, to alleviate excessive control signals, generated because of $Q(z^{-1}) = 0$, Clarke and Gawthrop (1979) assigned a value λ to this polynomial and called the algorithm detuned generalized minimum variance (GMV).



where,

$$\phi^T(t) = [-y(t-1), -y(t-2), \dots, -y(t-n_a), u(t-k-1), \dots, u(t-k-n_b-1)]$$

$$\theta(t) = [a_1, a_2, \dots, a_n, b_1, b_2, \dots, b_m]$$

and $\varepsilon(t)$ is an error at

The parameter estimation problem in this formulation involves a least-squares method, is to find the Controller $\theta(t)$ by minimizing the System cost function

$$J = \sum_{t=0}^N [y(t) - \phi^T(t) \theta(t)]^2 \quad (3.26)$$

Figure 3.14. Structure of the optimal controller

3.4.3 Parameter Estimation Methods

- The Recursive Least-Squares Algorithm

In adaptive control on-line sequential updating of the model parameters is necessary to ensure good regulation properties. Consequently, recursive estimation algorithms are better suited for this purpose. The recursive least-squares algorithm (RLS) widely described in the literature (Ljung and Soderstrom, 1983) falls into this category, and its formulation is reviewed below.

If the noise model polynomial in equation (3.14) is dropped for simplicity's sake, the same equation could be rewritten as:

$$y(t) = \Phi^T(t) \hat{\Theta}(t) + \varepsilon(t) \quad (3.25)$$

where,

$$\Phi^T(t) = \left[-y(t-1), -y(t-2), \dots, -y(t-na), u(t-k-1), \dots, u(t-k-nb-1) \right]$$

$$\hat{\Theta}(t) = \left[a_1, a_2, \dots, a_{na}, b_1, b_2, \dots, b_{nb} \right]$$

and $\varepsilon(t)$ is an error assumed independent of the input-output sequence.

The parameter estimation problem, whose formulation involves a least-squares method, is to find the estimates $\hat{\Theta}(t)$ by minimizing the following cost function:

$$J = \sum_{t=1}^N \left[y(t) - \Phi^T(t) \hat{\Theta}(t) \right]^2 \quad (3.26)$$

where N is the number of data points, and $y(t)$ is the measured value of the output.

The equations for recursive least-squares computation of the unknown parameters are given by the following set of expressions (Clarke, 1985a; Ljung and Soderstrom, 1983; Billings, 1985):

$$\begin{cases} \hat{\Theta}(t) = \hat{\Theta}(t-1) + K(t) \varepsilon(t) \\ K(t) = \frac{P(t-1) \Phi(t)}{1 + \Phi^T(t) P(t-1) \Phi(t)} \\ P(t) = [I - K(t) \Phi^T(t)] P(t-1) \\ \varepsilon(t) = y(t) - \Phi^T(t) \hat{\Theta}(t-1) \end{cases} \quad (3.27)$$

P is called the covariance matrix of the estimation error, $\varepsilon(t)$ the prediction error, I the identity matrix, and $K(t)$ the Kalman (feedback) filter gain.

The parameter estimates obtained using equation (3.27) are unbiased if the noise term $\varepsilon(t)$ has zero mean (white noise). In this case the polynomial $C(z^{-1})$ in equation (3.14) is equal to unity and $\hat{\Theta}$ represents, therefore, the minimum variance estimate. In environments where signals to noise ratios are low, however, other algorithms, such as the instrumental variable (Young, 1970), extended least-squares (Clarke, 1985a) could also be implemented. Ljung and Soderstrom (1983) give a full review of widely available algorithms.

One characteristic of equation (3.27), though, is that to start the algorithm, it is necessary to initialize P and $\hat{\Theta}$. Large initial value of P means that the user expresses little confidence in $\hat{\Theta}(0)$, while small values mean that $\hat{\Theta}(0)$ is good and therefore, no big fluctuations around this value are anticipated. Further characteristics of the same equation include the fact that $\|K\|$ and $\|P\|$ tend to zero as more data are processed making, thus, the corrections to $\hat{\Theta}$ smaller, meaning that the parameters have converged. While this parameter convergence is directly linked to the speed of process dynamics variations, the estimator sometimes loses sensitivity, especially in closed-loop environments. Therefore, and in order to maintain its sensitivity, the algorithm has been modified to include an exponential weighting factor, called 'the forgetting factor', in the cost function as expressed by the following equation:

$$J_m [\Theta(t)] = \sum_{i=1}^{i=t} \rho^{t-i} [y(i) - \Phi^T(i) \hat{\Theta}]^2 \quad (3.28)$$

where,

$$0 < \rho \leq 1$$

leading, hence, to the following modified algorithm

$$\begin{cases} \hat{\Theta}(t) = \hat{\Theta}(t-1) + K(t) \varepsilon(t) \\ K(t) = \frac{P(t-1) \Phi(t)}{\rho + \Phi^T(t) P(t-1) \Phi(t)} \\ P(t) = \frac{1}{\rho} [I - K(t) \Phi^T(t)] P(t-1) \\ \varepsilon(t) = y(t) - \Phi^T(t) \hat{\Theta}(t-1) \end{cases} \quad (3.29)$$

The effect of the exponential factor ρ is to prevent the elements of P from becoming too small. A small value of ρ implies fast forgetting of past data, whereas a value close to unity implies a slow forgetting of these data. Suffice to say here that the choice of this factor should allow a trade-off between the ability to track parameter variations and noise sensitivity.

- **Operating Problems of Parameter Estimation Algorithms**

When implemented in real-life environments, estimation algorithms, regardless of their type, may operate unsatisfactorily. Indeed, Anderson (1985) showed that 'bursting' or 'blow-up' phenomena can result from noise or unmodelled dynamics in the absence of persistent excitation. This particular problem is related to the covariance matrix $P(t)$ in equation (3.29), whose elements become large as time increases, causing the estimator to become overly sensitive to parameter changes and noise. As a result, large fluctuations and drifting in parameter estimates occur. Furthermore, Astrom and Wittenmark (1989) showed that large values of P lead usually to numerical problems.

There are a number of approaches to deal with such problems which include covariance resetting, use of perturbation signals, and variable forgetting factor. The following sections discuss each of these remedies.

1. Covariance Resetting

The method, first proposed by Young (1969), consists of adding a positive definite matrix D to $P(t - 1)$ at a specific period of time. This addition of D prevents $\|P\|$ from becoming too small. The magnitude of the elements of D depends upon the expected rate of variations of the parameters. How often this resetting operation occurs during one particular run could for instance be related to the value of the trace of $P(t)$, i.e., whenever this value falls below a certain threshold, D must be added.

2. Perturbation Signal

The assumption that the system under consideration is persistently excited has always been at the forefront of most convergence results established with adaptive control theory. However, as Anderson and Johnson (1982) pointed out, there is no guarantee of persistent excitability of the feedback signal, leading therefore to a non-uniqueness of the parameter estimates. One possibility which ensures that the process is adequately excited is to superimpose a perturbation in the form of a sine wave, or a pseudo-random binary sequence signal (PRBS) for instance. Vogel (1982) suggested that the chosen period and amplitude for the PRBS signal should comply with guidelines involving process dynamics. The same author postulated that the PRBS period should be longer than the duration of the process impulse response, while the amplitude is related to the trace of the $P(t)$ matrix in a linear relationship.

3. Variable Forgetting Factor

If the forgetting factor is constant and wrongly selected, old information is continually forgotten especially if the process is not excited enough to obtain new dynamic information. As equation (3.29) may suggest, this leads to the covariance matrix P growing exponentially causing 'blow-up'. In order to encourage tuning-in and later inhibit any excessive sensitivity of the RLS algorithm to new incoming data, another solution which consists of adjusting the forgetting factor periodically could be used. The strategy is known as the variable forgetting factor approach (Fortescue et al., 1981; Ydstie et al., 1985).

Fortescue et al. (1981), for instance, proposed an algorithm in which the forgetting factor ρ is a function of the prediction error $\varepsilon(t)$ such that:

$$\rho(t) = \frac{1}{\Sigma_0} \left[1 - (1 - \Psi^T(t) K(t)) \varepsilon^2(t) \right] \quad (3.30)$$

where $\varepsilon(t)$ is the prediction error and Σ_0 is a parameter expressed as $\Sigma_0 = \sigma^2 N_0$, where σ^2 is the anticipated measurement noise which acts on the process, and N_0 is a constant governing the speed of adaptation. Implemented according to equation (3.30), the forgetting factor decreases whenever a change in process dynamics occurs and approaches to unity under steady-state regulations. However, the choice of Σ_0 also has to follow a trade-off policy since small values assigned to this parameter leads to a quick adaptation, but if these values are too small 'blow-up' could occur. Although improvements with such procedures have been reported (Fortescue et al., 1981), authors such as (Goodwin et al., 1983) found that the method does not always lead to satisfactory results.

Another simplified algorithm was also proposed by Wellstead and Sanoff (1981) in which the variable forgetting factor expression is given by:

$$\rho(t) = \rho_1(t) \times \rho_2(t) \quad (3.31)$$

where,

$$\begin{aligned} \rho_1 &= \rho\rho + (1 - \rho\rho) (1 - e^{-\frac{t}{\tau}}) \\ 0.0 &\leq \rho\rho \leq 1.0 \\ \tau &= \text{desired memory of estimation} \end{aligned} \quad (3.32)$$

and,

$$\begin{aligned} \rho_2(t) &= 1.0 - \frac{\epsilon^2(t-1)}{\tau s(t)} \\ s(t) &= \frac{\tau-1}{\tau} s(t-1) + \frac{\epsilon^2(t-1)}{\tau} \end{aligned} \quad (3.33)$$

This method has been particularly found easily implementable with another version of the RLS algorithm and better known as the UDU factorization method (Bierman, 1976, 1977). This algorithm, which fulfils the same task as the RLS, consists of decomposing P into a multiplication of triangular and diagonal matrices. This modification has in fact a double role to play: first, it ensures that the matrix P is always positive definite, and second it reduces the computational burden and allows variable forgetting factor procedures to be easily and efficiently implemented.

To conclude, it should be stated that based upon a study of the background relative to the physiology of the human body, mathematical models associated with two well known muscle relaxant drugs were obtained. The results showed large patient-to-patient parameter variability. The study allowed one to realize feedback control of the physiological variable which is muscle relaxation. The closed-loop control was achieved using fixed PID controllers whose parameters were tuned in an off-line study involving available optimization routines. It has been shown that the fixed controller can perform well under certain conditions, but if the model parameters vary, the performance was seen to degrade considerably.

It was then concluded, that such form of control was not suitable and that a strategy which combines on-line estimation of the model parameters as well as control had to be considered if good quality control was the prime target. Adaptive control represented an attractive candidate. The overall scheme would use a fixed PI controller during the phase corresponding to the margin of safety period, then switch on to the self-adaptive mode assuming that the estimates have converged to reasonable values. An introduction into the technique was reviewed together with parameter estimation methods. The scheme should be able to cope with nonlinearities, large delays and variable dynamics. The next chapter is mainly dedicated to the application of an explicit type approach which is an extension to the well known PI controller and known as the Proportional-Integral-Plus (PIP) algorithm.

SHEFFIELD
UNIVERSITY
LIBRARY

CHAPTER 4

POLE-PLACEMENT PROPORTIONAL-INTEGRAL-PLUS APPLIED TO THE MUSCLE RELAXATION SYSTEM

4.1 INTRODUCTION

The next sections will endeavour to present the main theoretical results of a new method of state-variable feedback pole-assignment control for discrete-time systems. The method depends upon the specification of a non-minimal state-space (NMSS) representation of the system under consideration in which the state vector is composed only of the present and past input-output variables, together with an "integral of error" state which ensures type-1 servomechanism performance. It is perhaps worth noting that this new formulation is considered to be a direct development of the multivariable continuous-time servomechanism design procedures for continuous-time systems suggested by Young and Willems (1972).

4.2 A REVIEW OF STATE-SPACE FORMULATION

State-space (state-variable) representation and controller design suffered a rather long set-back because of their computational burden. However, the advent of digital processors with their remarkable power and speed made this alternative method and many others even more attractive by restoring their valuable contribution. As a result of this, state-space methods have reemerged to form a direct multivariable approach to linear control synthesis and design. These types of representations have always been linked to the multivariable character of systems which makes them rather complicated. In the following we will only present them in a single-input single-output (SISO) manner in the hope to get easily to grips

with the theory. The state-space representation of a continuous-time system is defined by a set of 'first order' differential equations called the state equations. These equations describe the dynamic behaviour of any system linearized around an operating point at any time 't', i.e:

$$\begin{aligned}\dot{x}_t &= F x_t + G u_t \\ y_t &= H x_t\end{aligned}\tag{4.1}$$

x_t is the vector of state-variables.

y_t is the system output.

F is a transition matrix continuous and bounded.

G is the input matrix continuous and bounded.

H a continuous and bounded matrix.

Complex SISO or multivariable systems rarely satisfy the assumption that the system state-vector is available for feedback control purposes, necessitates either a radical review of the state-space method itself at the loss of its most favourable properties, or the reconstruction of the missing state-variables as first proposed by Kalman (1958). Figure (4.1) illustrates such a scheme in open-loop. However, in closed-loop considerations if the control strategy is of the type:

$$u(t) = K x(t)\tag{4.2}$$

where K is a gain matrix, then the observer can be regarded as forming part of a linear feedback compensation scheme used to generate some sort of approximation $F\hat{x}(t)$ (O'Reilly, 1983). Figure (4.2) depicts such a configuration.

Consider physical systems whose dynamic behaviour can be modelled by discrete-time linear vector equations, i.e:

$$\begin{aligned}x_k &= \Phi x_{k-1} + \Gamma u_{k-1} \\ y_k &= H x_k\end{aligned}\tag{4.3}$$

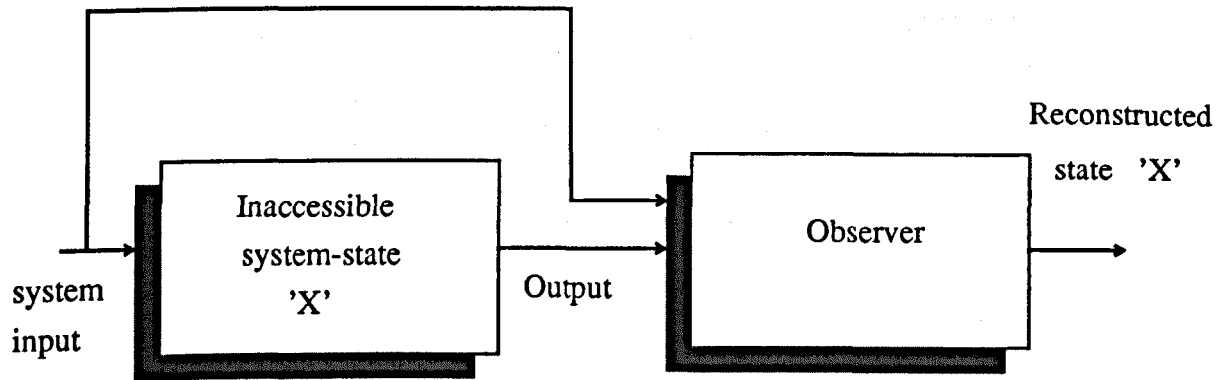


Figure 4.1. Open-loop system-state reconstruction

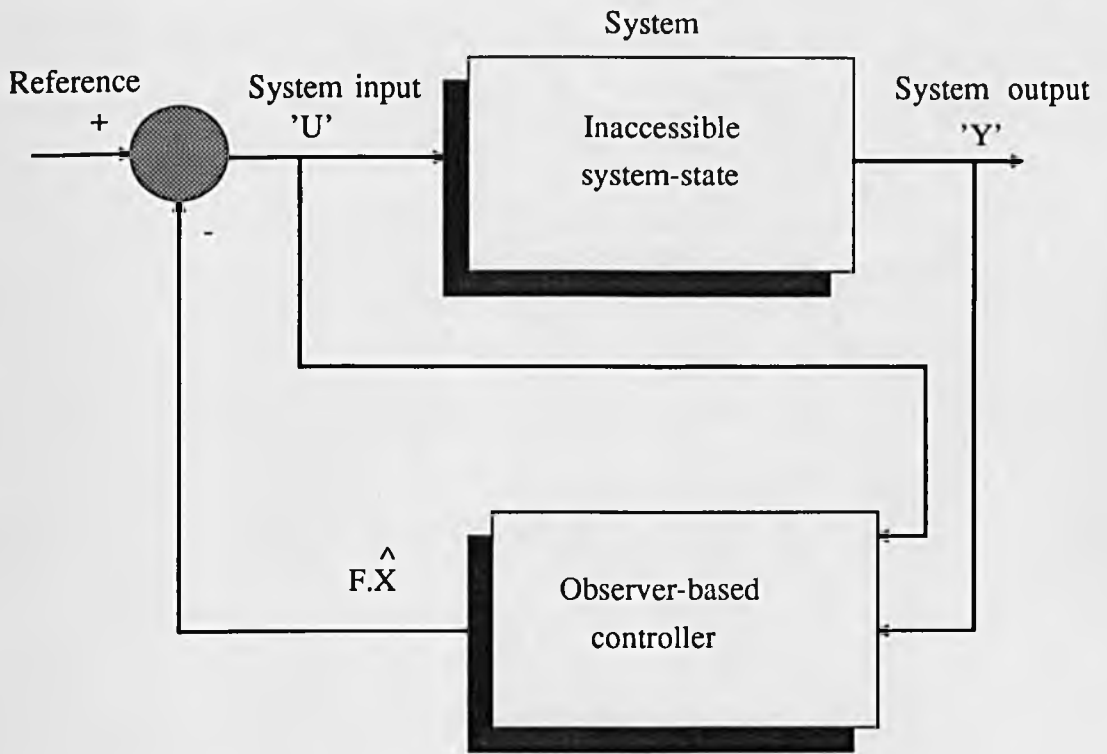


Figure 4.2. Closed-loop observer-based control system

Here all the variables are defined exactly in the same manner as previously in system equations (4.1). Taking the z-transform of system (4.3) leads to:

$$\begin{aligned} X(z) &= \Phi z^{-1} X(z) + \Gamma z^{-1} U(z) \\ Y(z) &= H X(z) \end{aligned} \quad (4.4)$$

Factorizing and rearranging gives:

$$\begin{aligned} [z I - \Phi] X(z) &= \Gamma U(z) \\ Y(z) &= H X(z) \end{aligned} \quad (4.5)$$

The open-loop transfer function could be obtained as:

$$\frac{Y(z)}{U(z)} = H [z I - \Phi]^{-1} \Gamma$$

It is worth noting at this stage that the system poles are defined by the eigenvalues of the matrix Φ . Similarly to the continuous case, we can define the feedback of a linear combination of all the states, i.e:

$$u = -K x = - [k_1 \ k_2 \ \dots] \begin{bmatrix} x_1 \\ x_2 \\ \cdot \\ \cdot \end{bmatrix} \quad (4.6)$$

From this, the closed-loop characteristic equation is of the form:

$$\det [z I - \Phi + \Gamma K] = 0 \quad (4.7)$$

Although this approach of the control problem is somewhat different from the so-called 'classical design methods', its aim is practically identical. Indeed, the strategy consists of selecting the elements k_1, k_2, \dots , so that the roots of the characteristic equation (4.7) lie at chosen locations in the complex z-plane. The approach is known as the 'State-Variable Feedback Pole-Placement approach (SVF)'.

At the time when significant results by many researchers in this field had been

reached namely by Popov (1964), Young and Willems (1972), and Kuo (1980), the method became more and more appealing to control engineers, especially when it has been shown that through the state-variable feedback control law, the closed-loop system characteristic polynomial poles can be arbitrarily assigned to selected positions in the z -plane providing that the system equations (4.3) are controllable. However, in this representation it is assumed that all the states are available to adequately realize a proper feedback, which in general is not the case, since not all the state-variables are always accessible for measurement. This obvious drawback of SVF system design has almost certainly restricted its practical use and discouraged many from showing enthusiastic interest in this area. To obviate this requirement, Kalman (1960, 1961) proposed an optimal state estimator followed later by many other contributions (Luenberger, 1966). However, these methods can only be used if the systems under investigation are observable. Early work by Young and Willems (1972) suggested a methodology in which attention should be focused on the non-minimal character of the state-space formulation, i.e. selecting state-variables to which primary emphasis should be given. One could possibly argue about the basis on which this selection may be made. The answer is simple: It should be linked to our ability to directly measure these carefully chosen states. For instance, in a digital system, these states could be the present and past values of the output variable, and the past values of the input. These variables can be considered as non-minimal state-variables which are used for SVF control. Therefore, the representation of systems in which the state vector is only composed of selected present and past inputs and outputs is named **Non-Minimal State-Space** representation (NMSS). It is worth noting that the use of these sampled data signals is not only proper to this particular strategy, but they are also used in several self-tuning control algorithms (Astrom and Wittenmark, 1980a). However, in this case it provides a special and valuable insight into the nature of

the resulting control design system (Young et al., 1987). Moreover, to add to the features that most recent algorithms have, an integral of error state is introduced which allows for an inherent type-1 servomechanism performance. The next section will describe the NMSS discrete-time model for the single-input single-output case and the associated SVF control system.

4.3 NON-MINIMAL STATE-SPACE FORM

Consider the following general discrete-time transfer function represented by the following n th order SISO system.

$$y_k = \frac{B(z^{-1})}{A(z^{-1})} u_k \quad (4.8)$$

Where $A(z^{-1})$ and $B(z^{-1})$ are polynomials of the form:

$$\begin{aligned} A(z^{-1}) &= 1 + a_1 z^{-1} + a_2 z^{-2} + \dots + a_n z^{-n} \\ B(z^{-1}) &= b_1 z^{-1} + b_2 z^{-2} + \dots + b_m z^{-m} \end{aligned}$$

z^{-1} is the backward-shift operator.

The transfer function $\frac{B(z^{-1})}{A(z^{-1})}$ may be marginally stable, unstable or possesses non-minimum phase characteristics.

Replacing the polynomials $A(z^{-1})$ and $B(z^{-1})$ by their respective expressions in equation (4.8) gives:

$$y_k = -a_1 y_{k-1} - a_2 y_{k-2} - \dots - a_n y_{k-n} + b_1 u_{k-1} + b_2 u_{k-2} + \dots + b_m u_{k-m}$$

The NMSS system can be represented by the following discrete-time state equation:

$$\begin{aligned} x_k &= F x_{k-1} + g u_{k-1} + d y_{dk} \\ y_k &= h x_k \end{aligned} \quad (4.9)$$

Where the state transition matrix F , input vector g , and output vector h are defined by the following expressions:

$$F = \begin{bmatrix} -a_1 & -a_2 & \dots & -a_{n-1} & -a_n & b_2 & b_3 & \dots & b_{m-1} & b_m & 0 \\ 1 & 0 & \dots & 0 & 0 & 0 & 0 & \dots & 0 & 0 & 0 \\ 0 & 1 & \dots & 0 & 0 & 0 & 0 & \dots & 0 & 0 & 0 \\ \cdot & \cdot & & \cdot & \cdot & \cdot & \cdot & & \cdot & \cdot & \cdot \\ \cdot & \cdot & & \cdot & \cdot & \cdot & \cdot & & \cdot & \cdot & \cdot \\ \cdot & \cdot & & \cdot & \cdot & \cdot & \cdot & & \cdot & \cdot & \cdot \\ 0 & 0 & \dots & 1 & 0 & 0 & 0 & \dots & 0 & 0 & 0 \\ 0 & 0 & \dots & 0 & 0 & 0 & 0 & \dots & 0 & 0 & 0 \\ 0 & 0 & & 0 & 0 & 1 & 0 & & 0 & 0 & 0 \\ 0 & 0 & & 0 & 0 & 0 & 1 & & 0 & 0 & 0 \\ \cdot & \cdot & & \cdot & \cdot & \cdot & \cdot & & \cdot & \cdot & \cdot \\ \cdot & \cdot & & \cdot & \cdot & \cdot & \cdot & & \cdot & \cdot & \cdot \\ \cdot & \cdot & & \cdot & \cdot & \cdot & \cdot & & \cdot & \cdot & \cdot \\ 0 & 0 & & 0 & 0 & 0 & 0 & & 1 & 0 & 0 \\ a_1 & a_2 & & a_{n-1} & a_n & -b_2 & -b_3 & & -b_{m-1} & -b_m & 1 \end{bmatrix}$$

$$g^T = \begin{bmatrix} b_1 & 0 & \dots & 0 & 1 & 0 & 0 & \dots & 0 & -b_1 \end{bmatrix}$$

$$h = \begin{bmatrix} 1 & 0 & \dots & 0 & 0 & 0 & 0 & \dots & 0 & 0 \end{bmatrix}$$

$$d^T = \begin{bmatrix} 0 & 0 & \dots & 0 & 0 & 0 & 0 & \dots & 0 & 1 \end{bmatrix}$$

The state vector x is defined as:

$$x^T = \begin{bmatrix} x_k & x_{k-1} & \dots & u_{k-1} & \dots & u_{k-m+1} & z_k \end{bmatrix}$$

Where z_k is the 'integral of error' state defined by:

$$z_k = z_{k-1} + y_{dk} - x_k \quad (4.10)$$

y_{dk} being the reference signal (command input to the servomechanism). The familiar integral action is automatically introduced by feedback of this state-variable. The non-minimal character of the state-space model described by equation (4.9) is

clearly justified by the simple fact that the state has been extended from its dimension n (degree of polynomial $A(z^{-1})$) to be able to accommodate in addition to the n sampled output data $x_k, x_{k-1}, \dots, x_{k-n+1}$, the $m-1$ past sampled values of input $u_k, u_{k-1}, \dots, u_{k-m+1}$ together with the integral of error state z_k .

Having shown the non-minimal feature of the new state-space formulation, the next section endeavours to consider the use of such representation as a basis for state-variable feedback (SVF) and the possibility of it retaining the property of assigning the poles of the closed system to a specific location in the z -plane.

4.4 THE PROPORTIONAL-INTEGRAL-PLUS CONTROL SYSTEM

From equation (4.9) for the definition of the vector h the following equations can be written:

$$\begin{cases} x_k = y_k \\ u_k = -V^T x_k \\ V^T = -[f_0, f_1, \dots, f_{n-1}, g_1, g_2, \dots, g_{m-1}, k_I] \end{cases} \quad (4.11)$$

Hence,

$$u_k = -f_0 x_k - \dots - f_{n-1} x_{k-n+1} - g_1 u_{k-1} - \dots - g_{m-1} u_{k-m+1} - k_I z_k$$

But from equation (4.10) it follows that:

$$z_k = \frac{1}{1-z^{-1}} (y_{dk} - x_k)$$

Substituting in equation (4.11) leads to:

$$u_k = -f_0 x_k - \dots - f_{n-1} x_{k-n+1} - \dots - g_{m-1} u_{k-m+1} - \frac{k_I}{1-z^{-1}} (y_{dk} - x_k)$$

Developing and rearranging yields:

$$\begin{cases} u_k = u_{k-1} - k_I (y_{kd} - x_k) - f_0 \Delta x_k - \dots - g_{m-1} \Delta u_{k-m+1} \\ \Delta = 1-z^{-1} \end{cases} \quad (4.12)$$

Equation (4.12) could alternatively be described in block diagram terms and figures (4.3) and (4.4) illustrate such representations which clearly show that the system includes a proportional action P, an integrator I, and two discrete time-filters G and F. Because of the presence of these latter components, this NMSS control system is considered as a direct extension of the classical PI controller reviewed in chapter 3. Consequently, it has been given the name of **Proportional Integral-Plus** control system or **PIP**. In order to develop the PIP control algorithm, first consider the block diagram model illustrated in figure (4.4) and find the expression of the closed-loop transfer function.

Hence, it follows that:

$$y_k = \frac{F}{G} \left[\frac{I}{F} (y_{dk} - y_k) - y_k \right] \frac{B(z^{-1})}{A(z^{-1})} \quad (4.13)$$

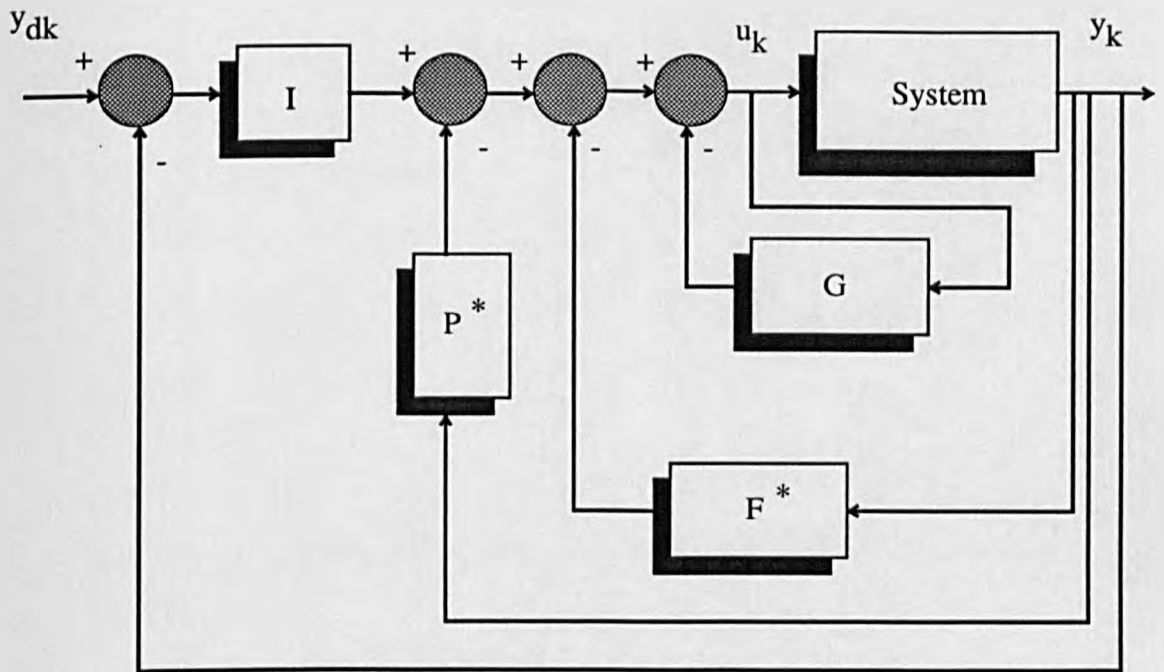
where,

$$\begin{aligned} F(z^{-1}) &= f_0 + f_1 z^{-1} + \dots + f_{n-1} z^{-n+1} \\ G(z^{-1}) &= 1 + g_1 z^{-1} + \dots + g_{m-1} z^{-m+1} \\ I &= k_I \end{aligned} \quad (4.14)$$

Using equation (4.8) and rearranging leads to:

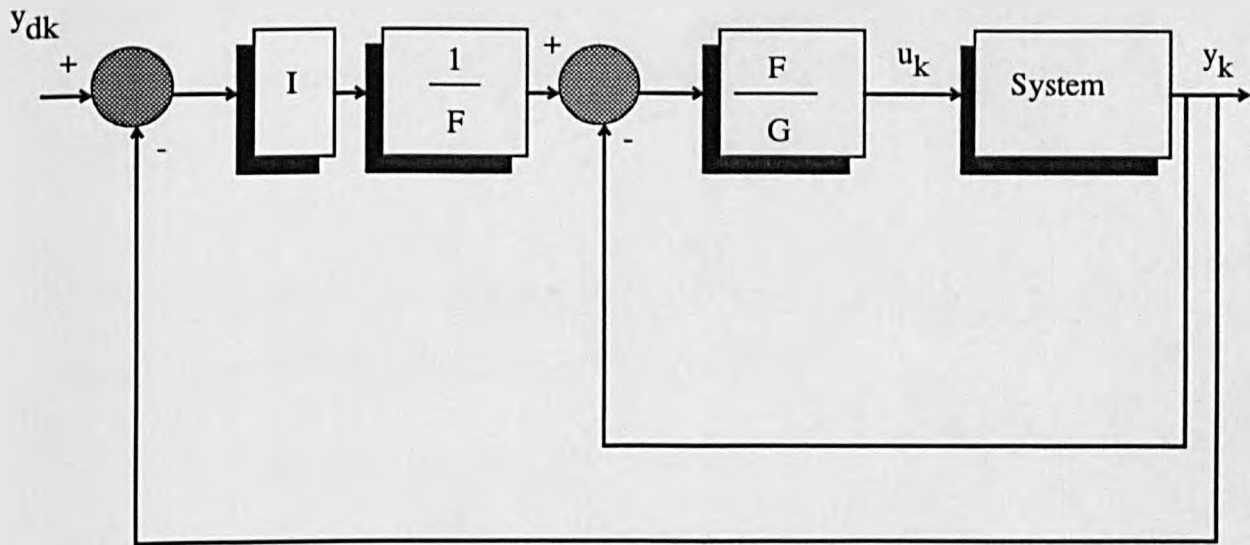
$$\begin{cases} y_k = \frac{N(z^{-1})}{D(z^{-1})} y_{dk} \\ N(z^{-1}) = k_I B(z^{-1}) \\ D(z^{-1}) = (1 - z^{-1}) [G(z^{-1}) A(z^{-1}) + F(z^{-1}) B(z^{-1})] + k_I B(z^{-1}) \end{cases} \quad (4.15)$$

System-equations (4.15) represent the closed-loop transfer function for the NMSS system. It is worth noting at this stage that both numerator and denominator possess an identical term, i.e: $k_I B(z^{-1})$. As we will see later, this is an important result which may have a direct consequence on the stability requirement of the algorithm.



- P^{*}** Proportional term
- F^{*}** Feedback filter
- G** Forward-path filter
- I** Integral term

Figure 4.3. The PIP servo-mechanism control system



F Proportional and feedback filter

G Forward-path filter

I Integral term

Figure 4.4. Another representation of the PIP servo-mechanism control system

If we ever wish to specify the desired closed-loop poles corresponding to the roots of:

$$d(z^{-1}) = 1 + d_1 z^{-1} + d_2 z^{-2} + \dots + d_{m+n+\delta} z^{-m+n+\delta} \quad (4.16)$$

with δ being the assumed value of time-delay, we only have to equate the polynomials $D(z^{-1})$ and $d(z^{-1})$ and identify term by term the coefficients of power z^{-i} , result of which is a set of $(n+m)$ linear simultaneous equations of the general matrix form of:

$$\Sigma \cdot V = \beta \quad (4.17)$$

Where Σ is a matrix of dimension $(n+m) \cdot (n+m)$, V the SVF control gain introduced in equation (4.11) and β a vector of the form:

$$\beta^T = \left[\beta_1 \ \beta_1 \ \dots \ \beta_{m+n} \right]$$

with

$$\begin{cases} \beta_i = d_i - (a_i - a_{i-1}) \\ a_0 = 1 \\ a_i = 0 \quad \text{for } i \geq n + 1 \end{cases}$$

d_i being the coefficients of the desired characteristic polynomial $d(z^{-1})$ in equation (4.16).

By using equations (4.15), (4.16), and by equating the two polynomials $D(z^{-1})$ and $d(z^{-1})$, we obtain the following Σ matrix

$$\Sigma = \left[\Sigma_f \ : \ \Sigma_g \ : \ \Sigma_k \right]$$

While the general forms of Σ_f , Σ_g , and Σ_k can be found in Young et al. (1987), section 4.5 below shows the form of Σ for a particular system order.

Having justified the NMSS form and derived the PIP control algorithm, the question of controllability of this representation is a problem of great interest. Indeed Wang's theorem (1988) states that:

Given a single-input single-output discrete-time system of equation (4.8), the non-minimal state representation of equation (4.9) is completely controllable if and only if:

a) The polynomials $A(z^{-1})$ and $B(z^{-1})$ are coprime.

$$b) \sum_{i=1}^{i=m} b_i \neq 0$$

Clearly condition a) relative to the coprimeness of the two polynomials means that there should not be pole-zero cancellations between their respective roots which would make the matrix Σ singular and therefore non-invertible. Whereas, condition b) is equivalent to the requirement that the numerator of the closed-loop transfer function described by equation (4.15) should not admit $z=1$ as a root. If it is the case, then the pole introduced by the integral action at $z=1$ would be cancelled out, making the system non-controllable.

4.5 A SIMPLE EXAMPLE OF APPLICATION

As an example, consider the pharmacokinetics of the muscle relaxation system associated with the Pancuronium-Bromide drug described in chapter 3. The linear dynamics correspond to a one minute sampling time, and the time-delay is omitted here for simplicity reasons.

$$y_k = \frac{B(z^{-1})}{A(z^{-1})} u_k = \frac{0.04 + 0.03 z^{-1}}{1 - 1.55 z^{-1} + 0.57 z^{-2}} u_{k-1}$$

Using equations (4.16) and (4.17) and assigning a relatively fast pole of 2 minutes the following expressions for respectively Σ , V , and β are therefore obtained.:

$$\Sigma = \begin{bmatrix} b_1 & 0 & 1 & b_1 \\ b_2 - b_1 & b_1 & a_1 - 1 & b_2 \\ -b_2 & b_2 - b_1 & a_2 - a_1 & 0 \\ 0 & -b_2 & -a_2 & 0 \end{bmatrix}$$

Replacing the a's and b's by their values leads to:

$$\Sigma = \begin{bmatrix} 0.04 & 0 & 1 & 0.04 \\ -0.01 & 0.04 & -2.55 & 0.03 \\ -0.03 & -0.01 & 2.12 & 0 \\ 0 & -0.03 & -0.57 & 0 \end{bmatrix}$$

$$V^T = [f_0 \ f_1 \ g_1 \ k_I]$$

$$\beta^T = [\beta_0 \ \beta_1 \ \beta_2 \ \beta_3]$$

Again replacing the a's and the d's by their respective values it follows that:

$$\beta^T = [1.95 \ -2.12 \ 0.57 \ 0.0]$$

Hence, the following system of 4 simultaneous equations written in matrix form is obtained:

$$\begin{bmatrix} b_1 & 0 & 1 & b_1 \\ b_2 - b_1 & b_1 & a_1 - 1 & b_2 \\ -b_2 & b_2 - b_1 & a_2 - a_1 & 0 \\ 0 & -b_2 & -a_2 & 0 \end{bmatrix} \begin{bmatrix} f_0 \\ f_1 \\ g_1 \\ k_I \end{bmatrix} = \begin{bmatrix} 1.95 \\ -2.12 \\ 0.57 \\ 0.0 \end{bmatrix}$$

Using a stable algorithm for matrix inversion (Jordan's algorithm) the following solution for this system in the form of a control law is obtained:

$$u_k = u_{k-1} - 25.83 \cdot \Delta y_k + 11.06 \cdot \Delta y_{k-1} - 0.58 \cdot \Delta u_{k-1} + 2.19 \cdot (y_{kd} - y_k)$$

Figure (4.5) illustrates the corresponding behaviour of the fixed gain PIP for a changing command signal of 80% then 70% at regular intervals of 50 iterations

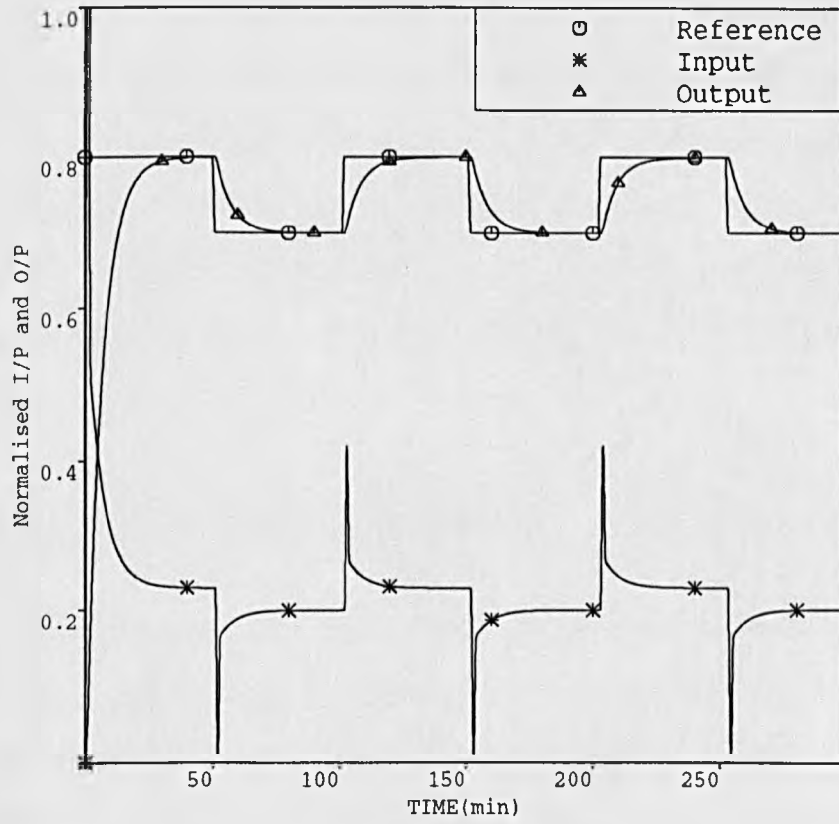


Figure 4.5. Closed-loop response of linear pharmacokinetics associated with Pancuronium model under fixed PIP control algorithm

each. The response is fast and well damped despite the position of these assigned closed-loop pole which implies fast transient performance. However this harsh choice should carefully be reviewed when using the algorithm in a self-tuning mode since great attention should be focused on the magnitude of the input signal fluctuations the algorithm is able to sustain in these conditions before maintenance of stability becomes impossible. This remark is particularly useful for the next study as the dynamics we will focus on vary from one subject to another and we will undoubtedly have to settle for a trade-off eventually.

The next section considers the application of the previously developed algorithm to the muscle relaxation system associated with both model drugs identified in the previous chapter.

4.6 ON-LINE PIP CONTROL OF MUSCLE RELAXATION SYSTEM

The relaxant dynamics identified in the previous chapter have shown a large variability from one subject to another. These variations, added to other phenomena such as time-delays, noise, non-linearities, make the design of a fixed gain controller for muscle relaxation system extremely difficult. As demonstrated in the previous chapters parameters of such controllers need to be adjusted in order to avoid degradation in the closed-loop performance when model parameters were varied, especially the dead-time. Although a significant reduction in the system's sensitivity particularly to changes in the dead-time has been claimed (Smith, 1959), inaccurate modelling of the system under consideration appears as a mismatch term between the actual process and its model in the Smith predictor leading consequently to a poor performance (Marshall, 1979).

Having said that, the development of a scheme which would combine the identification of the parameters of the process, and the use of these parameters to

calculate the control signal according to an a priori established law would seem to adequately counteract the problems previously faced. Therefore, the application of the previously developed PIP algorithm in a self-tuning manner rather than in a fixed gain one seems to be justified and its performance is assessed via the two models associated with Pancuronium-Bromide and Atracurium drugs already identified.

4.6.1 Self-Tuning Adaptive PIP Control of Muscle Relaxation System Associated with Pancuronium-Bromide

The overall non-linear muscle relaxant model describing Pancuronium-Bromide dynamics presented in section 3.2 is first considered here. The pharmacokinetics are given by a two-time-constant transfer function with a one unit time-delay, i.e:

$$G_1(s) = \frac{3.5 e^{-s}}{(1 + 20 s) (1 + 2 s)} \quad (4.18)$$

whereas the pharmacodynamics are modelled by a dead space of 50% together with a saturation element of 100%.

Whenever the controller operates in the non-linear region, parameter-estimation is frozen and control is maintained with the previously used fixed PI controller and the self-tuner takes over as soon as the non-linear region is passed. The block diagram in figure (4.6) shows the overall control system.

The gains for the fixed PI controller have been reduced to shape smoothly the transient response using the following optimized values obtained via the PSI package program (Van Den Bosch, 1979):

$$K_p = 0.4$$

$$K_I = 0.02$$

At this stage it is perhaps worth noting that the overall system was simulated in a

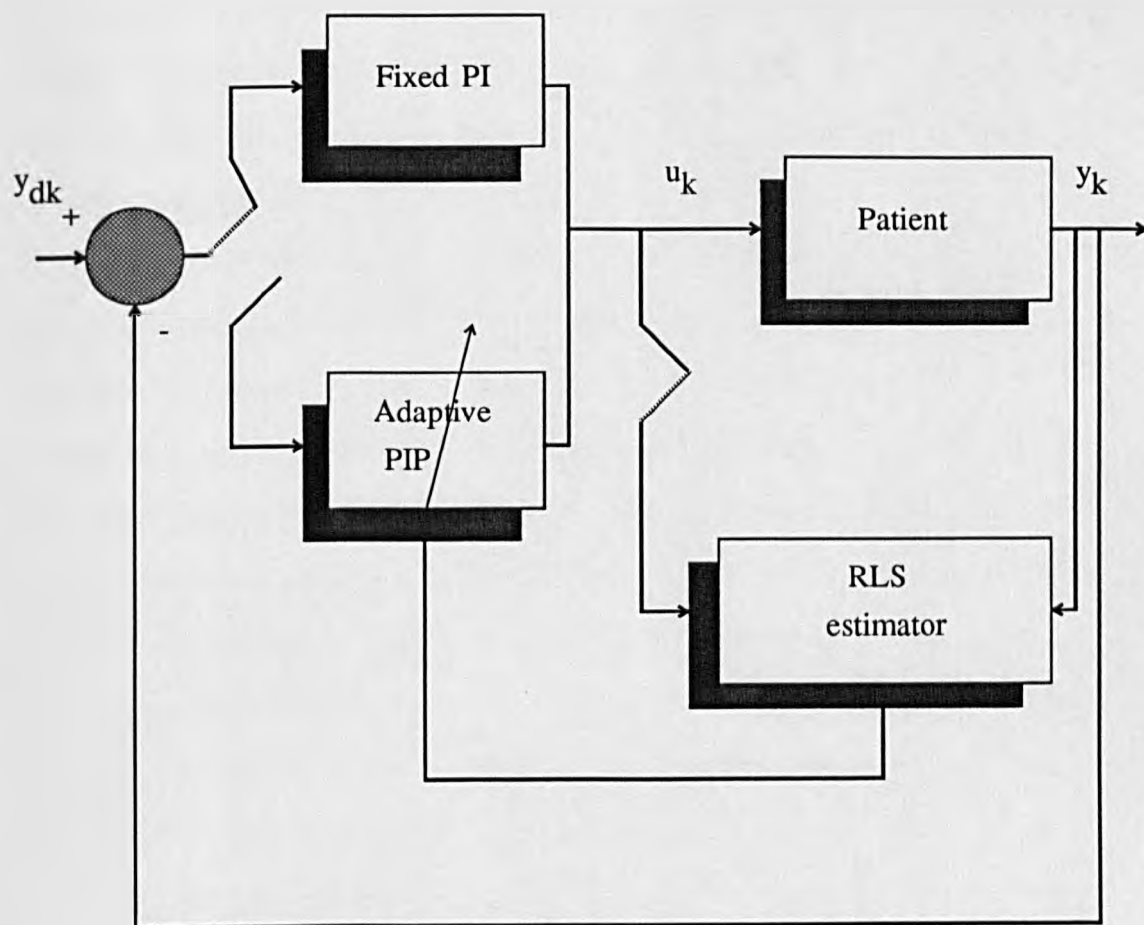


Figure 4.6. Block diagram of the self-adaptive PIP control system for muscle relaxation

continuous form using a fourth order Runge-Kutta integration method with a fixed-step of 0.1. The sampling interval was chosen according to Shannon's theorem (stating that the sampling frequency should be at least twice the largest frequency included in the dynamics), in our case a 1 minute sampling time was adopted throughout all of this study.

As pointed out earlier, because the system exhibits relatively large dead-zones, the previously optimized PI provides initial control for 20 samples then the self-tuner takes over. Parameter estimation, using full-valued data or positional data for the measurement vector, takes the form of a UDU factorization algorithm (Bierman, 1976, 1977), which is a modified version of the well known RLS algorithm.

Because the estimated model between u and y does not reflect in any way the process dynamics during the dead-zone period (Clarke, 1985a), the estimation routine is only triggered when the output reaches 10% of the output value. Parameter estimates are initially set at 0.0 unless otherwise specified, the covariance matrix is made equal to $10^4 \cdot I$, I being the identity matrix, and a value of 0.995 for the forgetting factor is adopted throughout.

Simulation Results

$$G_1(z^{-1}) = \frac{(b_1 z^{-1} + b_2 z^{-2})}{1 + a_1 z^{-1} + a_2 z^{-2}} z^{-1}$$

With $n = 2$ and $m = 3$, the PIP algorithm, coded in Fortran 77 and implemented on a SUN workstation, solves the system of equations (4.17), i.e:

$$\Sigma \cdot V = \beta$$

where Σ is a (5 \times 5) matrix of the following form:

$$\begin{bmatrix} 0 & 0 & 1 & 0 & 0 \\ b_1 & 0 & a_1 - 1 & 1 & b_1 \\ b_2 - b_1 & b_1 & a_2 - a_1 & a_1 - 1 & b_2 \\ -b_2 & b_2 - b_1 & -a_2 & a_2 - a_1 & 0 \\ 0 & -b_2 & 0 & -a_2 & 0 \end{bmatrix}$$

Note that because of the assumed time-delay of 1 sample, the matrix is one dimension larger than the one established in section 4.5.

$$V^T = [f_0 \ f_1 \ g_1 \ g_2 \ k_I]$$

If a second order closed-loop characteristics equation is assigned, i.e: $1 + d_1 z^{-1} + d_2 z^{-2}$ then,

$$\beta^T = [\beta_1 \ \beta_2 \ \beta_3 \ 0 \ 0]$$

where:

$$\beta_1 = d_1 - (a_1 - a_0)$$

$$\beta_2 = d_2 - (a_2 - a_1)$$

$$\beta_3 = a_2$$

If on the other hand a first order closed-loop characteristic equation is preferred, then,

$$\beta_1 = d_1 - (a_1 - a_0)$$

$$\beta_2 = a_1 - a_2$$

$$\beta_3 = a_2$$

Figure (4.7) shows the response of the muscle relaxation process for a changing

response of 0.75 after 100 min. This stability was due to 11 and 6 minutes were assigned leading to a polynomial of the following expression:

$$G(s) = s^2 - 1.78s + 0.77$$

The first zero which is considered to have more effect, needed to be modified.

but that 20% of the gain was the partially integrated controller to control the process. The response of the system will be shown and compared with good results. The process was controlled by the self-adaptive PIP controller. They converged to the following values:

$$k_1 = 0.3376 \quad k_2 = 0.3914 \quad b_1 = -0.0465 \quad b_2 = 0.2058$$

considering a continuous-time transfer function having a gain and time-constant

$$\text{Gain} = 2.96 \quad T_1 = 1.19 \text{ minutes} \quad T_2 = 10.94 \text{ minutes}$$

that was obtained by using the inverse z-transform (Powers and Simpson 1976)

which had the model reflects the dynamics of a non-linear model.

Increasing the value of the time constant, the system response is shown in Figure

4.7 and 4.10. These responses are shown in a plot of their poles of 6

minutes and 11 minutes and 6 minutes and 11 minutes. The process was good

the controller was able to control the process. The process was good

the process was good. The process was good. The process was good.

the process was good. The process was good. The process was good.

the process was good. The process was good. The process was good.

the process was good. The process was good. The process was good.

the process was good. The process was good. The process was good.

the process was good. The process was good. The process was good.

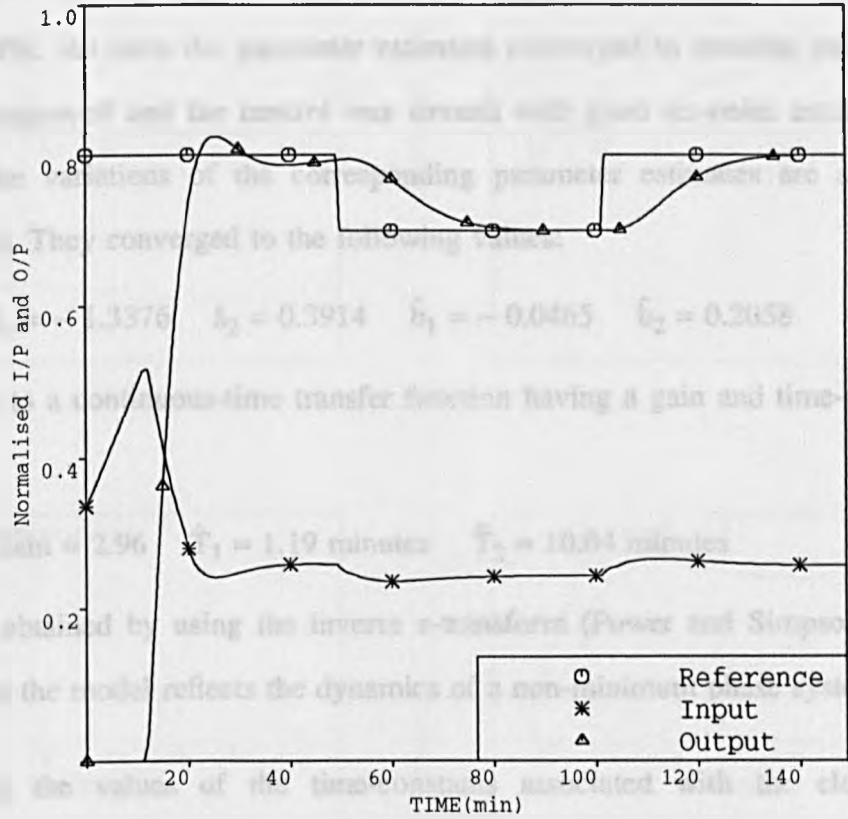


Figure 4.7. Closed-loop response of non-linear Pancuronium model under self-adaptive PIP control with two assigned closed-loop poles of 11 min. and 6 min.

$$s^2 + 1.78s - 0.77 = 0 \quad s_1 = -0.0465 \quad s_2 = 0.3376$$

$$\text{Gain} = 2.96 \quad T_1 = 1.19 \text{ minutes} \quad T_2 = 10.94 \text{ minutes}$$

set-point of 80% then 70%. Two relatively slow poles of 11 and 6 minutes were assigned leading to a polynomial of the following expression:

$$d(z^{-1}) = 1 - 1.76 z^{-1} + 0.77 z^{-2}$$

The first phase which is considered to be a tuning-phase, resulted in an overshoot less than 3%, but once the parameter estimates converged to sensible values. The response improved and the control was smooth with good set-point tracking properties. The variations of the corresponding parameter estimates are shown in figure (4.8). They converged to the following values:

$$\hat{a}_1 = -1.3376 \quad \hat{a}_2 = 0.3914 \quad \hat{b}_1 = -0.0465 \quad \hat{b}_2 = 0.2058$$

equivalent to a continuous-time transfer function having a gain and time-constants of:

$$\hat{G}\text{ain} = 2.96 \quad \hat{T}_1 = 1.19 \text{ minutes} \quad \hat{T}_2 = 10.04 \text{ minutes}$$

This was obtained by using the inverse z-transform (Power and Simpson, 1978). Notice that the model reflects the dynamics of a non-minimum phase system.

Decreasing the values of the time-constants associated with the closed-loop characteristic equation would speed-up the system response as shown in figures (4.9) and (4.10). These correspond respectively to a pair of faster poles of 5 minutes and 3 minutes, and 8 minutes and 5 minutes. The responses were good but for both cases the undershoot during the tuning-in phase increased respectively to 4% and 3%. The parameter estimates this time converged respectively to values of:

$$\hat{a}_1 = -1.4066 \quad \hat{a}_2 = 0.4562 \quad \hat{b}_1 = -0.0315 \quad \hat{b}_2 = 0.1167$$

$$\hat{G}\text{ain} = 1.72 \quad \hat{T}_1 = 1.47 \text{ minutes} \quad \hat{T}_2 = 9.42 \text{ minutes}$$

and

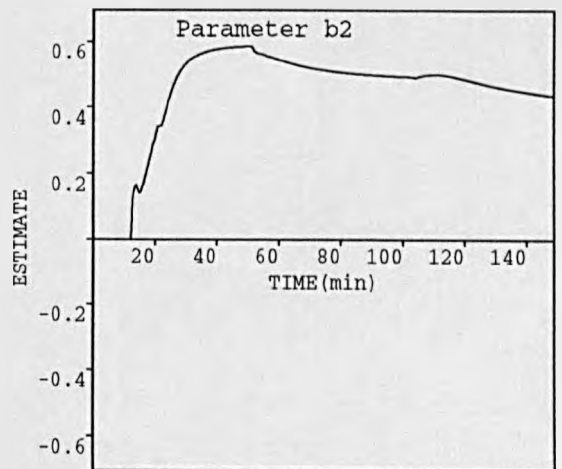
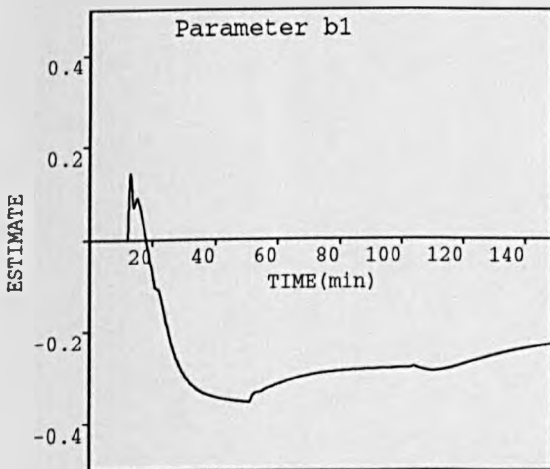
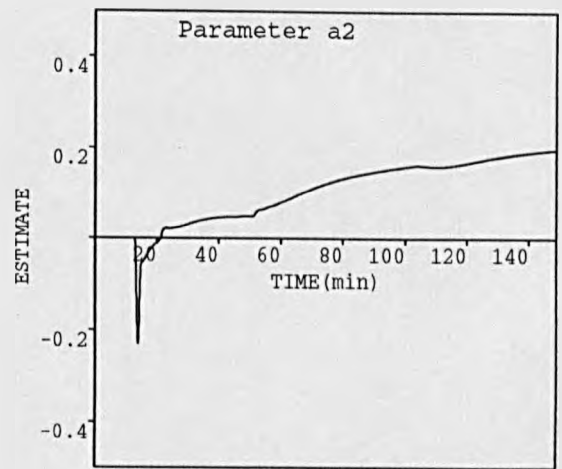
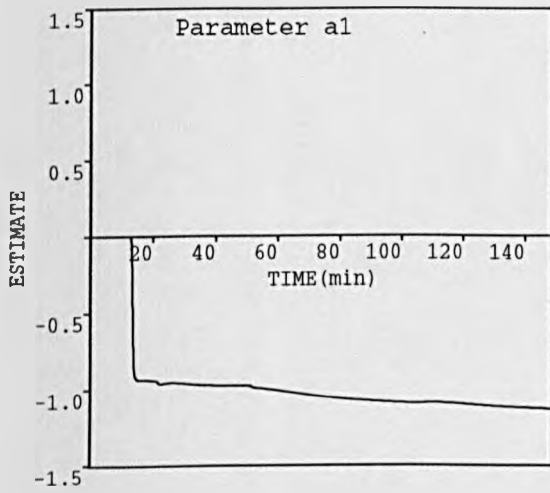


Figure 4.8. System parameter estimates corresponding to figure (4.7)

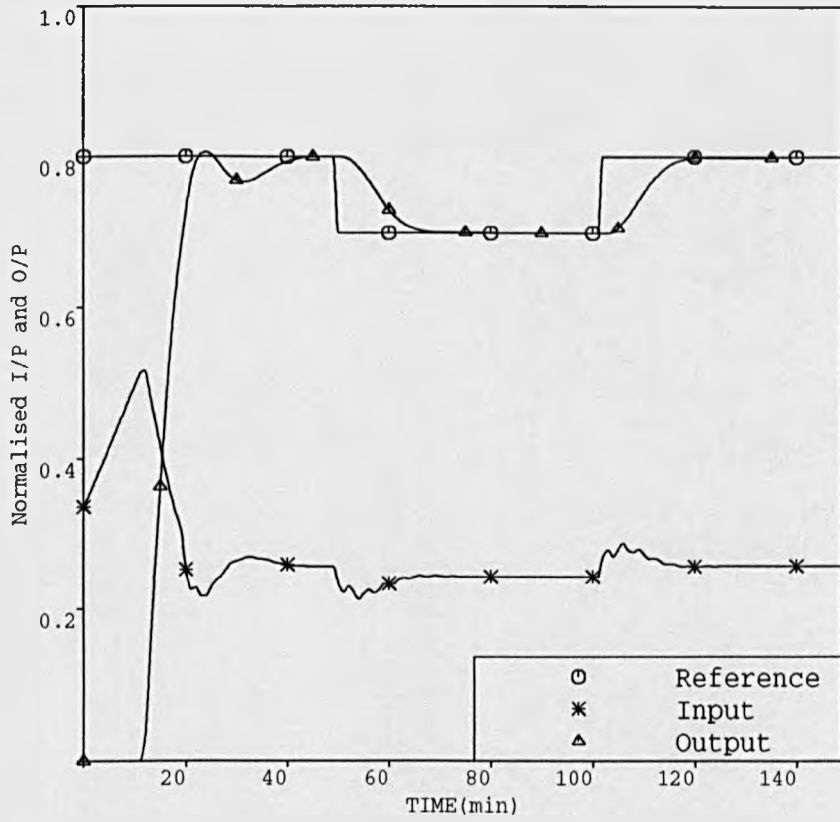


Figure 4.9. Same conditions as in figure (4.7) but with two assigned closed-loop poles of 5 min. and 3 min.

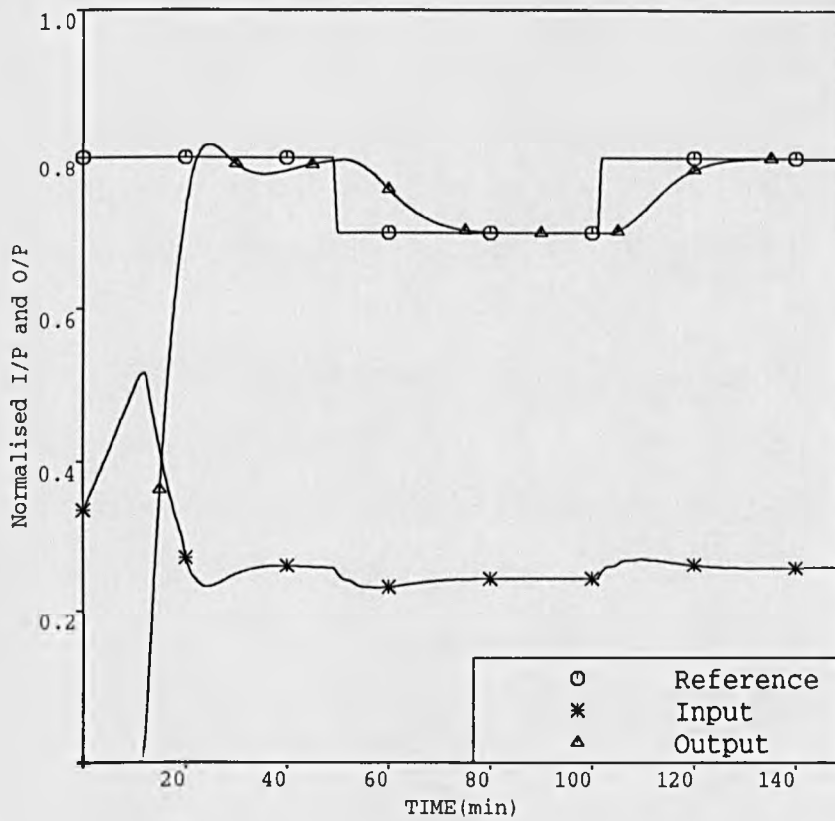


Figure 4.10. Same conditions as in figure (4.7) but with two assigned closed-loop poles of 8 min. and 5 min.

$$\hat{a}_1 = -1.3556 \quad \hat{a}_2 = 0.4082 \quad \hat{b}_1 = -0.0264 \quad \hat{b}_2 = 0.1840$$

$$\hat{G}_{\text{ain}} = 2.99 \quad \hat{T}_1 = 1.25 \text{ minutes} \quad \hat{T}_2 = 9.91 \text{ minutes}$$

Hitherto all the responses obtained demonstrated some overshoot or undershoot during the tuning-in phase. While both features are commonly considered acceptable, in the case of muscle relaxation they are undesirable: during the overshoot phase the output could reach saturation, and during the undershoot period the patient, not being totally relaxed, may create problems for the surgeon currently undergoing the operation. Both phenomena may be explained by two major factors:

1) The sudden transition between two different modes of control, i.e. The PI controller then the adaptive PIP.

2) The assignment of a second order closed-loop characteristic polynomial which normally induces overshoot.

An alternative strategy was then considered in which one unique pole is assigned rather than two, allowing the response to follow first order system characteristics.

This behaviour is shown in figure (4.11) where a slow pole of 11 minutes was chosen. The overshoot was removed altogether although the transition between the fixed control and the adaptive PIP was still energetic. At the end of the run the parameter estimates converged to:

$$\hat{a}_1 = -1.4047 \quad \hat{a}_2 = 0.4550 \quad \hat{b}_1 = 0.0722 \quad \hat{b}_2 = 0.0786$$

$$\hat{G}_{\text{ain}} = 2.99 \quad \hat{T}_1 = 1.47 \text{ minutes} \quad \hat{T}_2 = 9.30 \text{ minutes}$$

A faster assigned pole of 5 minutes produced a more rapid response as shown in figure (4.12), and the control was also fast to track the set-point changes occurring at regular intervals. Figure (4.13) displays the variations of the controller-parameters f_0 , f_1 , g_1 , g_2 , and k_I . Particular attention should be drawn to the last

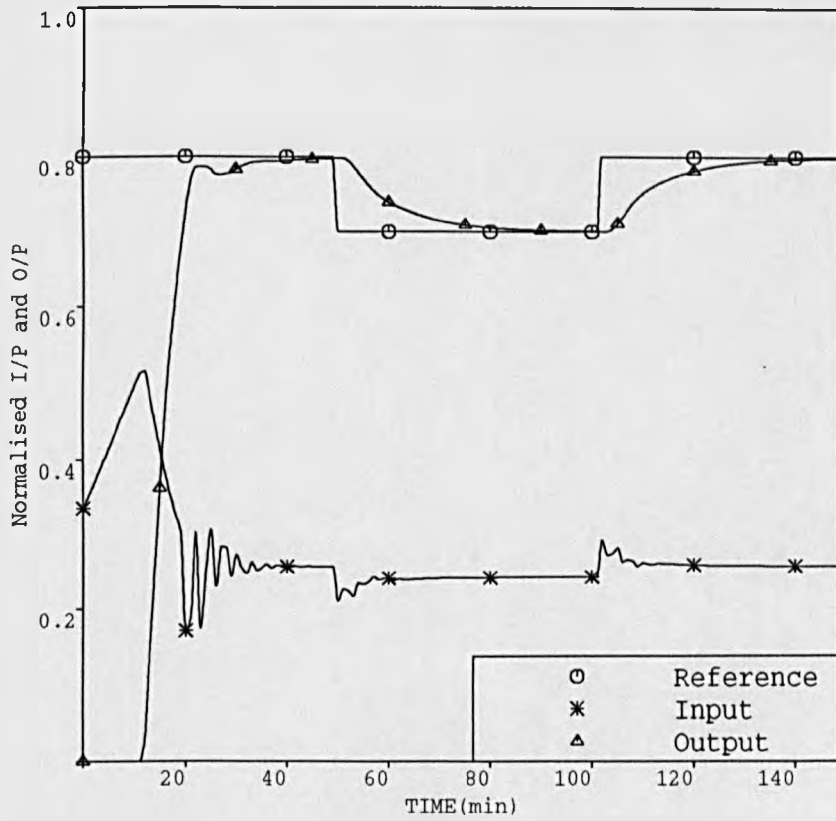


Figure 4.11. Same conditions as in figure (4.7) but with one assigned closed-loop pole of 11 min.

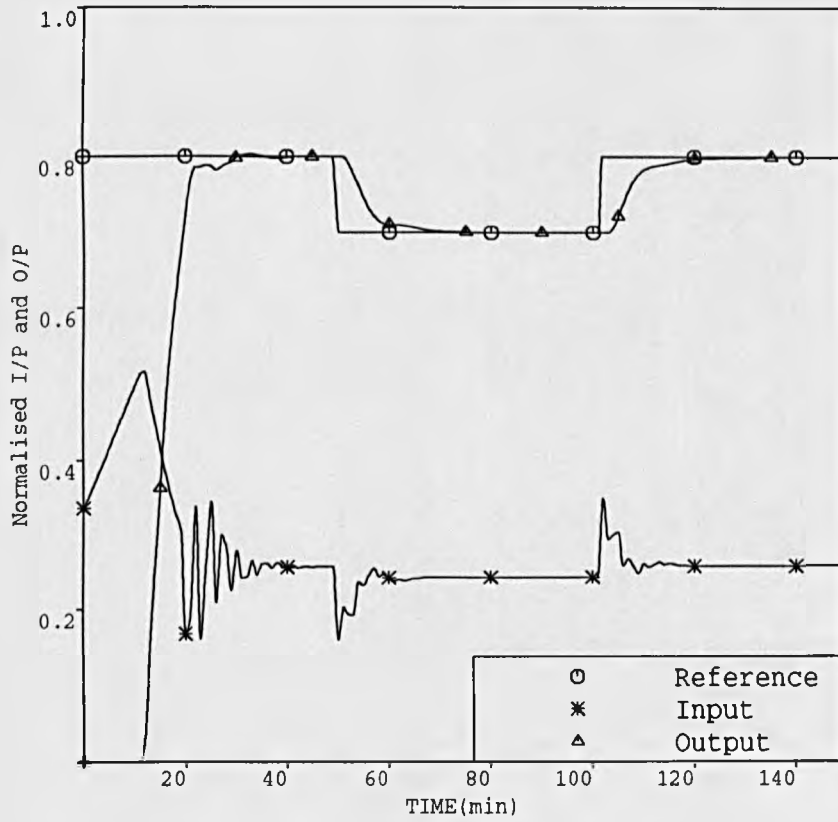


Figure 4.12. Same conditions as in figure (4.7) but with one assigned closed-loop pole of 5 min.

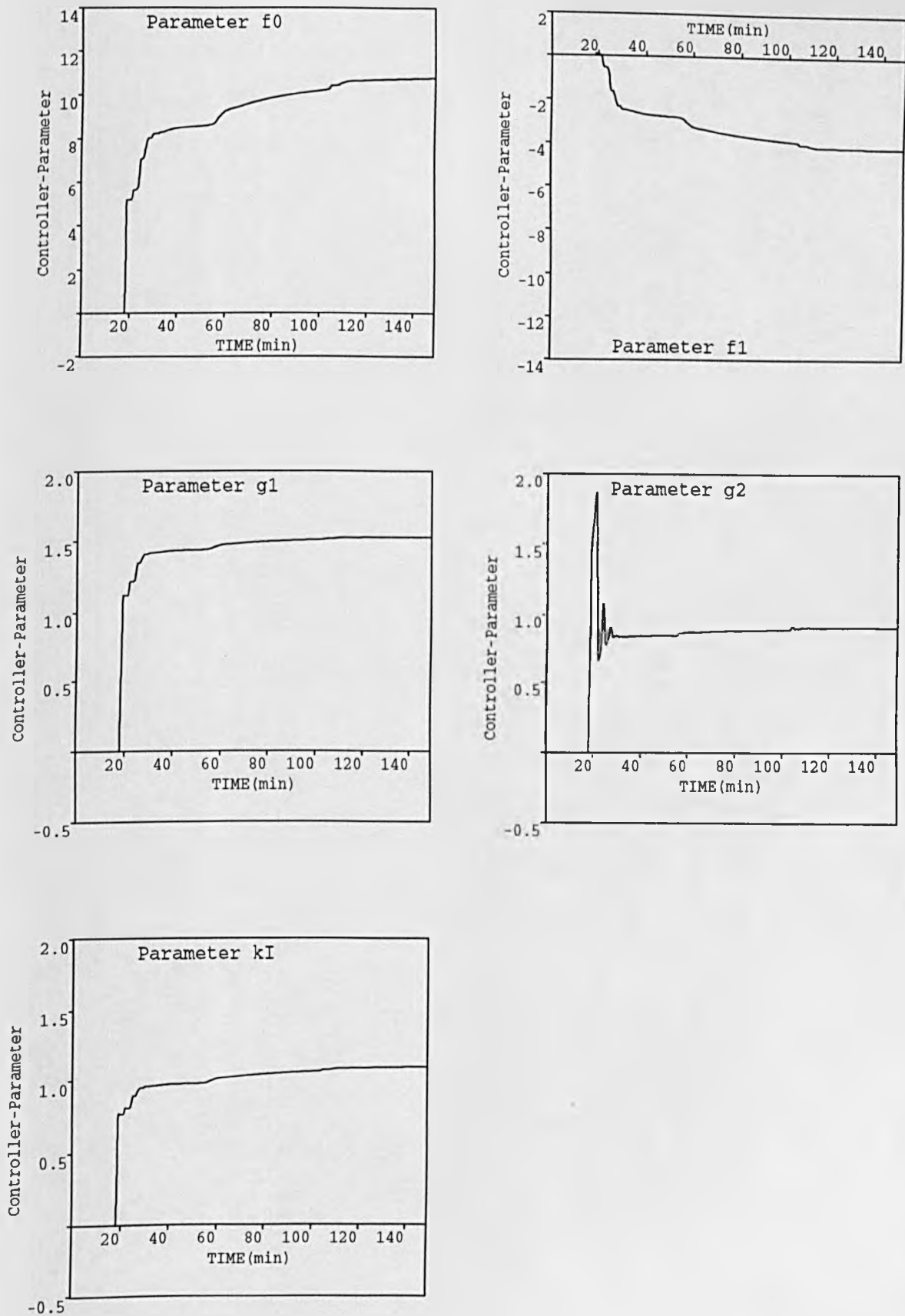


Figure 4.13. Variation of the controller parameters for conditions of figure (4.12)

parameter k_I which ensures an offset-free response. The plot shows how constant this parameter is along the three phases corresponding to the changing command signal, indicating therefore good control. The associated parameter estimates converged to values of:

$$\hat{a}_1 = -1.4513 \quad \hat{a}_2 = 0.4979 \quad \hat{b}_1 = 0.0705 \quad \hat{b}_2 = 0.0689$$

equivalent to a gain and time-constants of:

$$\hat{G}_{\text{ain}} = 2.99 \quad \hat{T}_1 = 1.70 \text{ minutes} \quad \hat{T}_2 = 9.01 \text{ minutes}$$

The objectives of a self-tuning regulator are to minimize with respect to system noise and disturbances, the variance of the systems error from the set-point. Some of the desired features may include:

- a) Fast step-responses
- b) Small overshoots
- c) Good disturbance rejection
- d) Absence of energetic control excursions
- e) A small tuning-in transient

As pointed out earlier, because it is believed that all these desirable features are interdependent, in some cases it could be practically impossible to realize all of them simultaneously, and instead one would settle for the best trade-off obtainable in these circumstances.

Experiments conducted during the last decade have clearly indicated that adequate initial conditions especially for the parameter estimates may speed up the convergence of the self-tuning controller (Zanker and Wellstead, 1979). In light of these considerations, another run was conducted in which initial parameter estimates of the following values were considered:

$$\Theta_i = \begin{bmatrix} -1.55 & 0.57 & 0.04 & 0.03 \end{bmatrix}$$

A smaller covariance matrix of $10^2 \cdot I$ was considered together with a forgetting factor value of 0.995, expressing therefore bigger confidence in these parameters. The same closed-loop pole as in figure (4.12) was assigned. Figure (4.14) shows an improved response of the muscle relaxation process which is well damped and fast. The control signal was also quick to reject the disturbance in terms of set-point changes. Eventually the parameter estimates converged to the following values:

$$\Theta_f = \begin{bmatrix} -1.4970 & 0.5406 & 0.0694 & 0.0609 \end{bmatrix}$$

equivalent to the following continuous parameters:

$$\hat{G}_{\text{ain}} = 2.99 \quad \hat{T}_1 = 2.01 \text{ minutes} \quad \hat{T}_2 = 8.47 \text{ minutes}$$

Another run was conducted under the same conditions but with a constant set-point, leading to the performance shown in figure (4.15). The parameter estimates converged to values of:

$$\Theta_f = \begin{bmatrix} -1.4360 & 0.4836 & 0.0807 & 0.0674 \end{bmatrix}$$

equivalent to:

$$\hat{G}_{\text{ain}} = 3.11 \quad \hat{T}_1 = 1.61 \text{ minutes} \quad \hat{T}_2 = 9.16 \text{ minutes}$$

The pharmacodynamics describing the relationship that exists between drug concentration and the resulting response could also be modelled in a context of a Hill equation (Whiting and Kelman, 1980; Weatherley et al., 1983) of the following form:

$$f_{\text{Hill}} = \frac{C^\alpha}{C^\alpha + C(50)^\alpha} \quad (4.19)$$

where,

α = Constant

$C(50)$ = drug concentration at 50% effect

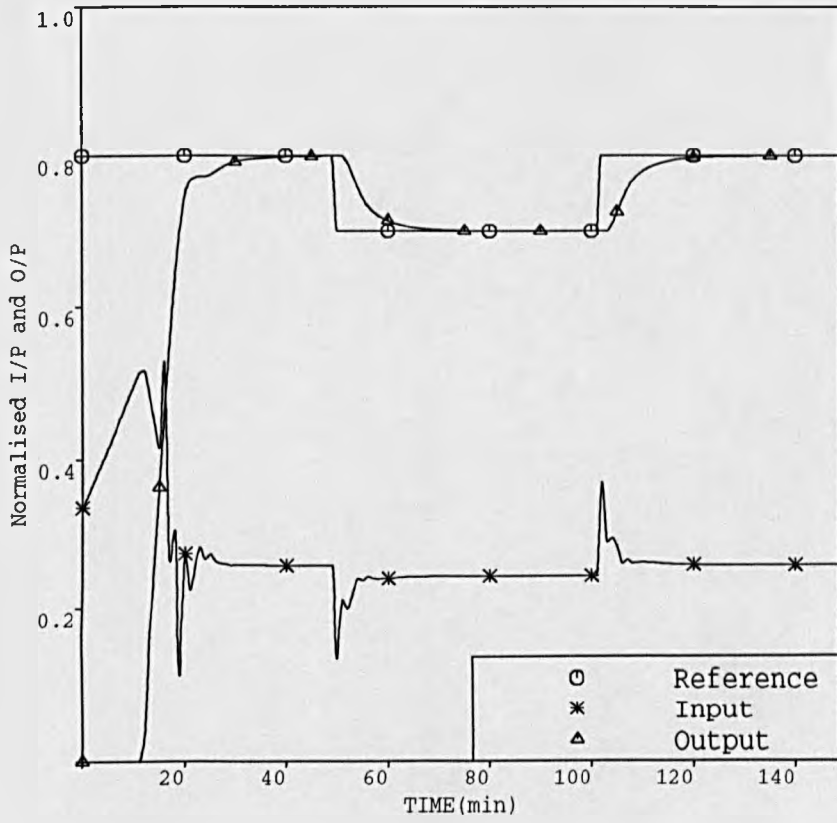


Figure 4.14. Same conditions as in figure (4.12)
but with non-zero initial parameter estimates

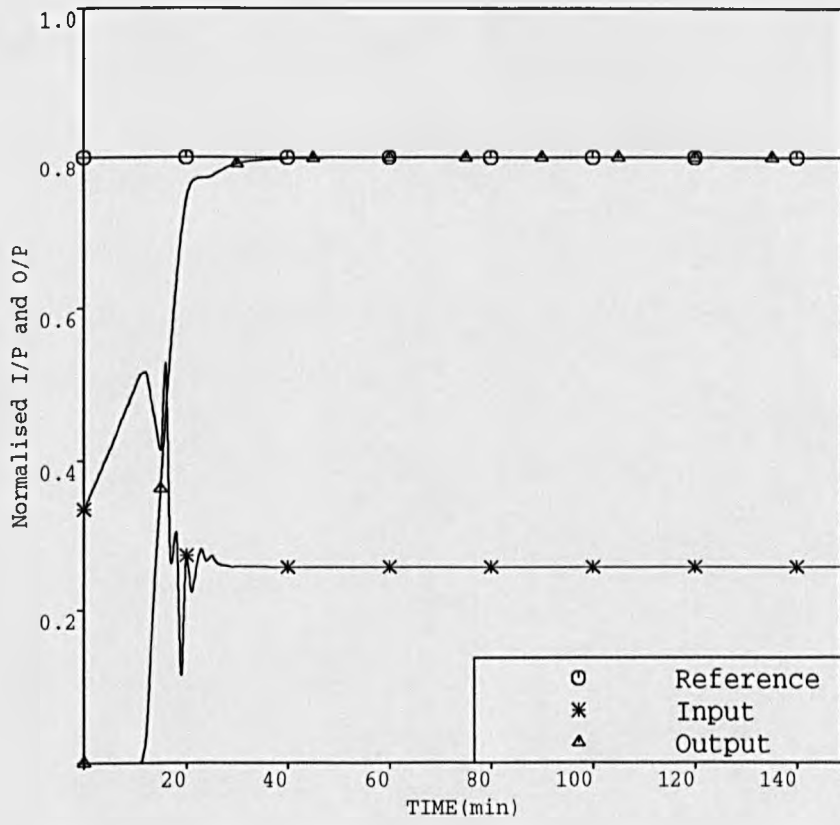


Figure 4.15. Same conditions as in figure (4.14)
but with constant command signal

Figure (4.16) illustrates the analogy between the Hill equation curve together with the dead-zone in series with a saturation element representation.

Comparing this with the non-linearity represented by the dead-zone and saturation, an approximate analogy between the two situations may well be drawn. Indeed, a dead-zone of DZ and a saturation element of SAT may be defined as:

$$E = \begin{cases} 0 & \text{if } C \leq \text{DZ} \\ \text{SL} * (C - \text{DZ}) & \text{if } \text{DZ} \leq C \leq \text{SAT} \end{cases} \quad (4.20)$$

SL being the associated slope value.

Taking the derivative of equation (4.19) with respect to C, gives the expression of the slope at some point in the characteristic, i.e:

$$\frac{\partial f_{\text{Hill}}}{\partial C} = \frac{\alpha C^{\alpha-1} (C^{\alpha} + C(50)^{\alpha}) - \alpha C^{\alpha-1} C^{\alpha}}{(C^{\alpha} + C(50)^{\alpha})^2}$$

Developing and rearranging leads to:

$$\frac{\partial f_{\text{Hill}}}{\partial C} = \frac{\alpha C^{\alpha-1} C(50)^{\alpha}}{(C^{\alpha} + C(50)^{\alpha})^2}$$

Substituting C by C(50) leads to::

$$\frac{\partial f_{\text{Hill}}}{\partial C} = \frac{\alpha}{4 C(50)} \quad (4.21)$$

Using equation (4.20) at C(50) yields:

$$C(50) = \frac{E(C(50)) + \text{SL} \cdot \text{DZ}}{\text{SL}}$$

Assuming that the slopes are identical at the concentration C(50) and using equation (4.21) leads to:

$$\alpha = 4 \text{SL} C(50)$$

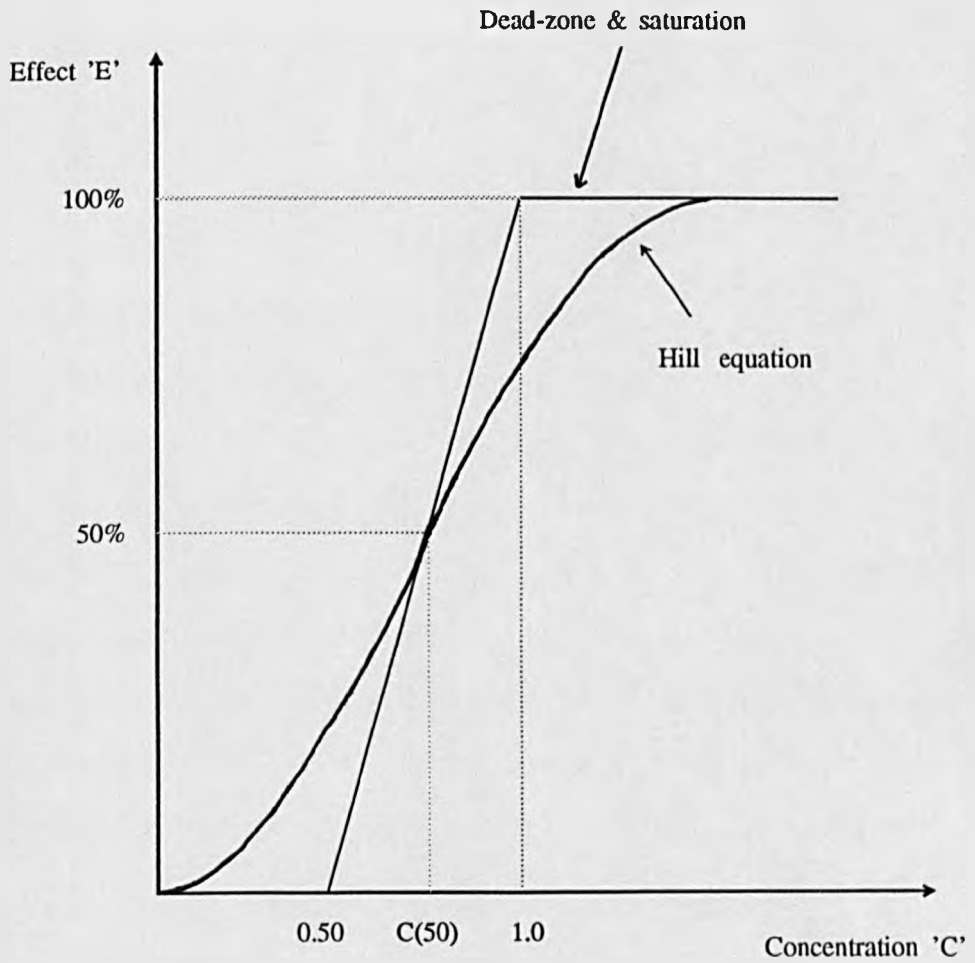


Figure 4.16. A comparative study between the non-linearity represented by the Hill equation and that of the dead-zone and saturation

Therefore, for a dead-zone of 50% and a saturation element of 100% it follows that:

$$\begin{cases} \text{SL} = 2.0 \\ \text{C}(50) = 0.75 \\ \alpha = 6 \end{cases}$$

The non-linear muscle relaxant model of section 3.2 is again simulated under the same conditions of section 4.6.1 except that the pharmacodynamics are represented by a Hill equation with power $\alpha = 6.0$ and $\text{C}(50) = 0.75$, values previously derived. The initial conditions are identical to those of figure (4.12), unless otherwise specified. The relatively fast response of figure (4.17) was to be expected due to the high value of α . The transition between the control modes, i.e the PI controller and the self-tuning controller PIP, was energetic although after the estimates converged to some steady values the response tracked better the set-point, as a result of which the parameter estimates assumed the following final values:

$$\hat{a}_1 = -1.6057 \quad \hat{a}_2 = 0.6348 \quad \hat{b}_1 = 0.0470 \quad \hat{b}_2 = 0.0374$$

equivalent to a gain and time-constants of:

$$\hat{\text{Gain}} = 2.90 \quad \hat{T}_1 = 2.85 \text{ minutes} \quad \hat{T}_2 = 9.66 \text{ minutes}$$

It is interesting to note that because of the type of non-linearity, the parameter estimates in this case did not assume a non-minimum phase system. Clearly the representation of the pharmacodynamics in the context of a Hill equation represents a more realistic image of the system's dynamics.

So far not much emphasis has been put on the values of the parameter estimates and their equivalent continuous gain and time-constants, and this is completely

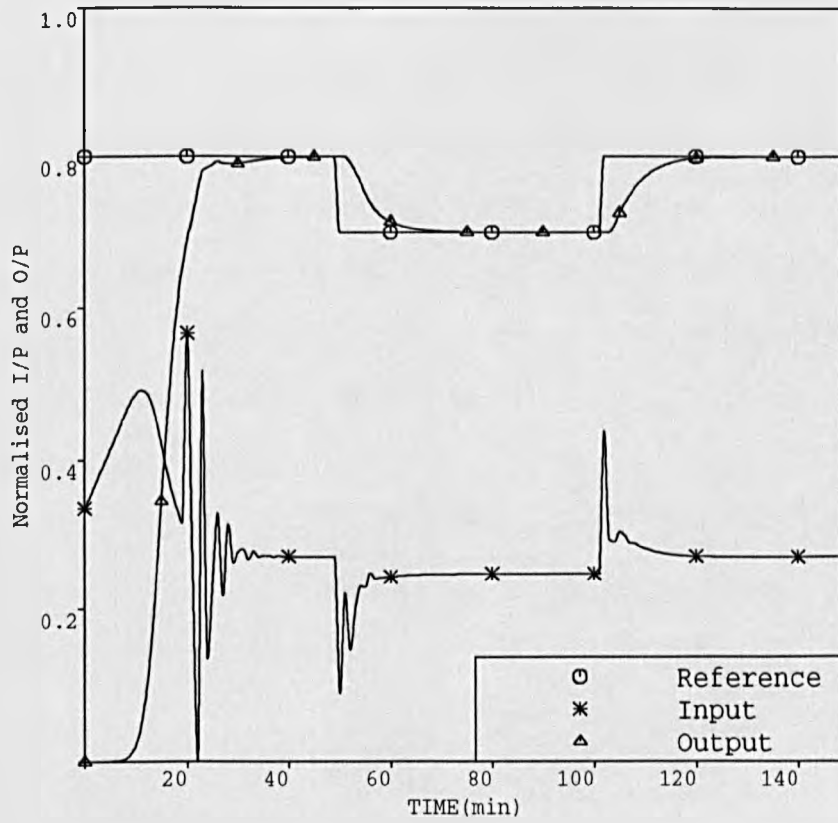


Figure 4.17. Same conditions as in figure (4.12) but with non-linearity represented by Hill equation ($\alpha=6.0$; $C_{50}=0.75$)

understandable since the corner-stone property of self-tuning controllers embodied in the principle of "certainty equivalence" (Astrom and Wittenmark, 1989) states that if those parameters are to be replaced by their estimates, self-tuning properties are normally conserved providing of course that the process is excited enough to give the best possible knowledge to the controller. It is known that non-linearities such as saturation and dead-zones are among the major problems that face the estimator. Consequently, the gain and time-constants of the system cannot be accurately estimated. On the other hand, it has been shown (Young, 1987) that prefiltering of the input and output data can produce optimal parameter estimates and can be especially useful when the signals are perturbed. Several digital filters have been widely reported in literature (Isermann, 1981; Young, 1984). One common practice before using the estimation algorithm is to remove any possible d.c. level which can result in a bias on the parameter estimates. One alternative to mean-removal is differencing, equivalent to the use of the operator $\Delta = 1-z^{-1}$. This is proved by the equations below:

If:

$$\bar{y}_1 = y_1 + d$$

$$\bar{y}_2 = y_2 + d$$

d represents the d.c.level

Then,

$$\bar{y}_1 - \bar{y}_2 = y_1 - y_2$$

One obvious consequence of this operation which is equivalent to the use of a high-pass digital filter, is the amplification of the high frequency components present in the data. To counteract this, another filter, this time with low-pass characteristics, is cascaded to the previous one making the overall operation equivalent to a band-pass digital filter amplifying the desirable frequencies and

attenuating the undesirable ones. The discrete-time transfer function of the filter is of the form:

$$G_F(z^{-1}) = \frac{\Delta}{T(z^{-1})} \quad (4.22)$$

where,

$$\Delta = 1 - z^{-1} \quad \text{and} \quad T(z^{-1}) = 1 + t_1 z^{-1} + t_2 z^{-2} + \dots + t_t z^{-t}$$

t_1, t_2, \dots, t_t represent the characteristics of the filter. For a chosen first order polynomial $T_1 = -e^{-T_s \cdot f_s}$, where T_s is the sampling time and f_s is the filter cut-off frequency.

The frequency f_s should be chosen such that its value encompasses the bandwidth of the system under investigation. It is important to note that this filter plays an important role in providing good estimates for the controller, and it (the filter) is a result of a new model-representation, different from the one described by equation (4.8) and named CARIMA model (Tuffs and Clarke, 1985) obtained as it will be seen in the next chapter by modelling differently the noise term which in the case of the PIP algorithm has been ignored for purposes of convenience .

For the system so far considered, a $T(z^{-1})$ polynomial of $T(z^{-1}) = 1 - 0.95 z^{-1}$ was chosen corresponding to a time-constant of 20 minutes (predominant time-constant of the previous model), leading to an overall digital band-pass filter of the form:

$$G_F(z^{-1}) = \frac{1 - z^{-1}}{1 - 0.95 z^{-1}}$$

$$z = e^{hs}$$

$$h = \text{sampling time} \quad (4.23)$$

Figure (4.18) illustrates the resulting control system.

Using filtered data for the measurement vector, a run was undertaken with a fixed

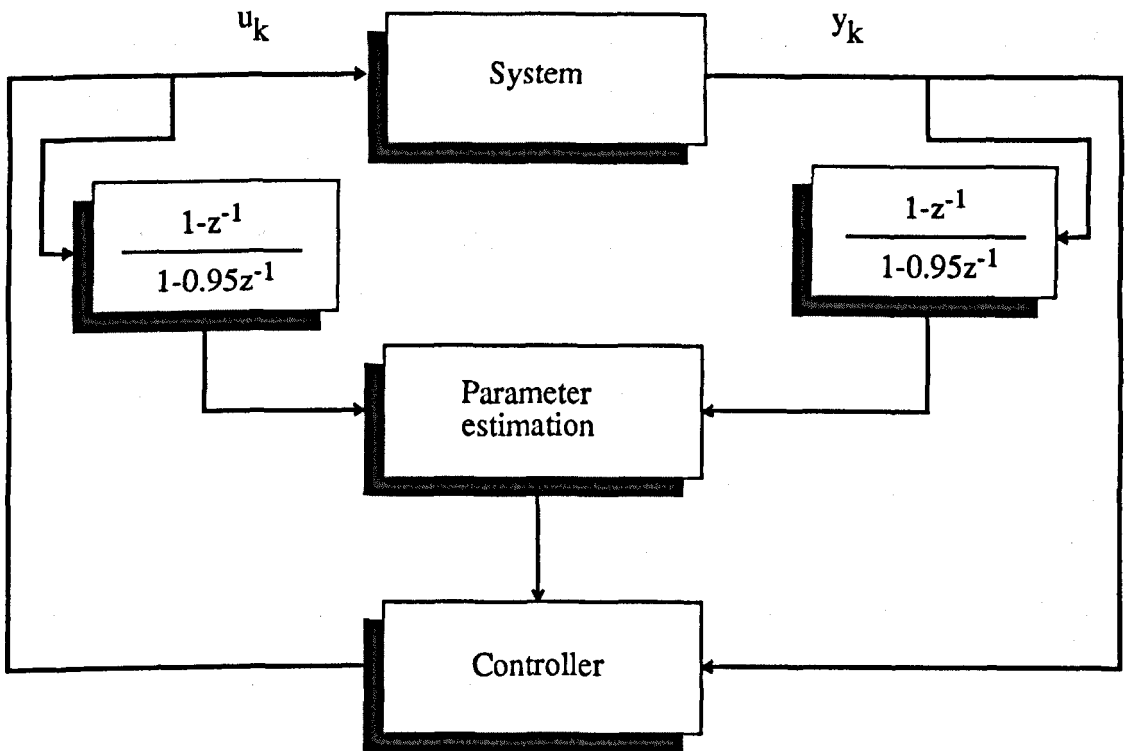


Figure 4.18. The overall control system including the band-pass filter

command signal of 80%, a covariance matrix of $P = 10^5 \cdot I$, and a forgetting-factor of $\rho = 0.995$. The initial parameter estimates were all set to 0.0. The estimation was started when the output reached 15% and the fixed PI was allowed to run for 20 samples before the adaptive PIP took over. The result shown in figure (4.19) demonstrates a good response well damped with no overshoot or undershoot. However, in contrast to the previous runs, the parameter estimates whose variations are shown in figure (4.20) look particularly interesting not so much for their stability during the run, but for their final values which were:

$$\hat{a}_1 = -1.5529 \quad \hat{a}_2 = 0.5719 \quad \hat{b}_1 = 0.0739 \quad \hat{b}_2 = 0.0632$$

Equivalent to:

$$\hat{G}ain = 7.21 \quad \hat{T}_1 = 1.96 \text{ minutes} \quad \hat{T}_2 = 20.52 \text{ minutes}$$

Clearly, as it has always been argued, filtering is often necessary, even if the signals are clean (Shook et al., 1991; Boucher et al., 1988), and this is equivalent to carefully choosing the right filter parameters in order to ensure that relevant information about the system is not lost.

4.6.2 Self-Tuning Adaptive PIP Control of Muscle Relaxation System Associated with Atracurium

When associated with the second order Pancuronium-Bromide drug model, the PIP algorithm (either a fixed or self-adaptive form) proved effective and flexible. The following will assess its performance further, this time associated with the more complicated model of Atracurium, the fast acting drug introduced in section 3.3. Its corresponding model is of a third order linear component followed by the non-linearity of a Hill equation type described earlier.

The pharmacokinetics are represented by the following third order transfer func-

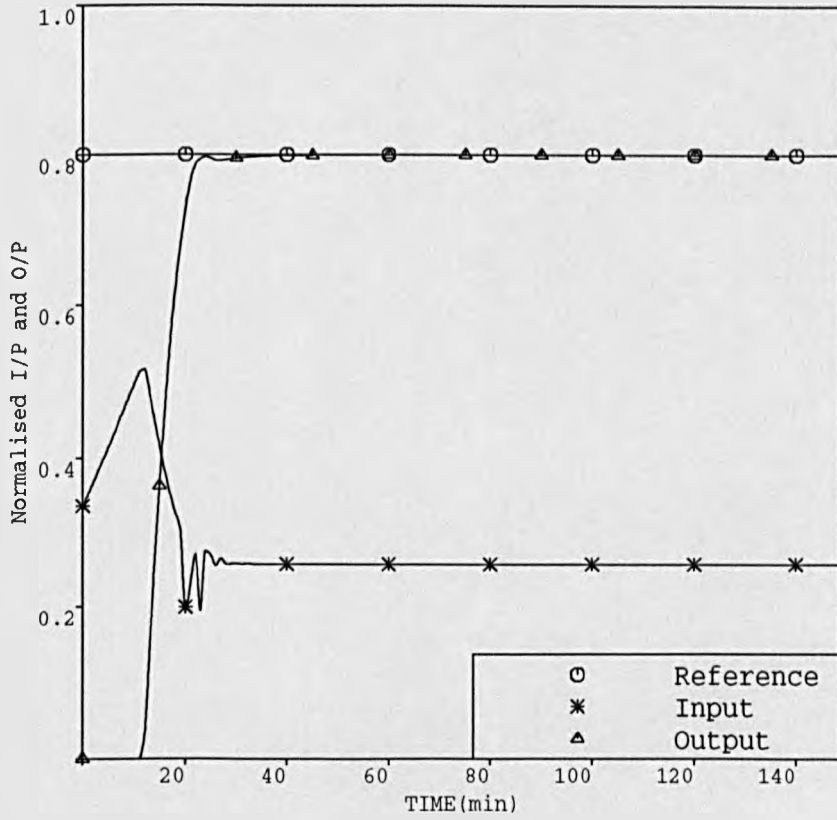


Figure 4.19. Same conditions as in figure (4.12)

but with filtered data for the estima-

tor ; $T(z^{-1}) = (1 - z^{-1}) ((1 - 0.95z^{-1}))^{-1}$

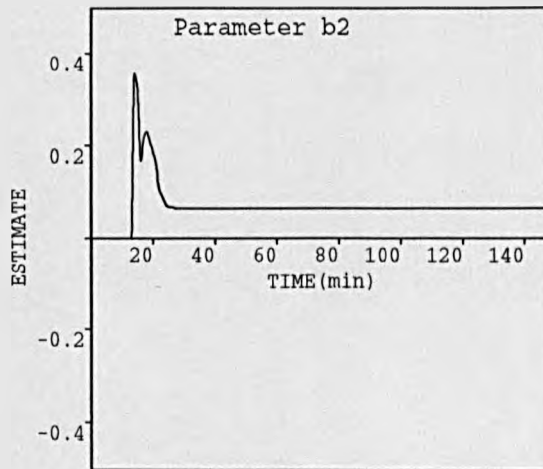
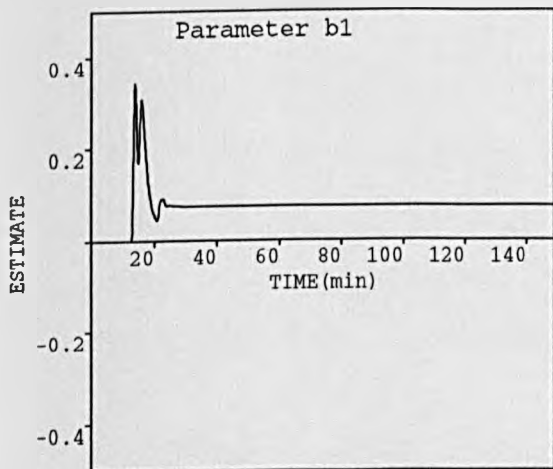
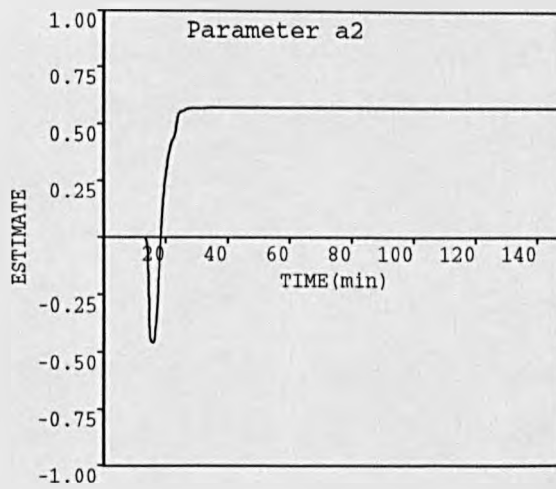
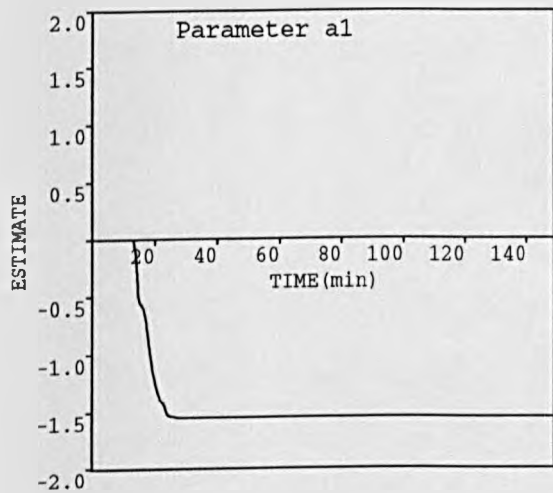


Figure 4.20. System parameter estimates corresponding to figure (4.19)

tion with time-delay:

$$G_2(s) = \frac{(1 + 10.64 s) e^{-s}}{(1 + 3.08 s) (1 + 4.81 s) (1 + 34.36 s)} \quad (4.24)$$

The pharmacodynamics are modelled by the Hill equation (4.19) with the power α and the concentration at 50% ($C(50)$) having the following parameters:

$$\begin{aligned} \alpha &= 2.98 \\ C(50) &= 0.404 \end{aligned}$$

Due to the low value of the open-loop gain, the parameters of the fixed PI controller were modified in order to achieve an acceptable response during the period where the estimator is gathering reasonable data, giving the following parameters:

$$K_p = 0.80$$

$$K_I = 0.04$$

The overall continuous system was simulated following the same steps as in the previous study as regards to the integration method as well as the step-length. A sampling interval of 1 minute was also used throughout all of this study. Conditions of jacketing and initial conditions for the estimation routine were similar to those adopted in the previous section.

Simulation Results

A third order linear discrete-time model with an assumed dead-time of 1 sample was considered throughout giving the following transfer function:

$$G_2(z^{-1}) = \frac{b_1 z^{-1} + b_2 z^{-2} + b_3 z^{-3}}{1 + a_1 z^{-1} + a_2 z^{-2} + a_3 z^{-3}} z^{-1}$$

With the values $n = 3$ and $m = 4$, the PIP algorithm this time solves the following system of equations:

$$\Sigma \cdot V = \beta$$

where,

$$\Sigma = \begin{bmatrix} 0 & 0 & 0 & 1 & 0 & 0 & 0 \\ b_1 & 0 & 0 & a_1 - 1 & 1 & 0 & b_1 \\ b_2 - b_1 & b_1 & 0 & a_2 - a_1 & a_1 - 1 & 1 & b_2 \\ b_3 - b_2 & b_2 - b_1 & b_1 & a_3 - a_2 & a_2 - a_1 & a_1 - 1 & b_3 \\ -b_3 & b_3 - b_2 & b_2 - b_1 & -a_3 & a_3 - a_2 & a_2 - a_1 & 0 \\ 0 & -b_3 & b_3 - b_2 & 0 & -a_3 & a_3 - a_2 & 0 \\ 0 & 0 & -b_3 & 0 & 0 & -a_3 & 0 \end{bmatrix}$$

V is such that:

$$V^T = [f_0, f_1, f_2, g_1, g_2, g_3, k_I]$$

Because of the size of the system to be solved, a more stable algorithm based on singular value decomposition algorithm for a matrix was used.

The first experiment whose response is shown in figure (4.21) considered a command signal of 80% then 70%. One unique pole of 30 minutes, close to the rise time of the system, was assigned for the closed-loop leading to a polynomial of the form:

$$d(z^{-1}) = 1 - 0.96 z^{-1}$$

As expected, the response was rather slow and smooth, and the control was sluggish. Figure (4.22) shows the variations of the parameter estimates which converged to:

$$\hat{a}_1 = -1.0544 \quad \hat{a}_2 = -0.2656 \quad \hat{a}_3 = 0.3437$$

$$\hat{b}_1 = 0.0978 \quad \hat{b}_2 = 0.0199 \quad \hat{b}_3 = 0.0659$$

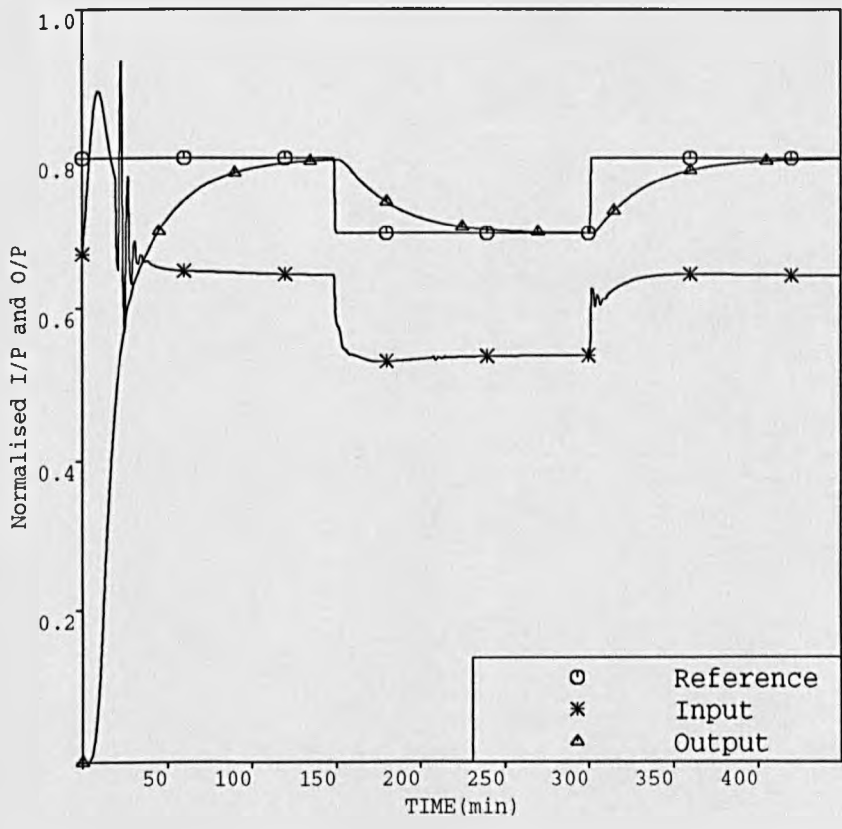


Figure 4.21. Closed-loop response of Atracurium model under self-adaptive PIP control with one assigned closed-loop pole of 30 min.

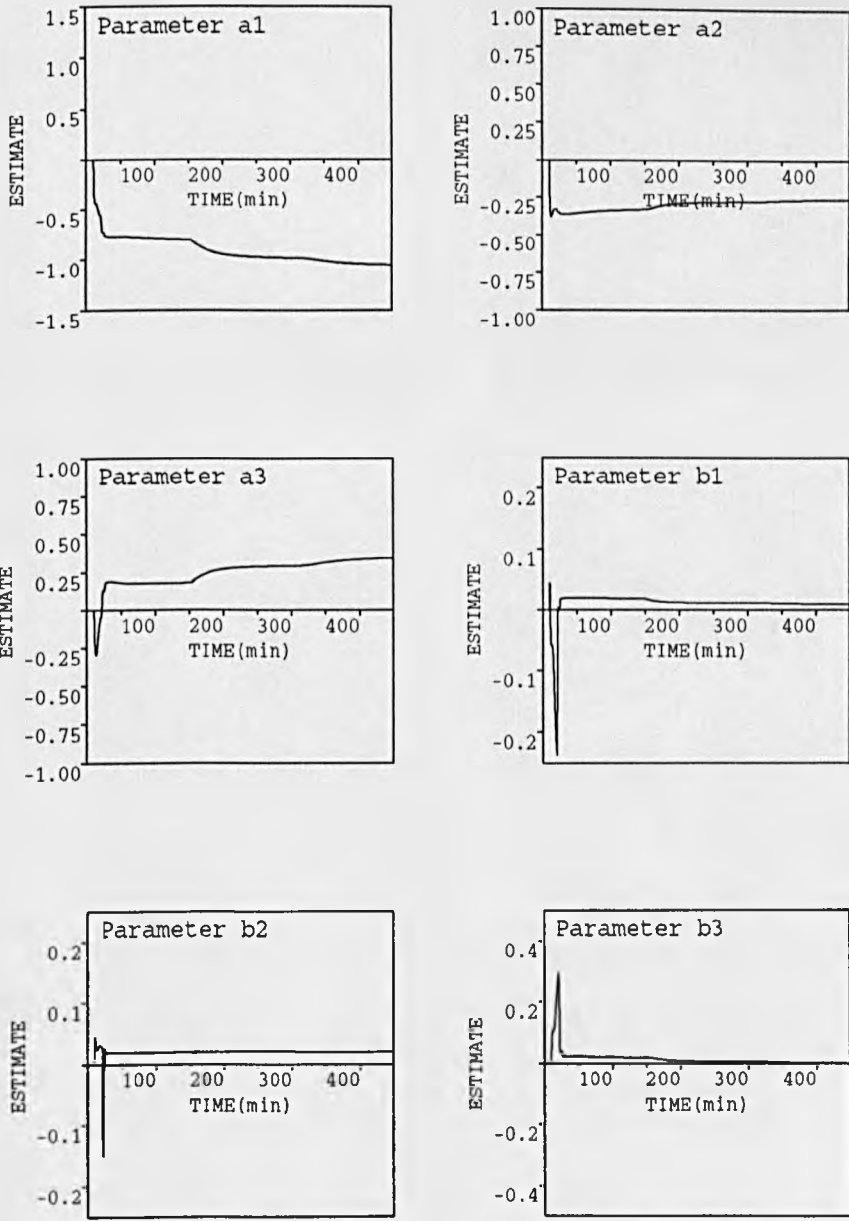


Figure 4.22. System parameter estimates corresponding to figure (4.21)

equivalent to the following positions in the z plane:

$$\begin{aligned} \text{zeros: } & (-0.1017 \pm 0.8145 i) \\ \text{poles: } & 0.9563 ; 0.6505 ; -0.5525 \end{aligned}$$

In the hope of increasing the control activity, another run was performed in which a faster pole of 15 minutes was assigned this time leading to the response of figure (4.23) which shows how the speed of the transient was improved without deteriorating the control signal. The parameter estimates converged to the following set of values.

$$\hat{a}_1 = -1.1053 \quad \hat{a}_2 = -0.2449 \quad \hat{a}_3 = 0.3699$$

$$\hat{b}_1 = 0.0089 \quad \hat{b}_2 = 0.0168 \quad \hat{b}_3 = 0.0011$$

equivalent to the following positions in the z plane:

$$\begin{aligned} \text{zeros: } & -1.8187 ; 0.0679 \\ \text{poles: } & 0.9577 ; 0.6996 ; -0.5521 \end{aligned}$$

Given the conditions for stability of the algorithm presented in section 4.4, it is stated that there should be no pole-zero cancellations in the transfer function $\frac{B(z^{-1})}{A(z^{-1})}$ and no conditions were imposed as to whether the transfer function estimated was stable, unstable, or exhibited non-minimum phase characteristics. clearly this explains why the self-tuning properties were maintained despite the poor position of one of the zeros.

In practice, if the excitation is poor, adding to the fact that the polynomials are of high orders, the estimated parameters could well suggest the unfortunate situation of a near pole/zero cancellation making the system uncontrollable. This situation could in fact be avoided by using powerful algorithms for matrix inversion or simply reducing the order of the model considered (Young et al., 1987). Hence, an underparameterized second order model with a unit time-delay was assumed and

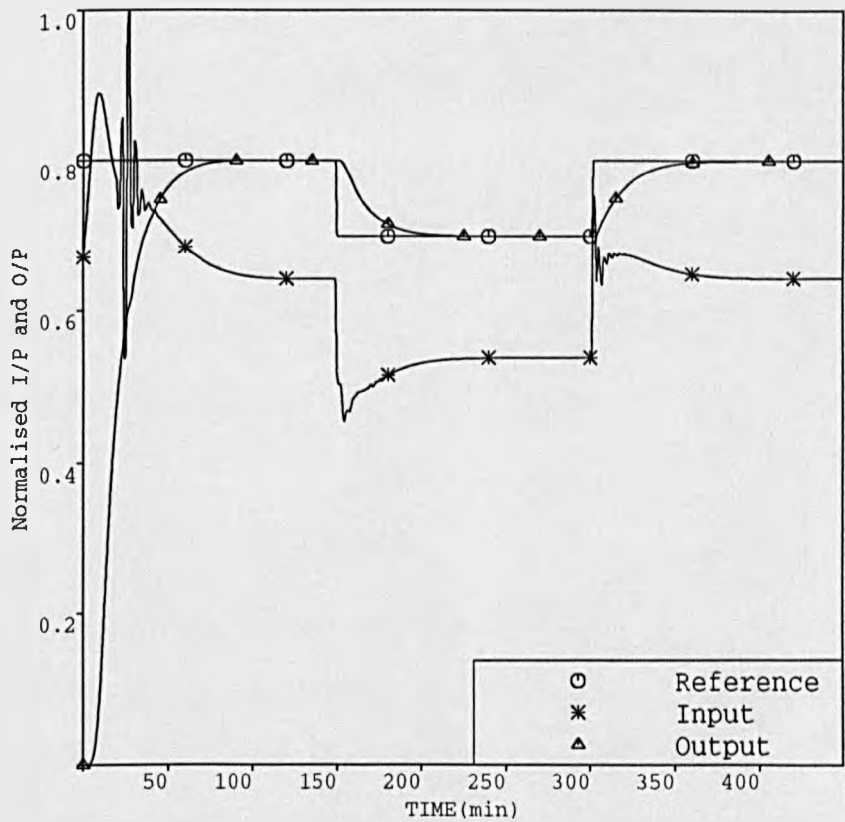


Figure 4.23. Same conditions as in figure (4.21) but with one assigned closed-loop pole of 15 min.

the same conditions as above were considered both for the estimation and the self-tuner. A 15 minute pole was assigned for the closed-loop characteristic equation. Figure (4.24) shows the response obtained which, compared with the previous one, seems to be smoother on the take-over phase from the fixed PI controller. The final parameter estimates have converged to the following values:

$$\hat{a}_1 = -1.2687 \quad \hat{a}_2 = 0.2959 \quad \hat{b}_1 = -0.014 \quad \hat{b}_2 = 0.02$$

equivalent to a continuous-time transfer function having a gain and time-constants of:

$$\hat{\text{Gain}} = 0.22 \quad \hat{T}_1 = 0.85 \text{ minute} \quad \hat{T}_2 = 24.94 \text{ minutes}$$

Finally, a last run was conducted in which the parameter estimates were initialised to:

$$\theta_i = [-1.51 \quad 0.54 \quad 0.02 \quad 0.01]$$

The covariance matrix was set to $P = 10^2 \cdot I$ and the forgetting factor to $\rho = 0.995$. Figure (4.25) representing the response obtained shows a well damped transient. The control signal however was highly activated when the adaptive PIP took over from the PI reflecting a high frequency component probably due to the initialization of the estimates, which this time converged to the following values:

$$\hat{a}_1 = -1.5571 \quad \hat{a}_2 = 0.5734 \quad \hat{b}_1 = 0.0108 \quad \hat{b}_2 = 0.0097$$

equivalent to a continuous-time transfer function having a gain and time-constants of:

$$\hat{\text{Gain}} = 1.2577 \quad \hat{T}_1 = 1.94 \text{ minutes} \quad \hat{T}_2 = 24.18 \text{ minutes}$$

The time-constants values indicate the presence of a predominant one, while the gain is close to the system's open loop gain of 1.0.

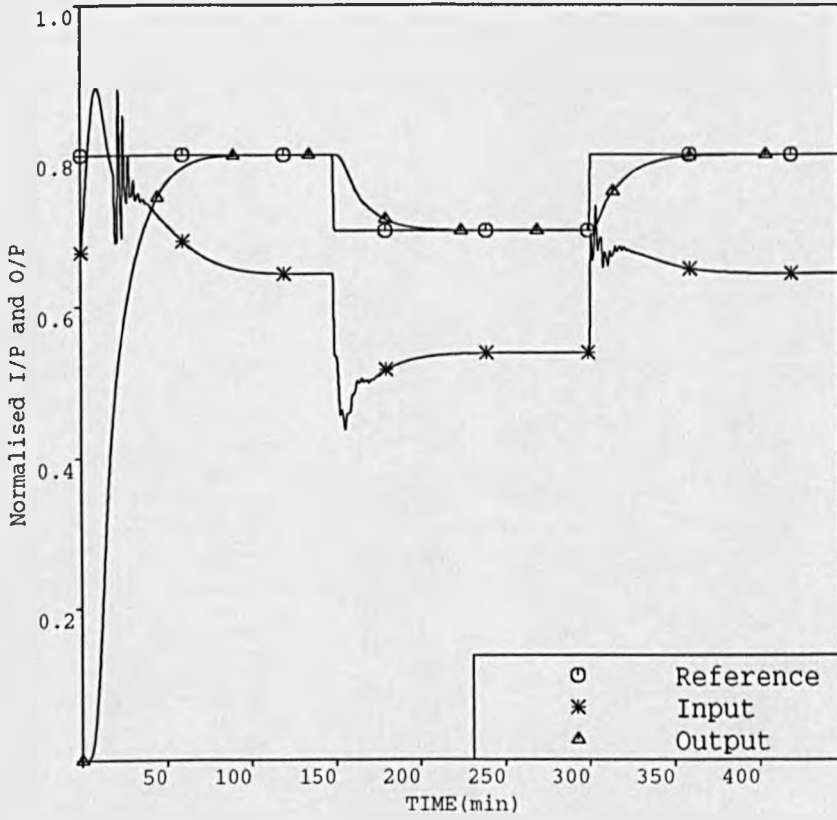


Figure 4.24. Same conditions as in figure (4.23)
but assuming a second order discrete-time model

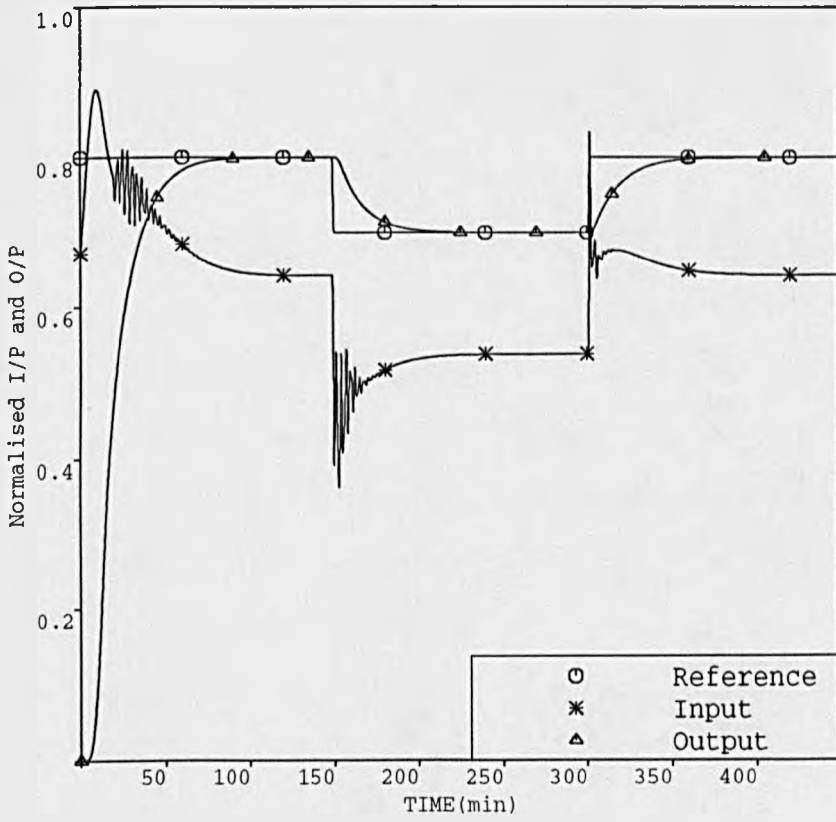


Figure 4.25. Same conditions as in figure (4.24) but with non-zero initial parameter estimates

4.7 SENSITIVITY OF THE PIP DESIGN TO THE PRESENCE OF TIME-DELAY

In the previous section emphasis has been placed on the requirement that one should have an idea about the frequency-range under which the process should operate in order to successfully filter the data for the estimator (i.e, not to cut-off any frequency relevant to the system). Also, one of the uncertainties that could be difficult to some currently designed self-tuning controllers is the knowledge of time-delay or dead-time. Hitherto, the self-adaptive PIP has been applied under the presumption that this precise value was known. Consequently, the parameter estimates were updated at each sample with this full knowledge and the performances were all acceptable. However, in most cases this value is unknown or subject to variations. For this reason and in order to assess further the robustness of the adaptive PIP controller, a series of experiments was performed in which the value of dead-time in the model was taken to be different from the one in the system. The experiment consisted of assuming a time-delay of 1 sample for the system associated with the drug Atracurium while the model included a changing time-delay between 1 to 2 samples every 100 minutes. A pair of relatively fast poles of 5 and 3 minutes was assigned for the closed-loop characteristic equation. Notice that the control signal in figure (4.26) was only active 40 samples after the set-point change took place due to the fact that the estimates did not have knowledge of the delay change until this time. At sample 300 where the delay went back to 1 sample the control tried to recover its steady level but it was slow due to the slow assigned pole. The parameter estimates finally assumed the following values:

$$\hat{a}_1 = -1.0682 \quad \hat{a}_2 = -0.2239 \quad \hat{a}_3 = 0.3159$$

$$\hat{b}_1 = 0.0128 \quad \hat{b}_2 = 0.0079 \quad \hat{b}_3 = 0.0099$$

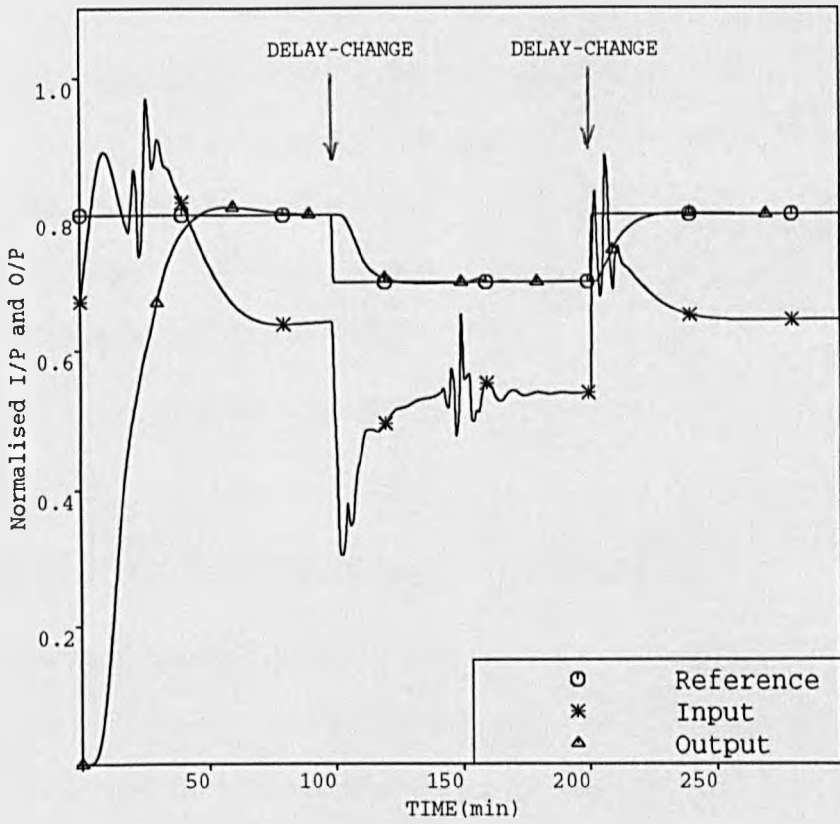


Figure 4.26. Closed-loop control performance of the self-adaptive PIP with Atracurium model under unknown and variable time delay. Two poles assigned; 5 min. and 3 min.

equivalent to the following positions in the z plane:

$$\begin{aligned} \text{zeros: } & (-0.3086 \pm 0.8235 i) \\ \text{poles: } & 0.9574 ; 0.6324 ; -0.5217 \end{aligned}$$

The same conditions were assumed for another run in which the Pancuronium-Bromide drug model was considered. Time-delay changes of 2 then 4 samples were made at iteration 70, and back to 2 samples again at iteration 140. Two poles of 5 and 3 minutes were assigned for that purpose. Figure (4.27) shows how the controller after being excited was aware of the change in time-delay, resulting in oscillations in the response. The parameter estimates suggesting a non-minimum phase system converged to the following values:

$$\hat{\Theta}_f = \begin{bmatrix} -1.4706 & 0.5089 & 0.0308 & 0.0819 \end{bmatrix}$$

equivalent to:

$$\hat{G}ain = 2.94 \quad \hat{T}_1 = 1.71 \text{ minutes} \quad \hat{T}_2 = 11.06 \text{ minutes}$$

If on the other hand a slower characteristic equation in the image of 2 poles of 8 and 5 minutes is assigned, the response is that of figure (4.28) which could be described as relatively slow. The control signal on the other hand remains smooth despite the big changes in time-delay.

4.8 PIP DESIGN WITH DEAD-TIME COMPENSATION

Time-delay problems are common phenomena with processes such as chemical, biological, or just industrial. This can be due to different factors such as measurement or control, and their difficulty resides in the dead-time between taking the control action and the direct effect of that action being seen at the output. Stimulation recordings of the EMG and control signals (Linkens et al., 1982) confirm the presence of such dead-time namely in Pancuronium induced muscle relaxation in

dogs. Space prohibits a full Nyquist-stability analysis widely available in the literature (Marshall, 1979), but it is worthwhile noting that stability problems arising from this delay are due to the excessive phase-lag. Conventional closed-loop compensations in the form of a phase-lead network would appear attractive as far as stability is concerned, but it is known that the maximum phase-lead readily available from this network cannot exceed 70 degrees. Therefore, for systems possessing effective phase lags greater than this value such idea would certainly be ineffective unless several of them are used in cascade, an undesirable solution since the overall network would act as a "noise-amplifier".

As time-delays inevitably form an integral part of a system, researchers sensed the need for alternative solutions. First, it was Smith (1957, 1959) who proposed a principle which bears his name and known as the **Smith predictor principle** which was to revolutionize the way in dealing with such situations. Several other ideas based on a classical or adaptive approach followed. For instance, Kurz and Goedecke (1981) proposed an interesting adaptive approach in which the value of time-delay could be estimated at regular sampling intervals: a model G^* of the process under consideration is assumed and a model G of the same process is estimated. Successive tests in a total of 4 are run to fit G^* with G . Good adaptive control is shown to be possible at the expense of course of an extra computational burden. However, good fitting cannot be guaranteed unless a reasonable excitation is present all the time the algorithm is run. Space prohibits investigating such approach, instead, the next section endeavours to review the idea of a Smith predictor together with the idea of the $B(z^{-1})$ expansion method.

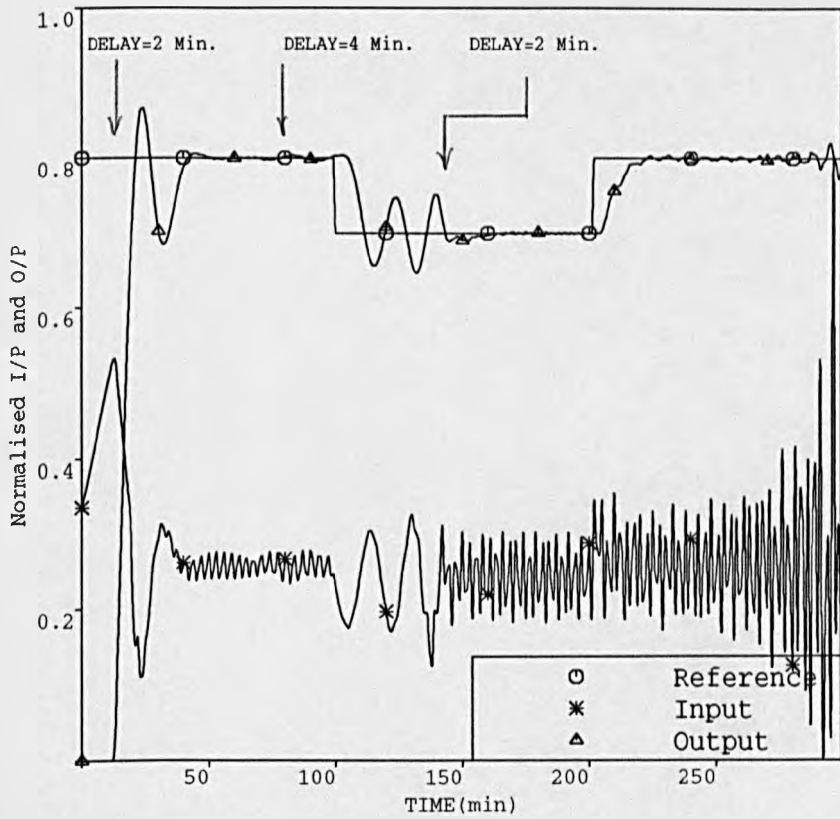


Figure 4.27. Closed-loop control performance of the self-adaptive PIP with Pancuronium model under unknown and variable time delay. Two poles assigned; 5 min. and 3 min.

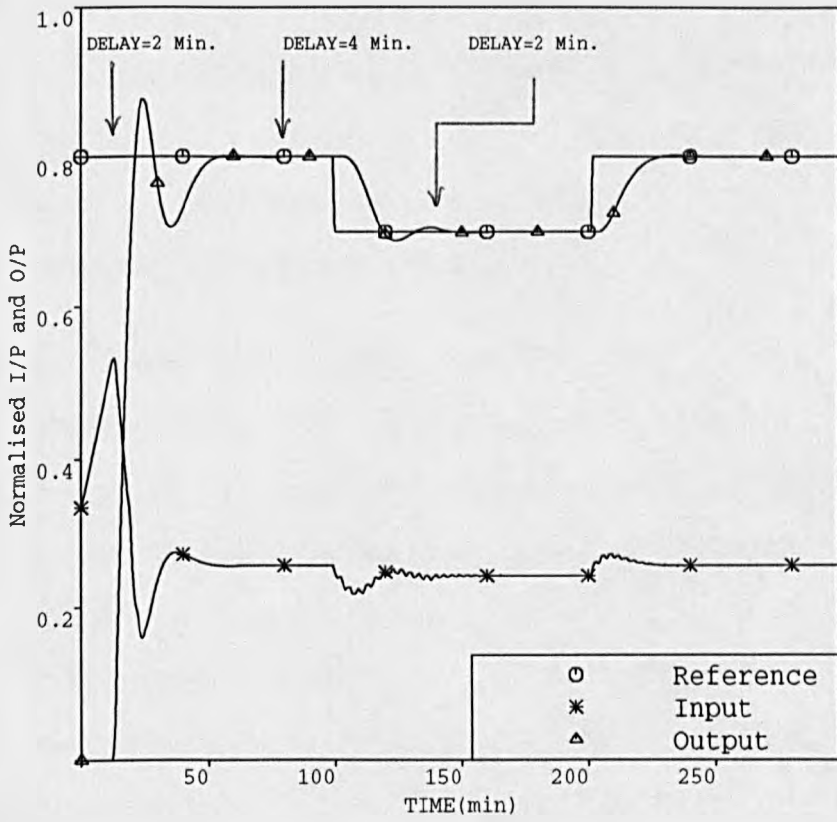


Figure 4.28. Same conditions as in figure (4.27) but with two assigned closed-loop poles of 8 min. and 5 min.

dogs. Space prohibits a full Nyquist-stability analysis widely available in the literature (Marshall, 1979), but it is worthwhile noting that stability problems arising from this delay are due to the excessive phase-lag. Conventional closed-loop compensations in the form of a phase-lead network would appear attractive as far as stability is concerned, but it is known that the maximum phase-lead readily available from this network cannot exceed 70 degrees. Therefore, for systems possessing effective phase lags greater than this value such idea would certainly be ineffective unless several of them are used in cascade, an undesirable solution since the overall network would act as a "noise-amplifier".

As time-delays inevitably form an integral part of a system, researchers sensed the need for alternative solutions. First, it was Smith (1957, 1959) who proposed a principle which bears his name and known as the **Smith predictor principle** which was to revolutionize the way in dealing with such situations. Several other ideas based on a classical or adaptive approach followed. For instance, Kurz and Goedecke (1981) proposed an interesting adaptive approach in which the value of time-delay could be estimated at regular sampling intervals: a model G^* of the process under consideration is assumed and a model G of the same process is estimated. Successive tests in a total of 4 are run to fit G^* with G . Good adaptive control is shown to be possible at the expense of course of an extra computational burden. However, good fitting cannot be guaranteed unless a reasonable excitation is present all the time the algorithm is run. Space prohibits investigating such approach, instead, the next section endeavours to review the idea of a Smith predictor together with the idea of the $B(z^{-1})$ expansion method.

4.8.1 The Classical Smith Predictor Scheme

Before being involved in any mathematical formulations, the following summarizes the idea of Smith's principle;

Suppose that a controller C has been designed for a delay free system represented by its transfer function G whose response is shown in figure (4.29).

As has been mentioned earlier, and since the time-delay is part of a system and cannot be removed, Smith's principle simply states that the response illustrated in figure (4.30) is ideally the response that should be obtained using a controller C^* for the same system but incorporating the time-delay. The response in figure (4.30) is that of figure (4.29) but delayed with τ . Consequently, it is interesting to note that all specifications for the system performance need only to be formulated considering the associated delay free system.

Now, consider the closed-loop transfer function associated with figure (4.29)

$$TF_1 = \frac{C G}{1 + C G} \quad (4.25)$$

whereas for figure (4.30):

$$TF_2 = \frac{C^* G e^{-s\tau}}{1 + C^* G e^{-s\tau}} \quad (4.26)$$

Smith's principle is equivalent to:

$$TF_2 = TF_1 e^{-s\tau}$$

i.e:

$$\frac{C^* G e^{-s\tau}}{1 + C^* G e^{-s\tau}} = \frac{C G}{1 + C G} e^{-s\tau}$$

Hence,

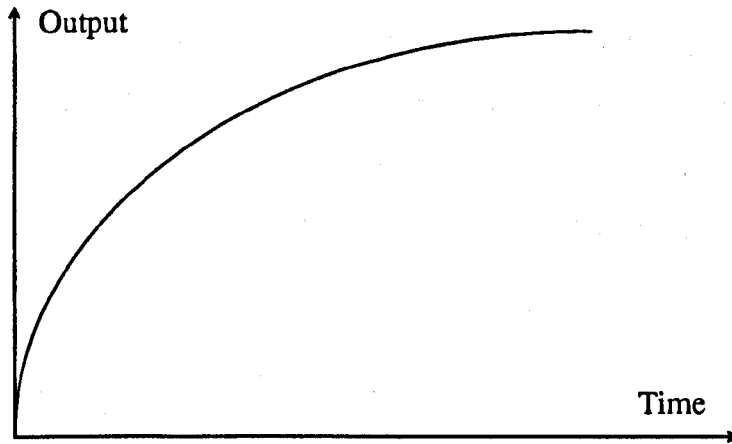


Figure 4.29. Output response of a delay-free system

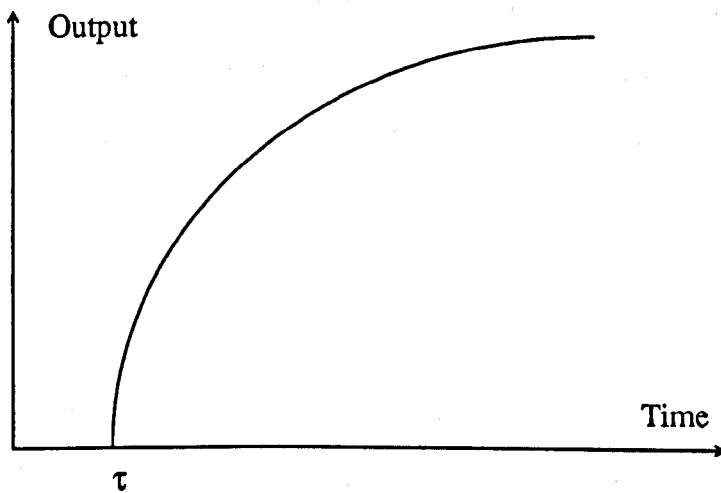


Figure 4.30. Output response of a delayed system

$$C^* = \frac{C}{1 + C G (1 - e^{-s\tau})} \quad (4.27)$$

The overall Smith's scheme could ideally be represented as in figure (4.31). However, this is an unrealistic representation since the model considered does not always coincide exactly with the true process. Instead, the representation of the scheme in figure (4.32) is adopted leading to an overall transfer function TF_2 of the form:

$$TF_2 = \frac{C G e^{\tau}}{1 + C G + C (G e^{-s\tau} - G_0 e^{-s\tau_0})} \quad (4.28)$$

The term $(G e^{\tau} - G_0 e^{\tau_0})$ is often called the mismatch-term.

The degree of the acceptable mismatch depends mainly on the magnitude of the controller considered and a full study of how this affects the stability properties of a system is of great interest and is reviewed in Marshall (1979). Nevertheless, in order to demonstrate this idea, the non-linear muscle relaxant model was simulated in the context of a Smith predictor and according to figure (4.33). The controller being considered in this case is the PID network derived in chapter 3 and whose parameters $p_0 = 3.82$, $p_1 = -6.39$, $p_2 = 2.62$ were optimized using the PSI package program (Van Den Bosch, 1979).

Simulation Results

First the scheme was tried under matched conditions. Figure (4.34) shows the performance of the PID controller when the muscle relaxant model associated with Pancuronium-Bromide was considered, and figure (4.35) the corresponding performance when the same system associated with Atracurium was used, both models using the nominal values previously specified. Even if the delay was increased to a higher value of 3 samples, the scheme under matched conditions still showed a

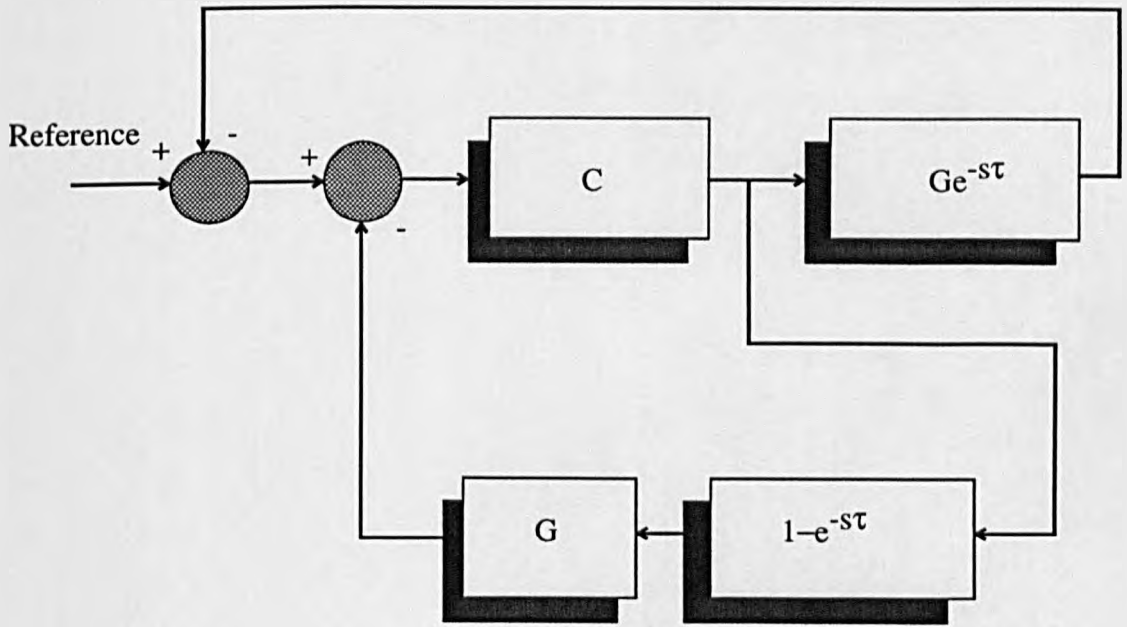


Figure 4.31. Block diagram of a Smith predictor

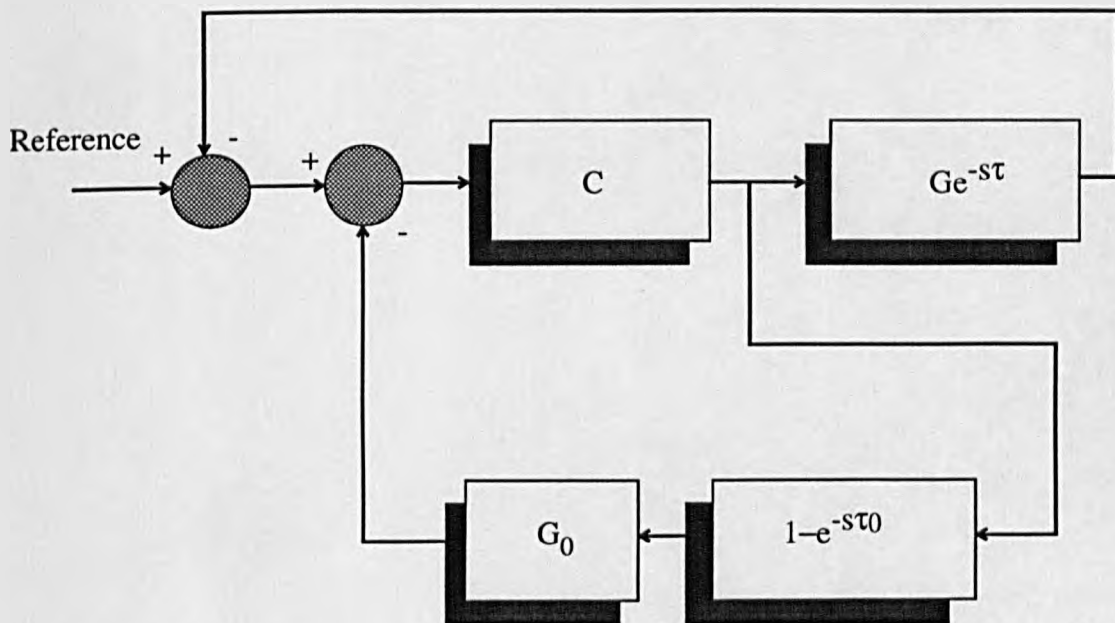


Figure 4.32. Block diagram of a Smith predictor :
mismatch conditions

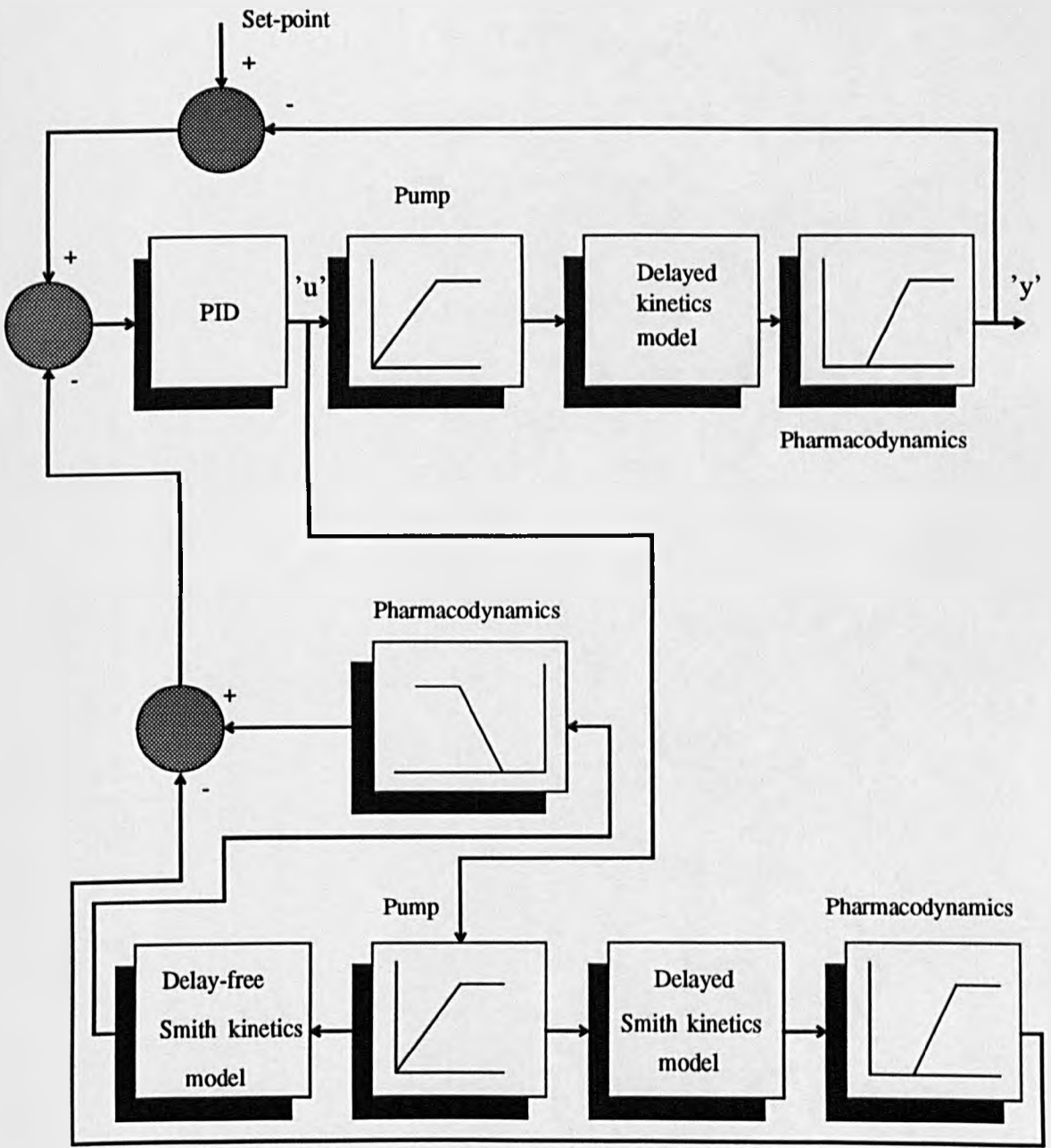


Figure 4.33. Muscle relaxation control system including a Smith predictor

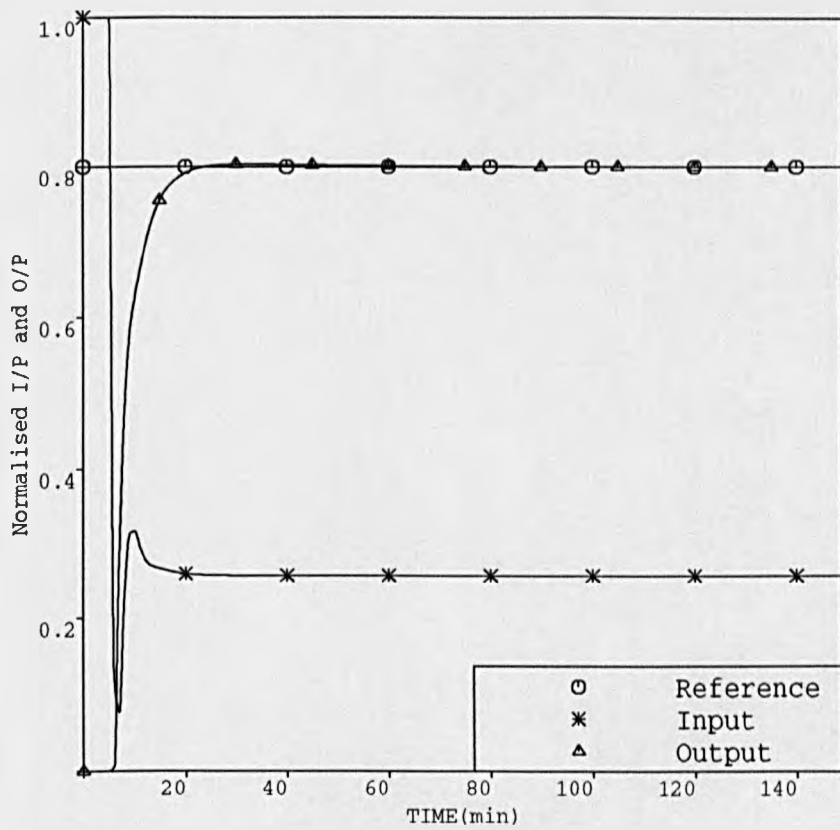


Figure 4.34. Closed-loop response of Pancuronium model under Smith predictor control (matched conditions)

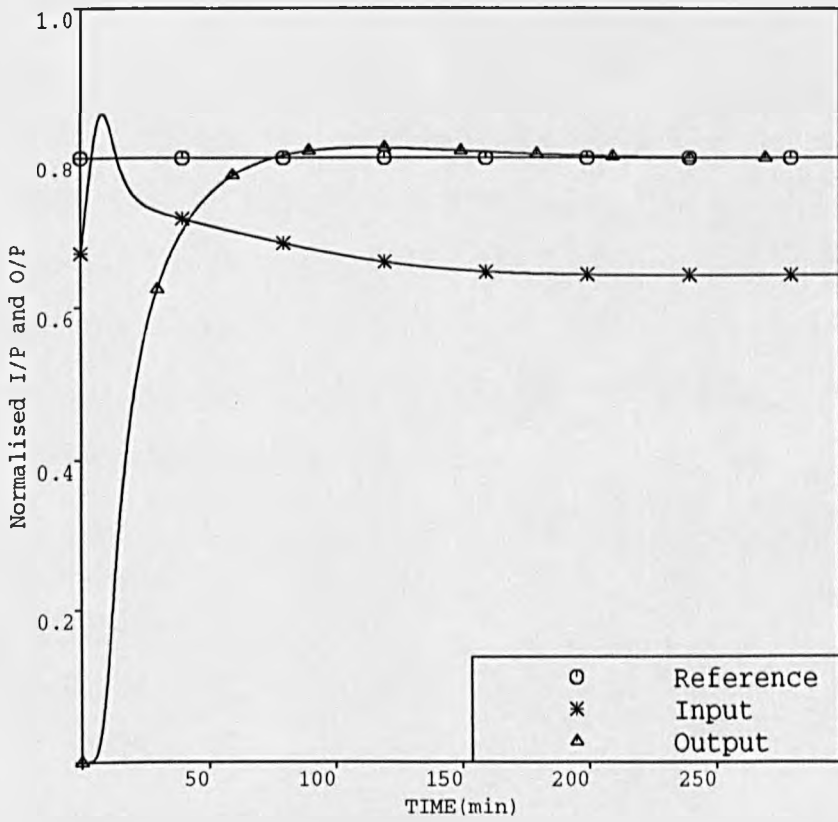


Figure 4.35. Closed-loop response of Atracurium model under Smith predictor control (matched conditions)

very good performance with both models as shown in figure (4.36) for Pancuronium and figure (4.37) for Atracurium. In order to assess the performance of the scheme under mismatch conditions, the system associated with Pancuronium was simulated with a time-delay of 4 samples, whereas the model assumed a delay of 1 sample only. Figure (4.38) shows how the performance deteriorated due to the phase-lag induced by this large dead-time. The performance was even worse when a mismatch in the dynamics was considered. Indeed, as figure (4.39) demonstrates, oscillations were produced when the system associated with Pancuronium was simulated with $K_1 = 3.5$ $T_1 = 1.0$ min. $T_2 = 10.0$ min. while the model assumed nominal values of $K_1 = 3.5$ $T_1 = 2.0$ min. $T_2 = 20.0$ min.. The performance also degraded when the system associated with Atracurium was considered. In this case the corresponding system was simulated with:

$$K_1 = 1.0$$

$$T_1 = 1 \text{ min.}$$

$$T_2 = 2 \text{ min.}$$

$$T_3 = 10 \text{ min.}$$

$$T_4 = 30 \text{ min.}$$

whereas the model assumed nominal values of :

$$K_1 = 1.0$$

$$T_1 = 4.81 \text{ min.}$$

$$T_2 = 3.08 \text{ min.}$$

$$T_3 = 34.36 \text{ min.}$$

$$T_4 = 10.64 \text{ min.}$$

The response of figure (4.40) shows the consequence of a wrong dynamics assumption.

The series of experiments conducted above demonstrated how the Smith predictor scheme could be robust in counteracting the effects of time-delay when a correct

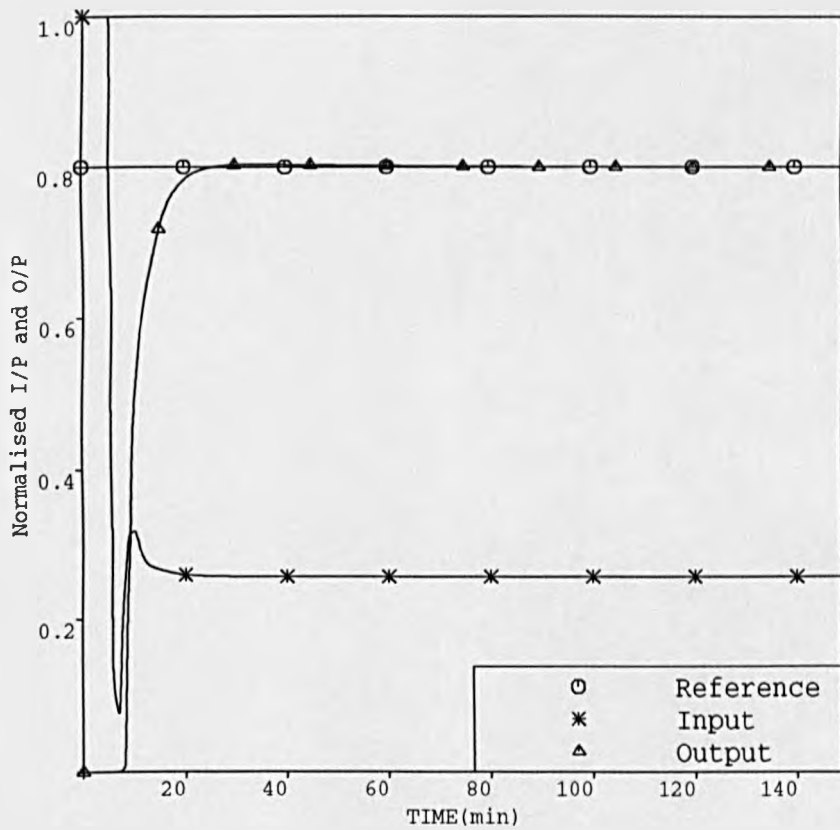


Figure 4.36. Same conditions as in figure (4.34) but with $\tau=3$ min.

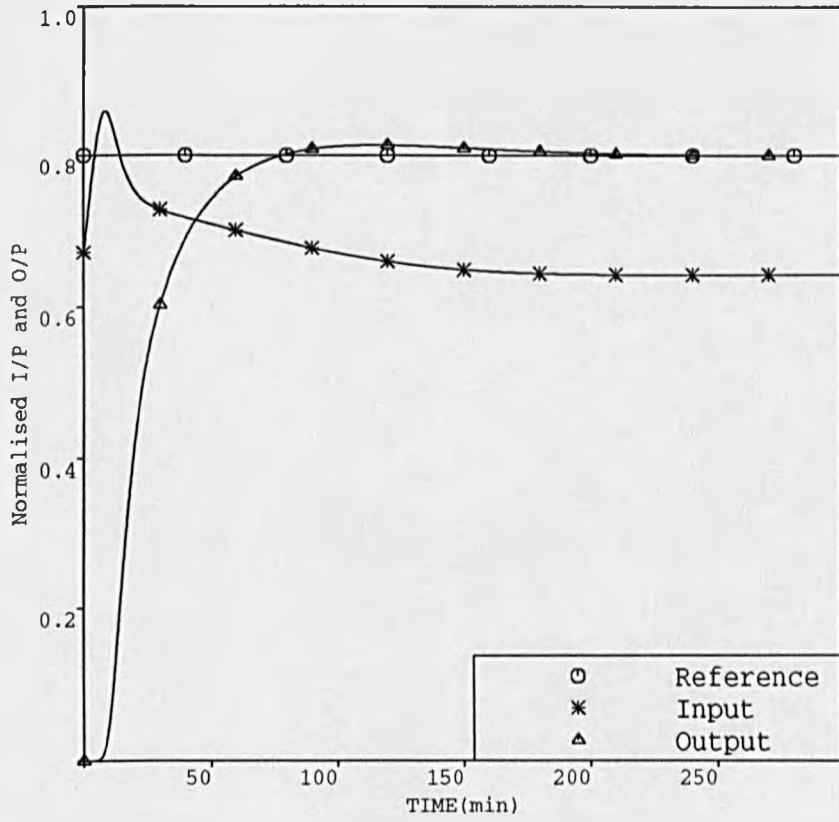


Figure 4.37. Same conditions as in figure (4.35)

but with $\tau=3$ min.

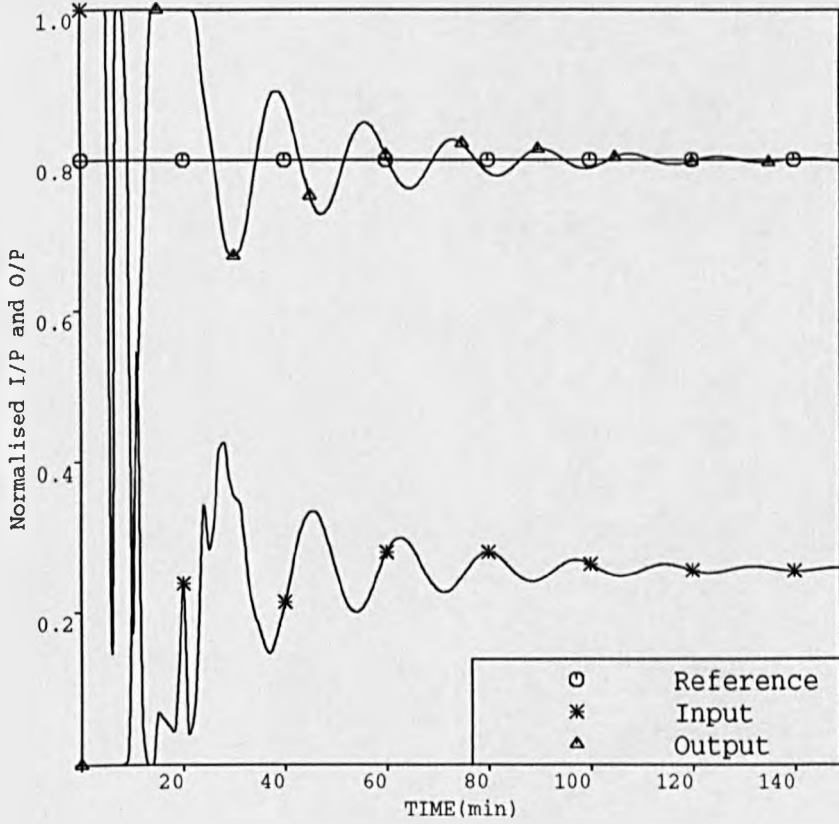


Figure 4.38. Closed-loop response of Pancuronium model under Smith predictor control (mismatch conditions; $\tau_m=1$ min. $\tau_s=4$ min.)

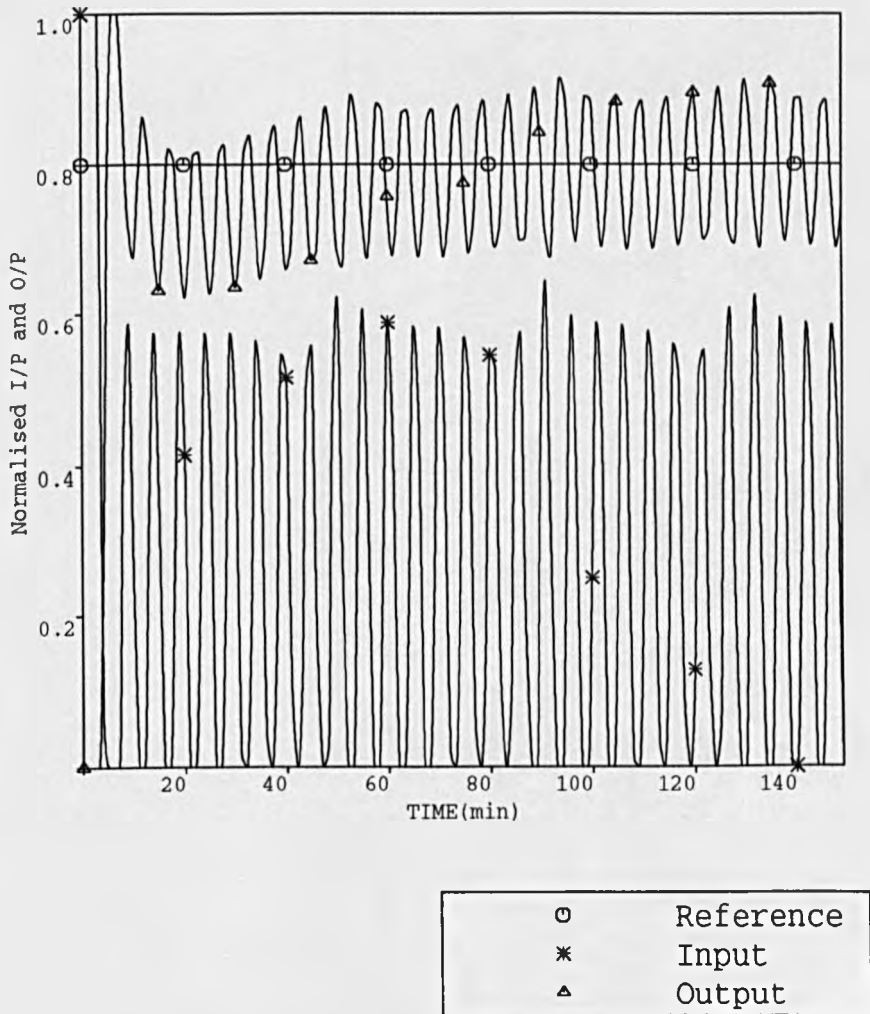


Figure 4.39. Closed-loop response of Pancuronium model under Smith predictor control (mismatch conditions; $T_2=10$ min. $T_1=1$ min.)

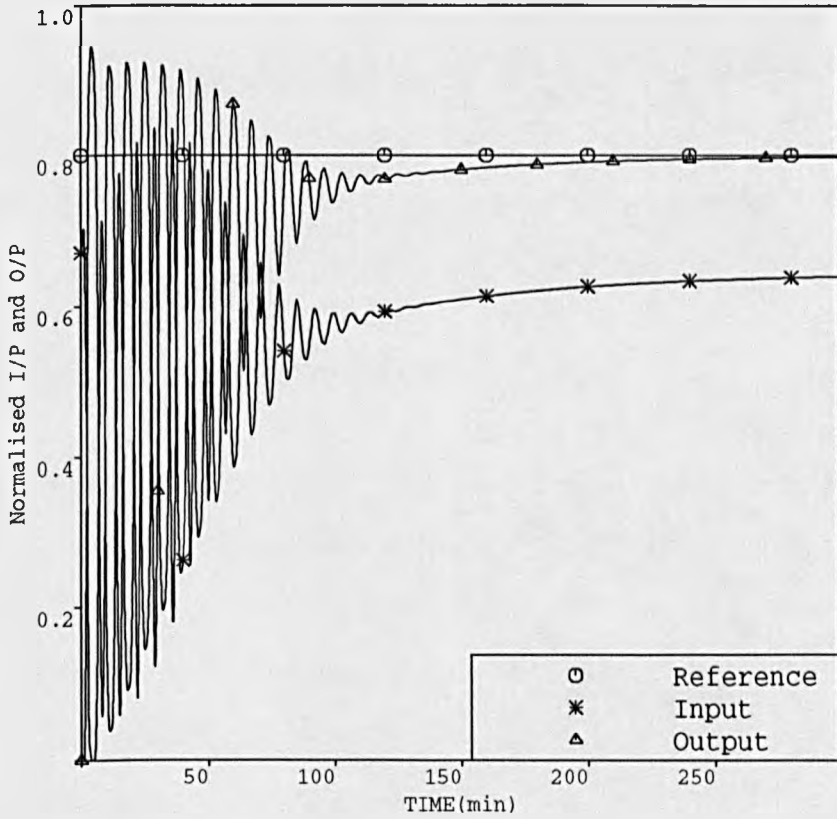


Figure 4.40. Closed-loop response of Atracurium model under Smith predictor control (mismatch conditions; $T_1=1$ min. $T_2=2$ min. ; $T_3=10$ min. $T_4=30$ min.)

model of the process is assumed. However the same technique could prove to have undesirable consequences when the magnitude of the error between the system dynamics and the dynamics assumed in the model is somewhat large. This, as already seen is reflected in the mismatch term which should be kept as near as possible to zero. Practically, this is not always possible as current identification tools guarantee only an approximate model rather than an accurate one.

With the advance witnessed in self-tuning and adaptive technique, the need for adapting the previous scheme was quickly sensed. This is the subject of the next section which looks at the digital version of the Smith predictor.

4.8.2 The Extended Smith Predictor (ESP)

Originally, the Smith predictor was developed for continuous-time control. However, the idea can be extended to include discrete-time control (Marshall, 1974) as illustrated by figure (4.41). In this figure, C is the controller designed in delay free conditions, δ' is the minimum assumed model time-delay (used in the forthcoming equations), \hat{B} and \hat{A} are the estimated polynomials in the backward shift z^{-1} . At this stage it is worth noting that the model parameters are estimated assuming the time-delay δ' , and it is the same parameters that are used to calculate the delayed as well as the free version of the output.

If the controller C is represented by the PIP algorithm, the diagram would be one of figure (4.42), where I , G , and F are as defined in section (4.4), i.e:

- I integral of error term.
- F proportional and feedback filter.
- G forward path filter.

Because of the inclusion of the PIP design method, the resulting control scheme might be termed as: **Extended Smith Predictor** or **ESP** (Chotai and Young,

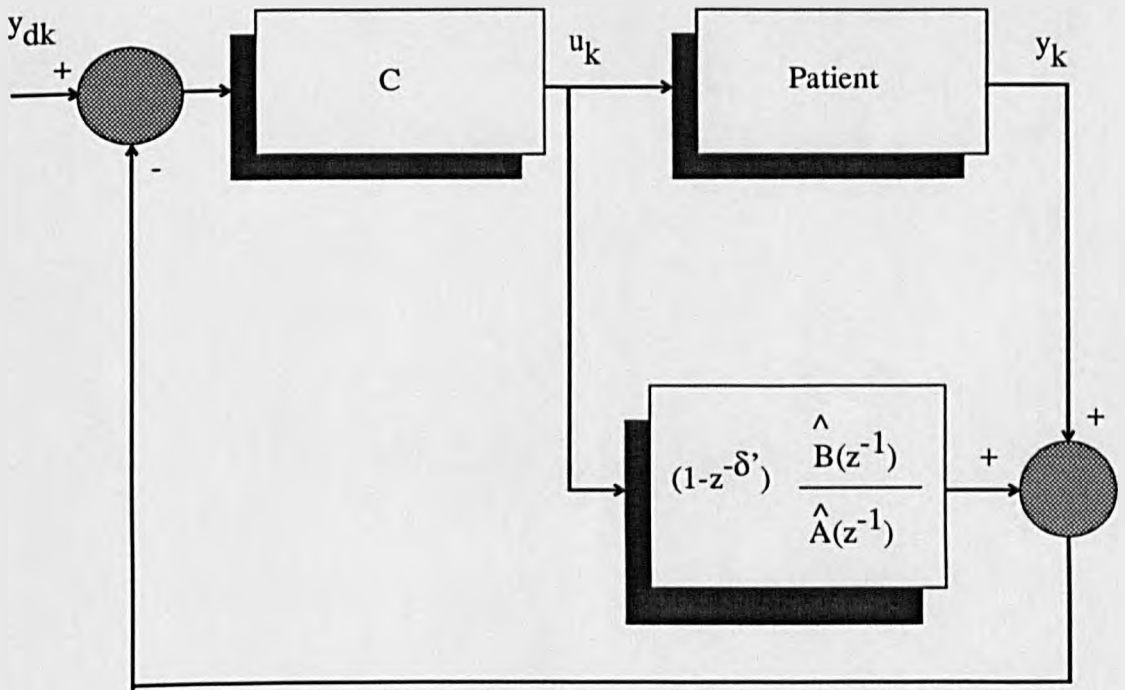


Figure 4.41. Block diagram of the Smith predictor in a digital form

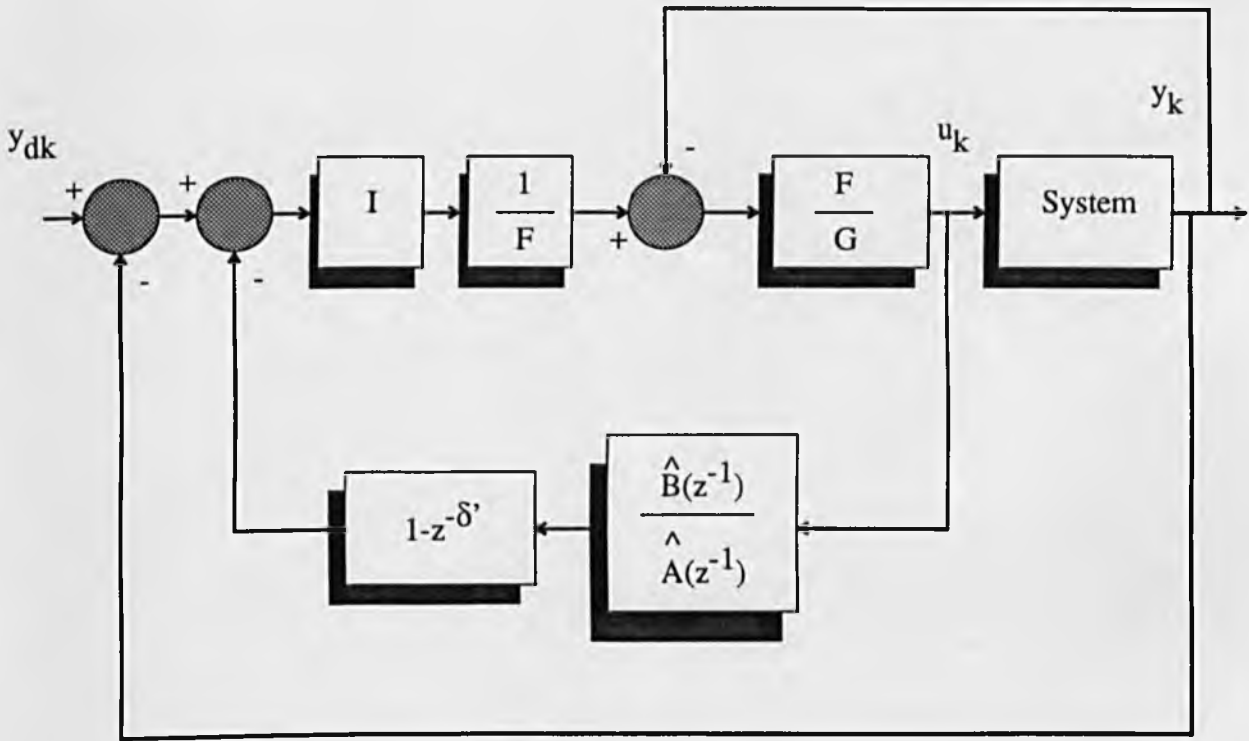


Figure 4.42. Block diagram of the extended Smith predictor (ESP) control system

1988).

From the last figure the corresponding closed-loop transfer function must be derived. For this purpose, assume that the process is linearized around an operating point by a discrete model of the usual form:

$$\frac{y_k}{u_k} = \frac{B(z^{-1})}{A(z^{-1})} z^{-\delta} \quad (4.29)$$

where $B(z^{-1})$ and $A(z^{-1})$ are the polynomials in the backward shift of the usual form:

$$\begin{aligned} B(z^{-1}) &= b_1 z^{-1} + b_2 z^{-2} + \dots + b_m z^{-m} \\ A(z^{-1}) &= 1 + a_1 z^{-1} + a_2 z^{-2} + \dots + a_n z^{-n} \end{aligned}$$

Using the latter figure it follows that:

$$u_k = \frac{1}{G} [I [D_k - [(y_k - y_{\text{delay}}) - y_{\text{free}}]] - F \frac{\hat{B}}{\hat{A}} u_k] \quad (4.30)$$

where:

$$\begin{aligned} y_{\text{free}} &= \frac{\hat{B}}{\hat{A}} u_k \\ y_{\text{delay}} &= \frac{\hat{B} z^{-\delta'}}{\hat{A}} u_k \\ y_k &= B \frac{z^{-\delta}}{A} u_k \end{aligned}$$

\hat{B} and \hat{A} and δ' represent the estimated model parameters

Substituting and rearranging leads to:

$$y_k = u_k \frac{I \frac{B z^{-\delta}}{A}}{G + I \left[\frac{B z^{-\delta}}{A} - \frac{\hat{B} z^{-\delta'}}{\hat{A}} \right] + I \frac{\hat{B}}{\hat{A}} + F \frac{\hat{B}}{\hat{A}}} \quad (4.31)$$

Hence, the specification of system performance can be obtained in familiar delay free PIP design terms. Consequently, the set of simultaneous equations of the form

$\Sigma \cdot V = \beta$ to be solved in this case reduces to a smaller size than the one that would be obtained if the delay was presumed to be known as it will be seen in the next section. If the parameters B , A , and δ are modelled exactly then the mismatch term mentioned in section 4.8.1 and represented here by the term:

$$\left[\frac{B z^{-\delta}}{A} - \frac{\hat{B} z^{-\delta'}}{\hat{A}} \right]$$

would be nil in equation (4.31) reducing it therefore to the following expression:

$$y_k = u_k \frac{I \frac{B z^{-\delta}}{A}}{G + I \frac{B}{A} + F \frac{B}{A}} \quad (4.32)$$

Clearly, it is important to acknowledge that this mismatch-term is typical of many time-delay control systems (Marshall, 1979). However, because the predictor is being used in a self-tuning context, the model parameters are updated at every sampling interval. Therefore, the parameters of the control-law governed by equation (4.31) are adjusted accordingly, making the overall loop less sensitive to the magnitude of this mismatch-term. It is concluded that the Smith predictor combined with self-tuning is in the long-term less sensitive to changes that may occur in the system compared to the classical version (Gawthrop, 1977).

Simulation Results

In order to verify some of the above assertions, a series of experiments was undertaken under such a scheme.

Throughout the following, a command signal of 80% then 70% was used. For estimating the model parameters, a UDU factorisation of the RLS routine was used with initial covariance matrix and forgetting factor set respectively at:

$$P = 10^4 \cdot I \quad \text{and} \quad \rho = 0.995 \quad \text{for Pancuronium model}$$

$$P = 10^3 \cdot I \quad \text{and} \quad \rho = 0.995 \quad \text{for Atracurium model}$$

The initial parameter estimates were all set to 0.0 unless otherwise specified. To allow the self-tuner to gather reasonable data, a fixed controller in a form of a PI was used for the first 20 samples with the following parameters:

$$\begin{aligned} K_p &= 0.4 & K_I &= 0.02 & \text{for Pancuronium drug model} \\ K_p &= 0.8 & K_I &= 0.04 & \text{for Atracurium drug model} \end{aligned}$$

The non-linear muscle relaxation system associated with Pancuronium-Bromide model or the Atracurium one was simulated in a continuous form using a fourth order Runge-Kutta method with fixed-step length of 0.1 and a sampling interval of 1 minute.

The first experiment considered the second order Pancuronium model with the nominal values presented in section 3.2 with a unit time-delay. The estimated model structure also assumed this exact value. A relatively fast pole of 5 minutes corresponding to a polynomial of

$$d(z^{-1}) = 1 - 0.8 z^{-1}$$

was assigned to the closed-loop characteristic equation. As shown in figure (4.43), the performance was good. During the first 50 samples the controller was still estimating the parameters, and after the first set-point change they converged to sensible values which allowed the self-tuner to track the set-point better. At the end of the run, these parameter estimates converged to:

$$\hat{a}_1 = -1.4746 \quad \hat{a}_2 = 0.5193 \quad \hat{b}_1 = 0.0660 \quad \hat{b}_2 = 0.0676$$

equivalent to a gain and time-constants of:

$$\hat{\text{Gain}} = 2.99 \quad \hat{T}_1 = 1.84 \text{ minutes} \quad \hat{T}_2 = 8.86 \text{ minutes}$$

The same run was repeated, this time with some initial values for the parameter estimates which assumed a gain and time-constants of:

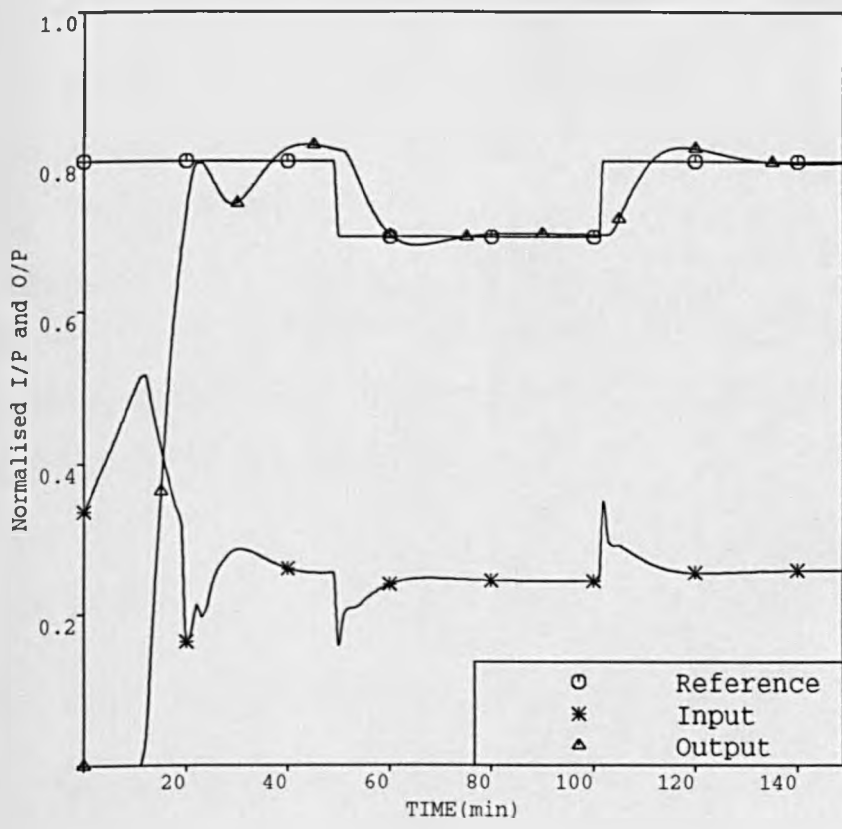


Figure 4.43. Closed-loop response of Pancuronium model under ESP control

$$\hat{G}_{\text{ain}} = 2.5$$

$$\hat{T}_1 = 2.0$$

$$\hat{T}_2 = 20.0$$

The resulting response shown in figure (4.44) produced an improvement since the parameters were better conditioned in this particular case. They indeed converged to:

$$\hat{a}_1 = -1.4268 \quad \hat{a}_2 = 0.4749 \quad \hat{b}_1 = 0.0741 \quad \hat{b}_2 = 0.0724$$

equivalent to a gain and time-constants of:

$$\hat{G}_{\text{ain}} = 3.04 \quad \hat{T}_1 = 1.57 \text{ minutes} \quad \hat{T}_2 = 9.28 \text{ minutes}$$

When associated with the third order Atracurium drug-model, the controller produced the response of figure (4.45). The control signal was smooth despite the fast pole assigned (5 minutes), and the parameter estimates gave the following final values:

$$\hat{a}_1 = -1.1239 \quad \hat{a}_2 = -0.2279 \quad \hat{a}_3 = 0.3705$$

$$\hat{b}_1 = 0.0106 \quad \hat{b}_2 = 0.0129 \quad \hat{b}_3 = -0.0004$$

equivalent to the following positions in the z plane:

$$\text{zeros: } -1.2472 ; 0.0303$$

$$\text{poles: } 0.9582 ; 0.7201 ; -0.5445$$

For the next series of experiments a delay of 1 minute was assumed in the model while the one in the system was set at 2 minutes for the Pancuronium and Atracurium models. A pair of 2 poles of 5 and 3 minutes was assigned to the closed-loop characteristic equation. Figures (4.46) and (4.47) respectively for Pancuronium-Bromide and Atracurium demonstrate some overshoot amounting to 4% as well as some undershoot due to the phase-lag introduced by the delay wrongly assumed in the respective models. The control signal in figure (4.47) did not deteriorate because the design specification was in delay free terms reducing therefore the Σ

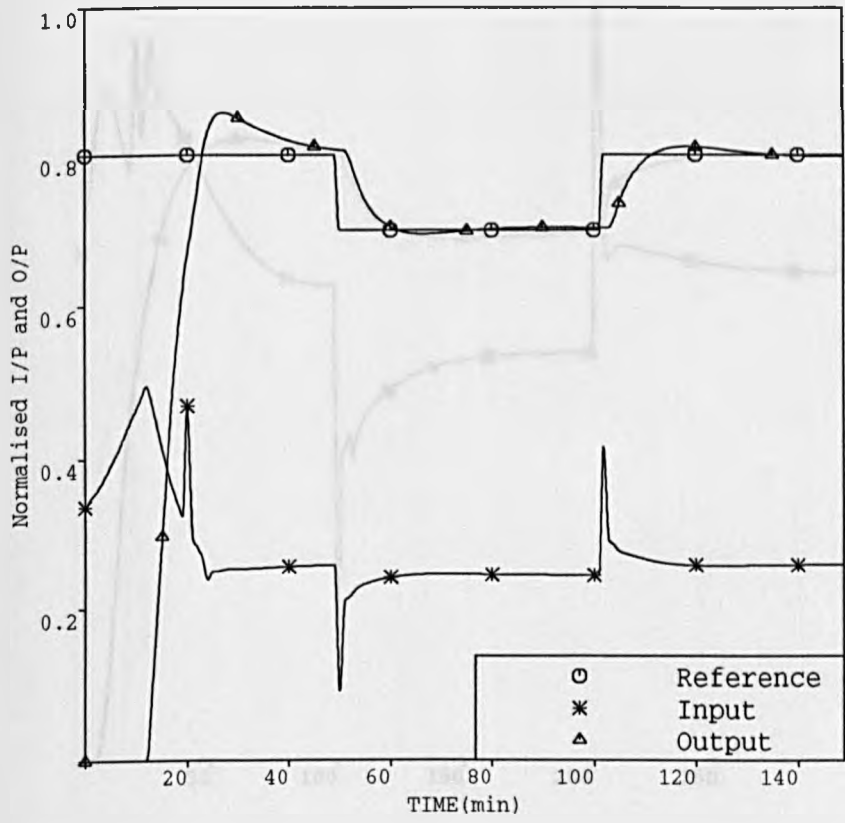


Figure 4.44. Same conditions as in figure (4.43) but with non-zero initial parameter estimates

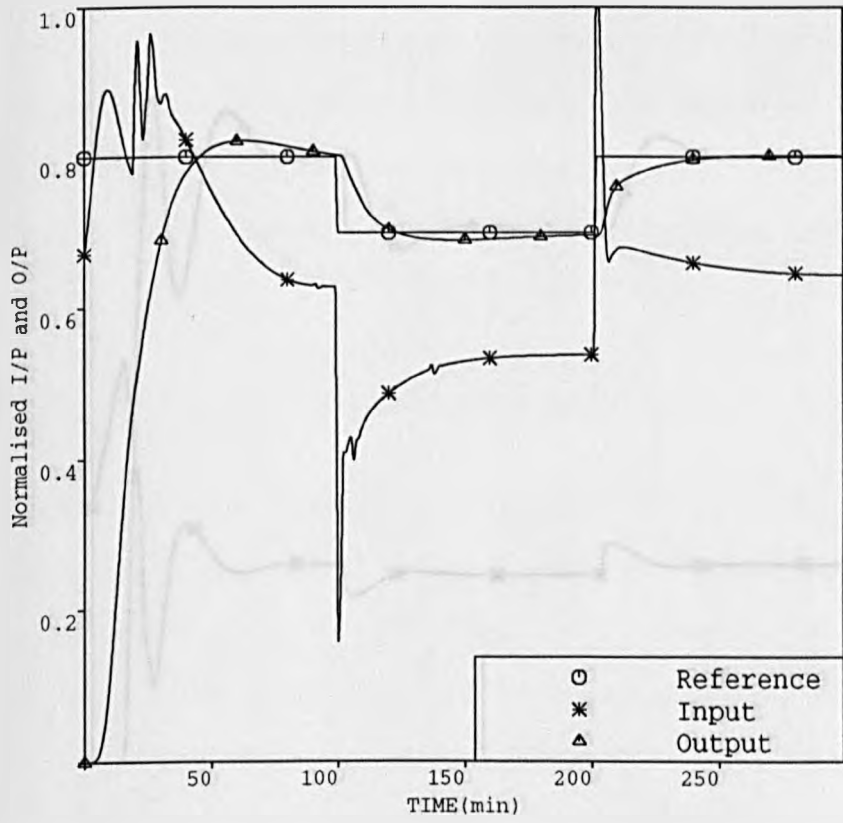


Figure 4.45. Closed-loop response of Atracurium model under ESP control

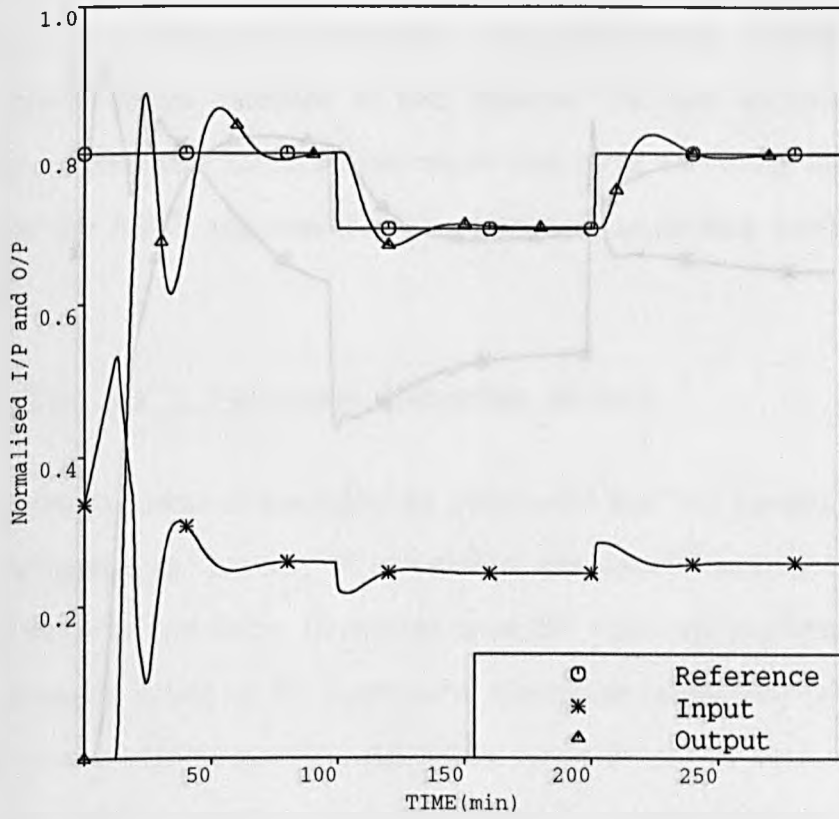


Figure 4.46. Closed-loop response of Pancuronium model under ESP control (mismatch conditions ; $\tau_s=2$ min.)

Figure 4.47 shows the closed-loop response of the Atracurium model under ESP control. The plot displays Normalised I/P and O/P versus TIME (min). The reference input (circles) is a step function that changes from 0.8 to 0.7 at 100 minutes and from 0.7 to 0.55 at 200 minutes. The input (asterisks) follows the reference input with some delay and oscillation. The output (triangles) follows the input with a significant time delay and some overshoot.

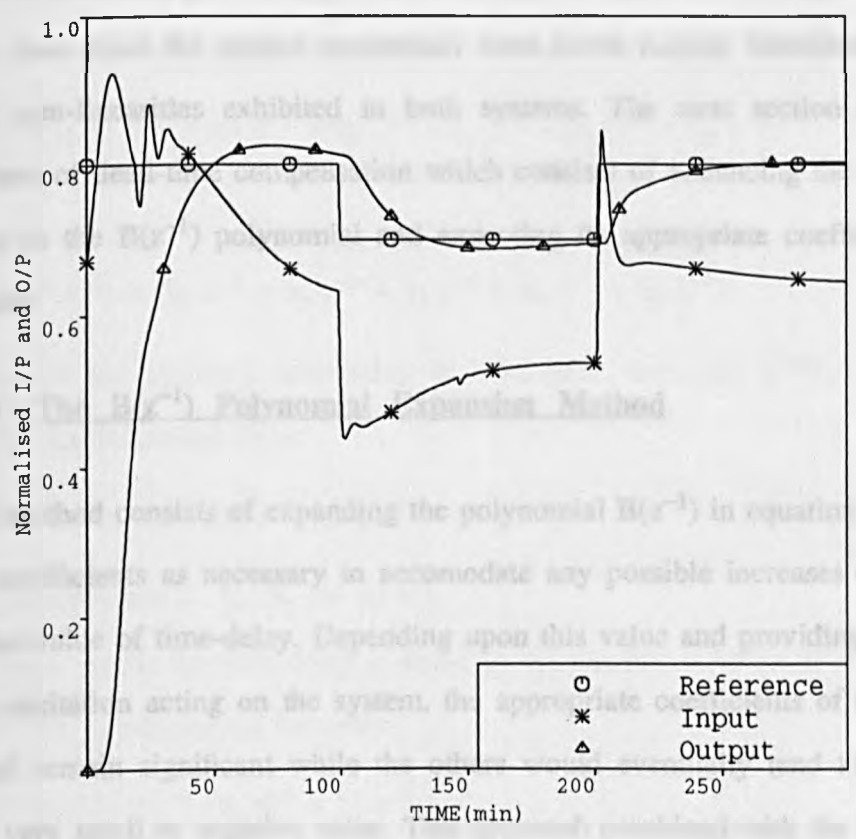


Figure 4.47. Closed-loop response of Atracurium model under ESP control (mismatch conditions ; $\tau_s=2$ min.)

matrix being inverted to a dimension of (3×3) rather than (4×4).

Clearly, the results presented above showed that the ESP scheme performs better than the classical Smith predictor either under matched or mismatch conditions. In fact, the 6 experiments previously performed could be considered as representing a mismatch case since the system parameters were never exactly identified due to the harsh non-linearities exhibited in both systems. The next section looks at another form of dead-time compensation which consists of enhancing the value of time-delay in the $B(z^{-1})$ polynomial and expecting its appropriate coefficients to tend to zero.

4.8.3 The $B(z^{-1})$ Polynomial Expansion Method

This method consists of expanding the polynomial $B(z^{-1})$ in equation (4.8) by as many coefficients as necessary to accommodate any possible increases or variations in the value of time-delay. Depending upon this value and providing there is sufficient excitation acting on the system, the appropriate coefficients of the same polynomial remain significant while the others would eventually tend to zero or assume a very small or negative value. This approach combined with the PIP control algorithm is considered to be more general than ESP, and for this reason it has been named **Generalized Smith Predictor control (GSP)** (Chotai and Young, 1988).

In order to understand the polynomial expansion method, consider the second order system describing the Pancuronium drug dynamics. For a delay free system the polynomial $B(z^{-1})$ would be written as:

$$B(z^{-1}) = b_1 z^{-1} + b_2 z^{-2}$$

If a minimum time-delay of 1 minute is assumed but knowing that this value is

subject to variations of a maximum of 4 minutes, then the $B(z^{-1})$ polynomial should be expanded by a number of coefficients N_c such that:

$$N_c = \text{Maximum expected delay} - \text{Minimum delay assumed}$$

In our case $N_c = 3$

Hence, the structure of the $B(z^{-1})$ becomes:

$$B^{\text{exp}}(z^{-1}) = z^{-1} (b_1 z^{-1} + b_2 z^{-2} + b_3 z^{-3} + b_4 z^{-4} + b_5 z^{-5})$$

or:

$$B^{\text{exp}}(z^{-1}) = (b_1 z^{-2} + b_2 z^{-3} + b_3 z^{-4} + b_4 z^{-5} + b_5 z^{-6})$$

If for instance the system's time-delay is 2 samples, then the $B^{\text{exp}}(z^{-1})$ would ideally have the following form:

$$B^{\text{exp}}(z^{-1}) = z^{-1} (b_2 z^{-2} + b_3 z^{-3})$$

where the coefficients b_1 , b_4 , b_5 are all nil.

If on the other hand, the time-delay is equal to the maximum value of 4 samples, then the $B^{\text{exp}}(z^{-1})$ polynomial becomes:

$$B^{\text{exp}}(z^{-1}) = z^{-1} (b_4 z^{-5} + b_5 z^{-6})$$

where this time, the coefficients b_1 , b_2 , b_3 are equal to zero.

Simulation Results

In order to demonstrate the above idea, one experiment for each of the two systems so far considered was carried out, in which the $B(z^{-1})$ polynomial in equation (4.8) was expanded according to the maximum value of the expected time-delay in the system.

The system describing the Pancuronium-Bromide drug dynamics was considered

first. The gain and time-constants are those corresponding to the nominal values. The delay in the system was made to vary from a value of 2 minutes to that of 4 minutes every 70 iteration-intervals. A one minute sample-delay was assumed in the second order linear model and the numerator $B(z^{-1})$ polynomial was expanded by N_c coefficients, $N_c = 3$, taking therefore, the number of estimated parameters to: $n + m = 2 + 5 = 7$.

Hence, the following model transfer function is adopted:

$$\frac{y_k}{u_k} = \frac{z^{-1} (b_1 z^{-1} + b_2 z^{-2} + b_3 z^{-3} + b_4 z^{-4} + b_5 z^{-5})}{1 + a_1 z^{-1} + a_2 z^{-2}}$$

Initial conditions include a covariance matrix of $P = 10^3 I$ and parameter estimates set at $\theta_i = [-1.55 \ 0.57 \ 0.04 \ 0.03 \ 0.0 \ 0.0 \ 0.0]$. Because of the large number of parameters involved in the estimation part, and to ensure that correct parameterization is achieved, a forgetting factor of $\rho = 0.95$ was adopted throughout. Figure (4.48) shows the performance of the controller when a pair of poles of 5 and 3 minutes was assigned to the closed-loop characteristic equation. Despite the heavy burden of having to estimate such a considerable number of parameters (whose time-variations are shown in figure (4.49)) as well as to invert a matrix of dimension (8×8), the overall strategy coped rather well following the two severe changes made in the delay respectively at iterations 70 and 140. The slight fluctuations in the control signal that appeared during the run were due to the variations in the coefficients of the $B(z^{-1})$ reflecting the actual system's time-delay. Table (4.1) illustrates the variations for these coefficients at the end of each phase.

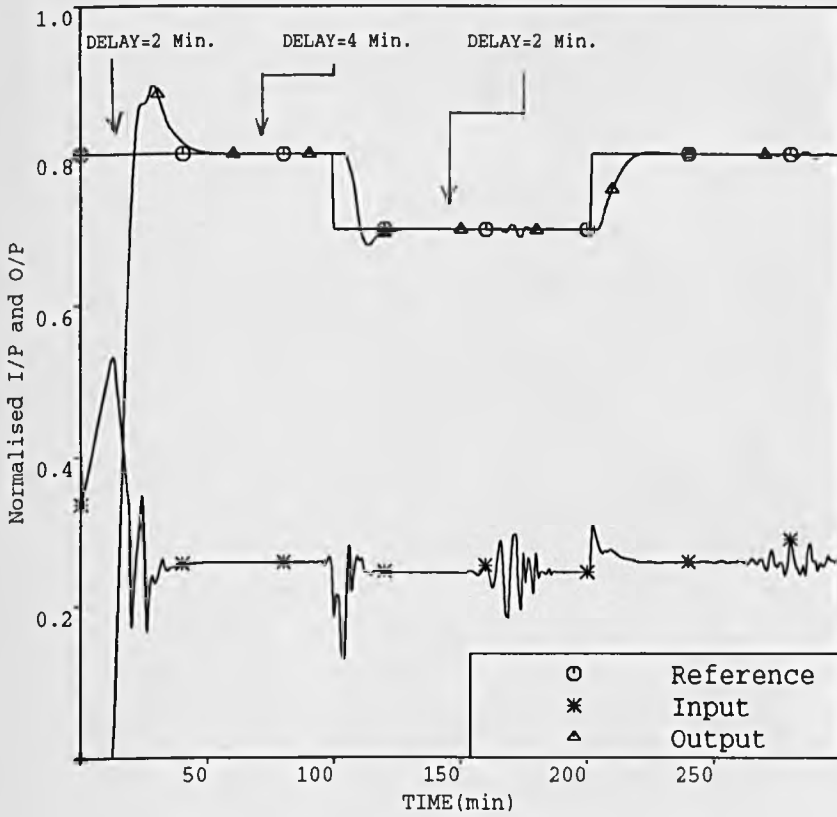


Figure 4.48. Closed-loop response of Pancuronium model under PIP control with overparameterized $B(z^{-1})$ polynomial

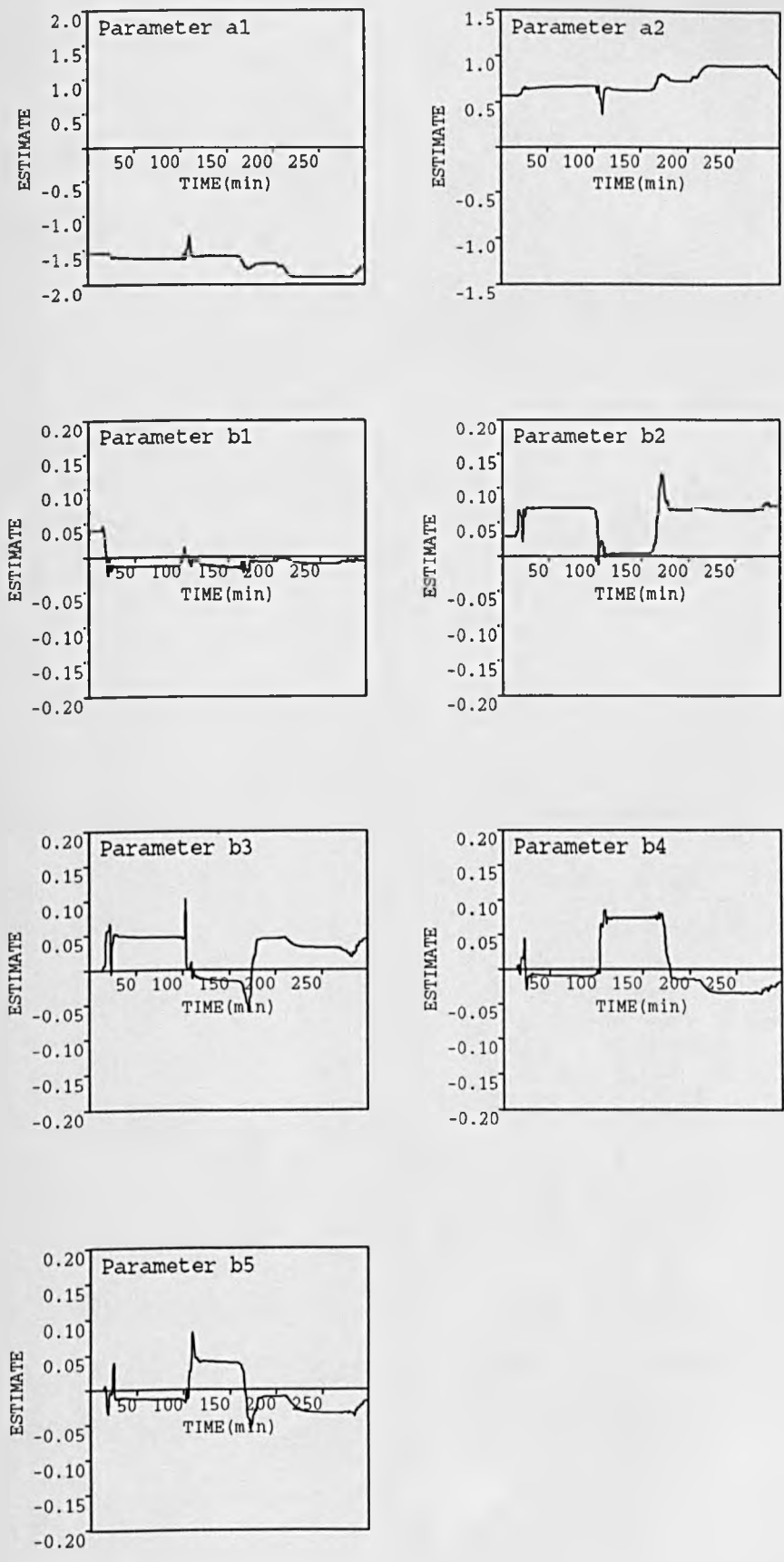


Figure 4.49. System parameter estimates corresponding to figure (4.48)

Parameter Estimates Convergence			
Parameter estimates	Time-delay value(Min.) from...to...		
	2 (0 to 70)	4 (71 to 140)	2 (141 to 300)
\hat{a}_1	-1.6377	-1.5937	-1.7386
\hat{a}_2	0.46639	0.6239	0.7632
\hat{b}_1	-0.0135	-0.0139	-0.00597
\hat{b}_2	0.0707*	-0.0042	0.0724*
\hat{b}_3	0.0476*	-0.0156	0.0446*
\hat{b}_4	-0.0099	0.0739*	-0.0185
\hat{b}_5	-0.0132	0.0396*	-0.0161

Table 4.1. Model parameter estimates for figure (4.48)

The second experiment considered the muscle relaxation system associated with Atracurium. The delay in the system was varied from 1 to 2 minutes every 100 minutes. A one minute delay was assumed in the model. The $B(z^{-1})$ polynomial was expanded by one coefficient leaving the following transfer function to be estimated:

$$y_k = \frac{z^{-1} (b_1 z^{-1} + b_2 z^{-2} + b_3 z^{-3} + b_4 z^{-4})}{1 + a_1 z^{-1} + a_2 z^{-2} + a_3 z^{-3}}$$

Figure (4.50) shows the resulting response when the same combination of poles as before was adopted for the characteristic equation. The response was good despite the harsh conditions of the run namely a changing delay simultaneously with a changing operating point. At the end of the run, the parameter estimates converged to:

* Significant values

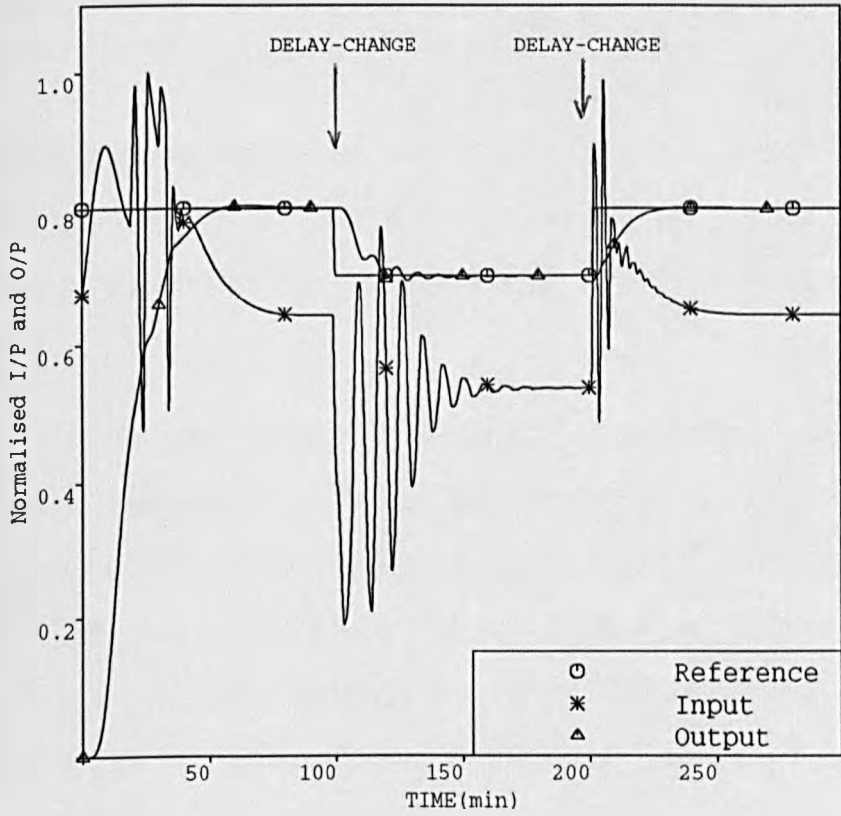


Figure 4.50. Closed-loop response of Atracurium model under PIP control with over-parameterized $B(z^{-1})$ polynomial

$$\hat{a}_1 = -1.7708 \quad \hat{a}_2 = +0.8474 \quad \hat{a}_3 = -0.0654$$

$$\hat{b}_1 = 0.0054 \quad \hat{b}_2 = 0.0090 \quad \hat{b}_3 = -0.0017 \quad \hat{b}_4 = 0.0013$$

equivalent to the following positions in the z plane:

$$\text{Zeros: } -1.8992 ; (0.1163 \pm 0.3365 i)$$

$$\text{poles: } 0.9558 ; 0.7200 ; -0.0950$$

The same technique was used in conjunction with the extended Smith predictor scheme previously reviewed in section 4.8.2. By so doing the whole concept contradicts Smith's principle but improvement over the basic case was proven to be possible.

Hence, assuming the same conditions as in figures (4.48) and (4.50) respectively, two experiments combining the ESP and GSP schemes at the same time were undertaken leading to the responses in figures (4.51) and (4.52) where it can be seen that the performances have greatly improved compared to figures (4.46) and (4.47) where the degree of the $B(z^{-1})$ polynomial was kept at its minimum value (i.e: degree 3 for Pancuronium-Bromide, and 4 for Atracurium).

Other techniques based around the same idea have since followed. For instance to improve the stability and speed of the response of the closed-loop system, Chien et al. (1984) proposed an algorithm by which the delay-free process model was redefined as being:

$$G_{\text{delay-free}} = \frac{B^{\text{exp}}(1)}{A(z^{-1})} \quad (4.33)$$

where:

$$B^{\text{exp}}(1) = \sum_{i=1}^m b_i$$

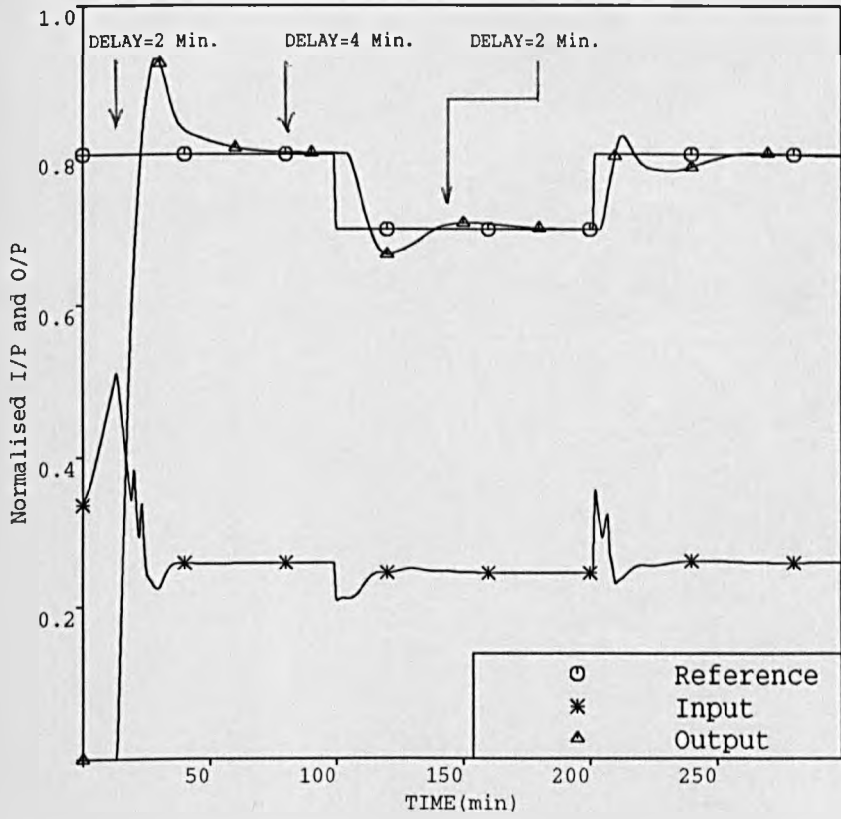


Figure 4.51. Closed-loop response of Pancuronium model under ESP control with overparameterized $B(z^{-1})$ polynomial

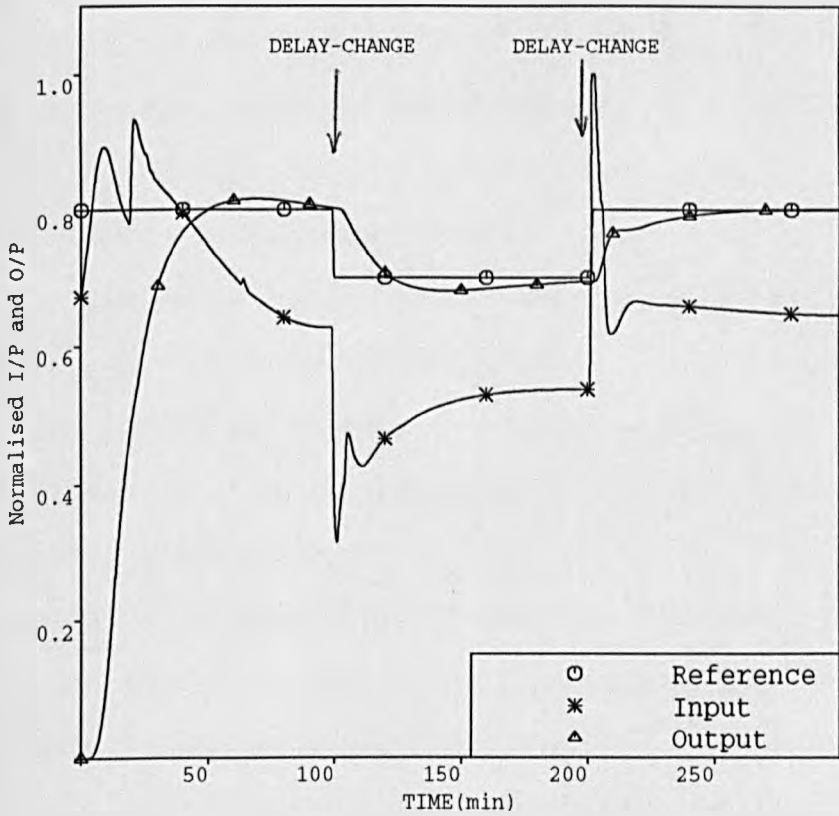


Figure 4.52. Closed-loop response of Atracurium model under ESP control with over-parameterized $B(z^{-1})$ polynomial

One implication of this formulation is that no delay term will appear in the closed-loop characteristic equation implicitly or explicitly, leading therefore to a larger stability zone. A slight improvement has been shown to be possible.

Clearly, the above technique demonstrated an improvement of performance of the controller at the cost of an increase in the number of estimated model-parameters. Very often it is necessary to take precautionary measures which would eventually ensure the obtaining of reasonable parameter estimates such as covariance-matrix resetting and variable forgetting factor. As these methods could be very effective in certain cases, they may well prove ineffective in a heavily noisy environment as far as the identification side is concerned. In the case of muscle relaxation system, the disturbances could be due to diathermy problems (severe electrical interference), and to movements of the patient's arm or parts of his (or her) body where the EMG signal is being picked-up.

In order to assess the robustness of the GSP algorithm under such conditions, an experiment was carried out in which an output disturbance with a 4% amplitude was introduced at iterations 50 and 70 respectively for Pancuronium and Atracurium and lasting 3 minutes. Initial conditions were similar to those adopted for figures (4.48) and (4.50). The upper traces of figures (4.53) and (4.54) show the output response for each system under such conditions. The control signals were energetic indeed in trying to reject the disturbance. Very often such behaviour is not always welcomed, a smooth reaction to load disturbances is rather preferred especially when actuators are part of the system. One way to counteract this is to assign slower poles to the closed-loop characteristic equation at the cost of a slower recovery from this disturbance.

The second experiment considered the muscle relaxation system corrupted with a sequence of white noise. In order to ensure that the latter is white, its

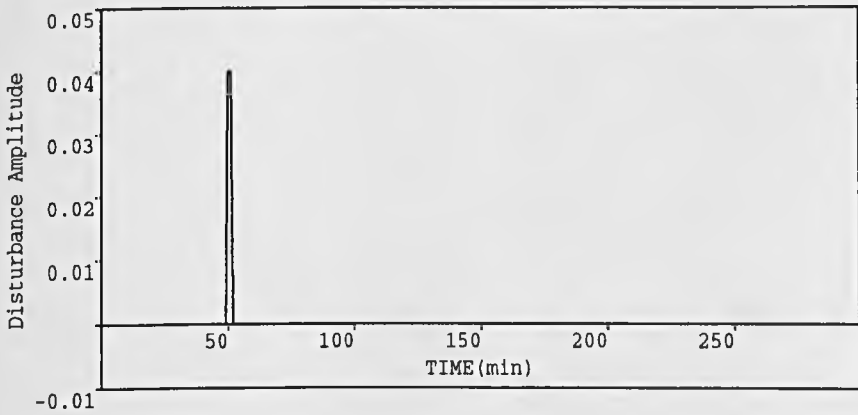
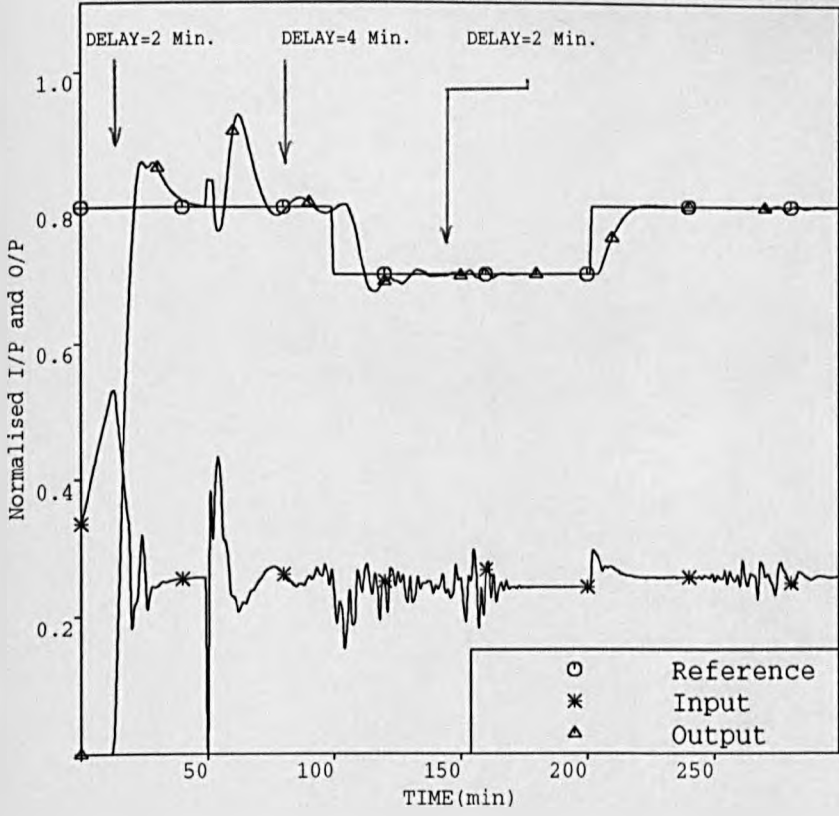


Figure 4.53. Same conditions as in figure (4.48) but with additive disturbance

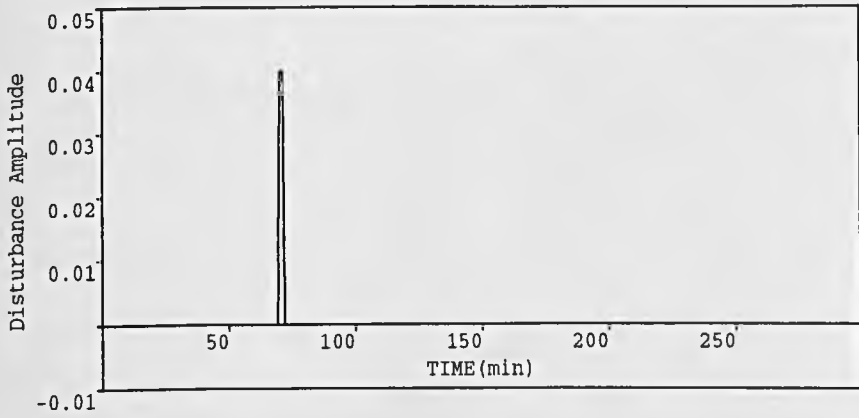
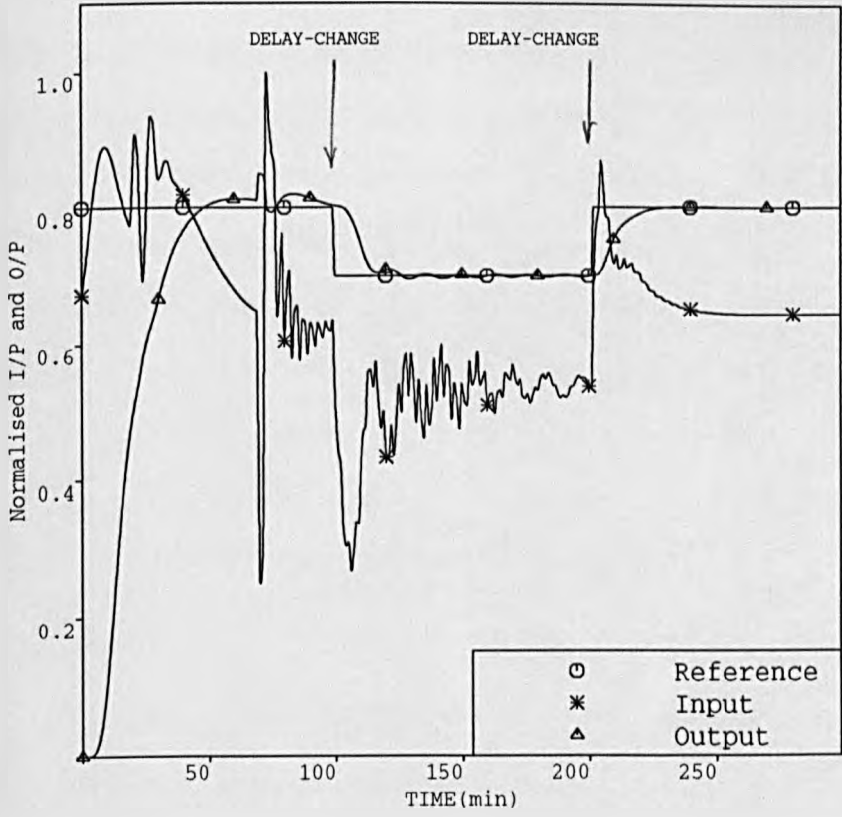


Figure 4.54. Same conditions as in figure (4.50)
but with additive disturbance

corresponding values at different values of time must be uncorrelated. In practice, it is rather difficult to generate such sequences but it is beyond the scope of this study to expand on the subject. However, a particularly attractive approximation to white or pseudo-random noise lies with the sequence normally known as PRBS (Pseudo-Random Binary Sequence). The technique is not complicated and moreover its associated amplitude and periodicity can easily be monitored. Many classes of such pseudo-noise sequences do exist and for the following the quadratic residue code or Legendre sequence was chosen. It corresponds to the following value of N (total number of bits in the sequence).

$$N = 4\alpha - 1 \quad (4.34)$$

where N is a Mersenne prime (Golomb, 1964), and α is an integer. In this way two levels of sequence x_i may be constructed by putting:

$$x_i = \begin{cases} + \text{ ampl.} & \text{if } i \text{ is a quadratic modulo } N \\ - \text{ ampl.} & \text{otherwise} \end{cases}$$

this is equivalent to finding those values of i for which:

$$i = t^2 - mN \quad (4.35)$$

where m is an integer such that:

$$mN + 1 \leq t^2 \leq (m + 1)N + 1 \quad (4.36)$$

Those values of i that satisfy these equations for $2 \leq t \leq \frac{(N-1)}{2} + 1$ give the locations in the sequence of one state in the binary digit. The state of the zeroth position may be chosen at will to make the average value of the sequence equal to either plus or minus $\frac{1}{N}$.

For the following experiments a value of 19 was chosen for N satisfying therefore equation (4.34) above. The amplitude of the PRBS was taken to be $\text{ampl.} = 1\%$.

Hence, the resulting sequence would be of the form:

- ampl. + ampl. - ampl. - ampl. + ampl. + ampl.
- + ampl. + ampl. - ampl. + ampl. - ampl. + ampl.
- ampl. - ampl. - ampl. - ampl. + ampl. + ampl. - ampl.

The whole sequence which was added to system's output was repeated as many times as the experiment required it. The conditions under which the muscle relaxation system was simulated are similar to those of figures (4.48) and (4.50). The value of the initial covariance matrix was taken to be $P = 10^2 \cdot I$, and the forgetting factor equal to 0.995. The initial parameter estimates were all taken to be 0.0. The results shown in figures (4.55) and (4.56) demonstrate how the adaptive controller coped well despite the persisting excitation of the PRBS signal, and the changing value of the time-delay. As a consequence, the parameter estimates obtained were poor and converged respectively to:

$$\begin{aligned} \hat{a}_1 &= -0.4345 & \hat{a}_2 &= -0.4346 & \hat{b}_1 &= 0.1399 & \hat{b}_2 &= -0.1518 \\ \hat{b}_3 &= 0.1478 & \hat{b}_4 &= 0.0395 & \hat{b}_5 &= 0.2228 \end{aligned}$$

for Pancuronium-Bromide, and

$$\begin{aligned} \hat{a}_1 &= -0.2716 & \hat{a}_2 &= -0.3515 & \hat{a}_3 &= -0.2963 \\ \hat{b}_1 &= -0.048 & \hat{b}_2 &= 0.0393 & \hat{b}_3 &= -0.0366 & \hat{b}_4 &= 0.0466 \end{aligned}$$

for Atracurium.

To conclude this chapter, it is worth mentioning that the foregoing results show clearly that the PIP scheme performed well under extensive simulation studies. Arising from the new concept of NMSS, it is simple to formulate. Moreover, because it is considered as an extension to the well known PI controller already applied to the muscle relaxation system, it represents an attractive candidate for a future clinical application. Results also showed little sensitivity of the algorithm to time-delay changes as the approach allowed for inclusion of the digital Smith

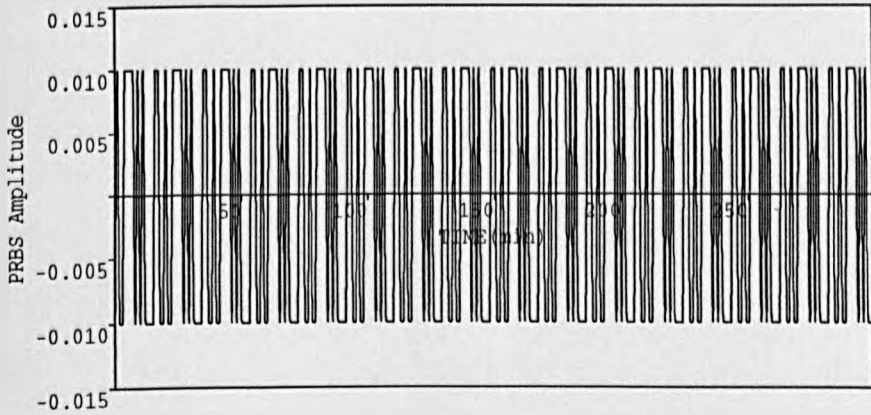
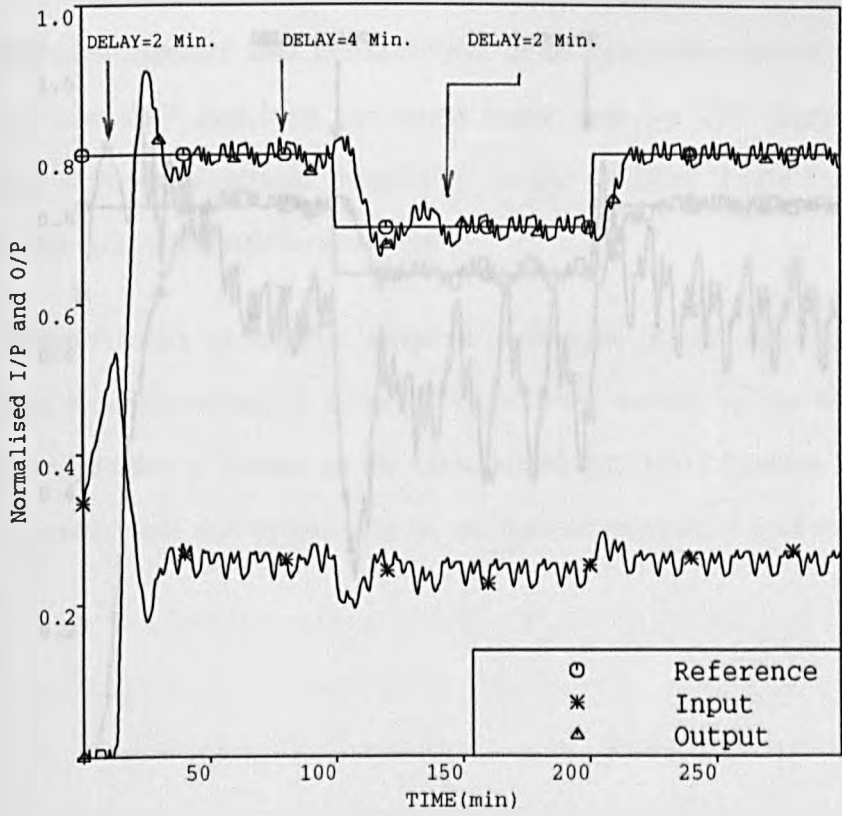


Figure 4.55. Same conditions as in figure (4.48)
but with additive noise

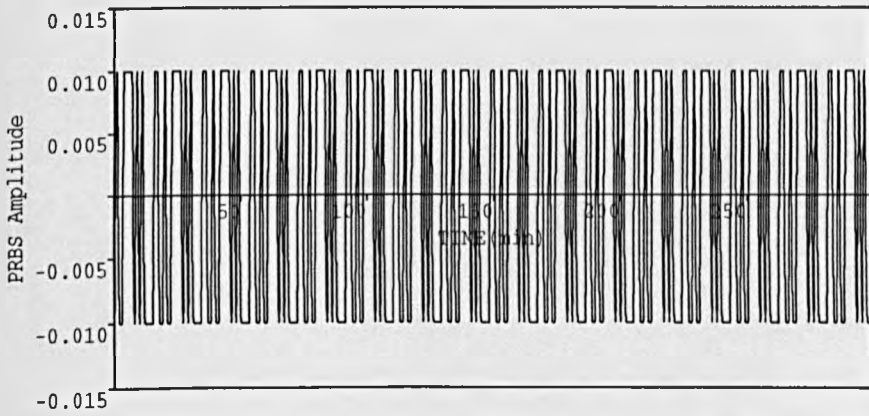
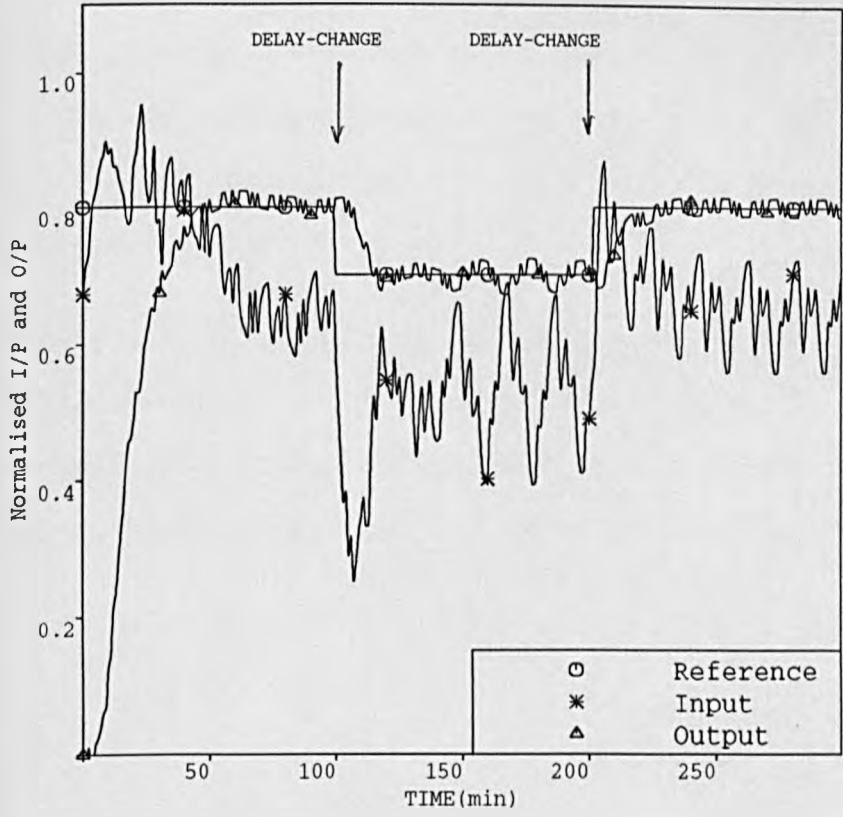


Figure 4.56. Same conditions as in figure (4.50)
but with additive noise

predictor ESP idea together with the technique of overparameterization under the GSP scheme. The GSP algorithm performed better than the ESP algorithm, but both schemes have demonstrated superiority to the classical Smith's approach, especially under heavy mismatch conditions.

The next chapter looks at another adaptive technique. Based on a predictive approach, it is specially aimed at solving the problems caused by the time-delay. Its associated algorithm is known as the Generalized Predictive Control algorithm (GPC). Its development and application to the muscle relaxation system will follow next.

CHAPTER 5

GENERALIZED PREDICTIVE CONTROL (GPC) OF MUSCLE RELAXANT ANAESTHESIA

5.1 INTRODUCTION

Designing controllers to overcome time-delays has always represented a serious challenge for engineers from almost all walks of life. Also the previous chapter proved that this challenge grows even bigger when the value of this time-delay is unknown or is prone to variations. PID controllers whose benefits are still so much praised within industry could prove ineffective in trying to overcome this problem. Indeed, despite their derivative action they are often unable to provide the right phase advance needed and consequently require retuning in order to encompass such variations, an operation which requires considerable trial and error efforts which could be tiresome and altogether time-consuming.

In cases with significant dead-times, the method of O.J.M Smith known as the **Smith predictor** has been shown to be very advantageous* indeed, but on the other hand its performance may deteriorate considerably in the presence of a large process mismatch, which has led industry to prefer the manually tuned classical PID networks which do not involve deriving realistic dynamic process models. This mismatch problem has always been one of the major topics for those who have been involved with time-delay systems (Marshall, 1979; Gawthrop, 1977) and the advent achieved in the computer technology in the 70's allowed self-tuning adaptive control, whose origin goes back to the 50's (Gregory, 1959), to emerge as another alternative for such a problem.

* See section 4.8.1

Early well known self-tuning adaptive algorithms included the minimum variance controller (MV) (Astrom and Wittenmark, 1973), the generalised minimum variance (GMV) with its refined version developed by Clarke and Gawthrop (1975, 1979), and the pole-placement algorithm (Wellstead et al., 1978a, 1978b). Over the years these methods proved to be far superior to the classical PID controllers providing the model order as well as the corresponding dead-time value are carefully selected. Indeed, the MV controller showed high sensitivity to a wrongly assumed or variable value of time-delay, whereas the improved version of Clarke and Gawthrop (GMV) was somewhat more robust providing it is rightly detuned. Practical work also showed that the pole-placement approach is robust against this assumption (the delay-value is enhanced within the numerator polynomial of the discrete-time transfer function), but overparameterization often leads to common factors in the estimated polynomials resulting in deterioration of the controller performance.

Since the emergence of self-tuning adaptive techniques as a powerful tool for handling complex design problems, it has always been the dream of plant engineers to be able to come up with an algorithm which would eventually assemble the advantages of the above cited approaches while rejecting their drawbacks. Long-range predictive control algorithms (LRPC) seem to some extent to satisfy such hopes. The principle of this approach will be clearer in the next sections. Suffice to say here that the late 70's witnessed the development of a number of computer control algorithms which used long-range predictions of the process output. Early work involved the development of the model algorithmic control algorithm (MAC) (Richalet et al., 1978), in which the output of a linear time-invariant system at discrete time instants is described by means of a discrete impulse response. The algorithm then makes use of an approximation of this system's impulse response

by a finite number of terms, which reflects the so called **prediction horizon**.

Also during that period, the dynamic matrix control algorithm (DMC) (Cutler and Ramaker, 1980) enjoyed great popularity. Evolving from a technique that represents process-dynamics with a set of numerical coefficients together with a least-squares formulation, it promised to solve complex control problems, especially those associated with systems exhibiting large dead-times.

In contrast to the MAC and DMC approaches where the process is described by dynamic impulses or step responses, the extended prediction self-adaptive control algorithm (EPSAC) (De Keyser and Van Cauwenberghe, 1979a, 1979b, 1985) uses an ARMA** model representation of the process dynamics. The one-step ahead predictor is computed by means of a prediction model whose parameters are estimated using a recursive (extended) least-squares method. The algorithm is also able to predict the process over a range which is usually taken greater than the maximum anticipated value of time-delay. The key assumption that all control increments beyond this prediction range are taken to be nil is one characteristic of this algorithm.

The extended adaptive control algorithm (EHAC) (Ydstie, 1984) uses almost the same parametric process model as in the EPSAC version. Its fundamental idea is to compute at each sampling instant a sequence of inputs that satisfy a criterion over the chosen prediction horizon which is the only design parameter in the method.

Reported applications within industry showed that Richalet's algorithm (MAC) is unsuitable for non-minimum phase plants, but the DMC, EPSAC as well as EHAC

** Auto-Regressive Moving Average

algorithms seem to be very effective. However, one criticism that was acknowledged is that they in fact either have a unique or relatively few design parameters. For instance, the EPSAC approach uses the prediction horizon, a weighting sequence and a model reference polynomial to accomplish a full design study, while the EHAC algorithm requires only the choice of the prediction horizon parameter. Consequently, albeit simple to formulate, the above methods do suffer from a certain loss of design flexibility vital for robustness. More recent research has seen the development of an algorithm based on the same idea of long-range predictive control (LRPC) but tailored, first to retain advantages of the previously formulated algorithms, i.e. easy to commission, and second to add more flexibility in its design, leaving therefore the user with a wider variety of parameters to arrive at the preset goal. It is known as the Generalized Predictive Control algorithm (GPC) (Clarke et al., 1987a, 1987b) and is considered to be the most robust technique yet to exist. Based on an explicit formulation, it combines the advantages of the GMV approach as well as those of the pole-placement algorithm while rejecting their respective drawbacks. The next section looks at the mathematical background behind this new approach and outlines the different steps that finally lead to the formulation of the general control law.

5.2 DEVELOPMENT OF THE BASIC SISO GPC ALGORITHM

5.2.1 The CARIMA Process Model Representation and Output Prediction

It is known that the so called ARMAX/CARMA*** models, which linearize processes locally, have been used in many self-tuning control algorithms (Seborg

*** Controlled Auto-Regressive Moving Average

et al., 1986). Following earlier work by Astrom and Wittenmark (1973), it was assumed that the disturbance is stationary with rational spectral density giving the following representation:

$$y(t) = \frac{B_1(z^{-1})}{A(z^{-1})} u(t - k) + \frac{C(z^{-1})}{A(z^{-1})} \zeta(t) \quad (5.1)$$

where $A(z^{-1})$, $B_1(z^{-1})$, and $C(z^{-1})$ are polynomials in the backward shift operator z^{-1} of the form:

$$\begin{aligned} A(z^{-1}) &= 1 + a_1 z^{-1} + a_2 z^{-2} + \dots + a_n z^{-n} \\ B_1(z^{-1}) &= b_1 + b_2 z^{-1} + b_3 z^{-2} + \dots + b_m z^{-m+1} \\ C(z^{-1}) &= 1 + c_1 z^{-1} + c_2 z^{-2} + \dots + c_p z^{-p} \end{aligned}$$

$y(t)$ is the process output, $u(t)$ is the control signal delayed by k samples, and $\zeta(t)$ is a sequence of random variables all having a variance σ^2 and a mean of zero. It is also assumed that all roots of the $C(z^{-1})$ lie inside the unit circle in the z -plane.

Although the above model formulation has provided good control basis for minimum variance (MV) regulators as well as pole-placement algorithms, it was on the other hand found to be sensitive to processes whose additive noise did not have zero-mean. To avoid offset, Clarke and Gawthrop (1979) extended the model of equation (5.1) to include a constant d leading to a general representation of the form:

$$y(t) = \frac{B_1(z^{-1})}{A(z^{-1})} u(t - k) + \frac{C(z^{-1})}{A(z^{-1})} \zeta(t) + d \quad (5.2)$$

When this term is constant this type of representation has proven quite effective, but difficulties may arise when it is varying. To alleviate this problem, an attempt could be made to estimate its value by extending the data measurement vector to include the "1" albeit this idea is not always successful since the "1" in the data

vector is not a persistent exciting signal (Tuffs and Clarke, 1985). Hence, in order to avoid this term and at the same time counteract its influence a model representation in which the zero-mean stochastic disturbance $\zeta(t)$ is assumed to be **integrated** before affecting the process was successfully used by Harris et al. (1980) and Belanger (1983). This latter paper considered its inclusion within the GMV design of Clarke and Gawthrop (1975), and Tuffs and Clarke (1985) did in fact use it as a basis for the same algorithm. Because of its integrating nature, this form of representation is better known as the **CARIMA®** model representation and takes the form of:

$$y(t) = \frac{B_1(z^{-1})}{A(z^{-1})} u(t - k) + \frac{C(z^{-1})}{A(z^{-1}) \Delta} \zeta(t) \quad (5.3)$$

Here Δ is the differencing operator in the backward shift z^{-1} .

Appending the common factor Δ to the polynomials $B_1(z^{-1})$ and $A(z^{-1})$ in the above equation leads to:

$$A(z^{-1}) \Delta y(t) = B_1(z^{-1}) \Delta u(t - k) + C(z^{-1}) \zeta(t) \quad (5.4)$$

equation (5.4) forms the basis of the model parameter estimation using a measurement vector and a data vector of the form:

$$\begin{aligned} \Phi^T &= [- \Delta y(t - 1), \dots, \Delta u(t - k - 1), \dots, \zeta(t - 1), \dots, \zeta(t - p)] \\ \varepsilon(t) &= \Delta y(t) - \Phi^T \hat{\Theta}(t-1) \end{aligned}$$

At this stage it is worth noting that the formulation of equation (5.3) is important, since the offset problem is inherently solved due to the zero-mean nature of the data leaving therefore the estimation of the "d" term no longer necessary.

As in the GMV case, to derive a "j" step ahead predictor of $y(t + j)$ based on the

® Controlled Auto-Regressive Integrated Moving Average

model of equation (5.4), let us consider the following identity:

$$C(z^{-1}) = E_j(z^{-1}) A(z^{-1}) \Delta + z^{-j} F_j(z^{-1}) \quad (5.5)$$

where $E_j(z^{-1})$, $F_j(z^{-1})$ are polynomials in the backward shift z^{-1} completely and uniquely defined given $A(z^{-1})$ and the integer "j", and of the form:

$$\begin{aligned} E_j(z^{-1}) &= e_0 + e_1 z^{-1} + e_2 z^{-2} + \dots + e_{j-1} z^{-j+1} \\ F_j(z^{-1}) &= f_{j0} + f_{j1} z^{-1} + f_{j2} z^{-2} + \dots + f_{jn} z^{-n} \end{aligned}$$

Equation (5.5) is better known as the Diophantine equation (Kucera, 1979).

Let $C(z^{-1}) = 1$ with no loss of generality and enhance the values of k which are greater than 1 within the $B_1(z^{-1})$ polynomial such that:

$$z^{-k} B_1(z^{-1}) = z^{-1} B(z^{-1})$$

Model (5.4) and equation (5.5) respectively become:

$$A(z^{-1}) \Delta y(t) = B(z^{-1}) \Delta u(t-1) + \zeta(t) \quad (5.6)$$

$$1 = E_j(z^{-1}) A(z^{-1}) \Delta + z^{-j} F_j(z^{-1}) \quad (5.7)$$

Multiplying equation (5.6) by $E_j z^j$ leads to:

$$E_j(z^{-1}) z^j A(z^{-1}) \Delta y(t) = E_j(z^{-1}) z^j (B(z^{-1}) \Delta u(t-1) + \zeta(t)) \quad (5.8)$$

Developing and rearranging by noting that:

$$\begin{aligned} z^j y(t) &= y(t + j) \\ z^j u(t) &= u(t + j) \end{aligned}$$

equation (5.8) becomes:

$$E_j(z^{-1}) \Delta y(t + j) = E_j(z^{-1}) B(z^{-1}) \Delta u(t + j - 1) + E_j(z^{-1}) \zeta(t + j) \quad (5.9)$$

but from equation (5.7) it follows that,

$$E_j(z^{-1}) A(z^{-1}) \Delta = 1 - z^{-j} F_j(z^{-1})$$

hence, equation (5.9) becomes:

$$y(t+j) = E_j(z^{-1}) B(z^{-1}) \Delta u(t+j-1) + F_j(z^{-1}) y(t) + E_j(z^{-1}) \zeta(t+j) \quad (5.10)$$

Because $E_j(z^{-1})$ is of degree $j-1$ only, the noise components are all in the future. If $\zeta(t)$ is an uncorrelated random sequence, the term $E_j(z^{-1}) \zeta(t+j)$ is moving average of order $j-1$. Therefore the optimal "j" step ahead predictor becomes:

$$\begin{aligned} \hat{y}(t+j) &= G_j(z^{-1}) \Delta u(t+j-1) + F_j(z^{-1}) y(t) \\ G_j(z^{-1}) &= E_j(z^{-1}) B(z^{-1}) \end{aligned} \quad (5.11)$$

This expression suggests that in contrast to Clarke and Gawthrop's algorithm which uses only one prediction of the form $y(t+k)$ the GPC approach considers a whole set of predictions depending on how far the prediction horizon "j" is extended. Also the same equation normally needs to be solved for each value of "j" considered, but instead a recursive formula is imposed on the Diophantine equation (5.7) leading to straightforward and less computational calculations in equation (5.11) as the next section endeavours to show.

5.2.2 Recursion of the Diophantine Equation

As pointed out earlier, the aim is to establish a recursion between the elements of equation (5.7) for one horizon and the elements of the one immediately next to it, so that starting with a value of $j = 1$, the elements of the same equation could be found for $j = 2$ which themselves would serve to find the elements for $j = 3$ and so forth.

For that purpose recall the expression of the Diophantine equation (5.7)

$$1 = E_j(z^{-1}) A(z^{-1}) \Delta + z^{-j} F_j(z^{-1}) \quad (5.7)$$

For notation purposes, it is assumed here that;

For the horizon "j", $E = E_j(z^{-1})$, and $F = F_j(z^{-1})$

and for the next horizon "j+1", $R = E_{j+1}(z^{-1})$, and $S = F_{j+1}(z^{-1})$

For the horizon "j" and immediately the horizon next to it "j+1" it follows that:

$$\begin{aligned} 1 &= E \tilde{A} + z^{-j} F \\ 1 &= R \tilde{A} + z^{-j+1} S \end{aligned} \quad (5.12)$$

where $\tilde{A} = A \Delta$

Subtracting the two identities leads to:

$$0 = (R - E) \tilde{A} + z^{-j} (z^{-1} S - F) \quad (5.13)$$

Recall that the polynomial E is of degree "j-1", consequently polynomial R is of degree "j" and so is polynomial R - E which could be split into two parts, i.e:

$$R - E = \tilde{R} + r_j z^{-j} \quad (5.14)$$

Substituting equation (5.14) into equation (5.13) gives:

$$\tilde{A} \tilde{R} + z^{-j} (z^{-1} S - F + \tilde{A} r_j) = 0 \quad (5.15)$$

Equation (5.15) is of the form:

$$\alpha \tilde{A} + z^{-j} \beta = 0$$

where

$$\begin{aligned} \alpha &= \tilde{R} \\ \beta &= r_j \tilde{A} + z^{-1} S - F \end{aligned}$$

and it is an equation system equivalent to:

$$\begin{cases} \alpha = 0 \\ \beta = 0 \end{cases}$$

i.e,

$$\begin{cases} \tilde{R} = 0 \\ r_j \tilde{A} + z^{-1} S - F = 0 \end{cases} \quad (5.16)$$

or:

$$\begin{cases} \tilde{R} = 0 \\ S = z (F - r_j \tilde{A}) \end{cases} \quad (5.17)$$

The polynomial $A(z^{-1})$ has "1" as a leading element and so does \tilde{A} . Because the second expression of equation (5.17) has "z" as an external factor and if " f_0 " is the leading element of polynomial "F", then:

$$r_j = f_0 \quad (5.18)$$

Let "i" be an index varying from 0 to the degree of polynomial $A(z^{-1})$ "n". Based upon equation system (5.17), the components of higher powers of polynomial S can be obtained by the following recursion formula:

$$\begin{cases} s_i = f_{i+1} - \tilde{a}_{i+1} r_j \\ 0 \leq i \leq n \end{cases} \quad (5.19)$$

Taking into account equation (5.16), equation (5.13) becomes:

$$R - E = r_j z^{-j} \quad (5.14)$$

i.e.,

$$R = E + r_j z^{-j}$$

or

$$E_{j+1}(z^{-1}) = E_j(z^{-1}) + r_j z^{-j} \quad (5.20)$$

and using equation (5.11) of section (5.2.1) yields:

$$G_{j+1}(z^{-1}) = B(z^{-1}) R \quad (5.21)$$

Finally, the solution of the Diophantine equation can be summarized by equations (5.18), (5.19) together with equations (5.20) and (5.21) as:

$$\begin{cases} r_j = f_0 \\ s_i = f_{i+1} - \tilde{a}_{i+1} r_j \\ E_{j+1} = E_j(z^{-1}) + r_j z^{-j} \\ G_{j+1}(z^{-1}) = B(z^{-1}) E_{j+1}(z^{-1}) \end{cases} \quad (5.22)$$

Equations (5.22) represent the procedure for implementing the GPC algorithm in a self-tuning manner. Because the four above expressions are based upon a recursive

formula, the first iteration has to be initialised. Therefore for $j = 1$ equation (5.7) becomes:

$$1 = E_1(z^{-1}) \tilde{A}(z^{-1}) + F_1(z^{-1}) \cdot z^{-1} \quad (5.23)$$

Because \tilde{A} has "1" as a leading element then:

$$E_1(z^{-1}) = 1$$

Substituting in equation (5.23) leads to:

$$F_1(z^{-1}) = z (1 - \tilde{A}(z^{-1}))$$

Summarizing:

For $j = 1$

$$\begin{cases} E_1(z^{-1}) = 1 \\ F_1(z^{-1}) = z (1 - \tilde{A}(z^{-1})) \end{cases} \quad (5.24)$$

Having established a useful recursion which will enable one to easily and quickly calculate the parameters of the Diophantine equation (5.7), the next section examines the main steps involved in the principle of long-range prediction and its correlation with the GPC control law which is later derived.

5.2.3 The Long-Range Predictive Control Principle and the GPC Control Law

It has always been the argument for predictive control that as the process-time-delay is "k", the first output that can be influenced by the current control $u(t)$ is $y(t + k)$. For a purely stochastic regulation, if an optimal prediction of the direct effect $\zeta(t + k)$ is available at time "t", the control $u(t)$ can be optimally chosen to neutralise it. Obviously, how effective this control is depends largely on the inter-

val along which the prediction is realised. A logical choice would undoubtedly suggest it to be at least made equal to the expected value of time-delay. In fact, the idea of extending the prediction interval over a range which possibly goes far beyond this value of dead-time is known as **Long-Range Prediction (LRP)** (De Keyser and Van Cauwenberghe, 1983) and whose strategy, which is also illustrated in figure (5.1), could be summarized in the following 3 steps:

Step 1

- At each present moment "t" a forecast is made of the process output, over a long-range prediction interval which we call the **horizon**, by means of a mathematical model of the process dynamics, and is a function of the future control policy that is only to be applied at this moment "t"

Step 2

- As a result of this forecast, several control actions will be proposed but only the strategy which drives the predicted output back to the predefined set-point in the best possible way* will be selected.

Step 3

- The retained candidate is then applied to the process as the control action at the moment "t".

The three steps are then repeated at the next sample.

To be able to duplicate the whole strategy (also known as the **Receding Horizon Approach**) on a digital computer, the mathematical background behind the GPC control law which uses the same principle is considered next.

* According to the criteria preset by the user himself

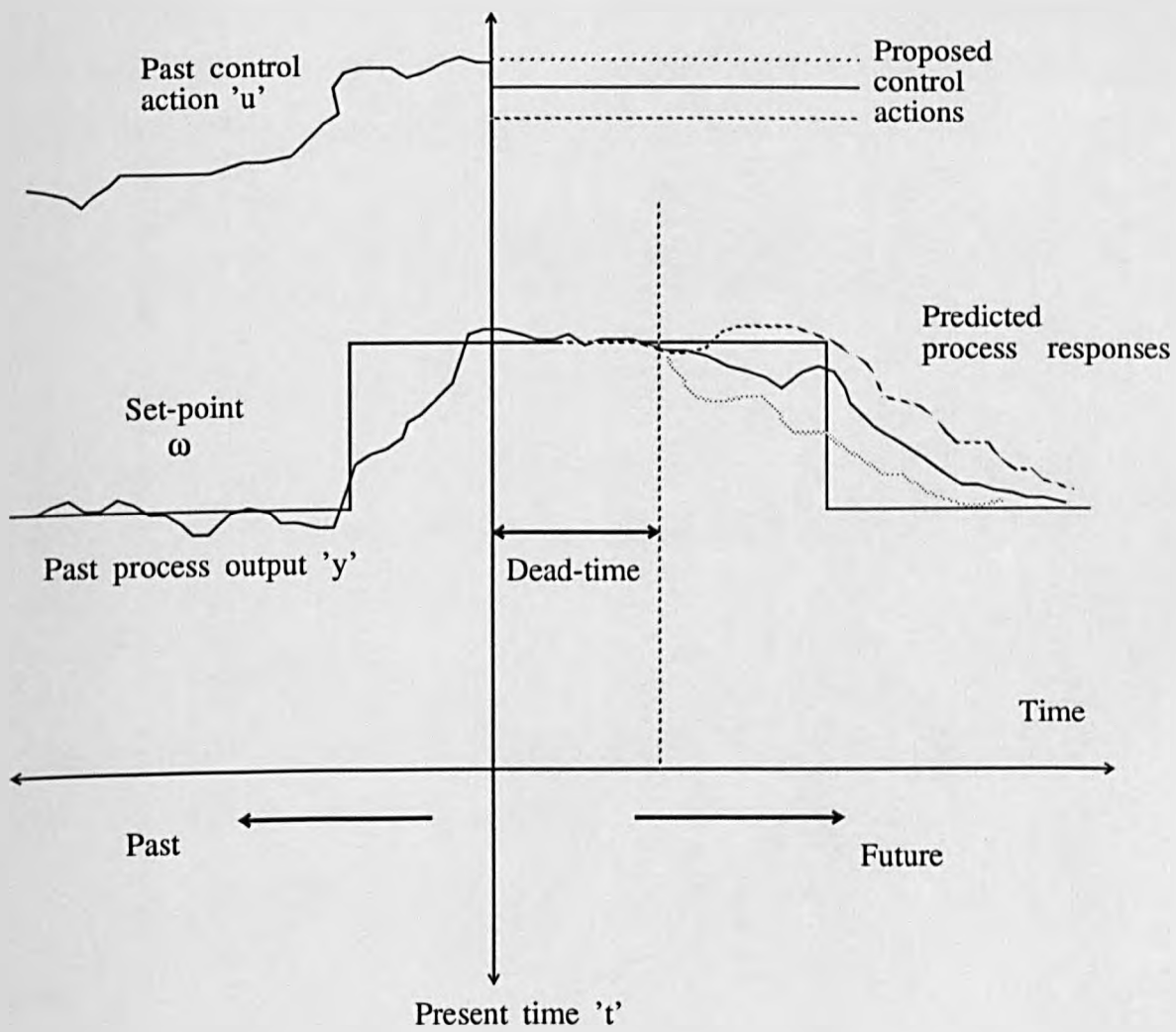


Figure 5.1. Long-range predictive control (LRPC)

Consider the following future set-point sequence, $\omega(t + j)$ $j = 1, 2, \dots$.

As is the case for most LRPC algorithms, a smooth rather than a sudden approach from the current output position $y(t)$ to the set-point $\omega(t)$ is preferred by filtering the present and future set-points using a first order lag model of the form:

$$\begin{cases} \omega(t) = y(t) \\ T_{\text{lag}}(z^{-1}) = \frac{1 + \alpha}{1 - \alpha z^{-1}} = \frac{\omega(t + j)}{\omega(t)} \quad j = 1, 2, \dots \\ \alpha = -e^{-\frac{T_s}{T_c}} \approx -1 \quad T_s \text{ is the sampling time} \end{cases} \quad (5.25)$$

As illustrated in figure (5.2), the objective of the GPC controller is to drive the process output close to the set-point. GPC also computes the vector of controls using a cost function of the form:

$$J = J_{\text{GPC}}(e, \bar{u})$$

where: \bar{u} is a vector of increments of u , and e is the predicted future system-errors. J is a quadratic function of the form:

$$J_{\text{GPC}} = \sum_{j=N_1}^{j=N_2} e^2(t + j) + \sum_{j=1}^{j=N_2} \lambda_j \Delta u^2(t + j - 1) \quad (5.26)$$

with:

N_1 : The minimum costing horizon

N_2 : The maximum costing horizon

λ_j : The control weighting sequence

Consider equation (5.11) which models the future outputs. For different values of j ranging from 1 to N it follows that:

$$\begin{aligned} y(t + 1) &= G_1(z^{-1}) \Delta u(t) + F_1(z^{-1}) y(t) + E_1(z^{-1}) \zeta(t + 1) \\ y(t + 2) &= G_2(z^{-1}) \Delta u(t + 1) + F_2(z^{-1}) y(t) + E_2(z^{-1}) \zeta(t + 2) \\ &\cdot \quad \cdot \quad \cdot \quad \cdot \quad \cdot \\ &\cdot \quad \cdot \quad \cdot \quad \cdot \quad \cdot \\ &\cdot \quad \cdot \quad \cdot \quad \cdot \quad \cdot \\ y(t + N) &= G_N(z^{-1}) \Delta u(t + N - 1) + F_N(z^{-1}) y(t) + E_N(z^{-1}) \zeta(t + N) \end{aligned} \quad (5.27)$$

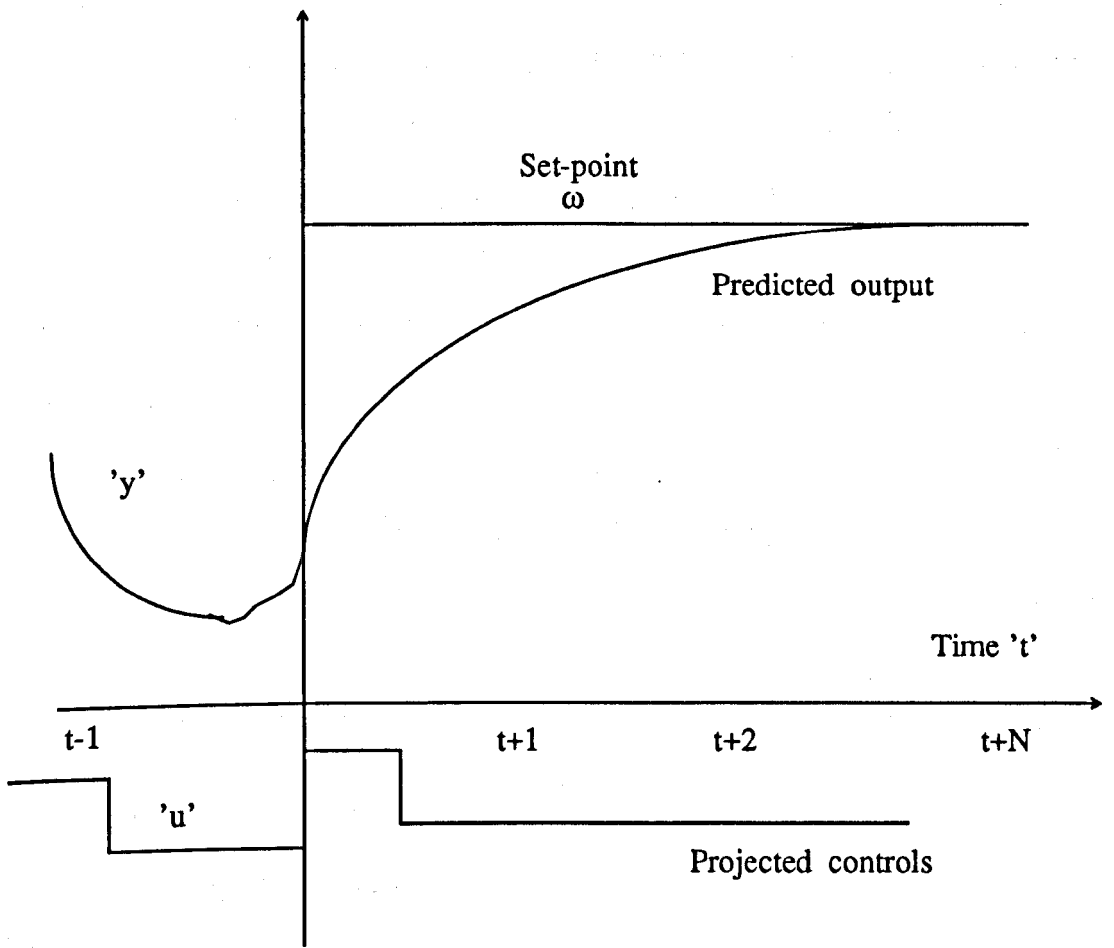


Figure 5.2. Preprogrammed set-point in GPC

Because $y(t + j)$ includes signals that are in the present and past time and consequently can be known, as well as signals in the future which are unknown, let its expression be split into those two categories. Hence, let $f(t + j)$ $j = 1, 2, 3, \dots$ be that component of the signals which are known at time "t", such that:

$$G_j(z^{-1}) = g_{j0} + g_{j1} z^{-1} + \dots + g_{j\delta B} z^{-j - \delta B + 1}$$

$\delta B = \text{degree of polynomial } B(z^{-1})$

then $f(t + j)$ would include all signals of $y(t + j)$ minus its future unknown components, i.e:

$$\begin{aligned} f(t + 1) &= [G_1(z^{-1}) - g_{10}] \Delta u(t) + F_1(z^{-1}) y(t) \\ f(t + 2) &= z [G_2(z^{-1}) - g_{21} z^{-1} - g_{10}] \Delta u(t) + F_2(z^{-1}) y(t) \\ &\quad \cdot \quad \quad \quad \cdot \quad \quad \quad \cdot \quad \quad \quad \cdot \\ &\quad \cdot \quad \quad \quad \cdot \quad \quad \quad \cdot \quad \quad \quad \cdot \\ &\quad \cdot \quad \quad \quad \cdot \quad \quad \quad \cdot \quad \quad \quad \cdot \\ f(t + N) &= z^{N-1} [G_N(z^{-1}) - \dots - g_{N0}] \Delta u(t) + F_N y(t) \end{aligned} \tag{5.28}$$

Note that,

$$g_{ji} = g_i \quad \text{for } i = 0, 1, 2, \dots < j$$

i.e.

$$\begin{aligned} g_{10} &= g_{20} = \dots = g_{N0} \\ g_{21} &= g_{31} = \dots = g_{N1} \\ &\quad \cdot \quad \quad \cdot \quad \quad \cdot \quad \quad \cdot \\ &\quad \cdot \quad \quad \cdot \quad \quad \cdot \quad \quad \cdot \end{aligned}$$

Written in matrix form, system (5.27) becomes:

$$\hat{y} = G \tilde{u} + f \tag{5.29}$$

where,

$$\begin{aligned} \hat{y} &= [\hat{y}(t + 1), \hat{y}(t + 2), \dots, \hat{y}(t + N)] \\ \tilde{u} &= [u(t), u(t + 1), \dots, u(t + N - 1)] \\ f &= [f(t + 1), f(t + 2), \dots, f(t + N)] \end{aligned}$$

and the matrix G which is associated with the present and future control

increments is lower triangular of dimension $N \times N$ and of the form:

$$G = \begin{bmatrix} g_0 & 0 & \dots & 0 \\ g_1 & g_0 & \dots & 0 \\ g_2 & g_1 & \dots & \cdot \\ g_3 & g_2 & \dots & \cdot \\ \cdot & \cdot & \dots & \cdot \\ \cdot & \cdot & \dots & 0 \\ \cdot & \cdot & \dots & 0 \\ g_{N-1} & g_{N-2} & \dots & g_0 \end{bmatrix}$$

At this stage the three steps generally formulated for the receding horizon philosophy could be adapted to the GPC case and are in effect equivalent to the following:

Step 1

- At each sampling instant "t", the free response of the process is computed based on known data [$y(t)$, $y(t-1)$, ..., $u(t-1)$,...]]

Step 2

- The control increment vector \tilde{u} is computed using the optimizing routine of equation (5.26) with given set-points.

Step 3

- The first control signal $u(t)$ is extracted and applied to the process and all sequences are shifted in preparation for the next sample to repeat the same procedure. Figure (5.3) in a form of a diagram illustrates such a prediction sequence.

Recall equation (5.26)

$$J_{GPC} = \sum_{j=N_1}^{j=N_2} e^2(t+j) + \sum_1^{j=N_2} \lambda_j \Delta u^2(t+j-1) \quad (5.26)$$

where,

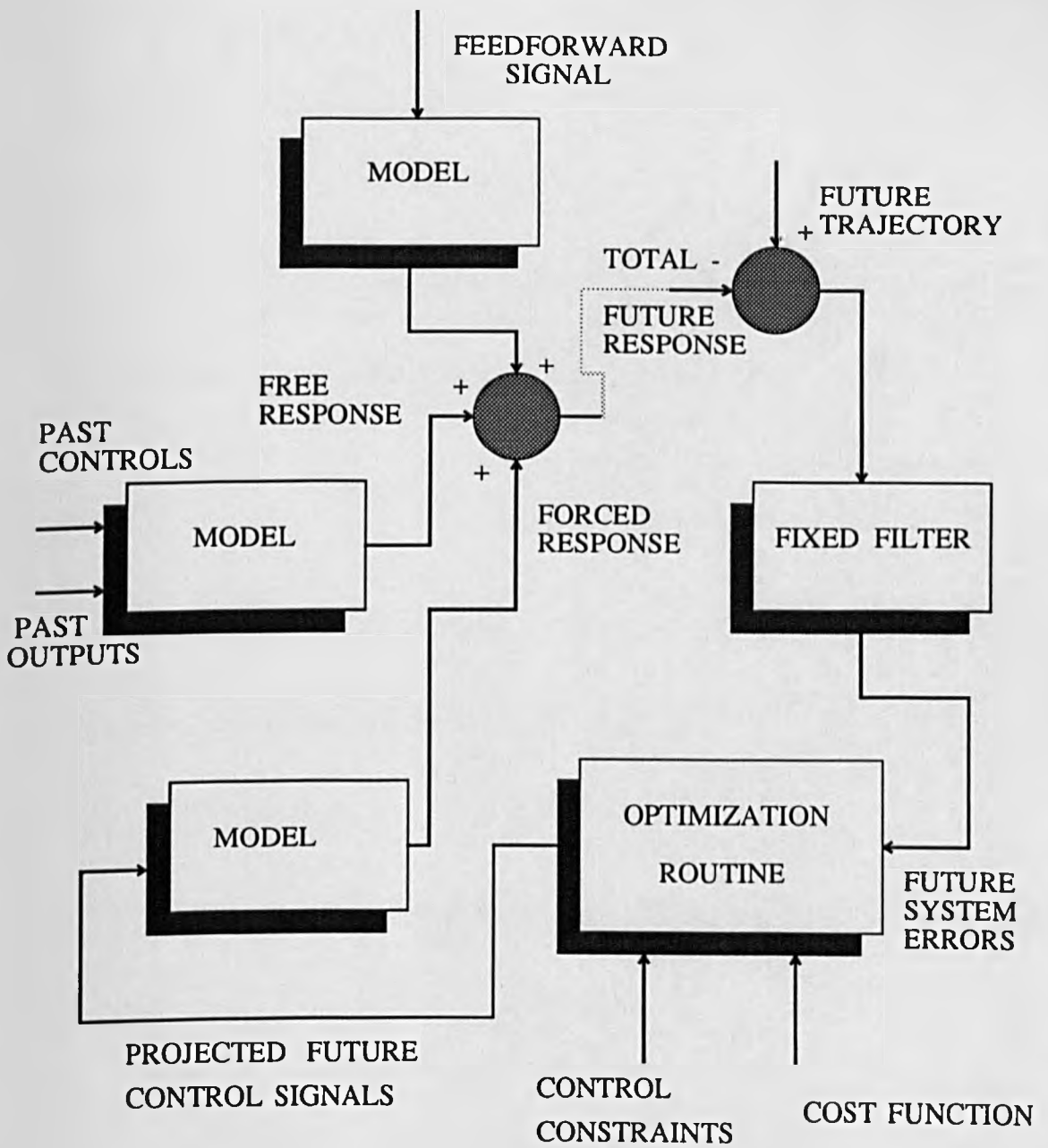


Figure 5.3. Optimization in GPC

$$e(t + j) = \hat{y}(t + j) - \omega(t + j)$$

$\omega(t + j)$ being the future set-points.

Therefore,

$$J_{\text{GPC}} = \sum_{j=N_1}^{j=N_2} (\hat{y}(t + j) - \omega(t + j))^2 + \sum_{j=1}^{j=N_2} \lambda_j \Delta u^2(t + j - 1) \quad (5.30)$$

The expectation of such a cost function can be expressed as:

$$J_1 = E \left\{ J_{\text{GPC}}(1, N) \right\}$$

or

$$J_1 = E \left\{ (\hat{y} - \omega)^T (\hat{y} - \omega) + \lambda_j \tilde{u}^T \tilde{u} \right\}$$

Using equation (5.29) for \hat{y} it follows that:

$$J_1 = E \left\{ (G \tilde{u} + f - \omega)^T (G \tilde{u} + f - \omega) + \lambda_j \tilde{u}^T \tilde{u} \right\}$$

The minimization of J_1 assuming **no constraints** on future controls requires:

$$\frac{\partial J_1}{\partial \tilde{u}^T} = 0$$

$$\frac{\partial}{\partial \tilde{u}^T} [(G \tilde{u} + f)^T (G \tilde{u} + f) - \omega^T (G \tilde{u} + f) - (G \tilde{u} + f)^T \omega + \omega^T \omega + \tilde{u}^T \lambda \tilde{u}] = 0$$

or,

$$\frac{\partial}{\partial \tilde{u}^T} [(\tilde{u}^T G^T + f^T) (G \tilde{u} + f) - \omega^T (G \tilde{u} + f) - (\tilde{u}^T G^T + f^T) \omega + \omega^T \omega + \tilde{u}^T \lambda \tilde{u}] = 0$$

Developing the expressions inside the external brackets and rearranging leads to:

$$2 G^T G \tilde{u} + 2 G^T f - 2 G^T \omega + 2 \lambda I \tilde{u} = 0$$

or,

$$(G^T G + \lambda I) \bar{u} + G^T (f - \omega) = 0$$

Finally,

$$\bar{u} = (G^T G + \lambda I)^{-1} G^T (\omega - f) \quad (5.31)$$

Since only the first increment is to be considered, the current control $u(t)$ is given by:

$$u(t) = u(t-1) + \bar{g}^T (\omega - f) \quad (5.32)$$

where,

\bar{g}^T is the first row of the matrix $(G^T G + \lambda I)^{-1} G^T$.

As it stands, the algorithm would constitute a heavy computational burden if used in a self-adaptive manner due to the inversion of the matrix $(G^T G + \lambda I)$ in equation (5.31), in addition to the difficulties that would emerge if the same matrix is ill conditioned (singular), an envisaged possibility especially if the value of the process dead-time is wrongly assumed.

Although the latter handicap could be avoided by choosing an appropriate value of the weighting sequence λ , a simpler and effective solution in which an assumption is made about future controls has been proposed and represents the real power of the GPC algorithm.

Indeed, the key question in long-range predictive control is what assumption to make about future control actions. In the DMC approach (Cutler and Ramaker, 1980), movements of the manipulated variable (input variable) are considered for a number of intervals of time into the future. How far into the future these movements are allowed to be free is left to the user. GPC has also borrowed the same idea by assuming that after an interval NU ($NU \leq N_2 - 1$) called the **control horizon**, projected control increments are assumed to be nil, i.e:

$$\Delta u(t + j - 1) = 0 \quad j \geq NU + 1$$

This has the advantage of stabilizing non-minimum phase systems even if $\lambda = 0$, as well as reducing the computational burden since the matrix G above reduces to the matrix G_1 of dimension $N \times NU$ instead of $N \times N$, i.e:

$$G_1 = \begin{bmatrix} g_0 & 0 & \dots & 0 \\ g_1 & g_0 & \dots & 0 \\ g_2 & g_1 & \dots & \cdot \\ g_3 & g_2 & \dots & \cdot \\ \cdot & \cdot & \dots & \cdot \\ \cdot & \cdot & \dots & 0 \\ \cdot & \cdot & \dots & 0 \\ g_{N-1} & g_{N-2} & \dots & g_{N-NU} \end{bmatrix}$$

leading therefore to a general control law of the form:

$$\bar{u} = (G_1^T G_1 + \lambda I)^{-1} G_1^T (\omega - f) \quad (5.33)$$

It is apparent from the above equation that the matrix to be inverted is only of dimension $(NU \times NU)$, and if $NU = 1$, the same operation reduces to the usual scalar inversion.

5.2.4 The GPC Algorithm and the Selection of its Tuning Parameters

Like all self-tuning algorithms GPC possesses parameters that should be tuned to allow one to satisfactorily reach a certain predefined point. These parameters which constitute "tuning knobs" have been introduced when formulating equation (5.26), i.e: the minimum output horizon N_1 , the maximum output horizon N_2 , the control weighting sequence λ , and last but not least the control horizon NU . In the following, interpretations as well as general guidelines for the selection of each of the above parameters are given and further details can be found in Clarke and

Mohtadi (1989).

a) The Minimum Output Horizon N_1

The choice of this parameter is directly related to the process time-delay k . If its value is exactly known, N_1 should be set to this value, since the $(k-1)$ rows of the matrix G_1 will be equal to zero. However, if this value is unknown or is subject to variations, N_1 should be set to 1 with no loss of generality.

b) The Maximum Output Horizon N_2

Theoretically, N_2 should be chosen to exceed the degree of polynomial $B(z^{-1})$, that is, if the delay is enhanced within the expression of this polynomial as seen in section 4.8.2 the prediction horizon (N_2) should go beyond the maximum value of this time-delay which is anticipated. It was also found that for first order systems, N_2 should be chosen such that it exceeds $\delta B + 1$ (Clarke and Mohtadi, 1989), and for higher order processes N_2 should be equal to $2n - 1$, n being the order of the plant integrator included (equal to $\max(\text{order } A(z^{-1}) + 1, \text{order } B(z^{-1}))$). However, larger values of N_2 which correspond to the rise time of the process were also considered appropriate.

c) The Control Horizon NU

As mentioned before this factor determines the degree of freedom in future control increments. A value of NU of 1 usually gives satisfactory results, while values greater than 1 lead to a more activated control.

d) The Control Weighting Sequence λ_1

It is known that the GMV algorithm (Clarke and Gawthrop, 1975) stabilizes non-minimum phase systems only by a careful choice of the parameter λ , the

weighting factor which is the same as for the LQG approach (Clarke et al., 1985c, 1985d). In contrast to both approaches, GPC can fulfil the same task even if $\lambda = 0.0$. However, the choice of this latter as a **fine tuning parameter** helps to improve the overall performance of the GPC algorithm which is robust with respect to this choice. In practice, λ may vary over a wide range (10^{-3} to 10^3).

(Lam, 1980) suggested a method in which it is stated that if the gain of the process under consideration depends on the $\hat{B}(z^{-1})^*$ polynomial, any gain variation will reflect itself in $\hat{B}(1)$ and in order to keep the closed-loop poles in the same positions despite these variations, λ should be rescaled by $\hat{B}(1)^2$ such that:

$$\lambda = \lambda_{\text{rel.}} (\hat{B}(1))^2$$

$$0 \leq \lambda_{\text{rel.}} \leq 1$$

5.3 EXAMPLES OF APPLICATION

Before being involved in any calculations, it is worth mentioning that the GPC law derivation can be performed in two ways:

- a) The Diophantine method
- b) The direct method

method a) is the method outlined previously and uses the Diophantine equation solution to calculate the matrix f in equation (5.28), whereas method b) does not, and instead notes that f is simply composed of signals that represent the response of the process assuming that future controls equal the previous control, and that the disturbance $C(z^{-1}) \zeta(t + j)$ is constant so that $\zeta(t + j) = 0$.

Computationally, method b) is more efficient than method a) since it involves half

* Estimated Polynomial

the number of operations required for method a) . However, the Diophantine method has the advantage of expressing the controller in a transfer function form if so desired, which can be useful since the closed-loop poles can be located easily as the next sections will show. For this reason method a) will be adopted throughout this study.

5.3.1 Example 1 (Non-Minimum Phase Plant)

Consider the non-minimum phase system reported in Clarke et al. (1987a):

$$(1 + a_1 z^{-1}) y(t) = (b_0 + b_1 z^{-1}) u(t - 1)$$

where,

$$\begin{cases} a_1 = -0.90 \\ b_0 = 1.0 \\ b_1 = 2.0 \end{cases}$$

and assume the following settings for the GPC algorithm:

$$\begin{cases} N_1 = 1 \\ N_2 = 1, 2, 3 \\ NU = 1 \\ \lambda = 0.0 \end{cases}$$

a) Calculation of the E and F polynomials

$$j = 1 \quad \begin{cases} E_1 = 1 \\ F_1 = 1.9 - 0.9 z^{-1} \end{cases}$$

$$j = 2 \quad \begin{cases} E_2 = 1 + 1.9 z^{-1} \\ F_2 = 2.71 - 1.71 z^{-1} \end{cases}$$

$$j = 3 \quad \begin{cases} E_3 = 1 + 1.9 z^{-1} - 1.71 z^{-2} \\ F_3 = 3.439 - 2.439 z^{-1} \end{cases}$$

b) Calculation of the $G(z^{-1})$ polynomial

$$j = 1 \quad G_1(z^{-1}) = 1 + 2 z^{-1}$$

$$j = 2 \quad G_2(z^{-1}) = 1 + 3.9 z^{-1} + 3.8 z^{-2}$$

$$j = 3 \quad G_3(z^{-1}) = 1 + 3.9 z^{-1} + 6.51 z^{-2} + 5.42 z^{-3}$$

c) Calculation of signals f known at time t

$$f(t + 1) = 2 \Delta u(t - 1) + 1.9 y(t) - 0.9 y(t - 1)$$

$$f(t + 2) = 3.8 \Delta u(t - 1) + 2.71 y(t) - 1.71 y(t - 1)$$

$$f(t + 3) = 5.42 \Delta u(t - 1) + 3.439 y(t) - 2.439 y(t - 1)$$

d) Calculation of the control sequence $u(t)$

Recall equation (5.33) in the previous sections:

$$\bar{u} = (G_1^T G_1 + \lambda I)^{-1} G_1^T (\omega - f)$$

For $j = 1$, i.e the prediction horizon $N_2 = 1$, it follows that,

$$\bar{u} = \frac{\omega - f(t + 1)}{g_0}$$

Using the values of g_0 and $f(t + 1)$ previously calculated leads to:

$$\Delta u(t) = \omega - 2 \Delta u(t - 1) - 1.9 y(t) + 0.9 y(t - 1)$$

In order to locate the corresponding closed-loop poles, first consider the following expression which is the general form of the control law associated with the GPC algorithm:

$$H(z^{-1}) \Delta u(t) = \omega(t) - M(z^{-1}) y(t) \quad (5.34)$$

where $H(z^{-1})$ and $M(z^{-1})$ are polynomials in the usual backward shift z^{-1} .

but,

$$A(z^{-1}) y(t) = B(z^{-1}) z^{-1} u(t)$$

or,

$$u(t) = \frac{A(z^{-1})}{B(z^{-1}) z^{-1}} y(t) \quad (5.35)$$

Substituting equation (5.35) in equation (5.34) and rearranging leads to:

$$\frac{y(t)}{\omega(t)} = \frac{B(z^{-1}) z^{-1}}{H(z^{-1}) \Delta A(z^{-1}) + B(z^{-1}) z^{-1} M(z^{-1})} \quad (5.36)$$

For the above case where $N_2 = 1$, the closed-loop characteristic equation is equivalent to:

$$H(z^{-1}) \Delta A(z^{-1}) + B(z^{-1}) z^{-1} M(z^{-1}) = 1 + 2 z^{-1}$$

because the non-minimum phase zero of the plant is cancelled by this zero, the system becomes unstable.

Increasing N_2 to 2 and following the same steps as previously yields:

$$\Delta u(t) = \frac{1}{16.21} [4.9 \omega - 16.82 \Delta u(t-1) - 12.469 y(t) + 7.569 y(t-1)]$$

This time:

$$H(z^{-1}) \Delta A(z^{-1}) + B(z^{-1}) z^{-1} M(z^{-1}) = 1 - 0.09 z^{-1}$$

which suggests a more stable system.

If N_2 is increased up to a value of 3, the control law then becomes:

$$\Delta u(t) = \frac{1}{58.591} [11.41 \omega - 52.104 \Delta u(t-1) - 34.857 y(t) + 23.447 y(t-1)]$$

and,

$$H(z^{-1}) \Delta A(z^{-1}) + B(z^{-1}) z^{-1} M(z^{-1}) = 1 - 0.416 z^{-1}$$

suggesting also better stability properties. Figure (5.4) shows the resulting

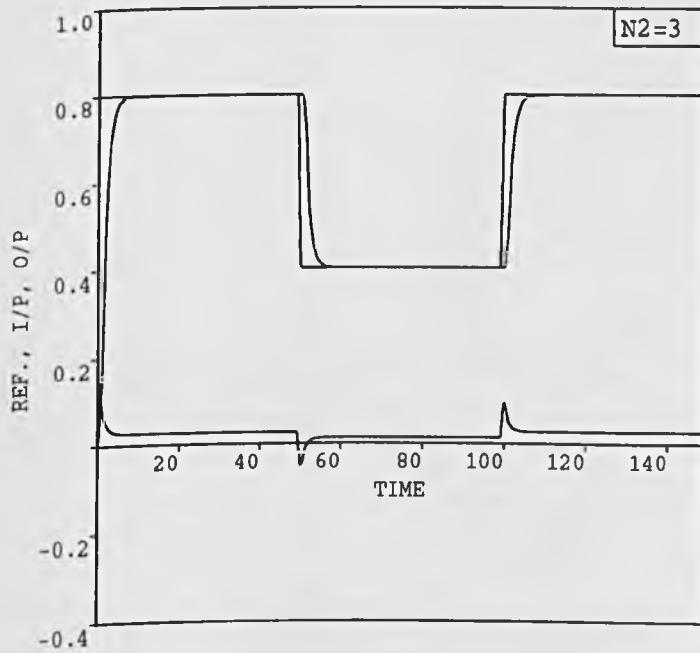
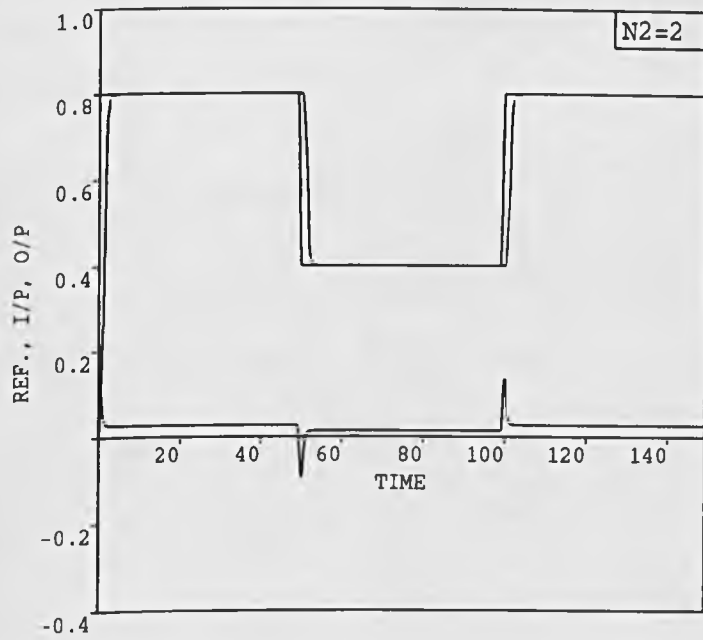


Figure 5.4. Closed-loop responses of the non-minimum phase plant under fixed GPC algorithm with $N_1=1$; $N_2=2$; 3 ; $NU=1$

responses corresponding to the last two cases considered for a command signal of 80% then 40% every 50 samples. Notice also how the control becomes more sluggish with the prediction horizon N_2 increasing.

5.3.2 Example 2 (Muscle Relaxation Process Pharmacokinetics)

As a second example, the linear pharmacokinetics of the muscle relaxation system associated with the drug Pancuronium-Bromide are considered here, i.e:

$$y_k = \frac{0.04 + 0.03 z^{-1}}{1 - 1.55 z^{-1} + 0.57 z^{-2}} u_{k-1}$$

Following similar steps to those adopted in section 5.3.1 and setting the GPC parameters at:

$$\begin{cases} N_1 = 1 \\ N_2 = 1, 3, 6, 10 \\ NU = 1 \\ \lambda = 0 \end{cases}$$

the following control laws for various N_2 are obtained:

a) $N_2 = 1$

$$\begin{aligned} \bar{u} = \frac{1}{0.0016} [0.04 \omega - 0.0012 \Delta u(t-1) - 0.102 y(t) \\ + 0.0848 y(t-1) - 0.0228 y(t-2)] \end{aligned}$$

b) $N_2 = 2$

$$\begin{aligned} \bar{u} = \frac{1}{0.0190} [0.172 \omega - 0.0112 \Delta u(t-1) - 0.6804 y(t) \\ + 0.72 y(t-1) - 0.0215 y(t-2)] \end{aligned}$$

c) $N_2 = 6$

$$\bar{u} = \frac{1}{0.9435} [1.9948 \omega - 0.4534 \Delta u(t-1) - 18.9798 y(t) + 25.5939 y(t-1) - 8.6135 y(t-2)]$$

d) $N_2 = 10$

$$\bar{u} = \frac{1}{4.9485} [5.9571 \omega - 2.2615 \Delta u(t-1) - 86.0828 y(t) + 123.0795 y(t-1) - 42.9683 y(t-2)]$$

Figure (5.5) shows the corresponding responses assuming the same conditions as in section 5.3.1. Notice also how the control activity decreases with increasing N_2

5.4 GENERALIZED PREDICTIVE CONTROL (GPC) APPLIED TO THE MUSCLE RELAXATION PROCESS

The previous chapter saw the application of a self-tuning technique based upon a pole-placement approach (PIP) on the muscle relaxation system associated with two drug models which had been duly identified. The performance of this algorithm which falls into the category of explicit self-tuners has been assessed. Similarly, this section is concerned with the application of the GPC algorithm, also explicit but based on a totally different principle (LRPC), to the above models.

The algorithm, coded in Fortran 77 and implemented on a SUN workstation, uses the solution of the Diophantine equation to establish the final control sequence $u(t)$. All models were simulated in a continuous form using a fourth order Runge-Kutta integration method with a fixed step length of 0.1. A sampling time of 1 minute was adopted throughout the study. The simulation studies are also divided into two parts, the first part concerning the Pancuronium-Bromide model, while

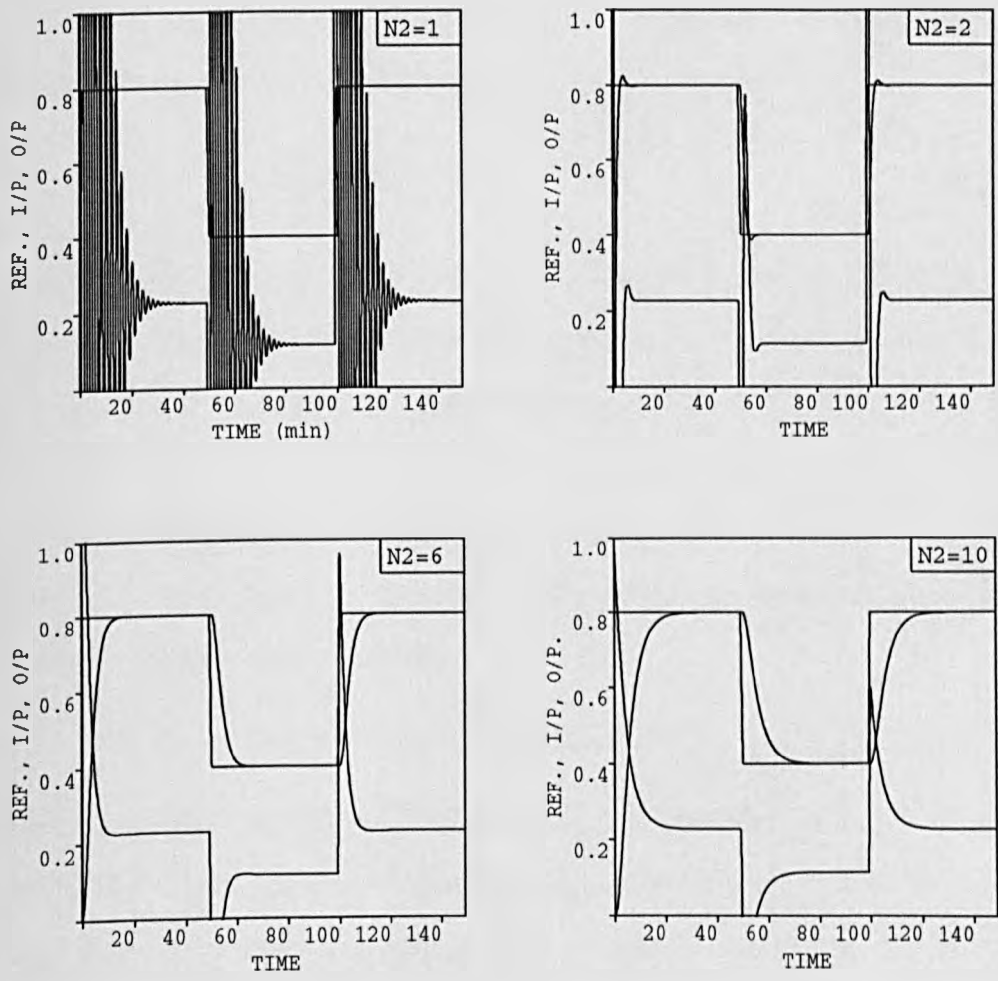


Figure 5.5. Closed-loop responses of linear pharmacokinetics associated with Pancuronium model under fixed GPC algorithm with $N_1=1$; $N_2=1$; 2 ; 6 ; 10 ; $NU=1$

the second deals with the Atracurium drug model.

5.4.1 The Pancuronium-Bromide Model

The non-linear muscle relaxant model describing the Pancuronium-Bromide dynamics of section 3.2 is considered, i.e:

$$G_1(s) = \frac{3.5 e^{-s}}{(1 + 20 s) (1 + 2 s)} \quad (5.37)$$

The pharmacodynamics are modelled by the dead-space of 50% and a saturation of 100%. Conditions for jacketting of the algorithm are similar to those adopted in section 4.6.1. Initial control is provided by an optimized PI with the same parameters as before.

Parameter estimation, triggered after the dead-zone has been traversed, also takes the form of a UDU algorithm (Bierman, 1976, 1977) this time using **incremental data** for the measurement vector, i.e:

$$\Phi^T = [- \Delta y(t), - \Delta y(t-1), \dots, \Delta u(t-k-1), \dots]$$

Parameter estimates are all set to 0.0 unless otherwise specified, the covariance matrix is made equal to $P = 10^4 \cdot I$, and a value of $\rho = 0.95$ is adopted for the forgetting factor. The control signal is clipped between maximum and minimum values of respectively 0.0 and 1.0. These limitations are also reflected back to the estimator by recomputing the **actual** control sequence which is asserted (Clarke, 1985a).

Simulation Results

A second order discrete-time model with an assumed delay of 1 minute was considered throughout, implying therefore that the leading element of the matrix G is nil, but in the following the value of the minimum output horizon N_1 is taken to

be 1 with no loss of generality.

The study is divided into different phases. Each phase is concerned with investigating the effect of the tuning knobs introduced in the technique, i.e. N_2 , NU , and λ . During phase 1 the control horizon NU was set to a constant value of 1, whereas λ was set at 0.0. The process being of order 3 (see section 5.2.4.b) the maximum output horizon was first set at $(2 \times 3) - 1 = 5$. Figure (5.6) shows the corresponding output response which demonstrated a slight overshoot evaluated at 3% during the first 50 samples. The control signal was quite active especially at every set-point change. Figure (5.7) shows the variations of the parameter estimates whose final values were:

$$\hat{a}_1 = -1.5173 \quad \hat{a}_2 = 0.5457 \quad \hat{b}_1 = 0.0718 \quad \hat{b}_2 = 0.0619$$

equivalent to a gain and time-constants of:

$$\hat{G}ain = 4.70 \quad \hat{T}_1 = 1.87 \text{ minutes} \quad \hat{T}_2 = 14.08 \text{ minutes}$$

Increasing N_2 to 8 made the response slower and the control signal less active as shown in figure (5.8). The parameter estimates settled to the following values:

$$\hat{a}_1 = -1.4274 \quad \hat{a}_2 = 0.4554 \quad \hat{b}_1 = 0.0742 \quad \hat{b}_2 = 0.0732$$

equivalent to a gain and time-constants of:

$$\hat{G}ain = 5.26 \quad \hat{T}_1 = 1.37 \text{ minutes} \quad \hat{T}_2 = 18.02 \text{ minutes}$$

For the third experiment N_2 was increased to 10 and the response of figure (5.9) was even slower than the previous one with a rather sluggish input signal. Parameter estimates suggested a non-minimum phase characteristics converging to:

$$\hat{a}_1 = -1.3857 \quad \hat{a}_2 = 0.4135 \quad \hat{b}_1 = 0.0735 \quad \hat{b}_2 = 0.0831$$

equivalent to a gain and time-constants of:

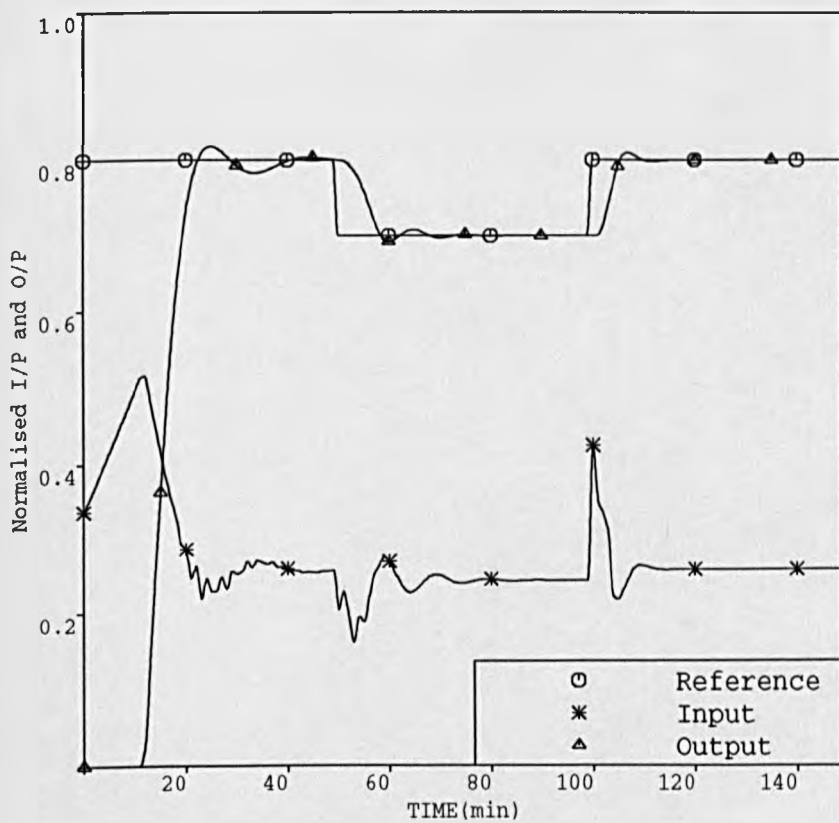


Figure 5.6. Closed-loop response of non-linear Pan-curonium model under self-adaptive GPC algorithm with $N_1=1$; $N_2=5$; $NU=1$

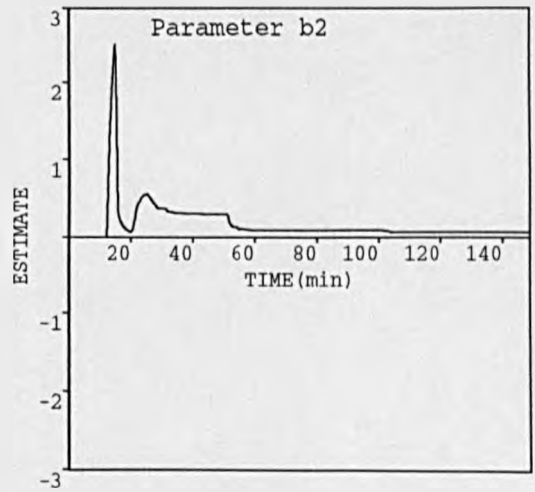
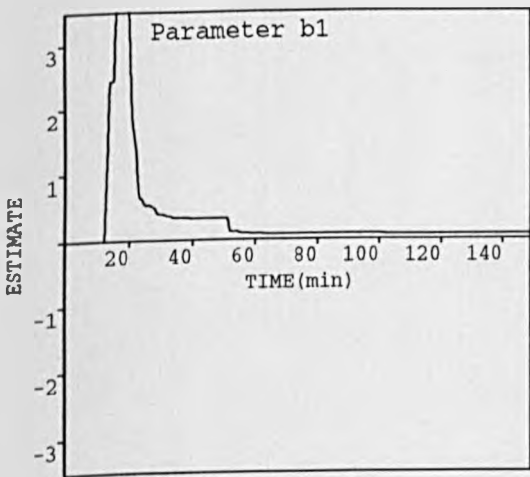
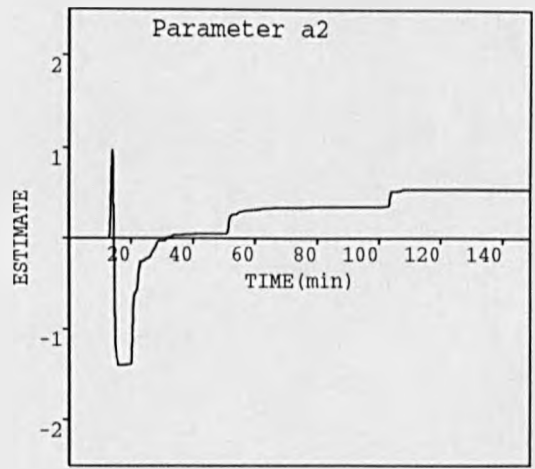
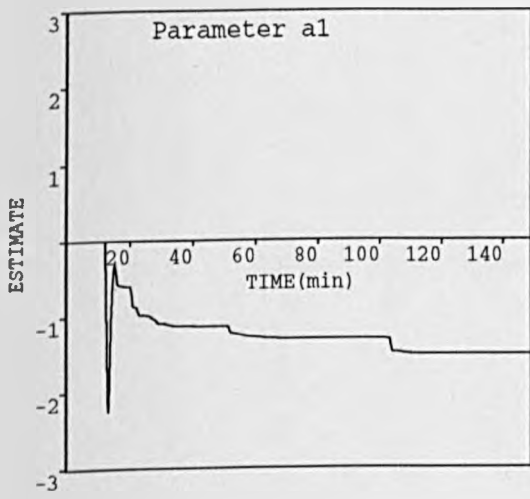


Figure 5.7. System parameter estimates corresponding to figure (5.6)

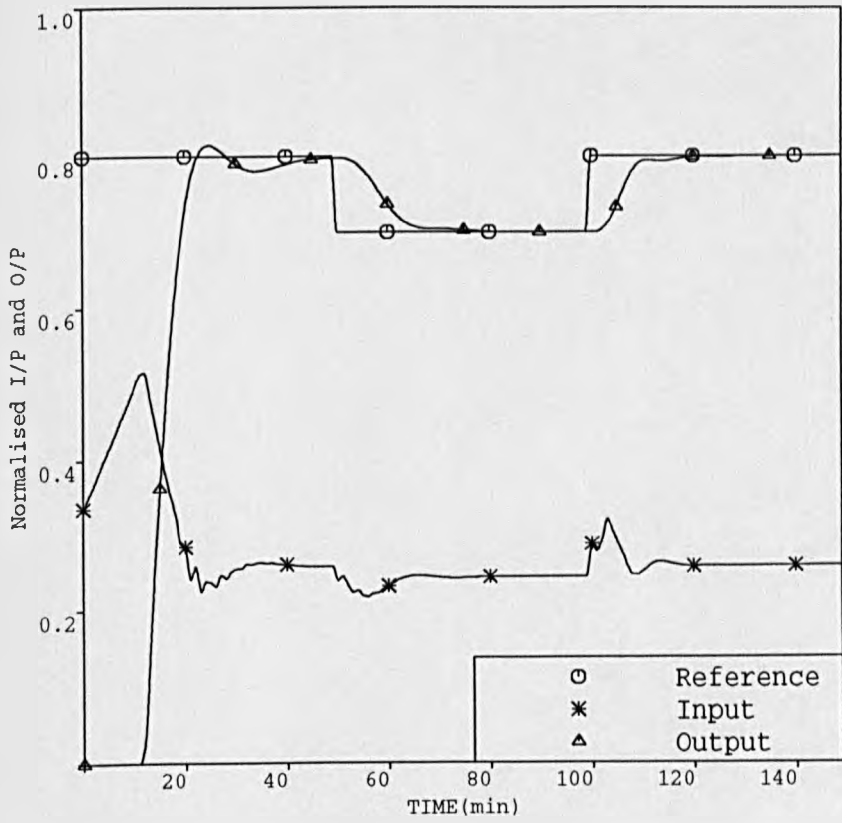


Figure 5.8. Same conditions as in figure (5.6) but with $N_2=8$

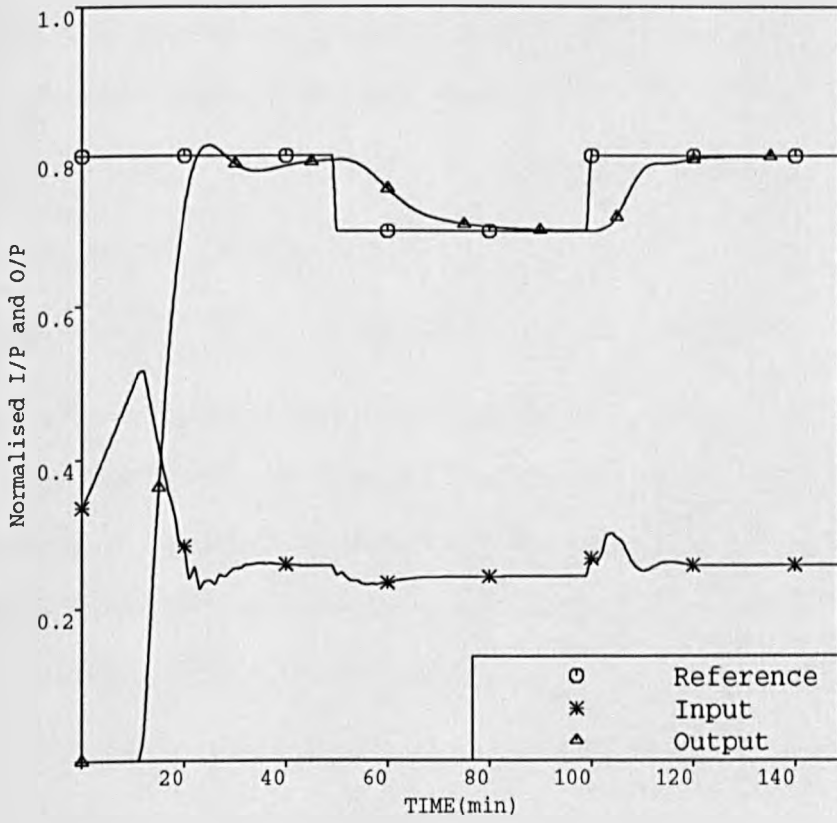


Figure 5.9. Same conditions as in figure (5.6) but with $N_2=10$

$$\hat{G}\text{ain} = 5.72 \quad \hat{T}_1 = 1.20 \text{ minutes} \quad \hat{T}_2 = 19.90 \text{ minutes}$$

Initializing the estimates to some values of $\theta_1 = [-1.38, 0.41, 0.08, 0.07]$ and assuming the same combination for (N_1, N_2, NU, λ) as before another run was conducted whose response is shown in figure (5.10). The performance was good, the overshoot was removed and the corresponding control signal was reasonably active. The associated parameter estimates settled to the following final values:

$$\hat{a}_1 = -1.3495 \quad \hat{a}_2 = 0.3847 \quad \hat{b}_1 = 0.1059 \quad \hat{b}_2 = 0.0919$$

equivalent to a gain and time-constants of:

$$\hat{G}\text{ain} = 5.62 \quad \hat{T}_1 = 1.12 \text{ minutes} \quad \hat{T}_2 = 16.28 \text{ minutes}$$

The second phase of the study considered a varying control horizon NU while the maximum output horizon N_2 was fixed at 10 and the weighting sequence λ at 0.0. The run with $NU = 2$ produced the output response of figure (5.11) whose performance during the first 50 samples was poor due to the high activity of the control signal. The estimates settled to the following values:

$$\hat{a}_1 = -1.5405 \quad \hat{a}_2 = 0.5689 \quad \hat{b}_1 = 0.0725 \quad \hat{b}_2 = 0.0606$$

equivalent to a gain and time-constants of:

$$\hat{G}\text{ain} = 4.67 \quad \hat{T}_1 = 2.05 \text{ minutes} \quad \hat{T}_2 = 13.03 \text{ minutes}$$

Taking NU up to 4 induced an even more active input signal leading to a poorer output response as illustrated in figure (5.12). The activity of such control signals could be reduced considerably by adopting a value of λ different from zero. This is demonstrated in figures (5.13) and (5.14) where the previous cases were considered but using $\lambda = 1$.

The last phase of this simulation study is concerned with the varying time-delay in the process. Because the GPC approach is based on an explicit formulation, the

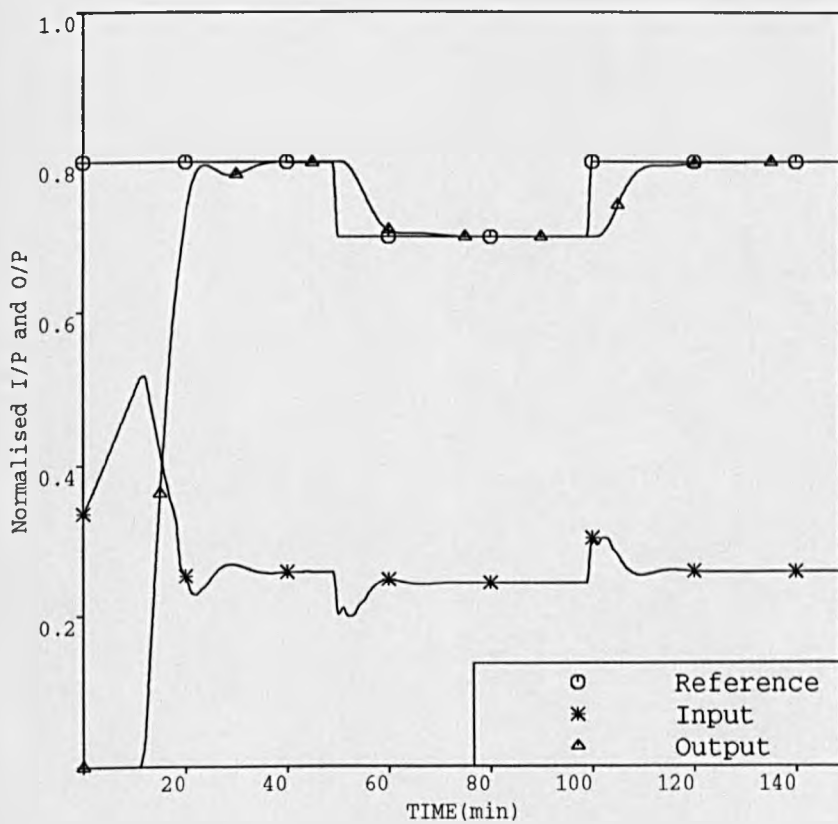


Figure 5.10. Same conditions as in figure (5.9) but with non-zero initial parameter estimates

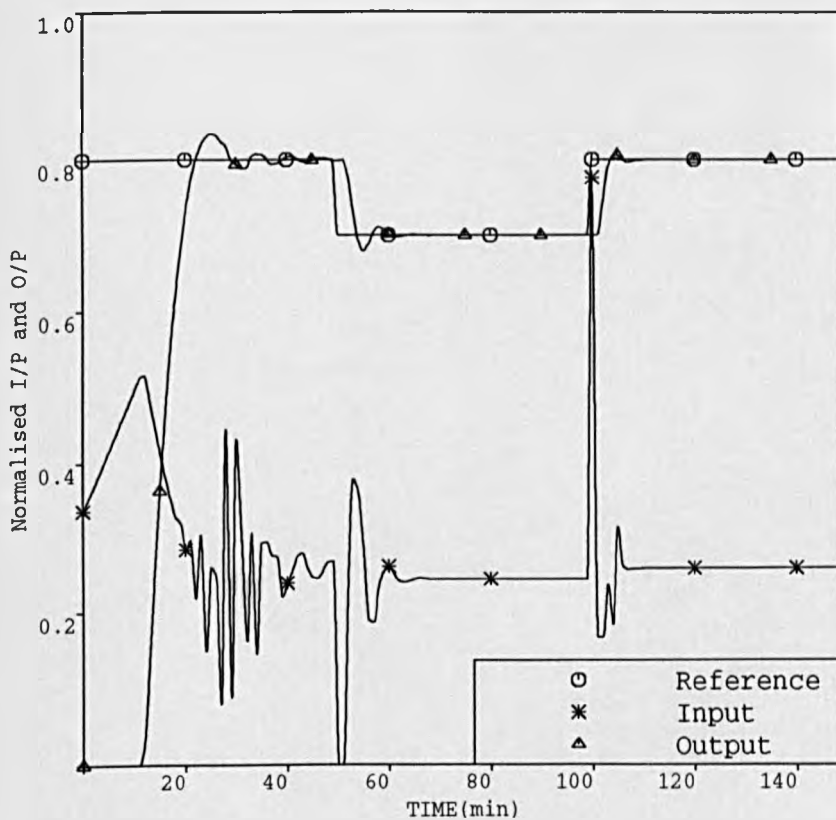


Figure 5.11. Closed-loop response of Pancuronium model under GPC algorithm with $N_1=1$; $N_2=10$; $NU=2$; $\lambda=0$

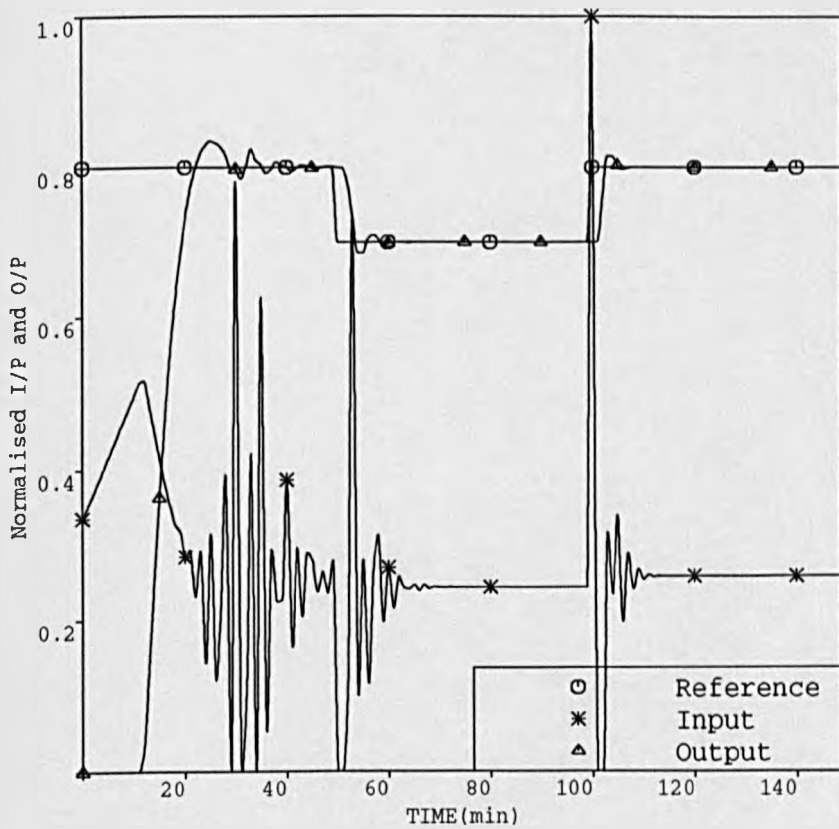


Figure 5.12. Closed-loop response of Pancuronium model under GPC algorithm with $N_1=1$; $N_2=10$; $NU=4$; $\lambda=0$

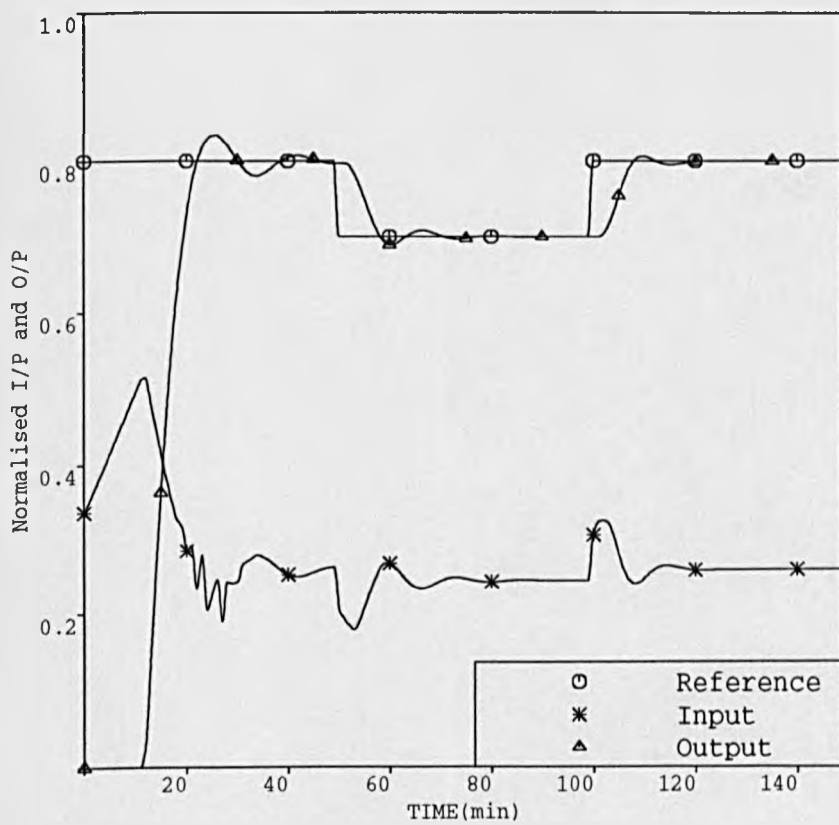


Figure 5.13. Same conditions as in figure (5.11)
but with $\lambda=1.0$

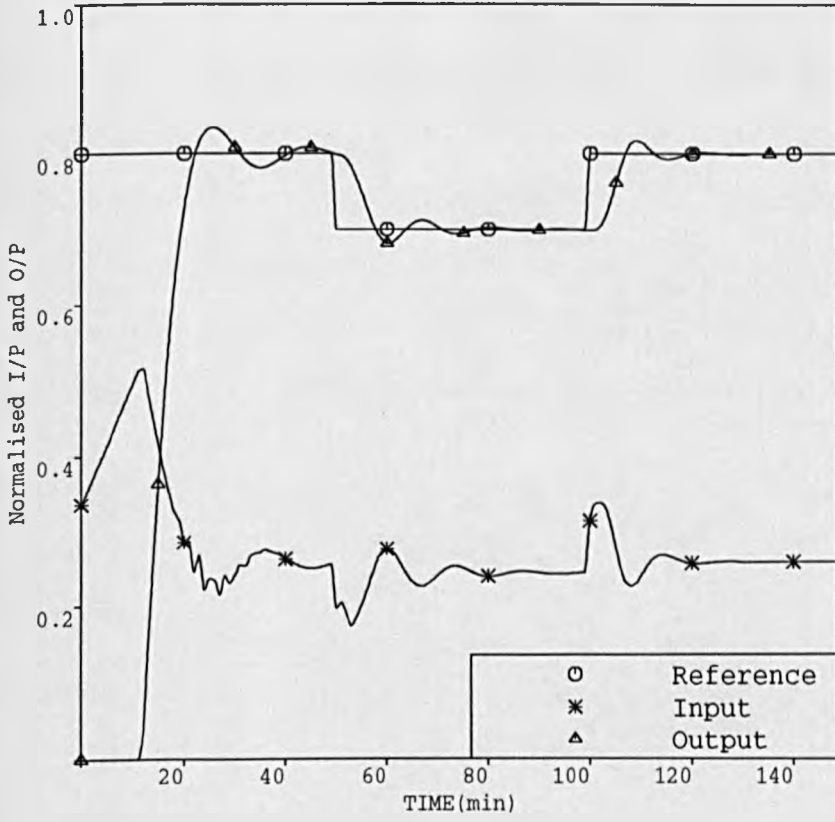


Figure 5.14. Same conditions as in figure (5.12) but with $\lambda=1.0$

uncertainty that may arise about the time-delay could be enhanced in the $B(z^{-1})$ polynomial without the usual problem of overparameterization encountered with pole-placement approaches. Therefore, in order to investigate the robustness of the algorithm in such a situation, an experiment was conducted in which time-delay changes from 2 to 4 samples were made at iteration 70 and back to 2 samples at iteration 140. Conditions for the controller and the estimator are identical to those of figure (5.10) except that three more 'b' coefficients were estimated to absorb any time-delay changes. The performance shown in figure (5.15) was good despite the severe delay changes. Parameter estimates, whose variations are shown in figure (5.16), settled to the values given in table (5.1). According to the time-delay, the appropriate "b" coefficients became negative or negligible quantities.

Parameter Estimates Convergence			
Parameter estimates	Time-delay value(Min.) from...to...		
	2 (0 to 70)	4 (71 to 140)	2 (141 to 300)
\hat{a}_1	-0.9753	-1.4867	-1.5506
\hat{a}_2	0.0253	0.5273	0.5714
\hat{b}_1	-0.0120	-0.0069	-0.0000
\hat{b}_2	0.0536*	-0.0022	0.0725*
\hat{b}_3	0.1133*	-0.0041	0.0609*
\hat{b}_4	0.0469	0.0677*	0.0010
\hat{b}_5	0.0960	0.0649*	0.0009

Table 5.1. Model parameter estimates for figure (5.15)

* Significant values

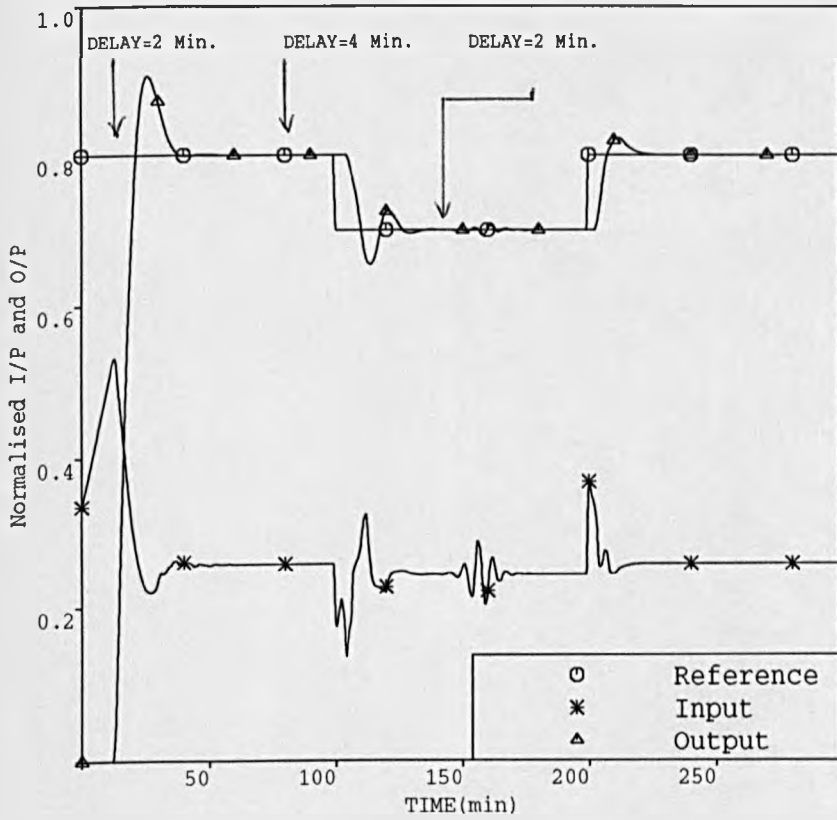


Figure 5.15. Closed-loop control of non-linear Pancuronium model with changing delay. $N_1=1$; $N_2=10$; $NU=1$ and overparameterized $B(z^{-1})$ polynomial

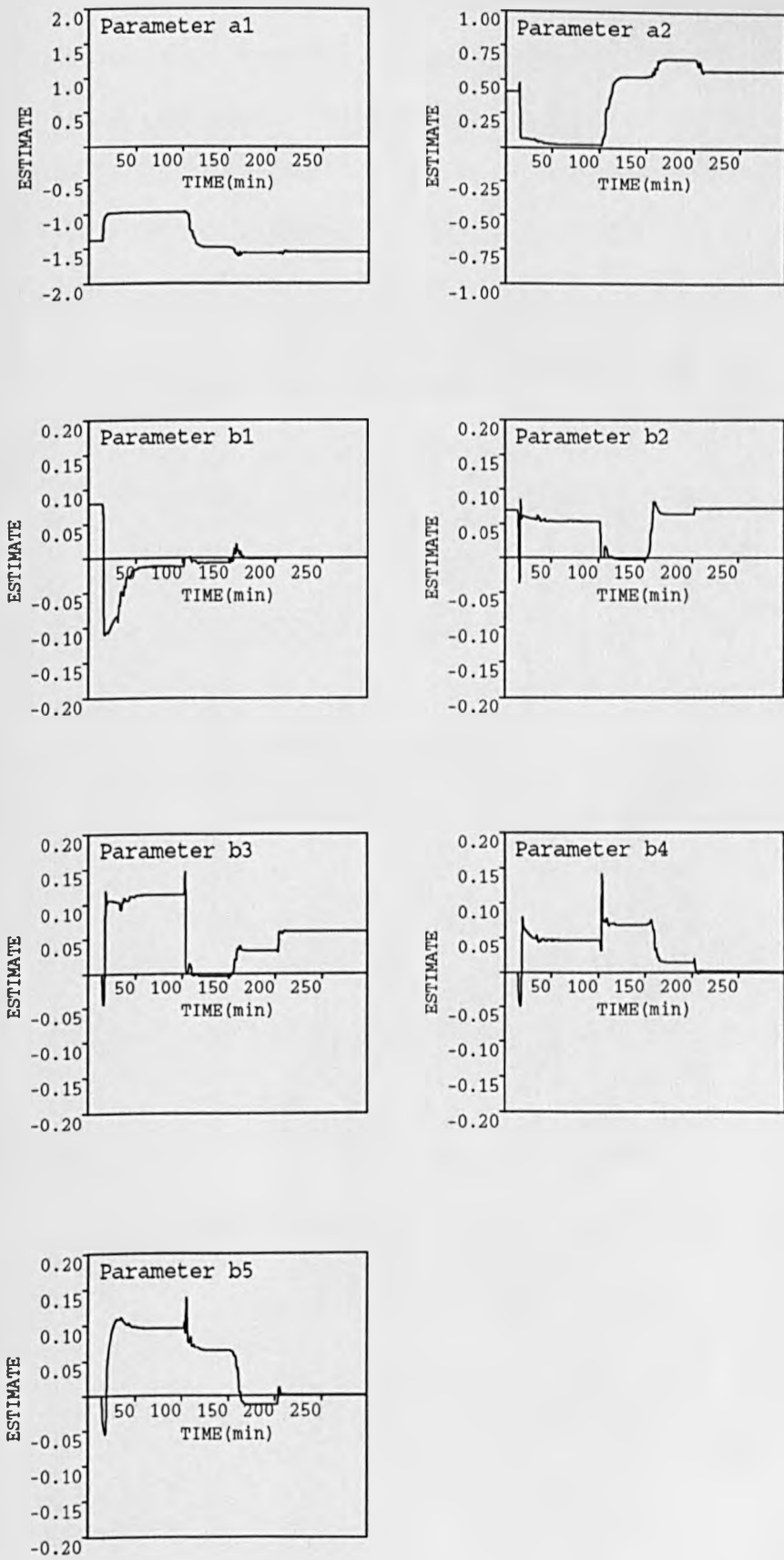


Figure 5.16. System parameter estimates corresponding to figure (5.15)

The same conditions were simulated this time taking N_2 to be 20 which is the value of the model predominant time-constant. The result of such experiment is shown in figure (5.17). The associated performance was good; less overshoot and less active control signal. Parameter estimates whose variations are shown in figure (5.18) settled to values according to table (5.2).

Parameter Estimates Convergence			
Parameter estimates	Time-delay value(Min.) from...to...		
	2 (0 to 70)	4 (71 to 140)	2 (141 to 300)
\hat{a}_1	-0.9765	-1.3415	-1.5247
\hat{a}_2	0.0.0271	0.3863	0.5451
\hat{b}_1	-0.0118	-0.0204	-0.0000
\hat{b}_2	0.0496*	-0.0009	0.0720*
\hat{b}_3	0.1106*	-0.0022	0.0625*
\hat{b}_4	0.0600	0.0695*	0.0038
\hat{b}_5	0.0861	0.0887*	0.0026

Table 5.2. Model parameter estimates for figure (5.17)

* Significant values

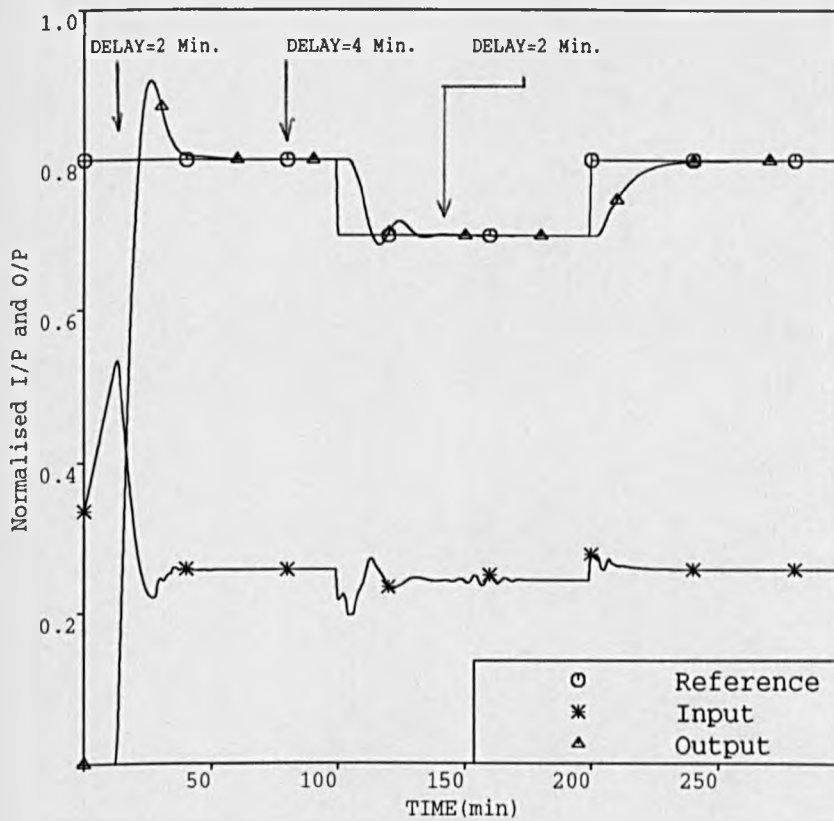


Figure 5.17. Same conditions as in figure (5.15)
 but with GPC parameter settings as;
 $N_1=1$; $N_2=20$; $NU=1$

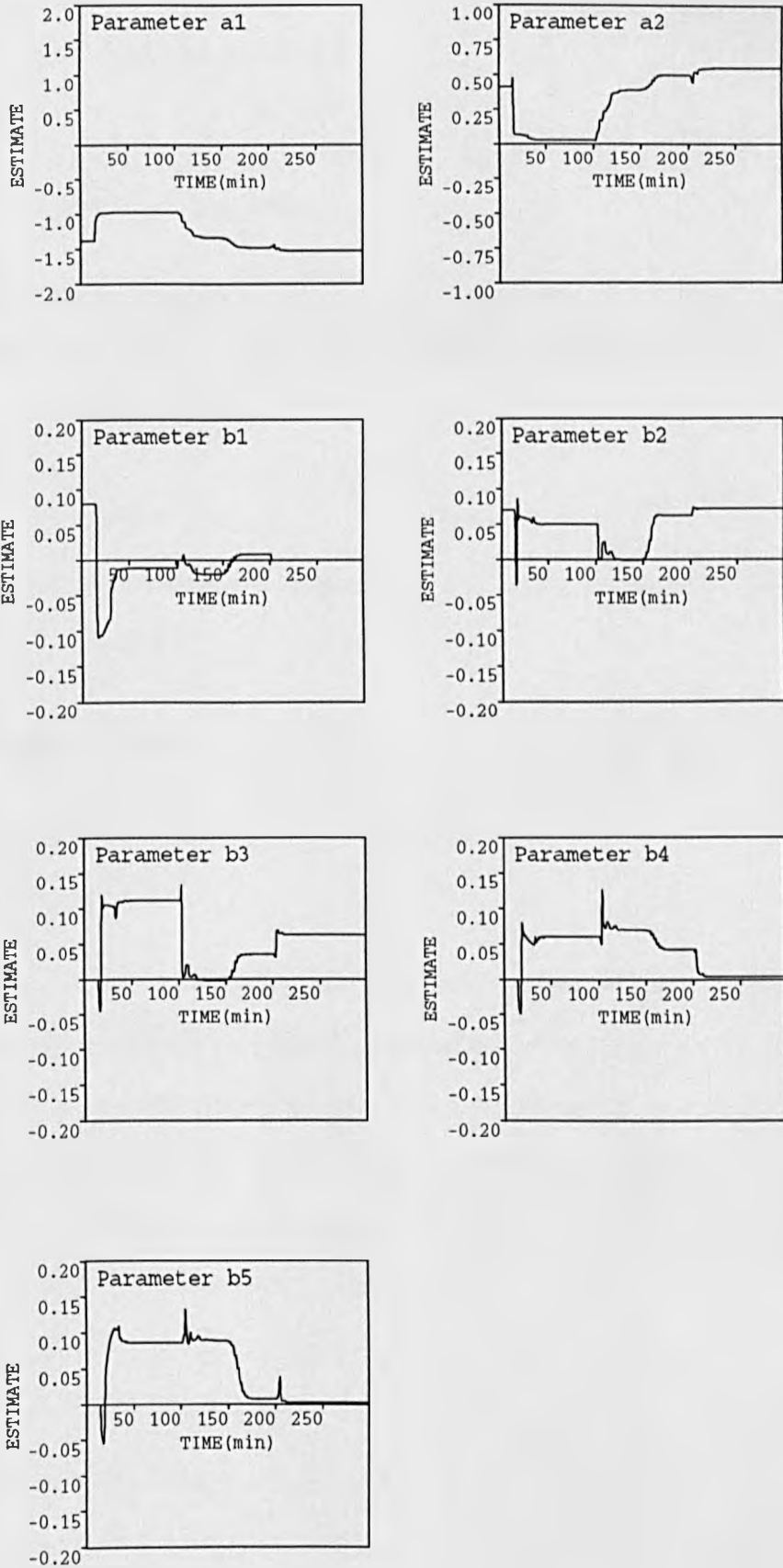


Figure 5.18. System parameter estimates corresponding to figure (5.17)

5.4.2 The Atracurium Model

For this model the pharmacokinetics are represented by the following third order transfer function of the form:

$$G_2(s) = \frac{(1 + 10.64 s) e^{-s}}{(1 + 3.08 s) (1 + 4.81 s) (1 + 34.36 s)} \quad (5.38)$$

The pharmacodynamics are modelled by the Hill equation (4.18) with the following parameters:

$$\begin{aligned} \alpha &= 2.98 \\ C(50) &= 0.404 \end{aligned}$$

Conditions for the estimation and jacketting are similar to those of section 5.4.1 unless otherwise specified.

Simulation Results

A third order discrete-time model with an assumed delay of 1 minute was considered throughout.

The process order being 4 (integrator included) a value of 7 was chosen for the maximum output horizon N_2 , while N_1 , NU , and λ were chosen to be 1, 1, and 0 respectively. With such controller-settings an experiment was conducted which produced the output response of figure (5.19). The performance was good although the control signal being rather active gave rise to a 2 % overshoot. Parameter estimates converged to the following values:

$$\begin{aligned} \hat{a}_1 &= -1.8946 & \hat{a}_2 &= 1.1500 & \hat{a}_3 &= -0.2361 \\ \hat{b}_1 &= 0.0099 & \hat{b}_2 &= 0.0047 & \hat{b}_3 &= -0.0029 \end{aligned}$$

equivalent to the following positions in the z plane:

$$\begin{aligned} \text{zeros: } & 0.35 ; 0.83 \\ \text{poles: } & 0.93 ; (0.48 \pm 0.15 i) \end{aligned}$$

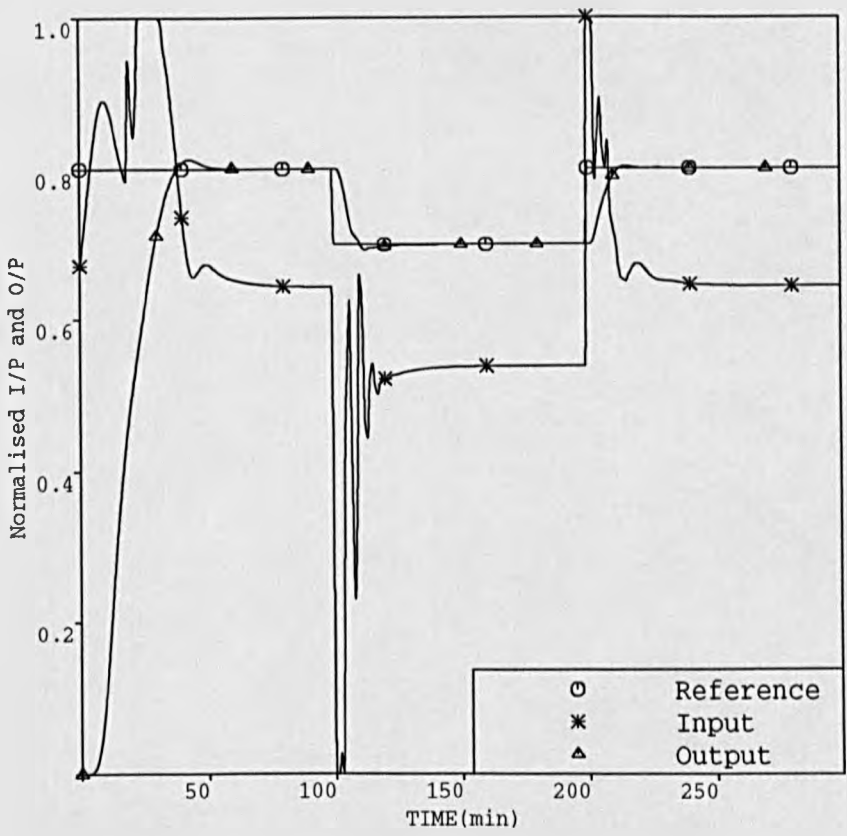


Figure 5.19. Closed-loop response of Atracurium model under self-adaptive GPC algorithm with $N_1=1$; $N_2=7$; $NU=1$

Increasing the value of N_2 to 10 led to the performance of figure (5.20) which saw the overshoot diminish and the control activity decrease. The parameter estimates whose variations are shown in figure (5.21) converged to:

$$\begin{aligned}\hat{a}_1 &= -2.1499 & \hat{a}_2 &= 1.5107 & \hat{a}_3 &= -0.3490 \\ \hat{b}_1 &= 0.0102 & \hat{b}_2 &= 0.0023 & \hat{b}_3 &= -0.0054\end{aligned}$$

equivalent to the following positions in the z plane:

$$\begin{aligned}\text{zeros: } & -0.85 ; 0.62 \\ \text{poles: } & 0.92 ; (0.61 \pm 0.04 i)\end{aligned}$$

The dominant time-constant in the model is 34 minutes, and so N_2 was now set to a value of 35 closer to the previous time-constant value. The estimates were initialized to some values to help improve the transient. Figure (5.22) shows how the response was well damped with a minimum percentage of overshoot due to the reasonably active input signal. This latter could be seen increasing if for instance NU was to be taken equal to 2 as figure (5.23) illustrates. The associated input signal saturated for approximately 15 samples before dropping to a reasonable level. In an industrial environment, this type of excessive control could be detrimental to the actuators, and in the muscle relaxation system case, the pump which operates with a small motor starts driving at saturation levels and that would certainly hinder its normal operation.

To simulate a situation where the patient's time-delay is subject to variations a final experiment was conducted in which the dead-time value was varied from 1 minute to 4 minutes every 100 minute-samples. The controller was chosen with a combination of (1, 10, 1, 0) for (N_1, N_2, NU, λ) , and any time-delay variations were enhanced in the $B(z^{-1})$ polynomial by estimating 3 extra 'b' coefficients. As shown in figure (5.24), the performance was good despite the harsh conditions under which the run was conducted; during the first 100 samples the response was

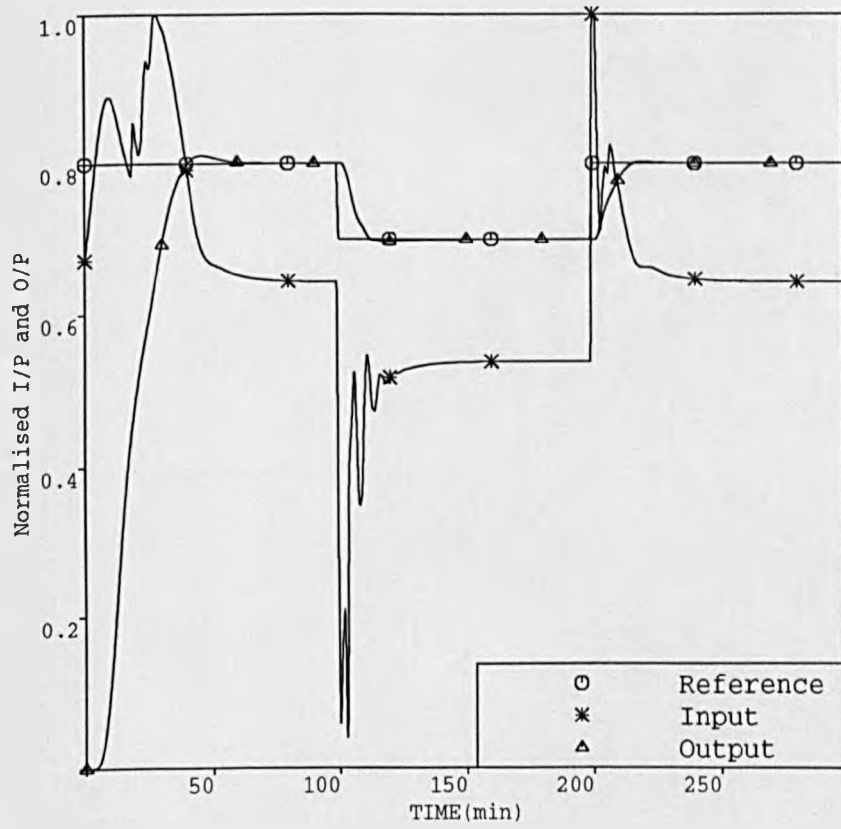


Figure 5.20. Same conditions as in figure (5.19)
but with $N_2=10$

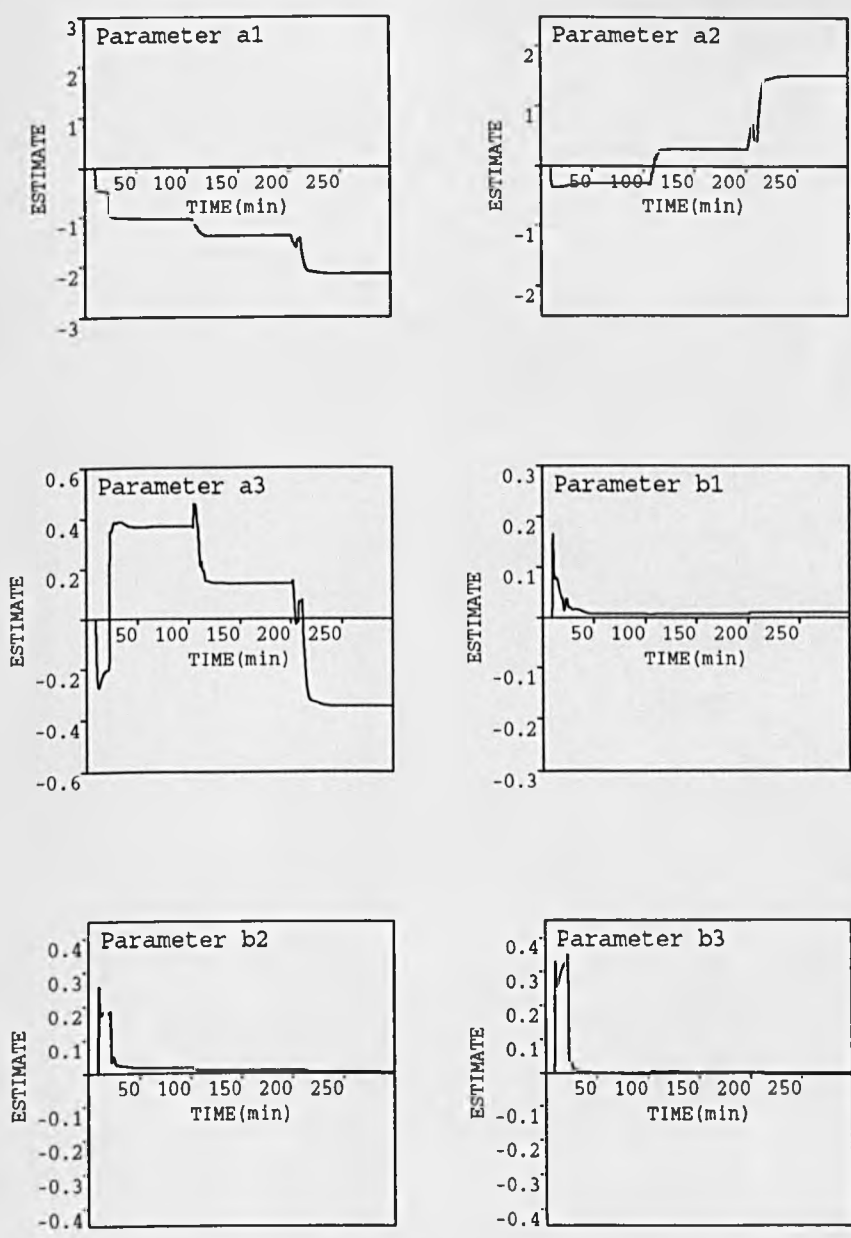


Figure 5.21. System parameter estimates corresponding to figure (5.20)

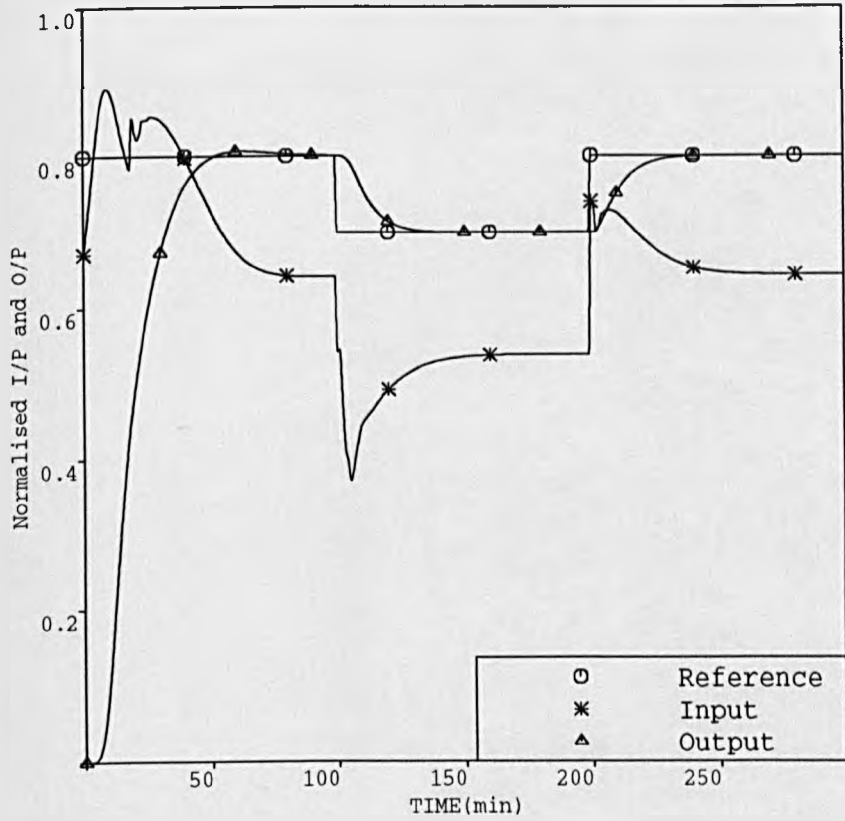


Figure 5.22. Closed-loop response of Atracurium model under self-adaptive GPC algorithm with $N_1=1$; $N_2=35$; $NU=1$ and non-zero initial parameter estimates

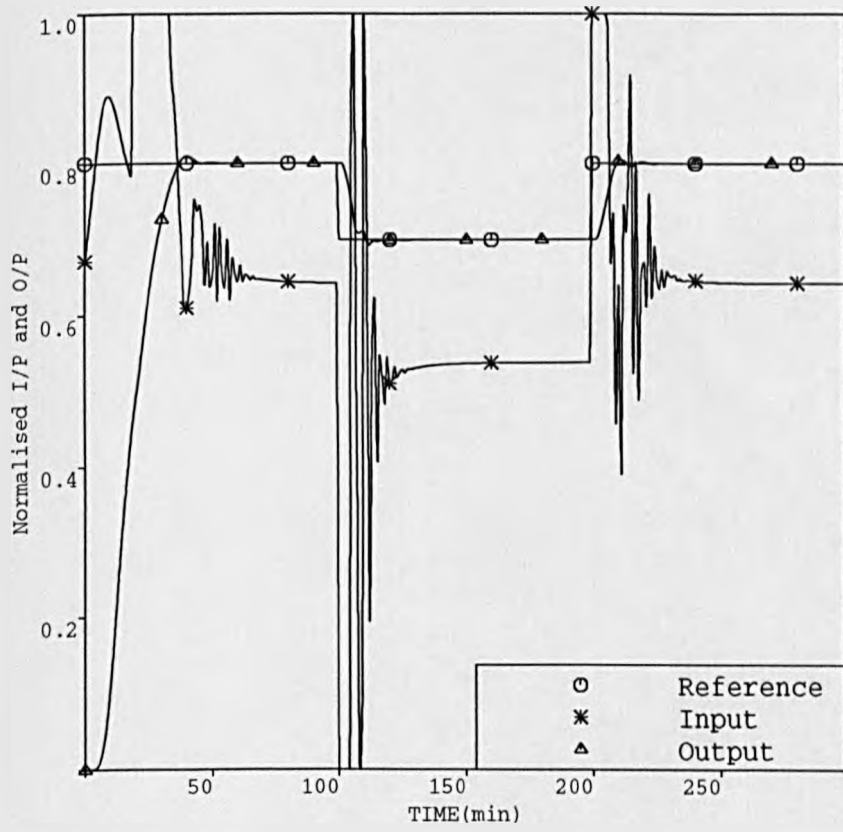


Figure 5.23. Same conditions as in figure (5.20)
but with $NU=2$

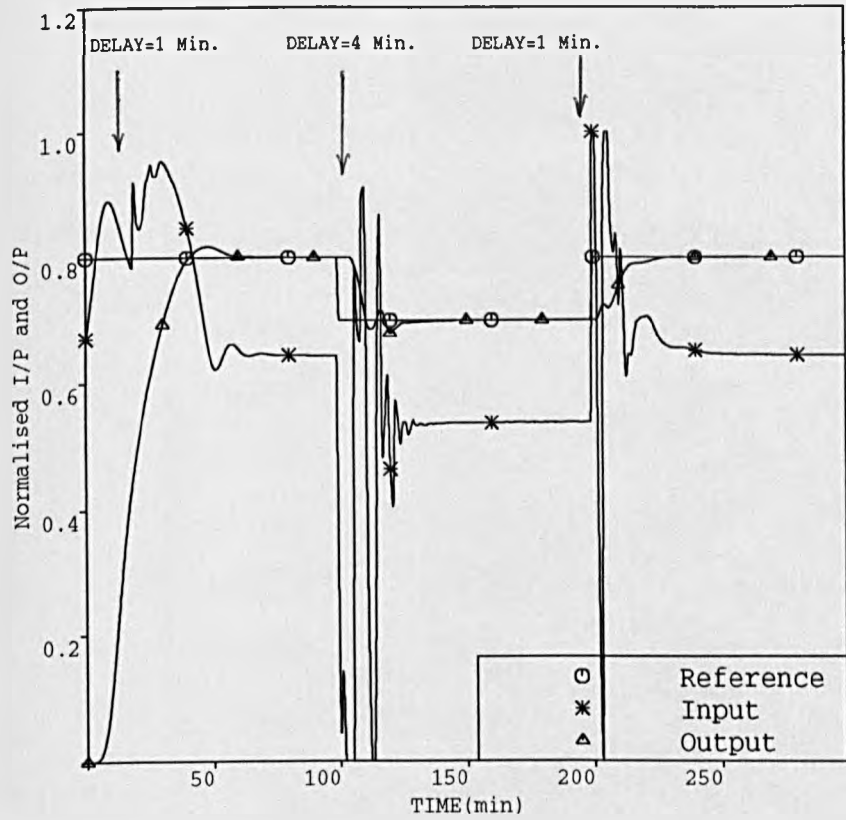


Figure 5.24. Closed-loop response of Atracurium model with variable time-delay and under self- adaptive GPC algorithm with $N_1=1$; $N_2=10$; $NU=1$ and overparameterized $B(z^{-1})$ polynomial

well damped with a reasonably active control signal, and when the delay changed to the value of 4 minutes the input signal was active making therefore, the output track the set-point very rapidly. Table (5.3) summarizes the values towards which the parameter estimates, whose variations are shown in figure (5.25), converged during the three phases of the run.

Parameter Estimates Convergence			
Parameter estimates	Time-delay value(Min.) from...to...		
	1 (0 to 99)	4 (100 to 199)	1 (200 to 300)
\hat{a}_1	-1.0502	-1.7449	-2.1166
\hat{a}_2	-0.2967	0.8820	1.7898
\hat{a}_3	0.3806	-0.1141	-0.6499
\hat{b}_1	0.0090*	0.0000	0.0091*
\hat{b}_2	0.0151*	-0.0004	0.0025*
\hat{b}_3	0.0009*	-0.0005	-0.0019*
\hat{b}_4	-0.0042	0.0009*	0.0038
\hat{b}_5	-0.0014	0.0074*	0.0019
\hat{b}_6	0.0002	-0.0011*	0.0000

Table 5.3. Model parameter estimates for figure (5.24)

5.5 THE EXTENDED GPC ALGORITHM

The question of how many tuning-parameters any particular self-tuning algorithm possesses is of great importance. Indeed, two main sources of concern arise

* Significant values

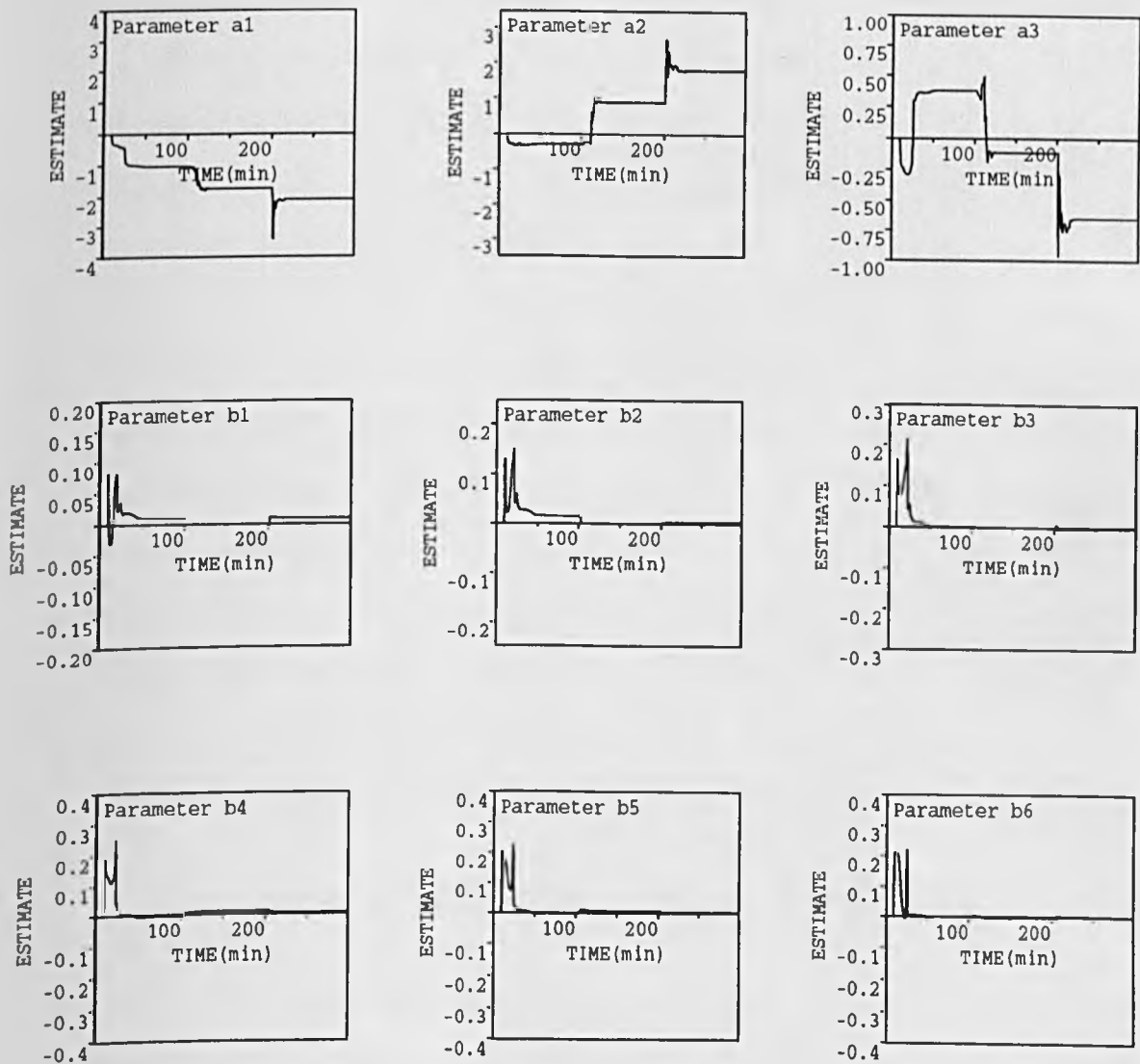


Figure 5.25. System parameter estimates corresponding to figure (5.24)

when designing any control strategy: prior specifications and requirements, as well as limitations associated with the system concerned. It is therefore important that the adopted control strategy includes design parameters that eventually relate to the above requirements and limitations. Hitherto, four tuning parameters were introduced in the basic GPC version studied in the previous sections., i.e N_1 , N_2 , N_U , and λ . GPC was shown to be effective with the use of such knobs. It is known that the early version of the GMV algorithm (Clarke and Gawthrop, 1975) which was found to be sensitive to the choice of dead-time and to the non-minimum phase characteristics exhibited by a process was later refined to include user-chosen transfer functions $P(z^{-1})$, $Q(z^{-1})$, and the observer polynomial $T(z^{-1})$. GPC being closely related to the same approach, has also considered the inclusion of such polynomials within its basic version in the hope of making the overall control design even more robust. The next sections will endeavour to consider the introduction of such polynomials, namely the user chosen polynomial $P(z^{-1})$ for specifying a desired closed-loop model, and the observer polynomial $T(z^{-1})$ for tailoring the controlled response to load disturbances and unmodelled dynamics.

5.5.1 Inclusion of the Model Reference Polynomial $P(z^{-1})$

Situations where excessively energetic control signals are required are often discouraged by control engineers who would rather prefer a smoother reaction to disturbances or set-point changes. As already seen in section 5.2.3, prefiltering the set-point using a first order lag is one way of achieving this, i.e:

$$\begin{cases} \omega'(t) = L(z^{-1}) \omega(t) \\ L(z^{-1}) \text{ represents the prefilter transfer function} \end{cases} \quad (5.39)$$

Because this approach does not involve modifications in the closed-loop behaviour, a method in which an auxiliary output $\Psi(t)$ is defined in the model as:

$$\Psi(t) = P(z^{-1}) y(t) \quad (5.40)$$

seems to solve the problem. Indeed, because $P(z^{-1})$ is included in the loop (that is the model is internal rather than being external) and as $L(z^{-1})$ would have a phase lag, $P(z^{-1})$ introduces a phase lead, a property which is very often favoured by engineers. The following will explore the mathematical background behind the use of such a polynomial within the GPC approach:

Consider the auxiliary output $\Psi(t)$ such that:

$$\begin{cases} \Psi(t) = P(z^{-1}) y(t) \\ P(z^{-1}) = \frac{P_n(z^{-1})}{P_d(z^{-1})} \end{cases} \quad (5.41)$$

with $P(1) = 1$ to ensure offset-free control.

This time the controller minimizes the following cost function:

$$J(N_1, N_2) = \sum_{j=N_1}^{j=N_2} (\hat{\Psi}(t+j) - \omega(t+j))^2 + \sum_{j=1}^{j=N_2} \lambda_j \Delta u^2(t+j-1) \quad (5.42)$$

all the variables having the same definitions as before.

Recall the CARIMA model of equation (5.4)

$$A(z^{-1}) \Delta y(t) = B_1(z^{-1}) \Delta u(t-k) + C(z^{-1}) \zeta(t) \quad (5.4)$$

where $C(z^{-1}) = 1$ for simplicity reasons.

Consider the following Diophantine identity:

$$\frac{P_n}{P_d} = E_j A \Delta + z^{-j} \frac{F_j}{P_d} \quad (5.43)$$

Following the same steps as in section 5.2, we obtain the following predictor:

$$\begin{aligned} \Psi(t+j/t) &= G_j(z^{-1}) \Delta u(t+j-1) + \frac{F_j(z^{-1})}{P_d} y(t) + E_j \zeta(t+j) \\ G_j(z^{-1}) &= E_j(z^{-1}) B(z^{-1}) \end{aligned} \quad (5.44)$$

or,

$$\left\{ \begin{array}{l} \Psi(t+1) = G_1(z^{-1}) \Delta u(t) + \frac{F_1}{P_d} y(t) + E_1 \zeta(t+1) \\ \Psi(t+2) = G_2(z^{-1}) \Delta u(t+1) + \frac{F_2}{P_d} y(t) + E_2 \zeta(t+2) \\ \cdot \quad \quad \cdot \quad \quad \cdot \quad \quad \cdot \quad \quad \cdot \\ \cdot \quad \quad \cdot \quad \quad \cdot \quad \quad \cdot \quad \quad \cdot \\ \cdot \quad \quad \cdot \quad \quad \cdot \quad \quad \cdot \quad \quad \cdot \\ \Psi(t+N) = G_N(z^{-1}) \Delta u(t+N-1) + \frac{F_N}{P_d} y(t) + E_N \zeta(t+N) \end{array} \right. \quad (5.45)$$

Let $ff(t+j)$ be that component of $\Psi(t+j)$ composed of signals which are known at time "t", i.e:

$$\left\{ \begin{array}{l} ff(t+1) = [G_1(z^{-1}) - g_0] \Delta u(t) + \frac{F_1}{P_d} y(t) \\ ff(t+2) = [G_2(z^{-1}) - g_0 - g_{21} z^{-1}] \Delta u(t) + \frac{F_2}{P_d} y(t) \\ \cdot \quad \quad \cdot \quad \quad \cdot \quad \quad \cdot \\ \cdot \quad \quad \cdot \quad \quad \cdot \quad \quad \cdot \\ \cdot \quad \quad \cdot \quad \quad \cdot \quad \quad \cdot \\ ff(t+N) = [G_N(z^{-1}) - \dots - g_0] \Delta u(t) + \frac{F_N}{P_d} y(t) \end{array} \right. \quad (5.46)$$

Therefore, equation (5.44) could be expressed in matrix form as:

$$\hat{\Psi}(t) = G \bar{u} + ff$$

where,

$$\begin{aligned} \hat{\Psi} &= [\hat{\Psi}(t+1), \hat{\Psi}(t+2), \dots, \hat{\Psi}(t+N)]^T \\ \bar{u} &= [\Delta u(t), \Delta u(t+1), \dots, \Delta u(t+N-1)]^T \\ ff &= [ff(t+1), ff(t+2), \dots, ff(t+N)]^T \end{aligned}$$

The expectation of the cost function in (5.42) could hence be written as:

$$J_1 = E [(\Psi - \omega)^T (\Psi - \omega) + \lambda \bar{u}^T \bar{u}]$$

i.e.,

$$\bar{u} = (G^T G + \lambda I)^{-1} G^T (\omega - ff) \quad (5.47)$$

or,

$$u(t) = u(t-1) + \bar{g}^T (\omega - ff) \quad (5.48)$$

where \bar{g}^T is the first row of the matrix $(G^T G + \lambda I)^{-1} G^T$.

At this stage it is worth noting that the Diophantine equation (5.43) could be solved by following the same steps already outlined previously and by noting that for the first horizon:

$$\begin{aligned} E_1 &= \frac{P_n(0)}{P_d(0)} \\ F_1 &= z [P_n(z^{-1}) - E_1 \tilde{A}] \\ \text{where } \tilde{A} &= A \Delta P_d(z^{-1}) \end{aligned} \quad (5.49)$$

Simulation Results

In order to demonstrate the effect of $(P(z^{-1}))$, cases from the previous section and where the control activity was high were considered, i.e. $NU \geq 2$. First, assuming the same conditions as in figure (5.11) with an additional polynomial $P(z^{-1}) = \frac{1 - 0.7 z^{-1}}{0.3}$, a run was conducted with the Pancuronium-Bromide model. Figure (5.26) shows how the control activity was considerably reduced and the output response reasonably fast and well damped. The same conditions were maintained when the Atracurium model was considered, leading to the output response of figure (5.27) and showing the input signal to be less active than the one of figure (5.23). If the root of $P_n(z^{-1})$ is this time chosen to give a slower time-constant, e.g: $P(z^{-1}) = \frac{1 - 0.9 z^{-1}}{0.1}$, the performance of figure (5.28) is even

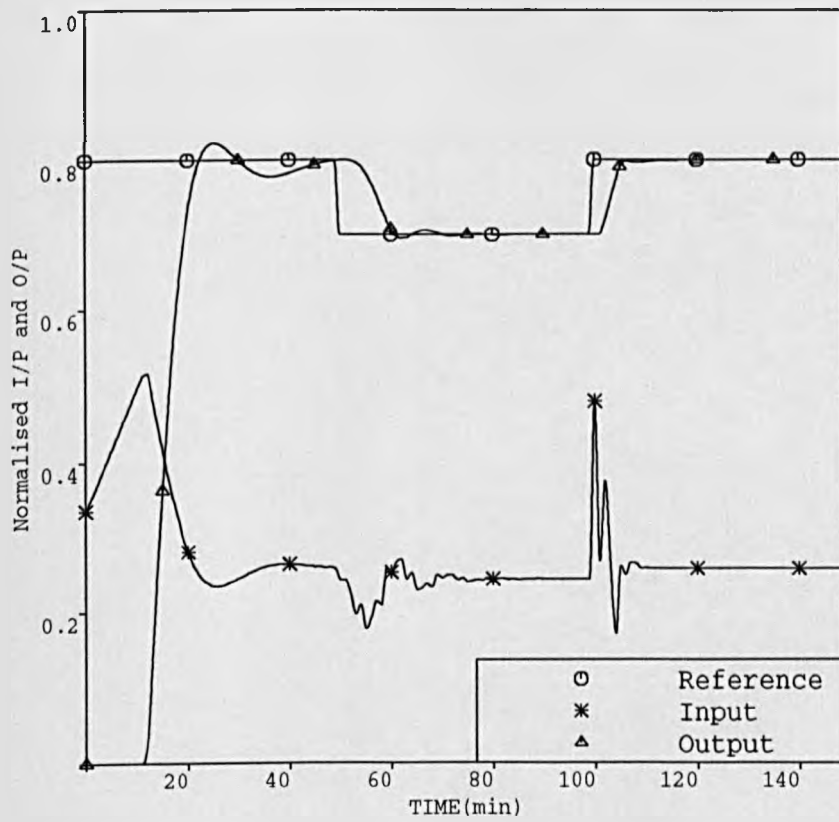


Figure 5.26. Closed-loop response of Pancuronium model; extended GPC algorithm with model following polynomial $P(z^{-1})$; $N_1=1$; $N_2=10$; $NU=2$ and $P(z^{-1})=3.33(1-0.7z^{-1})$

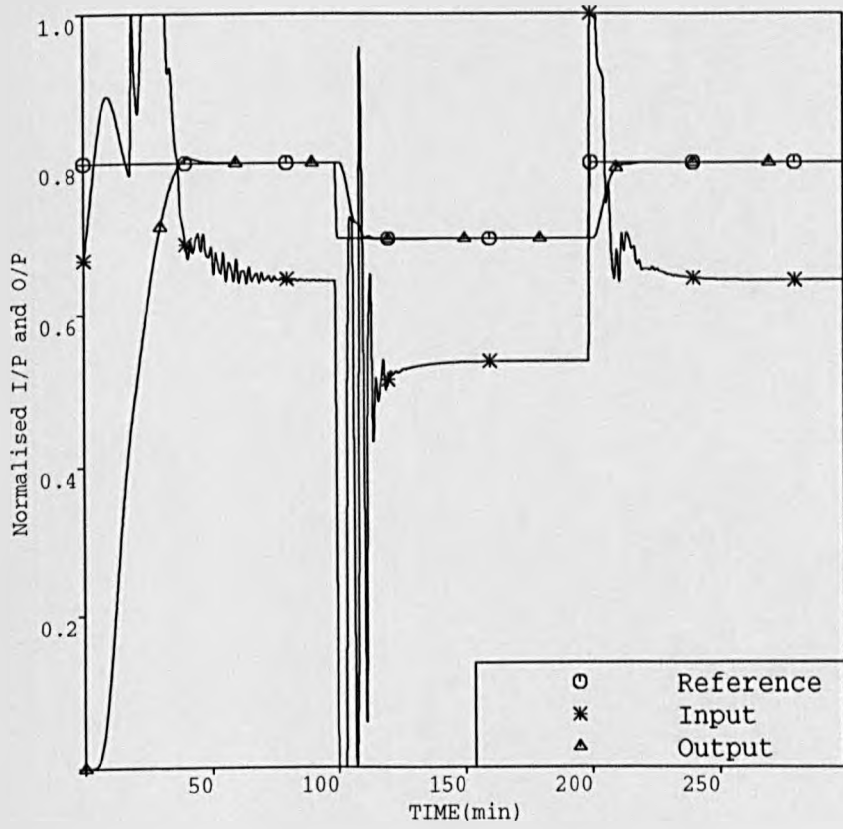


Figure 5.27. Closed-loop response of Atracurium model under the same conditions as those of figure (5.26)

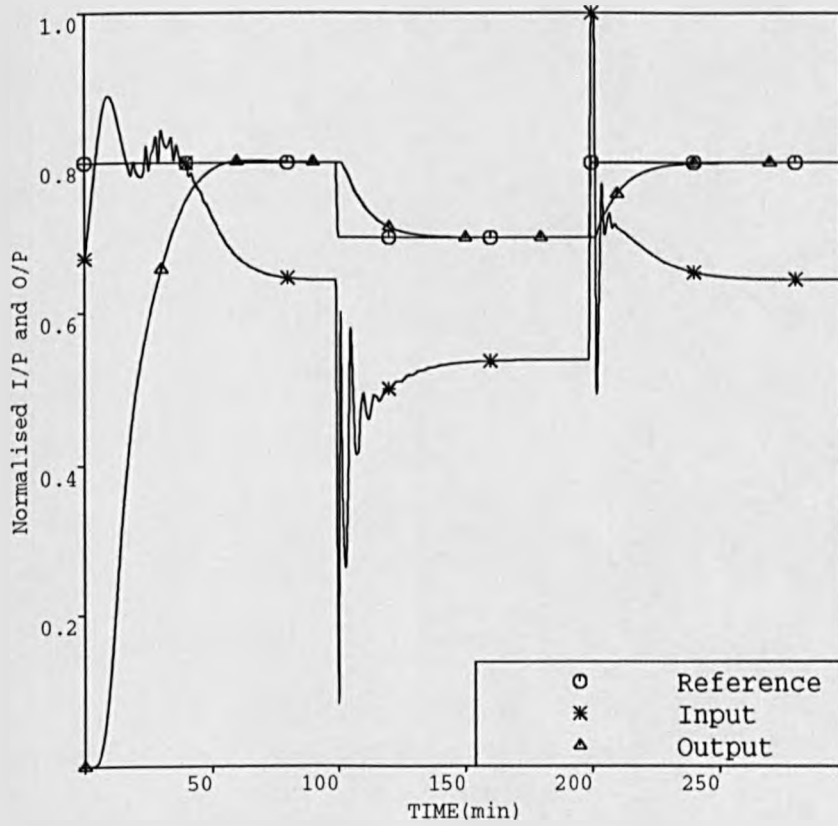


Figure 5.28. Same conditions as in figure (5.27)
but with $P(z^{-1})=10(1-0.9z^{-1})$

better; the response is very well damped and the input signal activity is reduced to a minimum. Table (5.4) summarizes the different values of ISE (Integral of Squared Errors) and ITAE (Integral of Time and Absolute Errors) criteria for cases when $P(z^{-1})$ is used or not for both models. Clearly, the table below indicates how the control activity is reduced at the expense of more sluggishness in the response.

Figure Number	Time-Phases(Min.) from...to...	ISE	ITAE
5.12	0 to 150	9.48	158.40
5.26	0 to 150	9.53	198.98
5.23	0 to 300	9.23	342.36
5.27	0 to 300	9.26	354.40
5.28	0 to 300	9.49	568.75

Table 5.4. Table representing the ISE and ITAE criteria for varying $P(z^{-1})$

5.5.2 GPC and the Observer Polynomial $T(z^{-1})$

In the previous sections, a simplified process model has been adopted when deriving the GPC law such that the $C(z^{-1})$ has been truncated to 1. In practice, because several disturbance and noise sources act on most processes, a formulation is preferred in which the full expression of this polynomial seems to be as close to reality as possible, i.e.,

$$y(t) = \frac{B(z^{-1})}{A(z^{-1})} u(t-1) + \frac{C_1}{A \Delta} \zeta_1(t) + \dots + \frac{C_p}{A \Delta} \zeta_p(t) \quad (5.50)$$

This structure suggests that the measurement vector should include the data

$\zeta_1(t), \dots, \zeta_p(t)$ if C_1, \dots, C_p are to be estimated on-line. However, since most processes are usually subject to different disturbances at different times, any attempt to estimate those terms would be fruitless (Clarke et al., 1987b).

Alternatively, a polynomial $T(z^{-1}) = t_1 + t_1 z^{-1} + \dots + t_{nt} z^{-nt}$ can be used to represent a knowledge of the process noise, leading to a model of the form:

$$y(t) = \frac{B(z^{-1})}{A(z^{-1})} u(t-1) + \frac{T(z^{-1}) \zeta(t)}{A(z^{-1}) \Delta} \quad (5.51)$$

It is clear from the above expression that $T(z^{-1})$ can only affect the disturbance rejection properties of the system unlike $P(z^{-1})$ which affects both. For this reason this polynomial is better known as the **observer polynomial** $T(z^{-1})$. It acts as an observer for the prediction of future (pseudo) outputs (Astrom and Wittenmark, 1984). Another consequence resulting from the introduction of such a polynomial is that the predictions will not be optimal, but if $T(z^{-1}) = C(z^{-1})$, the model (5.4) will be valid and the variances of the output will also be minimum (Astrom and Wittenmark, 1973).

Consider now the following Diophantine equation:

$$T(z^{-1}) = E_j A \Delta + z^{-1} F_j \quad (5.52)$$

where,

$$T(z^{-1}) = t_1 + t_1 z^{-1} + \dots + t_{nt} z^{-nt}$$

Operating in the usual manner, the following prediction equations are obtained:

$$\hat{y}(t+j/t) = G_j(z^{-1}) \Delta u^f(t+j-1) + F_j y^f(t) \quad (5.53)$$

where f denotes a quantity filtered by $\frac{1}{T(z^{-1})}$.

In order to express the above set of equations in terms of Δu rather than Δu^f , consider the following identity:

$$G_j(z^{-1}) = G'_j(z^{-1}) T(z^{-1}) + z^{-j} \Gamma_j(z^{-1}) \quad (5.54)$$

where the coefficients of polynomial $G'_j(z^{-1})$ are similar to those of $G_j(z^{-1})$ for which $T(z^{-1}) = 1$.

$G'_j(z^{-1})$ and $\Gamma(z^{-1})$ are polynomials of the form:

$$\begin{aligned} G'_j(z^{-1}) &= g'_0 + g'_1 z^{-1} + \dots + g'_{j-1} z^{-(j-1)} \\ \Gamma(z^{-1}) &= \gamma_0 + \dots + \gamma_q z^{-q} \end{aligned}$$

Substituting equation (5.54) into equation (5.53) leads to:

$$\begin{aligned} \hat{y}(t+j/t) &= G'_j(z^{-1}) \Delta u(t+j-1) + z^{-j} \Gamma_j(z^{-1}) \Delta u^f(t+j-1) \\ &\quad + F_j y^f(t) \end{aligned}$$

or,

$$\hat{y}(t+j/t) = G'_j(z^{-1}) \Delta u(t+j-1) + \Gamma_j(z^{-1}) \Delta u^f(t-1) + F_j y^f(t) \quad (5.55)$$

In the above expression the signals which are known at time "t" could be extracted as being:

$$f(t+j) = \Gamma_j \Delta u^f(t-1) + F_j y^f(t)$$

and the expression of the control sequence is identical to that of equation (5.32). It is also worth noting that the coefficients of polynomials $G'(z^{-1})$ and $\Gamma(z^{-1})$ are obtained using a recursive formula outlined in appendix A.

In order to understand how the introduction of such a polynomial affects the disturbance properties of a system, consider the following formulation:

Recall from section 5.3 the expression describing the general GPC control law, i.e:

$$H(z^{-1}) \Delta u(t) = \omega(t) - M(z^{-1}) y(t) \quad (5.34)$$

or,

$$u(t) = \frac{\omega(t) - M(z^{-1}) y(t)}{H(z^{-1}) \Delta}$$

If the filter $T(z^{-1})$ is used, equation (5.34) could be rewritten as:

$$u(t) = \frac{\omega(t) - \frac{M(z^{-1})}{T(z^{-1})} y(t)}{\frac{H(z^{-1}) \Delta}{T(z^{-1})}} \quad (5.56)$$

leading to the diagram of figure (5.29). If the disturbances, which are of high frequency nature, occur, they affect the output, and the expression fed-back to the loop contains the filter $\frac{M(z^{-1})}{T(z^{-1})}$. The feedback gain is therefore attenuated providing that the same filter possesses low-pass frequency characteristics. Moreover, the use of $T(z^{-1})$ also has the advantage of low-pass filtering the data for the estimator, considering that the Δ operator is normally equivalent to a high-pass filter, this leads to an overall filter having band-pass characteristics.

In practice there are no well supported rules for choosing the filter parameters. Clarke and Robinson (1991) conducted a study in which the notion of stability bound was introduced, the bound having to be kept as high as possible to ensure robustness. Slow observer roots were found to satisfy this requirement. However, if these roots are too slow, loss of performance could be obtained in some cases due to the appearance of unstable poles (zeros of $H(z^{-1})$). Another study carried out by Shook et al. (1991), also focussed on the same subject, proposed a method in which the RLS estimator was replaced by an identification scheme called Long-Range Predictive identification (LRPI) and which uses the minimization of some cost function including the assumed linear model. Faster convergence of the estimates was shown to be possible. Nevertheless, if the RLS is still to be used, the research work hitherto conducted agreed on the following:

To ensure good robustness properties, choose $T(z^{-1})$ such that its cut-off frequency coincides with the dominant time-constant of \hat{A} , i.e:

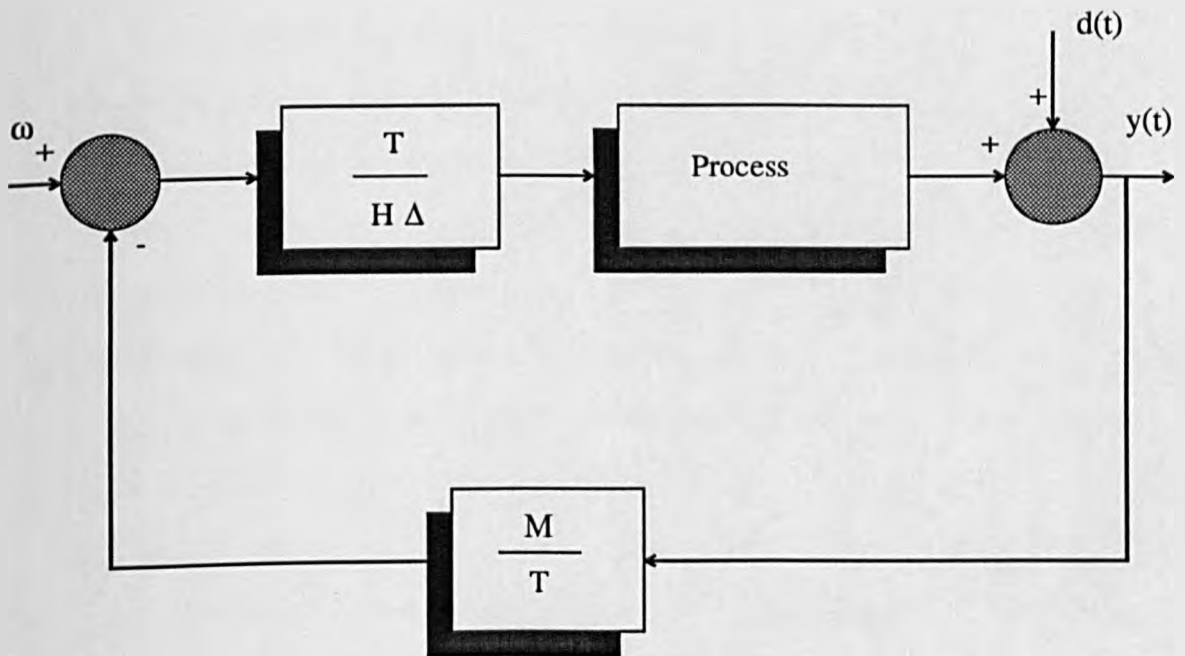


Figure 5.29. Diagram representing the standard control-loop

$$T(z^{-1}) = (1 - \beta z^{-1})^n$$

$$n = (\text{degree of } \hat{A}(z^{-1})) + 1$$

Simulation Results

In order to test the effect of the observer polynomial $T(z^{-1})$ on the overall GPC performance, two tests were undertaken; introduction of a sudden disturbance during the run, and inclusion of a noise sequence. As pointed out previously for the muscle relaxation system, these phenomena are commonly due to sudden patient's movements or diathermy (severe electrical interference). To test the robustness of GPC under such circumstances, a series of experiments was conducted in which both models were considered. Assuming the same conditions as those of figure (5.15) and introducing a disturbance of 4% at iteration 70, a run was undertaken using a filter of the form $T(z^{-1}) = 1 - 0.95 z^{-1}$ (corresponding to a time-constant of $T_s = 20$ minutes). Figure (5.30) shows how the controller was quick to reject the disturbance without its performance deteriorating. In fact the control signal was better conditioned than the one in figure (5.15) despite the severe changes in time-delay. For Atracurium, similar conditions to those for figure (5.24) were considered except that a disturbance was introduced at the same iteration 70 as before. The filter considered was of the form $T(z^{-1}) = 1 - 0.97 z^{-1}$. Figure (5.31) demonstrated a good performance of the GPC algorithm despite the range between which the delay was varying. Finally, the conditions were repeated with the inclusion of a PRBS sequence of 1% amplitude. Figures (5.32) and (5.33) show the performances of GPC for Pancuronium and Atracurium respectively which were both acceptable since the outputs were kept within a reasonable band. The parameter estimates were somewhat biased and converged respectively to:

$$\hat{a}_1 = -0.2226 \quad \hat{a}_2 = -0.5413 \quad \hat{b}_1 = 0.6001 \quad \hat{b}_2 = -0.3299$$

$$\hat{b}_3 = 0.2377 \quad \hat{b}_4 = -0.0400 \quad \hat{b}_5 = 0.3360$$

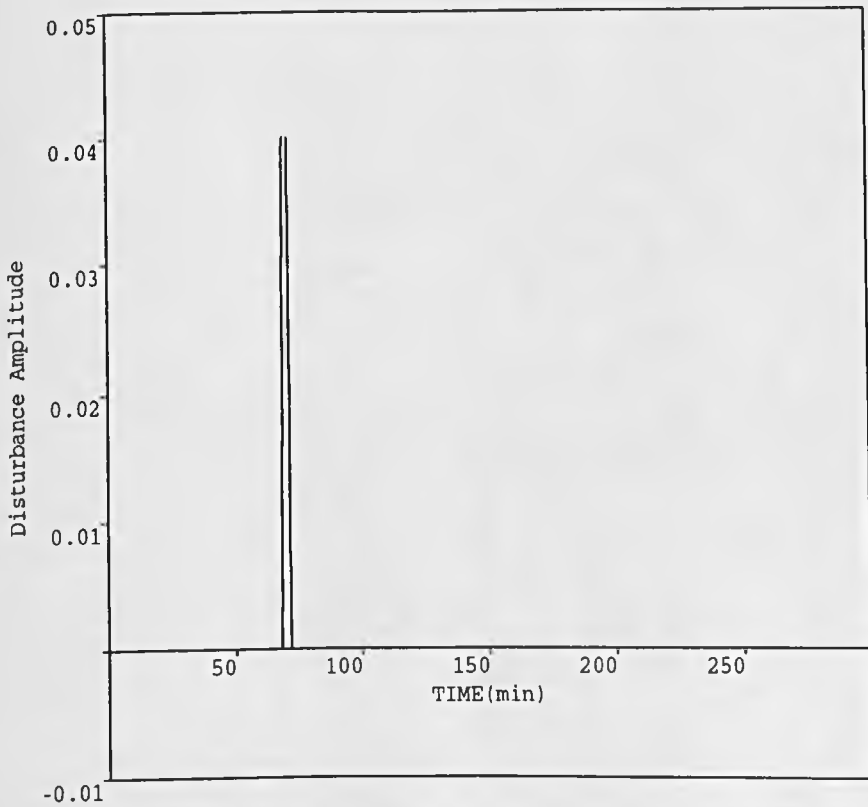
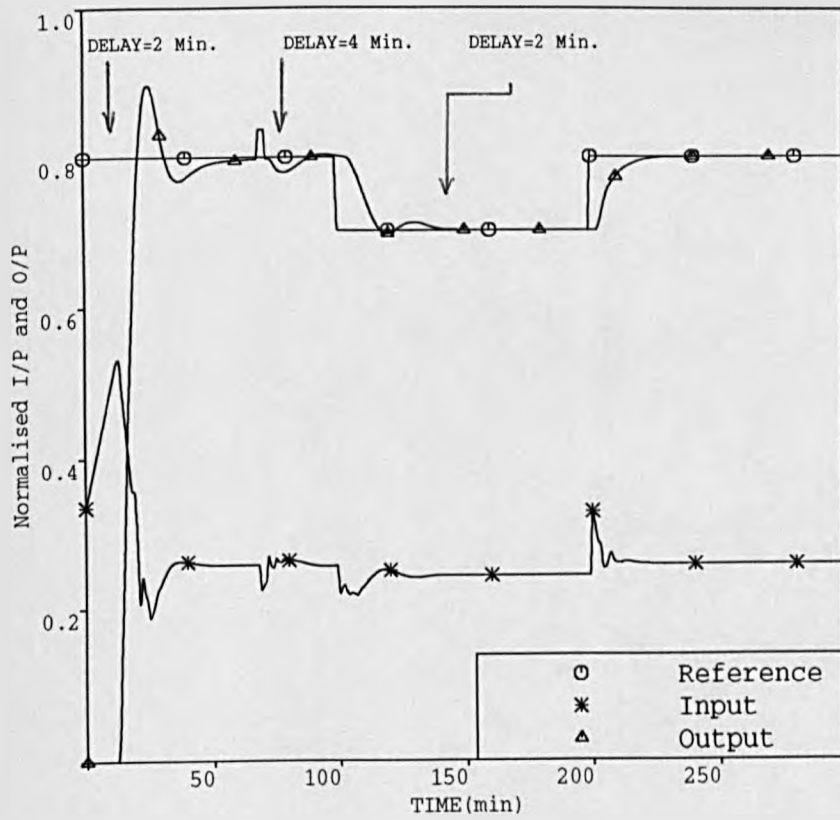


Figure 5.30. Closed-loop response of Pancuronium model with additive disturbance; extended algorithm with $T(z^{-1})=1-0.95z^{-1}$

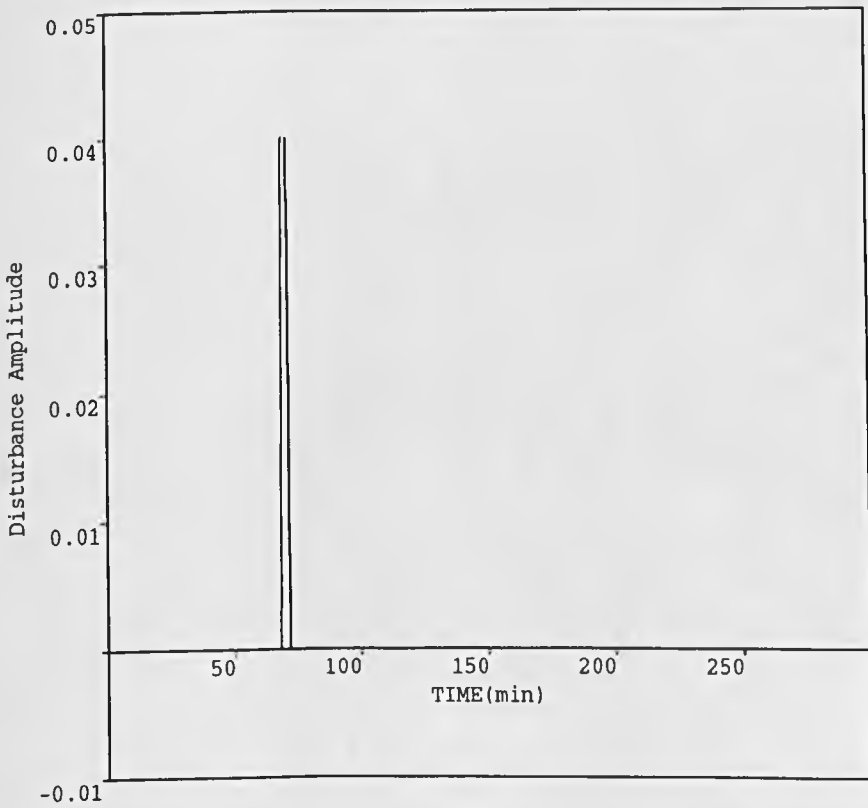
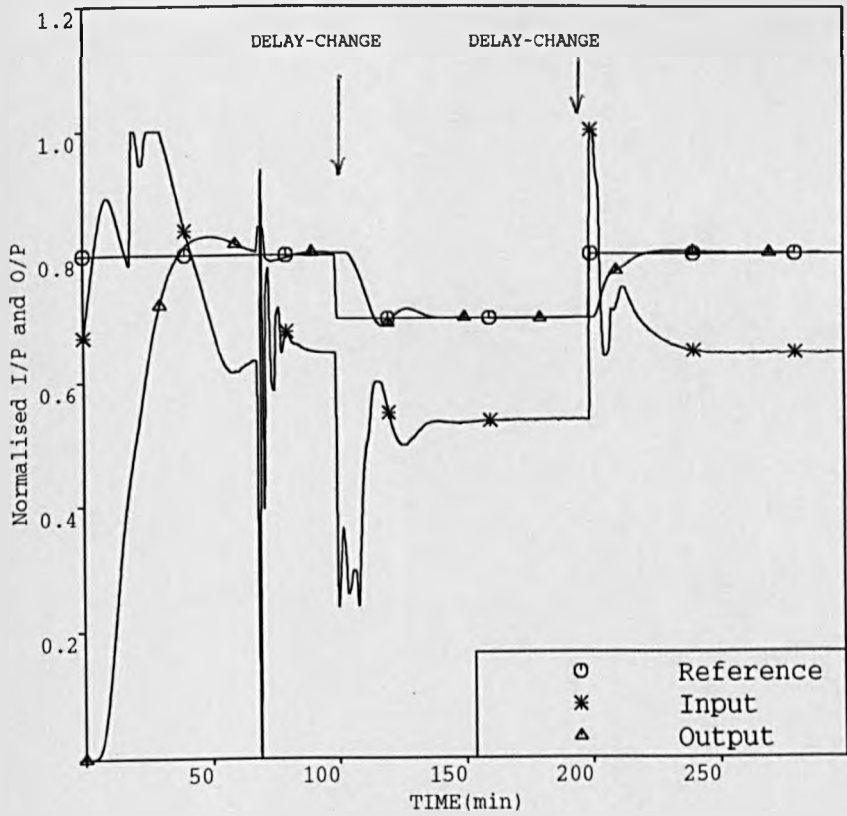


Figure 5.31. Closed-loop response of Atracurium model with additive disturbance; extended algorithm with $T(z^{-1})=1-0.97z^{-1}$

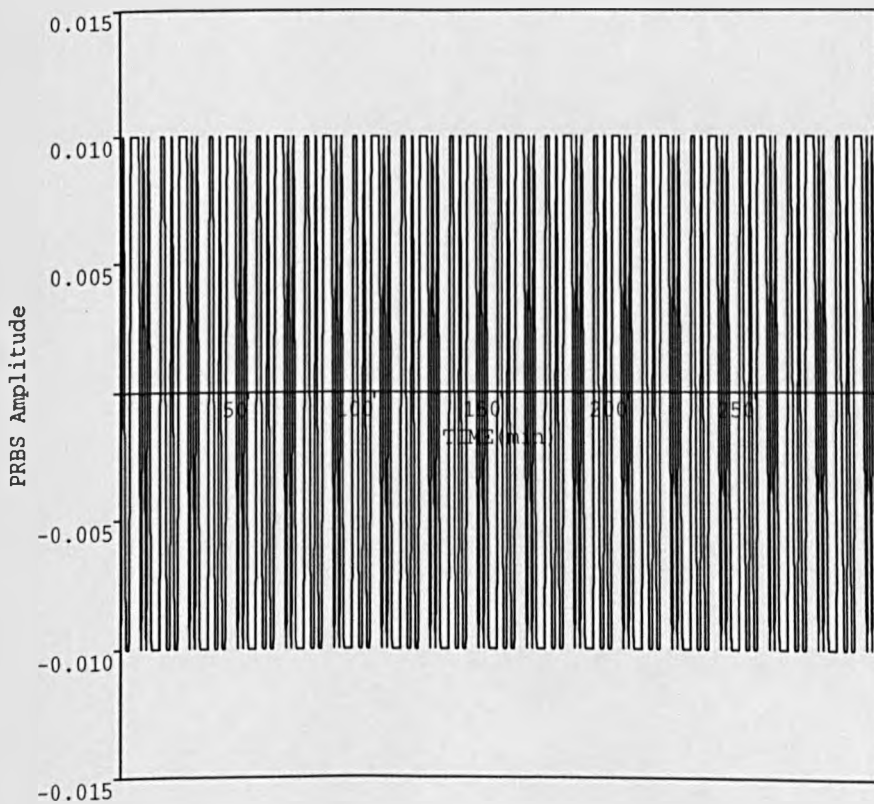
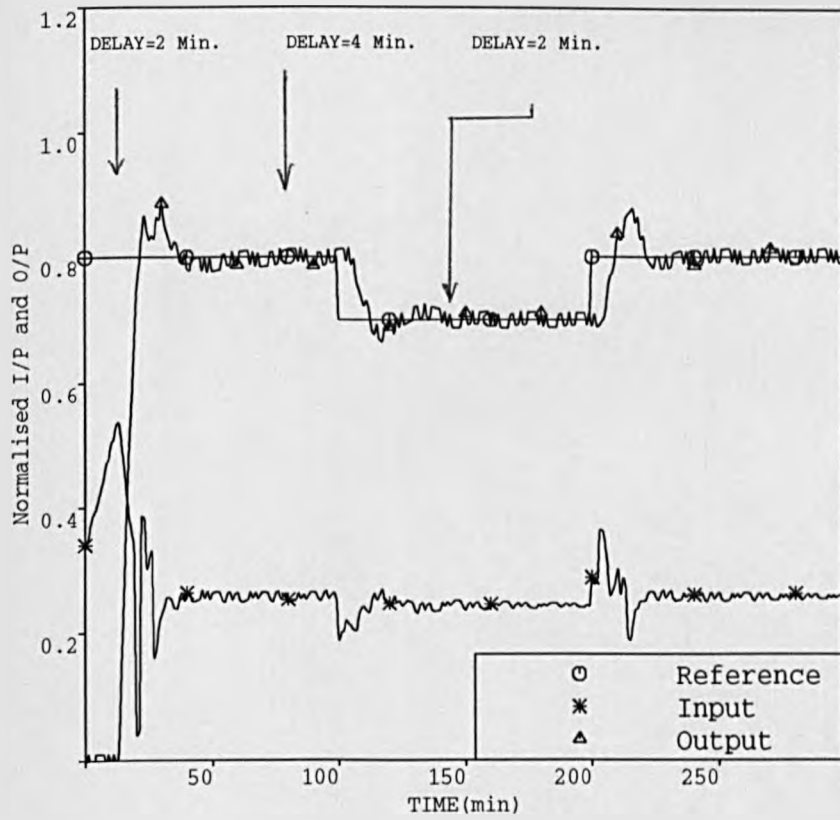


Figure 5.32. Same conditions as in figure (5.30)
but with additive noise

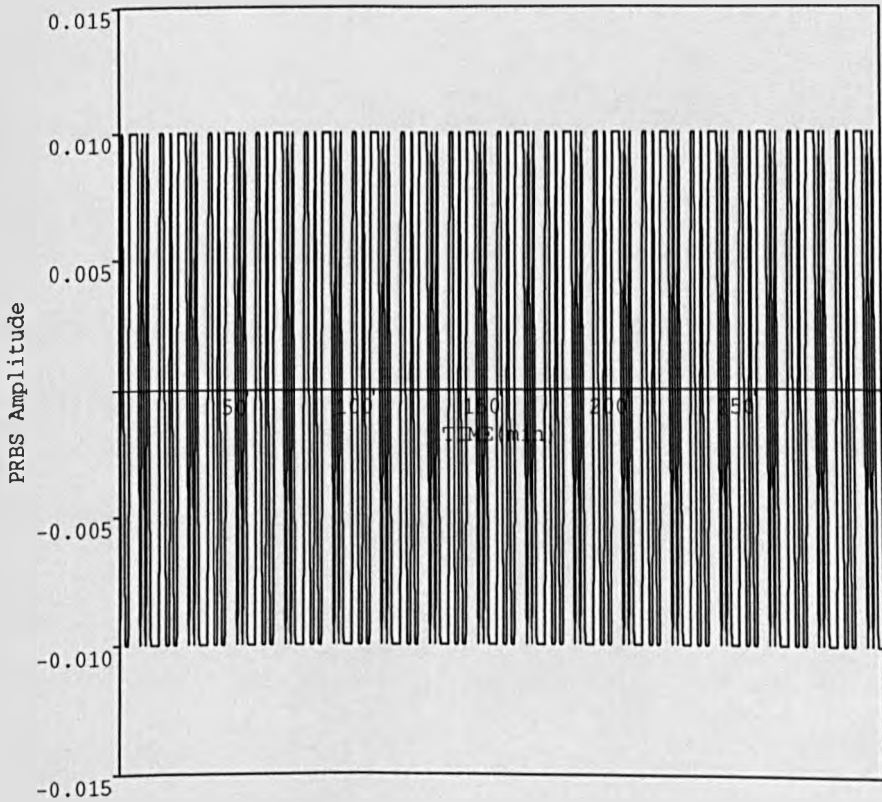
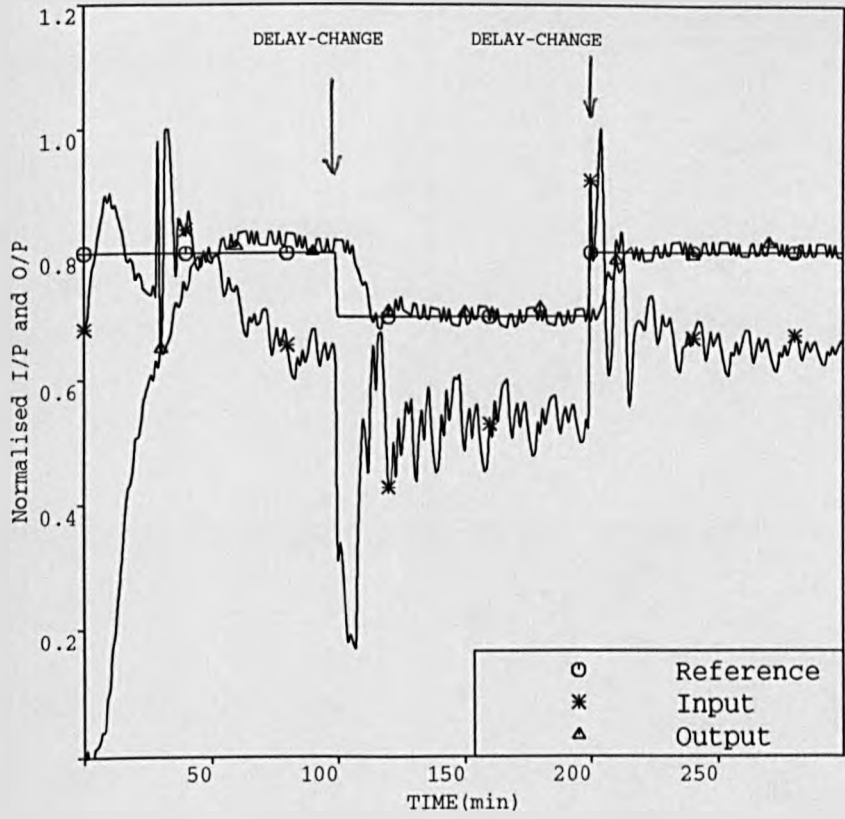


Figure 5.33. Same conditions as in figure (5.31)
but with additive noise

for Pancuronium-Bromide,

and

$$\begin{aligned}\hat{a}_1 &= -0.1083 & \hat{a}_2 &= -0.4559 & \hat{a}_3 &= -0.2606 \\ \hat{b}_1 &= 0.1623 & \hat{b}_2 &= 0.0280 & \hat{b}_3 &= -0.0869 \\ \hat{b}_4 &= 0.0425 & \hat{b}_5 &= 0.0389 & \hat{b}_6 &= 0.0109\end{aligned}$$

for Atracurium.

5.6 GENERALIZED PREDICTIVE CONTROL WITH INPUT CONSTRAINTS

The standard GPC algorithm giving the best unconstrained control increment $\Delta u(t)$ necessary to calculate the control sequence $u(t)$, is found by minimizing some cost function J (equation (5.30)). While it was possible to obtain performances where the input signal did not reach the maximum and minimum limits imposed by the system, other parameter settings such as $NU \geq 2$, were found to cause the control signal to be highly active. Theoretical results, confirmed by simulation experiments of the previous sections, showed that the use of λ and $P(z^{-1})$ can reduce considerably this activity at the expense of modifying the overall closed-loop characteristics. Research work namely by Tsang and Clarke (1988) considered the inclusion of such constraints (saturation) directly within the cost function J before deriving the control increments. This was shown to lead to better performances.

The constraints could be of two types: rate constraints and amplitude constraints. The following sections look at each of them separately and derive the associated modified control algorithms.

5.6.1 GPC and the Soft Rate Limits

Because GPC calculations are based on increments rather than amplitudes, consider the following limitations:

$$\alpha_j \leq \Delta u(t + j - 1) \leq \beta_j \quad j = 1, 2, \dots, NU \quad (5.57)$$

where α_j and β_j represent the minimum and maximum limits considered constant over the interval 'j', and let $\Delta u^*(t + j - 1) \quad j = 1, 2, \dots, NU$ be the solution obtained using the unconstrained GPC algorithm.

When $NU = 1$, the best solution $\Delta u(t)$ is obtained by clipping $\Delta u^*(t)$ between α_j and β_j . In this case, and as illustrated in figure (5.34) the "J = constant" contours are described by a set of circles (for visual purposes) whose common centre represents the unconstrained minimum control increment $\Delta u(t)^*$ and where the clipped minimum as well as the constrained one are the same, while figure (5.35) shows that for $NU = 2$ the "J = constant" contours are represented by a set of ellipses showing combinations of inputs giving the same value for the cost function. The two minima are different in this case. In figure (5.35) 'ü' represents the vector of components formed by $\Delta u(t)$, and $\Delta u(t+1)$.

For this latter case of $NU = 2$ consider the following inequality:

$$\alpha_1 \leq \Delta u^*(t + j - 1) \leq \beta_1 \quad j = 2, 3, \dots, NU \quad (5.58)$$

where * denotes that the quantities are the ones derived under the unconstrained algorithm.

If this condition is satisfied for all the control increments over the interval 'j', then the best control increment is given by clipping $\Delta u^*(t)$ between α_j and β_j . However, if condition (5.58) is only verified for some of the increments, then the best

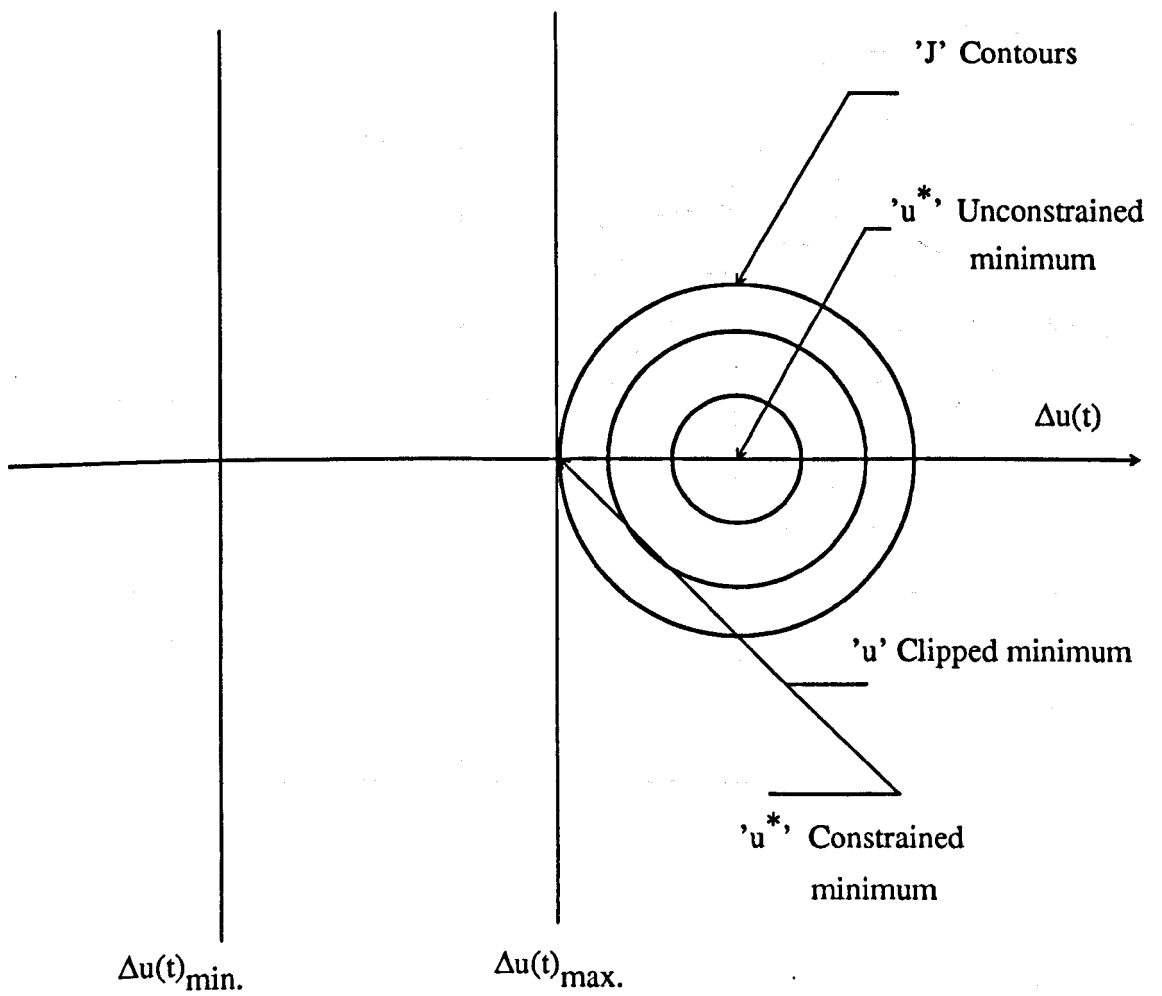


Figure 5.34. Positions of the clipped and constrained minimum for $NU=1$

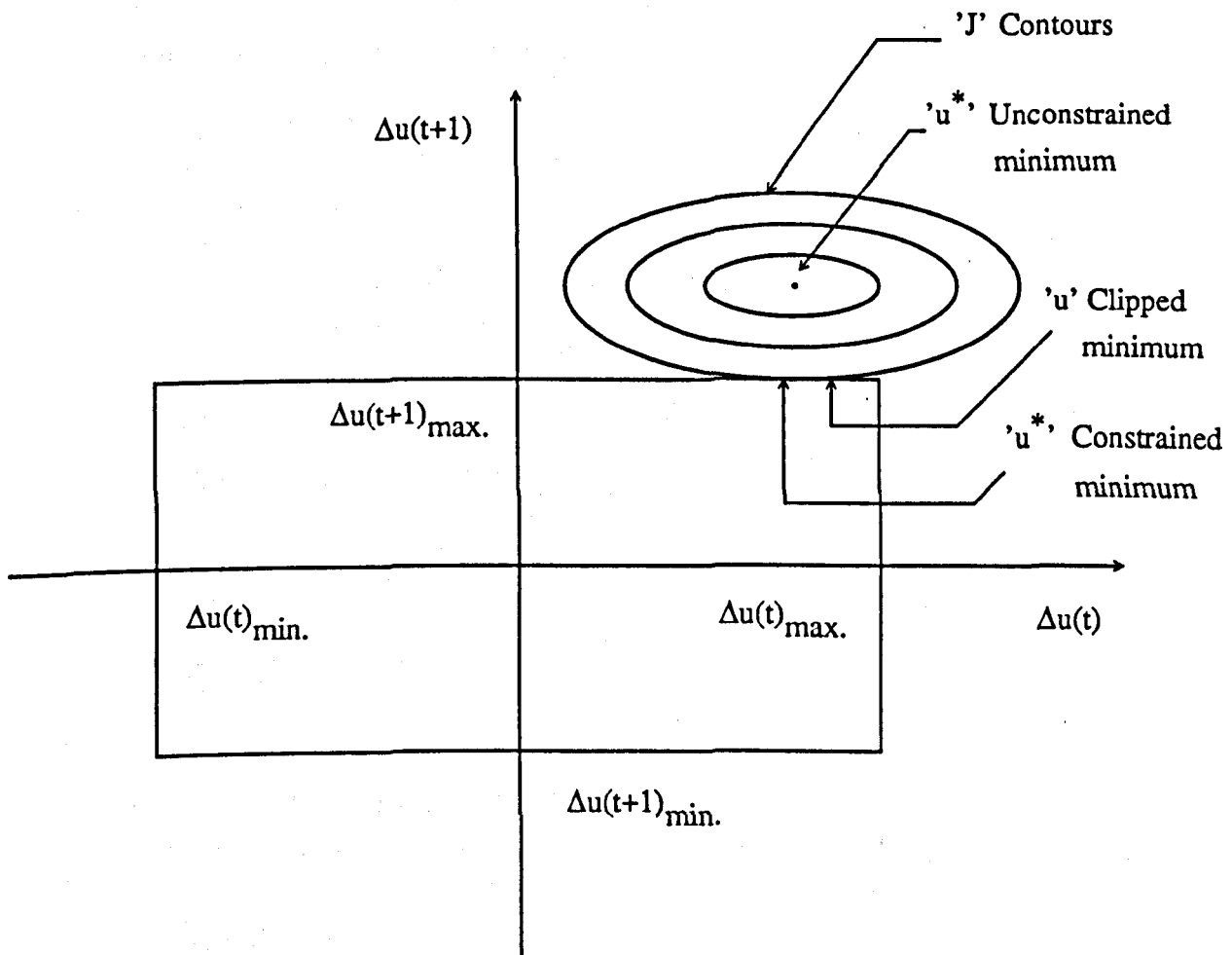


Figure 5.35. Positions of the clipped and constrained minimum for $NU=2$

control sequence is obtained by reoptimizing the cost function in equation (5.30) and taking into account NU. Hence, consider the case where the constrained optimum has one control just on the constraint boundary, i.e:

$$\Delta u(t + j - 1) = \alpha_j \quad (5.59)$$

Consider the function:

$$L = (G_1 \bar{u} + f - \omega)^T (G_1 \bar{u} + f - \omega) + \lambda \bar{u}^T \bar{u} + 2 \mu_j [\Delta u(t + j - 1) - \alpha_j] \quad (5.60)$$

where, μ_j is the Lagrange multiplier, and α_j the limit of the boundary. All other variables are as defined previously.

Deriving L with respect to \bar{u}^T leads to:

$$\frac{\partial L}{\partial \bar{u}^T} = 0$$

or,

$$2 G_1^T (G_1 \bar{u} + f - \omega) + 2 \lambda I \bar{u} + 2 \mu_j e_j = 0$$

Because only the j th increment is assumed to violate the boundary, it follows that:

$$e_j = [0, 0, \dots, 1, \dots, 0]^T$$

Therefore, the full expression of the new constrained optimum becomes:

$$\begin{aligned} \bar{u} &= \bar{u}^* - (G_1^T G_1 + \lambda I)^{-1} \mu_j e_j \\ \bar{u}^* &= (G_1^T G_1 + \lambda I)^{-1} G_1^T (\omega - f) \end{aligned} \quad (5.61)$$

where \bar{u}^* represents the GPC unconstrained solution.

The Lagrange multiplier could be found by using equation (5.59), i.e:

$$\alpha_j = \Delta u(t + j - 1) = \Delta u^*(t + j - 1) - h_{jj} \mu_j \quad (5.62)$$

where h_{jj} represents the j th term of the matrix $(G_1^T G_1 + \lambda I)^{-1}$.

Hence,

$$\mu_j = \frac{-\alpha_j + \Delta u^*(t+j-1)}{h_{jj}}$$

Summarizing, the constrained GPC solution is:

$$\begin{aligned} \bar{u} &= \bar{u}^* + (G_1^T G_1 + \lambda I)^{-1} \mu_j e_j \\ \mu_j &= \frac{-\alpha + \Delta u^*(t+j-1)}{h_{jj}} \end{aligned} \quad (5.63)$$

In the case of the muscle relaxation system, the sequence $u(t)$ is implemented rather than $\Delta u(t)$. Therefore, limits on $\Delta u(t)$ have to be imposed taking into account those already existing on $u(t)$ (Clarke, 1985a). The method is called "soft rate limiting".

5.6.2 GPC and Amplitude Limits

For the simple reason already mentioned in section 5.6.1, it is difficult to establish an expression for the constrained minimum using constraints on the amplitude rather than on the increment, unless the QP approach is involved (Lawson and Hanson, 1974) which on the other hand is computationally demanding. However, the simple case of $NU = 2$ is considered here.

Suppose that the condition $\alpha_1 \leq u^*(t+1) \leq \beta_1$ is violated, then the expression for the new control sequence taking into account the new constraints needs to be formulated.

Consider the following inequalities:

$$\begin{aligned} \alpha_1 &\leq u(t) \leq \beta_1 \\ \alpha_2 &\leq u(t+1) \leq \beta_2 \end{aligned} \quad (5.64)$$

Subtracting $u(t-1)$ from both sides of each inequality leads to:

$$\begin{aligned}\alpha_1 - u(t-1) &\leq u(t) - u(t-1) \leq \beta_1 - u(t-1) \\ \alpha_2 - u(t-1) &\leq u(t+1) - u(t-1) \leq \beta_2 - u(t-1)\end{aligned}\quad (5.65)$$

or,

$$\begin{aligned}\alpha'_1 &\leq \Delta u(t) \leq \beta'_1 \\ \alpha'_2 &\leq \Delta u(t+1) + \Delta u(t) \leq \beta'_2 \\ \alpha'_1 &= \alpha_1 - u(t-1) \\ \beta'_1 &= \beta_1 - u(t-1) \\ \alpha'_2 &= \alpha_2 - u(t-1) \\ \beta'_2 &= \beta_2 - u(t-1)\end{aligned}\quad (5.66)$$

Consider the following expression:

$$\begin{aligned}L &= (G_1 \bar{u} + f - \omega)^T (G_1 \bar{u} + f - \omega) + \lambda \bar{u}^T \bar{u} \\ &\quad + 2 \mu_j [\Delta u(t) + \Delta u(t+1) - \alpha'_2]\end{aligned}\quad (5.67)$$

Minimization of L leads to :

$$\begin{aligned}\bar{u} &= \bar{u}^* - (G_1^T G_1 + \lambda I)^{-1} \mu e \\ e &= [1 \ 1]^T\end{aligned}$$

Because $\alpha'_2 = \Delta u(t) + \Delta u(t+1)$, it follows that:

$$\begin{aligned}\alpha'_2 &= \Delta u^*(t) + \Delta u^*(t+1) - \mu (\sigma_1 + \sigma_2) \\ \sigma_i &\text{ being the sum of the } i\text{th rows of } (G_1^T G_1 + \lambda I)^{-1}\end{aligned}$$

Therefore,

$$\mu = \frac{-\alpha'_2 + \Delta u^*(t) + \Delta u^*(t+1)}{\sigma_1 + \sigma_2}\quad (5.68)$$

Hence, the final constrained solution when $NU = 2$ could be summarized as:

$$\Delta u(t) = \Delta u^*(t) - \frac{\sigma_1}{\sigma_1 + \sigma_2} [-\alpha'_2 + \Delta u^*(t) + \Delta u^*(t+1)]\quad (5.69)$$

Simulation Results

In order to test the robustness of the revised GPC algorithm, a series of 5 experiments was undertaken in which the same controller settings as in figure (5.23) were considered, i.e (1, 10, 2, 0) for (N_1, N_2, NU, λ) . Only the Atracurium model was used here. Figure (5.36) to figure (5.39) show the performances of the constrained GPC with "soft rate limits". Limits on the control increments of $\pm 0.20, \pm 0.15, \pm 0.10, \pm 0.05$ were imposed respectively. Clearly, the control activity has considerably decreased for the three last cases without modifying the overall closed-loop characteristic. Table (5.5) summarizes the number of times the condition for constraints $(\alpha_1 \leq \Delta u^*(t+1) \leq \beta_1)$ was violated. Notice that the smaller these boundaries became the more times the condition was violated, and therefore the less active the control signal was. This is understandable, since the cost function is more often reoptimized to include the constraints. Finally, the GPC with amplitude constraints produced exactly the same output as that of figure (5.23) since the condition $\alpha_1 \leq u^*(t+1) \leq \beta_1$ was never violated.

Fig.Nbr.	Constr.Type	Rate (Ampl.) Limits	Viol. Freq.
5.36	Soft Rate Limits	± 0.20	36
5.37	Soft Rate Limits	± 0.15	42
5.38	Soft Rate Limits	± 0.10	47
5.39	Soft Rate Limits	± 0.05	69
Same as 5.23	Amplitude Limits	0.0 – 1.0	0

Table 5.5 Table representing the frequency of condition violation versus the rate (ampl.) limits

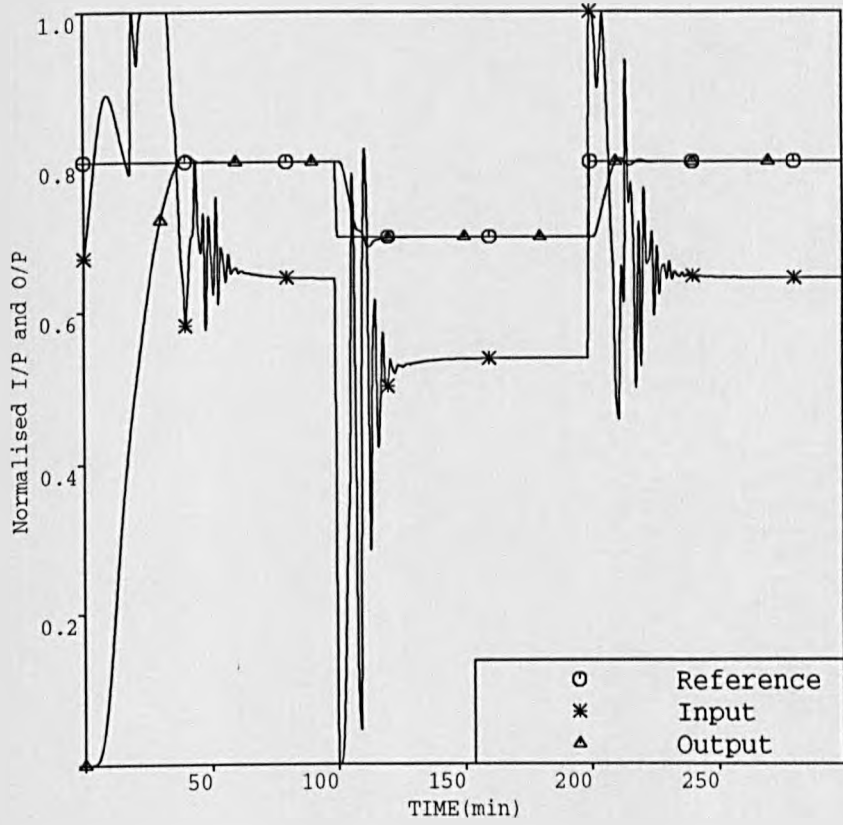


Figure 5.36. Closed-loop response of Atracurium model under GPC algorithm with input constraints; soft rate limiting method with rate limits of ± 0.20 ; $N_1=1$; $N_2=10$; $NU=2$

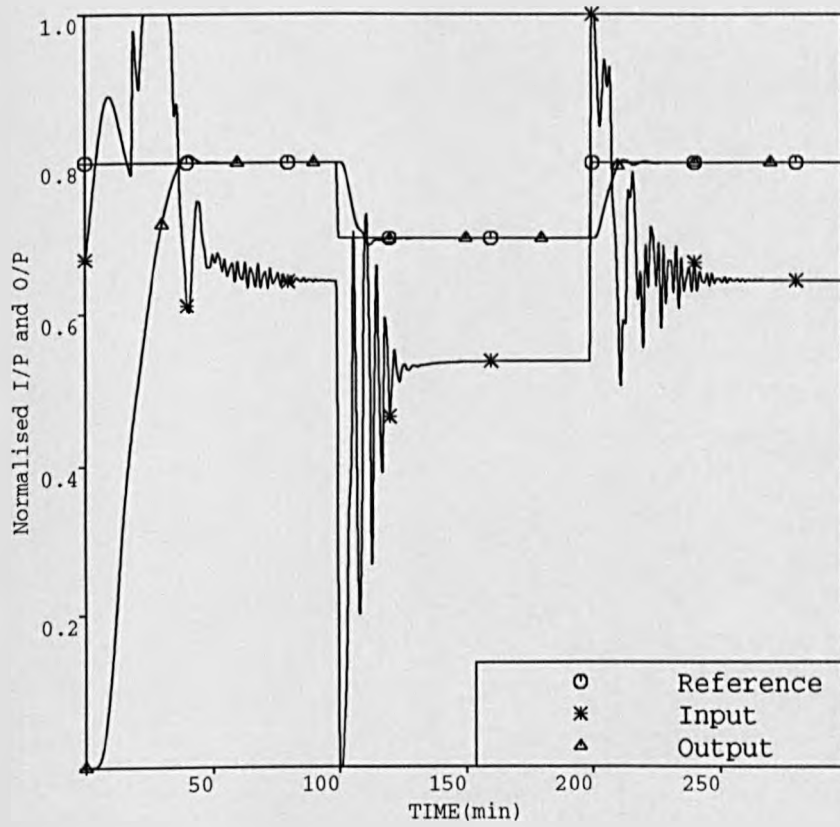


Figure 5.37. Same conditions as in figure (5.36)
but with rate limits of ± 0.15

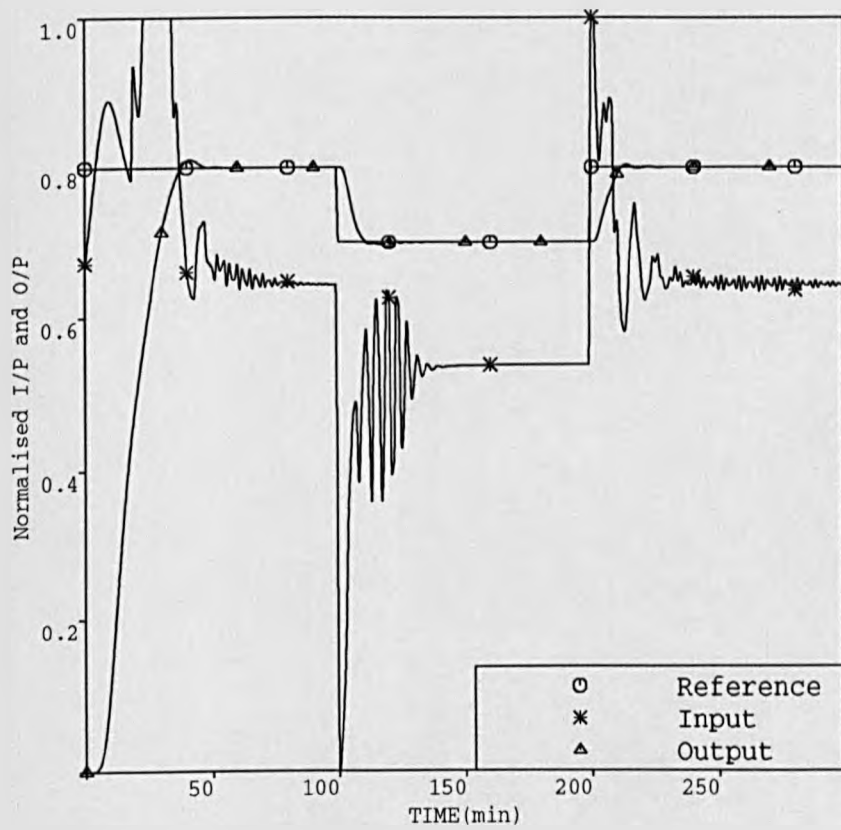


Figure 5.38. Same conditions as in figure (5.36)
but with rate limits of ± 0.10

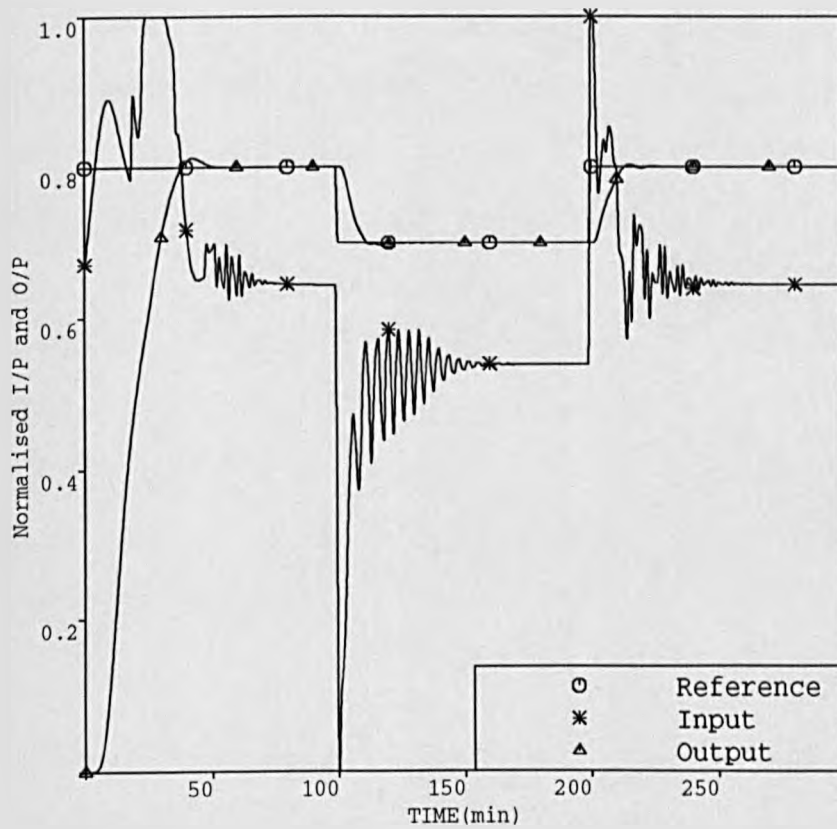


Figure 5.39. Same conditions as in figure (5.36)
but with rate limits of ± 0.05

In conclusion to this chapter, it can be stated that the application of a self-tuning adaptive control technique known as GPC and based on a long-range predictive approach (LRPC) to the muscle relaxation system associated with two drug models (Pancuronium-Bromide and Atracurium) proved very effective indeed. The algorithm was reviewed in its basic form as well as in its extended version. The performance of the former algorithm, which includes four tuning knobs, i.e: N_1 , N_2 , NU , λ , under harsh simulation conditions was good. The later inclusion of the model following polynomial $P(z^{-1})$ and the observer polynomial $T(z^{-1})$ added more robustness and flexibility to the algorithm. Experimental results, supported by performance criteria, showed that $P(z^{-1})$ affected the disturbance rejection of the system as well as the set-point response, whereas the $T(z^{-1})$ affected only its disturbance rejection. Also experiments carried out under corrupted noise measurements and sudden disturbances, showed that the use of this polynomial prevented the manipulated variable from highly active or unstable modes.

Because high values of the control horizon NU induced unnecessarily active signals often well beyond saturation limits, it was argued that the cost function whose minimization provided the GPC solution, had to include such constraints in order to extract the best possible control sequence. Smoother input signals without modification of the set-point response were proved possible.

The next chapter considers the implementation of the same algorithm, whose robustness has been demonstrated, under real-time conditions using an analogue computer.

CHAPTER 6

MICROCOMPUTER IMPLEMENTATION AND PERFORMANCE EVALUATION OF THE GPC CONTROLLER: A SIMULATION STUDY FOR PANCURONIUM AND ATRACURIUM

6.1 INTRODUCTION

The previous chapters 4 and 5 have described mainly the application of different control strategies to different drug models in simulated environments that were as close as possible to real conditions. The modelling study included the existing knowledge of the Pancuronium and Atracurium kinetics resulting from PRBS identification studies and bolus injections respectively, and pharmacodynamic characteristics such as the Hill equation (Whiting and Kelman, 1980; Weatherley et al., 1983) or a dead-space and a saturation element. The later incorporation in the simulated model of a noise model, sudden disturbances and varying time-delay made the whole system realistic.

The simulation results obtained were very encouraging. To further demonstrate the robustness of the control strategies, it was judged necessary to assess their performances under real-time conditions. Previous research studies by Menad (1984) and Denai et al. (1990) who undertook a similar task using different self-tuning algorithms (pole-placement and self-tuning PID respectively) demonstrated this to be very useful prior to any trials in theatre.

The real-time simulation study which will follow in the next sections concerns only the GPC control strategy, and it has been made possible by combining a Research Machines 380Z disk-based microcomputer system and a VIDAC 336

analogue computer. Interface between the two devices is made via 10 bits analogue to digital-digital to analogue (AD/DA) hardware converters.

The system that forms the 380Z disk-based microcomputer uses the Fortran 80 as a high level language. Several other routines are available for use with the system to perform well defined functions. Among these routines, the interrupt routines could be cited as forming an important part of the overall system, since it is these which allow one to set-up the real-time clock from the background processing unit. The frequency of the interrupts on all the channels (AD/DA) was chosen to be 1Hz corresponding to a 1 second sampling time which represents 60 times faster real-time performance.

The VIDAC 336 analogue computer is an important instrument that spans between symbolism and the physical problem. Operational amplifiers, together with potentiometers, diodes, and resistors constitute the main equipment used to solve many complex problems by patching their corresponding equations on a 'patch board'. The machine operates within a range of ± 10 volts and the limit voltage used is referred to as the machine unit (1 M.U=10 volts). This voltage reference is available both in positive and negative forms and constitutes the basis for any scaling of the variables which are normally generated in the background program segment. Section 6.2 below will be concerned with the representation of the Pancuronium dynamics on the analogue computer and the application of the GPC algorithm in a series of simulations, whereas section 6.3 will consider the Atracurium model.

6.2 CONTROL OF PANCURONIUM ADMINISTRATION USING GPC

6.2.1 Model Representation on the VIDAC 336

In order to obtain a model representation relative to Pancuronium on the analogue computer recall first the transfer function describing the kinetics of the drug, i.e:

$$\frac{X(s)}{U(s)} = \frac{K_1}{(1 + T_1 s)(1 + T_2 s)} \quad (6.1)$$

or,

$$\frac{X(s)}{U(s)} = \frac{r_0}{q_0 + q_1 s + s^2} \quad (6.2)$$

Decomposing and rearranging leads to the following:

$$\begin{aligned} -\frac{d}{dt}(-\dot{X}) &= -q_1 \dot{X} - q_0 X + r_0 U \\ -\frac{d}{dt} X &= -\dot{X} \end{aligned} \quad (6.3)$$

For this equation to be adequately patched on the VIDAC computer it is particularly important to normalize the outputs X and \dot{X} with respect to the range within which the machine is operating, i.e 1 M.U., by taking into account the respective maximum values X_m and \dot{X}_m of X and \dot{X} respectively. This consideration is even more useful in the Atracurium case, as it will be shown later, where the previous quantities greatly exceed the 1 M.U. range. Thus, the above equations could be rewritten as:

$$\begin{aligned} -\frac{d}{dt} \left[-\frac{\dot{X}}{\dot{X}_m} \right] &= -q_1 \left[\frac{\dot{X}}{\dot{X}_m} \right] + q_0 \frac{X_m}{\dot{X}_m} \left[-\frac{X}{X_m} \right] + r_0 \frac{U}{\dot{X}_m} \\ -\frac{d}{dt} \left[\frac{X}{X_m} \right] &= \frac{\dot{X}_m}{X_m} \left[-\frac{\dot{X}}{\dot{X}_m} \right] \end{aligned} \quad (6.4)$$

Open-loop studies showed that the maximum values at the outputs of the first and second integrator were:

$$\dot{X}_m = X_m = 1.0$$

Thus, using the nominal values for Pancuronium kinetics as specified in chapter 2, it follows that:

$$\begin{aligned} -\frac{d}{dt} \begin{bmatrix} -\frac{\dot{X}}{1.0} \end{bmatrix} &= 0.5500 \begin{bmatrix} -\frac{\dot{X}}{1.0} \end{bmatrix} + 0.0250 \begin{bmatrix} -\frac{X}{1.0} \end{bmatrix} \\ &+ 0.0875 \begin{bmatrix} U \end{bmatrix} \\ -\frac{d}{dt} \begin{bmatrix} \frac{X}{1.0} \end{bmatrix} &= 1.0000 \begin{bmatrix} -\frac{\dot{X}}{1.0} \end{bmatrix} \end{aligned} \quad (6.5)$$

Or, if amplifiers are used, the above system becomes:

$$\begin{aligned} -\frac{d}{dt} \begin{bmatrix} -\frac{\dot{X}}{1.0} \end{bmatrix} &= 0.0550 (10) \begin{bmatrix} -\frac{\dot{X}}{1.0} \end{bmatrix} + 0.0250 (1) \begin{bmatrix} -\frac{X}{1.0} \end{bmatrix} \\ &+ 0.0875 (1) \begin{bmatrix} U \end{bmatrix} \\ -\frac{d}{dt} \begin{bmatrix} \frac{X}{1.0} \end{bmatrix} &= 1.0000 (1) \begin{bmatrix} -\frac{\dot{X}}{1.0} \end{bmatrix} \end{aligned} \quad (6.6)$$

Figure (6.1) shows the analogue representation of the non-linear model which does not include the delay element which it was not possible to represent adequately. A Pade approximation such as:

$$e^{-s\tau} = \frac{1 - 0.5 s \tau}{1 + 0.5 s \tau} \quad (6.7)$$

could have been made and realized practically if enough summers were available, but this was not the case. Instead it was decided to include it digitally in the control program. However, the non-linear part is represented by a dead-space in series with a saturation element.

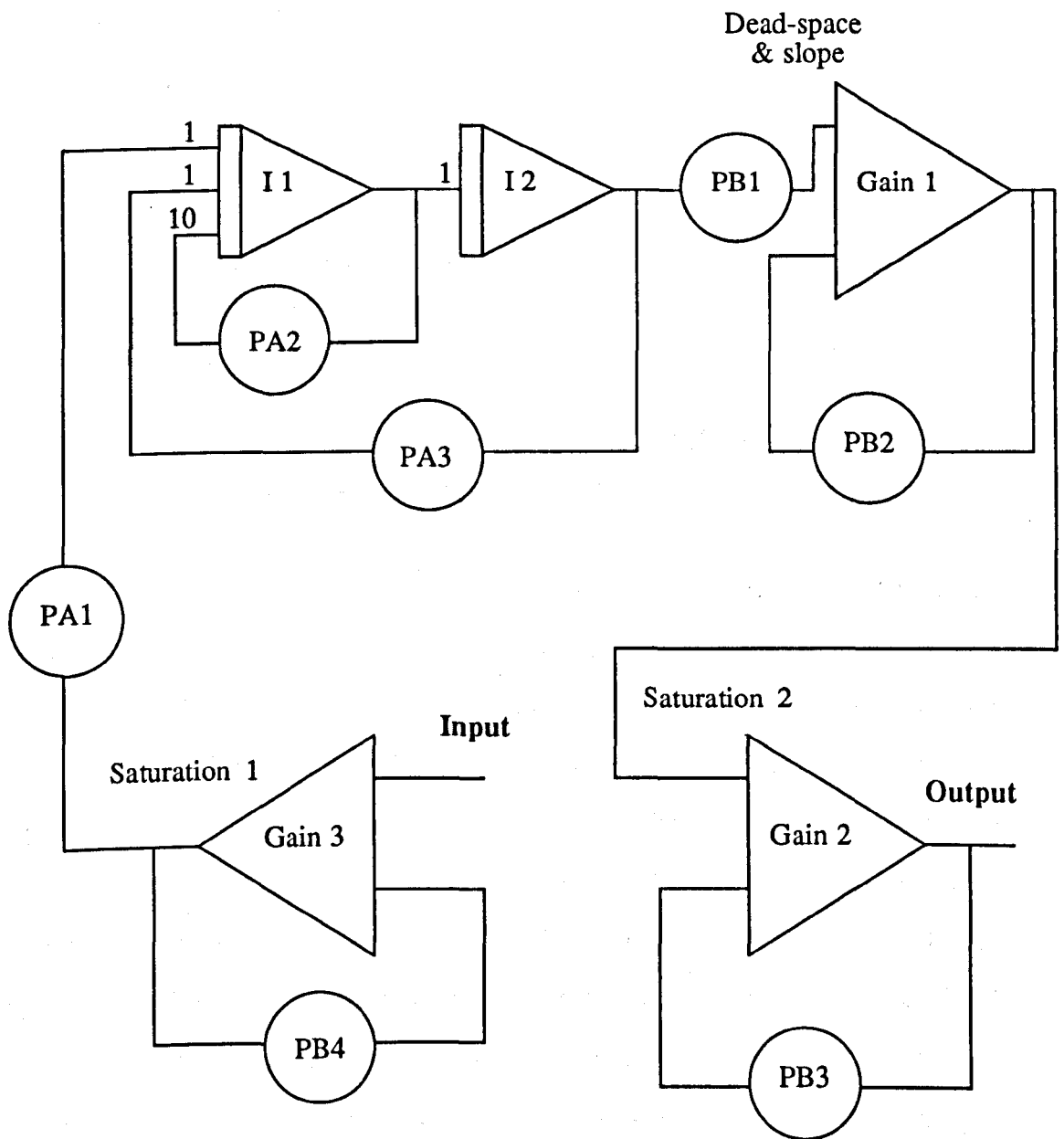


Figure 6.1. VIDAC representation of the non-linear Pancuronium model.

Settings for the potentiometers were:

$$PA_1 = 0.0875$$

$$PA_2 = 0.055$$

$$PA_3 = 0.025$$

$$PB_1 = 0.2867 \text{ (Dead-space)}$$

$$PB_2 = 0.3916 \text{ (Slope)}$$

$$PB_3 = PB_4 = 0.9980 \text{ (Saturation)}$$

6.2.2 Implementation and Application of the GPC Algorithm Using the 380Z Machine

Because the original GPC algorithm was coded in Fortran 77, it had to be rewritten in Fortran 80 and altered to include the 380Z interrupt routines, as well as the scaling formulae corresponding to the AD/DA converters emerging from a calibration operation. Figure (6.2) illustrates the flowchart of the overall control sequence. At this stage it is worth noting that the background processing time should not exceed the time period between interrupts, which in this case is 1 second. Figure (6.3) is a picture taken of the overall real-time system including the VIDAC 336-analogue computer bearing the patch board, and the 380Z machine set-up in the biomedical laboratory located within the Department of Automatic Control and Systems Engineering. A real-time oscilloscope using a multi-channel facility, was also included in the overall set-up to monitor the input-output as well as the potentiometer values, especially those involving the pharmacodynamics of the model.

The non-linear muscle relaxant model describing the Pancuronium-Bromide dynamics having been patched on the VIDAC, a series of trials was carried out. A combination of (1, 10, 1, 0) for (N_1, N_2, NU, λ) was chosen as part of the GPC

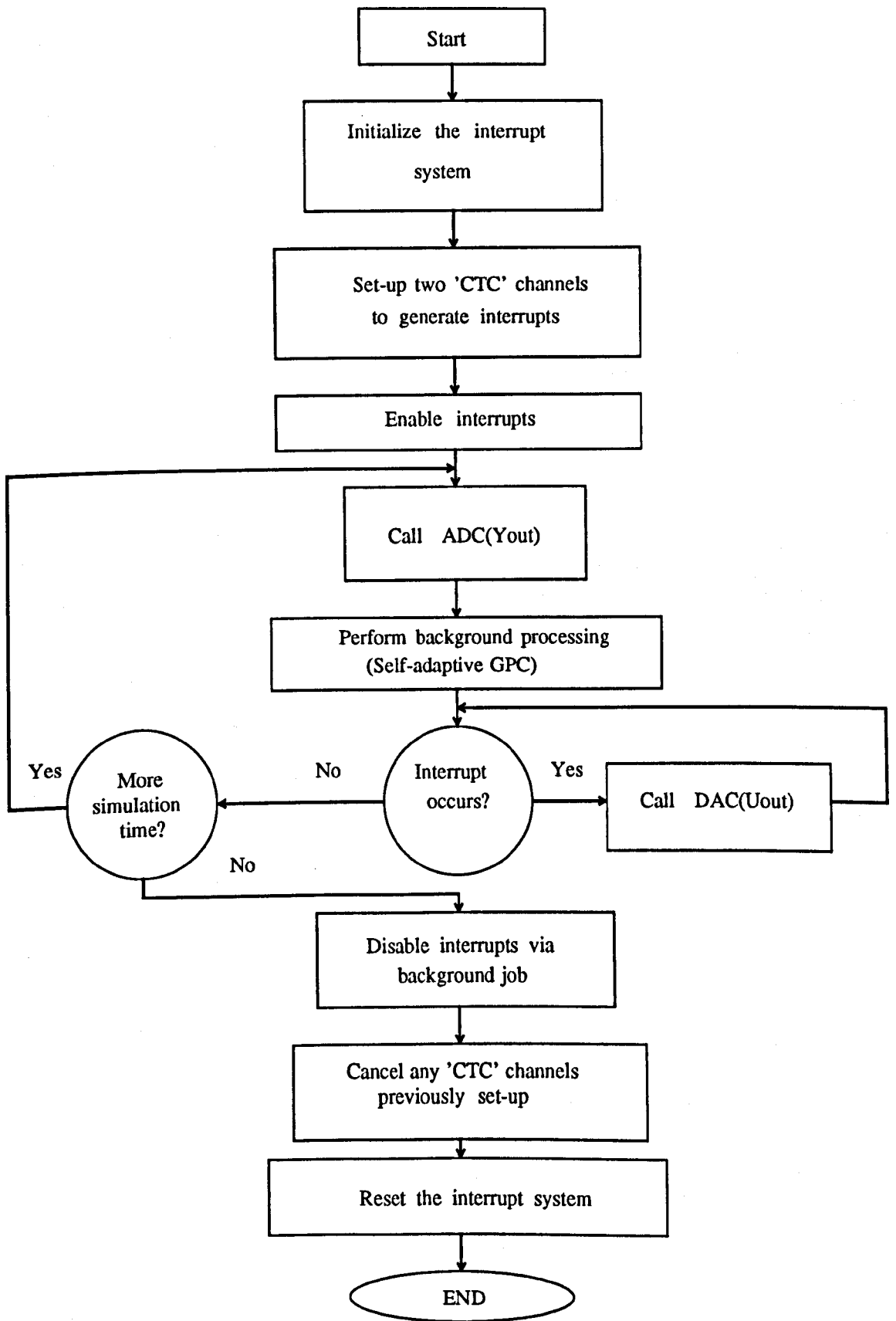


Figure 6.2. Flowchart describing the control sequence on the 380 Z disk-based microcomputer

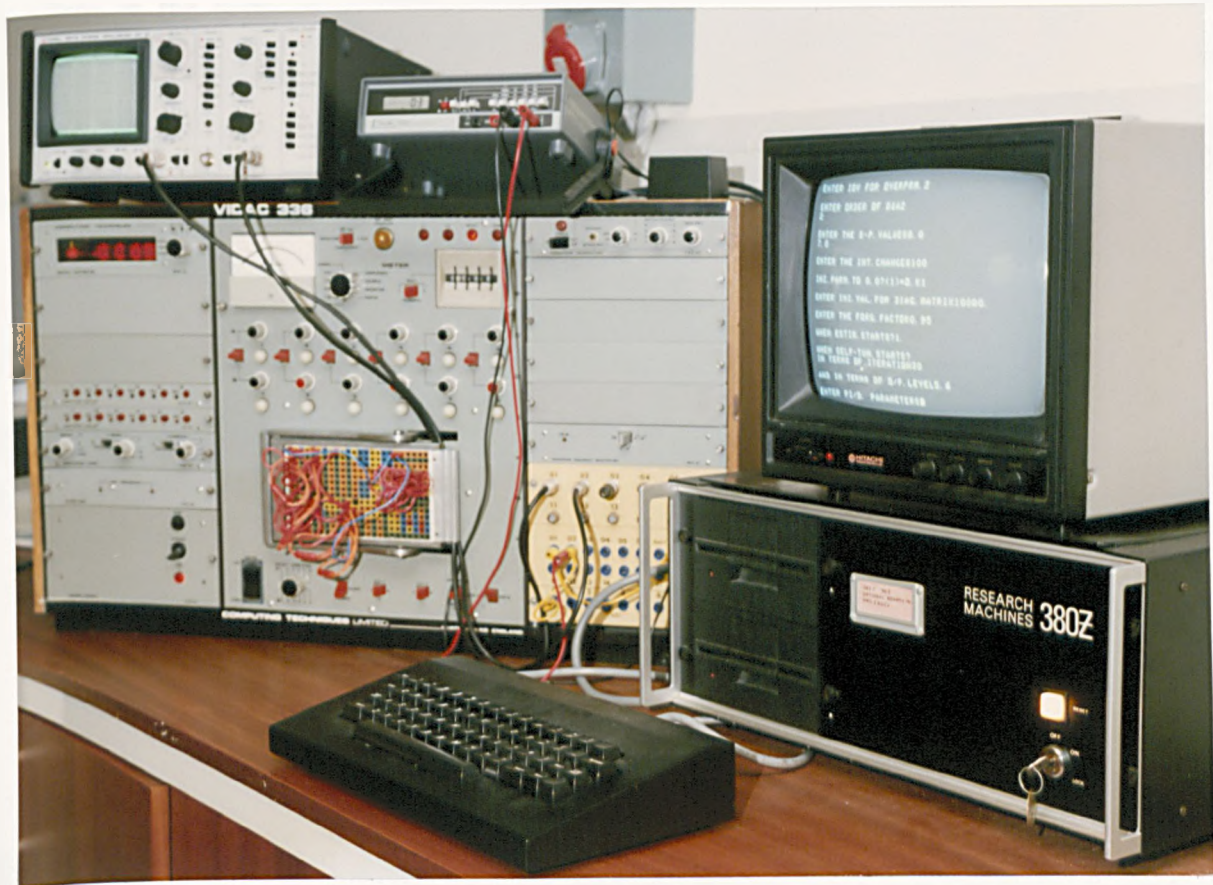


Figure 6.3. Picture showing the overall real-time system including the VIDAC 336-analogue computer, the patch board, the real-time oscilloscope, and the 380 Z machine

settings. Initial control is provided by an optimized PI whose parameters are identical to those used in the previous chapter and for the same drug. Parameter estimation also in the form of a UDU algorithm used the same initial conditions as before. In order to eliminate any drift in the estimates, a low-pass first order filter of the form $T(z^{-1}) = 1 - 0.8 z^{-1}$ is used. Because this filter is also included in the control derivation, it will reduce the overall feedback gain, leading therefore to a more stable input signal.

Because incremental data are normally fed to the measurement vector, the addition of this filter characteristics leads to an overall band-pass filter often favoured by engineers and which is of the form:

$$G_F(z^{-1}) = \frac{1 - z^{-1}}{1 - 0.8 z^{-1}} \quad (6.8)$$

Simulation Results

A second order discrete-time model was considered throughout. To account for the digital delay incorporated in the external program segment and any other forms of delay due to the hardware itself, the degree of the polynomial $B(z^{-1})$ was extended to 4 leading to a transfer function of the form:

$$G_1(z^{-1}) = \frac{b_1 z^{-1} + b_2 z^{-2} + b_3 z^{-3} + b_4 z^{-4}}{1 + a_1 z^{-1} + a_2 z^{-2}} \quad (6.9)$$

The closed-loop system response to a set-point command change of 80% then 70% every 100 seconds is shown in figure (6.4). The output response is good, although an undershoot of approximately 4% was produced during the first phase. The speed of the transient response was relatively high due to the system's gain which was high. This high gain-value was caused by the non-linearity which is represented by a small dead-space not quite equivalent to 50% due to the

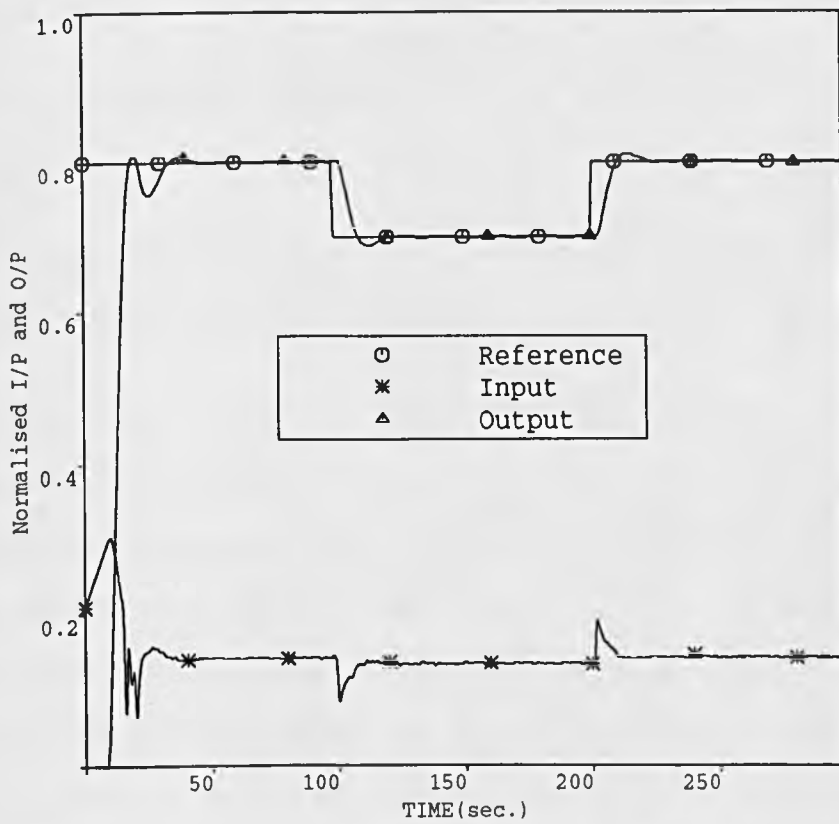


Figure 6.4. Closed-loop response of Pancuronium model under self-adaptive GPC algorithm with $N_1=1$; $N_2=10$; $NU=1$ and observer polynomial $T(z^{-1})=1-0.8z^{-1}$

limitations of the hardware. Parameter estimates whose variations are shown in figure (6.5) have converged to the following values:

$$\begin{aligned}\hat{a}_1 &= -1.4849 & \hat{a}_2 &= 0.5243 \\ \hat{b}_1 &= 0.0172 & \hat{b}_2 &= -0.0389 \\ \hat{b}_3 &= 0.1360 & \hat{b}_4 &= 0.1034\end{aligned}$$

equivalent to a gain and time-constants of:

$$\hat{\text{Gain}} = 5.52 \quad \hat{T}_1 = 1.83 \text{ seconds} \quad \hat{T}_2 = 10.19 \text{ seconds}$$

It is worth noting that the \hat{b}' estimates suggest that the overall time-delay might be higher than 1 since only the values of the estimates \hat{b}_3 and \hat{b}_4 are significant.

A second experiment was performed in which the time-constant T_2 of the continuous system was increased from 20 seconds to 40 seconds. Another GPC run produced the output response of figure (6.6) which was free from overshoot and undershoot due to the slow dominant time-constant. The input signal was slightly noisy because of the filter cut-off frequency (0.2Hz) which allowed some other high frequency components to be included in the overall spectrum. The parameter estimates variations are shown in figure (6.7). They finally converged to the following values:

$$\begin{aligned}\hat{a}_1 &= -1.5453 & \hat{a}_2 &= 0.5653 \\ \hat{b}_1 &= 0.0079 & \hat{b}_2 &= -0.0173 \\ \hat{b}_3 &= 0.0630 & \hat{b}_4 &= 0.0406\end{aligned}$$

corresponding to a second order continuous model with a gain and time-constants of:

$$\hat{\text{Gain}} = 4.71 \quad \hat{T}_1 = 1.92 \text{ seconds} \quad \hat{T}_2 = 19.79 \text{ seconds}$$

If a comparison is drawn between these real-time simulations and the digital ones conducted in chapter 5, it can be seen that the results are similar despite the

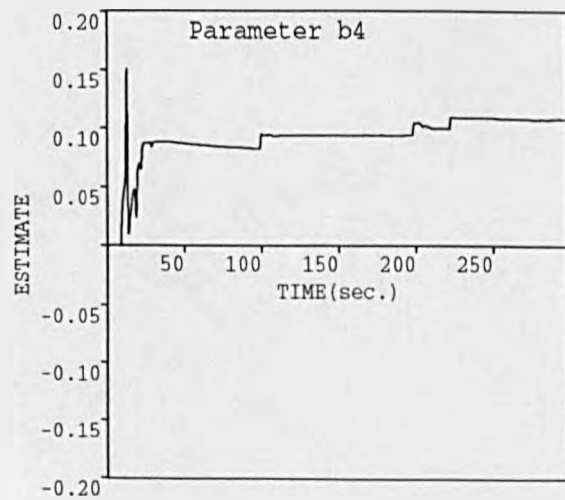
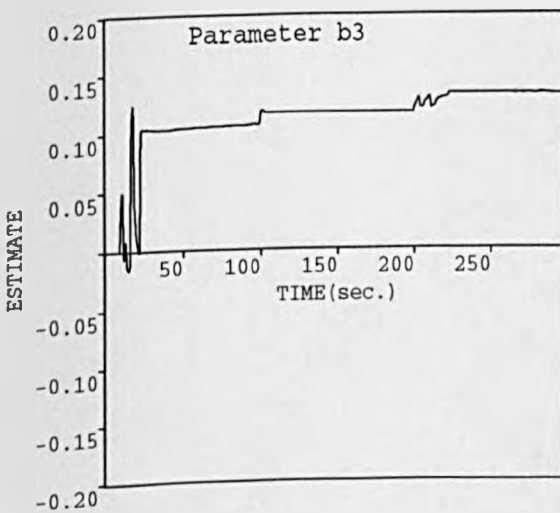
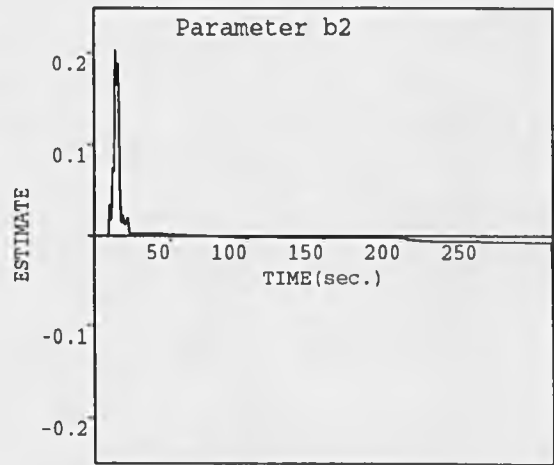
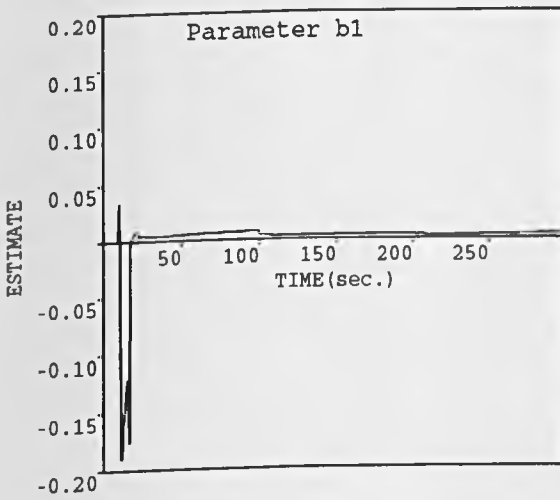
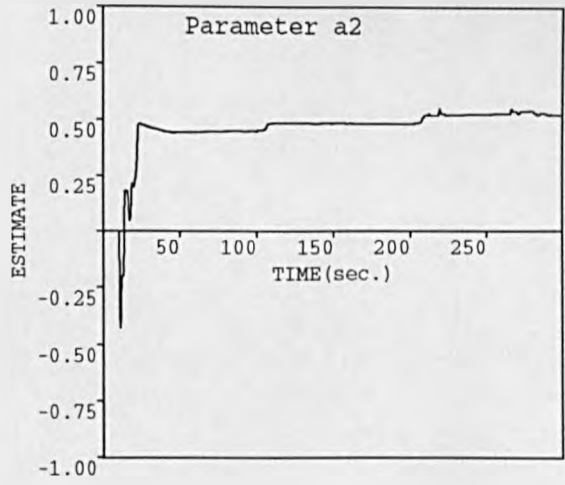
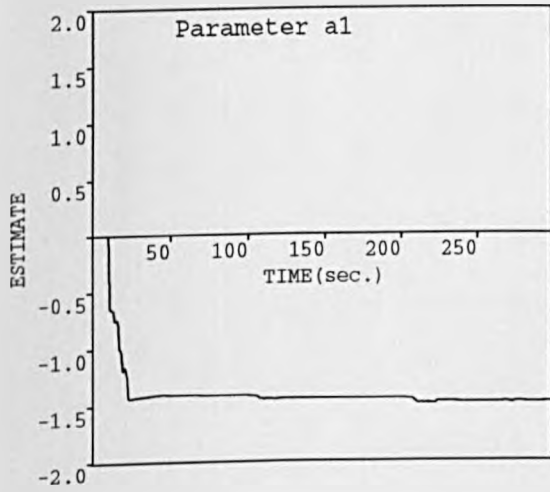


Figure 6.5. System parameter estimates corresponding to conditions of figure (6.4)

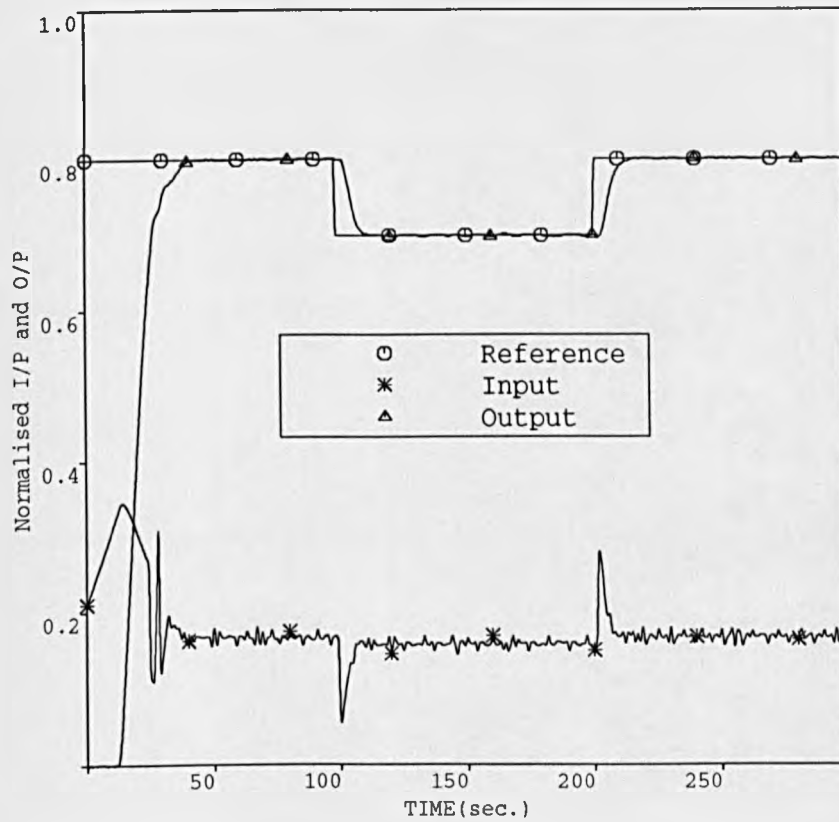


Figure 6.6. Closed-loop response of Pancuronium model when $T_2=40$ seconds

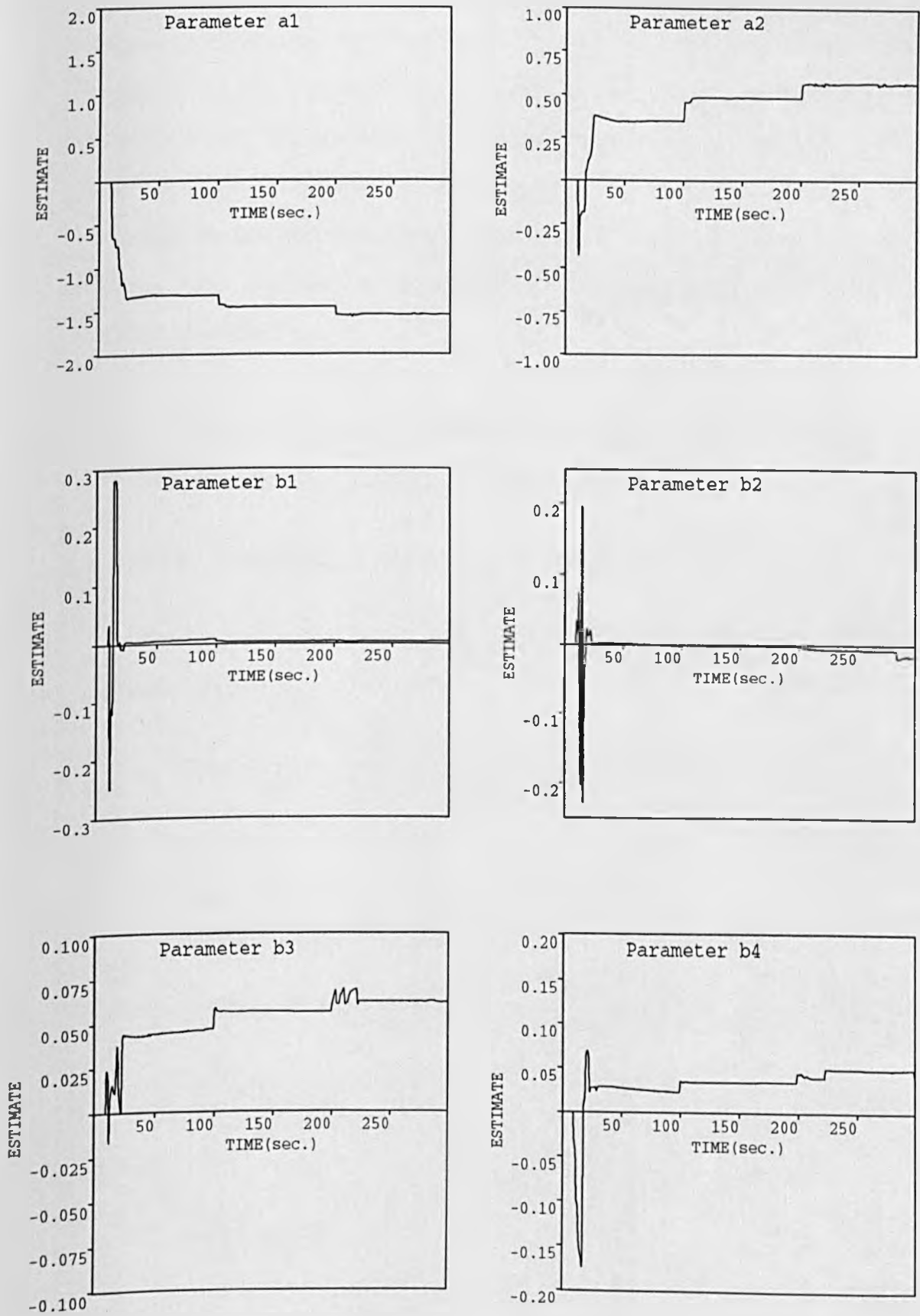


Figure 6.7. System parameter estimates corresponding to conditions of figure (6.6)

different conditions set for the estimation routine. Moreover, the estimated time-constants fell within an acceptable range although the value of the dominant time-constant is only half the true value. As for the open-loop gain, its value in both cases was slightly higher than the one obtained in the digital case due as explained earlier to the non-linearity represented by a short dead-space. The overall performances were good despite the inaccuracy in the transfer of data through the AD/DA converters.

6.3 MICROCOMPUTER-CONTROLLED ANALOGUE COMPUTER MODEL OF ATRACURIUM DYNAMICS

6.3.1 Simulation of Atracurium Model on the VIDAC 336

Similarly to section 6.2.1, consider the transfer function relative to the kinetics of the drugs, i.e:

$$G_2(s) = \frac{K_1 (1 + T_4 s)}{(1 + T_1 s) (1 + T_2 s) (1 + T_3 s)} \quad (6.10)$$

or,

$$\frac{X_E(s)}{U(s)} = \frac{r_0 + r_1 s}{q_0 + q_1 s + q_2 s^2 + s^3} \quad (6.11)$$

This equation may be decomposed as:

$$\frac{X_E(s)}{U(s)} = \frac{X_E(s)}{X(s)} \cdot \frac{X(s)}{U(s)} \quad (6.12)$$

where:

$$\frac{X_E(s)}{X(s)} = r_0 + r_1 s \quad (6.13)$$

and,

$$\frac{X(s)}{U(s)} = \frac{1}{q_0 + q_1 s + q_2 s^2 + s^3} \quad (6.14)$$

after developing and rearranging it follows that:

$$-\frac{d}{dt} [\ddot{X}] = q_2 \ddot{X} + q_1 \dot{X} + q_0 X - U \quad (6.15)$$

and,

$$X_E = r_0 X + r_1 \dot{X} \quad (6.16)$$

Similarly, introducing the quantities \ddot{X}_m , \dot{X}_m , and X_m respectively for \ddot{X} , \dot{X} , and X , equations (6.15) and (6.16) become:

$$\begin{aligned} -\frac{d}{dt} \left[\frac{\ddot{X}}{\ddot{X}_m} \right] &= q_2 \left[\frac{\ddot{X}}{\ddot{X}_m} \right] + q_1 \frac{\dot{X}_m}{\ddot{X}_m} \left[\frac{\dot{X}}{\dot{X}_m} \right] + q_0 \frac{X_m}{\ddot{X}_m} \left[\frac{X}{X_m} \right] - \frac{U}{\ddot{X}_m} \\ -\frac{d}{dt} \left[-\frac{\dot{X}}{\dot{X}_m} \right] &= \frac{\ddot{X}_m}{\dot{X}_m} \left[\frac{\ddot{X}}{\ddot{X}_m} \right] \\ -\frac{d}{dt} \left[-\frac{X}{X_m} \right] &= \frac{\dot{X}_m}{X_m} \left[-\frac{\dot{X}}{\dot{X}_m} \right] \end{aligned} \quad (6.17)$$

and,

$$X_E = r_0 \left[\frac{X}{X_m} \right] + r_1 \left[\frac{\dot{X}}{\dot{X}_m} \right] \quad (6.18)$$

An open-loop step response study suggested that:

$$\ddot{X}_m = 2.0 \quad \dot{X}_m = 20.0 \quad X_m = 500.0$$

Consequently, after combining these values together with those of r_i and q_i of chapter 3 and substituting them in equations (6.17) and (6.18), it follows that:

$$\begin{aligned} -\frac{d}{dt} \left[\frac{\ddot{X}}{2.0} \right] &= [0.562] (1) \left[\frac{\ddot{X}}{2.0} \right] + [0.8309] (1) \frac{\dot{X}}{20.0} \\ &\quad + [0.49] (1) \left[\frac{X}{500.0} \right] - [0.5] (1) U \end{aligned}$$

$$-\frac{d}{dt} \left[-\frac{\dot{X}}{20.0} \right] = [0.10] (1) \left[\frac{\ddot{X}}{2.0} \right] \quad (6.19)$$

$$-\frac{d}{dt} \left[-\frac{X}{500.0} \right] = [0.04] (1) \left[-\frac{\dot{X}}{20.0} \right]$$

and,

$$X_E = [0.9835] (1) \left[\frac{X}{500.0} \right] + [0.4185] (1) \left[\frac{\dot{X}}{20.0} \right] \quad (6.20)$$

Introducing amplifiers within equations (6.19) leads to:

$$\begin{aligned} -\frac{d}{dt} \left[\frac{\ddot{X}}{2.0} \right] &= [0.562] (1) \left[\frac{\ddot{X}}{2.0} \right] + [0.08309] (10) \frac{\dot{X}}{20.0} \\ &\quad + [0.049] (10) \left[\frac{X}{500.0} \right] - [0.5] (1) U \end{aligned}$$

$$-\frac{d}{dt} \left[-\frac{\dot{X}}{20.0} \right] = [0.10] (1) \left[\frac{\ddot{X}}{2.0} \right] \quad (6.21)$$

$$-\frac{d}{dt} \left[-\frac{X}{500.0} \right] = [0.04] (1) \left[-\frac{\dot{X}}{20.0} \right]$$

Figure (6.8) shows the corresponding VIDAC representation of the model. The same remark as in section 6.2.1 about the time-delay applies here, and the non-linearity is still represented by a dead-space and a saturation element.

A detailed list of the potentiometers includes the following values:

$$\begin{aligned} PA_1 &= 0.562 & PA_4 &= 0.04 \\ PA_2 &= 0.100 & PA_5 &= 0.049 \\ PA_3 &= 0.580 & PA_6 &= 0.98 \end{aligned}$$

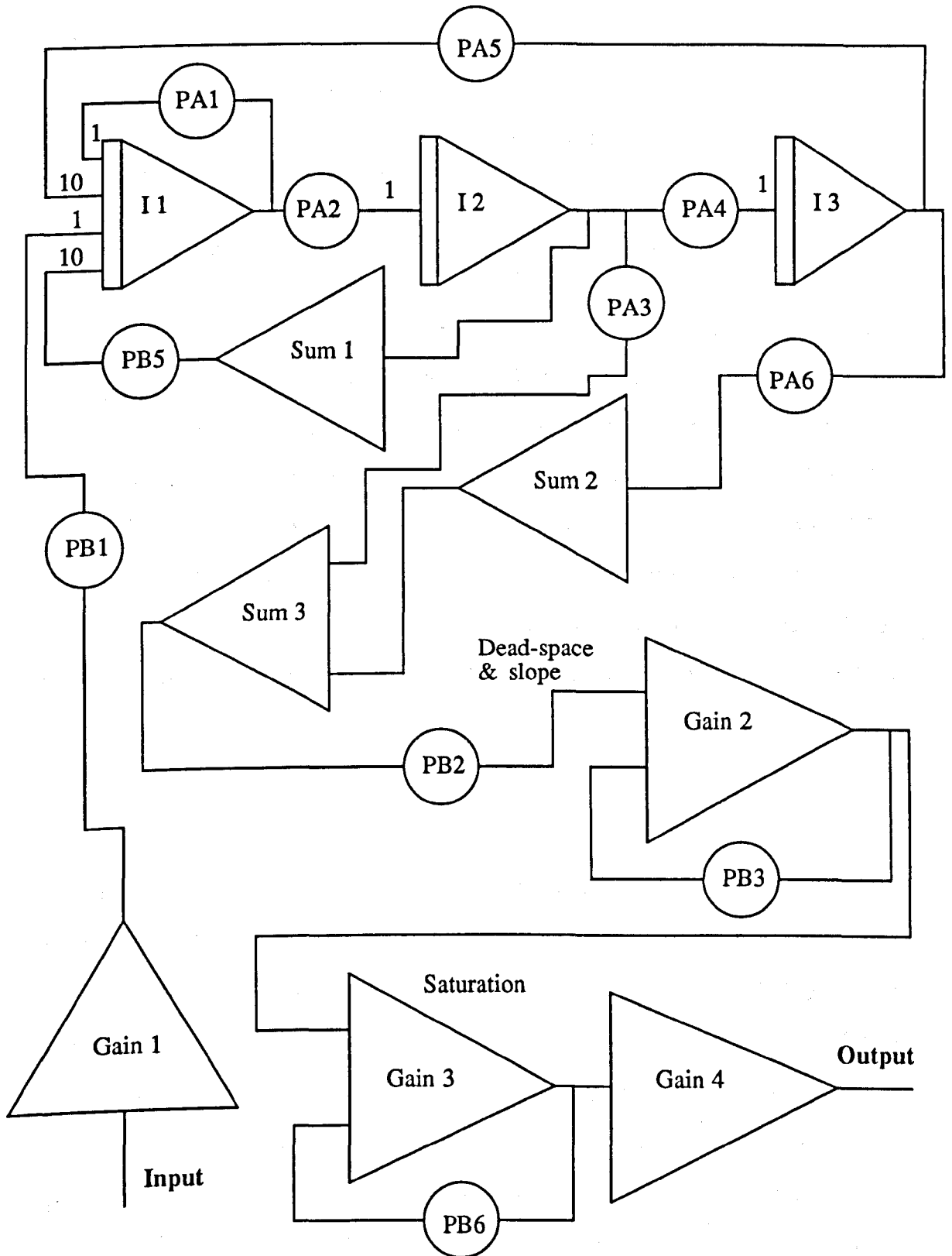


Figure 6.8. VIDAC representation of the non-linear third order Atracurium model

and,

$$\begin{aligned} PB_1 &= 0.500 & PB_5 &= 0.08309 \\ PB_2 &= 0.3916 \text{ (Slope)} & PB_6 &= 0.9980 \text{ (Saturation)} \\ PB_3 &= 0.2867 \text{ (Dead-space)} \end{aligned}$$

6.3.2 Control of Atracurium Administration Using GPC

For this third order non-linear model, the GPC algorithm used the same parameter settings as those of section 6.2.2. The fixed PI, allowed to provide initial control, included similar parameters to those used in chapter 4 for the same drug. The UDU estimation routine is started when the output reached a 10% value. If initial estimates are taken to be zero, the diagonal matrix is set to $10^4 \cdot I$, I being the identity matrix, and consequently, the PI is allowed to run for 20 samples, whereas if the estimates are set to non-zero values, the diagonal matrix is set to $10^2 \cdot I$ and therefore the self-adaptive GPC takes over from the PI at the 15th sample.

Simulation Results

If a full order model is considered here, the 380Z machine which uses a slow microprocessor chip known as the Z80 would fail to keep its processing time below the time period between interrupts as required, due to the heavy burden imposed by the estimation routine and the control sequence. Therefore, the idea of underparameterizing the model to a lower order (2 for instance) was adopted throughout all the simulations. This can safely be done knowing that the use of the previous $T(z^{-1})$ polynomial would compensate for any unmodelled dynamics. The structure of the estimated transfer function is similar to that of equation (6.9), i.e:

$$G_2(z^{-1}) = \frac{b_1 z^{-1} + b_2 z^{-2} + b_3 z^{-3} + b_4 z^{-4}}{1 + a_1 z^{-1} + a_2 z^{-2}} \quad (6.22)$$

Figure (6.9) shows the performance of the GPC controller for a changing set-point of 80% then 70% every 100 seconds interval. The output demonstrated an overshoot of 3%, then tended to approach the set-point smoothly to avoid undershoot during the first phase. This is typical of GPC when used with the observer polynomial $T(z^{-1})$, although if a slower root was chosen for this polynomial, the slight undershoot during the second and the third phase would have undoubtedly been eliminated. As for the control signal, it kept a steady level despite the repeated disturbances that have been noticed on the oscilloscope from the other electronic and electrical components that were part of different rigs currently used in the laboratory. Parameter estimates, initially taken to be zero, did not seem to be affected by these disturbances as their variations are shown in figure (6.10). Here again, the estimates \hat{b}_1 and \hat{b}_2 had a very small positive quantity and a negative small quantity respectively, whereas the values of the estimates \hat{b}_3 and \hat{b}_4 were significant, suggesting a time-delay of 2 seconds. At the end of the run these estimates converged to the following values:

$$\begin{aligned} \hat{a}_1 &= -1.4044 & \hat{a}_2 &= 0.4346 \\ \hat{b}_1 &= 0.0043 & \hat{b}_2 &= -0.0076 \\ \hat{b}_3 &= 0.0318 & \hat{b}_4 &= 0.0289 \end{aligned}$$

corresponding to an estimated gain and time-constants of:

$$\hat{\text{Gain}} = 1.90 \quad \hat{T}_1 = 1.29 \text{ seconds} \quad \hat{T}_2 = 17.36 \text{ seconds}$$

Using the same model-parameters, another run was conducted in which the estimates were initialized to initial values equivalent to a second order continuous-time system with a gain and time-constants of:

$$\theta_1 = [\hat{\text{Gain}} = 2.0, \hat{T}_1 = 1.27 \text{ Seconds}, \hat{T}_2 = 18.0 \text{ Seconds}]$$

The result of this experiment is that of figure (6.11) where no significant change

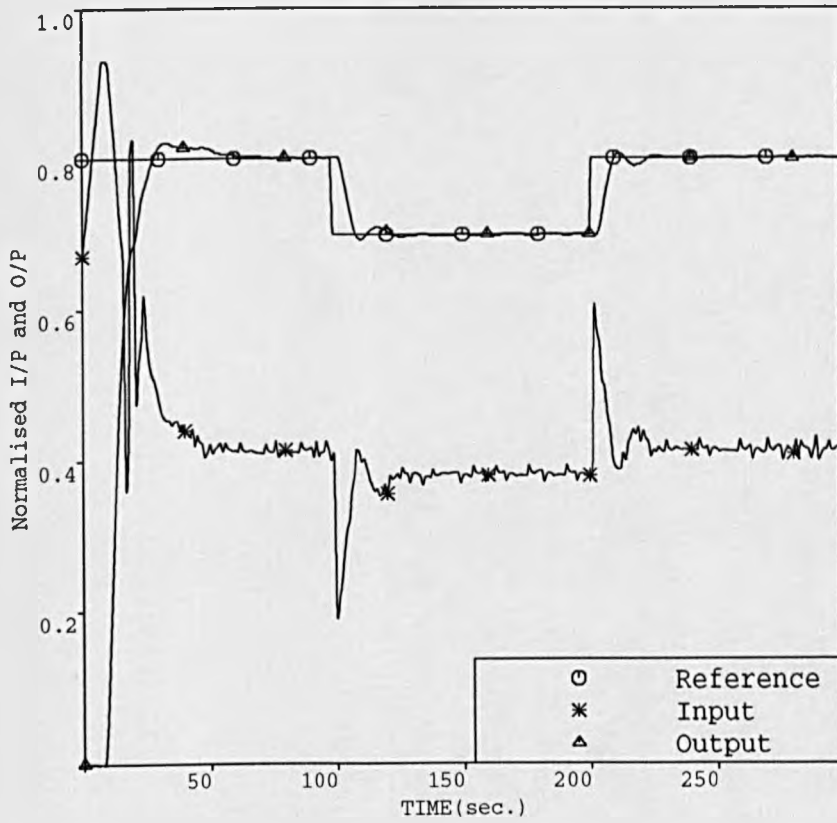


Figure 6.9. Closed-loop response of Atracurium model under self-adaptive GPC algorithm with $N_1=1$; $N_2=10$; $NU=1$ and observer polynomial $T(z^{-1})=1-0.8z^{-1}$

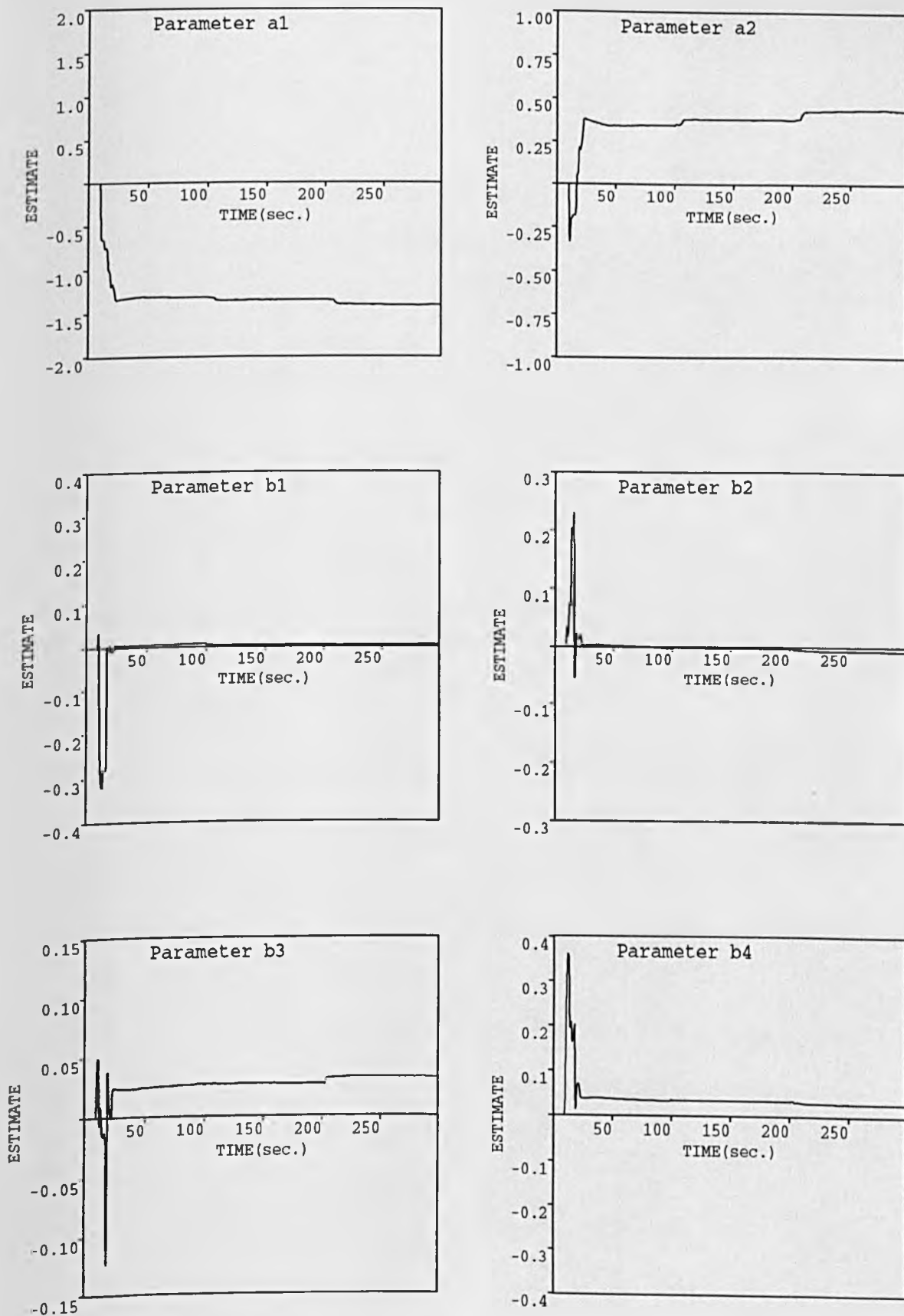


Figure 6.10. System parameter estimates corresponding to conditions of figure (6.9)

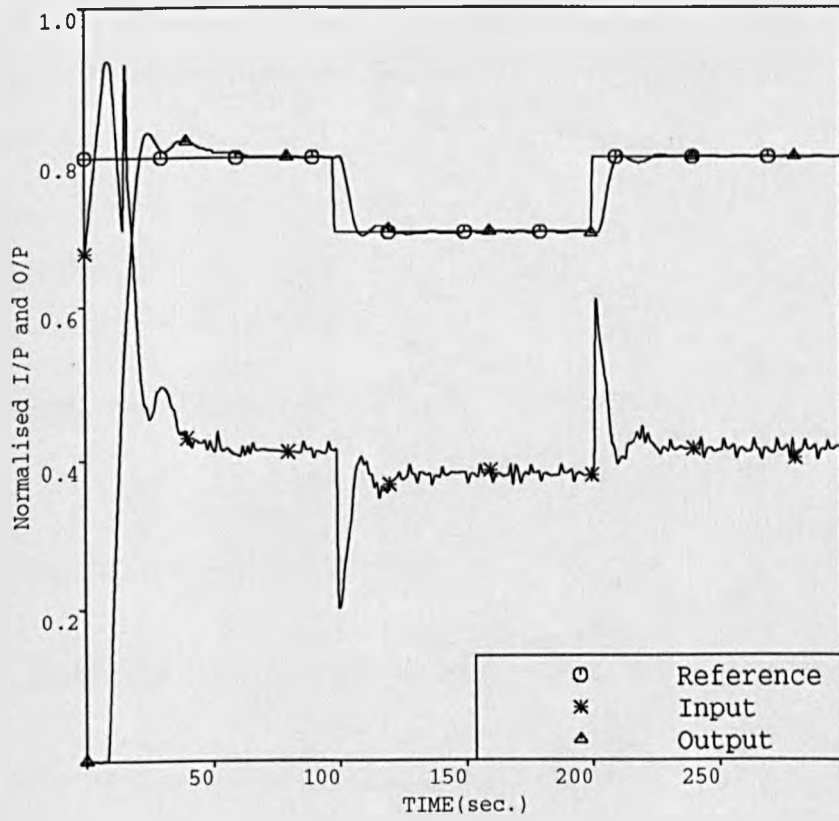


Figure 6.11. Same conditions as figure (6.9) but with non-zero initial parameter estimates

could be observed except that the output, after having overshoot once, overshoot a second time due to the fact that at that precise moment the value of the potentiometer fixing the value of the slope in the non-linearity part and monitored via the real time oscilloscope, showed a significant drift from its initial position. But, on the whole, the performance was similar to the previous one, although parameter estimates whose variations are shown in figure (6.12) were steadier and converged to the following:

$$\begin{aligned}\hat{a}_1 &= -1.3997 & \hat{a}_2 &= 0.4306 \\ \hat{b}_1 &= 0.0023 & \hat{b}_2 &= -0.0058 \\ \hat{b}_3 &= 0.0325 & \hat{b}_4 &= 0.0296\end{aligned}$$

corresponding to the following estimated gain and time-constants:

$$\hat{\text{Gain}} = 1.89 \quad \hat{T}_1 = 1.27 \text{ seconds} \quad \hat{T}_2 = 17.08 \text{ seconds}$$

values which are close to the previous ones.

6.3.3 Sensitivity of the Self-Adaptive GPC to Patient Variability

The aim of this section is to assess the robustness of the self-adaptive GPC when model parameters vary. Indeed, it has been shown previously that the parameters of the drug models vary from one subject to another, which originally led to the argument that a self-adaptive scheme would be more adequate in this case rather than a fixed one. It is believed that this variability may be due to the interaction between the drug concentration and the organs and tissues to which it is distributed. For instance, patients with too much fat would normally require large amounts of Atracurium than those with less fat, in order to reach the same degree of muscle relaxation. The concept of sensitivity was later introduced to describe patients who are highly, average, and less sensitive to the drug. Using the mathematically derived model of equation (6.10), this could be interpreted as

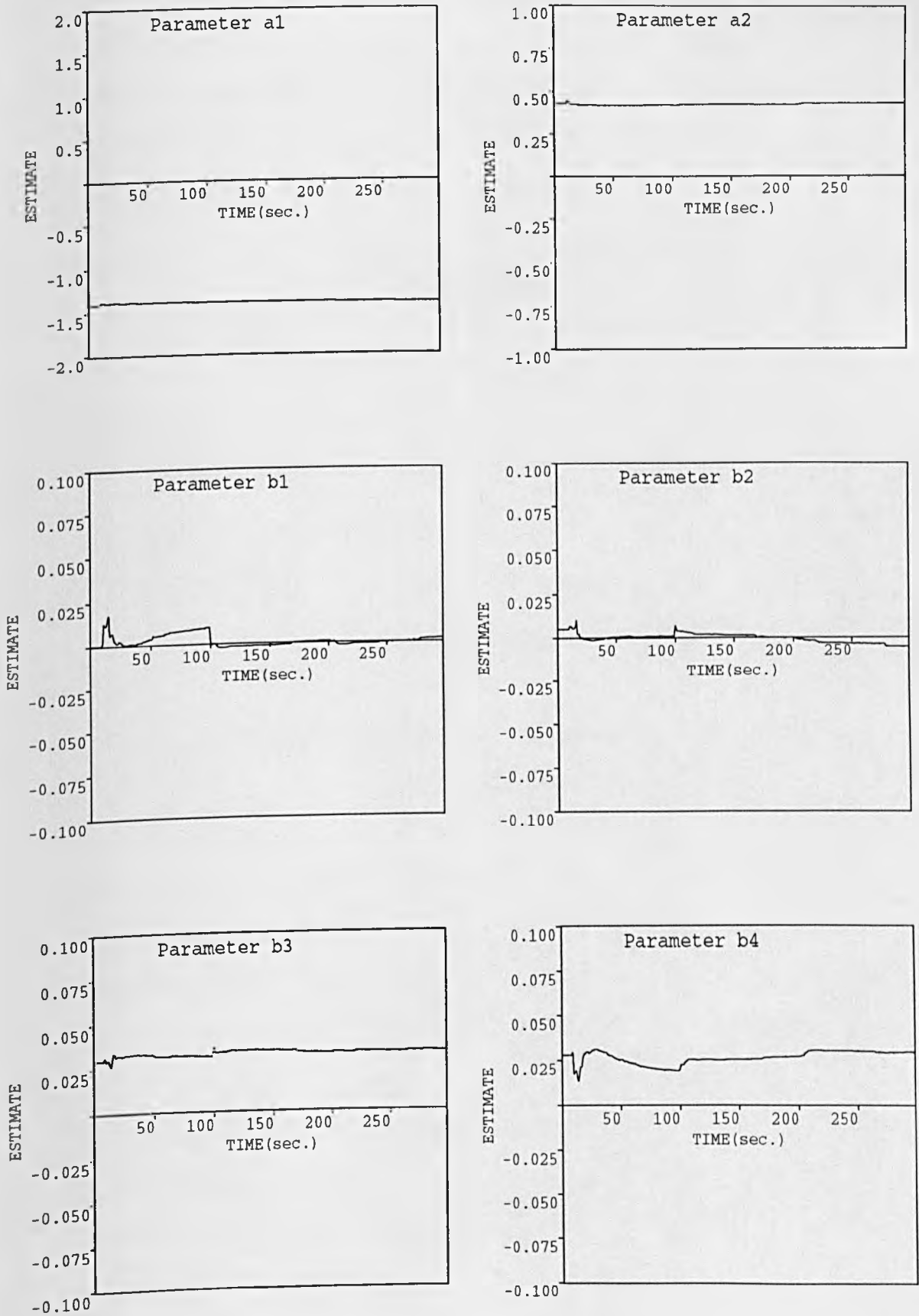


Figure 6.12. System parameter estimates corresponding to conditions of figure (6.11)

patients having high, average, and low gain respectively. To illustrate this idea, a series of simulations was undertaken, in which patient parameters were varied using equation (3.10) and according to table (6.1). At this stage, it is worth noting that only one parameter was allowed to vary at a time.

Sensitivity Study					
Figure number	Atracurium Model parameters				
	K_1	T_1 (Sec.)	T_2 (Sec.)	T_3 (Sec.)	T_4 (Sec.)
6.13	2.00*	3.08	4.81	34.36	10.64
6.14	1.00	4.00*	4.81	34.36	10.64
6.15	1.00	3.08	3.0*	34.36	10.64
6.16	1.00	3.08	4.81	20.00*	10.64
6.17	1.00	3.08	4.81	34.36	15.00*

Table 6.1. Atracurium model parameter variation reflecting patient variability.

For this series of simulations and throughout, parameter estimates were all initialized at zero. Figure (6.13) shows the performance of the GPC controller when the open-loop gain was increased to 2.0 (high sensitivity patient). Because the parameters of the fixed PI controller were kept exactly the same (previously optimized for $K_1 = 1$), the output response demonstrated an overshoot of almost 29% and a 12% undershoot. The adaptive GPC responded quickly to this by making the output track the set-point better. The control signal was reasonably active and was quick to reject the disturbance, here in the form of a set-point change, leading to a

* Model parameter subject to variation

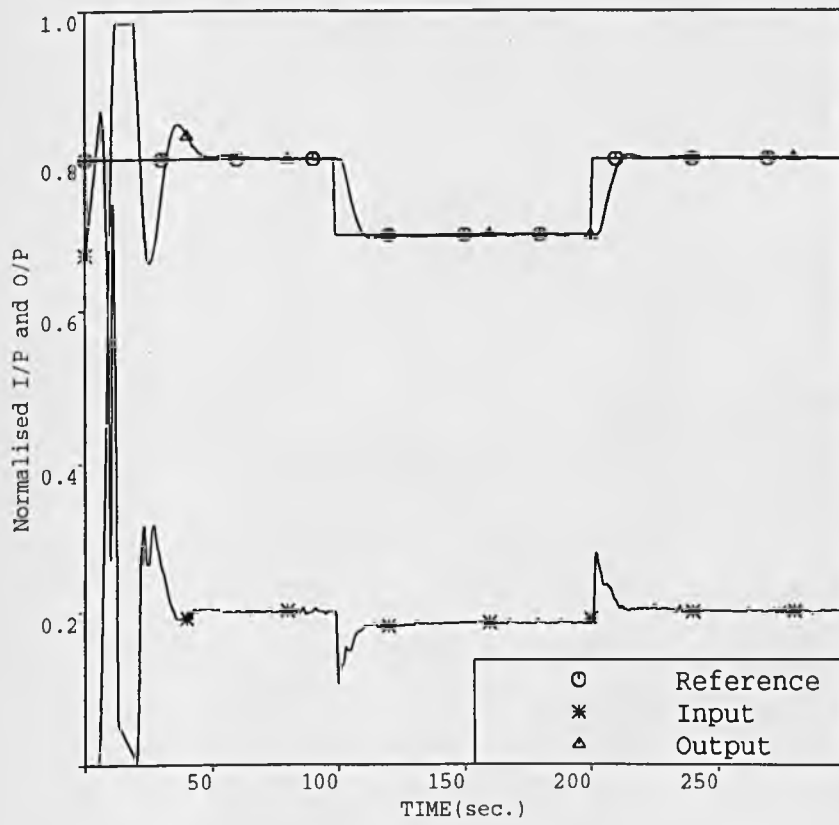


Figure 6.13. Closed-loop response of Atracurium model when $K_1=2.0$

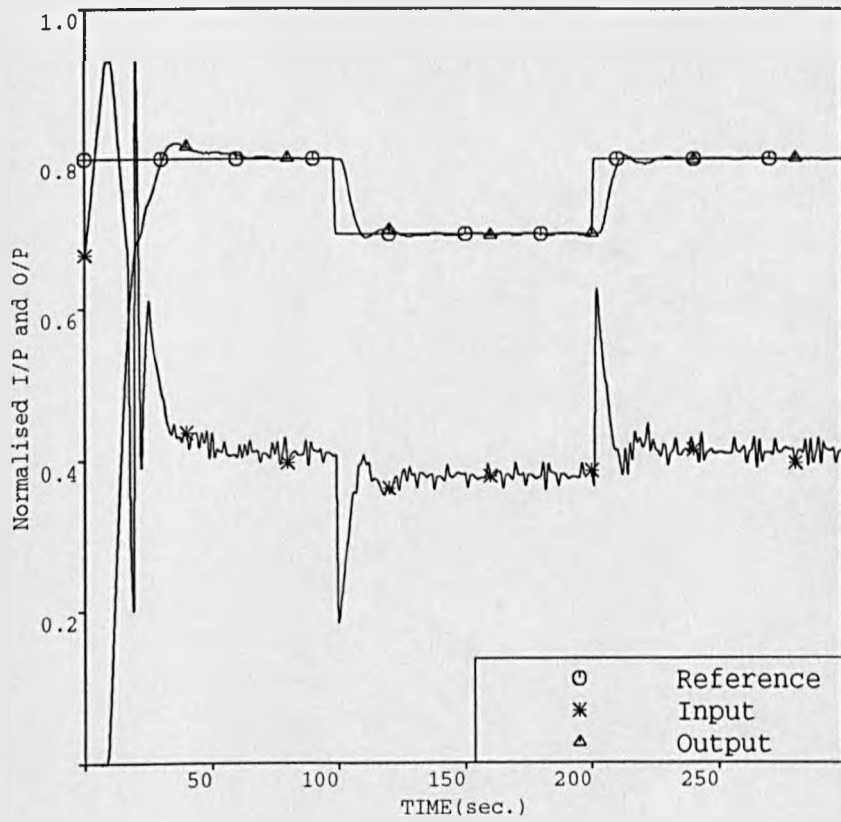


Figure 6.14. Closed-loop response of Atracurium model when $T_1=4$ seconds

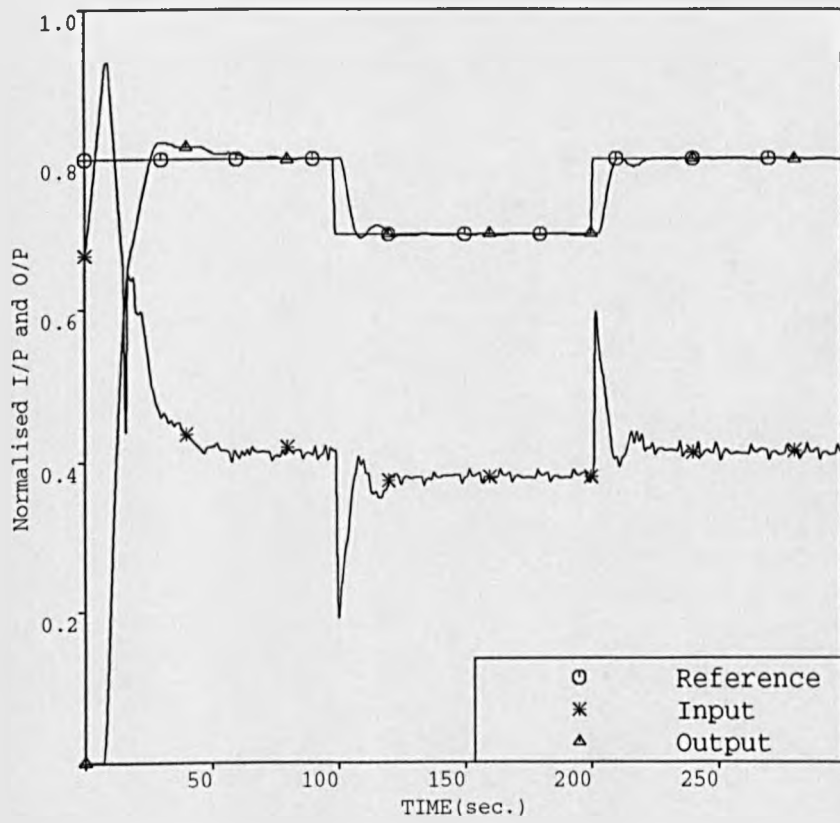


Figure 6.15. Closed-loop response of Atracurium model when $T_2=3$ seconds

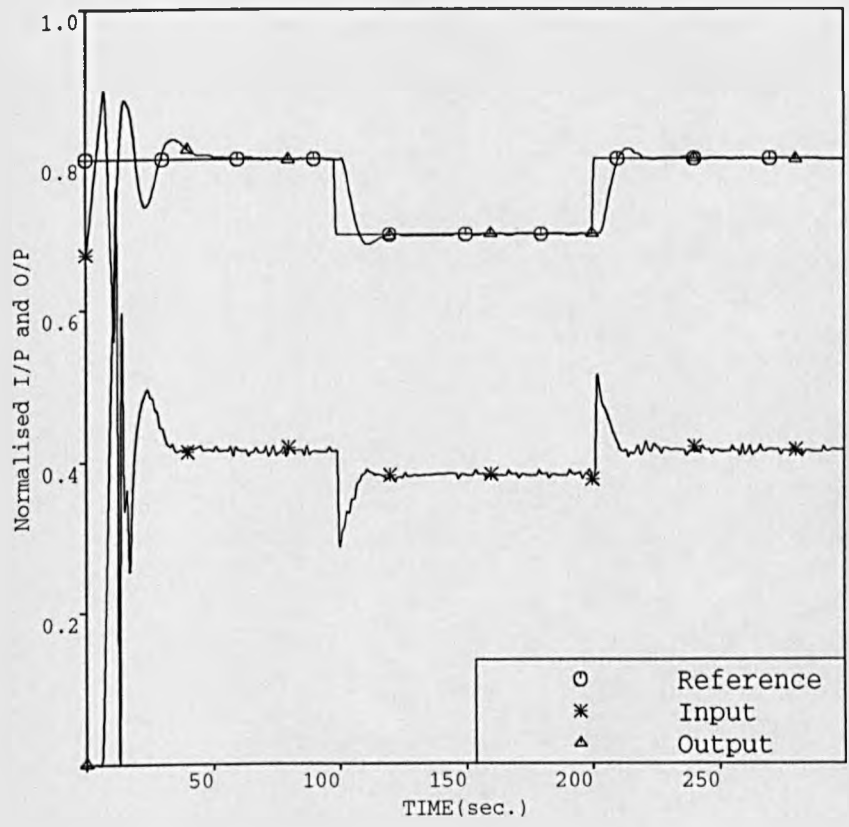


Figure 6.16. Closed-loop response of Atracurium model when $T_3=20$ seconds

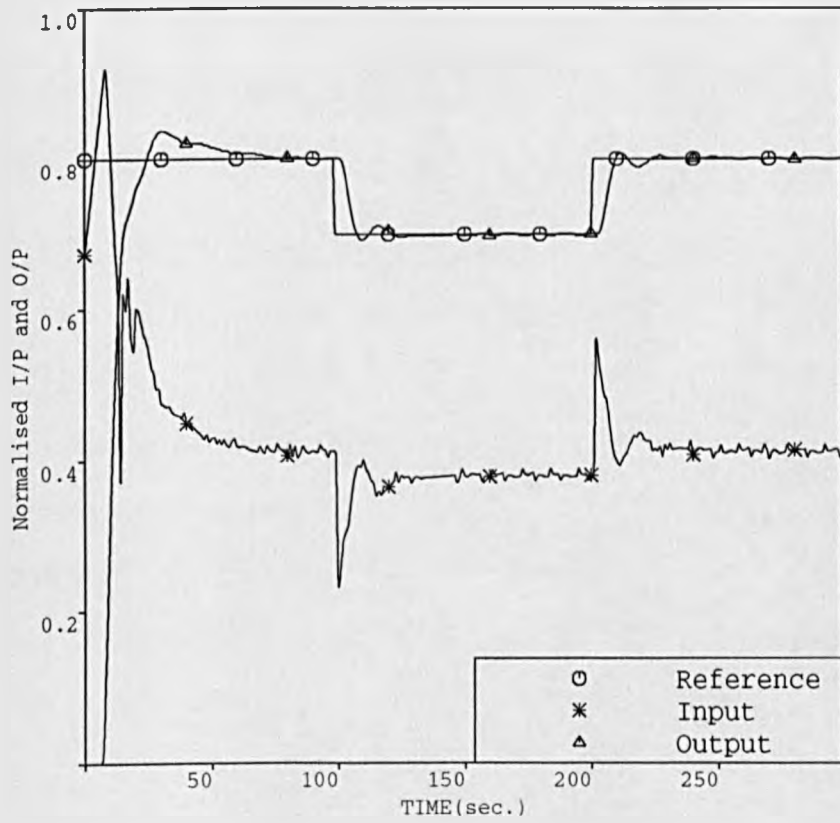


Figure 6.17. Closed-loop response of Atracurium model when $T_4=15$ seconds

response almost free from undershoot and overshoot during the second and third phase. Parameter estimates converged to the following values:

$$\begin{aligned}\hat{a}_1 &= -1.3648 & \hat{a}_2 &= 0.4051 \\ \hat{b}_1 &= 0.0028 & \hat{b}_2 &= -0.0077 \\ \hat{b}_3 &= 0.0357 & \hat{b}_4 &= 0.1104\end{aligned}$$

corresponding to the following continuous values:

$$\hat{\text{Gain}} = 3.88 \quad \hat{T}_1 = 1.20 \text{ seconds} \quad \hat{T}_2 = 13.48 \text{ seconds}$$

Figures (6.14), (6.15), and (6.17) also show the performance of the GPC controller when the model parameters T_1 , T_2 , and T_4 took values of 4, 3, and 15 seconds respectively. Little change could be observed in the corresponding performances which were characterized by an overshoot of approximately 3% during the first phases, whereas during the first and third phases, GPC was quick to reject the disturbances caused by the set-point changes and allow the outputs to track the set-point better. Parameter estimates for the three cases converged to the following values:

(i)

$$\begin{aligned}\hat{a}_1 &= -1.4880 & \hat{a}_2 &= 0.5131 \\ \hat{b}_1 &= 0.0049 & \hat{b}_2 &= -0.0050 \\ \hat{b}_3 &= 0.0249 & \hat{b}_4 &= 0.031\end{aligned}$$

equivalent to a gain and time-constants of:

$$\hat{\text{Gain}} = 2.22 \quad \hat{T}_1 = 1.64 \text{ seconds} \quad \hat{T}_2 = 17.71 \text{ seconds}$$

for figure (6.14)

(ii)

$$\begin{aligned}\hat{a}_1 &= -1.3040 & \hat{a}_2 &= 0.3406 \\ \hat{b}_1 &= 0.0008 & \hat{b}_2 &= -0.0056 \\ \hat{b}_3 &= 0.0385 & \hat{b}_4 &= 0.0360\end{aligned}$$

equivalent to a gain and time-constants of:

$$\hat{G}\text{ain} = 1.90 \quad \hat{T}_1 = 0.99 \text{ second} \quad \hat{T}_2 = 16.95 \text{ seconds}$$

for figure (6.15)

(iii)

$$\begin{aligned} \hat{a}_1 &= -1.3610 & \hat{a}_2 &= 0.4030 \\ \hat{b}_1 &= 0.0011 & \hat{b}_2 &= -0.0014 \\ \hat{b}_3 &= 0.0401 & \hat{b}_4 &= 0.0395 \end{aligned}$$

equivalent to a gain and time-constants of:

$$\hat{G}\text{ain} = 1.89 \quad \hat{T}_1 = 1.20 \text{ seconds} \quad \hat{T}_2 = 12.94 \text{ seconds}$$

for figure (6.17)

The experiment whose result is shown in figure (6.16) was undertaken by assigning a smaller value to the dominant time-constant, i.e. $T_3 = 20$ seconds. The response, as expected, was fast. The response tried to reach the set-point quickly during the fixed PI phase, and because a different controller mode was switched on (i.e. GPC), the response demonstrated an undershoot first, then, due to the $T(z^{-1})$ filter, the approach to the set-point became smoother. The control signal was good and reasonably active. At the end of the run the estimates converged to the following values:

$$\begin{aligned} \hat{a}_1 &= -1.4056 & \hat{a}_2 &= 0.4629 \\ \hat{b}_1 &= 0.0002 & \hat{b}_2 &= -0.0004 \\ \hat{b}_3 &= 0.0539 & \hat{b}_4 &= 0.0545 \end{aligned}$$

equivalent to a gain and time-constants of:

$$\hat{G}\text{ain} = 1.90 \quad \hat{T}_1 = 1.56 \text{ seconds} \quad \hat{T}_2 = 7.75 \text{ seconds}$$

To summarize the previous 5 performances, table (6.2) outlines the corresponding

ISE and ITAE criteria defined in the previous chapter.

Figure Number	ISE	ITAE
6.13	5.38	352.51
6.14	8.59	368.34
6.15	7.44	334.31
6.16	5.69	314.41
6.17	6.65	341.12

**Table 6.2. ISE and ITAE criteria for varying
Atracurium model parameters**

A quick analysis of the table confirms what was already said about the cases corresponding to figures (6.13) to (6.17). Indeed, cases for which the non-dominant time-constants varied, i.e figures (6.14), (6.15), and (6.17), produced ITAE and ISE values which were quite comparable. However, the lowest ITAE value was recorded for the case of figure (6.16) which used a faster dominant time-constant ($T_3 = 20$ seconds). As time increased, the error was minimized meaning a reward rather than a penalty for minimizing the error. As for the smallest ISE, surprising as it may seem looking at the shapes of the different responses, it was achieved for the case of figure (6.13) which used a gain of 2.00. The 20% overshoot followed by a 12% undershoot would indeed have suggested otherwise. But, because the transient response was fast, it soon tracked the set-point leaving the ISE value smaller.

As pointed out earlier, the patient population can be divided into 3 categories: highly sensitive, average sensitive, and less sensitive patients, corresponding respectively to a high, average, and low gain. This gain could also vary for one

patient and on-line. Hence, the self-adaptive GPC should not exhibit any unstable mode as a result of this. The estimator should signal to the GPC so that it would tune in accordingly. To test the robustness of the algorithm under such conditions, a run was conducted in which the open-loop gain was made to vary using the potentiometers PA_3 and PA_6 in figure (6.8) from 1.00 to 0.90 (sudden change) at iteration 70, from 0.90 to 0.80 (sudden change) at iteration 150, from 0.80 to 0.90 (sudden change) at iteration 210, and finally back to 1.00 at iteration 260 (sudden change). Figure (6.18) shows how the GPC with the help of the observer polynomial $T(z^{-1})$ rejected the 4 disturbances quickly without deteriorating its performance despite the harsh changes made. The variations of the parameter estimates illustrated in figure (6.19) showed little drift in the dynamics, whereas the \hat{b} estimates changed accordingly, i.e a decrease in their value whenever the gain decreased, and an increase whenever the gain increased. Table (6.3) summarizes the values of the parameter estimates at the end of each phase, as well as the gain and time-constants of the corresponding continuous-time system.

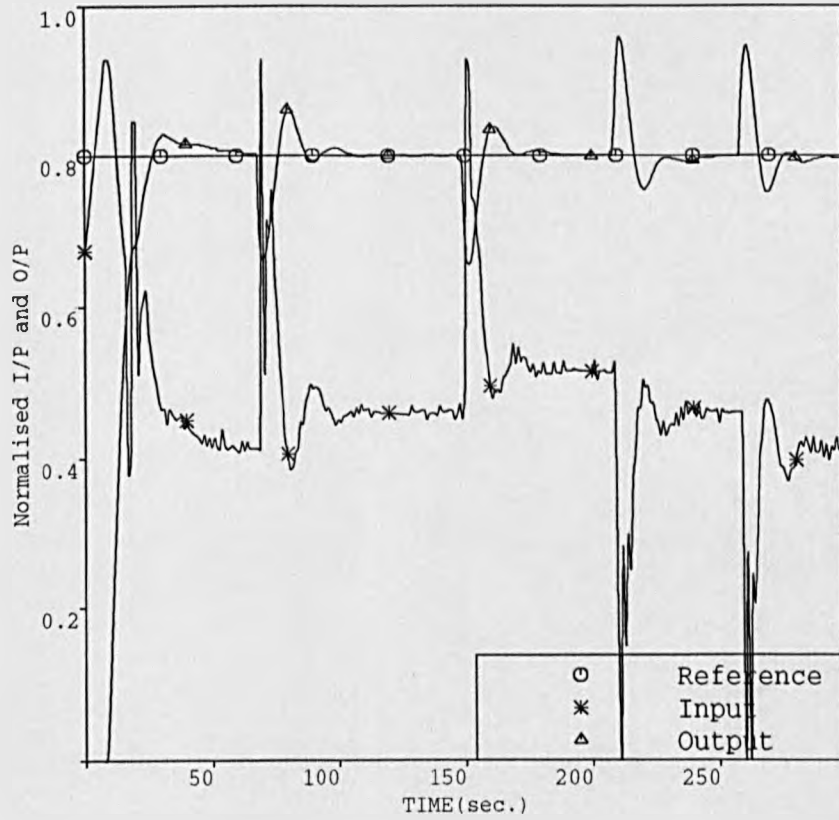


Figure 6.18. Closed-loop response of Atracurium model with additive gain change disturbances at iterations 70, 150, 210, and 260 seconds

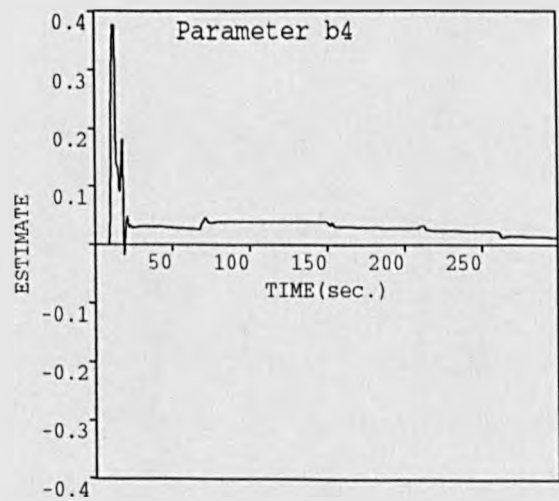
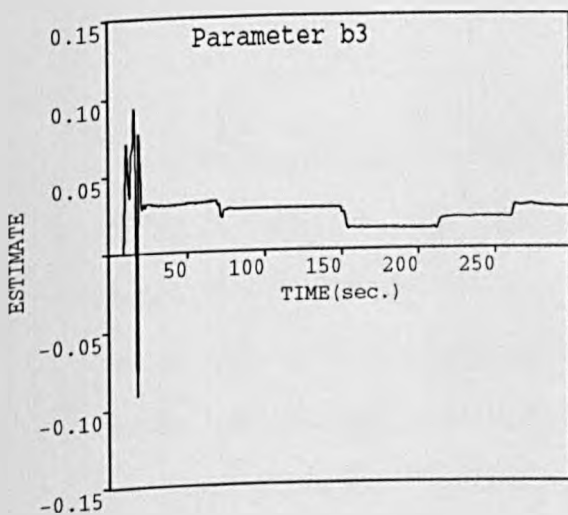
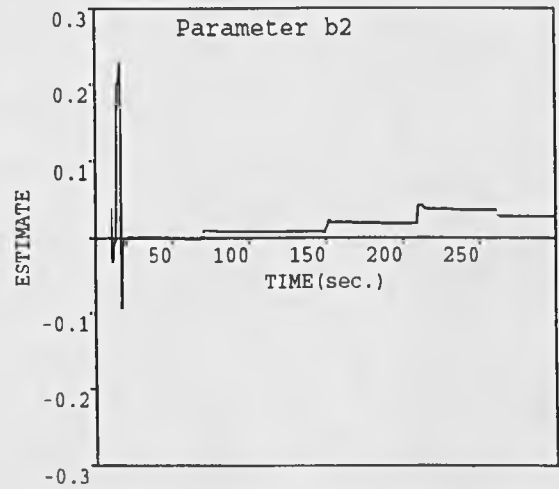
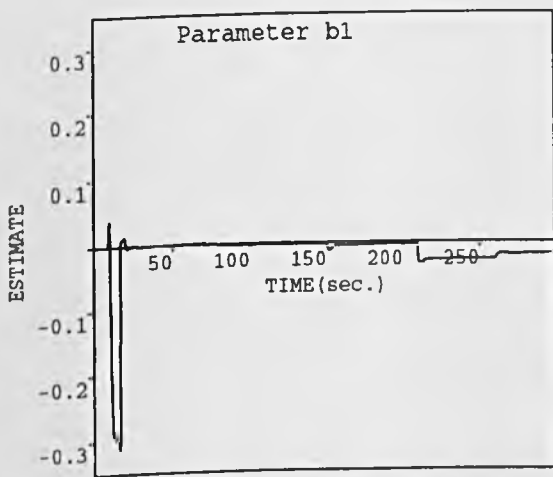
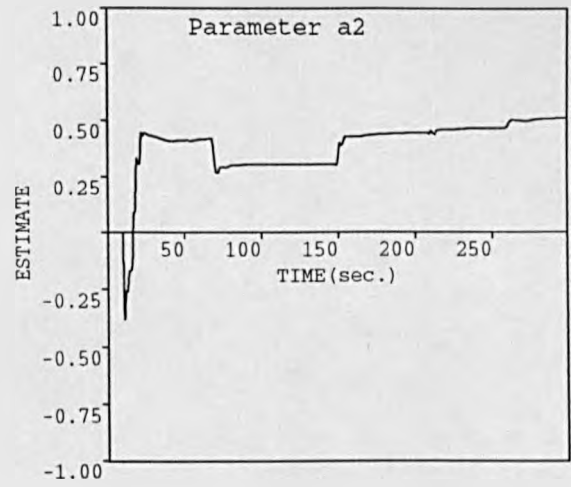
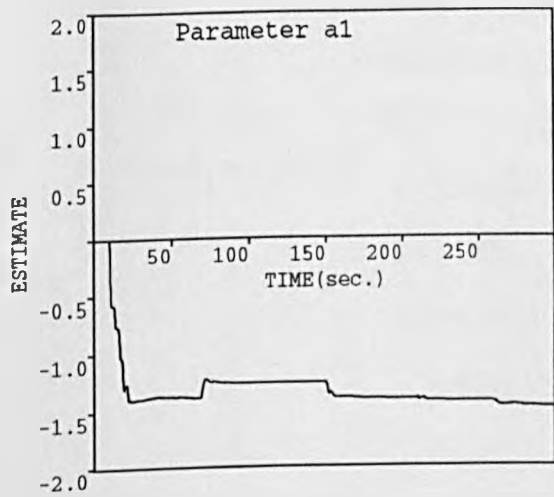


Figure 6.19. System parameter estimates corresponding to conditions of figure (6.18)

Parameter Estimates Convergence				
Parameter estimates	Time phase (from...to...) (Seconds)			
	(0-70)	(70-150)	(150-260)	(260-300)
\hat{a}_1	-1.3208	-1.2925	-1.4371	-1.4824
\hat{a}_2	0.3613	0.3346	0.4677	0.5105
\hat{b}_1	-0.0001	-0.0051	-0.0263	-0.0181
\hat{b}_2	0.0023	0.0126	0.0371	0.0283
\hat{b}_3	0.0295	0.0236	0.0195	0.0262
\hat{b}_4	0.0359	0.0394	0.0221	0.0131
Gain	1.75	1.67	1.71	1.76
\hat{T}_1 (Sec.)	1.05	0.97	1.4347	1.64
\hat{T}_2 (Sec.)	14.63	14.74	15.90	15.72

Table 6.3. Model parameter estimates for an on-line varying gain

Notice that this time the 2 seconds time-delay is not clearly demonstrated by the \hat{b} estimates during the phases corresponding to the iterations between 150-260 (sec.) and 260-300 (sec.) .

The conditions under which the GPC algorithm was investigated were closely related to reality, as far as the uncertainty of the model parameters were concerned, which themselves reflect patient parameters variability. The controller proved very robust in making the output track the set-point command efficiently despite non-linearities, and offsets induced by the hardware available. These later conditions emphasized the realistic character of the simulations. Corresponding

control signals were reasonably active, due to the observer polynomial $T(z^{-1})$, which undoubtedly attenuated the high frequency components originating from the hardware, and later amplified by the Δ operator. As a result of this, parameter estimates were good and were characterized only by a slight drift or none at all in some cases. Further simulations combining bolus dose administration and closed-loop infusions of Atracurium were scheduled as part of this real-time study, but because of serious hardware problems, related mainly to the AD/DA converters, they were impossible to conduct. Finally, it should be said that these real-time simulations were very useful in assessing the robustness of the algorithm over a wide range of subjects parameters before its implementation and evaluation in operating theatre. The next chapter is concerned with the implementation and application of this control strategy in operating theatre.

CHAPTER 7

SELF-ADAPTIVE GENERALIZED PREDICTIVE CONTROL (GPC) OF ATRACURIUM INDUCED MUSCLE RELAXATION IN OPERATING THEATRE

7.1 INTRODUCTION

The previously successful implementation and application of the GPC control algorithm in simulations as well as in real-time experiments motivated the work reported in this chapter which is concerned with the clinical evaluation of the same control strategy (GPC), using the fast acting drug Atracurium. The experiments to be presented have been undertaken during the period spreading between November 1990 to July 1991, in collaboration with the Department of Anaesthesia, Western Infirmary Hospital, Glasgow, and the Department of Anaesthesia and Anaesthesiology, Hallamshire Hospital, Sheffield, and with the respective Ethics Committee approvals.

A new configuration for the closed-loop control scheme had to be considered for that purpose, suggesting therefore, that a number of modifications and additions for both the existing hardware and the original developed software had to be included, details of which will be reviewed in the next section. Moreover, to provide a closer insight into the anaesthesia technique, a brief description of the clinical preparation of the patients just before surgery will also be given. Finally, results of the conducted clinical trials will be presented, analysed and discussed.

7.2 MODIFICATION OF THE MUSCLE RELAXATION CONTROL SYSTEM PRIOR TO CLINICAL EVALUATION

The muscle relaxation control system used in operating theatre and illustrated in figure (7.1), consists of the following components:

- A 380Z-D Research Machines disk-based microcomputer system (similar to the one used in the previous study and reported in chapter 6, except that its density has been doubled allowing for more RAM memory space), and which includes the control algorithm.
- A Relaxograph system for measuring the degree of muscle relaxation (paralysis).
- A digital pump driving a disposable syringe containing a solution of Atracurium.

Before describing the overall control loop, the following sections will endeavour to describe each of the previous components.

7.2.1 The Relaxograph Measurement System

The Datex RelaxographTM neuromuscular transmission (NMT) monitor is designed for monitoring neuromuscular blockade by electrically stimulating a peripheral nerve and displaying the resulting EMG (electromyograph) response. It employs the Train-of-Four principle (TOF) and features an automatic search for supramaximal stimulation current level. Five electrodes are needed for monitoring NMT with the Relaxograph. Two are for electrically stimulating a peripheral nerve (over the ulnar nerve), while two others are for measuring the resulting response from the corresponding muscle (hypothenar muscle). The fifth electrode serves for grounding the apparatus, and is placed above the wrist. NMT monitoring is

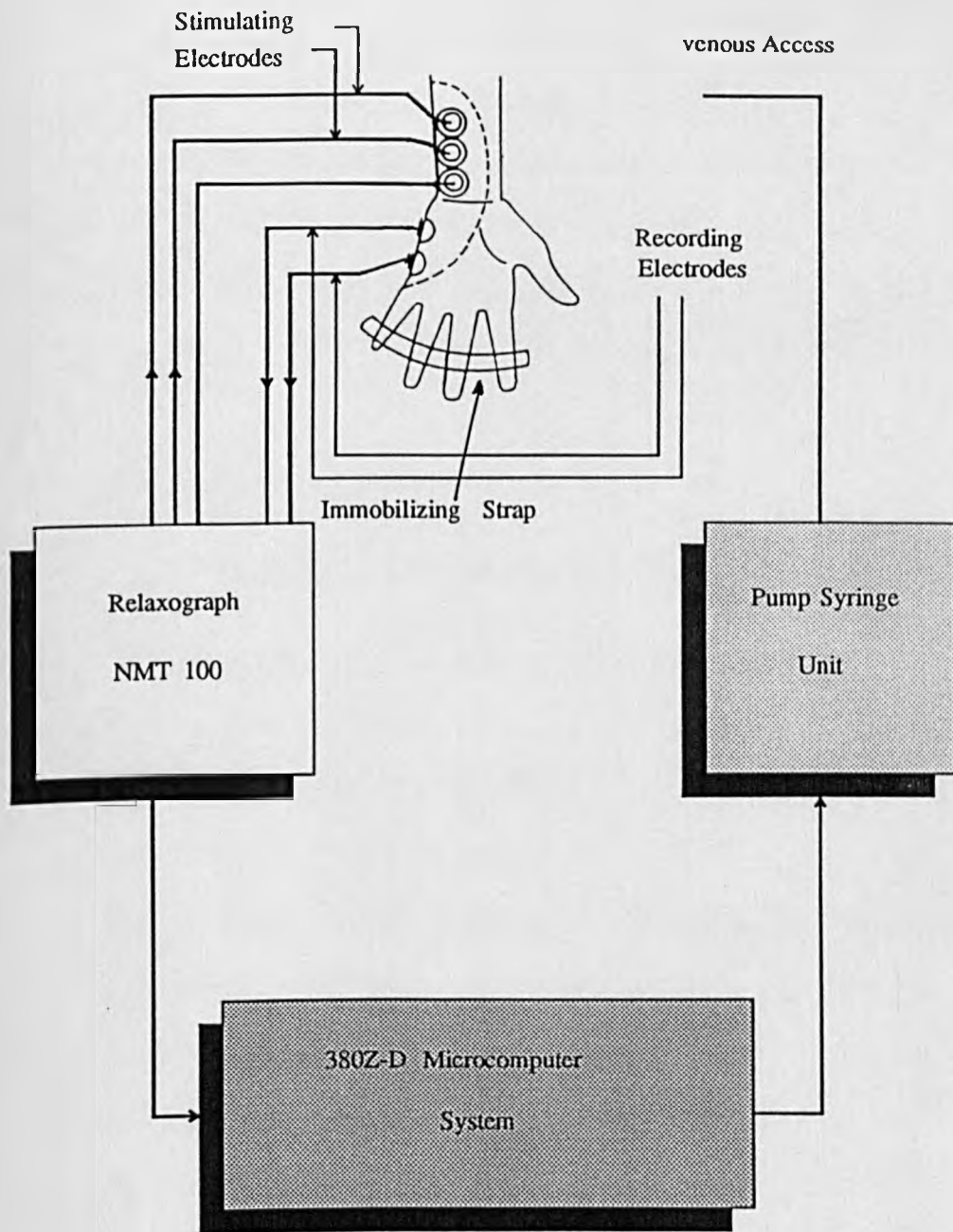


Figure 7.1. A schematic diagram of the muscle relaxation control system used in theatre.

usually begun after the induction of sleep to prevent voluntary muscle contractions. Calibration, which consists of a search for 100% reference response, is initiated after sleep is induced, but before administration of muscle relaxant drugs. The Train-of-Four (TOF) stimulation is delivered by the Relaxograph every 20 seconds. Stimuli of the corresponding sequence are given at a rate of 2 pulses per second. The device displays T1% and TR% values given by the following formulae:

$$T1 = \frac{\text{first twitch}}{\text{control}} \times 100\%$$
$$TR = \frac{\text{last twitch}}{\text{first twitch}} \times 100\% = \text{TOF ratio}$$

In this case T1 represents the value of the EMG level.

The information output from the device comes in the form of a 41 character string in ASCII code. It includes the following data:

- The actual time (in hours and minutes).
- The marker number (signal generated by the user to point to a particular event during the operation).
- The values of the four twitches (T1, T2, T3, and T4).
- The reference EMG values (100% control).
- The error codes.

To provide the access to this information, which is available in the buffer every 20 second interval, the NMT machine includes a built-in 9-pin serial input-output connector for any microcomputer interface. And finally, the Relaxograph monitor contains also a built-in two speed printer. The slow speed mode (used throughout the study) will allow only the T1 and T4 values to be printed. High frequency disturbances, such as diathermy, are usually displayed as broken or dotted lines.

7.2.2 The Pump-Syringe Unit

Two different types of digital syringe pumps were used during the trials conducted in the previously mentioned hospitals. For the Glasgow trials, a VICKERS Treonic digital syringe pump was made available. Originally set for conventional use (speed of the pump set by means of three thumbwheels operated manually), it was modified to allow the BCD signals which control the rate multipliers to be provided by the computer. This BCD signal transmits to the rate multipliers which control the pump's timing circuitry to produce pulses that drive a stepper motor at a speed which is proportional to the signal generated by the controller segment. A simple mechanism included in the hardware transforms the rotating movements of the motor into linear ones. 50/60 ml disposable syringes can be used with the device. The syringe barrel is fixed to the pump body with a barrel holder, while the plunger is attached to the pump carriage. The linear movements are directly transmitted to the pump carriage which pushes the plunger into the barrel, causing the Atracurium solution to be expelled through an administration line. As for the experiments conducted in Sheffield, a CRITIKON SYRINGE-MINDER 90 syringe pump was provided. No modifications were necessary in the hardware, since an RS232 input was already available. The principle of functioning is the same, except that this pump allows only integer signals to be input in, i.e 1 to 999 corresponding to 0.1 to 99.9 ml.hr⁻¹, whereas the former pump demanded signals between 0.1 to 99.9 corresponding to 0.1 to 99.9 ml.hr⁻¹.

7.2.3 The Control Algorithm and the Sampling Period

Because the Relaxograph delivers signals only at precise intervals of 20 seconds, a change in the existing program had to be made to accommodate the use of a one minute sampling interval which was found to give adequate results both

in simulations and in real-time experiments. This was done by using a 3 point non-recursive averaging filter of the form:

$$G_{AF}(z^{-1}) = \frac{1}{3} \sum_{i=0}^2 z^{-i} \quad (7.1)$$

where:

$$\begin{aligned} z^{-1} &= e^{-s h} \\ h &= 20 \text{ seconds} \end{aligned} \quad (7.2)$$

Expanding equation (7.1) leads to the following expression:

$$G_{AF}(z^{-1}) = \frac{1 + z^{-1} + z^{-2}}{3} \quad (7.3)$$

By noting that:

$$1 - z^{-3} = (1 + z^{-1} + z^{-2})(1 - z^{-1}) \quad (7.4)$$

equation (7.3) could then be replaced by the following expression:

$$G_{AF}(z^{-1}) = \frac{1 - z^{-3}}{3(1 - z^{-1})} \quad (7.5)$$

Substituting equation (7.2) into equation (7.5), yields:

$$F(s) = \frac{1 - e^{-60s}}{3(1 - e^{-20s})} \quad (7.6)$$

Substituting $s = j\omega$ in equation (7.6) leads to the following expression:

$$F(j\omega) = \frac{1 - e^{-60j\omega}}{3(1 - e^{-20j\omega})} \quad (7.7)$$

In order to extract the equation that governs the magnitude plot of equation (7.7), it is necessary to transform it as follows:

$$\frac{1 - e^{-60j\omega}}{3(1 - e^{-20j\omega})} = \frac{1 - (\cos 60\omega - j \sin 60\omega)}{3(1 - (\cos 20\omega - j \sin 20\omega))} \quad (7.8)$$

Isolating real and imaginary part for this equation, yields:

$$F(j \omega) = \frac{(1 - \cos 60 \omega) + j \sin 60 \omega}{3 ((1 - \cos 20 \omega) + j \sin 20 \omega)} \quad (7.9)$$

After manipulating this equation, the mathematical expression of the magnitude plot is given by:

$$|F(j \omega)| = \frac{1}{3} \sqrt{\frac{1 - \cos 60 \omega}{1 - \cos 20 \omega}} \quad (7.10)$$

or, if expressed in decibels, it becomes

$$|F(j \omega)| = 20 \log_{10} \left[\frac{1}{3} \sqrt{\frac{1 - \cos 60 \omega}{1 - \cos 20 \omega}} \right] \quad (7.11)$$

Hence, equation (7.11) represents the equation governing the magnitude-plot of the above filter.

The log-magnitude plot response of the filter is shown in figure (7.2), where the characteristic shows a frequency of 0.008 Hz at -3 dB.

When closed-loop control is initiated, a PI controller is used to provide initial control allowing the parameter estimation routine to gather reasonable data. The PI parameters were obtained using Ziegler-Nichols techniques (Ziegler and Nichols, 1942) applied to open-loop step responses in an off-line study. The dose of Atracurium is expressed in ml.hr^{-1} and is obtained using the following known formula:

$$\text{Output of Atrac. (ml.hr}^{-1}\text{)} = K_p e + K_i (\sum e + P) \quad (7.12)$$

where,

$$K_p = k_p W_t$$

$$K_i = k_i W_t$$

$$k_p = 0.02 \text{ Kg.}^{-1}, \quad k_i = 0.0021 \text{ Kg.}^{-1}$$

W_t represents the actual patient's weight

e is the difference between the actual T1% and the target T1%

At this stage it is worth noting that when a bolus dose is preloaded to induce mus-

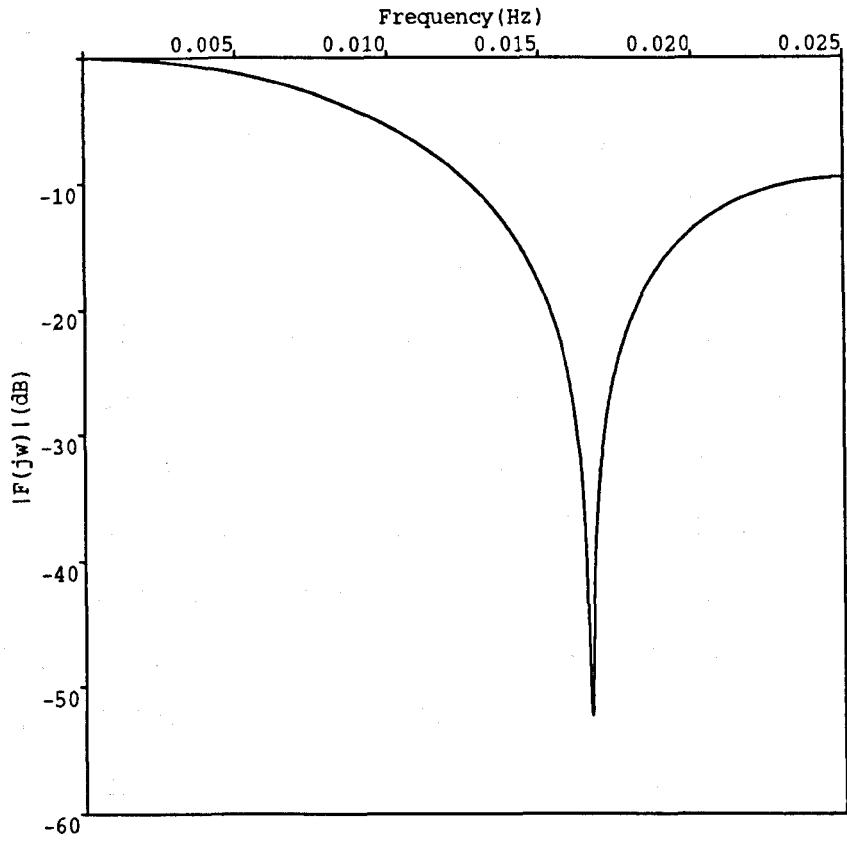


Figure 7.2. Frequency response corresponding to the filter of equation (7.11)

cle relaxation, the PI controller is initialized with some integral value P , so as to shorten the stabilization period when closed-loop control mode is entered. Nominal values between 150 and 333 were used throughout.

7.2.4 The Overall Control Program

The control program whose flowchart of figure (7.3) illustrates the different steps, is implemented on the 380Z-D microcomputer system. The link between the machine, the Relaxograph device as well as the syringe pump drive unit is via the serial and parallel input-output ports. Once the run command is entered, the program reads first the default data values relative to the control segment settings from off-line stored files. The user then enters the information concerning the patient such as, initials, age, and importantly the weight. To allow communication between the microcomputer and the Relaxograph, the 380Z-D library provides the routine INTSI which initializes the serial port SIO-4 and sets the baud transfer rate to 300 baud. The program then checks the Relaxograph buffers for any relevant information using the functions ISIKTL(4) and ISIKIN(4) which are both included in the subroutine Relax called by the main program segment. The information in a form of a 41 character string is decoded by the same subroutine which also separates the relevant numerical quantities mainly the time, mark, T1, and T4. In case of high frequency disturbances (diathermy for instance), the character string is stripped of its 41 characters. To counteract this, the subroutine was written so as to check that this string is complete. For convenience purposes, T1% which indicates the value of the EMG level is scaled in the program so as to reflect the paralysis level (values between 0.0 and 1.0) using the following transformation formula:

$$\text{Paralysis} = \frac{100 - \text{EMG}\%}{100} \quad (7.13)$$

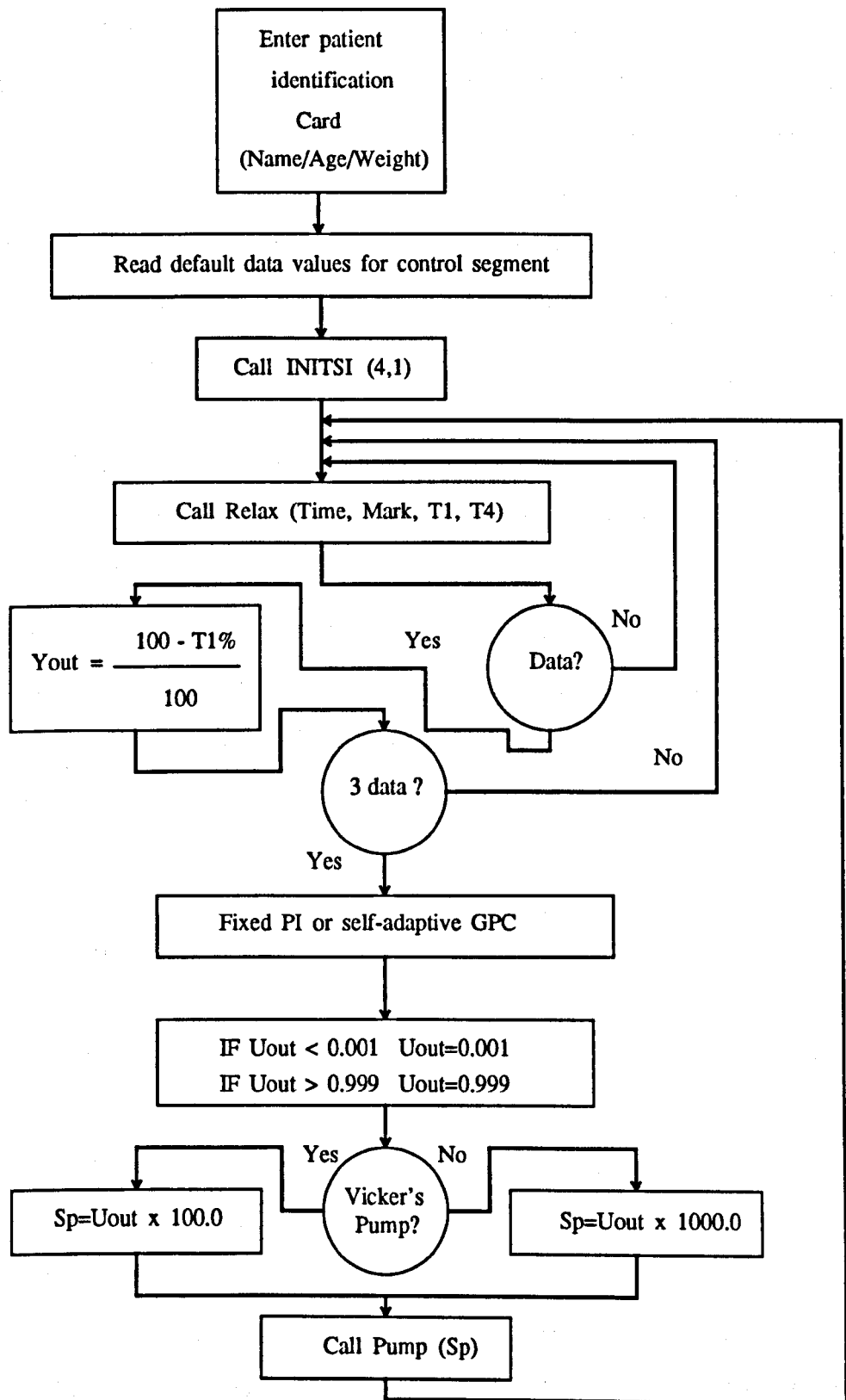


Figure 7.3. Flowchart representing the muscle relaxation control system used in operating theatre.

Once three data values have been gathered, the 3 point non-recursive averaging filter is applied to smooth these data. The single value of the output obtained is then used by the control program (fixed PI or self-adaptive GPC) to generate the input signal clipped between minimum and maximum values of 0.001 and 0.999 respectively. The input value is then scaled by a factor depending on the type of syringe pump which is made available and sent to the subroutine Pump which interfaces the 380Z-D machine to the syringe pump device. For the VICKERS pump, this subroutine initializes the PIO channel and separates the pump speed into a three digit number of decades, units, and decimals, then sends the final result to the PIO board. However, if the Critickon syringe pump is the one to be used, the same subroutine initializes the second available serial port and sets the baud-rate at 9600. The 16 bits rate-data is sent as two bit numbers into two addresses. The first address is HI byte, whereas the second address is LO byte. The link between the 380Z-D machine and the pump is in this case realized via an RS232 connector.

7.3 CLINICAL PREPARATION OF THE PATIENTS BEFORE SURGERY

The patients upon which this study was based were all selected knowing that they did not suffer from any known sensitivity to anaesthetic drugs or myoneural disorders, or have not been taking drugs known to affect neuromuscular transmission. They all underwent abdominal or orthoepedic surgery which normally requires muscle relaxation.

Approximately 60 minutes before surgery, they were all premedicated with Temazepam by mouth. Anaesthesia was induced with Methohexitane 1 mg.Kg.⁻¹. The trachea was intubated when T1 reached a 15% to a 10% value. The lungs

were inflated with 30% oxygen, 70% nitrous oxide and 1% Enflurane. During surgery, Enflurane anaesthesia was supplemented with boluses of Fentanyl $1\mu\text{g.Kg.}^{-1}$. While the patient was still in the anaesthetic room, the Relaxograph electrodes were adequately placed on the patient's arm, then the calibration proceeded. Once transferred to the theatre, the patient, already connected to the control system, was intravenously given an initial bolus dose of Atracurium of 0.15 to 0.25 mg.Kg.^{-1} . Atracurium concentration varied from 500 $\mu\text{g.ml}^{-1}$ to 1 mg.ml^{-1} .

The automatically controlled infusion was started when T1 (induced by the initial bolus) reached a level judged adequate by the anaesthetist (usually 10% to 15% of the 100% baseline* value). Muscle relaxation level was monitored until the surgeon ordered cessation of relaxation. The control was then switched off immediately and residual blockade was reversed using antagonist agents such as Neostigmine 2.5 mg. and Atropine 0.8 mg. Figure (7.4) is a picture taken in hospital showing the patient connected to the overall muscle relaxation control system ready to undergo surgery.

7.4 RESULTS AND DISCUSSIONS

After local Ethics Committee approvals, 10 patients (8 females, 2 males) were selected as being suitable for the experiments. Information relative to the patients are presented in table (7.1). Atracurium concentrations used were all 1mg.ml^{-1} unless otherwise specified.

*A 100% EMG corresponds to 0% paralysis, whereas 0% EMG is equivalent to maximum paralysis.



Figure 7.4. Picture showing the patient in the anaesthetic room while connected to the overall control system which includes (clockwise); the 380 Z μ computer system, the DATEX Relaxograph, and the CRITIKON syringe pump

Patients' Identification Cards					
Patients' initials	Sex	Age (Yr)	Weight (Kg.)	Type of surgery	Figure number
EXC*	F	68	50	Orthoepedic	7.5, 7.6
MGM*	F	33	60	Cholecystectomy	7.7, 7.8
TXC*	F	21	68	Cholecystectomy	7.9, 7.10
AXM*	F	69	50	truncal Vagatomy	7.11, 7.12
MMG*	F	65	58	Cholecystectomy	7.13, 7.14
MUU*	F	37	60	Cholecystectomy	7.15, 7.16
SMC*	F	17	56	Cholecystectomy	7.17, 7.18
JOD*	M	32	69	-	7.19, 7.20
ANM**	M	46	73	Truncal Vagatomy	7.21, 7.22
MCB**	F	41	71	Cholecystectomy	7.23, 7.24

Table 7.1. Table summarizing the patients' personal details including the type of surgery they underwent (-): not communicated by the anaesthetist

All ten trials were conducted using a sampling time interval of 1 minute. Consequently, the previous 3 point non-recursive averaging filter was included in all experiments. Control and estimation were performed every one minute, while EMG readings were obtained every 20 seconds. Parameter estimation was based on the UDU factorization algorithm and was triggered at the same time as the closed-loop control with a covariance matrix and forgetting factor values of

* Western Infirmary Hospital, Glasgow

** Hallamshire Hospital, Sheffield

$P = 10^2.I$ and $\rho = 0.995$ respectively. A 20% reference EMG level (T1%) was required by the operating surgeon in all trials except for the last case corresponding to patient MCB, where a 15% EMG reference level was targeted. Results corresponding to each patient were divided into two parts: the first part consists of two traces; the upper trace representing the recorded EMG level (T1%) in a form of segments, whereas the lower trace shows the variations of the infusion rate of Atracurium in ml.hr^{-1} . The time axis is labelled in samples of 20 seconds, and it is worth noting that the infusion rate is constant over three samples of 20 seconds each. As for the second part of the results, it includes the parameter estimates variations plotted every one minute interval.

Patient EXC

A combination of (1, 10, 1, 4) was chosen for (N_1, N_2, NU, λ) as part of the GPC settings. A first order observer polynomial $T(z^{-1}) = 1 - 0.85 z^{-1}$ was also included to compensate for any unmodelled dynamics. The parameter estimation routine, using incremental filtered data, assumed an underparameterized second order model with a minimum time-delay of 1 minute. Parameter estimates were initialized at 0.0 except estimate b_1 which was taken to be 1.0. The EMG recording of figure (7.5) shows how this patient was resistant to the initial bolus dose of Atracurium of 7 mg. administered at mark (2). It took the anaesthetist five other bolus doses of 2 mg. each respectively at mark (3), mark (4), mark (5), mark (7), and mark (9) to bring the EMG down to 19%, level which was still above the value of 15% which was suggested by the anaesthetist as being the safety margin normally allowing for the time-delay between the time of the infusion and the time at which its corresponding effect takes place. Closed-loop control was then

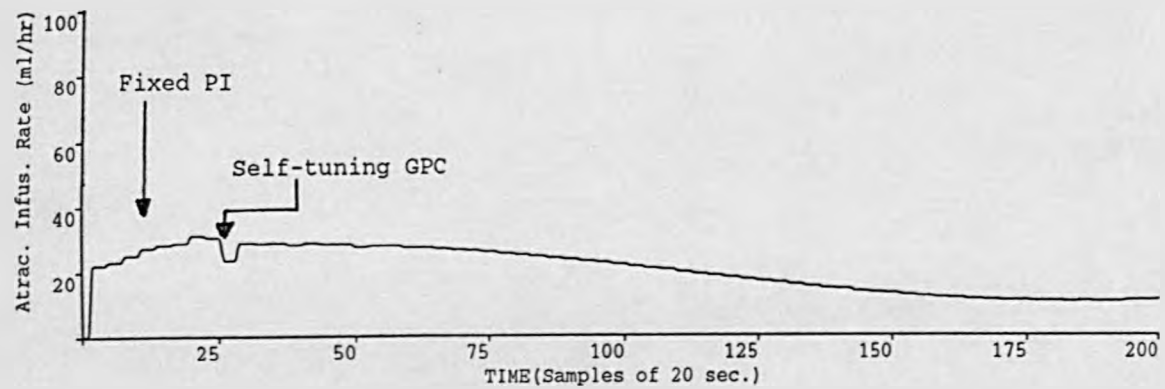
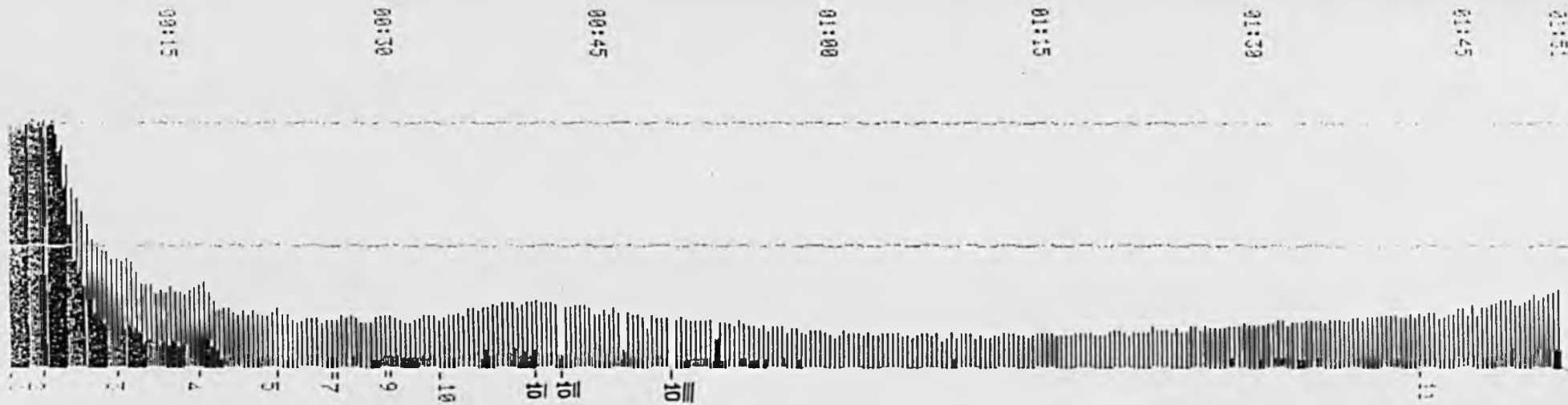


Figure 7.5. Recorded EMG and pump infusion-rate during surgery.

Patient EXC

started at mark (10) with the optimized PI allowed to run for 10 minutes within which an overshoot of 8% was produced. When the self-adaptive GPC took over at mark $\overline{(10)}$ on the trace, it tried to overcome this overshoot, but was rather slow to do so, despite the relatively fast time-constant of the filter, and produced the input signal which is represented by the lower trace of the same figure. The EMG undershot 5% below the target and started recovering at the end of the run. The overall performance, however, was acceptable and the controller did not exhibit any unstable mode despite diathermy problems appearing several times namely at mark $\overline{(10)}$, and mark $\overline{\overline{(10)}}$. Parameter estimates variations illustrated in figure (7.6) showed little drift, and the estimates finally converged to the following values:

$$\begin{aligned}\hat{a}_1 &= -0.6552 & \hat{a}_2 &= 0.0732 \\ \hat{b}_1 &= 0.3556 & \hat{b}_2 &= -0.0930\end{aligned}$$

These correspond to an estimated gain and time-constants of:

$$\hat{\text{Gain}} = 0.63 \quad \hat{\text{TC}}_1 = 0.51 \text{ minute} \quad \hat{\text{TC}}_2 = 1.49 \text{ minutes}$$

Patient MGM

For this experiment, the GPC protocol assumed a combination of (1, 30, 1, 0) for (N_1, N_2, NU, λ) and a second order observer polynomial of $T(z^{-1}) = (1 - 0.70 z^{-1})^2$. The idea was to use a faster root to quickly reject any disturbance and also to double the roll-off for enhancing robustness (Clarke and Robinson, 1991; Shook et al., 1991). Similar conditions to the previous case were adopted for the estimation routine. Mark (1) on the upper trace of figure (7.7) is when a bolus dose of Atracurium of 10 mg. was given to the patient leading to a

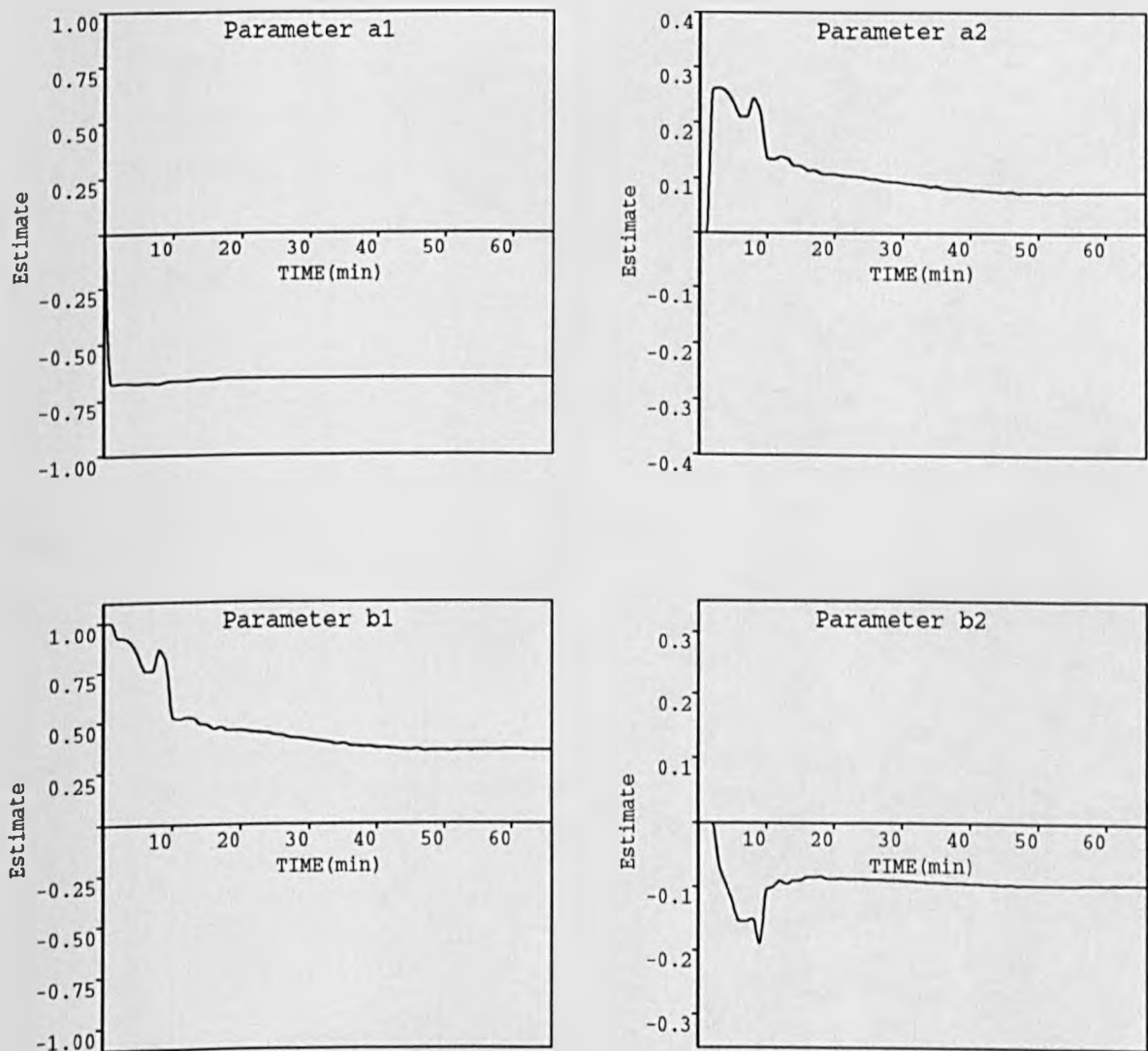


Figure 7.6. System parameter estimates corresponding to figure (7.5)

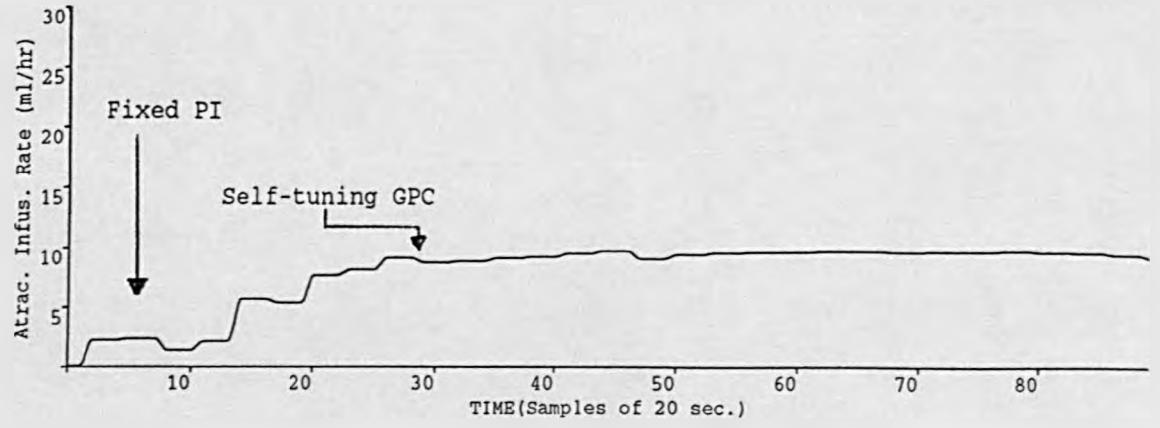
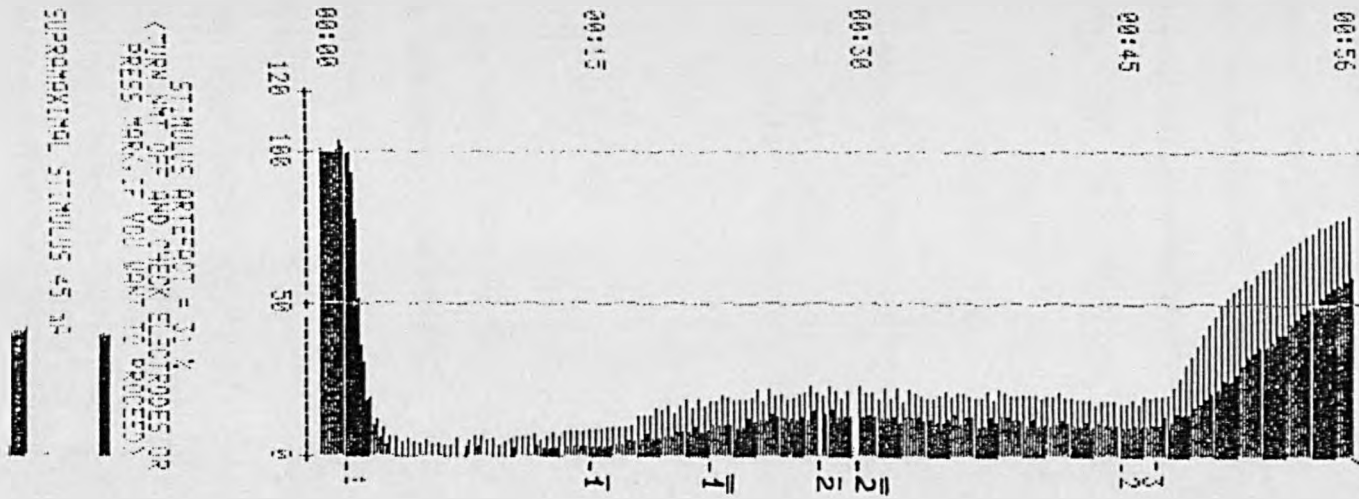


Figure 7.7. Recorded EMG and pump infusion-rate during surgery.

Patient MGM

fast decrease in the EMG level to approximately 4%, and hence no further drug was administered until mark $\overline{(1)}$ where the loop was closed with the fixed PI providing initial control for 10 minutes. Mark $\overline{(1)}$ is when the self-adaptive GPC took over. During that period, the EMG level was remarkably steady until mark (2) where the controller was switched off and the blockade reversed with Neostigmine. The infusion rate for the whole run was smooth in spite of diathermy problems which occurred mainly at mark $\overline{(2)}$ and mark $\overline{(2)}$. Parameter estimates were steady as figure (7.8) shows and finally converged to the following values:

$$\begin{aligned}\hat{a}_1 &= -1.3742 & \hat{a}_2 &= 0.4880 \\ \hat{b}_1 &= 0.5073 & \hat{b}_2 &= -0.4078\end{aligned}$$

Corresponding to the following pole/zero positions in the z-plane:

$$\begin{aligned}\text{zero: } & 0.8039 \\ \text{poles: } & (0.6871 \pm 0.1261 i)\end{aligned}$$

Patient TXC

For this experiment whose results are shown in figure (7.9), the Atracurium drug concentration was halved to $500 \mu\text{g.ml}^{-1}$. Conditions for the controller were similar to those of the previous case. However, a third order model with a minimum time-delay of 1 minute was assumed this time. Mark (1) and mark (2) on the upper trace of the same figure represent the times at which the anaesthetist administered bolus doses of respectively 7.5 mg. and 2.5 mg. in order to bring the EMG level down to approximately 15%. At mark (3), the closed-loop control mode was entered with the fixed PI allowed to run for 30 minutes, after which the self-adaptive GPC took over at mark (4). Both control modes succeeded in keeping a remarkably steady level of paralysis with hardly any fluctuations at all, but

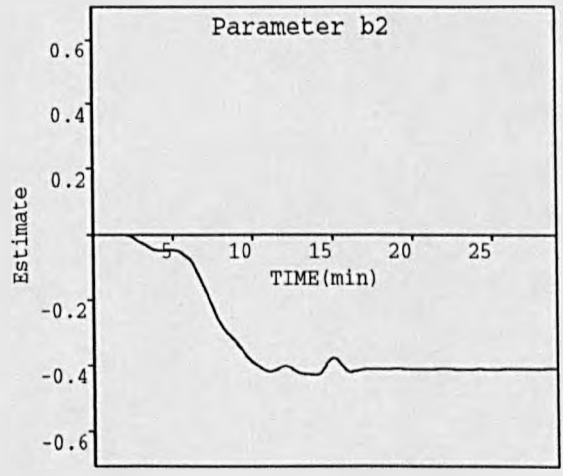
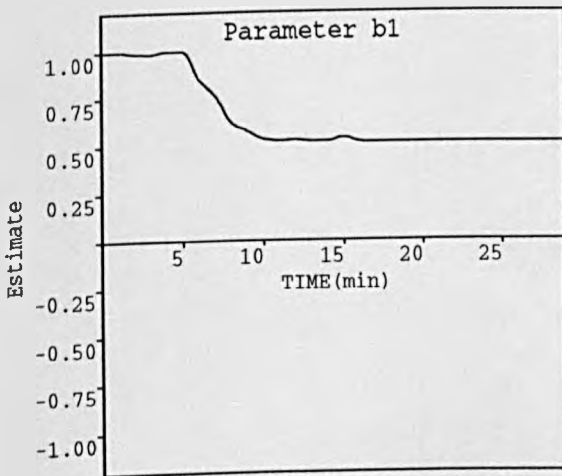
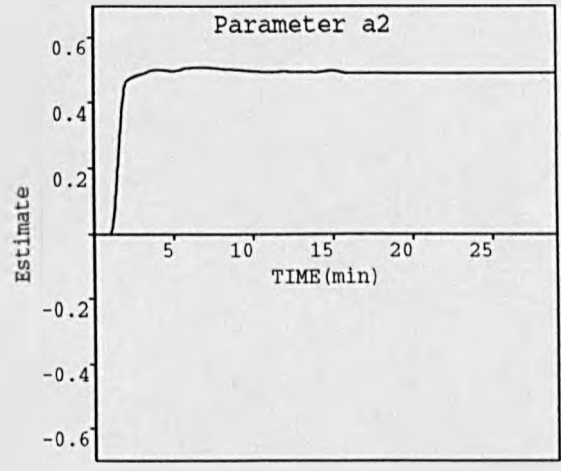
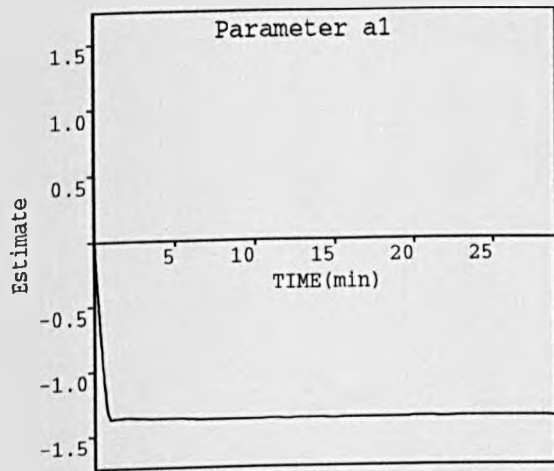


Figure 7.8. System parameter estimates corresponding to figure (7.7)

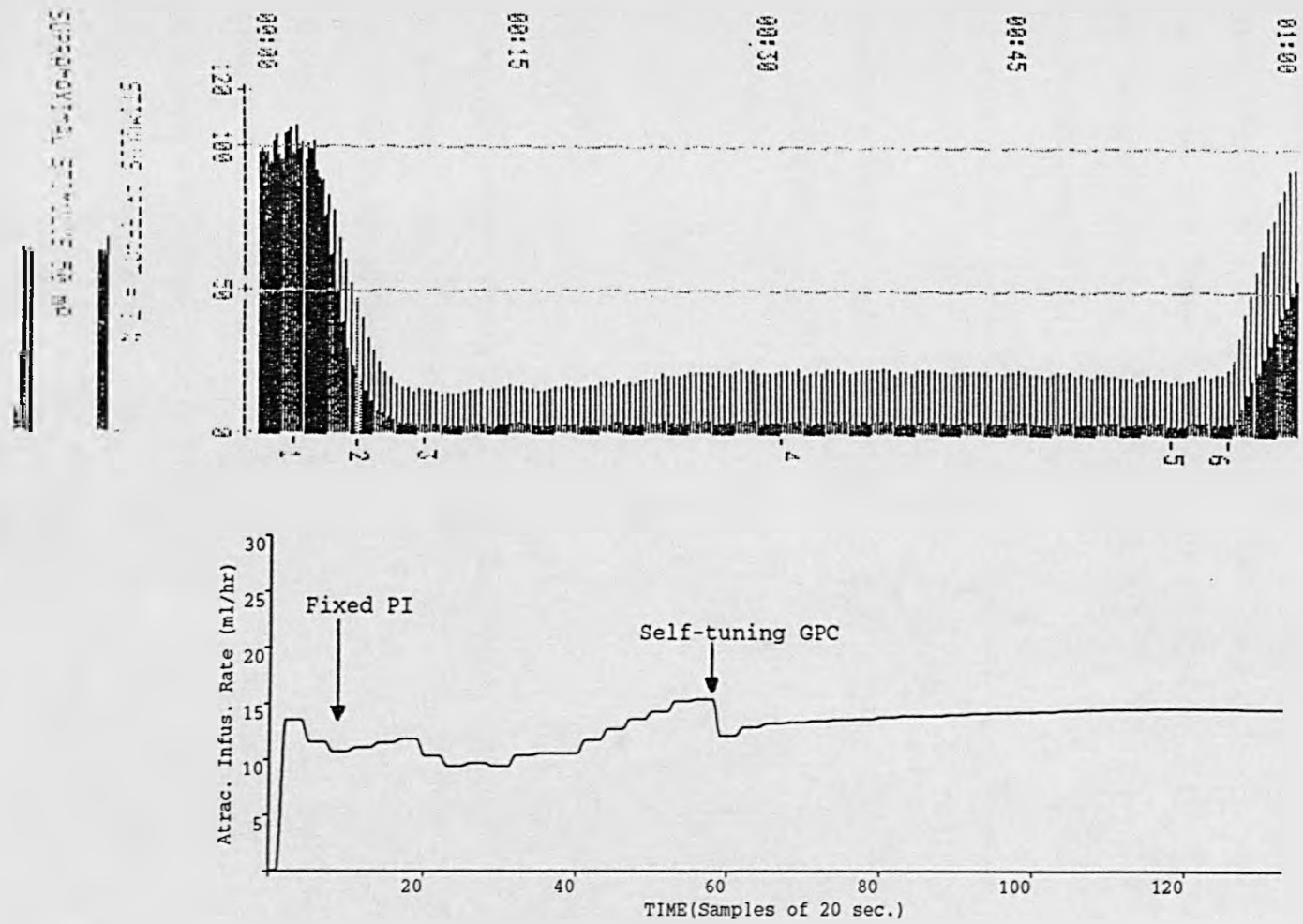


Figure 7.9. Recorded EMG and pump infusion-rate during surgery.

Patient TXC

looking at the infusion rate plot, the period corresponding to the GPC protocol was steadier. Finally at mark (5) the controller was switched off and the blockade reversed at mark (6). Notice the return to a 100% baseline suggesting that no unnecessary drug has been administered and therefore little drift in the relaxation level has been recorded. Figure (7.10) illustrates the variations of the parameter estimates which were steadier during the course of this trial. They finally converged to the following values:

$$\begin{aligned} \hat{a}_1 &= -1.1926 & \hat{a}_2 &= 0.3059 & \hat{a}_3 &= 0.0745 \\ \hat{b}_1 &= 0.8109 & \hat{b}_2 &= -0.1358 & \hat{b}_3 &= -0.0740 \end{aligned}$$

Corresponding to the following pole/zero positions in the z-plane:

$$\begin{aligned} \text{zeros: } & 0.3972 ; -0.2297 \\ \text{poles: } & (0.6702 \pm 0.2342 i) ; -0.1478 \end{aligned}$$

Patient AXM

During this particular experiment, the subject, a young female, demonstrated unusual resistance to the muscle relaxant drug. Indeed, as the EMG recording in figure (7.11) shows, the patient was insensitive to the first bolus dose of respectively 9 mg. intravenously administered at mark (2). Another 2 mg., then 3 mg. were given at mark (3) and mark (4) respectively. At this stage, the anaesthetist decided to enter automatic control of the infusion at mark (5) with the fixed PI allowed to run only for 5 minutes. The infusion rate of Atracurium at $500\mu\text{g.ml}^{-1}$ began at approximately 60 ml.hr^{-1} then started increasing gradually to reach 80 ml.hr^{-1} , and that did not cause the EMG to drop below the 50% line. However, when the GPC took over at mark (5), with a combination of (1, 10, 1, 0) for (N_1, N_2, NU, λ) and $T(z^{-1}) = (1 - 0.95 z^{-1})^2$, it was quick to drive the EMG level

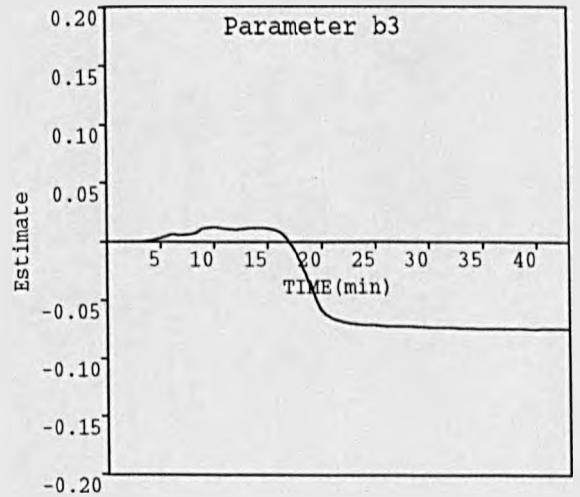
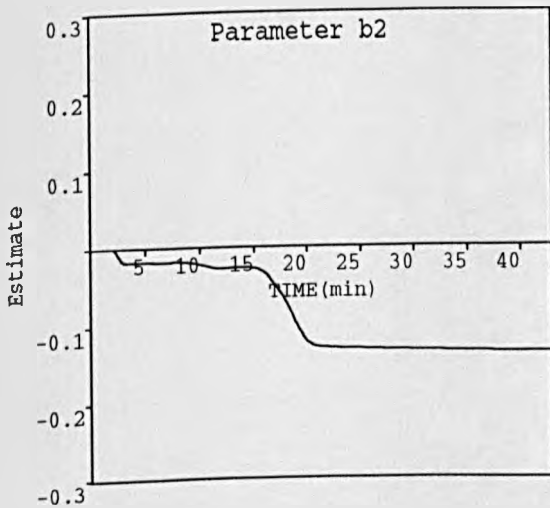
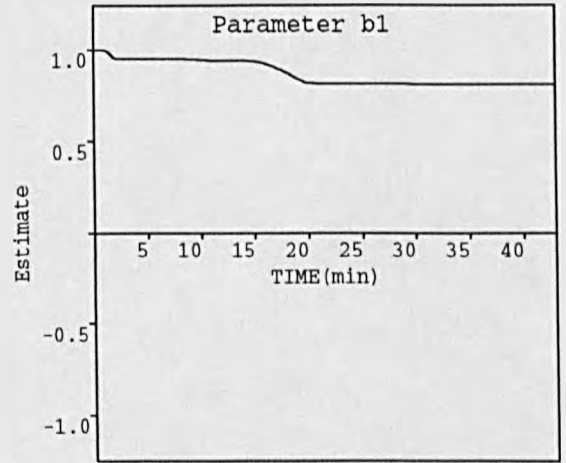
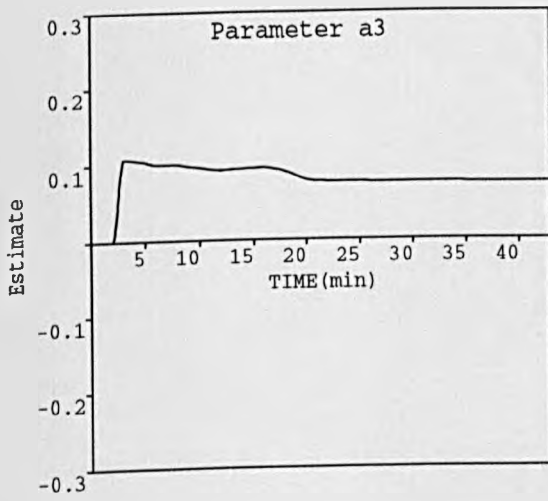
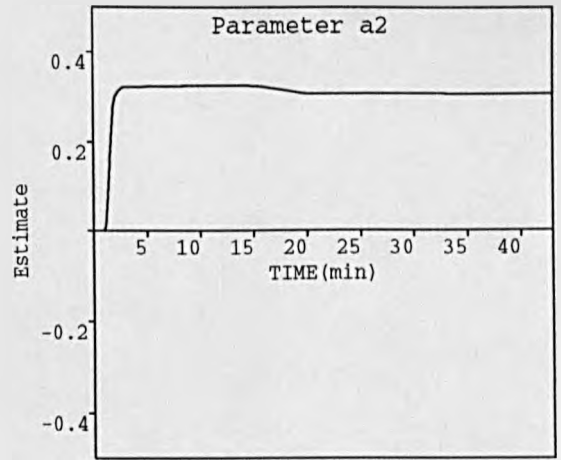
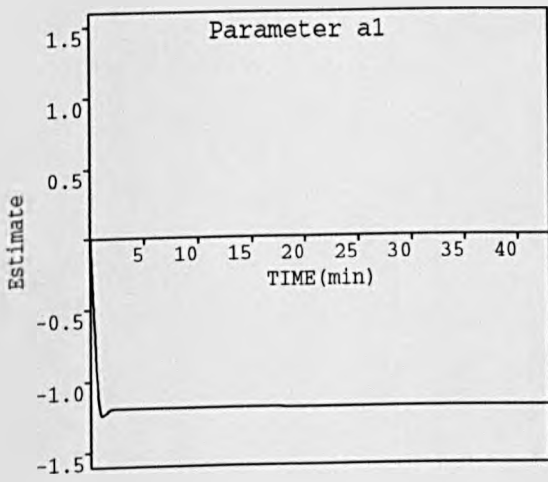


Figure 7.10. System parameter estimates corresponding to figure (7.9)

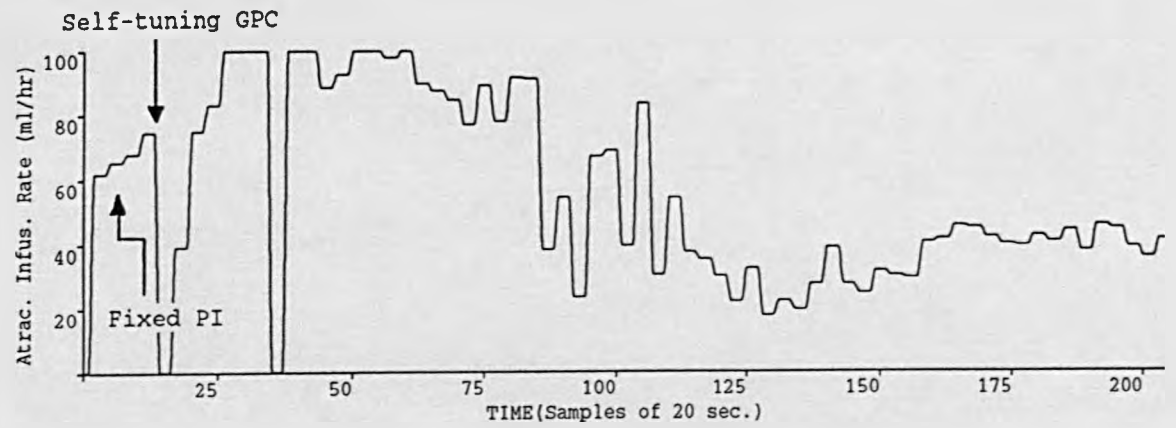
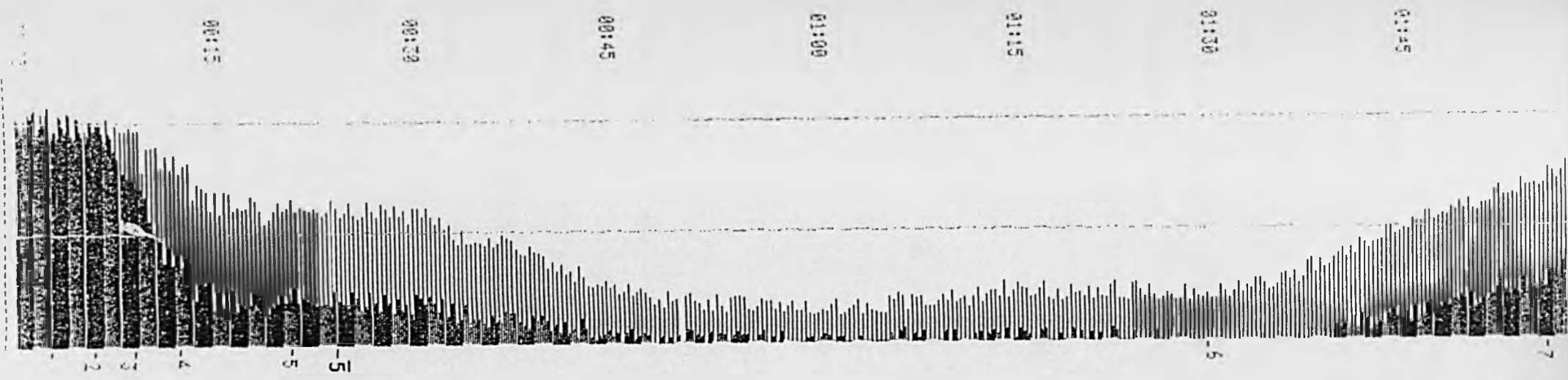


Figure 7.11. Recorded EMG and pump infusion-rate during surgery.

Patient AXM

to the target in spite of the noise level estimated at $\pm 3\%$ persistently acting on the output. The controller behaved rather well by rejecting these disturbances and produced a control signal, illustrated on the lower trace of the same figure, which was reasonably active. Undoubtedly, the use of a slower root in the $T(z^{-1})$ polynomial made the controller more robust. The parameter estimation routine, which in this case assumed a second order model with a one minute time-delay, used filtered incremental data for the measurement vector. The variations of the parameter estimates are shown in figure (7.12). They, on the other hand, finally converged to the following values:

$$\begin{aligned} \hat{a}_1 &= -1.7674 & \hat{a}_2 &= 0.7717 \\ \hat{b}_1 &= 0.0471 & \hat{b}_2 &= -0.0386 \end{aligned}$$

equivalent to a continuous second order system of the following gain and time-constants:

$$\hat{\text{Gain}} = 1.97 \quad \hat{\text{TC}}_1 = 4.19 \text{ minutes} \quad \hat{\text{TC}}_2 = 48.88 \text{ minutes}$$

Before describing the remaining six clinical trials, it is worth noting that throughout the following, full valued data (positional data) rather than incremental data were used in the measurement vector for estimation purposes. Although this constitutes a violation of the GPC approach based on a CARIMA model, it was found to give satisfactory performances as the following results will demonstrate. Parameter estimation assumed a second order model with a minimum time-delay of 1 minute unless otherwise specified, and initial conditions included a covariance matrix and a forgetting factor of respectively $P = 10^2 \cdot I$, and $\rho = 0.995$. Parameter estimates were initialized so as to reflect a continuous second order system with the following gain and time-constants (taken from one of the experiments conducted in hospital previously (Denai et al., 1990)):

$$\theta_i = \left[1.15, 0.34', 16.13' \right]$$

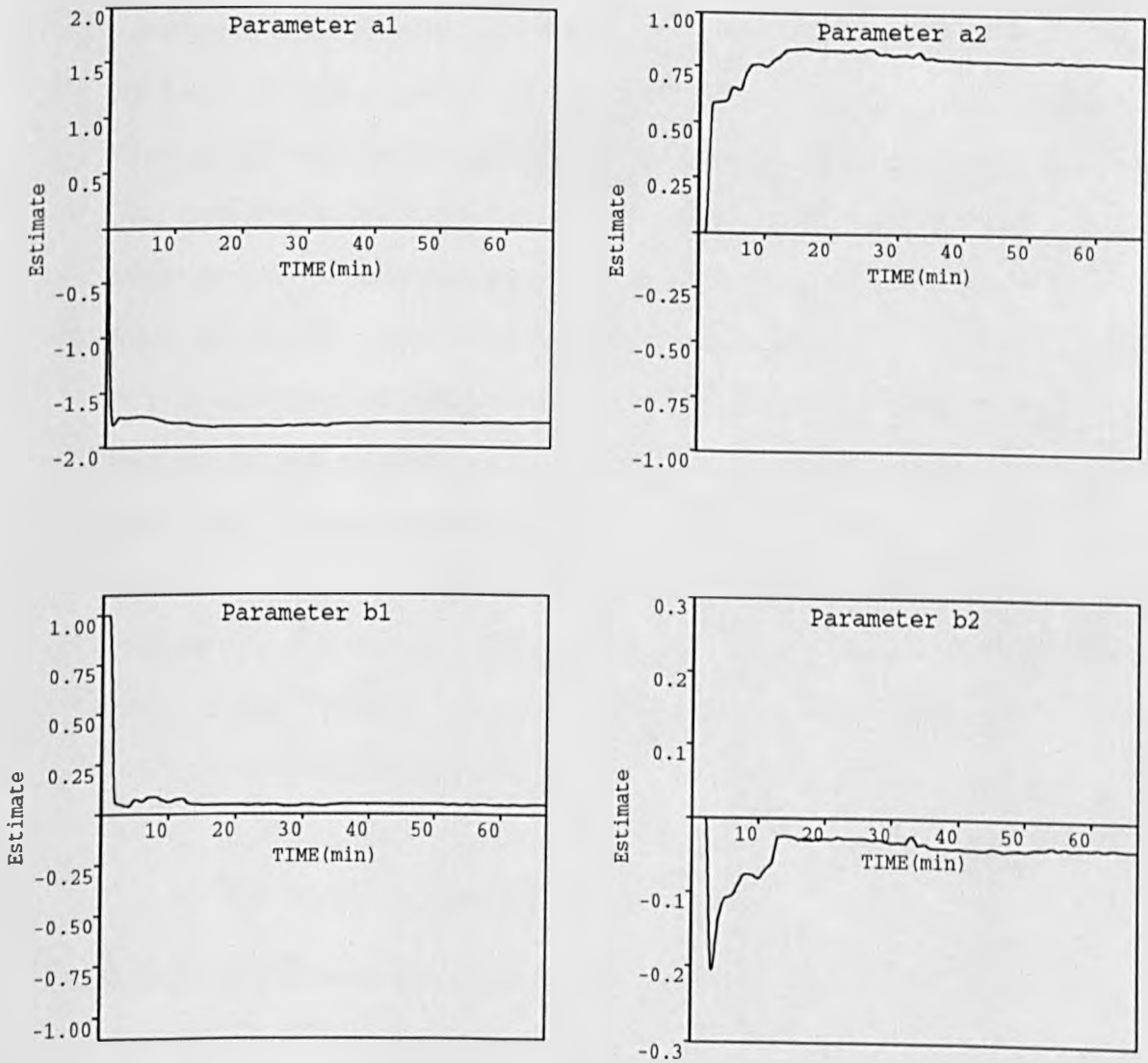


Figure 7.12. System parameter estimates corresponding to figure (7.11)

Patient MMG

Mark (1) of figure (7.13) is when a bolus of 6 mg. was administered to the patient, and mark (2) when another bolus dose of 2 mg. was added which brought the EMG down to a level of approximately 15%. Closed-loop control was started at mark (3) with the PI operating for 10 minutes, after which the self-adaptive GPC took over at mark (3̄). The control was switched off at mark (4), where at the same time Neostigmine was given to reverse the blockade. During the first phase (PI) the EMG response demonstrated an overshoot of almost 5% due to the PI parameters which probably needed readjustments, but when the GPC was switched on with a combination of (1, 20, 1, 5) for (N_1, N_2, NU, λ) , the output tracked the set-point better and with minimum fluctuations. The control was surprisingly good and reasonably active despite the absence of the filter $T(z^{-1})$. Here the use of a non-zero weighting sequence λ was adopted to introduce fine control tuning. Parameter estimates whose variations are shown in figure (7.14) converged to the following values:

$$\begin{aligned} \hat{a}_1 &= -1.0165 & \hat{a}_2 &= 0.0258 \\ \hat{b}_1 &= 0.0292 & \hat{b}_2 &= 0.0003 \end{aligned}$$

equivalent to a continuous second order system of the following gain and time-constants:

$$\hat{\text{Gain}} = 3.17 \quad \hat{T}C_1 = 0.27 \text{ minute} \quad \hat{T}C_2 = 104.23 \text{ minutes}$$

Patient MUU

In this experiment the control horizon was increased to 2 and all other parameters were similar to the ones assumed previously. Mark (1) on the upper

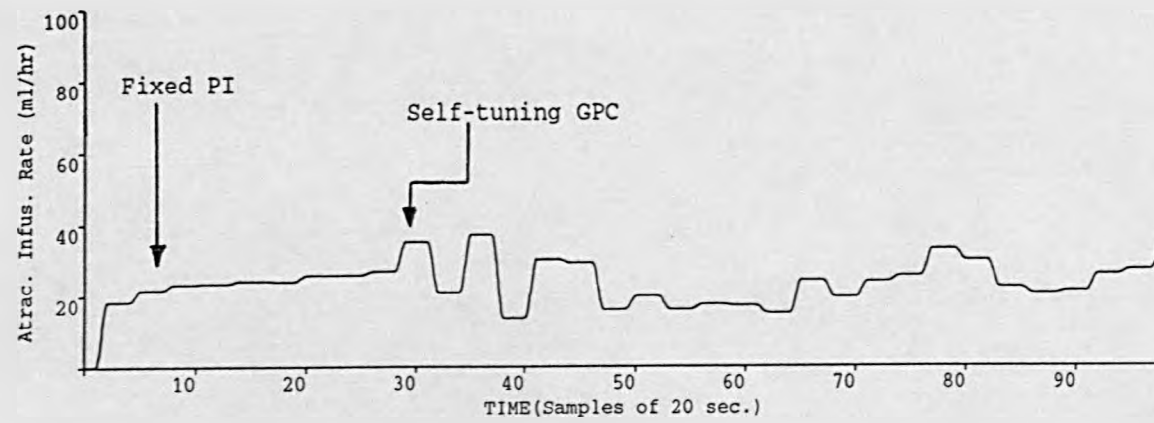
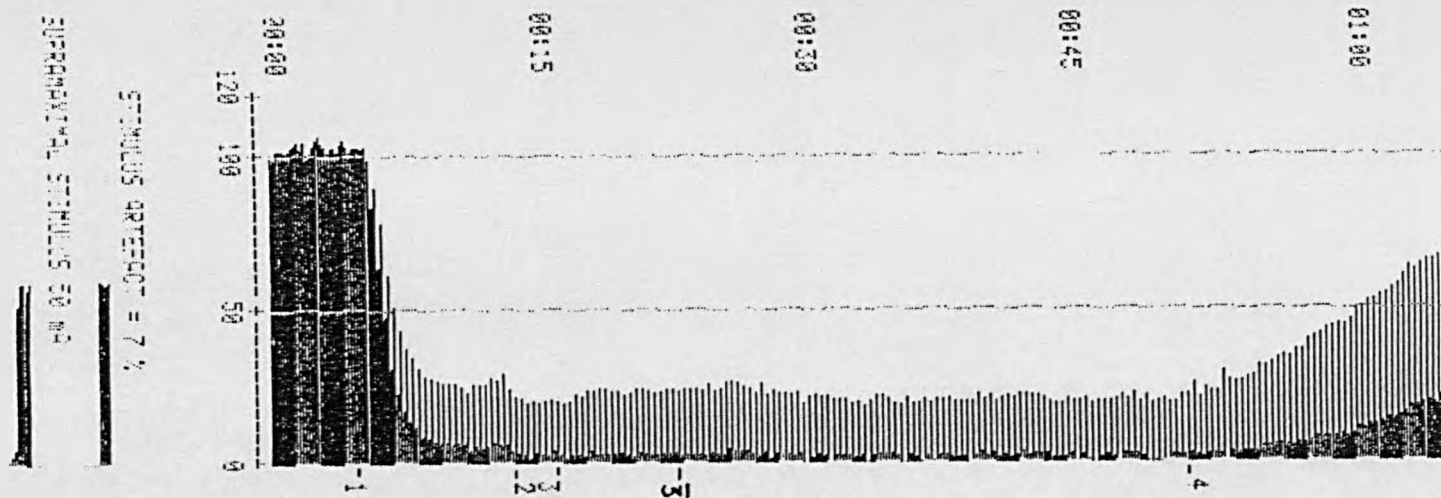


Figure 7.13. Recorded EMG and pump infusion-rate during surgery.

Patient MMG

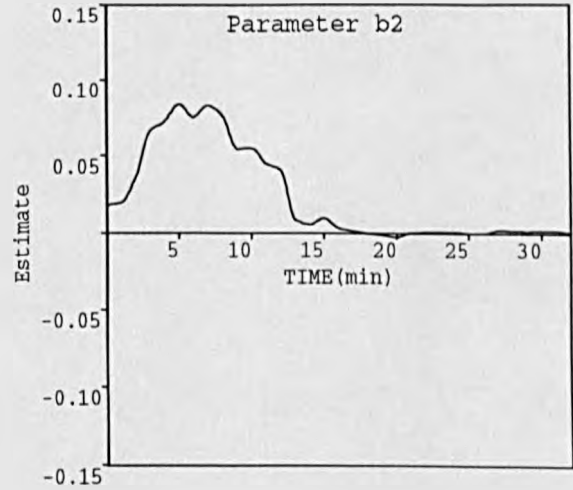
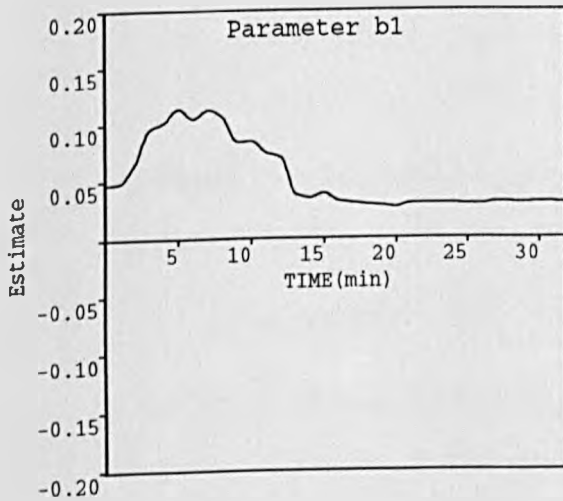
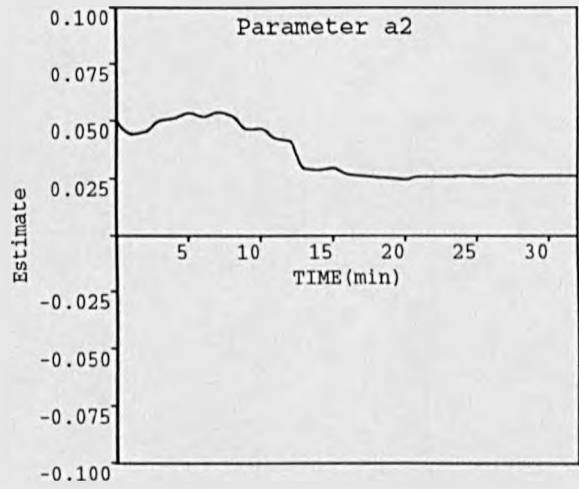
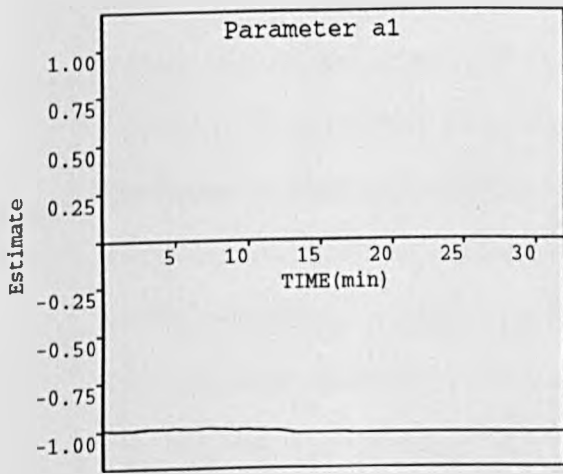


Figure 7.14. System parameter estimates corresponding to figure (7.13)

trace of figure (7.15) represents the time at which the anaesthetist administered a bolus dose of Atracurium of 10 mg. which completely wiped out the patient's EMG tracing as it began to appear again 2 minutes later. At **mark (2)** automatic control started and **mark (3)** is when the self-adaptive GPC was triggered. As shown, GPC was quick to overcome the 7% overshoot induced by the PI and maintained a relatively steady level of paralysis despite the presence of diathermy occurring several times mainly at **mark (4)**, **mark (5)**, and **mark (5)**. The use of a control weighting sequence $\lambda \neq 0.0$ counteracted the effect of a control horizon $NU \geq 2$ which normally makes the control signal highly activated. Finally at **mark (6)**, blockade was reversed with Neostigmine leading to a 100% baseline. Variations of the parameter estimates during the run are shown in figure (7.16). They converged to the following values:

$$\begin{aligned} \hat{a}_1 &= -1.0004 & \hat{a}_2 &= 0.0437 \\ \hat{b}_1 &= 0.1149 & \hat{b}_2 &= 0.0604 \end{aligned}$$

equivalent to a continuous second order system of the following gain and time-constants:

$$\hat{\text{Gain}} = 4.05 \quad \hat{\text{TC}}_1 = 0.32 \text{ minute} \quad \hat{\text{TC}}_2 = 21.53 \text{ minutes}$$

Suggesting a relatively high sensitivity patient with fast time-constants.

Patient SMC

The experiment conducted with this subject is quite interesting in that it allowed one to test the robustness of the algorithm when the drug concentration varied on-line. Figure (7.17) shows the corresponding EMG recording as well as the infusion rate variations. **Mark (1)** represents the time at which a 12 mg. bolus

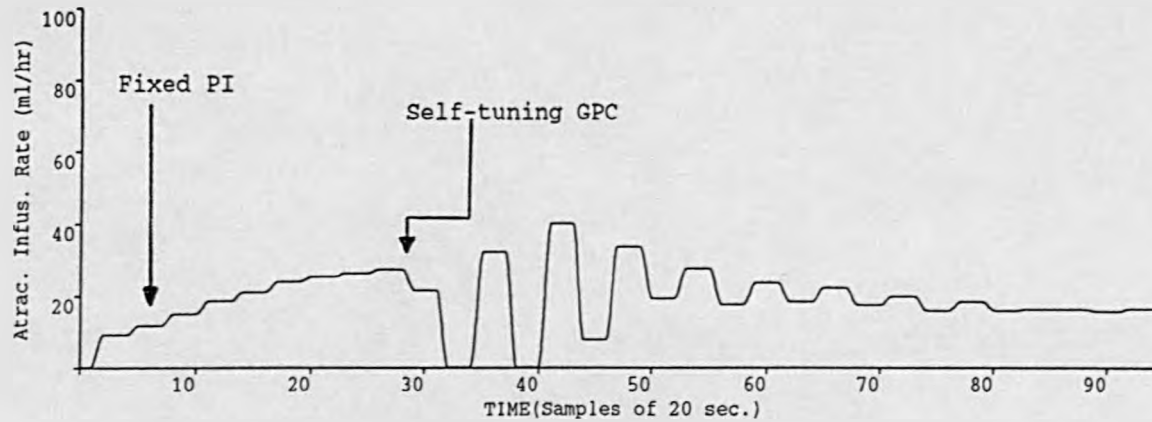
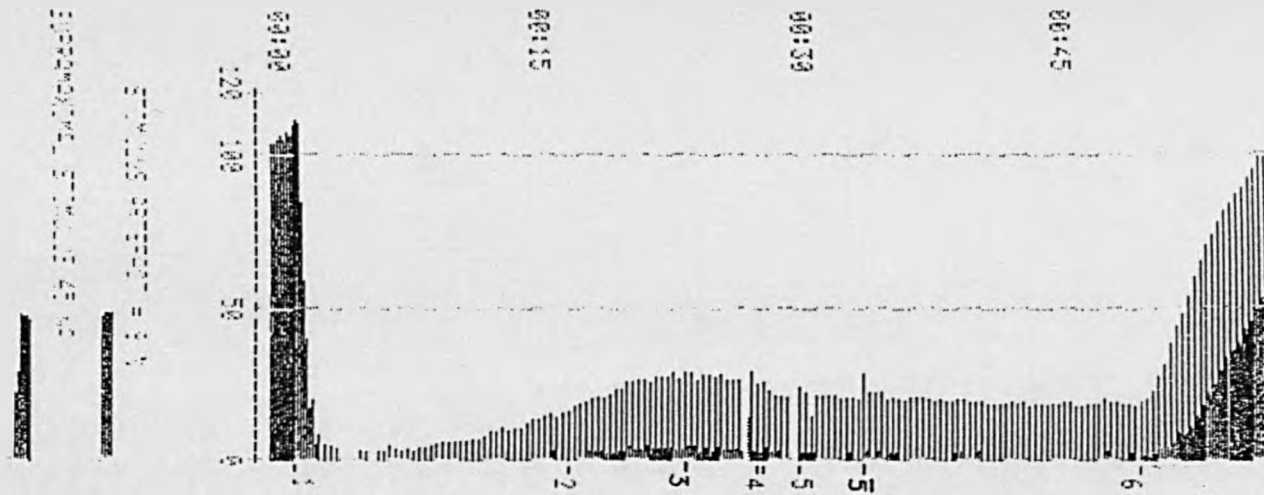


Figure 7.15. Recorded EMG and pump infusion-rate during surgery.

Patient MUU

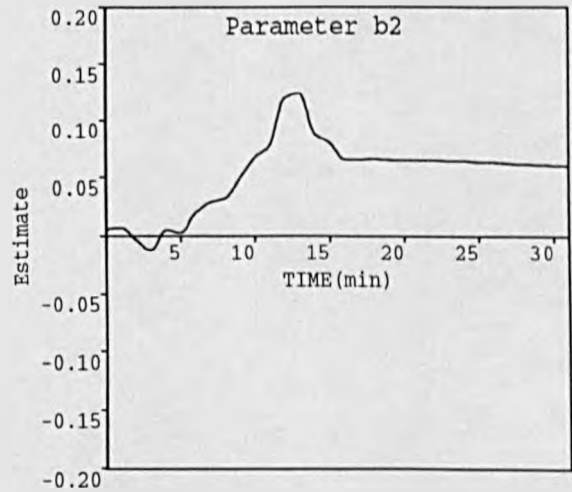
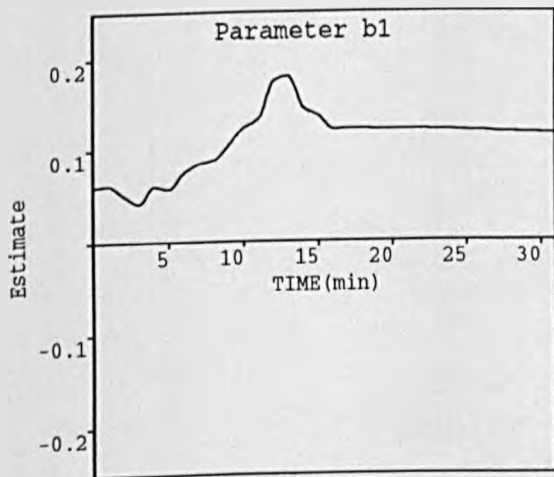
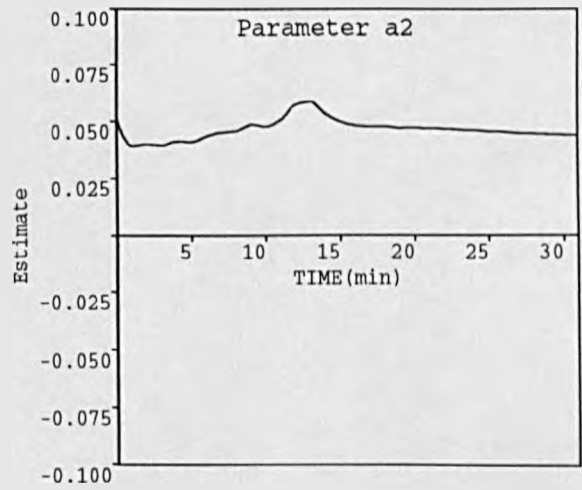
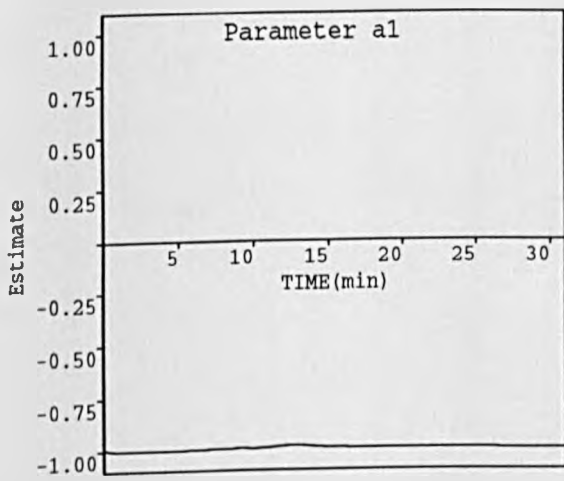


Figure 7.16. System parameter estimates corresponding to figure (7.15)

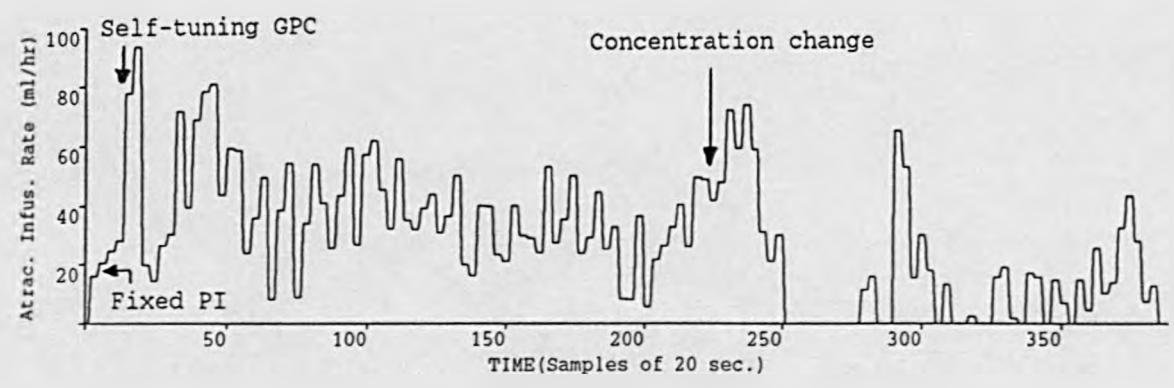


Figure 7.17. Recorded EMG and pump infusion-rate during surgery.

Patient SMC

dose of muscle relaxation drug was intravenously administered and **mark (2)** is when automatic control (PI) was initiated using a solution of the same drug diluted at $500 \mu\text{g.ml}^{-1}$. **Mark (2)** shows when the self-adaptive GPC took over (5 minutes later) with a combination of (1, 30, 1, 5) for (N_1, N_2, NU, λ) . The Atracurium concentration was doubled to 1 mg.ml^{-1} at **mark (3)**. The controller was later switched off at **mark (5)**, and the blockade reversed at **mark (6)**. The 22% overshoot induced by the PI was quickly accounted for by the GPC by generating abrupt control actions, which because of the low concentration reached a mean level of 40 ml.hr^{-1} . Control activity which was high during the first 100 samples decreasing slightly between samples 100 and 200, as a result of which the EMG level was kept steady with 2% fluctuations around the 20% target. When the change in Atracurium concentration was brought into effect at **mark (3)**, and because of the delay (definitely more than the minimum delay of 1 minute which was assumed in the model), the EMG level still assumed a 20% values for a few samples then dropped 5% below the target, while the pump tried to overcome this by driving sometimes at 0.1 ml.hr^{-1} (minimum speed) and other times at 20 ml.hr^{-1} . Figure (7.18) shows how the parameter estimates were affected by this change. As illustrated in the same figure, they did not settle at all, and this may be due to the wrong assumption of time-delay and the absence of the filter $T(z^{-1})$ to compensate for the unmodelled dynamics. In fact, at the end of the run, the estimates final values suggested a non-minimum phase system as the following values demonstrate:

$$\begin{aligned} \hat{a}_1 &= -0.9655 & \hat{a}_2 &= -0.0316 \\ \hat{b}_1 &= -0.0072 & \hat{b}_2 &= 0.0195 \end{aligned}$$

Corresponding to the following pole/zero positions in the z-plane:

$$\begin{aligned} \text{zero: } & 2.7083 \\ \text{poles: } & 0.9972 ; -0.0317 \end{aligned}$$

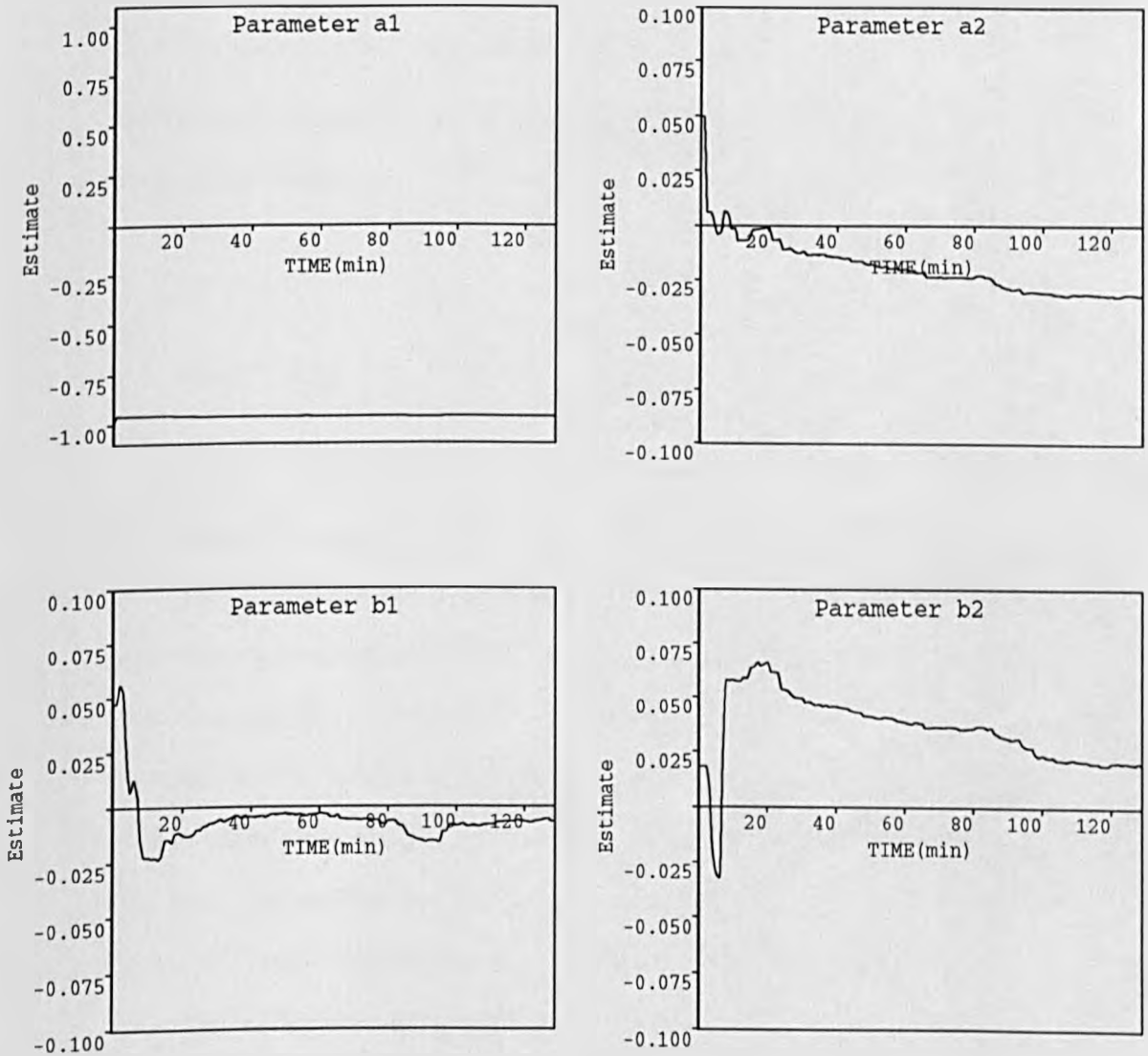


Figure 7.18. System parameter estimates corresponding to figure (7.17)

The estimated patient's open loop gain assumed the following values at the end of each of the two phases corresponding to the different concentrations:

$$\hat{G}_{\text{ain}} = 2.15 \quad \text{for concentration } 500 \mu\text{g.ml}^{-1}$$

$$\hat{G}_{\text{ain}} = 4.24 \quad \text{for concentration } 1 \text{ mg.ml}^{-1}$$

results which reflect the levels at which the pump was driving before and after the concentration change.

Patient JOD

After bolus doses of 8 mg. then 3 mg. administered at **mark (1)** and **mark (2)** respectively on the upper trace of figure (7.19), the loop was closed at **Mark (3)** where the EMG level reached approximately 28%. The PI was allowed to run for 5 minutes and produced therefore an overshoot of 12%. When the GPC took over at **mark (3)** assuming the same controller parameters as before, it was quick to reduce the overshoot by making the EMG track efficiently the 20% target. The control signal whose variations are shown on the lower trace of the same figure was good and reasonably active. Parameter estimates started to converge as soon as the GPC was in operation as figure (7.20) illustrates. At the end of the run they converged to the following values:

$$\hat{a}_1 = -0.9623 \quad \hat{a}_2 = -0.0120$$

$$\hat{b}_1 = 0.0320 \quad \hat{b}_2 = 0.0451$$

Corresponding to the following pole/zero positions in the z-plane:

$$\text{zero: } -1.4094$$

$$\text{poles: } 0.9746 ; -0.0123$$

It is worth noting that these values suggested a non-minimum phase system.

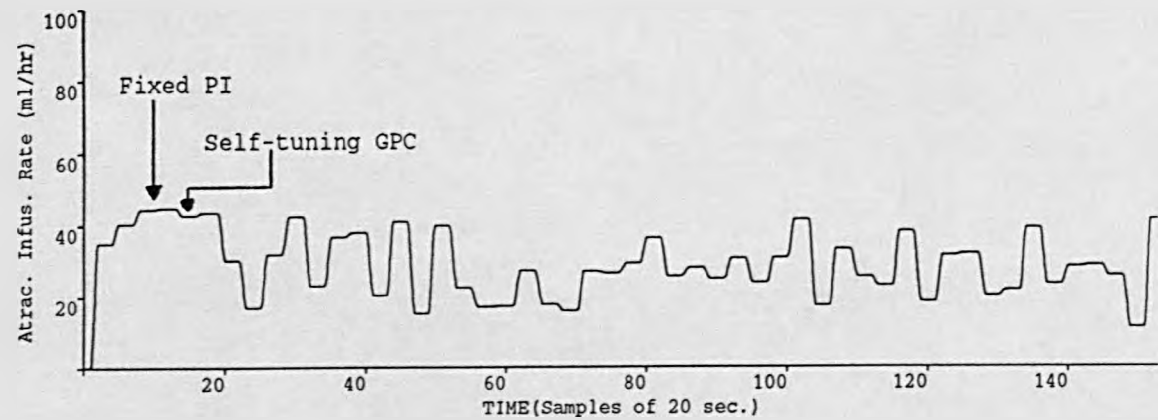


Figure 7.19. Recorded EMG and pump infusion-rate during surgery.

Patient JOD

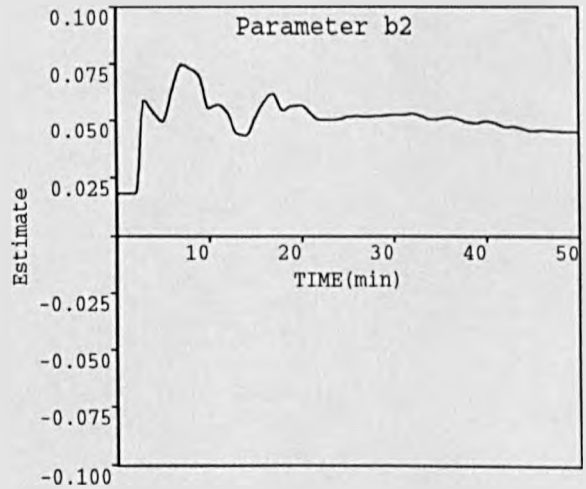
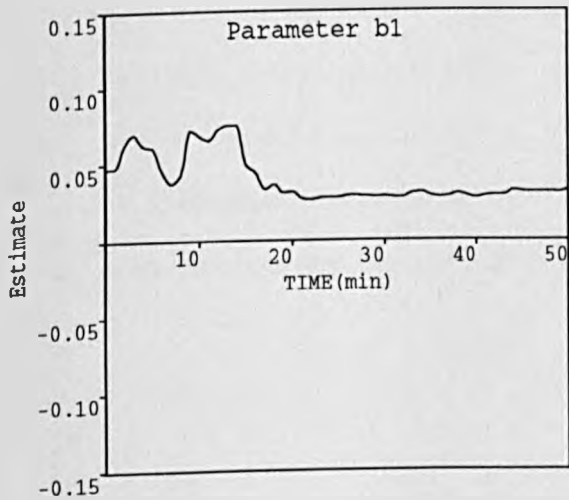
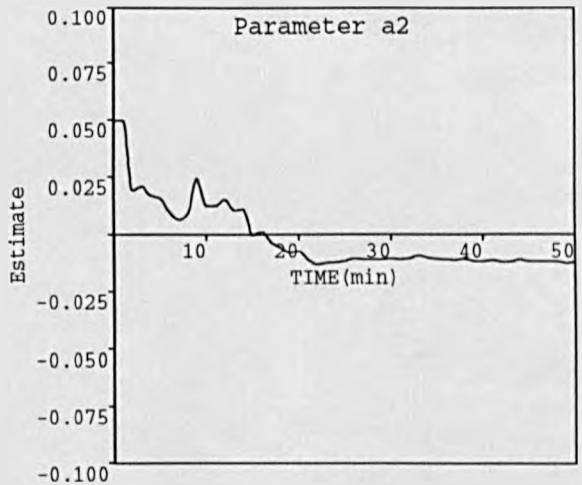
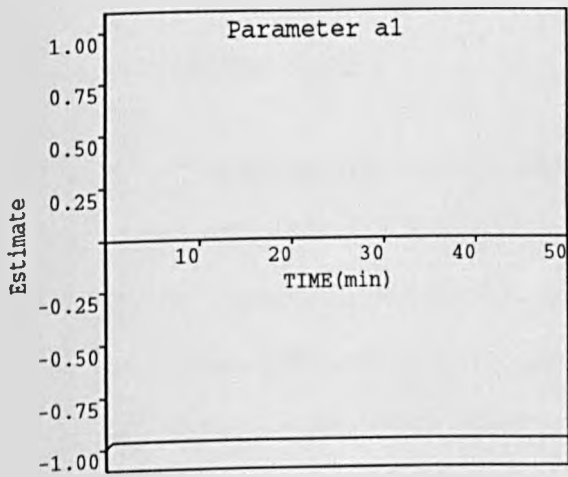


Figure 7.20. System parameter estimates corresponding to figure (7.19)

Finally, mark (4) is when the blockade was reversed.

Patient ANM

This experiment was the longest in this series of trials. The subject, a young male, underwent a 3 hour surgery requiring muscle relaxation. Mark (1) on the trace of figure (7.21) is the time at which Suxamethonium was administered before the trachea was intubated. A return to a 100% EMG level was achieved at mark (4) when a large bolus dose of muscle relaxant drug of 24 mg. was given intravenously, and this wiped out completely the EMG tracing, which only started to reappear again 12 minutes later. At mark (5) the automatic control mode was entered with the PI providing initial control for 30 minutes until mark (6) when the GPC took over with the same controller and estimation parameters as before, except that instead of assuming a minimum delay of 1 minute, the $B(z^{-1})$ polynomial structure was extended by one coefficient to absorb this value. Initial conditions for the estimates were taken to be:

$$\hat{a}_1 = -0.9927$$

$$\hat{a}_2 = 0.0496$$

$$\hat{b}_1 = 0.0$$

$$\hat{b}_2 = 0.0471$$

$$\hat{b}_3 = 0.0183$$

these were chosen to reflect the same gain, time-constants, and time-delay as in the previous case.

At mark (7) the control had to be switched off due to a lack of disk-space. Later at that stage (mark (8) and mark (9)), the anaesthetist had to resume manual con-

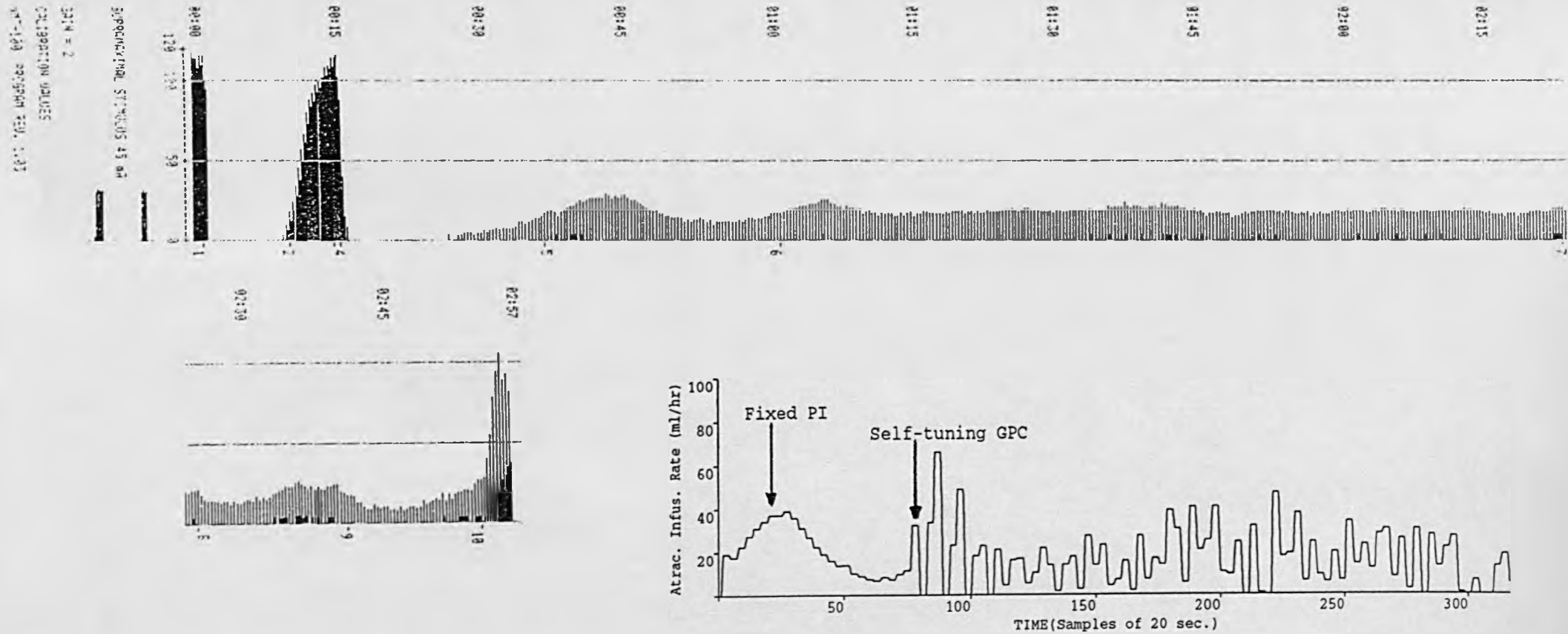


Figure 7.21. Recorded EMG and pump infusion-rate during surgery.

Patient ANM

trol with bolus doses of 10 mg. each. Mark (10) is when the blockade was reversed with Neostigmine. As shown by the same figure, the PI induced an 8% overshoot followed by a 10% undershoot of the EMG level, but was quickly eliminated as soon as the GPC took over. The EMG level was quite steady, fluctuating between 17% and 20% leading to a highly activated control signal as the lower trace of the same figure illustrates, and this despite the relatively large value of the output horizon and the non-zero control weighting sequence. Parameter estimates whose variations are shown in figure (7.22) did suggest indeed a value of time-delay greater or equal than 1 minute, since \hat{b}_1 assumed an insignificant value. These parameter estimates converged to the following final values:

$$\begin{aligned} \hat{a}_1 &= -1.0149 & \hat{a}_2 &= 0.0284 \\ \hat{b}_1 &= 0.0048 & \hat{b}_2 &= 0.0228 & \hat{b}_3 &= 0.0353 \end{aligned}$$

equivalent to a continuous second order system of the following gain and time-constants:

$$\hat{G}_{\text{ain}} = 4.66 \quad \hat{T}C_1 = 0.28 \text{ minute} \quad \hat{T}C_2 = 71.44 \text{ minutes}$$

Again these values suggest a high sensitivity patient with a slow dominant time-constant.

Patient MCB

In contrast to all 9 previous trials, a reference EMG level of 15% was targeted this time, moving therefore the operating point closer to the non-linear region. After a bolus dose given at mark (1) of figure (7.23), automatic control was switched on at mark (2) with the PI providing initial control for only 5 minutes, after which self-tuning control under the same conditions as before was initiated to counteract the overshoot induced previously. A remarkably steady

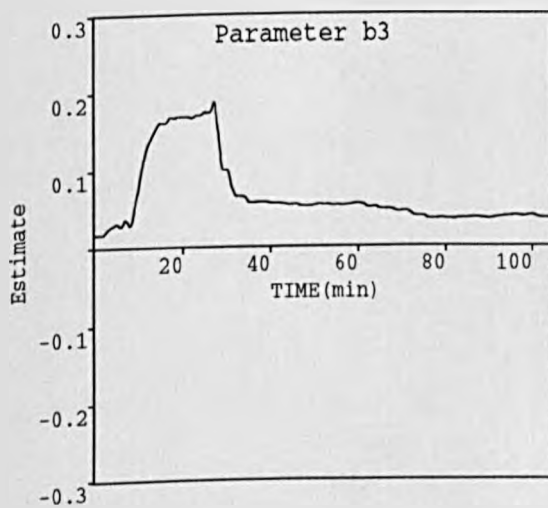
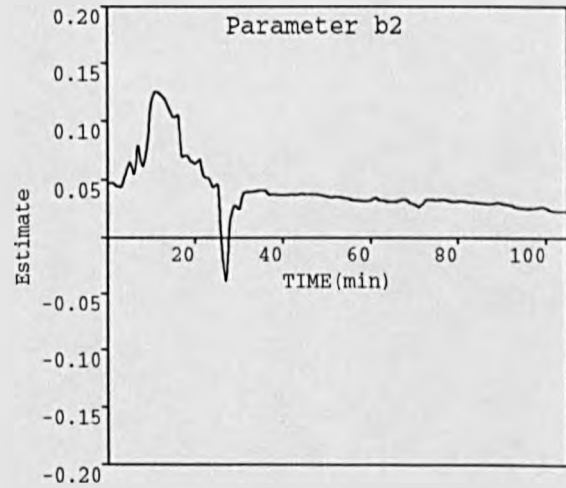
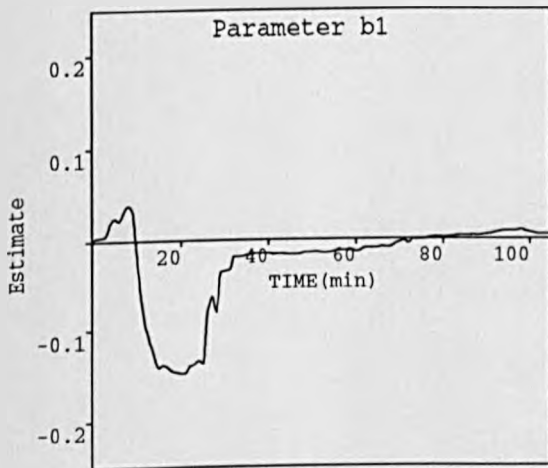
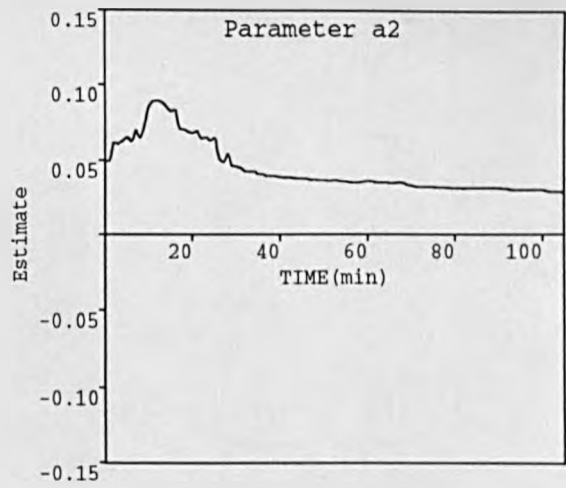
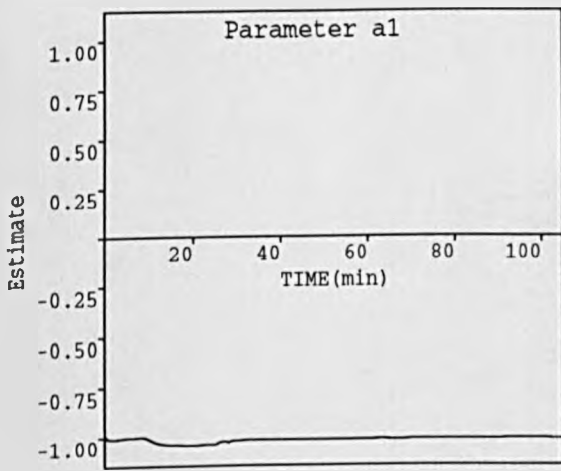


Figure 7.22. System parameter estimates corresponding to figure (7.21)

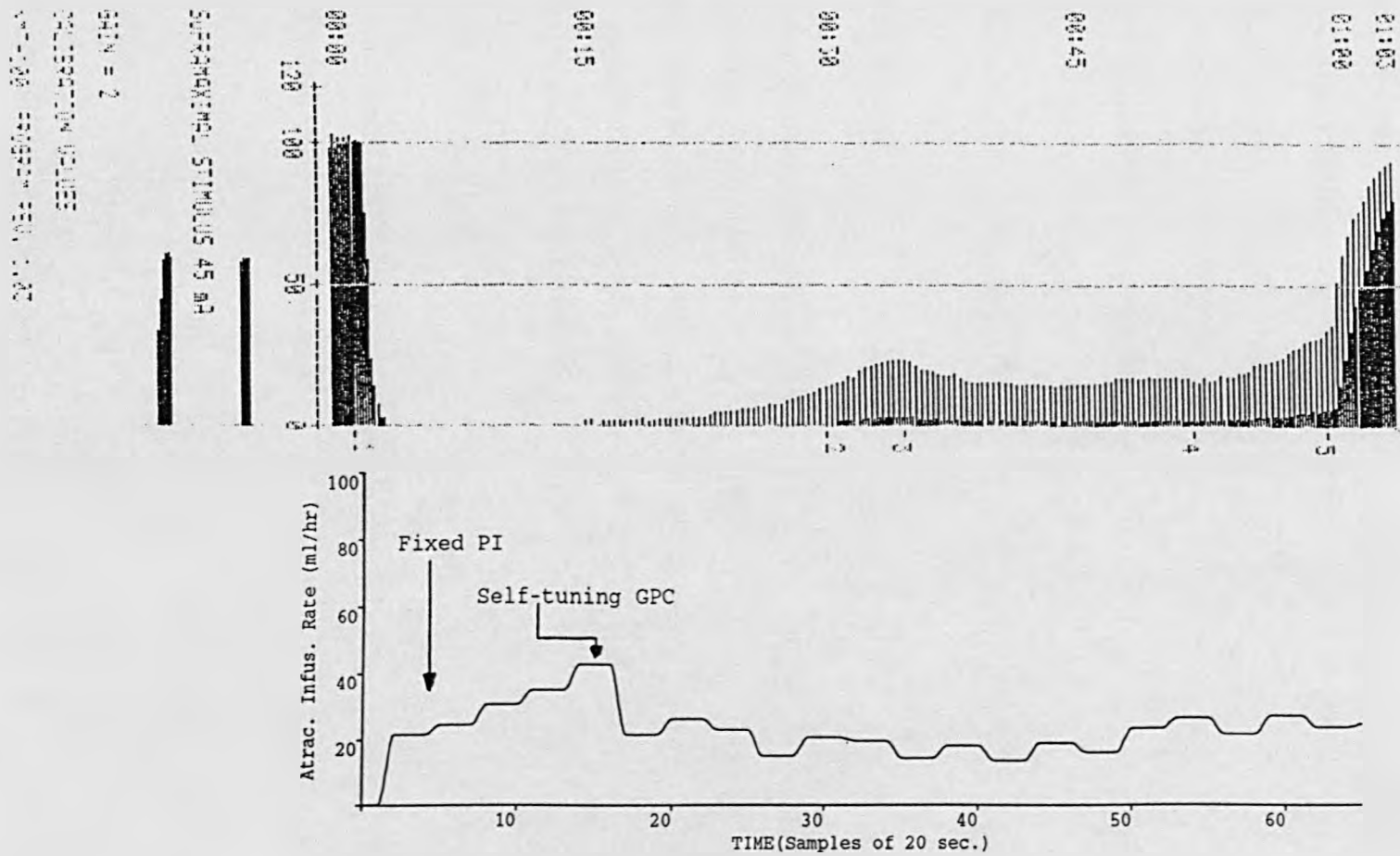


Figure 7.23. Recorded EMG and pump infusion-rate during surgery.

Patient MCB

EMG level of approximately 15% was achieved together with a well behaved control signal, until mark (4) where the controller was switched off only to reverse the blockade at mark (5). Parameter estimates varied according to the plot showed in figure (7.24) and finally converged to the following values:

$$\begin{aligned}\hat{a}_1 &= -0.9852 & \hat{a}_2 &= 0.0153 \\ \hat{b}_1 &= 0.0418 & \hat{b}_2 &= 0.0695\end{aligned}$$

equivalent to a continuous second order system of the following gain and time-constants:

$$\hat{G}_{\text{ain}} = 3.70 \quad \hat{T}C_1 = 0.24 \text{ minute} \quad \hat{T}C_2 = 32.20 \text{ minutes}$$

Analysis of the data

In order to analyse the data, three indices were used: The mean value, the standard deviation (SD), and the root mean square deviation (RMSD). These last two indices are also commonly used to give an indication about the spread of a set of values around the mean value as well as the target respectively. They are both defined by the following two formulae:

$$SD = \sqrt{\frac{1}{N} \sum (X_i - \bar{X})^2} \quad (7.14)$$

where X_i , \bar{X} , and N are the current measurement, the mean value, and the total number of points considered respectively.

and,

$$RMSD = \sqrt{\frac{1}{N} \sum (X_i - TRGT)^2} \quad (7.15)$$

here X_i is as defined previously and TRGT is the reference target.

Note that the effect of squaring the deviations before adding them is to emphasize

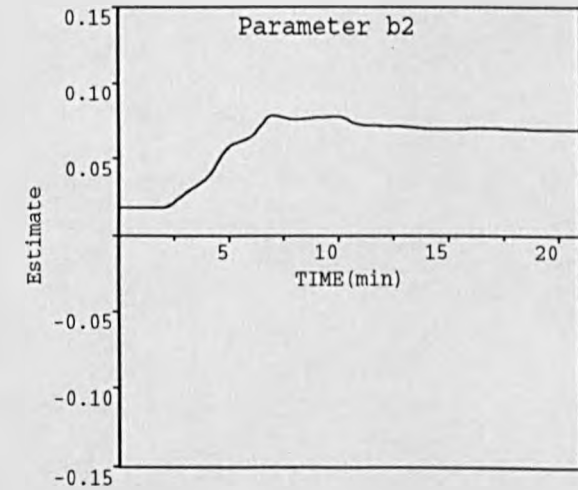
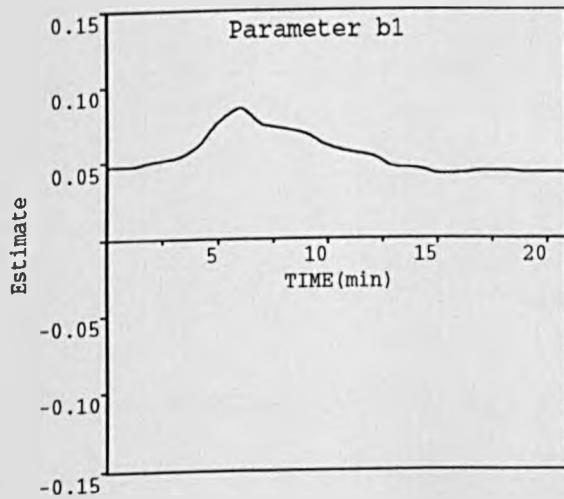
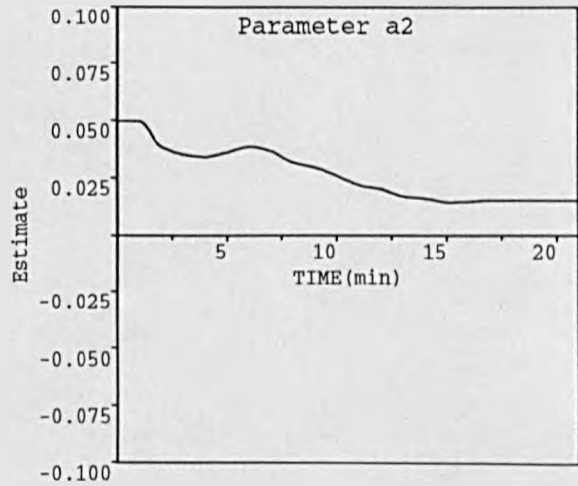
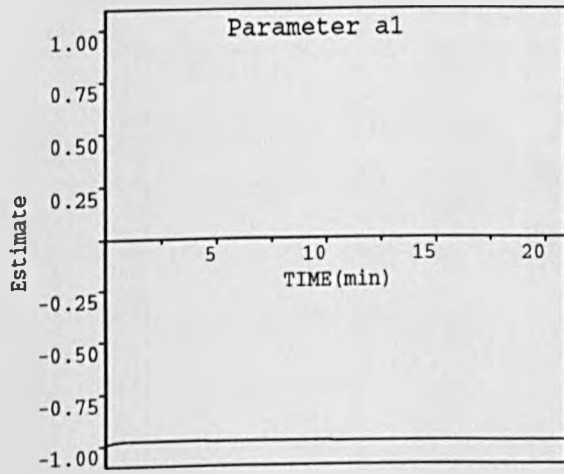


Figure 7.24. System parameter estimates corresponding to figure (7.23)

those quantities which differ most from the mean value or the reference target. Table (7.2) summarizes these values for each of the 10 patients studied.

Patients' initials	Total points	Mean T1 (%)	SD (%)	RMSD (%)
EXC*	197	17.50	4.13	4.83
MGM*	58	19.92	1.36	1.37
TXC*	134	19.43	2.56	2.63
AXM*	123	18.49	3.51	3.82
MMG*	97	21.85	1.76	2.56
MUU*	94	21.59	3.57	3.91
SMC*	387	20.14	6.89	6.89
JOD*	99	20.29	1.02	1.07
ANM*	318	18.42	3.31	3.67
MCB**	66	16.91	2.64	3.26

Table 7.2. Summary of each patient's data

(*): 20% T1 target

(**): 15% T1 target

The mean value of T1% for each patient was calculated for those trials where closed-loop infusion has been started when T1% returned to 15% after administration of the initial bolus dose of Atracurium (Patients TXC, MUU, ANM, and MCB). For those experiments where closed-loop control was initiated earlier, the mean was evaluated from the moment T1% crossed the target point for the first time. As shown in table (7.2), the mean values of T1% suggest that the degree of neuromuscular blockade obtained with the 10 patients was very satisfactory. Maximum overshoots were recorded with patients SMC (22%), ANM (8%), EXC (7%), and MUU (8%). The cause is directly linked to the wrong time at which the

closed-loop mode was entered. Indeed, with patient SMC, automatic control was operational when T1 reached 19% after recovery from the bolus, and the preloaded PI dose (P) was not large enough to shorten the stabilization period. This is probably the biggest problem facing such a controller because it is not always possible to switch to automatic control at $T1 = 15\%$ as experiments with patients EXC, MGM, MMG, JOD, and AXM have demonstrated. These patients have shown remarkable resistance to the drug, that even large bolus doses did not induce the expected drop in the EMG baseline. One solution to this problem of initial overshoot is of course to switch to the self-adaptive GPC a lot sooner as was the case for the experiment with patients JOD, and MCB which both produced a mean T1% level close to the target, i.e 20.29 (SD 1.02)% and 16.91 (SD 2.64)% respectively. Perhaps more justice would have been done to the self-adaptive GPC, as far as table (7.2) is concerned, if its corresponding values were evaluated only during the period GPC was operating, since all bigger overshoots were induced by the PI controller. Obviously, the initiation of the self-tuning GPC at an earlier stage is prone to some danger due to the fact that the estimator would not have gathered enough information about the patient to ensure adequate control, which may therefore produce a poor performance, especially if the wrong filter is used in case of incremental data being used in the measurement vector. The use of positional data in this case would be more advantageous. This has been demonstrated in the experiment with patient MCB where despite the use of an operating point close to the non-linear region (15% T1 target), the controller behaved sensibly by producing a good response and a reasonably active control. The same table also shows that the RMSD as well as the SD values were relatively low for all patients except those of patient SMC which reached a value of $SD = RMSD = \pm 6.89$, but again, these values correspond to the case where the concentration was doubled halfway through the run, meaning that the pump should

start driving at approximately half speed and waiting for the effect of the previous higher infusions to wear off. For patient EXC, the RMSD and SD values were outside the 4% range (4.83% and 4.13% respectively) due to the wrong choice of the filter $T(z^{-1})$ order, although otherwise the performance was good.

As for the infusion rate variations for the 10 patients, an analysis in which the mean Atracurium drug consumption per minute and per kilogram body weight was evaluated in each case, given the corresponding muscle relaxant drug concentration. Table (7.3) summarizes such evaluation.

Patients' initials	Total points	Mean dose ($\mu\text{g.Kg.}^{-1}.\text{min.}^{-1}$)	SD (%)
EXC*	197	6.65	2.35
MGM*	58	2.65	0.07
TXC**	134	1.57	0.28
AXM**	123	6.81	2.78
MMG*	97	6.77	1.64
MUU*	94	5.27	2.39
SMC***	387	5.38	4.43
JOD*	99	6.34	1.75
ANM*	318	4.03	2.98
MCB*	66	5.30	1.81

Table 7.3. Summary of each patient's drug consumption dose

(*) : 1 mg.ml^{-1} concentration

(**) : $500 \mu\text{g.ml}^{-1}$ concentration

(***) : Both concentrations used

As shown in the same table, the highest dose of muscle relaxant drug was

recorded with patient AXM ($6.89 \mu\text{g.Kg}^{-1}.\text{min}^{-1}$) who had a relatively low gain (1.97) adding to the fact that the closed-loop control mode was switched on at a very early stage. The lowest drug dose was that for patients TXC and MGM, where the GPC algorithm used the filter polynomial $T(z^{-1})$ which, as already seen, reduces the overall feedback gain leading to smoother control actions. The mean dose consumed by SMC was surprisingly low at $5.38 \mu\text{g.Kg}^{-1}.\text{min}^{-1}$. Despite the severe concentration change made during the trial, the algorithm performed well by administering the right amount of muscle relaxant drug. With this latter trial full valued data were used for the estimator and no filter was included to compensate for any unmodelled dynamics and reduce high frequency components. A summary of the nine patients' ($n = 9$) results is given in table (7.4) where the mean, and SD indices are displayed for the age, weight, duration of automatic control, mean drug dose consumption, the mean, RMSD, and the SD. The last experiment was excluded since the 15% target was different from the other trials.

Parameter	Mean	SD	Range
Age (Yr)	43.11	18.89	17-69
Weight (Kg.)	60.44	7.69	50-73
Automatic Control Duration (Min.)	62.33	33.04	30-130
Dose ($\mu\text{g.Kg}^{-1}.\text{min}^{-1}$)	5.05	1.80	1.57-6.81
Mean of T1 (%)	19.74	1.37	17.50-21.85
RMSD of T1 (%)	3.41	1.69	1.07-6.89
SD of T1 (%)	3.12	1.68	1.02-6.89

Table 7.4. Summary of patients' data ($n = 9$)

The value of 3.12% for the mean of standard deviation of T1 indicates that, gen-

erally, a steady level of blockade was obtained. Moreover, the fact that this value was so close to the value of the mean of the root-mean square deviation of T1 (3.41%) implies that the degree of neuromuscular blockade was close to the target. The mean value of Mean of T1% of 19.74% reinforces the argument that the individual T1% values were also close to the target. At this stage it is too soon to draw any conclusions about any existing correlation between the patient's reaction to the initial bolus and the overall control performance, as further experiments with a larger number of patients should be conducted. Suffice to say that from the three control modes currently used (manual, fixed controller, self-adaptive), the self-adaptive scheme proved more robust and efficient. Indeed, the experiment conducted with patient ANM, which clearly highlights the three phases, showed that during the manual control the anaesthetist administered a total dose of $9.13 \mu\text{g.Kg}^{-1}.\text{min}^{-1}$, whereas during the automatic control only $4.03 \mu\text{g.Kg}^{-1}.\text{min}^{-1}$ were given to the patient. The mean dose of muscle relaxant drug of $5.05 \mu\text{g.Kg}^{-1}.\text{min}^{-1}$, however, was far lower than the one obtained by the anaesthetist when using bolus doses, and most of all lower than the range recommended by the Atracurium manufacturers.

In conclusion, it could be said that the application of the self-adaptive GPC algorithm to control muscle relaxation was successful in achieving the two preset goals, i.e: in maintaining a steady level of paralysis with minimum deviation from the target, and reducing the total muscle relaxant dosage. The overall control system proved very easy to manage as most of these experiments were carried out single-handedly by an anaesthetist (A.J. Asbury). The GPC algorithm on the other hand, with its tuning knobs, allows more flexibility in the design.

Different aspects of the algorithm were exploited, although it was hoped to conduct more experiments. The one aspect that is probably the highlight of this chapter is the parameter estimation side. An approach in which full valued data for

the estimator rather than incremental ones were used was experimented and proved to give satisfactory results. Although the aspect of eliminating the offset from the data would be absent, the estimates provided were consistent and hardly biased, a problem which would have certainly occurred with incremental data and a wrong filter choice.

Summarizing the best settings for all GPC knobs would lead to a combination of (1, 20, 1, 5) for (N_1, N_2, NU, λ) if full valued data are used for the measurement vector, and a combination of (1, 10, 1, 0) for (N_1, N_2, NU, λ) together with a second order filter with slow roots of the form $T(z^{-1}) = (1 - 0.95 z^{-1})^2$ if filtered incremental data are to be fed to the estimator.

Finally, these encouraging results have provided the basis for another study in which simultaneous control of muscle relaxation and anaesthesia (unconsciousness) was considered. This is the subject of the next chapter which envisages such a scheme.

CHAPTER 8

IDENTIFICATION AND CONTROL OF NON-LINEAR MULTIVARIABLE ANAESTHETIC MODEL

8.1 INTRODUCTION

Various SISO self-adaptive techniques have been successfully applied to muscle relaxant anaesthesia in simulations and clinical trials as the previous chapters have clearly demonstrated. SISO generalized predictive control (GPC) is among these techniques. This chapter describes the extension of the previous work to the multivariable case involving simultaneous control of unconsciousness as well as muscle relaxation. The multivariable model has been elicited via a combination of literature surveys and clinical experiments conducted in hospital. The multivariable version of GPC in its basic form as well as its different extensions to include model following and observer polynomials is outlined. The strategy was then applied to the previous model assuming nominal parameter values. Further experiments in which the model parameters were chosen according to a Monte-Carlo method were also conducted. The robustness of the control strategy is investigated and the results presented and discussed.

8.2 IDENTIFICATION OF THE NON-LINEAR MULTIVARIABLE ANAESTHETIC MODEL

A number of on-line drug infusion systems in medicine have been developed in recent years, a survey of such schemes being given in (Linkens and Hacisalihzade, 1990). On-line control of neuromuscular blockade (muscle relaxation) and depth of anaesthesia (unconsciousness) have been investigated by many

researchers (Robb et al., 1988) and (Schwilden et al., 1987, 1989). Both of these areas are prime responsibilities for anaesthetists in operating theatre. As already seen, for muscle relaxation, measurements are made via evoked EMG responses obtained from supramaximal stimulation at the wrist. Resulting EMG signals at the hand are rectified and integrated giving a proportional measurement of the degree of relaxation (i.e induced paralysis). The drug used throughout this study is similar to the one previously considered, i.e Atracurium which is a modern fast acting agent suitable for continuous infusion via a motor driven syringe pump.

In contrast, depth of anaesthesia is more difficult to quantify accurately. Thus, one approach has been to merge a number of clinical signs and on-line data to produce an expert system advisor for the anaesthetist. This system called RESAC, has been developed and validated in a recent series of clinical trials (Linkens et al., 1990). In spite of the multi-sensor nature of the above approach, it appears that during the majority of operating periods when no unusual emergency conditions occur, a good indication of unconsciousness can be obtained from a single on-line monitored variable. Thus, the use of arterial blood pressure, monitored via an inflatable cuff using a Dinamap instrument, has been investigated for feedback control with simple PI strategies by Robb et al. (1988). In this case the control actuation is via a stepper motor driving the dial on a gas vaporiser. This concept forms the basis for the modelling and control aspects of unconsciousness in the following work. In particular, the drug Isoflurane has been used in these studies, it being commonly used in modern surgery.

The necessary transfer function components for the model used in these studies have been obtained in various ways. The two drugs considered in the model for human beings are Atracurium (for producing muscle relaxation) and Isoflurane (for inducing unconsciousness). The individual pathways are described in the following

sections.

8.2.1 The Atracurium Mathematical Model

- **Pharmacokinetics**

The study conducted and reported in chapter 3 allowed one to obtain the following equation:

$$\frac{X_1}{U_1} = \frac{9.94 (1 + 10.64 s)}{(1 + 3.08 s) (1 + 34.36 s)} \quad (8.1)$$

Equation (8.1) describes the pharmacokinetics of the muscle relaxation system relating to the Atracurium drug.

- **Pharmacodynamics**

Similarly, to characterize the drug effect the Hill equation is used to relate to a specific concentration giving the following expression:

$$E_{\text{eff}} = \frac{E_{\text{max}}}{1 + \frac{(0.404)^{2.98}}{X_E^{2.98}}} \quad (8.2)$$

Finally, the overall transfer function describing the Atracurium mathematical model is given by the following equation:

$$G_{11}(s) = \frac{X_E}{U_1} = \frac{K_1 e^{-\tau_1 s} (1 + T_4 s)}{(1 + T_1 s) (1 + T_2 s) (1 + T_3 s)} \quad (8.3)$$

where,

$$K_1 = 1.0$$

$$\tau_1 = 1 \text{ min.}$$

$$T_1 = 4.81 \text{ min.}$$

$$T_2 = 34.36 \text{ min.}$$

$$T_3 = 3.08 \text{ min.}$$

$$T_4 = 10.64 \text{ min.}$$

8.2.2 The Isoflurane Unconsciousness Model

Anaesthesia or unconsciousness is defined as being the state in which the body is insensitive to pain or other stimuli. There is no direct method of measuring depth of anaesthesia. Previous research work namely by Schwilden et al. (1987, 1989) and Savage et al. (1978) used quantitative EEG (electroencephalogram) analysis in human to give an indication of the anaesthetic state in humans. However, the interpretation of the tracings is a difficult and subjective task. The information proved unreliable even when interpreted by experienced staff, since the characteristic patterns are often disturbed by factors such as anoxia, surgical stimulations, and anaesthetic agents used (Breckenridge and Aitkenhead, 1983). Consequently, anaesthetists had to resort to the merger of several clinical signs such as blood pressure, respiration, etc... to obtain the closest possible indication of how lightly anaesthetised the patient is. Indeed, in a study conducted by Asbury (1990), anaesthetists were asked to give a personal rank for the relative importance of 10 clinical signs. These signs were ranked on a scale of 1 to 10 based on the mean of these personal ranks assigned to each one of them. Table (8.1) illustrates the result of such survey:

Clinical sign	Mean of raw ranks	Order of mean rank
Movement and response to surgery	7.4	1
Respiration rate	5.8	2
Heart rate	5.3	3
Low muscle tone	5.0	4
Lacrimation	4.9	5
Arterial pressure	4.84	6
Sweating	4.77	7
Pupil position	4.6	8
Pupil diameter	3.4	9
Capillary refill	2.5	10

Table 8.1. Anaesthetists' classification of the 10 clinical signs by order of importance

From these 10 clinical signs investigated, blood pressure has been used as one variable to give indication of depth of anaesthesia. Gray and Asbury (1986) describe a system that controls systolic arterial pressure (SAP). The algorithm, a simple PI controller, achieved a quality of control ranging from good to fairly poor, and in most operations the patient recovered fairly quickly. It has been concluded then from this study, that when no emergency conditions occur, blood pressure could be used to provide good indication of the patient's anaesthetic state. In fact, recent published work by Schils and coworkers (1987) used mean arterial pressure and a measure of EEG frequency to control Halothane anaesthesia in an on-off control strategy which was found to be less sensitive to parameter mismatches. It has also been argued that the lowest blood pressure that occurs normally during sleep is 15% to 20% less than the average pressure whilst awake.

Elderly and hypotensive persons kept the margin at 10%. Consequently, mean arterial pressure (MAP) is used as the second variable for the multivariable model considered throughout this study.

Off-line identification techniques such as maximum likelihood or instrumental variables methods should ideally be used to obtain an adequate and parsimonious discrete-time transfer function model of a locally linearized controllable system in adaptive control applications. Indeed, it is widely known from the literature that system identification has been possible in some biomedical applications, such as PRBS excitation of muscle relaxant drug response (Linkens et al., 1982). However, it is not always possible to apply these methods during clinical environments, partly because of ethical considerations and also because of limitations in time. Anaesthetic drugs normally have stable and slow acting responses, consequently, step and bolus responses are the most common identification procedures used by clinicians even though the signal to noise ratios are often very low. In light of the above considerations, a study was conducted by Millard et al. (1988b, 1988a), in which step response trials of each patient's response to Isoflurane were carried out before and after self-tuning control of blood pressure during surgery implementations. This was considered essential for safety reasons, because the authors used the early version of Clarke and Gawthrop's algorithm (1975) to control mean arterial blood pressure, and which was found to be sensitive to wrong time-delay assumption. In a tranquil anaesthetised state, step responses to changes in inspired concentration of Isoflurane from a vaporiser were performed. The patient's blood pressure response showed a transport delay. This pure dead-time is likely to vary slightly due to the breathing cycle of about 6 seconds. In fact, in the 55 patients studied, including 12 others in similar experiments conducted by the same author (Millard et al., 1986), dead-times in the range 16-30 seconds have

been observed. If the changes in inhaled Isoflurane concentration are small (0-5%), then the responses could be approximated to linear characteristics. However, if the changes do not fall within this range, the responses are in general non-linear and time-varying.

Thus, a first order linear model with dead-time has been adopted, having a time-constant of 1-2 minutes. The magnitude of this time-constant is long enough to absorb some inaccuracy of dead-time estimate due to breathing variations. On the other hand, in order to estimate the steady-state gain, it is assumed that a relatively sensitive patient needs 2% Isoflurane for a 30 mmHg reduction of the mean arterial pressure (Millard et al., 1988b). Therefore, the model describing variation of blood pressure to small changes in inhaled Isoflurane concentration can be written as:

$$G_{22}(s) = \frac{\Delta \text{MAP}}{U_2} = \frac{K_2 e^{-\tau_2 s}}{(1 + T_5 s)} \quad (8.4)$$

where,

$$\tau_2 = 25 \text{ seconds.}$$

$$T_5 = 2 \text{ min.}$$

$$K_2 = -15 \text{ mmHg/\%}$$

8.2.3 Interactive Component Model

- 'Atracurium to Mean Arterial Pressure' interaction

This interaction has been investigated in human beings and there seems to be small (clinically insignificant) changes in blood pressure. Most of these changes as a result of Atracurium occur because this latter has a slight ability to release Histamine. This is a very transient chemical in the blood lasting for no more than a

minute and it does not appear in every patient (Asbury, 1990) .

- 'Isoflurane to Muscle Relaxation' Interaction

In order to identify this type of interaction which is small but significant, an experiment was performed by Asbury (1990), in which a patient, a man of 47 without a kidney but having a renal transplant, had to be anaesthetised. The following gives a description of the procedure adopted.

With the patient set-up and control readings of the Dinamap as well as of the Relaxograph taken, the patient was given a dose of Atracurium of 10 mg. which completely wiped out his E.M.G tracing (figure (8.1)) which began to reappear at 20 minutes later. The infusion of Atracurium of 5 mg/hr was then commenced. This took up to some 50 minutes by which time a steady level had been achieved and this corresponding place on the trace is 1A on figure (8.2) where a step-change in Isoflurane concentration from 0-1% was introduced. At 2A on the trace of figure (8.3), the Isoflurane was switched off. Now at this stage the experiment had already taken 1 hour 35 minutes, at which time a new equilibrium was achieved. The Isoflurane was again switched on at 3A on the trace of figure (8.4), another 1% step-on. Once the changes were observed, the Isoflurane was finally switched off at 4A on the trace of figure (8.5). At 5A on the trace of the same figure the effect of Atracurium was reversed using a dose of Neostigmine and Glycopyrrolate with a satisfactory return to 100% baseline, suggesting that there has been very little drift.

In order to analyse this whole tracing, it is perhaps more interesting to divide the experiment into two main parts:

- The on-phases part (Marks 1A and 3A)

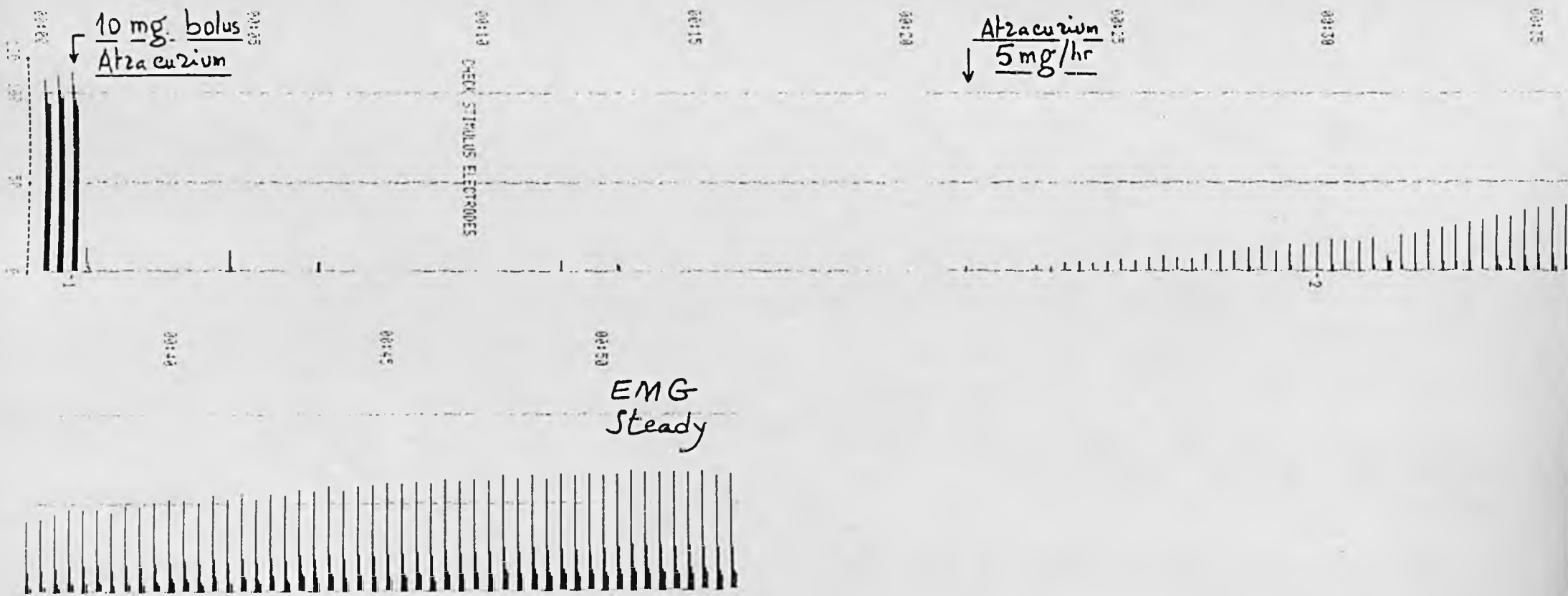


Figure 8.1. Recorded EMG corresponding to the first phase which follows the injection of the initial Atracurium bolus dose

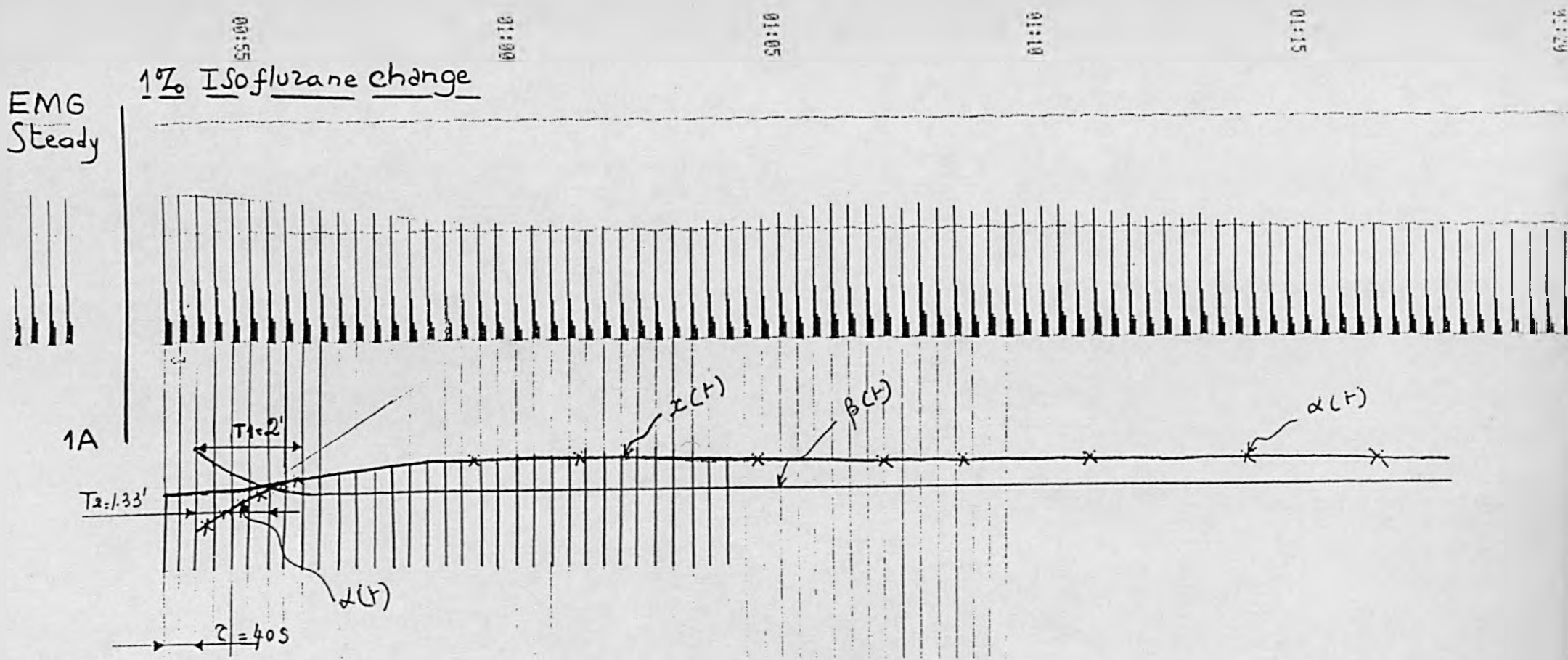


Figure 8.2. Recorded EMG corresponding to the phase which follows the introduction of a 1% Isoflurane change at mark 1A

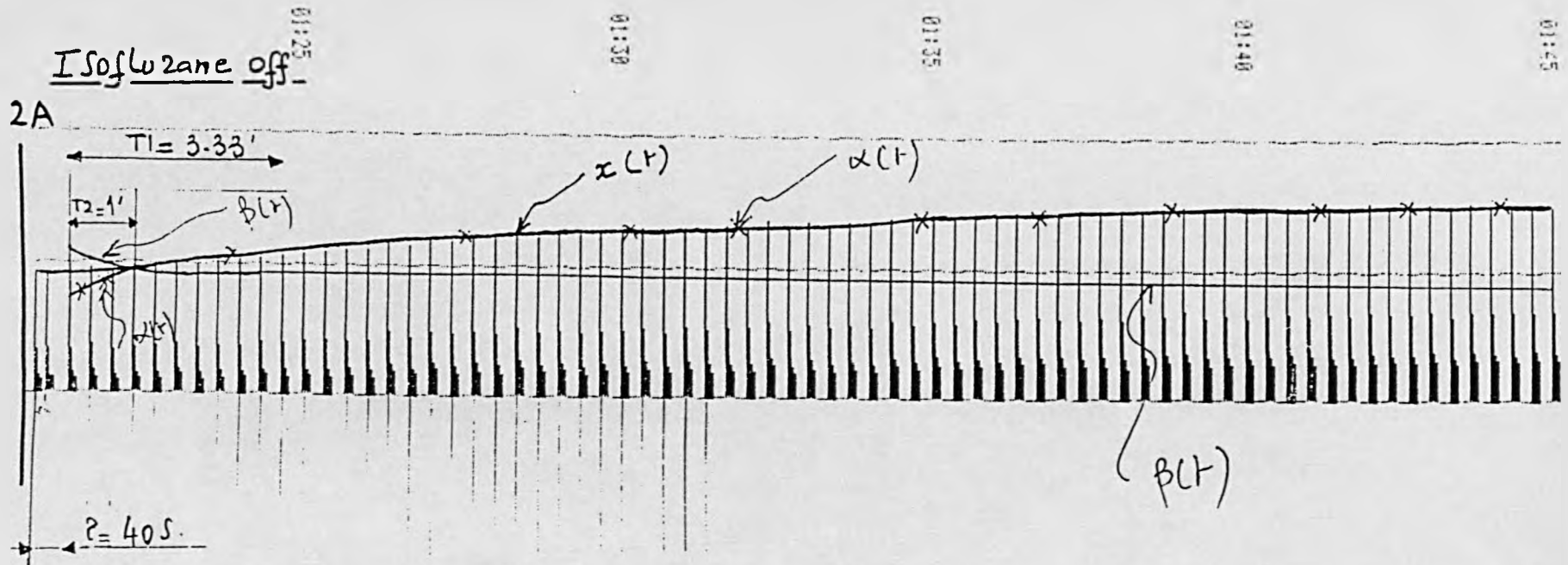


Figure 8.3. Recorded EMG when Isoflurane was switched-off at mark 2A

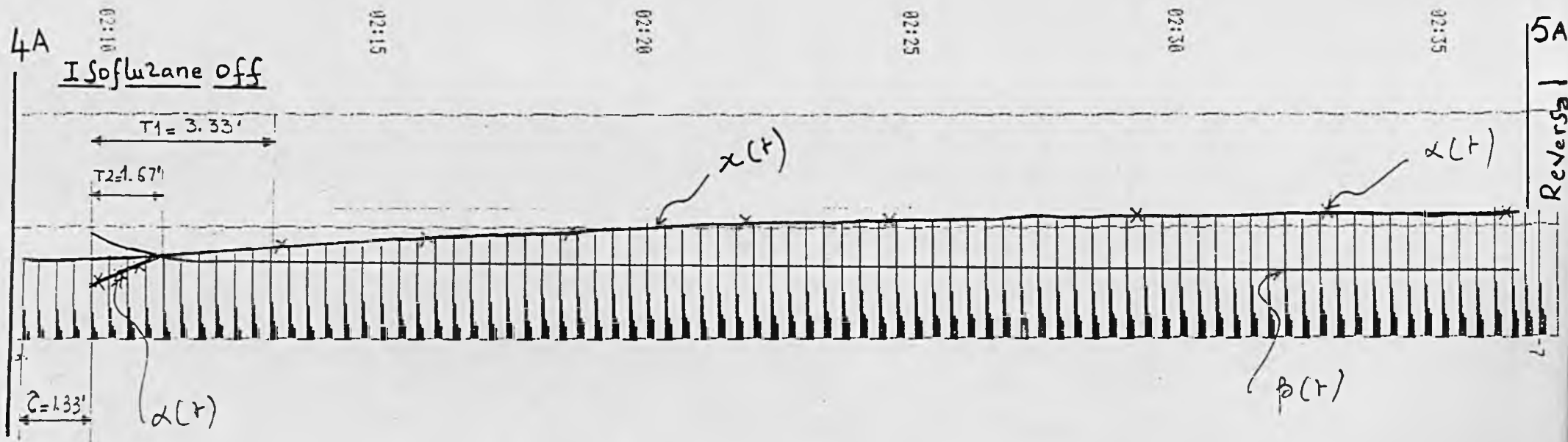


Figure 8.5. Recorded EMG when Isoflurane was switched-off at mark 4A and the blockade reversed at mark 5A

- The off-phases part (Marks 2A and 4A)

The point in proceeding in such manner will become clearer in the forthcoming sections.

a) The on-phases part

From figure (8.2) where the E.M.G signal versus time is represented, it can be seen that after 1% of Isoflurane change has been introduced, the E.M.G signal started to decline following a time-delay sequence of about 40 seconds. Moreover, if the Isoflurane change is kept within a relatively small range (as in this very case), the shape of the transient clearly suggests a second order linear model with a pure time-delay of the form:

$$G_{1on}(s) = \frac{K_{on} e^{-\tau s}}{(1 + T_{1on} s) (1 + T_{2on} s)} \quad (8.5)$$

Using the identification methods described in (Graupe, 1976), an attempt was made to evaluate the parameters in the above equation. It is however worth noting that for convenience the signal (100 - E.M.G) which is the paralysis was plotted. In order to evaluate the first time-constant T_{1on} , it is assumed that for large t 's the curve referred to by $x(t)$ on the same figure is approximated by

$$x(t) = x_{\infty} - x(t) = \text{coefficient}_1 e^{-\frac{t}{T_{1on}}} = \alpha(t)$$

where T_{1on} represents the dominant time-constant.

Drawing the tangent at this curve referred to by $\alpha(t)$ gives:

$$T_{1on} \cong 6 \text{ segments} \cong 120 \text{ seconds} = 2 \text{ minutes}$$

If the curve given by the following equation is drawn, i.e:

$$\beta(t) = x(t) - \alpha(t) = \text{coefficient}_2 e^{-\frac{t}{T_{2on}}}$$

where T_{2on} is the smallest time-constant, then drawing the tangent at the same curve leads to:

$$T_{2on} \equiv 4 \text{ segments} \equiv 80 \text{ seconds} = 1.33 \text{ minutes}$$

The final value-theorem allows one to evaluate the steady-state gain, i.e:

$$x_{\infty} = 15\%$$

Therefore,

$$K = 15\%/1\% \text{ or } K = 0.15 \text{ (normalised I/P and O/P)}$$

Hence, the identified second order model for this phase can be summarized by the following transfer function:

$$G_{1on}(s) = \frac{0.15 e^{-0.67s}}{(1 + 2 s) (1 + 1.33 s)} \quad (8.6)$$

Following the same procedure as previously for the trace starting at 3A on figure (8.4) the following transfer function was obtained:

$$G_{2on}(s) = \frac{0.33 e^{-s}}{(1 + 2.67 s) (1 + s)} \quad (8.7)$$

Taking the mean values for the two transfer functions yields:

$$G_{on}(s) = \frac{0.24 e^{-0.84s}}{(1 + 2.33 s) (1 + 1.17 s)} \quad (8.8)$$

b) The off-phases part

The point in analysing these parts of the transient where the Isoflurane was switched off after a certain equilibrium has been reached, is mainly to establish the symmetry of a possible linear model reinforcing hence its validity, and perhaps justifying the assumption of it (the model) being linear for small changes

of input.

In light of these considerations, the same procedure of section a) above was conducted using figures (8.3) and (8.5), leading to the following results:

$$G_{1\text{off}}(s) = \frac{0.31 e^{-0.67s}}{(1 + 3.33 s) (1 + s)} \quad (8.9)$$

$$G_{2\text{off}}(s) = \frac{0.28 e^{-1.33s}}{(1 + 3.33 s) (1 + 1.67 s)} \quad (8.10)$$

Taking the mean values for the two transfer functions (8.9) and (8.10) yields:

$$G_{\text{off}}(s) = \frac{0.29 e^{-s}}{(1 + 3.33 s) (1 + 1.33 s)} \quad (8.11)$$

A quick analysis of the two transfer functions above obtained could indeed suggest that the model is more or less symmetrical considering the fact that the study has been performed entirely by eye.

Hence, if an overall model describing the effect that Isoflurane has on muscle relaxation had to be drawn, mean values should be taken between the two models, thus giving:

$$G_{12}(s) = \frac{K_4 e^{-\tau_3 s}}{(1 + T_6 s) (1 + T_7 s)} \quad (8.12)$$

where,

$$K_4 = 0.27\%/%$$

$$\tau_3 = 1 \text{ minute}$$

$$T_6 = 1.25 \text{ minutes}$$

$$T_7 = 2.83 \text{ minutes}$$

Equation (8.12) represents the linear transfer function which describes the effect of the inhaled agent 'Isoflurane' on muscle relaxation during surgery.

8.2.4 The Overall Multivariable Anaesthetic Model

In light of the above identification studies, the overall linear multivariable system combining muscle relaxation together with anaesthesia (in terms of mean arterial blood pressure measurements), whose components are also illustrated in figure (8.6), can be summarized by the following equation:

$$\begin{bmatrix} \text{Paralysis} \\ \Delta \text{MAP} \end{bmatrix} = \begin{bmatrix} G_{11}(s) & G_{12}(s) \\ 0 & G_{22}(s) \end{bmatrix} \begin{bmatrix} U_1 \\ U_2 \end{bmatrix} \quad (8.13)$$

where,

$$\begin{aligned} G_{11}(s) &= \frac{1.0 e^{-s} (1 + 10.64 s)}{(1 + 3.08 s) (1 + 4.81 s) (1 + 34.36 s)} \\ G_{12}(s) &= \frac{0.27 e^{-s}}{(1 + 2.83 s) (1 + 1.25 s)} \\ G_{22}(s) &= \frac{-15.0 e^{-0.42 s}}{(1 + 2 s)} \end{aligned} \quad (8.14)$$

Finally, the overall non-linear multivariable system combining all the effects is obtained by including the non-linearity described in section 8.2.1 which involves the Atracurium drug only, since the other drug-effects are considered to reflect linear characteristics within a range already specified in sections 8.2.2 and 8.2.3.

8.3 DEVELOPMENT OF THE MULTIVARIABLE GPC CONTROLLER

8.3.1 The Basic Algorithm

Consider the m-input m-output linear discrete-time system:

$$A(z^{-1}) y(t) = z^{-k_{ij}} B_1(z^{-1}) u(t-1) + \frac{C(z^{-1}) \xi(t)}{\Delta} \quad (8.15)$$

where,

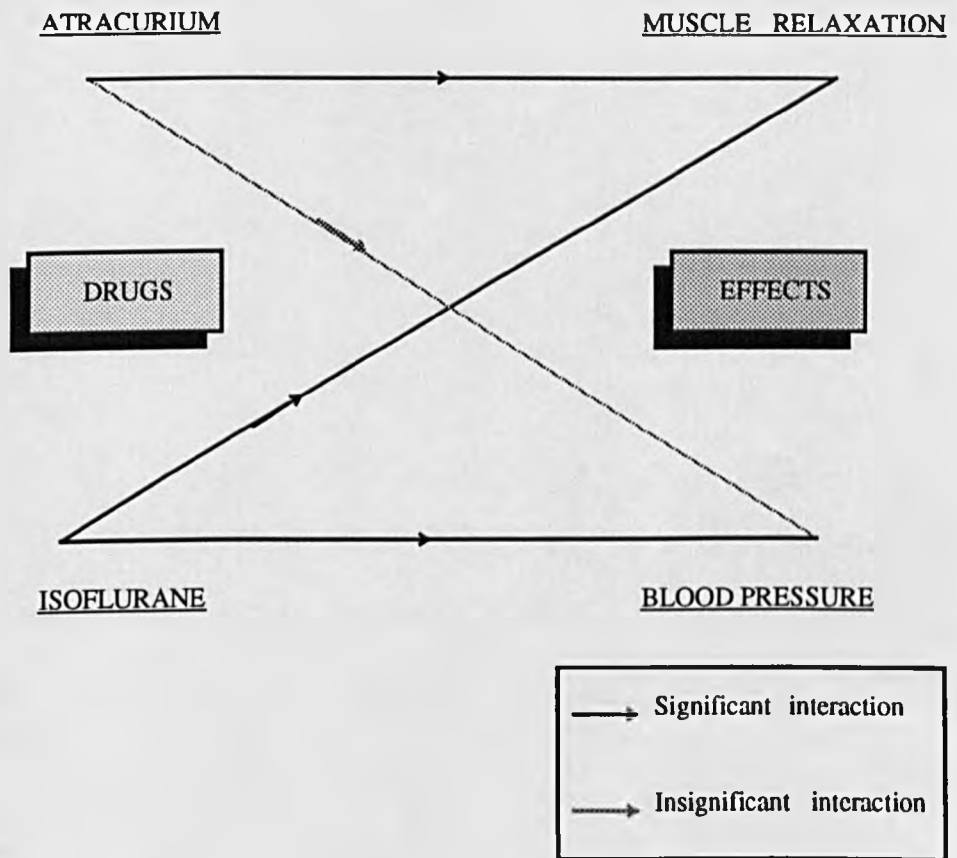


Figure 8.6. A schematic diagram representing the different components forming the multivariable anaesthetic model

$$\begin{aligned}
A(z^{-1}) &= I + A_1 z^{-1} + A_2 z^{-2} + \dots + A_n z^{-n} \\
B_1(z^{-1}) &= B_0 + B_1 z^{-1} + B_2 z^{-2} + \dots + B_m z^{-m} \\
C(z^{-1}) &= C_0 + C_1 z^{-1} + C_2 z^{-2} + \dots + C_p z^{-p} \\
y(t) &= \begin{bmatrix} y_1(t), y_2(t), \dots, y_m(t) \end{bmatrix} \\
u(t) &= \begin{bmatrix} u_1(t), u_2(t), \dots, u_m(t) \end{bmatrix} \\
\text{and } \Delta &= 1 - z^{-1}
\end{aligned}$$

$y(t)$, $u(t)$ are vectors of 'm' measurable outputs and 'm' measurable inputs respectively. k_{ij} is the integral time-delay of the ij th element of $B_1(z^{-1})$ and $\xi(t)$ denotes a vector of 'm' uncorrelated sequences of random variables with zero mean and covariance σ .

In order to derive a j -step ahead predictor of $y(t+j)$ based on equation (8.15), assume that $C(z^{-1}) = I$ with no loss of generality and consider the following Diophantine equation:

$$I = E_j A(z^{-1}) \Delta + z^{-j} F_j(z^{-1}) \quad (8.16)$$

where E_j and F_j are matrix polynomials defined given the matrix polynomial $A(z^{-1})$ and the prediction interval j . Following the same procedure as in the SISO case of chapter 5, it can be shown that the predictor becomes:

$$\begin{aligned}
\hat{y}(t+j) &= G_j \Delta u(t+j-1) + F_j(z^{-1}) y(t) \\
G_j &= E_j(z^{-1}) B(z^{-1})
\end{aligned} \quad (8.17)$$

Equation (8.17) can be rewritten as:

$$\begin{cases}
\hat{y}(t+1) = G_1 \Delta u(t) + F_1 Y(t) \\
\hat{y}(t+2) = G_2 \Delta u(t+1) + F_2 y(t) \\
\vdots \\
\hat{y}(t+N) = G_N \Delta u(t+N-1) + F_N y(t)
\end{cases} \quad (8.18)$$

Consider a cost function of the form:

$$\begin{cases} J_{GPC} = E [(Q1 + Q2)] \\ Q1 = \sum_{j=N_1}^{N_2} [y(t+j) - \omega(t+j)]^T [y(t+j) - \omega(t+j)] \\ Q2 = \sum_{j=1}^{N_2} [\Delta u(t+j-1)]^T \Lambda(j) \Delta u(t+j-1) \end{cases} \quad (8.19)$$

N_1 represents the minimum costing horizon

N_2 the maximum costing horizon

ω the future set-points usually presumed known

$\Lambda(j)$ the control weighting sequence (diagonal matrix)

Since only the first increment is considered, the solution for the minimization of the previous cost can be summarized as:

$$\bar{u} = (G^T G + \Lambda D)^{-1} G^T (\omega - f)$$

f denoting signals in equation (8.18) which are known at time 't'.

or,

$$\Delta u(t) = (I_m, 0, 0, \dots, 0) (G^T G + \Lambda D)^{-1} G^T (\omega - f) \quad (8.20)$$

where,

$$G = \begin{bmatrix} H_0 & 0 & \dots & 0 \\ H_1 & H_0 & \dots & \dots \\ H_2 & H_1 & \dots & \dots \\ H_3 & H_2 & \dots & \dots \\ \dots & \dots & \dots & \dots \\ \dots & \dots & \dots & \dots \\ \dots & \dots & \dots & \dots \\ H_{N_2-1} & H_{N_2-2} & \dots & H_0 \end{bmatrix}$$

H_0, \dots, H_{N_2-1} being submatrices of dimension $m \times m$, m being the number of chan-

nels within the matrix G which itself is of dimension $(m \times N_2) \cdot (m \times N_2)$ (Clarke et al., 1987a).

As in the SISO case the GPC approach uses the powerful assumption that after a certain horizon NU , all control increments are equal to zero, and that reduces considerably the computational burden as the matrix G becomes:

$$\bar{G} = \begin{bmatrix} H_0 & 0 & \dots & 0 \\ H_1 & H_0 & \dots & \cdot \\ H_2 & H_1 & \dots & \cdot \\ H_3 & H_2 & \dots & \cdot \\ \cdot & \cdot & \dots & \cdot \\ \cdot & \cdot & \dots & \cdot \\ \cdot & \cdot & \dots & \cdot \\ H_{N_2-1} & H_{N_2-2} & \dots & H_{N_2-NU} \end{bmatrix}$$

The above development undermines the fact that the output costing horizons N_{2m} and the control costing horizons NU_m could be different for the m different channels. If however the user judges the need to choose them to be different, some modifications have to be made to the algorithm, thus adding more flexibility and robustness to the design, especially if the process dealt with reflects a large difference in the dynamics from one channel to another. If the " m " channels have different output costing horizons $N_2(\text{Ch1}), N_2(\text{Ch2}), \dots$, then every channel would have its rows in the \bar{G} matrix equal to zero values from its own horizon+1 to the greatest horizon. If however, the " m " channels have different control horizons, $NU(\text{Ch1}), NU(\text{Ch2}), \dots$, then all the columns in the matrix \bar{G} corresponding to the associated control increments would be made equal to zero and taken out from the matrix to avoid singularity.

Finally for fine tuning, Λ , the control weighting sequence, can be used to reduce control activity and improve robustness. A suitable form for Λ is:

$$\Lambda = \lambda \Sigma G^T.G$$

where λ can take values between 0.0 and 1.0. If a value of 1.0 is used for instance, then the term $(G^T.G + \Lambda)^{-1}$ would have $\frac{1}{2}$ as an external coefficient halving therefore the control activity.

8.3.2 Inclusion of the Model-Following Polynomial $P(z^{-1})$

For this purpose let us consider the auxiliary output $\Psi(t)$ such that:

$$\begin{aligned}\Psi(t) &= P(z^{-1}) y(t) \\ P(z^{-1}) &= P_N(z^{-1}) (P_D(z^{-1}))^{-1}\end{aligned}\quad (8.21)$$

The controller minimizes therefore the following cost function which is in fact the expectation subject to data available at time 't'.

$$J(N_1, N_2) = \sum_{j=N_1}^{j=N_2} [\Psi(t+j) - \omega(t+j)]^2 + \sum_{j=1}^{j=N_2} \Lambda(j) (\Delta u(t+j-1))^2 \quad (8.22)$$

In this case the following Diophantine equation is considered:

$$P_N(z^{-1}) (P_D(z))^{-1} = E_j A(z^{-1}) \Delta + z^{-j} F_j (P_D(z^{-1}))^{-1} \quad j=1,2,\dots \quad (8.23)$$

It can be shown that this reduces to the following system of two equations:

$$\begin{cases} \Psi(t+j) = G_j(z^{-1}) \Delta u(t+j-1) + F_j(z^{-1}) (P_D(z^{-1}))^{-1} y(t) \\ G_j(z^{-1}) = E_j(z^{-1}) B(z^{-1}) \end{cases} \quad (8.24)$$

Following the same procedure as in the previous section the operation of minimization results in the projected control increment vector of the form:

$$\begin{cases} \bar{u} = (G^T G + \Lambda I)^{-1} G^T (\omega - ff) \\ u(t) = u(t-1) + g^T (\omega - ff) \end{cases} \quad (8.25)$$

where ff denotes signals in equation (8.24) known at time t , and g^T is the 'm'

rows of the matrix $(G^T G + \Lambda I)^{-1} G^T$.

Finally, it is worth noting at this stage that, as in the SISO case, and in process control $P(z^{-1})$ could be interpreted as being a model-reference polynomial which could penalize the overshoot, or reject a disturbance. It is particularly helpful when the value of NU is greater than 1 which causes the control signal to be highly active. The use of $P(z^{-1})$ affects both the set-point response as well as the disturbance rejection properties of the process under consideration.

8.3.3 Inclusion of the Observer Polynomial $T(z^{-1})$

Following the same procedure adopted in the previous sections, consider the following Diophantine equation:

$$T(z^{-1}) = E_j A \Delta + z^{-j} F_j \quad (8.26)$$

$T(z^{-1})$ defined as a polynomial in the backward shift z^{-1} of degree "s" and of the form:

$$T(z^{-1}) = I + T_1 z^{-1} + T_2 z^{-2} + \dots + T_s z^{-s}$$

The resulting prediction-equations can be summarized as follows:

$$\begin{aligned} y(t+j) &= T^{-1} [G_j \Delta u(t+j-1) + F_j y(t)] + T^{-1} E_j x(t+j) \\ G_j &= E_j B \end{aligned} \quad (8.27)$$

For the controller to be optimal, the residual $T^{-1} E_j x(t+j)$ must be orthogonal to data at time 't', suggesting that T , E_j , and $x(t+j)$ are uncorrelated which is not always the case, leading therefore, to sub-optimal predictions. However, the choice of T as diagonal and with identical elements in each row implies commutativity of the product of matrices in equation (8.27) reducing considerably the computational burden. The following set of prediction equations is finally obtained:

$$\begin{aligned}
y(t+j) &= G_j \Delta u^f(t+j-1) + F_j y^f(t) \\
y^f(t) &= T^{-1} y(t) \\
u^f(t) &= T^{-1} u(t)
\end{aligned} \tag{8.28}$$

Because the minimization of the cost function is in terms of Δu and not Δu^f , the following equation is considered:

$$G_j = G'_j T + z^{-j} \Gamma_j \tag{8.29}$$

where the coefficients of G'_j are equivalent to those of G_j when $T(z^{-1}) = I$. Consequently, equation (8.28) could be rewritten as:

$$y(t+j) = G'_j \Delta u(t+j-1) + z^{-j} \Gamma \Delta u^f(t+j-1) + F_j y^f(t) \tag{8.30}$$

The minimization procedure follows the same steps as in the previous sections. It is however worth noting that in contrast to the use of $P(z^{-1})$, $T(z^{-1})$ affects only the disturbance rejection properties of the system considered and offers the advantage of the data being filtered for the estimator eliminating hence any high frequency components.

Finally, in order to achieve more robustness, $P(z^{-1})$ and $T(z^{-1})$ could be combined to be used simultaneously (Clarke and Robinson, 1991). In this case, the Diophantine equation to be considered and the prediction equations obtained will be of the form:

$$\begin{aligned}
TP &= E_j A \Delta + z^{-j} F_j P_D^{-1} \\
\Psi &= G_j \Delta u^f(t) + F_j P_D^{-1} y^f(t)
\end{aligned} \tag{8.31}$$

It is worth noting that the solution of the Diophantine equation follows the same steps outlined previously (see chapter 5).

Note on the Process Model Representation

Modelling of multivariable system dynamics is usually expressed in terms of

a set of ordinary differential equations which can be translated into the state-space form as:

$$\begin{cases} \dot{\mathbf{x}}(t) = \mathbf{A} \mathbf{x}(t) + \mathbf{B} \mathbf{u}\mathbf{z}(t-\tau_{ij}) \\ \mathbf{y}(t) = \mathbf{C} \mathbf{x}(t) + \mathbf{D} \mathbf{u}\mathbf{z}(t) \end{cases} \quad (8.32)$$

Where $\mathbf{x}(t)$, $\mathbf{u}\mathbf{z}(t)$, and $\mathbf{y}(t)$ are $(n \times 1)$, $(r \times 1)$ and $(m \times 1)$ vectors representing the state, the input and the output variables respectively. \mathbf{A} , \mathbf{B} , \mathbf{C} and \mathbf{D} are matrices characterizing the system dynamics, and τ_{ij} the pure time-delay for the ij th element of \mathbf{B} .

The Laplace transforms of the above system is given by:

$$\begin{cases} s \mathbf{X}(s) - \mathbf{x}(0) = \mathbf{A} \mathbf{X}(s) + e^{-\tau_{ij}s} \mathbf{B} \mathbf{U}\mathbf{Z}(s) \\ \mathbf{Y}(s) = \mathbf{C} \mathbf{X}(s) + \mathbf{D} \mathbf{U}\mathbf{Z}(s) \end{cases} \quad (8.33)$$

Assuming zero initial conditions and rearranging to solve for $\mathbf{X}(s)$ yields:

$$\begin{cases} \mathbf{Y}(s) = \mathbf{G}(s) \mathbf{U}\mathbf{Z}(s) \\ \mathbf{G}(s) = \mathbf{C} [s \mathbf{I}_n - \mathbf{A}]^{-1} \mathbf{B} e^{-\tau_{ij}s} + \mathbf{D} \end{cases} \quad (8.34)$$

The continuous-time state-space equations of system (8.33) have an equivalent time-representation which is generally given by:

$$\begin{cases} \mathbf{x}[(t+1)h] = \Phi \mathbf{x}(ht) + \Delta \mathbf{u}\mathbf{z}[(t-k_{ij})h] \\ \mathbf{y}(ht) = \mathbf{H} \mathbf{x}(ht) + \mathbf{L} \mathbf{u}\mathbf{z}(ht) \end{cases} \quad (8.35)$$

Where h is the sampling time and t is the time index $t = 0, 1, 2, \dots$. The matrices Φ and Δ can be evaluated using discrete integration of the continuous-time equations expressed in system (8.33) or using Laplace transforms. Using the z operator on system equations (8.35) and dropping h for simplicity's sake leads to:

$$\begin{cases} \mathbf{x}(t) = [z \mathbf{I}_n - \Phi]^{-1} z^{k_{ij}} \mathbf{u}\mathbf{z}(t) \\ \mathbf{y}(t) = \mathbf{H} \mathbf{x}(t) + \mathbf{L} \mathbf{u}\mathbf{z}(t) \end{cases} \quad (8.36)$$

Substituting one equation into another in the above system results in the following equation:

$$\begin{cases} y(t) = G(z^{-1}) uz(t) \\ G(z^{-1}) = H [z I_n - \Phi]^{-1} \Delta z^{-k_{ij}} + L \end{cases} \quad (8.37)$$

Equation (8.37) is the sampled-data system equivalent to the Laplace transforms relation equation (8.34). Therefore the polynomial transfer function matrix $G(z^{-1})$ can be derived directly from $G(s)$.

For each element $G(s)$, the corresponding function of z is given by:

$$G_{ij}(z^{-1}) = Z \left\{ \frac{(1-e^{-sh}) G_{ij}(s)}{s} \right\} \quad (8.38)$$

Where $\frac{1-e^{-sh}}{s}$ is the the transfer function of the zero-order hold which is the most commonly used as data extrapolator. The polynomial transfer function matrix can be written as:

$$G(z^{-1}) = \begin{bmatrix} \frac{G_{n_{11}}}{G_{d_{11}}} & \cdots & \frac{G_{n_{1r}}}{G_{d_{1r}}} \\ \cdot & \cdot & \cdot \\ \cdot & \cdot & \cdot \\ \cdot & \cdot & \cdot \\ \frac{G_{n_{m1}}}{G_{d_{m1}}} & \cdots & \frac{G_{n_{mr}}}{G_{d_{mr}}} \end{bmatrix} \quad (8.39)$$

Reducing these polynomial fractions into their common denominator row by row leads to the following:

$$G'_{n_{ij}}(z^{-1}) = G_{n_{ij}} \times \prod_{\substack{k=1 \\ k \neq j}}^r G_{d_{ik}}(z^{-1}) \quad \text{for } i=1, \dots, m$$

$$G'_{d_{ii}}(z^{-1}) = \prod_{k=1}^m G_{d_{ik}}(z^{-1}) \quad \text{for } k=1, \dots, m$$

Using these equations, the transfer function matrix $G(z^{-1})$ can be written in terms of $G_n(z^{-1})$ and $G_d(z^{-1})$ as:

$$G_n(z^{-1}) = \begin{bmatrix} G'_{n_{11}} & \dots & G'_{n_{1r}} \\ \vdots & \ddots & \vdots \\ G'_{n_{m1}} & \dots & G'_{n_{mr}} \end{bmatrix} \quad \text{and} \quad G_d(z^{-1}) = \begin{bmatrix} \frac{1}{G'd_{11}} & 0 & 0 & 0 \\ 0 & \frac{1}{G'd_{22}} & \cdot & \cdot \\ \cdot & \cdot & \cdot & \cdot \\ 0 & 0 & 0 & \frac{1}{G'd_{mm}} \end{bmatrix}$$

Consider now partitioning the input vector $uz(t)$ into $(mx1)$ vector $u(t)$, and $(mx1)$ vector $\xi(t)$ of random variables, such that:

$$G_n(z^{-1}) = [z^{-k_{ij}} B(z^{-1}) C(z^{-1})] \begin{bmatrix} u(t) \\ \Phi(t) \end{bmatrix}$$

$$\text{and} \quad A(z^{-1}) = G_d(z^{-1})$$

Therefore system equations (8.37) can be written as:

$$A(z^{-1}) y(t) = z^{-k_{ij}} B(z^{-1}) u(t) + C(z^{-1}) \xi(t) \quad (8.40)$$

or including the Δ operator, equation (8.40) becomes:

$$A(z^{-1}) \Delta y(t) = z^{-k_{ij}} B(z^{-1}) \Delta u(t) + C(z^{-1}) \xi(t) \quad (8.41)$$

$A(z^{-1})$ and $C(z^{-1})$ are diagonal matrices as it has been established. Details on the estimation routine are given in the appendix B.

Finally, as pointed out earlier this representation is typical of many industrial processes, although additional interactions between different outputs could in fact be a possibility.

8.4 SIMULATION RESULTS

8.4.1 Simulation Studies Using Nominal Parameter Values

Different stages of the work involved the simulation of the model described in section 8.2. using fourth order Runge-Kutta method with a fixed step integration interval of 0.1 and a sampling interval of 1 minute. Command signals of 80% then 70% for relaxation, and 110 mmHg then 120 mmHg for blood pressure were assumed throughout. Initial conditions were 0% relaxation and 140 mmHg mean arterial pressure. During the first 25 samples, initial control was provided by the self-tuner itself but with fixed parameter estimates obtained from the nominal linear model. The input signal was clipped between 0 and 1.0 for Atracurium drug input, and between 0% and 5% for the Isoflurane input. For parameter estimation a UDU factorization method (Bierman, 1977) was used on incremental data, with an initial covariance matrix and forgetting factor given by:

$$P = 10^2.I \quad , \quad \rho = 0.995$$

A discrete multivariable model of 5 diagonal A's and 6 B's was estimated with an assumed time-delay of 1 sample. The experiments were conducted in 6 phases. Phase 1 to 4 reflect the basic algorithm, in contrast to phase 5 and 6 which are concerned with the extended algorithm using respectively the model following $P(z^{-1})$ and the observer polynomial $T(z^{-1})$.

Phase 1

Effect of The Output Horizon N_2			
Fig.Nbr	N_1	N_2	NU
8.7	1	10	1

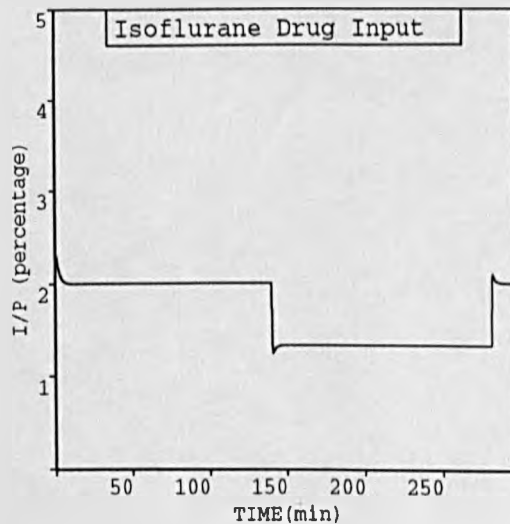
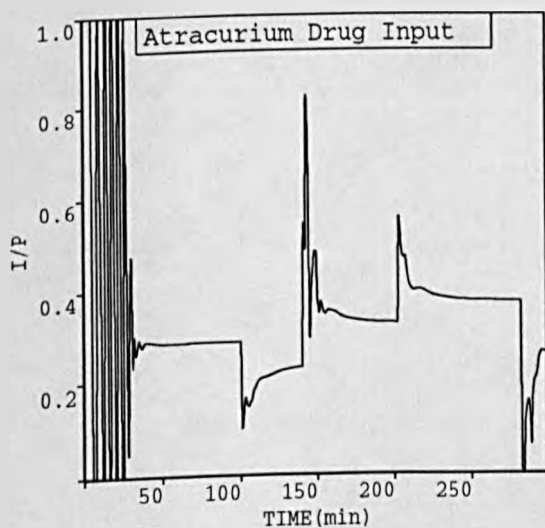
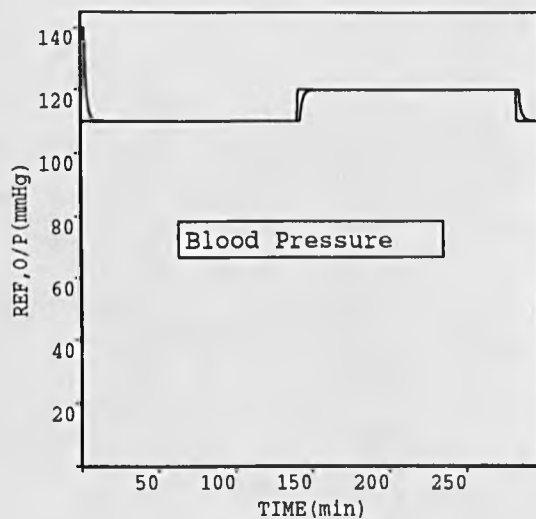
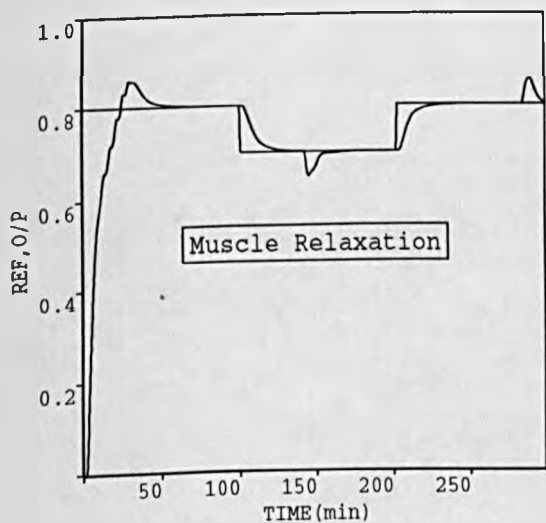


Figure 8.7. Closed-loop responses of the multivariable anaesthetic model under basic GPC algorithm with ; $N_1=1$; $N_2=10$; $NU=1$

Phase 2

Effect of The Control Horizon NU			
Fig.Nbr	N_1	N_2	NU
8.8	1	10	2

Phase 3

Effect of Different Horizons N_2 &NU					
Fig.Nbr	N_1	$N_2(\text{Ch1})$	$N_2(\text{Ch2})$	NU(Ch1)	NU(Ch2)
8.9	1	10	20	1	2

Phase 4

Effect of The Control Weighting λ				
Fig.Nbr	N_1	N_2	NU	λ
8.10	1	10	2	1

Phase 5

Effect of The Model-Following Polynomial $P(z^{-1})$					
Fig.Nbr	N_1	N_2	NU	$P_1(z^{-1})$	$P_2(z^{-1})$
8.11	1	10	2	$\frac{1.0-0.9z^{-1}}{0.1}$	$\frac{1.0-0.9z^{-1}}{0.1}$

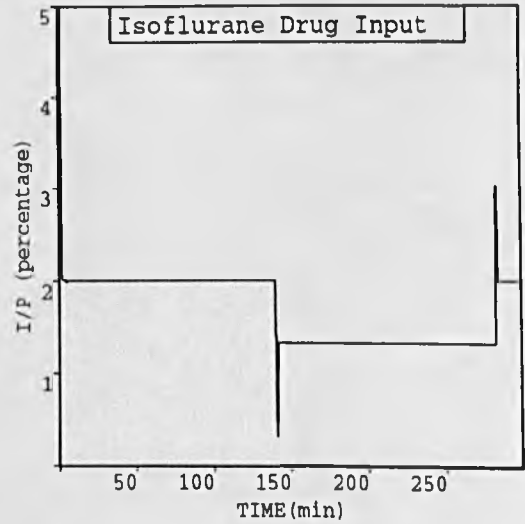
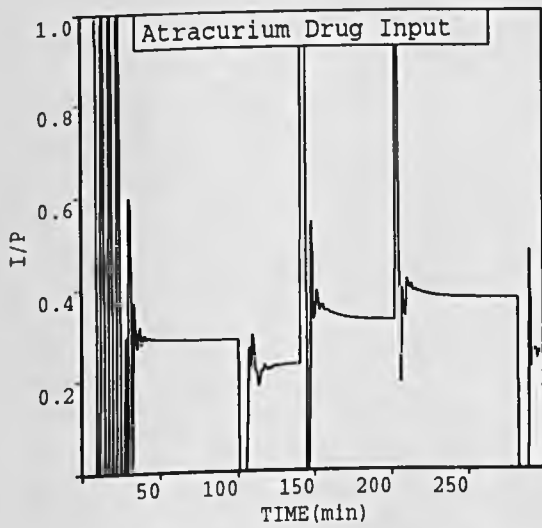
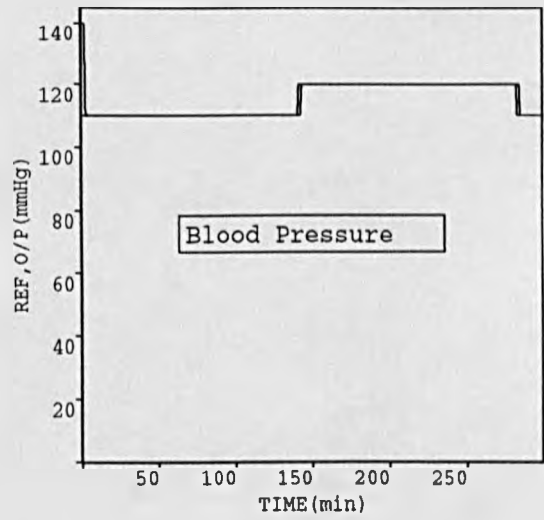
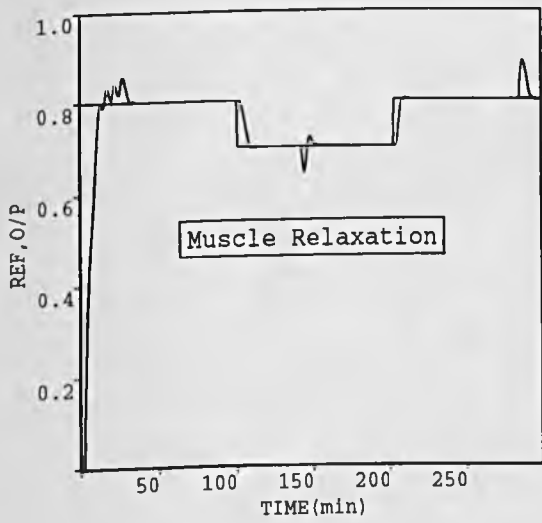


Figure 8.8. Closed-loop responses of the multivariable anaesthetic model under basic GPC algorithm with ; $N_1=1$; $N_2=10$; $NU=2$

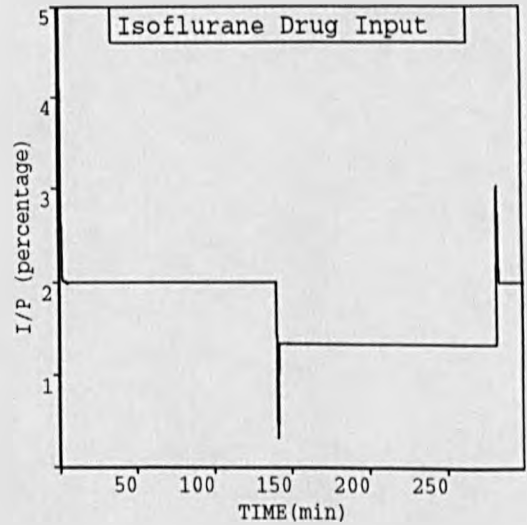
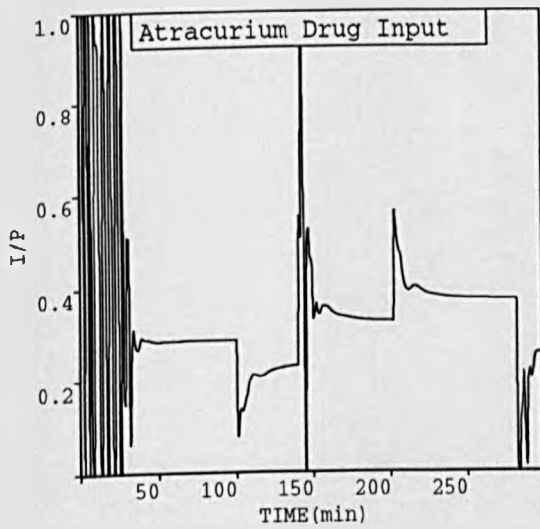
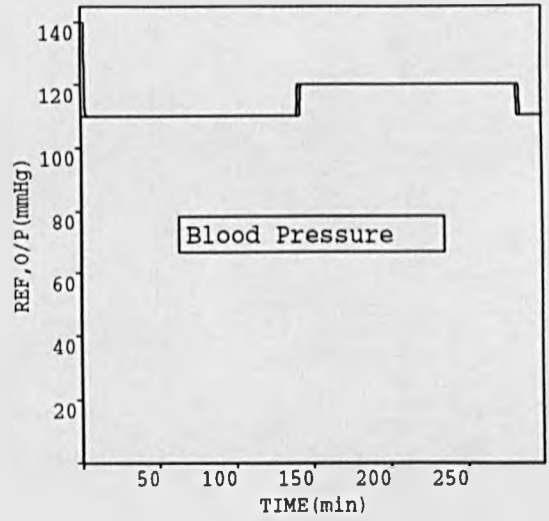
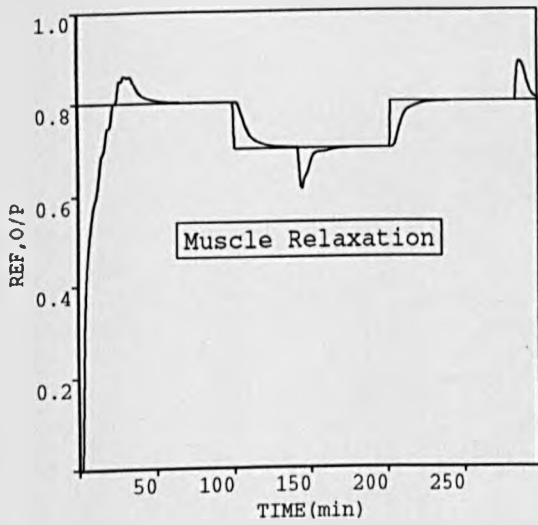


Figure 8.9. Investigation of differential channel parameters ; $N_1=1$; $N_2(\text{Ch1})=10$;
 $N_2(\text{Ch2})=20$; $\text{NU}(\text{Ch1})=1$; $\text{NU}(\text{Ch2})=2$

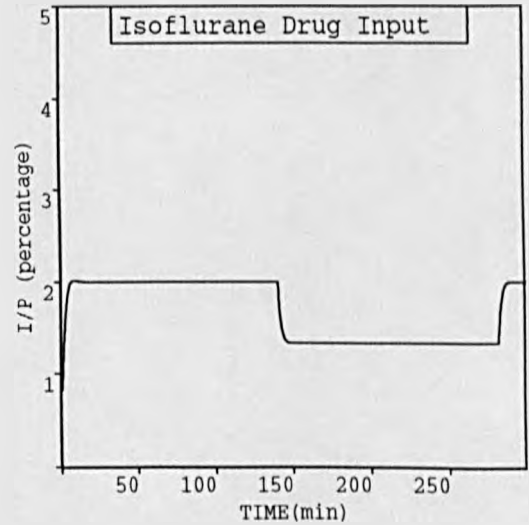
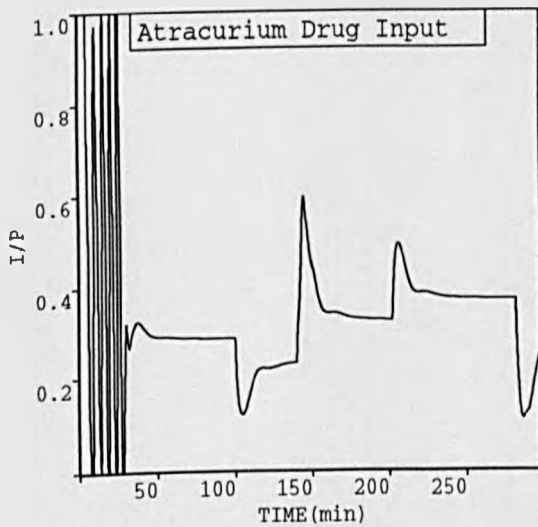
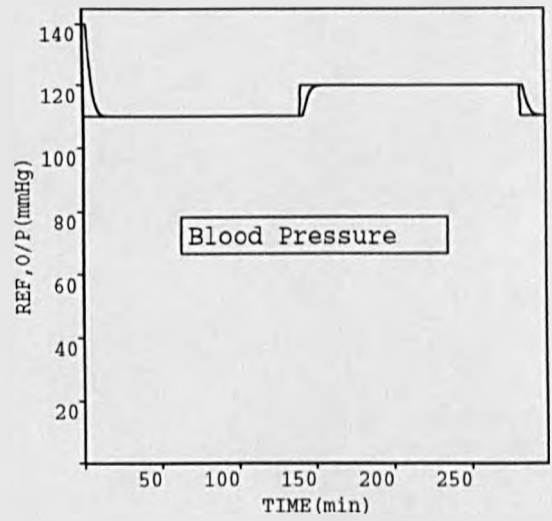
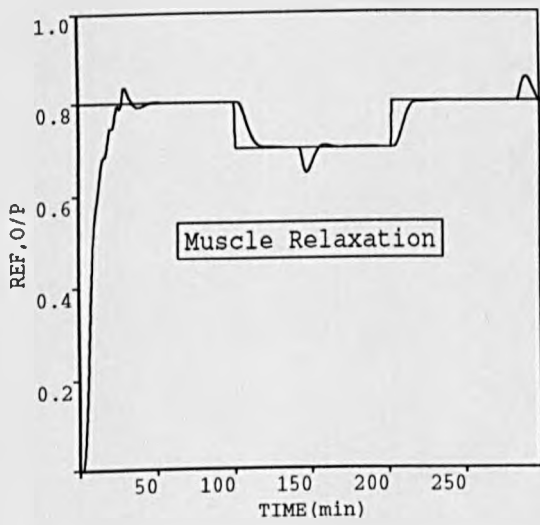


Figure 8.10. Same conditions as figure (8.8) but with control weighting sequence $\lambda=1.0$

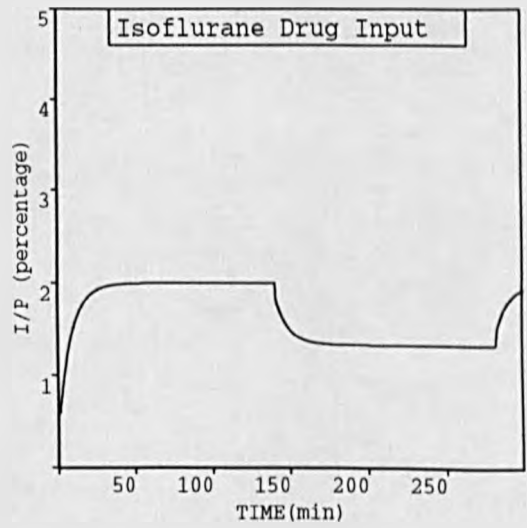
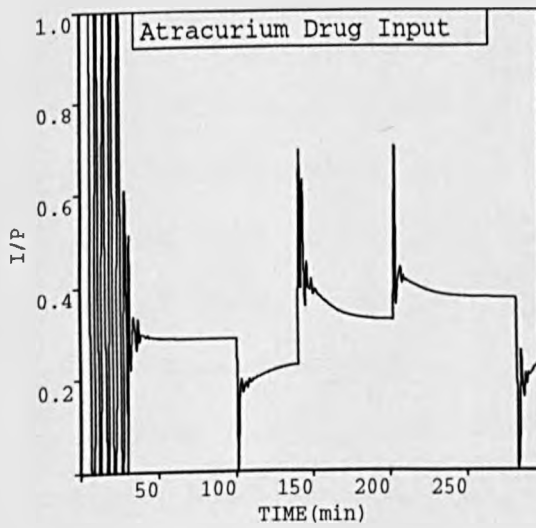
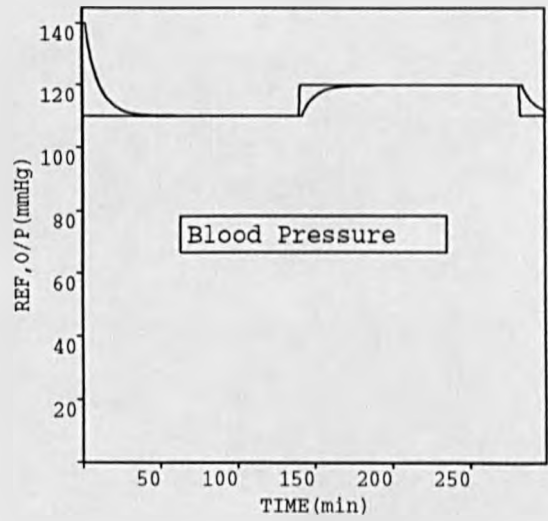
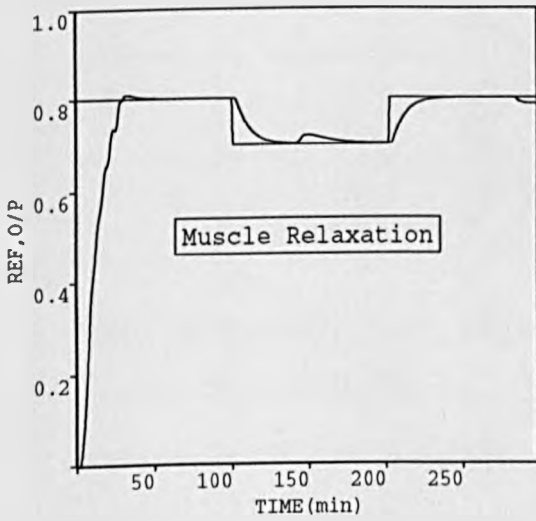


Figure 8.11. Extended GPC algorithm with model-following polynomial $P(z^{-1})$. $N_1=1$;
 $N_2=10$; $NU=2$; $P_1=P_2=10 (1-0.9z^{-1})$

Phase 6

Effect of The Polynomials $T(z^{-1})$ and $P(z^{-1})$					
Fig.Nbr	N_1	N_2	NU	$T(z^{-1})$	$P(z^{-1})$
8.12.a	1	10	2	$1.0 - 0.9z^{-1}$	$\frac{1.0 - 0.9z^{-1}}{0.1}$
8.12.b	1	10	1	$1.0 - 0.9z^{-1}$	$\frac{1.0 - 0.5z^{-1}}{0.5}$

Figure (8.7) shows a result from phase 1 where the controller parameter settings were (1, 10, 1, 0) for (N_1, N_2, NU, λ). This result gave fast responses with a 5% overshoot in the relaxation response but a well damped arterial pressure. Phase 2 was concerned with the control horizon parameter NU which is considered to represent the corner-stone of the GPC algorithm (Clarke et al., 1987a). In this experiment, its value was taken to be 2 and therefore, produced the response of figure (8.8) where the transients in both channels were very fast. However, the response in the relaxation channel oscillated for a period of 6 iterations before tracking finally the set-point efficiently. This was to be expected, since a value of $NU \geq 2$ always causes high control activity. Notice also the magnitude of the interactions due to the blood pressure changes. Phase 3 shows how the controller-parameter settings can be chosen to be different between the two channels: $N_1 = 1, N_2(\text{Ch1}) = 10, N_2(\text{Ch2}) = 20, NU(\text{Ch1}) = 1, NU(\text{Ch2}) = 2$. This result shown in figure (8.9) also gave fast responses with an overshoot in the relaxation response, as well as a well damped arterial pressure. Figure (8.10) shows how the high control activity induced by a large control horizon NU can be reduced by the use of a non-zero control weighting sequence λ ($\lambda = 1.0$). Another alternative also is the use of extended GPC algorithm with the important model following polynomial $P(z^{-1})$. Based on the particular dynamics as well as the sampling period, a

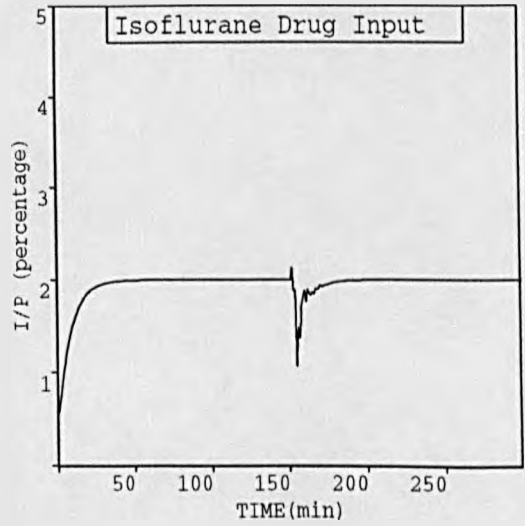
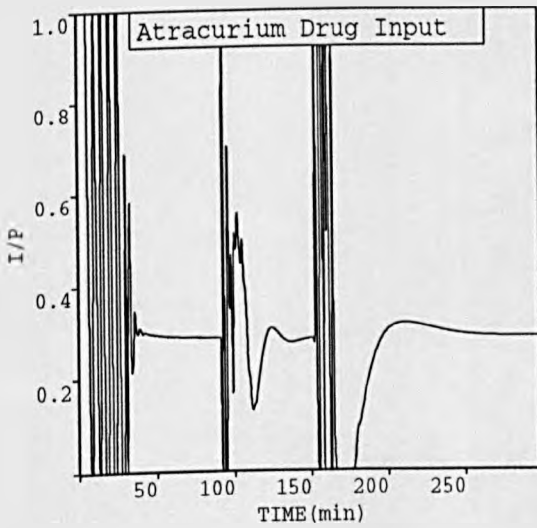
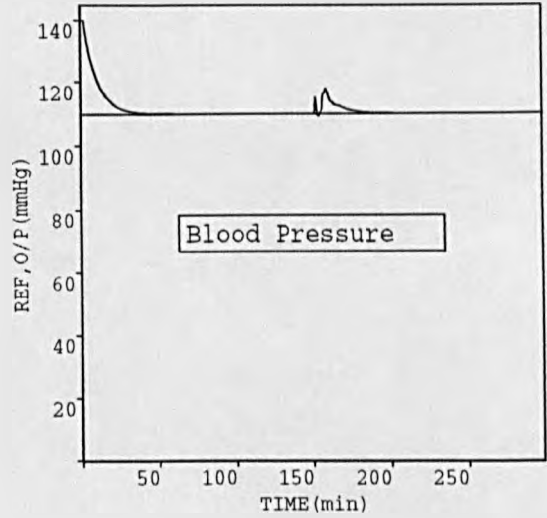
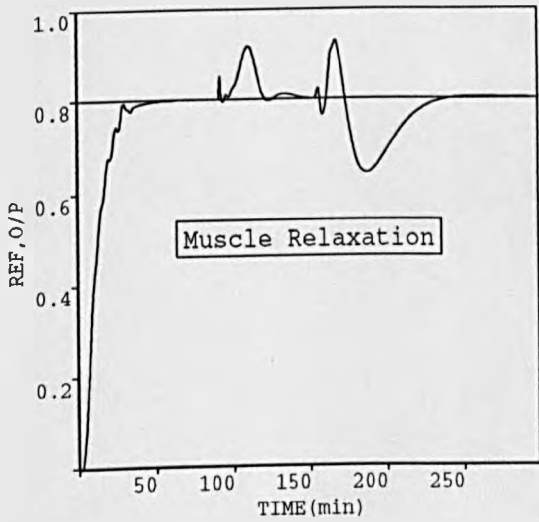


Figure 8.12.a. Effect of gain-change disturbances with observer polynomial $T(z^{-1})=1-0.9z^{-1}$, and model following polynomial $P(z^{-1})$. $P_1=P_2=10(1-0.9z^{-1})$; $N_1=1$; $N_2=10$; $NU=2$

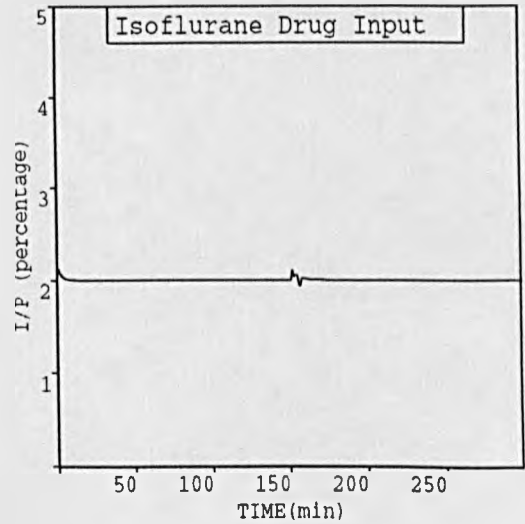
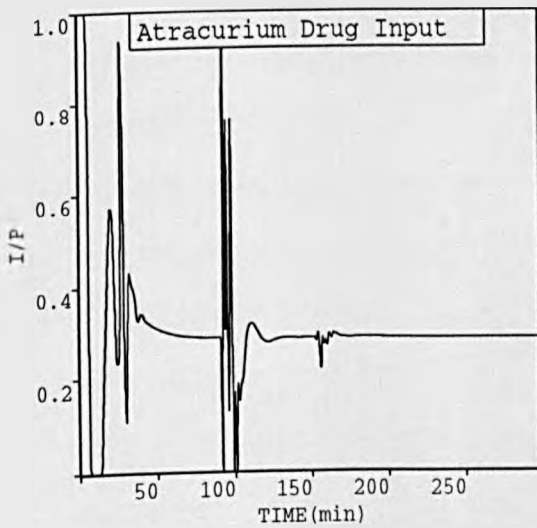
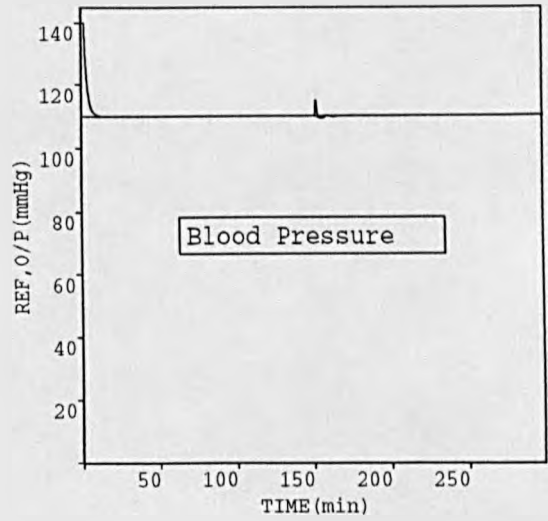
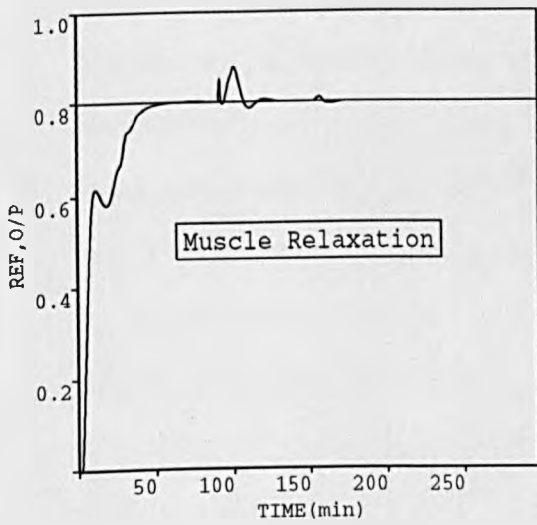


Figure 8.12.b. Effect of gain-change disturbances with observer polynomial $T(z^{-1})=1-0.9z^{-1}$, and model following polynomial $P(z^{-1})$.
 $P_1=P_2=2(1-0.5z^{-1})$; $N_1=1$; $N_2=10$;
 $NU=1$

value of $T_c = 9.49$ minutes (identical for both channels) was selected for assignment of the P matrix. Figure (8.11) shows how this can be used to reduce the previous overshoot in relaxation as well as minimizing the interaction, at the cost of overdamping the arterial pressure. Finally, phase 6 considered the inclusion of the observer polynomial $T(z^{-1})$ together with the previous polynomial $P(z^{-1})$ in order to enhance further the robustness of the whole control strategy (Clarke and Robinson, 1991). Figures (8.12.a) and (8.12.b) show how the effect of disturbances can be reduced but at the same time affecting the overall closed-loop responses with the use of the $P(z^{-1})$ polynomial. In this result gain changes were made during the run, being 5% at time 90 minutes in the relaxation dynamics, and 17% at time 150 minutes in the arterial pressure model.

From these figures it can be seen that the basic algorithm produced severe control actions for Atracurium during the initial transient, but this was reduced significantly by introducing the model following and observer polynomials. Through these simulation studies, experience had been gained in the selection of the crucial design parameters for GPC. Like many biomedical systems, however, anaesthetic models show very large inter-patient variability for which there is no information prior to an operation. The next section describes the use of this experience gained from the nominal model in the case of randomised model investigations.

8.4.2 Simulation Studies via Monte-Carlo Parameter Selection Method

Clearly, the application of the GPC algorithm to this particular multivariable non-linear anaesthetic model demonstrated that many design-parameters could be selected and this selection is very important in a safety-critical situation such as an

operating theatre. The previous chapter has particularly reflected this idea since patient parameters were ranging from low to high gains, and from slow to fast time-constants. Therefore, in order to validate further the robustness of these control strategies, Monte-Carlo simulations were chosen to undergo such tests. Equation (8.42) describes the anaesthetic model with parameters which are known to vary from patient-to-patient:

$$\begin{bmatrix} \text{Paralysis} \\ \Delta \text{MAP} \end{bmatrix} = \begin{bmatrix} G_{11}(s) & G_{12}(s) \\ 0 & G_{22}(s) \end{bmatrix} \begin{bmatrix} U_1 \\ U_2 \end{bmatrix} \quad (8.42)$$

where,

$$G_{11}(s) = \frac{K_1 e^{-s} (1 + T_4 s)}{(1 + T_1 s) (1 + T_2 s) (1 + T_3 s)}$$

$$G_{12}(s) = \frac{K_4 e^{-s}}{(1 + T_6 s) (1 + T_7 s)}$$

$$G_{22}(s) = \frac{K_2 e^{-s}}{(1 + T_5 s)}$$

The non-linearity is still represented by the Hill equation (8.2) described in section 8.2.1 using the same parameters, although these also could have been randomised.

The Monte-Carlo simulations consisted of choosing the model parameters in a random manner using the following formula:

$$\text{Monte-Carlo parameter} = \text{Min.} + \text{RANDOM} \times (\text{Max.} - \text{Min.})$$

where ($0 \leq \text{RANDOM} \leq 1$), and RANDOM is obtained from a random number generator. The minimum and maximum values for each parameter were chosen to reflect probable pharmacological ranges known to exist. In this way many combinations could be produced. Table (8.2) shows a sample of 10 cases which were studied but for simplicity only 3 of these will be selected on which to base the discussions. All time-constants are expressed in minutes.

Monte-Carlo Simulation Method										
Case	Anaesthetic model parameters									
	T ₁	T ₂	T ₃	T ₄	K ₁	T ₅	K ₂	T ₆	T ₇	K ₄
1	2.54	4.17	27.88	14.89	2.01	1.57	-17.26	2.79	1.19	0.24
2	2.45	4.28	16.44	7.3	1.69	1.54	-17.7	3.01	1.33	0.27
3	2.35	5.95	27.88	10.88	2.16	1.15	-14.61	3.06	1.26	0.24
4*	1.18	5.1	31.26	10.31	1.34	1.14	-15.94	2.99	1.26	0.24
5*	1.36	3.84	32.0	7.31	2.46	1.2	-10.48	2.42	1.25	0.27
6	1.55	2.58	32.74	13.31	2.08	1.26	-15.02	2.85	1.24	0.25
7*	1.73	5.32	33.48	10.31	1.71	1.31	-19.55	3.28	1.22	0.27
8	1.91	4.06	34.22	7.31	1.33	1.37	-14.09	2.71	1.21	0.25
9	2.09	2.8	34.96	13.3	2.45	1.43	-18.63	3.14	1.2	0.27
10	2.27	5.54	15.7	10.3	2.07	1.49	-13.16	2.57	1.18	0.25

Table 8.2. Selected model parameters using Monte-Carlo method

Cases 4, 5, and 7 were selected for the application of the algorithm. These cases were chosen to indicate the best, worst and medium performance conditions for the algorithm. The same conditions as described above remained unchanged except that the control signal for channel 1 during the first 10 samples (where the parameter estimates are fixed) was clipped between 0.0 and 0.5, whereas for channel 2 the corresponding control signal was clipped between 0.0 and 2.5 allowing the self-adaptive GPC to take over under better conditions.

Figure (8.13) shows the performance of the extended version of GPC with model

* Cases to be considered for analysis and discussions

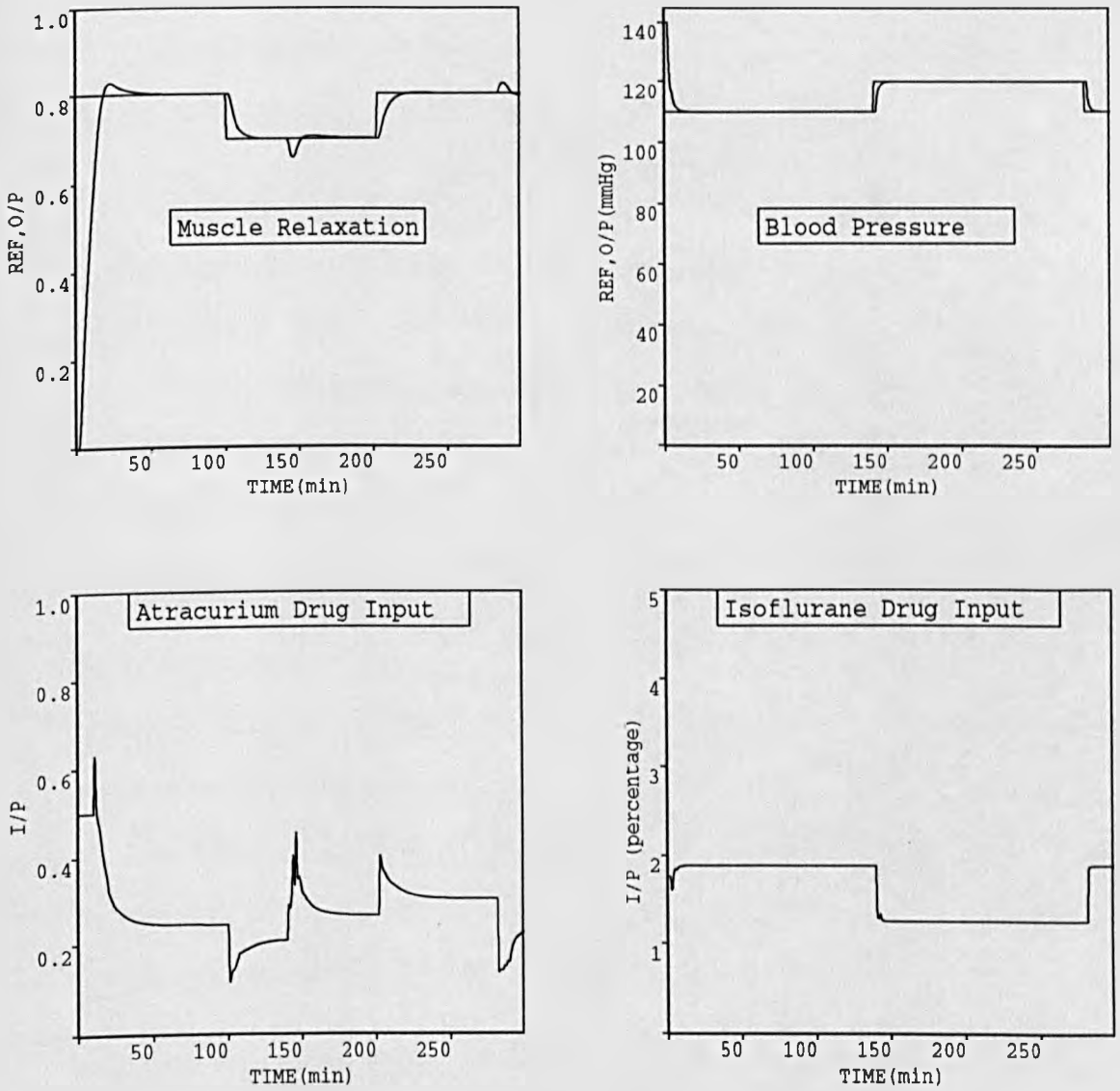


Figure 8.13. Monte-Carlo simulations; extended

GPC algorithm Case 4 with model-follo-

wing polynomial $P(z^{-1})$. $N_1=1$; $N_2=10$;

$NU=1$; $P_1=P_2=2 (1-0.5z^{-1})$

following polynomial $P(z^{-1})$ assuming the model-parameters of case 4 and a combination of (1, 10, 2, 0) for (N_1, N_2, NU, λ) . A relatively fast time-constant of 1.44 minutes was chosen for the polynomial. The response in both channels was fast and well-damped with the overshoot as well as the interactions reduced to a low level in channel 1 which exhibits severe non-linearities.

Case 5 represented a severe test for the chosen GPC configuration. It corresponds to a high gain paralysis model, and a low gain blood pressure model. Figure (8.14) shows a good performance for blood pressure, a heavy initial overshoot in paralysis and subsequent saturation of drug signals and correspondingly large interaction from the blood pressure channel. Finally, case 7 represented a medium condition with inferior blood pressure response to that of figure (8.13), but similar paralysis behaviour as shown in figure (8.15).

To complement the visual indications of control performance from figures (8.7)-(8.15), an objective measure of error performance over the simulation runs was made using ISE (Integral of Squared Errors) and ITAE (Integral of Time and Absolute Error) criteria. Table (8.3) gives such values for the above figures. The unit of time for the ITAE criterion was minutes. The criteria were evaluated for the 100 minute stretches for each set-point change.

In general all ITAE values were greater than the ISE values, because of the time scale involved. Similarly, all of the blood pressure ITAE and ISE values were greater than the paralysis, simply because of the non-normalised values for blood pressure. Approximate normalisation of blood pressure ISE could be obtained via division by 10,000 and ITAE via division by 100. This would give relatively lower figures for blood pressure than paralysis. This reflects clearly the better dynamic performance for the simpler and linear dynamic of that channel. Case 4

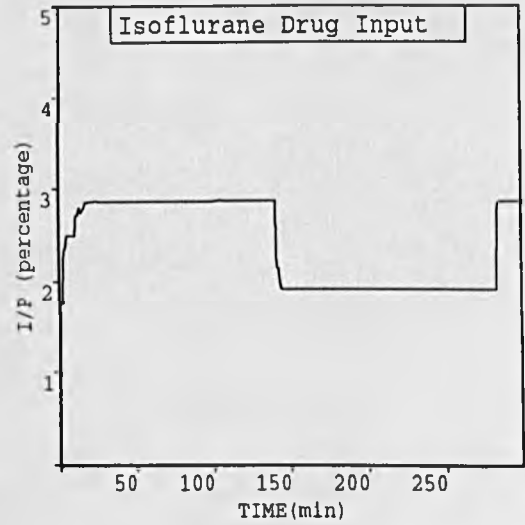
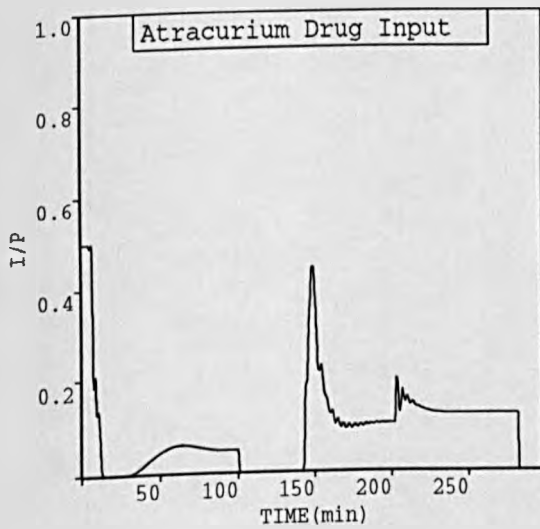
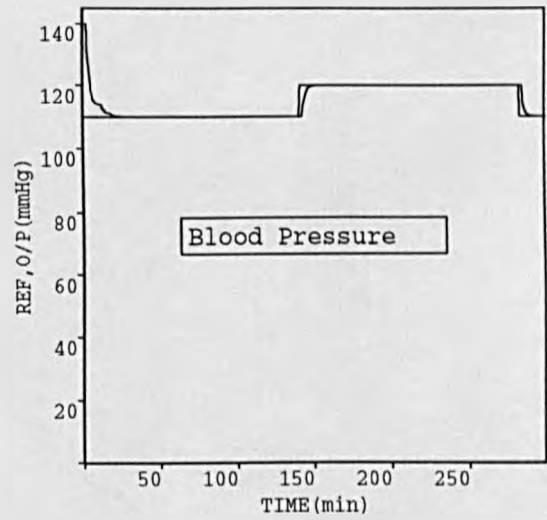
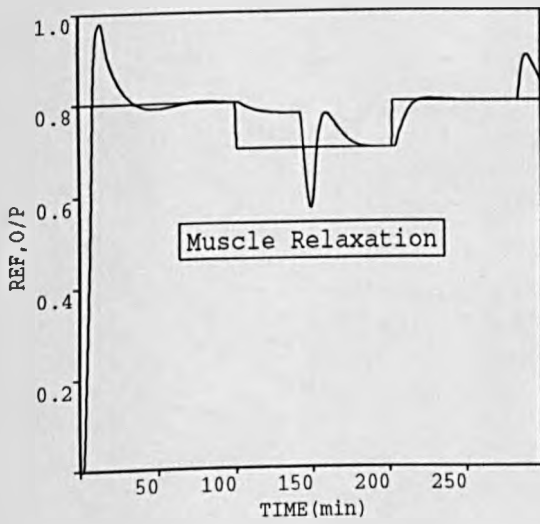


Figure 8.14. Monte-Carlo simulations; extended
 GPC algorithm Case 5 with model-follo-
 wing polynomial $P(z^{-1})$. $N_1=1$; $N_2=10$;
 $NU=1$; $P_1=P_2=2 (1-0.5z^{-1})$

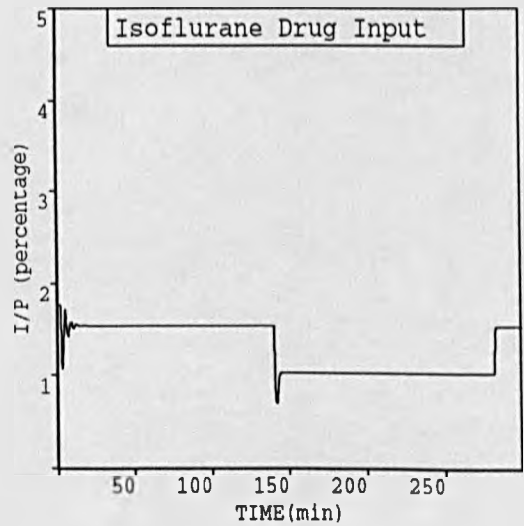
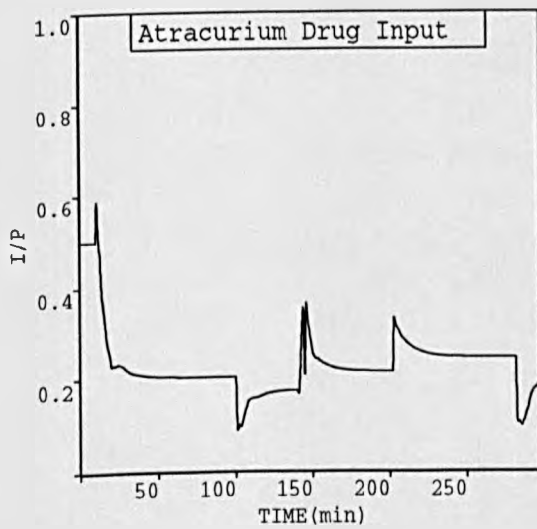
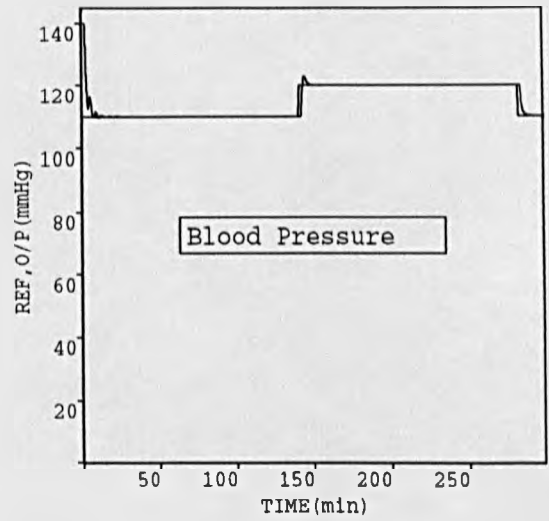
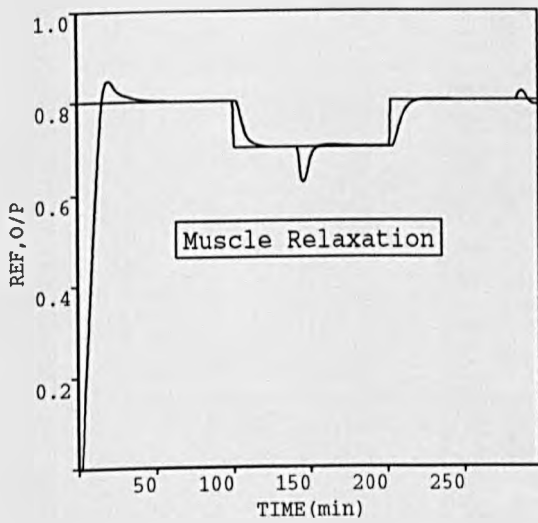


Figure 8.15. Monte-Carlo simulations; extended
 GPC algorithm Case 7 with model-follo-
 wing polynomial $P(z^{-1})$. $N_1=1$; $N_2=10$;
 $NU=1$; $P_1=P_2=2(1-0.5z^{-1})$

Figure number	Time-phases(Min.)	Paralysis		Blood-Pressure	
		ISE	ITAE	ISE	ITAE
8.7	0 to 99	3.27	64	2186	144
	100 to 200	0.08	167	242	4536
	201 to 300	0.07	298	243	9132
8.8	0 to 99	2.48	24	1800	31
	100 to 200	0.05	87	200	2819
	201 to 300	0.06	198	200	5650
8.9	0 to 99	2.78	61	1800	32
	100 to 200	0.09	197	200	2821
	201 to 300	0.09	364	200	5654
8.10	0 to 99	3.92	49	3144	349
	100 to 200	0.08	153	349	6774
	201 to 300	0.08	291	349	13561
8.11	0 to 99	5.17	74	5096	2315
	100 to 200	0.07	176	567	14491
	201 to 300	0.06	272	559	24951
8.12.a	0-300	5.89	1420	5395	14592
8.12.b	0-300	3.81	193	2288	1902
8.13	0 to 99	3.75	41	2126	163
	100 to 200	0.05	119	233	4389
	201 to 300	0.05	192	227	8102
8.14	0 to 99	2.98	58	2706	581
	100 to 200	0.41	689	256	4971
	201 to 300	0.14	486	227	8100
8.15	0 to 99	3.84	43	1979	138
	100 to 200	0.08	153	216	4017
	201 to 300	0.05	203	226	7993

Table 8.3. Table representing the ISE and ITAE criteria for different GPC runs

which the GPC found easy to control produced the lowest values of ISE for paralysis as well as for blood pressure during the last 200 iterations. Lowest ITAE values were also recorded in this case for paralysis. However, GPC found case 5 difficult to manage, which is not surprising because of the extreme nature of the parameters. The algorithm provided reasonable control except for the second transient in paralysis, where movement towards the set-point only occurred after the interactive disturbance from the blood pressure set-point change. The third case selected as moderate performance (visually determined) indicated somewhat comparable ISE and ITAE with case 4.

8.4.3 Execution-Time Considerations

An execution-time evaluation for the GPC algorithm was conducted for 7 of the previously carried out experiments. The multivariable GPC was run on a SUN 4 computer. The study produced table (8.4) where the corresponding execution-times in seconds for each type of algorithm are shown for a standard simulation run of 5 hours. The study suggests that the algorithm did rather well considering a real-time sampling of 1 minute. Indeed, it took on average 0.38 second for the GPC to finish one iteration of calculations. It is however worth noting that the choice of controller parameters is crucial not only for the final performance but also for the computation burden. For instance, large N_2 , NU induce large matrix calculations.

However, given the nature of the model which includes only one significant interaction path, the scheme which consists of using two single loop controllers and incorporating feedforward in one of the loops for the interaction seems to be interesting and the general idea is explored in the next section.

Speed Performances Relative to GPC: 5 Hour Simulation Run		
Figure number	Type of algorithm	Execution-time (seconds)
8.9	Basic Multivariable Algorithm; $N_2(\text{ch.1}) = 10 ; N_2(\text{ch.2}) = 20 ;$ $NU(\text{ch.1}) = 1 ; NU(\text{ch.2}) = 2$	124.76
8.11	Extended Multivariable Algorithm with model-following Polynomial $P(z^{-1})$; $N_1 = 1 ; N_2 = 10 ;$ $NU = 2 ; P_1 = P_2 = \frac{1 - 0.9 z^{-1}}{0.1}$	116.30
8.12.a	Extended Multivariable Algorithm with observer polynomial $T(z^{-1})$; and model-following Polynomial $P(z^{-1})$; $N_1 = 1 ; N_2 = 10 ;$ $NU = 2 ; T_1 = T_2 = 1 - 0.9 z^{-1} ;$ $P_1 = P_2 = \frac{1 - 0.9 z^{-1}}{0.1}$	120.45
8.12.b	Extended Multivariable Algorithm with observer polynomial $T(z^{-1})$; and model-following Polynomial $P(z^{-1})$; $N_1 = 1 ; N_2 = 10 ;$ $NU = 1 ; T_1 = T_2 = 1 - 0.9 z^{-1} ;$ $P_1 = P_2 = \frac{1 - 0.5 z^{-1}}{0.5}$	100.00
8.13;8.14;8.15	Extended Multivariable Algorithm with model-following Polynomial $P(z^{-1})$; $N_1 = 1 ; N_2 = 10 ;$ $NU = 1 ; P_1 = P_2 = \frac{1 - 0.5 z^{-1}}{0.5}$	99.42

Table 8.4. Table representing the speed of execution for different settings of the multivariable GPC algorithm

8.5 MULTIVARIABLE GPC ALGORITHM USING FEEDFORWARD

Many processes have some disturbances which are measurable. With interacting processes the disturbances in one loop may be controlled variables of other loops. These measurable disturbances added to the model structure in a feedforward manner could be a 'white noise' affecting the output as much as $\zeta(t)$ does. The more accurate the model of the process is the better predictive model becomes and hence, the more reduced the variance of the measured output is. In this event, the controlled behaviour is improved. As many feedforward terms as required can be included; by using variables from other loops the interaction between loops can be reduced (Astrom and Wittenwark, 1989).

8.5.1 Development of the SISO GPC

Algorithm with Feedforward

The main idea of this controller is as follows: an m-input and m-output MIMO system can be represented by m SISO loops with interactions within the MIMO system considered as measurable disturbances to each of the SISO loops. In order to develop the multivariable GPC algorithm with feedforward, it is necessary to formulate first the algorithm relative to the SISO GPC algorithm but including feedforward.

Consider the CARIMA model structure of equation (5.4) including feedforward and with $C(z^{-1}) = 1$ without any loss of generality.

$$A(z^{-1}) \Delta y(t) = B_1(z^{-1}) \Delta u(t - k) + D_1(z^{-1}) \Delta v(t - kv) + \zeta(t) \quad (8.42)$$

where, $A(z^{-1})$, $B_1(z^{-1})$, and $D_1(z^{-1})$ are the usual polynomials in the backward shift operator z^{-1} , i.e.,

$$\begin{aligned}
 A(z^{-1}) &= 1 + a_1 z^{-1} + a_2 z^{-2} + \dots + a_n z^{-n} \\
 B_1(z^{-1}) &= b_1 + b_2 z^{-1} + b_3 z^{-2} + \dots + b_m z^{-m+1} \\
 D_1(z^{-1}) &= d_0 + d_1 z^{-1} + d_2 z^{-2} + \dots + d_v z^{-v}
 \end{aligned}$$

and $y(t)$ is the measurable output, $u(t)$ the input delayed by k samples, and $v(t)$ is the measurable disturbance delayed by kv samples.

To simplify the derivations, if the dead-times ' k ' and ' kv ' are enhanced within the polynomials $B_1(z^{-1})$ and $D_1(z^{-1})$ respectively such that:

$$\begin{aligned}
 D(z^{-1}) \Delta v(t-1) &= D_1(z^{-1}) \Delta v(t-kv) \\
 B(z^{-1}) \Delta u(t-1) &= B_1(z^{-1}) \Delta u(t-k)
 \end{aligned}$$

then, following the same procedure as in section 5.2 it can easily be shown that the prediction equations will be of the following form (the operator z^{-1} has been dropped for simplicity's sake):

$$\hat{y}(t+j/t) = E_j B \Delta u(t+j-1) + E_j D \Delta v(t+j-1) + F_j y(t) \quad (8.43)$$

or,

$$\begin{aligned}
 \hat{y}(t+j/t) &= G_j \Delta u(t+j-1) + S_j \Delta v(t+j-1) + F_j y(t) \\
 G_j &= E_j B \\
 S_j &= E_j D
 \end{aligned} \quad (8.44)$$

where,

$$\Delta v(t+j-1) = 0 \quad \text{for } j \geq 2$$

If ' f ' is a vector composed of signals which are known at time ' t ' and ' ω ' the set-points command vector, the control sequence will be of the following form:

$$\Delta u(t) = (G_1^T G_1 + \lambda I)^{-1} G_1^T (\omega - f) \quad (8.45)$$

All variables bear the same definitions as the ones given in section 5.2 except ' f ' whose components are of the following form:

$$f = \left[f(t+1), f(t+2), \dots, f(t+N) \right]$$

with:

$$\begin{aligned} f(t+1) &= [G_1(z^{-1}) - g_{10}] \Delta u(t) + F_1(z^{-1}) y(t) + S_1 \Delta v(t) \\ f(t+2) &= z [G_2(z^{-1}) - g_{21} z^{-1} - g_{10}] \Delta u(t) + F_2(z^{-1}) y(t) + S_2 \Delta v(t+1) \\ &\vdots \\ &\vdots \\ &\vdots \\ f(t+N) &= z^{N-1} [G_N(z^{-1}) - \dots - g_{N0}] \Delta u(t) + F_N y(t) + S_N \Delta v(t+N-1) \end{aligned} \quad (8.46)$$

8.5.2 Development of the Multivariable GPC

Algorithm with Feedforward (GPCF)

Now, the same technique can be modified to be applied to multivariable systems. Thus, consider the dual-input dual-output system of the form:

$$\begin{aligned} A_1(z^{-1}) y_1(t) &= B_1(z^{-1}) u_1(t-k_{11}) + D_1(z^{-1}) u_2(t-k_{12}) \\ A_2(z^{-1}) y_2(t) &= B_2(z^{-1}) u_2(t-k_{22}) + D_2(z^{-1}) u_1(t-k_{21}) \end{aligned} \quad (8.47)$$

In the above, it assumed that u_1 is the input which is most strongly correlated with y_1 , and u_2 is the other input which is the most strongly correlated with y_2 . In practice, it is equivalent to say that u_1 is the signal that influences y_1 with the least time-delay in channel 1. The same situation applies in channel 2.

Summarizing leads to the following double inequality:

$$\begin{aligned} k_{11} &\leq k_{12} \\ k_{22} &\leq k_{21} \end{aligned} \quad (8.48)$$

Conditions (8.48) are indeed satisfied in the case of the previously derived anaesthetic model (8.13). Therefore, from equations (8.44) and (8.47), the expressions for calculating u_1, u_2 are thus given by the following equations:

$$\Delta u_1(t) = (G_1^T G_1 + \lambda_1 I)^{-1} G_1^T (\omega_1 - f_1) \quad (8.49)$$

$$\Delta u_2(t) = (G_2^T G_2 + \lambda_2 I)^{-1} G_2^T (\omega_2 - f_2) \quad (8.50)$$

where G_i is the same matrix as the matrix G defined in section 5.2.3 but for the i th channel, ω_i is the i th set-point command, and f_i is the vector for the i th channel composed of signals known at time 't' as described in equation (8.46).

The values of the control signals are then obtained as the solutions to the simultaneous equations (8.49) and (8.50). For reference purposes, this multivariable self-tuning controller will be referred to throughout as the MIMO generalized predictive controller incorporating feedforward (GPCF). It is however, worth noting that in the case of the multivariable anaesthetic model which only includes one interaction loop, the vector f_2 in equation (8.50) reduces only to:

$$f_2(t+1) = F_{21} y_2(t) + (g_{21} - g_0) \Delta u_2(t) \quad (8.51)$$

$$\begin{matrix} \cdot & \cdot & \cdot \\ \cdot & \cdot & \cdot \\ \cdot & \cdot & \cdot \end{matrix}$$

and when implemented, the scheme would consist of calculating the second control sequence u_2 first from equation (8.50), then substituting its present and past values in equation (8.49) to obtain the value of u_1 .

8.6 SIMULATION RESULTS WITH GPCF

The simulation study with GPCF involved the same conditions for the continuous simulated model and jacketting procedure as in section 8.4.1. For parameter estimation, the UDU factorization method (Bierman, 1977) was used on incremental data with an initial covariance matrix and forgetting factor given by:

$$P = 10^2 I, \quad \rho = 0.995$$

A third order model with a minimum time-delay of 1 minute and with two coefficients for the feedforward was considered for the first channel, whereas for

the second channel, a first model also with a 1 minute time-delay was considered.

The first experiment considered the same conditions as in figure (8.11) of phase 5. The result of the run, shown in figure (8.16), gave responses with slightly better transients and with the interaction in channel 1 slightly reduced adding to the fact that the control activity was lower than that of figure (8.11).

For the second experiment, conditions of phase 6 were considered this time. Figure (8.17.a) shows that the transients in both channels are fast and better damped than the ones in figure (8.12.a). Notice also that the interaction from channel 2 due to the disturbance has been considerably reduced with a minimum control activity. Similar results could be observed in figure (8.17.b) when compared with figure (8.12.b).

Similarly to section 8.4.2, the visual indications of control performances are complemented by ISE and ITAE measurements. Table (8.5) summarizes such values for figures (8.16), (8.17.a), and (8.17.b). The table indicates in general lower values for channel 1 than those obtained for figures (8.11), (8.12.a), and (8.12.b) and summarized in table (8.3), and comparable ones for channel 2.

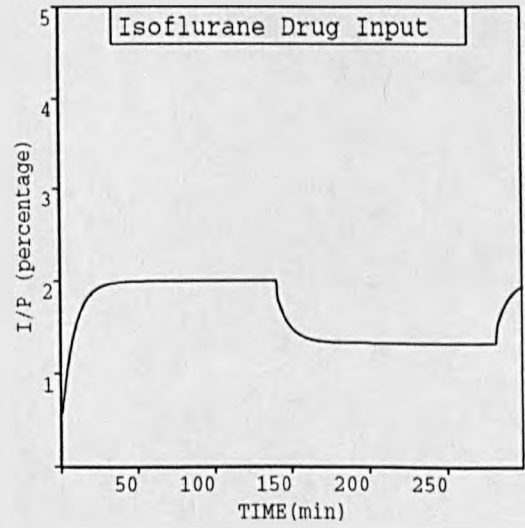
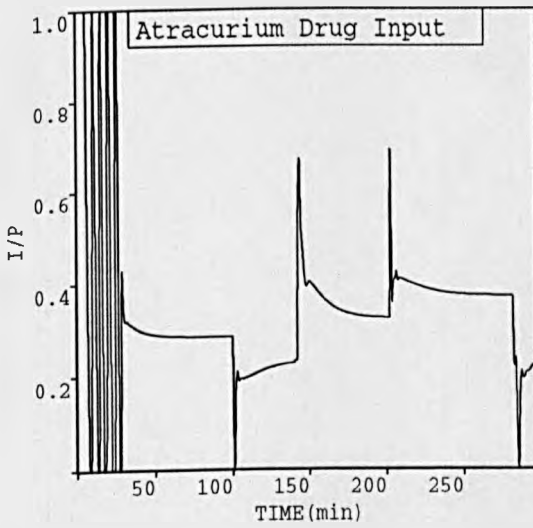
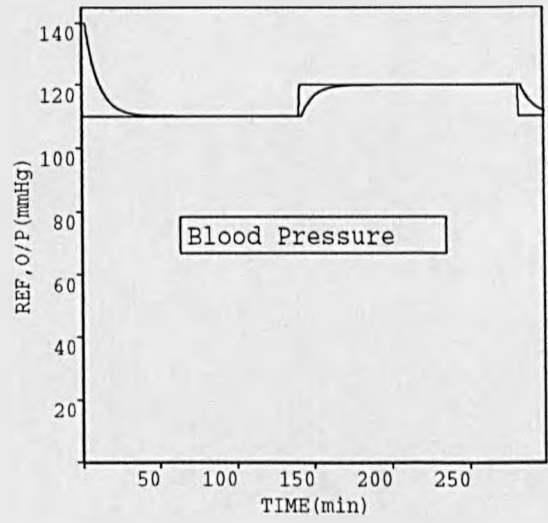
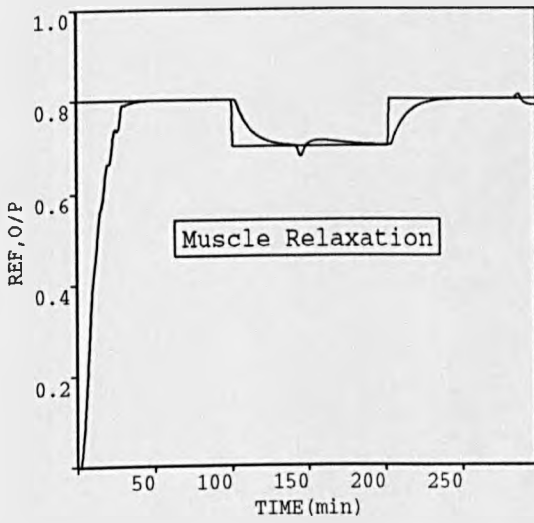


Figure 8.16. Extended GPC algorithm using feedforward (GPCF) and with model following polynomial $P(z^{-1})$. $N_1=1$; $N_2=10$; $NU=2$
 $P_1=P_2=10 (1-0.9z^{-1})$

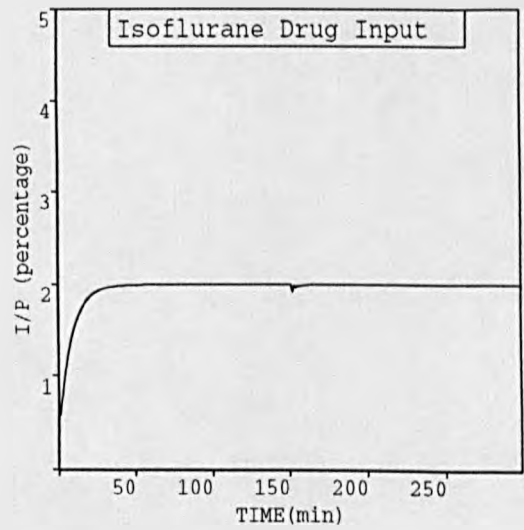
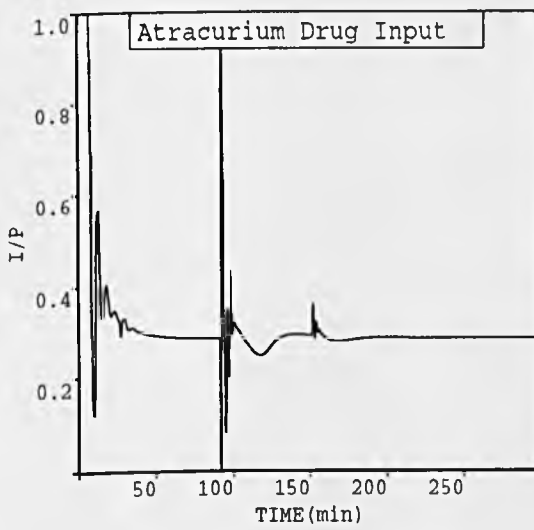
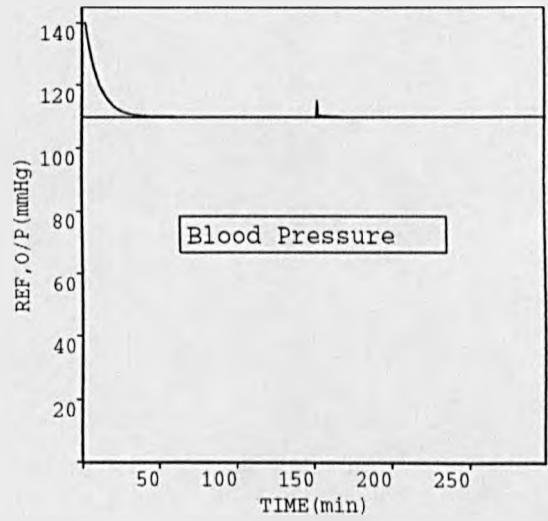
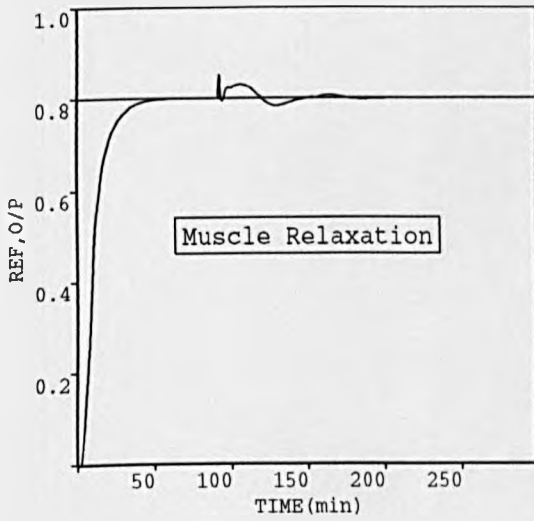


Figure 8.17.a. Same conditions as in figure (8.12.a) but using GPC algorithm with feedforward (GPCF)

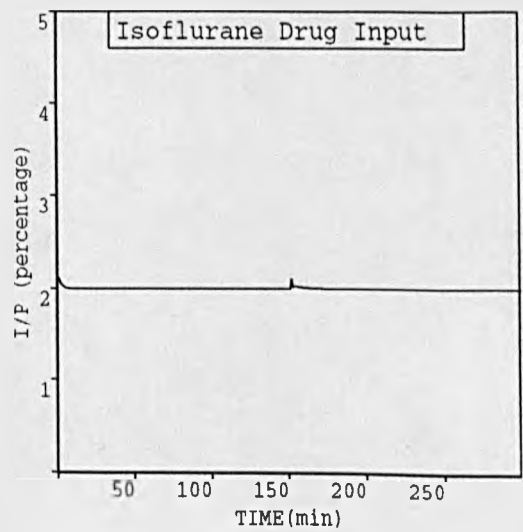
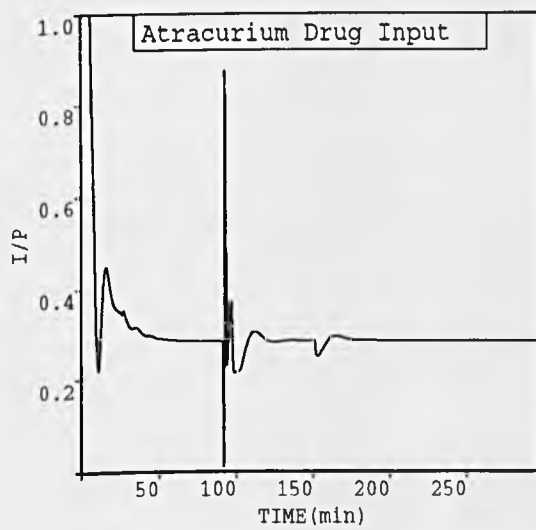
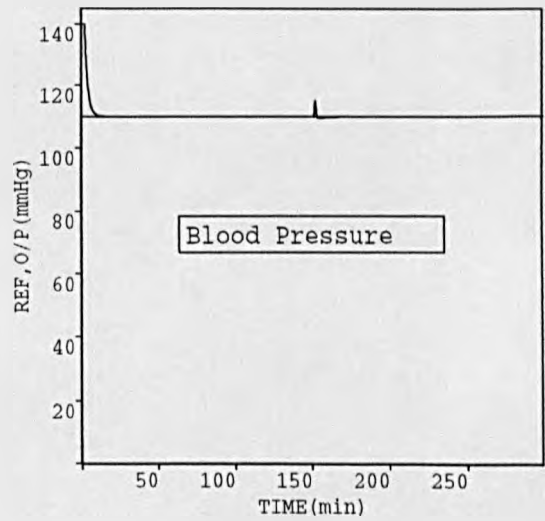
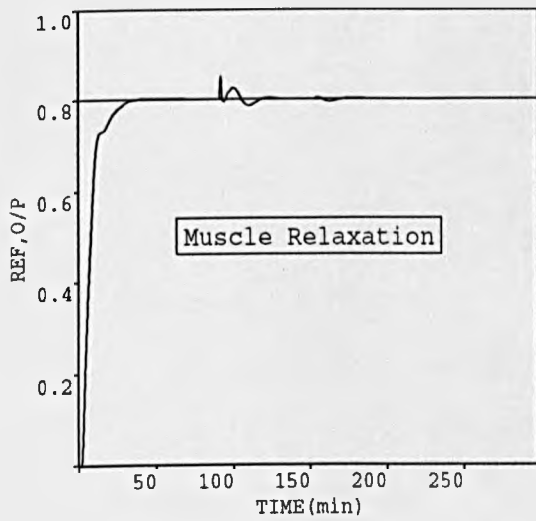


Figure 8.17.b. Same conditions as in figure (8.12.b) but using GPC algorithm with feedforward (GPCF)

Figure Number	Time-Phases(Min.)	Paralysis		Blood-Pressure	
		ISE	ITAE	ISE	ITAE
8.16	0 to 99	5.16	76	5101	2326
	100 to 200	0.07	179	566	14492
	201 to 300	0.07	274	559	24953
8.17.a	0-300	4.83	187	5127	3771
817.b	0-300	3.13	83	2292	1947

Table 8.5. Table representing the ISE and ITAE criteria for different GPCF runs

Finally, an execution-time evaluation of the GPCF algorithm was conducted for the previous 3 experiments. Run on a SUN 4 computer, the study produced table (8.6) showing the different execution-times in seconds for a 5-hour simulation run. As illustrated in the same table, the use of the GPCF algorithm reduced considerably the execution-time by almost a factor of 2 hence, making the GPCF scheme speedier despite the choice of a control horizon greater than 1 in some cases.

Speed Performances relative to GPC: 5 hour simulation run		
Figure Number	Type of Algorithm	Execution-Time (seconds)
8.16	Same as in figure (8.11)	43
8.17.a	Same as in figure (8.12.a)	44
8.17.b	Same as in figure (8.12.b)	38

Table 8.6. Table representing the speed of execution for different settings of the multivariable GPCF algorithm

A multivariable model combining muscle relaxation and anaesthesia has been identified. The Atracurium drug and the Isoflurane agent were considered in the study. The system dynamics are of moderate complexity. This model complexity consists of severe non-linearities as well as large patient-to-patient variability in model parameters. It is because of the inability of fixed controllers to cope with controlling such systems (Linkens et al., 1982; Slate, 1980), that the use of adaptive control techniques was justified. The GPC algorithm which has been evaluated in the muscle relaxation SISO case both in simulations and clinical trials represented a very attractive candidate for the above task. The GPC extension to include the multivariable case was straightforward and the results show a good performance both in examples of figures (8.7)-(8.12) and in the Monte-Carlo runs of figures (8.13)-(8.15). Control of relaxation was obviously harder than unconsciousness via blood pressure measurements. This was mainly due to the non-linear pharmacodynamics. Results also demonstrated that in order to obtain smoother control actions, the basic algorithm needed to be extended to include the model-following polynomial $P(z^{-1})$, the observer polynomial $T(z^{-1})$ or both (figures (8.13)-(8.15)), especially if disturbances occur or the control horizon NU is taken greater than 1. Because the use of $P(z^{-1})$ affects both the disturbance rejection properties of the system as well as its overall closed-loop characteristics, it was possible to reach a trade-off relating stability and rise-time between the two channels as the ITAE and ISE evaluations have shown (figures (8.7)-(8.12)). Perhaps the use of the $P(z^{-1})$ could have been avoided altogether, especially when $NU \geq 2$, if the algorithm was modified to include the input constraints in the cost function (Tsang and Clarke, 1990) as already seen in section 5.6. Lagrange multipliers would have been used to extract the best possible input solution, though the method is known to have some limitations. However, recent work by Wilkinson and Tham (1990) showed that the use of a quadratic approach (QP) (Lawson and

Hanson, 1974) would be more advantageous as far as data storage, execution-time, and quality of the solution are concerned. In fact, an evaluation of the execution-time showed that the algorithm, the extended version with $NU = 2$ (figures (8.11), (8.12)) performed rather adequately taking into account the considerable calculations involved. However, the later inclusion of the control strategy which consists of using two single GPC loops together with the feedforward in one of the loops for the interaction proved to be more efficient as far as the control performances and the computer burdens were concerned, making it altogether a more attractive protocol.

In conclusion, it can be stated that the overall results obtained are very encouraging and it is hoped that clinical trials under multivariable GPC and multivariable GPCF algorithms will be forthcoming.

CHAPTER 9

CONCLUSIONS AND RECOMMENDATIONS

During surgical operations which require muscle relaxation, the anaesthetist is faced with two important tasks; keeping a steady level of relaxation and at the same time administering the right amount of muscle relaxant so as to avoid over-paralysis at the end of the operation ensuring therefore, a quick and total recovery of the patient. Since the anaesthetist may not always fulfil such tasks, automatic feedback control emerges as a powerful tool which can assist in meeting the above objectives.

Fixed gain controllers in the form of P, PI, and PID networks which are simple to implement, have achieved good results in some cases, but in others they have failed to cope with non-linearities, large patient-to-patient variability in the dynamics, as well as other unexpected changes that may occur during surgery such as modification of operating point, sudden disturbances, change in muscle relaxant concentration, but most importantly changes in the physiological state of the patient.

With the above situation, strategies based on adaptive control techniques have proved to be a very powerful asset capable of having a major impact. The controllers adopted in this study were designed on the assumption of a second order linear discrete-time model representing a Pancuronium-Bromide continuous model, whereas a third order linear discrete-time model was assumed for a Atracurium continuous model. Both continuous models exhibit severe non-linearities including dead-zone and saturation. The chosen control strategy consists of using a fixed

controller (PI) for a few samples, enough to allow the estimator to converge towards reasonable estimates, then immediately switch on to the self-adaptive scheme after that.

First, the self-tuning PIP control algorithm was selected primarily for its attractive features including its ability to cope with systems exhibiting non-minimum phase characteristics. This is due to non-minimum phase zeros becoming unstable poles in closed-loop conditions and resulting from fractional time-delays (Wellstead and Zanker, 1979; Clarke, 1984). PIP can also produce good control in the case of unknown and variable time-delay. The PIP control algorithm is formulated on the basis of a new definition of non-minimal state space definition which draws a parallel between the powerful structure of state-space models and the world of digital systems. The estimated model, based on an ARMA model structure, is considered linear around a chosen operating point although the muscle relaxation process is severely non-linear. The PIP scheme performed well even under such conditions. Its later extensions to handle unknown and variable time-delays using the Extended Smith Predictor (ESP) and Generalized Smith Predictor (GSP) schemes showed its robustness. The GSP algorithm was shown to be superior to ESP, confirming similar claims by its authors (Chotai and Young, 1988).

Although the principle of certainty equivalence guarantees good self-tuning properties when the true process parameters are substituted by their estimated ones, sometimes, and particularly in muscle relaxation, a good set of these estimates is very useful in providing a deep insight into the pharmacokinetics of the drug without resorting to the usual blood-sample analysis to find out the concentration. The use of a pass-band filter of the form of $\frac{\Delta}{T(z^{-1})}$, where $\Delta = 1 - z^{-1}$ possesses high-pass properties and $T(z^{-1})$ is a low-pass filter (suggested by Boucher et al. (1988)) allows one to obtain parameter estimates close to the true

ones and which are better than those obtained when positional data is fed to the measurement vector.

The algorithm which includes the Δ operator in its assumed model structure is the GPC algorithm. Indeed, the approach uses a CARIMA model leading therefore to the elimination of the usual offset problem (Tuffs and Clarke, 1985) which may be met with the ARMA structure. Being based on an explicit process formulation it can deal with variable dead-time, but as it is a predictive method it can also cope with overparameterization. The method can also cope with systems exhibiting non-minimum phase characteristics.

The control algorithm clearly involves more complicated calculations than the PIP approach which requires only the specification of the positions of the closed-loop poles to be assigned. While this could be seen as a drawback, it only adds to the flexibility of the approach by providing the user with a wide range of tuning factors enabling him to achieve the best possible result. This flexibility was later enhanced when the model following $P(z^{-1})$ as well as the observer $T(z^{-1})$ polynomials were introduced. While $P(z^{-1})$ affected both the output and the disturbance rejection properties of the muscle relaxation process, $T(z^{-1})$ affected only its disturbance rejection properties. Unlike the PIP approach, the overall filter $\frac{\Delta}{T(z^{-1})}$ as well as being included in the estimator, is involved in the control calculations thus reducing the overall feedback gain in case of high frequency noise components or sudden disturbances.

Among the 4 tuning factors involved in the GPC design procedure, the control horizon is considered to be of great importance. Indeed, simulation results showed that a value of $NU=1$ always led to reasonably good control, whereas values greater than 1 induced relatively high control activity. This phenomenon

can be explained by the fact that the solution of the minimization procedure of the cost function involved moves further away from the optimal one. In order to obtain the best possible solution, i.e. as near as possible to the optimal one, while retaining the advantages of high control horizon values, i.e. fast set-point tracking abilities, modification of the original algorithm to include the input constraints in the cost function, either by means of rate limits or amplitude limits, showed reduction of the control activity without modifying the process output behaviour.

Because of the several advantages specific to this algorithm, GPC was selected for simulations under real-time conditions. The previous simulation study was helpful in providing guidelines relating to the selection of the design knobs, particularly that the output horizon should be taken close to the rise time of the process and the control horizon up to a value of 2. The respective values of 10 and 1 were confirmed to be sufficiently adequate. This study proved also very useful in the sense that the observer polynomial $T(z^{-1})$ enhanced the robustness of the control strategy over a wide range of process dynamics and compensated for the unmodelled dynamics because of the underparameterized discrete-time model assumed in the case of Atracurium.

The self-adaptive GPC algorithm was later evaluated in theatre during a series of trials on humans. The muscle relaxant Atracurium was chosen for continuous infusion, because of its relatively short duration of action and its non-cumulative properties. To allow the surgeon to proceed with the operation as soon as the patient is transferred to the operating theatre, preliminary muscle relaxation is induced by administering a bolus dose, the size of which is determined from the experience of the anaesthetist. As a result, automatic control beginning initially with a fixed optimized PI, has to start only when the level of T1 is judged appropriate (ideally 15%). At this particular point two major points have to be

taken into consideration; first avoiding the non-linearity region, and second inducing as little overshoot of the EMG level as possible before the self-tuner takes over. This latter precaution is particularly important, because the fixed PI was only optimized for an average population model. For this reason the initial preloaded bolus dose was considered to represent a serious challenge in itself for the control protocol, since it does not allow proper estimation of the system dynamics, discouraging therefore the self-adaptive GPC from being switched on earlier.

In practice, it is widely agreed (Tham, 1989) that the use of the observer polynomial $T(z^{-1})$ to counteract the effect of Δ which possesses high-pass properties is no longer a choice but a necessity, and because of its inclusion in the control calculations, the wrong choice of this filter characteristics would undoubtedly lead to poor performances. In the case of the muscle relaxation process associated with Atracurium, the choice of a second order filter to double the roll-off was found to be adequate in all cases. The overall performances obtained were remarkably good. Moreover, when enough excitation is provided, good control is achieved and reasonable parameter estimates are obtained (e.g. patient AXM). On the other hand, the exercise of choosing the filter characteristics was shown to be avoidable, by feeding positional data to the estimator. This was found to lead to good set-point tracking properties, although the control signals may not be as good as when filtered incremental data is used, due perhaps to the inherent structure of the GPC which requires differenced data rather than positional data. This could be seen as a violation of the GPC principle (a similar situation was observed when the digital Smith predictor was proposed (Gawthrop, 1977; Marshall, 1979) in opposition to Smith's principle which was designed in continuous systems). It did, however, lead to satisfactory results and allowed the GPC algorithm to take over as early as 5 minutes after automatic control was initiated. A resemblance could be found between this idea and the one proposed by McIntosh et al. (1989) who

used different filter characteristics for the controller and the estimator. Perhaps the scheme proposed by Shook et al. (1991) and which consists of replacing the RLS estimator by a scheme called long-range predictive identification (LRPI) would be more appropriate since at every iteration the estimates are optimized over the same horizon range as the control sequence itself. However, as the statistical study conducted in chapter 7 has demonstrated, the main aims of the study have been achieved. Nevertheless the previous points could be explored in the hope of improving the scheme even further .

The present research work has also included another interesting area in modern anaesthesia which is unconsciousness. Because no direct measurement is available for such a variable, mean arterial blood pressure was chosen as an inferential variable to give an accurate indication of how deep the patient is anaesthetised, when no emergency conditions such as blood loss, which causes a sharp fall in blood pressure level, occur. A non-linear multivariable model combining the effect of Atracurium on muscle relaxation and the effect of inhaled Isoflurane on mean arterial pressure was derived and successfully controlled using the multivariable GPC algorithm in a series of extensive simulations including Monte-Carlo model parameters selection for robustness studies. Further simulation studies considering the GPC algorithm with feedforward (GPCF) showed its superiority to the previous multivariable GPC algorithm in reducing the interactions as well as reducing the computer burden. In light of these considerations, the scheme represents a likely candidate for future clinical trials which will hopefully be undertaken.

Further investigations in the SISO case could involve the application of the PIP algorithm in theatre and the application of the GPC algorithm with other drugs such as Vecuronium (Khelfa, 1990) whose model which has been modelled

by a class of non-linear systems known as NARMAX* models (Billings and Leontaritis, 1982). Research work in the Department of Automatic Control and Systems Engineering by Sales (1988) led to the development of a non-linear GMV algorithm applied to this class of models. Since GPC uses a cost function of similar structure to GMV, it would be interesting to develop a non-linear version of the GPC algorithm using the same philosophy.

As for the multivariable case, the use of multivariable GPC with input constraints and involving the quadratic programming approach (QP) as described by Lawson and Hanson (1974) could also be pursued (Wilkinson and Tham, 1990). This would be particularly appropriate especially if other variables are involved in the multivariable model, particularly the path concerning the indication of depth of anaesthesia. The heart-rate variable is one possibility, and this coupled with mean arterial pressure measurements would make the indication of depth of anaesthesia more reliable. To improve this reliability even further, the idea of an intelligent measurement which would filter out any unreliable indication about the state of unconsciousness seems to be very interesting. In fact the possibility of a supervisory layer above GPC, to provide overall jacketing is not new since Zhang and Cameron (1989) suggested a strategy based on the same philosophy and applied the scheme to the area of ventilation treatment for new born babies.

As a conclusion to this research work, it should be said that adaptive control has proved successful in this very challenging area of life sciences (i.e medicine) and its contribution to this area has not gone unnoticed. However, for it to be used routinely in theatre, there is a need to evaluate it even further and provide anaesthetists with proper training; this having the advantage of boosting the confidence of the medical staff towards this theory which, it is deeply felt, has so

*Non-Linear Auto-Regressive Moving Average

much to offer.

REFERENCES

1. Ali, H.H., Utting, J.E., and Gray, T.C. (1971) "Quantitative assessment of residual antidepolarizing block (Part I)", *Br. J. Anaesthes.*, Vol.43, p.473.
2. Anderson, B.D.O., and Johnson, C.R. (1982) "Exponential convergence of adaptive identification and control algorithms", *Automatica*, Vol.18, p.1.
3. Anderson, B.D.O. (1985) "Adaptive systems, lack of persistency of excitation and bursting phenomena", *Automatica*, Vol.21, p.247.
4. Asbury, A.J., Brown, B.H., and Linkens, D.A. (1980) "Control of neuromuscular blockade by external feedback mechanism", *Br. J. Anaesthes.*, No.52, pp 633p-634p.
5. Asbury, A.J. (1990) "Private communication".
6. Astrom, K.J. (1970) "Introduction to Stochastic Control Theory", Academic Press, New York.
7. Astrom, K.J., and Wittenmark, B. (1973) "On self-tuning regulators", *Automatica*, Vol.9, p.185.
8. Astrom, K.J., Borisson, U., Ljung, L., and Wittenmark, B. (1977) "Theory and applications of self-tuning regulators", *Automatica*, Vol.13, pp 457-476.
9. Astrom, K.J. (1980a) "Self-tuning regulators- Design principles and applications", in *Applications of Adaptive Control*, K.S. Narendra and R.V. Monopoli, Eds., Academic Press, N.Y.
10. Astrom, K.J., and Wittenmark, B. (1980b) "Self-tuning controllers based on pole-zero placement, *IEE Proc.*, Vol.127, pp 120-130.
11. Astrom, K.J. (1983) "Theory and applications of adaptive control- A survey", *Automatica*, Vol.19, No.5, pp 451-486.
12. Astrom, K.J., and Wittenmark, B. (1984) "Computer-Controlled Systems-Theory and Design", Prentice-hall, Englewood Cliffs, N.J.
13. Astrom, K.J., and Wittenmark, B. (1989) "Adaptive Control", Addison-Wesley Publ. Comp., U.S.A.
14. Baird, W.L.M., and Kerr, W.J. (1983) "Reversal of Atracurium with Edrophonium", *Br. J. Anaesthes.*, Vol.55, p.63S.
15. Barnett, S.G., and Cameron, R.G. (1985) "Introduction to Mathematical Control Theory", Clarendon Press.
16. Bars, R. , and Haber, R. (1990) "Long-range predictive control of non-linear systems on the basis of the Hammerstein model", *IEE conference, Control 90*, Glasgow, pp 675-679.

17. **Belanger, P.R.** (1983) "On type-1 systems and the Clarke-Gawthrop regulator", *Automatica*, Vol.19, No.1, pp 91-94.
18. **Bierman, G.J.** (1976) "Measurement updating using the U-D factorization", *Automatica*, Vol.12, pp 375-382.
19. **Bierman, G.J.** (1977) "Factorization Methods for Discrete Sequential Estimates", Academic press, New York.
20. **Billings, S.A., Sterling, M.J.H.** (1975) "SPAID- A users guide", Department of Automatic Control and Systems Engineering, University of Sheffield, England.
21. **Billings, S.A., and Leontaritis, I.J.** (1982) "Parameter estimation techniques for non-linear systems", 6th Symposium on identification and systems parameter estimation, Washington D.C, U.S.A, pp 505-510.
22. **Billings, S.A.** (1985) lecture notes.
23. **Birks, R., Huxley, H.E., and Katz, B.** (1960) "The fine structure of neuromuscular junction", *J. Physiol. (Lond.)*, Vol.150, p.134.
24. **Boucher, A.R., Cox, C.S., and Young, P.C.** (1988) "True digital control and integrated environment for the design of direct digital and adaptive control systems", IEE conf. Public., Vol.285, pp 93-98.
25. **Borisson, U.** (1979) "Self-tuning regulators for a class of multivariable systems", *Automatica*, Vol.15, pp 209-215.
26. **Breckenridge, J.L., and Aitkenhead, A.R.** (1983) "Awareness during anaesthesia: a review.", *Annals of the royal college of surgeons of England*, Vol.65, pp 93-96.
27. **Brown, R.F., and Godfrey, K.R.** (1978) "Problems of determinacy in compartmental modelling with applications to Bilirubin kinetics", *Math. Biosc.*, Vol.40, pp 205-225.
28. **Brown B.H., Asbury A.J., Linkens D.A., Perks P., and Anthony M.** (1980) "Closed-loop control of muscle relaxation during surgery", *Clin. Phys. & Physiol. Meas.*, Vol.1, pp 203-210.
29. **Burns, B.D., and Paton, W.D.M.** (1951) "Depolarization of the motor-end-plate by Decamethonium and Acetylcholine", *J. Physiol. (Lond.)*, 115, p.41.
30. **Carter, J.A., Arnold, P.M., Yate, P.M., Flynn, P.J.** (1986) "Assessment of the Datex Relaxograph during anaesthesia and Atracurium-induced neuromuscular blockade", *Br. J. Anaesthes.*, 58, pp 1447-1452.
31. **Cass, N.M., Lampard, D.G., Brown, W.A., and Coles, J.R.** (1976) "Computer-controlled muscle relaxation: A comparison of four muscle relaxants in sheep", *Anaesth. Intens. Care*, Vol.4, p.16.

32. Chien, I.L., Seborg, D.E., and Millichamp, D.A. (1984) "A self-tuning controller for systems with unknown or varying time-delays", *Int. J. Control*, Vol.42, No.4, p.949.
33. Chotai, A., and Young, P.C. (1988) "Pole-placement design for time-delay systems using a generalized discrete-time Smith predictor", *IEE conf. Public.*, 285, pp 218-223.
34. Clarke, D.W., and Gawthrop, P.J. (1975) "Self-tuning controller", *IEE Proc.*, Vol.122, No.9, pp 929-934.
35. Clarke, D.W., and Gawthrop, P.J. (1979) " Self-tuning control", *IEE Proc.*, Vol.126, pp 633-640.
36. Clarke, D.W., Hodgson, A.J.F., and Tuffs, P.S. (1983) "The offset problem and k-incremental predictors in self-tuning control", *IEE Proc.*, Vol.139, Pt.D., No.5, pp 217-225.
37. Clarke, D.W. (1983) "The application of self-tuning control", *Trans. Inst. Meas. Contr.*, Vol.5, No.2, pp 59-69.
38. Clarke, D.W. (1984) "Self-tuning of non-minimum phase systems", *Automatica*, Vol.20, No.5, pp 501-517.
39. Clarke, D.W. (1985a) "Implementation of self-tuning controllers", in 'self-tuning and adaptive control: theory and application', edit. Harris, C.J., and Billings, S.A, *IEE Contr. Eng.*, series 15, pp 146-147.
40. Clarke, D.W., and Zhang, L. (1985b) "Does long-range predictive control work?", *IEE Confer.*, Control 85, Cambridge, pp 13-19.
41. Clarke, D.W., Kanjilal, P.P., and Mohtadi, C. (1985c) "A generalized LQG approach to self-tuning control- Part I. Aspects and design", *Int. J. Control*, Vol.41, No.6, pp 1509-1523.
42. Clarke, D.W., Kanjilal, P.P., and Mohtadi, C. (1985d) "A generalized LQG approach to self-tuning control- Part II. Implementations and simulations", *Int. J. Control*, Vol.41, No.6, pp 1524-1544.
43. Clarke, D.W., Mohtadi, C., and Tuffs, P.S. (1987a) "Generalized predictive control- part I. The basic algorithm", *Automatica*, Vol.23, No.2, pp 137-148.
44. Clarke, D.W., Mohtadi, C., and Tuffs, P.S. (1987b) "Generalized predictive control- part II. Extensions and interpretations", *Automatica*, Vol.23, No.2, pp 149-160.
45. Clarke, D.W., and Mohtadi, C. (1989) "Properties of generalized predictive control", *Automatica*, Vol.25, No.6, pp 859-875.
46. Clarke, D.W., and Robinson, B.D. (1991) "Robustness effects of a prefilter in generalized predictive control", *IEE Proc.*, Pt.D., Vol.138, No.1, pp 2-8.

47. **Cutler, C.R., and Ramaker, B.L. (1980)** "Dynamic matrix control- A computer control algorithm", JACC, San-Francisco, paper WP5-B.
48. **Dale, H.H., and Feldberg, W. (1934)** "Chemical transmission at motor nerve endings in voluntary muscle", J. Physiol. (Lond.), 81, p.39.
49. **Davies, W.D.T. (1970)** "System Identification for Self-Adaptive Control", Wiley and Sons Ltd.
50. **De Keyser, R.M.C., and Van Cauwenberghe, A.R. (1979a)** "A self-tuning predictor as operator guide", 5th IFAC Sympos. on identification and system parameter estimation, Dramstadt.
51. **De Keyser, R.M.C., and Van Cauwenberghe, A.R. (1979b)** "A self-tuning multistep predictor application", Automatica, Vol.17, pp 167-174.
52. **De Keyser, R.M.C., and Van Cauwenberghe, A.R. (1983)** "Microcomputer-controlled servo system based on self-tuning adaptive long-range prediction", Methods and applications of measurement and control, Trafestas, S.G., and Hamza, M.H. (editors), pp 583-587.
53. **De Keyser, R.M.C., and Van Cauwenberghe, A.R. (1985)** "Extended prediction self-adaptive control", 7th IFAC Sympos. on identification and system parameter estimation, invited session on applications of adaptive and self-tuning control, York, pp 1255-1260.
54. **De Keyser, R.M.C., and Van Cauwenberghe, A.R. (1986)** "Towards robust adaptive control with extended predictive control", IEEE Proc., 25th Confer. on decision and control, Athens (Greece).
55. **De Keyser, R.M.C., Van De Velde, Ph.G.A., and Dumortier, F.A.G. (1988)** "A comparative study of self-tuning long-range predictive control methods", Automatica, Vol.24, No.2, pp 149-163.
56. **Denai M., Linkens, D.A., Asbury, A.J., Macleod, A.D., and Gray, M.W. (1990)**. "Self-tuning PID control of Atracurium-induced muscle relaxation in surgical patients", Proc. IEE, Pt.D, 137, pp 261-272.
57. **De Vries, J.W., Ros, H.H., Booij, L.H.D.J. (1986)** "Infusion of Vecuronium controlled by a closed-loop system", Br. J. Anaesthes., 58, pp 1100-1103.
58. **Dion, J.M., Dugard, L., and N'Guyen Minh, T. (1991)** "Decoupling and constraints aspects of multivariable GPC", Proc. First European Control Conference ECC1, Grenoble (France), 2nd. July, Vol.2, pp 1075-1080.
59. **Ebert, J., Carroll, S.K., Bradley, E.L. (1986)** "Closed-loop feedback control of muscle relaxation with Vecuronium in surgical patients", Anaesthesia and Anaesthesiology, Vol.65, p.S44.
60. **Epstein, R.M., and Epstein, R.A. (1975)** "Electromyography in evaluation of the response to muscle relaxants", in R.L. Katz (Ed.), Muscle relaxants, Amsterdam: Excerpta Medica.

61. Fortescue, T.R., Kershenbaum, L.S., and Ydstie, B.E. (1981) "Implementation of self-tuning regulators with variable forgetting factors", *Automatica*, Vol. 17, NO.6, pp 831-835.
62. Garcia, C.E. (1984) "Quadratic/dynamic matrix control of non-linear processes: an application to a batch reaction process", AIChE meeting, San-Francisco, pp F3-G13.
63. Garcia, C.E., and Morshedi, A.M. (1986) "Quadratic programming solution of dynamic matrix control (QDMC)", *Chem.Eng.Commun.*, Vol.46, pp 073-087.
64. Gawthrop, P.J. (1977) "Some interpretations of the self-tuning controller", *IEE Proc.*, Vol.124, No.10, pp 889-894.
65. Gawthrop, P.J. (1979) "Smith's method and self-tuning control", *IEE Colloq. Digest*, No. 1979/39.
66. Gibaldi, M., Levey, G., and Hayton, W. (1972) "Kinetics of the elimination and neuromuscular blocking effect of d-Tubocurarine in man", *Anaesthesiology*, Vol.36, pp 213-218.
67. Gibaldi, M., and Perrier, D. (1975) "Pharmacokinetics. Drugs and pharmaceutical sciences", Vol.1, Marcel Dekker, New York.
68. Golomb, S.W. (1964) "Digital communications with space applications", Prentice-hall Inc., Englewood cliffs, N.J.
69. Goodwin, G.C., Elliot, H., and Teoh, E.K. (1983) "Deterministic convergence of a self-tuning regulator with covariance resetting", *Proc. IEE on control theory and appl.*, Vol.130, NO.1, p.6.
70. Goodwin, G.C., and Sin, K.S. (1984) "Adaptive Filtering Prediction and Control", Prentice-hall.
71. Graupe, D. (1976) "Identification of Systems", Robert Krieger Publ.Compa., Malabar, Florida, U.S.A.
72. Gray, W.M., and Asbury, A.J. (1986) "Measurement and control of depth of anaesthesia in surgical patients", Third IMEKO conference on 'Measurement in clinical medicine', Edinburgh, pp 167-172.
73. Greco, C., Menga, G., Mosca, E., and Zappa, G. (1984) "Performance improvements of self-tuning controllers by multistep horizons: The MUSMAR approach", *Automatica*, Vol.20, No.5, pp 681-699.
74. Gregory, P.C. (1959), Proc. self-adaptive flight control symposium, WADC report, No.59-49.
75. Ham, J., Miller, R.D., Sheiner, L.B., and Matteo, R.S. (1979) "Dosage schedule in dependence of d-Tubocurarine pharmacokinetics and pharmacodynamics and recovery of neuromuscular functions", *Anaesthesiology*, Vol.50, pp 528-533.

76. Harris, T.J., Mac Gregor, J.F., and Wright, J.D. (1980) "Self-tuning and adaptive controllers: an application to catalytic reactor control", *technometrics*, Vol.22, p.153.
77. Hull, C.J., English, M.J.M., and Sibbald, A. (1980) "Fazadinium and Pancuronium: a pharmacodynamic study", *Br. J. Anaesthes.*, 52, pp 1209-1220.
78. Hull, C.J., Van Beem, B.H., McLeod, K., Sibbald, A., and Watson, M.J. (1978) "A pharmacodynamic model for Pancuronium", *Br. J. Anaesth.*, No.50, p.113.
79. Hunt, K.J. (1986) "A survey of recursive identification algorithms", *Trans. Inst. Meas. Contr.*, Vol.18, No.5, pp 273-278.
80. Isermann, R. (1981) "Digital control systems", Springer-Verlag.
81. Isermann, R. (1982) "Parameter adaptive control algorithms- A tutorial", *Automatica*, Vol.18, No.5, pp. 513-528.
82. Jazwinski, A.H. (1970) " Stochastic Processes and Filtering Theory", Academic press, New York.
83. Kalman, R.E. (1958) "Design of a self-optimizing control system", *ASME Trans. J. Bas. Eng.*, Vol.80, pp 468-478.
84. Kalman, R.E. (1960) "A new approach to linear filtering and prediction problems", *Trans.ASME, series D, J. of Bas. Eng.*, Vol.82, pp 35-45.
85. Kalman, R.E., and Bucy, R.S. (1961) "New results in linear filtering and prediction theory", *J. of Bas. Eng.*, Vol., pp 95-108.
86. Khelfa, M. (1990) "Non-linear identification and control of muscle relaxant dynamics", PhD thesis, Department of Automatic Control and Systems Engineering, University of Sheffield, England.
87. Koivo, H.N. (1980) "A multivariable self-tuning controller", *Automatica*, Vol.16, pp 351-366.
88. Kucera, V. (1979) "Discrete Linear Control", Ed. Wiley.
89. Kuo, B.C. (1980) "Digital Control Systems", HRW series in electrical engineering, New York.
90. Kurz, H., and Goedecke, W. (1981) "Digital parameter-adaptive control for processes with unknown dead-time", *Automatica*, Vol.17., No.1, pp 245-252.
91. Lam, K.P. (1980) "Implicit and explicit self-tuning controllers", DPhil thesis, Oxford University Engineering Laboratory.
92. Landau, I.D. (1974) "A survey of model-reference adaptive techniques: theory and applications", *Automatica*, Vol.10, pp 353-379.

93. Lawson, C.L., and Hanson, R.J. (1974) "Solving least-squares problems", Prentice-hall series in automatic computation.
94. Lee, T.H., Lim, K.W., and Lai, W.C. (1991) "Real-time multivariable self-tuning controller using a feedforward paradigm with application to a coupled electric-drive pilot plant", to appear in IEEE Trans. on Industrial Electronics.
95. Linkens, D.A., Asbury, A.J., and Brown, B.H. (1981) "On-line control of muscle relaxant administration during anaesthesia", IEE Confer.on control and its applic., Warwick, pp 33-36.
96. Linkens, D.A., Asbury, A.J., Rimmer, S.J., and Menad, M. (1982). "Identification and control of muscle relaxant anaesthesia", IEE Proc., 129, pp 136-141.
97. Linkens, D.A., Menad, M., and Asbury, A.J. (1985). "Smith predictor and self-tuning control of muscle relaxant drug administration". Proc. IEE, Pt.D., 132, pp 212-218.
98. Linkens, D.A., Greenhow, S.G., and Asbury, A.J. (1990). "Clinical trials with the anaesthetic expert advisor RESAC", Expert systems in medicine 6, June, London, pp 11-18.
99. Linkens, D.A., and Haciosalihzade, S.S. (1990). "Computer control systems and pharmacological drug administration", J. Med. Eng.& Tech., 14, pp 41-54.
100. Linkens D.A., Mahfouf, M., Asbury, A.J., and Gray, W.M. (1991) "Generalized predictive control applied to muscle relaxant anaesthesia", IEE conference on adaptive control, Control 91, Edinburgh, March, pp 790-794 .
101. Linkens, D.A., Mahfouf, M., and Asbury, A.J. (1991) "Multivariable generalized predictive control for anaesthesia", Proc. First European Control Conference ECC1, Grenoble (France), 2nd. July, Vol.2, pp 1687-1683.
102. Ljung, L., and Soderstrom, T. (1983) "Theory and Practice of Recursive Identification", MIT Press, Cambridge MA.
103. Luenberger, D.G. (1966) "Observers for multivariable systems", IEEE, Trans.Auto. Control., Ac-11, pp 190-197.
104. MacLeod, A.D., Asbury, A.J., Gray, W.M., and Linkens, D.A. (1989) "Automatic control of neuromuscular block with Atracurium", Br. J. Anaesthes., 63, pp 31-35.
105. Marshall, J.E. (1974) "Extensions of O.J.M. Smith predictors to digital and other systems", Int. J. Control, Vol.19, No.5, pp 933-939.
106. Marshall, J.E. (1979) "Control of time-delay systems", IEE Control Engineering series 10, Peter Peregrinus Ltd., Stevenage, U.K.
107. Mayne, D.Q. (1973) "The Design of Linear Multivariable Systems", Automatica, Vol.9, pp 201-207.

108. McIntosh, A.R., Shah, S.L., and Fisher, D.G. (1989) "Selection of tuning parameters for adaptive generalized predictive control", Proceedings of the Amer. Contr. Conf., Pittsburgh, pp 1828-1833.
109. Menad, M. (1984) "Feedback Control of Drug Administration for Muscle Relaxation", PhD thesis, Department of Automatic Control and Systems Engineering, University of Sheffield, England.
110. Mendonca, T.F., Lemos, J.M., and Lago, P.J.A. (1989) "Long-range adaptive control of muscle relaxation with input constraints", IFAC Confer. on control in biomedicine, City Univ., London., pp 231-241.
111. Millard R.K., Hutton P., Pereira E., and Roberts C.Prys. (1986). "On using a self-tuning controller for blood pressure regulation during surgery", in 'IMEKO conference on measurement in clinical medicine', Edinburgh, pp 173-178.
112. Millard R.K., Monk C.R., Woodcock T.E., and Roberts C.Prys. (1988a) "Controlled hypotension during ENT surgery using self-tuners", Biomed. Meas. Info. Contr., Vol.2, No.2, pp 59-72.
113. Millard R.K., Monk, C.R., and Roberts C.Prys. (1988b) "Self-tuning control of hypotension during ENT surgery using a volatile anaesthetic", IEE Proc., Pt.D, 125, pp 95-105.
114. Mohtadi, C., Shah, S.L., and Fisher, D.G. (1991) "Frequency response characteristics of MIMO GPC", Proc. First European Control Conference ECC1, Grenoble (France), 2nd.July, Vol.2., pp 1845-1850.
115. Montague, G.A., and Morris, A.J. (1985) "Application of adaptive control: a heat exchanger system and a penicillin fermentation process", Third workshop on the theory and applications of self-tuning and adaptive control, Oxford, U.K.
116. Mosca, E., Zappa, G., and Lemos, J.M. (1989) "Robustness of multipredictor adaptive regulators: MUSMAR", Automatica, Vol.25, No.24, pp 521-529.
117. O'Reilly, J. (1983) "Observers for Linear Systems", Academic Press, London.
118. Owens, D.H., and Warwick, K. (1990) "Extended predictive control", IEE Confer., Control 90, Glasgow, pp 622-627.
119. Paton, W.D.M., and Waud, D.R. (1967) "The margin of safety of neuromuscular blockade transmission", J. Physiol. (Lond.), Vol.191, p.59.
120. Popov, V.M. (1964) "Hyperstability and optimality of automatic systems with several control functions", Rev. Roum. Sci. Tech., Ser. Electro. Tech. Energ., 9, pp 629-690.
121. Power, H.M., and Simpson, R.J. (1978) "Introduction to dynamics and control", London McGraw-Hill Book Co. (U.K) Ltd.

122. Prager, D.L., and Wellstead, P.E. (1980) "multivariable pole-assignment self-tuning regulators", IEE Proc., Pt.D, Vol.128, pp 9-18.
123. Richalet, J., Rault, A., Testud, J.L., and Papon, J. (1978) "Model predictive heuristic control: applications to industrial processes", Automatica, Vol.14, No.5, pp 413-428.
124. Ritchie, L.B., Ebert, J.P., Janett, T.C., Kissin, I., and Sheppard, L.C. (1985) "A microcomputer-based controller for neuromuscular block during surgery", IEEE Trans. Biomed. Eng., Vol.13, p.3.
125. Robb, H.M., Asbury, A.J., Gray, W.M., and Linkens, D.A. (1988) "Towards automatic control of general anaesthesia", Confer. 'Medical informatics '88', Nottingham, pp 121-126.
126. Rowland, M. (1978) "Drug administration and regimens in clinical pharmacology: Basic principles in therapeutics", Melnon and Morrelli (Eds), New York: Mac Millan, pp 25-70.
127. Sales, R.K. (1988) "Self-tuning control of non-linear systems", PhD thesis, Department of Automatic Control and Systems Engineering, University of Sheffield, England.
128. Savege, T.M., Dubois, M., Frank, M., Holly, J.M.P. (1978) "Preliminary investigation into a new method of assessing the quality of anaesthesia: the cardiovascular response to a measured noxious stimulus", Br. J. Anaesthesia, Vol.50, pp 481-487.
129. Schils, G.F., Sasse, F.J., and Rideout, V. (1987) "Automatic control of anaesthesia using two feedback variables", Annals of biomedical engineering, Vol.15, pp 19-34.
130. Schwilden, H. (1981) "A general method for calculating the dosage in linear pharmacokinetics", Europ. J. Clin. Pharmacol., 20, pp 379-386.
131. Schwilden, H., Scuttler, J., and Stoeckel, H. (1987) "Closed-loop feedback control of methohexital anaesthesia by quantitative EEG analysis in humans", Anaesthesiology, Vol.67, pp 341-347.
132. Schwilden, H., Stoeckel, H., and Scuttler, J., (1989) "Closed-loop control of propofol anaesthesia by quantitative EEG analysis in humans", Br. J. Anaesth., Vol.62, pp 290-296.
133. Seborg, D.E., Edgar, T.F., and Shah, S.L. (1986) "Adaptive control strategies for process control: a survey", AIchem journal, Vol.32., No.6, pp 881-913.
134. Shanks, C.A., Somogyi, A.A., Ranzqa, M.I., and Triggs, E.J. (1980) "d-Tubocurarine and Pancuronium: a pharmacokinetics view", Anaesthesiology Intens. Care 8, 4.
135. Sheiner, L.B., Stanski, D.R., Vozeh, S. (1979) "Simultaneous modelling of pharmacokinetics and pharmacodynamics: Application to d-Tubocurarine", Clin. Pharm. and Therap., Vol.25, p.358.

136. Sheppard, L.C., Shotts, J.F., Roberson, N.F., Wallace, F.D., and Kouchoukos, N.T. (1979) "Computer-controlled infusion of vasoactive drugs in cardiac patients", Proc. 1st Annual Conf. IEEE Eng. in Medic. and Biol. Society, Denver, Colorado, p.280.
137. Shook, D.S., Mohtadi, C., and Shah, S.L. (1991) "Identification for long-range predictive control", IEE Proc., Pt.D., Vol.138, No.19, pp 75-84.
138. Slate, J.B. (1980) "Model-based design of a controller for infusion Sodium Nitroprusside during post-surgical hypertension", PhD thesis, University of Wisconsin in Madison, U.S.A.
139. Smith, O.J.M. (1957) "Closer control of loops with dead-time", Chem. Eng. Prog., Vol.53, No.5, pp 217-219.
140. Smith, O.J.M. (1959) "A controller to overcome dead-time", ISA J., Vol.6, No.2.
141. Smith, N.TY., and Schwede, H.O. (1972) "The response of arterial pressure to Halothane: a systems analysis", Med. & Biol. Eng., Vol.10, pp 207-221.
142. Smith, N.TY., Rampil, I.J., Sasse, F.J., Hoff, B.H., and Fleming, D.C. (1980) "The Dynamic response to Enflurane and Halothane", Anaesthesiology, Vol.53, No.3, p.337.
143. Stanski, D.R., Ham, S., Miller, R.D. (1979) "Pharmacokinetics and pharmacodynamics of d-Tubocurarine during nitrous-oxide, narcotic and Halothane anaesthesia in man", Anaesthesiology, Vol.5, pp 235-241.
144. Tham, M.J. (1989) "Private communication".
145. Tsang, T.T.C., and Clarke, D.W. (1988) "Generalized predictive control with input constraints", IEE Proc., Pt.D., Vol.135, No.6, pp 451-460.
146. Tuffs, P.S., and Clarke, D.W. (1985) "Self-tuning control of offset: a unified approach", IEE Proc., Vol.132, Pt.D., pp 100-110.
147. Van Den Bosch, P.P.J. (1979) "PSI: an extended interactive block oriented simulation program", IFAC Symp. CAD Control Syst., Zurich, pp 223-228.
148. Vogel, E.F. (1982) "Adaptive control of chemical processes with variable dead-time", PhD thesis, Univ. Texas, Austin.
149. Wait, C.M., Goat, V.A., Blogg, C.E. (1987) "Feedback control of neuromuscular blockade. A simple system for infusion of Atracurium", Anaesthesia, Vol.42, pp 1212-1217.
150. Wang, C.L., and Young, P.C. (1988) "On the pole-assignment of linear, discrete-time servomechanism systems via state-variable input-output feedback", internal report No.54, centre for research on environmental systems, Institute of environmental and biological sciences, Lancaster University.

151. Ward, S., Neill, E.A.M., Weatherly, B.C., and Corall, I.M. (1983) "Pharmacokinetics of Atracurium Besylate in healthy patients (after a single iv bolus dose)", *Br. J. Anaesthes.*, Vol.55, p.113.
152. Warwick, K., and Clarke, D.W. (1988) "Weighted input predictive controller", *IEE Proc., Pt.D.*, Vol.135, No.1, pp 16-20.
153. Waud, D.R., and Waud, B.E. (1971) "The relation between tetanic fade and receptor occlusion in the presence of competitive neuromuscular block", *Anaesthesiology*, Vol.35, p.456.
154. Waud, D.R. (1972) "Biological assays involving quantal responses", *J. Pharmacol. Exp. Theor.*, Vol.183, p.577.
155. Weatherley, B.C., Williams, S.G., and Neil, E.A.M. (1983). "Pharmacokinetics, pharmacodynamics and dose response relationship of Atracurium administered i.v", *Br. J. Anaesthes.*, 55, p.39S.
156. Webster, N.R., Cohen, A.T. (1987) "Closed-loop administration of Atracurium. Steady-state neuromuscular blockade during surgery using a computer controlled closed-loop Atracurium infusion", *Anaesthesia*, 42, pp 1085-1091.
157. Wellstead, P.E., and Gale, S. (1978a) "Self-tuning pole/zero assignment predictions", Control Systems Centre, Report No.412, UMIST, Manchester, U.K.
158. Wellstead, P.E., Prager, D., Zanker, P., and Edmunds, J.M. (1978b) "Self-tuning pole/zero regulators", Control Systems Centre, Report No.404, UMIST, Manchester, U.K.
159. Wellstead, P.E., and Zanker, P. (1979) "The techniques of self-tuning control systems", Control Systems Centre, Report No.432, UMIST, Manchester, U.K.
160. Wellstead, P.E. (1980) "Self-tuning control systems: the pole-zero assignment approach", SRC vacation school on computer control, University of Sheffield, September, pp 9.1-9.34.
161. Wellstead, P.E., and Sanoff, S.P. (1981) "Extended self-tuning algorithm", *Int. J. Control*, Vol.34, No.3, pp. 433-455.
162. Whiting, B. , and Kelman, A.W (1980). "The modelling of drug response", *Cli. Scien.*, 59, pp 311-314.
163. Wilkinson, D.J., and Tham, M.J. (1990) "Predictive control with constrained optimisation", Internal report, Dept.of Chem.Eng., New-Castle University, U.K.
164. Wood, R.K., Berry, M.W. (1973) "Terminal Compensation of a Binary Distillation Column", *Chem. Eng. Scien.*, Vol.28, pp 1707-1717.
165. Woodcock, T.E., Millard R.K., Dixon, J., and Roberts, C.Prys. (1988) "Clonidine Premedication for Isoflurane-Induced Hypotension", *Br. J. Anaesthesia*, Vol.60, pp 388-394.

166. Ydstie, B.E. (1984) "Extended horizon adaptive control", IFAC Proc., 9th triennial world congress, Budapest (Hungary), pp 911-815.
167. Ydstie, B.E., Kershenbaum, L.S., Sargent, R.W.H. (1985) "Theory and application of an extended horizon self-tuning controller", AIChE J., Vol.31, No.1, p.771.
168. Young, P.C. (1969) "Applying parameter estimation to dynamic systems", Control Eng., Vol.16, p.119.
169. Young, P.C. (1970) "An instrumental variable method for real-time identification of a noisy process", Automatica, Vol.16, p.271.
170. Young, P.C., and Willems, J.C. (1972) "An approach to the linear multivariable servomechanism problem", Int. J. Control, Vol.15, No.5, Pt.2, pp 961-979.
171. Young, P.C. (1984) "Recursive Estimation and time-series analysis", Springer verlag, Berlin.
172. Young, P.C. (1987) "Recursive Estimation forecasting and adaptive control", chapter in Leondes, C.T. Ed. Control and Dynamic Systems, Vol.XXVIII, Academic Press.
173. Young, P.C., Behzadi, M.A., Wang, C.L., and Chotai, A. (1987) "Direct digital and adaptive control by input-output state-variable feedback pole-placement", Int. J. Control, Vol.46, pp 1867-1881.
174. Zanker, P., and Wellstead, P.E. (1978), Control Systems Centre, Report No.422, UMIST, Manchester, U.K.
175. Zhang, L., and Cameron, R.G. (1989) "A real-time expert control strategy for blood gas management in neonates under ventilation treatment", IEE colloquium on exploiting the knowledge base: Application of rule based control, London, pp 4/1-4/7.
176. Ziegler, J.G., and Nichols, N.B. (1942) "Optimum settings for automatic controllers", Trans. Eng., Vol.64, p.759.

APPENDIX A

Solution of the Diophantine Equation- The Extended Version

Consider the following expressions extended respectively to the horizons "j" and "j+1", and where the operator z^{-1} has been dropped for simplicity:

$$\begin{cases} G_j = E_j B = (e_0 + e_1 z^{-1} + e_2 z^{-2} + \dots + e_{j-1} z^{-j+1}) B \\ G_{j+1} = E_{j+1} B = (e_0 + e_1 z^{-1} + e_2 z^{-2} + \dots + e_{j-1} z^{-j+1} + e_j z^{-j}) B \end{cases} \quad (A1)$$

$$\begin{cases} G'_j = g'_1 + g'_2 z^{-1} + \dots + g'_j z^{-j+1} \\ G'_{j+1} = g'_1 + g'_2 z^{-1} + \dots + g'_j z^{-j+1} + g'_{j+1} z^{-j} \end{cases} \quad (A2)$$

$$\begin{cases} \Gamma_j = \gamma_j^0 + \gamma_j^1 z^{-1} + \dots + \gamma_j^i z^{-i} \\ \Gamma_{j+1} = \gamma_{j+1}^0 + \gamma_{j+1}^1 z^{-1} + \dots + \gamma_{j+1}^i z^{-i} \end{cases} \quad (A3)$$

Where $i = \max(\delta B, \delta T)$.

Now, recall equation (5.54) from section 5.5.2 and labelled here (A4).

$$G_j = T G' + z^{-j} \Gamma_j \quad (A4)$$

For the next horizon 'j+1' it follows that:

$$G_{j+1} = T G' + z^{-(j+1)} \Gamma_{j+1} \quad (A5)$$

Subtracting (A4) from (A5) yields:

$$z^{-j} e_j B = z^{-j} T g'_{j+1} + z^{-j} (z^{-1} \Gamma_{j+1} - \Gamma_j) \quad (A6)$$

After simplifying z^{-j} in equation (A6) it follows that:

$$\begin{cases} e_j (b_0 + b_1 z^{-1} + \dots) = (t_0 + t_1 z^{-1} + \dots) g'_{j+1} + z^{-1} \Gamma_{j+1} - \Gamma_j \\ z^{-1} \Gamma_{j+1} - \Gamma_j = z^{-1} (\gamma_{j+1}^0 + \gamma_{j+1}^0 z^{-1} + \dots) - (\gamma_j^0 + \gamma_j^1 z^{-1} + \dots) \end{cases} \quad (A7)$$

Identifying the two sides of the above equations using the powers of 0, -1, -2,... of z leads to:

Power zero of z:

$$e_j b_0 = t_0 g'_{j+1} - \gamma_j^0$$

Leading to the following expression of g'_{j+1} :

$$g'_{j+1} = t_0^{-1} (e_j b_0 + \gamma_j^0) \quad (A8)$$

And,

$$\text{power -1 of z} \quad e_j b_1 = t_1 g'_{j+1} + \gamma_{j+1}^0 - \gamma_j^1$$

$$\text{power -2 of z} \quad e_j b_2 = t_2 g'_{j+1} + \gamma_{j+1}^1 - \gamma_j^2$$

$$\begin{matrix} \cdot & \cdot & \cdot & \cdot & \cdot \\ \cdot & \cdot & \cdot & \cdot & \cdot \\ \cdot & \cdot & \cdot & \cdot & \cdot \end{matrix}$$

The common expression for the γ coefficients is given by the following:

$$\begin{aligned} \gamma_{j+1}^{i-1} &= e_j b_i - t_i g'_{j+1} + \gamma_j^i \\ i &= \max (\delta B, \delta T) \end{aligned} \quad (A9)$$

Finally, summarizing the solution of equation (A4), yields:

$$\begin{cases} g'_{j+1} = t_0^{-1} (e_j b_0 + \gamma_j^0) \\ \gamma_{j+1}^{i-1} = e_j b_i - t_i g'_{j+1} + \gamma_j^i \\ i = \max (\delta B, \delta T) \end{cases} \quad (\text{A10})$$

APPENDIX B

Recursive Least-Squares Algorithm- The Multivariable case

A discrete-time model equation may be rewritten in the following way:

$$y_t^i = x_t^{iT} \hat{\theta}_t^i + \epsilon_t^i \quad i=1, 2, \dots, p \quad (\text{B1})$$

Where,

- y_t^i is the i th component of the output vector y_t
- ϵ_t^i is the i th component of the residual vector ϵ_t
- x_t^i is the data vector
- θ_t^i is the associated parameter vector

From the standard recursive least-squares algorithm of chapter 3, the parameters are found using the following algorithm assuming that the A_i matrices are diagonal:

$$\hat{\theta}_{t+1}^i = \hat{\theta}_t^i + \gamma_t p_{t+1} x_{t+1}^i [y_{t+1}^i - x_{t+1}^{iT} \hat{\theta}_t^i] \quad (\text{B2})$$

where,

$$x_t^i = [y_{t-1}^i, y_{t-2}^i, \dots, y_{t-na}^i, u_{t-1}^1, \dots, u_{t-nb}^1, \dots, u_{t-1}^p, \dots, u_{t-nb}^p]^T$$

Since the measurement vectors are different for every channel, the gain γ , and the covariance matrix p_t need to be updated p times in addition to the updating of the parameters $\hat{\theta}_i$.